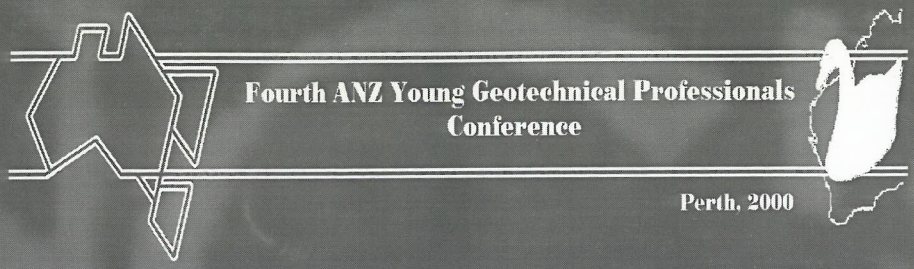

Proceedings of

THE FOURTH AUSTRALIA NEW ZEALAND YOUNG GEOTECHNICAL PROFESSIONALS CONFERENCE

Andrew House
Phil Watson
(Editors)

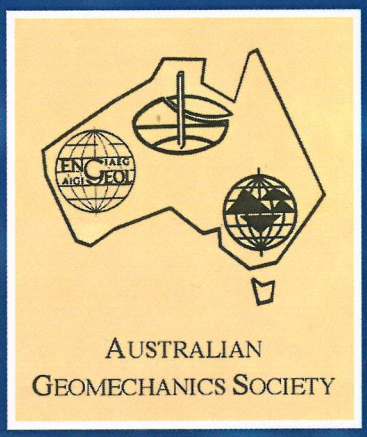

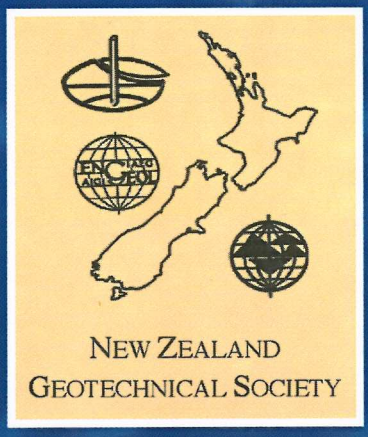

16 - 19 FEBRUARY 2000

St George's College

The University of Western Australia

Perth Australia

A gift in support of

Golder's commitment to technical

knowledge and excellence

Max Ervin

MAX ERVIN

WELCOME TO DELEGATES

WELCOME to the Fourth Australia New Zealand Young Geotechnical Professionals Conference, and for those visiting the west for the first time, welcome to Perth. First held in Sydney in 1994, from a joint initiative of the Australian Geomechanics Society and the New Zealand Geotechnical Society, the conference has since been successfully held in Auckland (1996) and Melbourne (1998).

In recent years, there has been a strong push for increased participation by "young" geotechnical engineers in society matters. This topic was first discussed at the Third ANZ YGPC, where the topic "How could the AGS and NZGS better serve their younger members" was debated in an open forum. Since then, the "Young Australian Geomechanics Society Corner" was established in the AGS journal (Australian Geomechanics), in which young geotechnical engineers are encouraged to contribute anything from seminar advertisements to stories on "life's little lessons". In addition, there is an ever increasing amount of direct input in AGS/NZGS affairs, with many committees now including at least one young representative.

With this in mind, I hope that all delegates attending the Fourth ANZ YGPC are able to both increase their own involvement in the geomechanics community, and encourage others within their organisation to do the same. This can come in the form of an active involvement by joining your local AGS/NZGS committee, by attending technical meetings, or by writing articles for society magazines or newsletters. It all counts. Please feel free to contact me (philw@cyllene.uwa.edu.au or at Centre for Offshore Foundation Systems, The University of Western Australia, Nedlands, AUSTRALIA 6907) if you would like any further information on becoming involved in the AGS or NZGS. If I can't help you myself, I will point you in the direction of someone who can.

As is always the case with events like this, there are a large number of people to thank for their involvement. Firstly, I must thank the other (past and present) organising committee members : Mike O'Neill, Andrew House, Davide Bruno and Gerard Dyson. All of them have put in a tremendous amount of time and energy to ensure the conference is a success. In addition, there have been a number of industry representatives (IR) and senior mentors (SM) who have provided great assistance at various stages of the conference organisation, with thanks going to : Dr Anthony de Nicola (IR), Dr Stephanie Watson (IR), Ms Eloise Browne-Cooper (IR), A/Prof. Martin Fahey (SM), Prof. Mark Randolph (SM), Dr Mohamed Khorshid (SM) and Mr Charles Waterton (SM). I would also like to thank the members of the Western Australian Chapter of the AGS, and acknowledge the support of the AGS National Committee. Thanks also to the various paper reviewers. In addition, thanks also to the NZGS (particularly Debbie Fellows and Jaime Bevin) for their support in organising what is a very strong New Zealand contingent.

In respect to conference events, I would like to thank the Fremantle Port Authority for providing their facilities for the site visit, and Mr Matthew Tutton (from Golder Associates) for organising the schedule for the afternoon, and for offering to act as 'tour guide'. I would also like to thank the various keynote speakers and session organisers, each of whom have agreed to give up their time to help make the conference a success. Thanks also to St George's College for providing the conference facilities and assisting with organisation, and to Golder Associates for arranging (and sponsoring!) the conference barbecue.

With this said, I would like to wish all delegates an enjoyable conference. I hope each of you benefit from the opportunity to present your own research, from the opportunity to 'network', and from an active participation in all formal and social aspects of the conference. The organising committee and myself are looking forward to meeting you at the conference.

Best regards,

Phil Watson
Chairman of the Organising Committee

Organising Committee

Mr Phil Watson
Mr Mike O'Neill
Mr Andrew House
Mr Davide Bruno
Mr Gerard Dyson

Industry Representatives

Dr Stephanie Watson
Dr Anthony de Nicola
Ms Eloise Browne-Cooper

Senior Mentors

Associate Professor Martin Fahey
Professor Mark Randolph
Dr Mohamed Khorshid
Mr Charles Waterton

Paper Reviewers

Mr Marc Woodward
Mr Trevor Osborne
Dr Doug Stewart
Professor Mark Randolph
Dr Chris Martin
Mr Robert Smith
Dr Sasha Galybin
Mr Ian Smith
Mr John Waterton
Dr Chris Swindells
Associate Professor Richard Jewell
Dr Yves Potvin
Mr David Foulsham
Dr Elio Novello
Dr Mohamed Khorshid
Dr Hackmet Joer
Associate Professor Martin Fahey
Dr Tam Larkin

All papers accepted for publication at this conference were independently reviewed by a senior geotechnical engineer. Papers were reviewed to check technical accuracy, relevance and presentation.

THE ORGANISING COMMITTEE WOULD LIKE TO ACKNOWLEDGE THE GENEROUS FINANCIAL SUPPORT OBTAINED FROM THE CONFERENCE SPONSORS. WITHOUT THEIR CONTRIBUTION, THE CONFERENCE WOULD NOT HAVE BEEN POSSIBLE.

ADVANCED GEOMECHANICS

Providing leading edge geotechnical design solutions

Offshore

- Site investigation definition, planning and supervision
- Advanced analytical and numerical modelling
- Foundation/structure interaction
- Pile design - driven, drilled and grouted, driven grouted
- Engineering of terrigenous and calcareous soils
- Design, supervision and interpretation of laboratory testing programs
- Drag anchor, suction pile and gravity anchor design
- Pipeline stability, ploughability and scour evaluation
- Probabilistic cost risk analyses

Onshore

- Site characterisation and parameter interpretation
- Development of novel, economic foundation concepts
- Design of in situ testing programs
- Piled and shallow foundation analysis and design
- Seepage, groundwater & dewatering assessments
- Soil and rock slope design (eg. reinforced earth/soil nailing)
- Soil stabilisation and ground improvement
- Pile drivability, integrity testing & verification services
- Expert advice for litigation

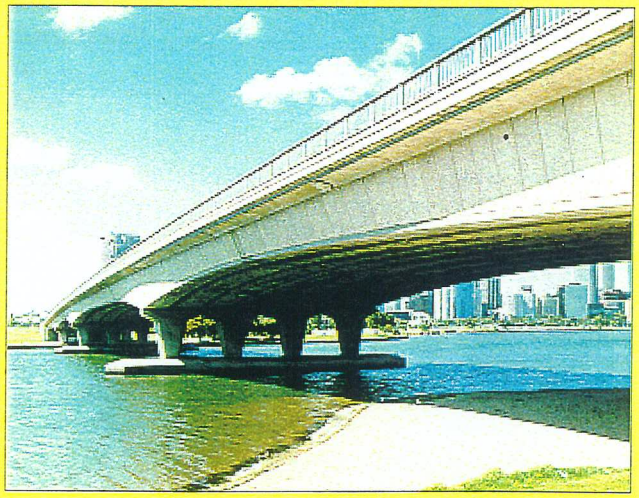

ADVANCED GEOMECHANICS

Contact Details

Perth
Advanced Geomechanics
4 Leura Street, Nedlands
Western Australia 6009
Phone: +61 8 9389 5033
Fax: +61 8 9389 5066
E-mail: info@ag.com.au

Sydney
Advanced Geomechanics
40 Canonbury Grove, Dulwich Hill
New South Wales 2203
Phone: +61 2 9558 1535
Fax: +61 2 9559 4771
Web Site: http://www.ag.com.au

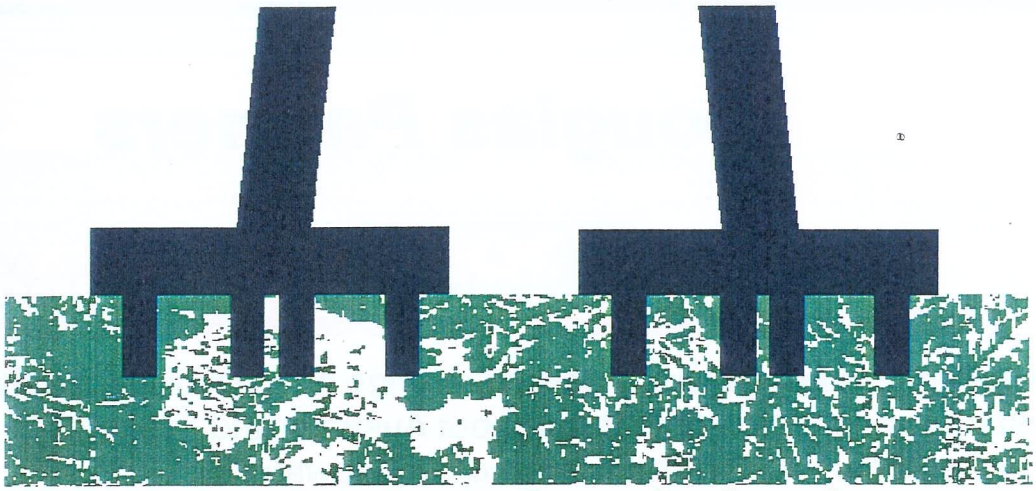

The ***Centre for Offshore Foundation Systems (COFS)*** at The University of Western Australia and The University of Sydney, undertakes fundamental research into the properties of offshore soils and the response of foundation systems for offshore oil and gas production facilities. It has been established under the direction of Professor Mark Randolph (UWA).

COFS three major research streams are

(1) micro-mechanics and stress strain response of seabed soils,
(2) response of foundation systems, particularly under cyclic loading, and
(3) soil-structure-fluid interaction for thin-walled shells and pipelines

COFS brings together top Australian and international researchers to advise and assist industry in all aspects of safe and economic foundation design and operation. COFS also supervises PhD students.

Complex tests are conducted using sophisticated facilities and COFS research personnel utilise world-class modelling capabilities. These include two geotechnical centrifuges, a large calibration chamber and advanced laboratory testing equipment. COFS houses the only centrifuge modelling facility in Australia.

For further information on COFS, its capacity to assist industry or the possibility of undertaking research work as a PhD student or postdoctoral fellow please contact:

Mark Randolph
Centre for Offshore Foundation Systems
UWA, Nedlands, WA, 6907.
Phone: 61 (0)8 9380 3094
Fax: 61(0)8 9380 7320
email: cofs@uwa.edu.au.

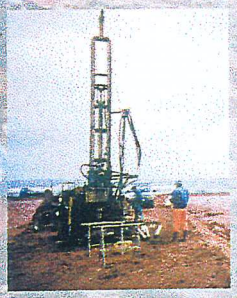

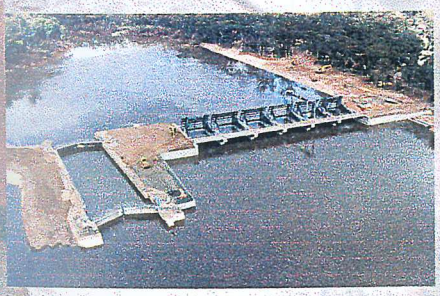

EXPERTS IN
GEOTECHNICAL ENGINEERING

GHD is an international company providing leadership in management, engineering, environmental, planning and design services with a commitment to sustainable development.

Our geotechnical division is a key element of our practice. Engineering skills and state of the art technology are only the starting points - it is the years of experience in local conditions together with common sense and judgment that lead to our safe, economical and creative engineering solutions.

Clients throughout Australia and the Asia Pacific region have benefited from our world class geotechnical skills in :

- ☐ mining
- ☐ dams and tailings
- ☐ soft ground engineering
- ☐ stability and landslides
- ☐ transportation

Our geotechnical staff are located in major regional centres and their services are available in the remotest areas through our integrated network of offices.

Adelaide	adlmail@ghd.com.au
Brisbane	bnemail@ghd.com.au
Canberra	cbnmail@ghd.com.au
Cairns	cnsmail@ghd.com.au
Darwin	drwmail@ghd.com.au
Hobart	hbamail@ghd.com.au
Melbourne	melmail@ghd.com.au
Perth	permail@ghd.com.au
Sydney	sydmail@ghd.com.au

Top to bottom:
Alpine Way reconstruction, NSW
Rock slope monitoring, NSW
Eurallumina SpA bauxite residue disposal, Italy
Hobart dams safety and security, Tas
Torrumbarry Weir, Vic
Tailings testing, WA
Background photo:
"Rock grooming", Whale Beach, NSW

GHD
MANAGEMENT
ENGINEERING
ENVIRONMENT

www.ghd.com.au

MARINE & CIVIL CONSTRUCTION CO PTY LTD

SPECIALISING IN PILED FOUNDATIONS SINCE 1993, PROUD SPONSORS OF THE FOURTH A-NZ YOUNG GEOTECHNICAL PROFESSIONALS CONFERENCE.

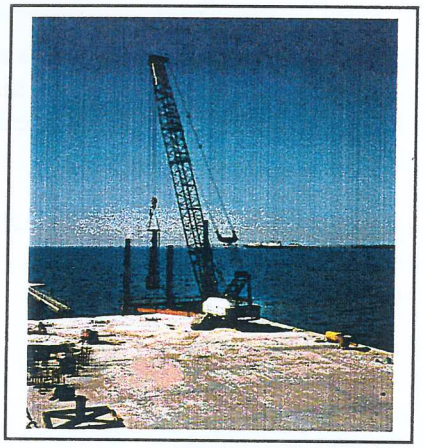

DAMPIER PUBLIC WHARF EXTENTION

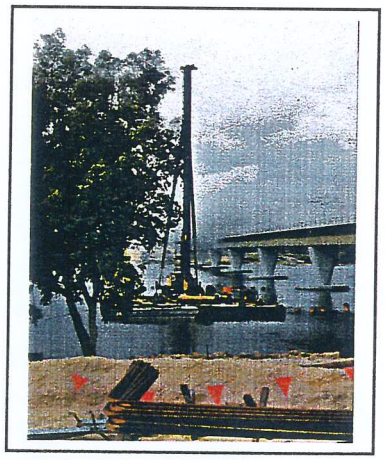

GRAHAM FARMER FREEWAY

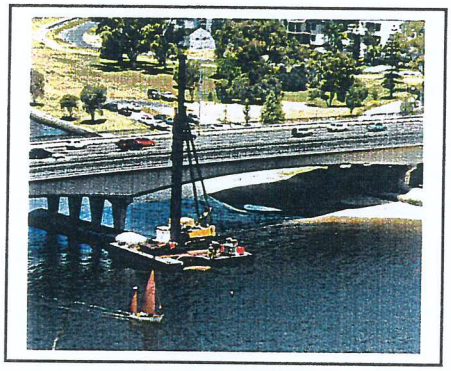

NARROWS BRIDGE
DUPLICATION PROJECT

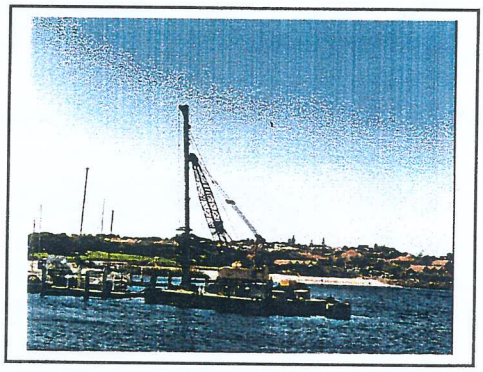

HILLARYS YACHT CLUB

LOT N13 RUDDERHAM DRIVE, O'CONNOR HOUSE,
NORTH FREMANTLE WA 6159
PH: 9336 4166
FAX: 9336 4706 EMAIL: marine@bekkers.com.au

PELLS SULLIVAN MEYNINK PTY LTD

Specialist Engineering Consultants in:

Soil

- Thredbo Landslide; advisors to NSW Coroner
- Kelian Gold Mine, Indonesia; 70m and 128m high embankment dams
- Sydney Airport; trafficability of off runway areas

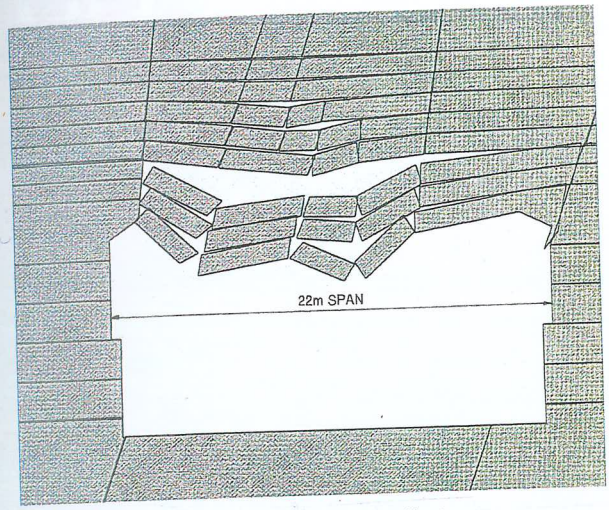

22m Span Eastern Distributor
No Support

Rock

- Eastern Distributor, Sydney; engineering geology and design of tunnel support
- Hamersley Iron, WA; open pit slope design
- Savage River, Tas; hydrology, engineering geology, design and documentation of river diversion tunnel

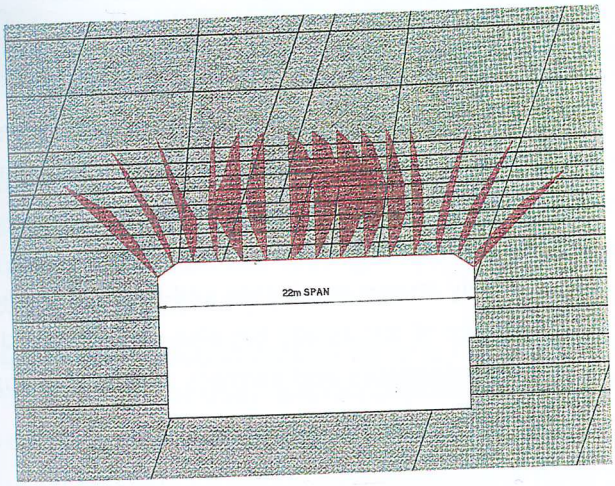

Design Support

Water

- Cadia Mine, NSW; flood hydrology for tailings dam
- Freeport Mine, Iran Jaya; mill water supply and tailings disposal
- Catchment Rainfall Simulation Software Development

PSM is very pleased to be a sponsor of the 4th ANZ Young Geotechnical Professionals Conference. We see these conferences as the key to the future strength of our profession in Australia and New Zealand.

Sydney: Ph: 02 9874 8855
Fax: 02 9874 8900
Email: pjnp@psm.com.au

Brisbane: Ph: 07 3217 5195
Fax: 07 3369 5062
Email: wjcm@psm.com.au

PSM

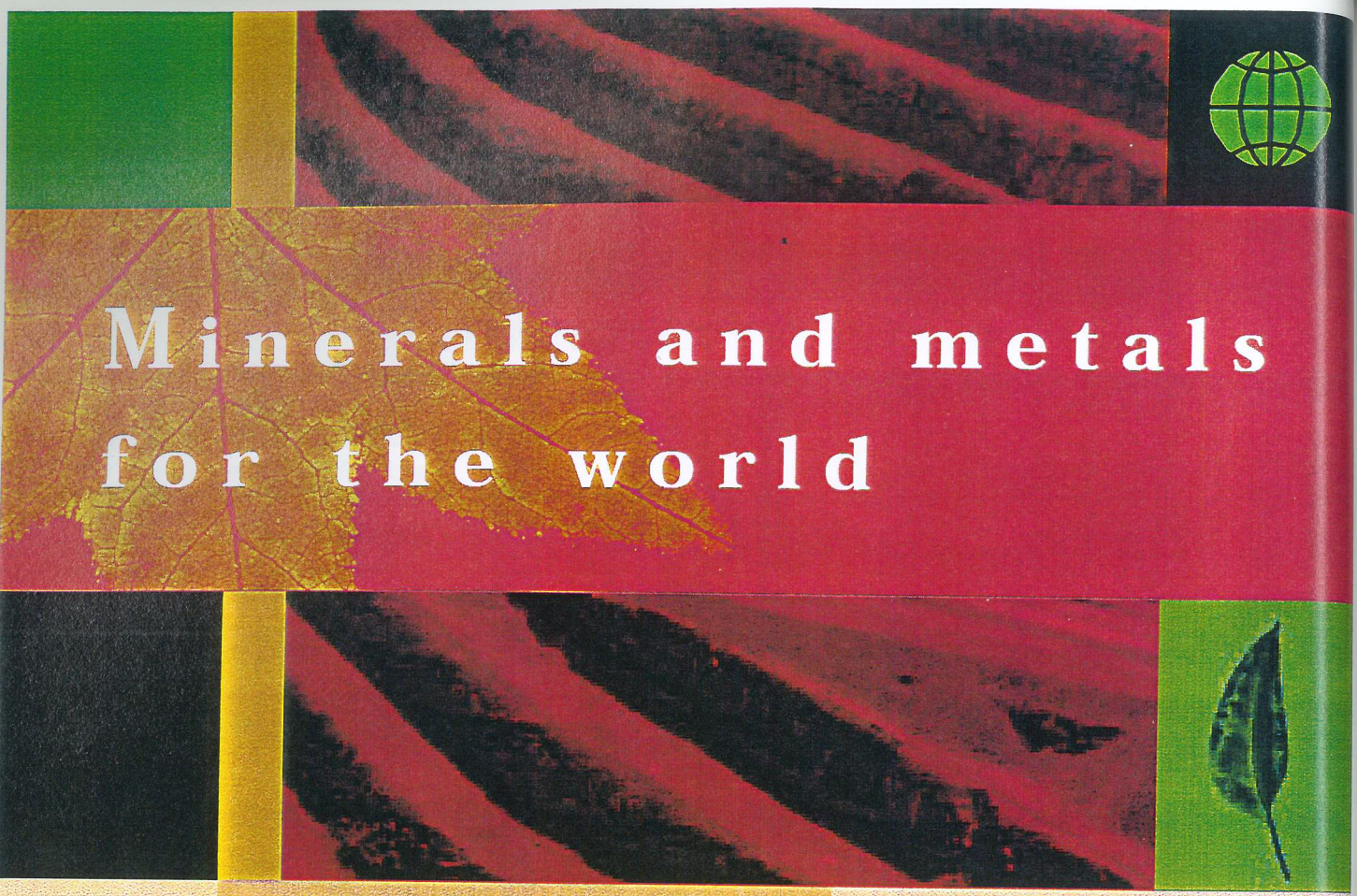

Minerals and metals for the world

Rio Tinto is a world leader in finding, mining and processing the earth's mineral resources.

In order to deliver superior returns to our shareholders over many years, we take a long term and responsible approach to exploring for first class ore bodies and to developing large efficient operations capable of sustaining competitive advantage. In this way, we help to meet the global need for minerals and metals which contribute to essential improvements in living standards, as well as making a direct contribution to economic development and employment in those countries where we invest.

Wherever we operate, we work as closely as possible with our hosts, respecting laws and customs, minimising adverse impacts and ensuring transfer of benefits and enhancement of opportunities. We believe that our competitiveness and future success depend not only on our employees and the quality and diversity of our assets but also on our record as good neighbours and partners around the world.

Accordingly, we set ourselves high environmental and community standards. Our commitment to health, safety and the enhancement of the skills and capabilities of our employees is second to none in mining. We seek to make lasting contributions to local communities and to be sensitive to their culture and way of life.

RIO TINTO

Minerals and metals for the world

Worley Limited
Resources & Energy

Worley was established in the US in the 1960s, and expanded to the Asia Pacific region in the 1970s. Today, Worley Limited is the largest Australian owned engineering organisation in the international arena.

Worley provides project management and multidiscipline engineering services to the energy, resources, infrastructure and maritime industries.

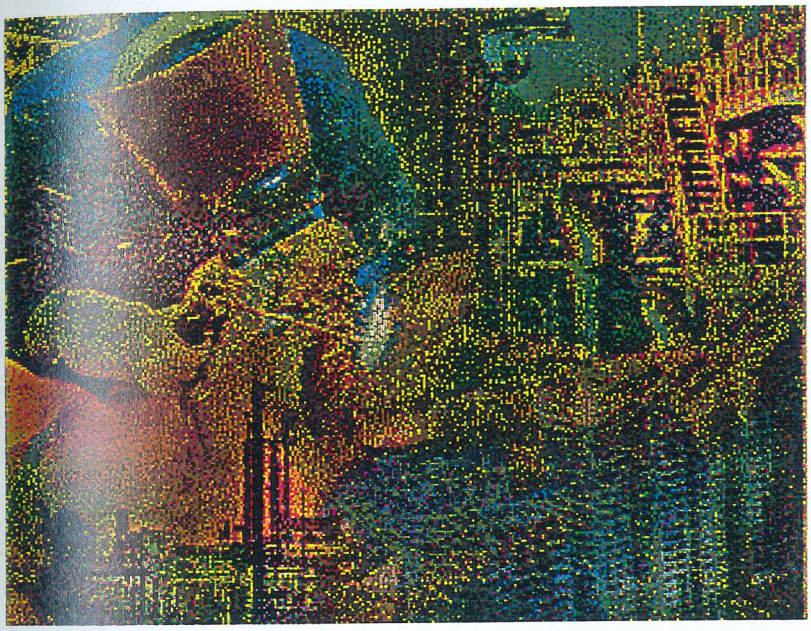

Worley has offices in most capital cities in the Asia Pacific region, as well as Houston in the US.

Worley offers a full range of services including process, mechanical, instrumentation, electrical, civil, structural, pipeline, dynamics, safety, environmental and marine engineering.

Worley keeps abreast of advancements in technology using state-of-the-art software in the areas of communications, information technology, 3D design and analysis and project management.

Worley handles projects of all types and sizes from the full engineering, procurement and construction management (EPCM), and operation/maintenance (EPC) of major facilities, through to minor troubleshooting exercises. Worley is the largest provider of such services to the terminals industry in Australia.

Worley is committed to setting up long term alliances, or partnering arrangements, with its clients based upon trust, shared objectives and mutual understanding of expectations and values.

Worley has a proven record of achievement, having successfully completed a wide range of projects throughout the world, particularly in Australia, New Zealand and Asia Pacific region.

Level 16, QV1, 250 St Georges Terrace
Perth Western Australia 6000
Telephone +61 8 9278 8111
Facsimile +61 8 9278 8110
Web: http://www.worleylimited.com

TABLE OF CONTENTS

ADDITIONAL DELEGATE PRESENTATIONS

Seismic Microzoning of the Ground Shaking Hazard from Soil Geotechnical Properties, Gisborne, New Zealand.

Jaime Bevin
BSc(Tech), MSc(Hons), TG.IPENZ
Engineering Geologist, Foundation Engineering, Auckland, New Zealand

SUMMARY

Gisborne is an urban area built upon young, soft, unconsolidated sediments. The extent of damage in the magnitude 6.3 Ormond earthquake near Gisborne in August 1993, and subsequent felt intensity surveys (MM V-VI) confirmed that the pattern of shaking and damage was not uniform. Geotechnical testing was undertaken to investigate the strength and deformation properties of the soils underlying Gisborne. Analysis and modelling of Earthquake Commission (EQC) claims from the Ormond earthquake were carried out to construct a claim density contour map. The map revealed two anomalous areas of high claim density in the northern suburbs of Mangapapa and Whataupoko compared to the rest of the city. Investigation of the underlying Neogene basement topography revealed the presence of sediment infilled valleys underneath or very close to each of the two claim density highs. The greater damage and anomalous claim density highs may have been caused by ground motion amplification at frequencies close to natural site periods, enhanced by resonance effects within the infilled sediment.

1. INTRODUCTION

Gisborne (45,780 people - 1996 census), is located on the eastern coast of the North Island of New Zealand (Figure 1). The region is part of a seismically active zone where the oceanic lithosphere of the Pacific Plate is being subducted beneath continental crust of the Australian Plate. In an average year around 13 earthquakes of magnitude 4.0 or larger, and less than 60 km in depth, occur within 100 km of Gisborne (Hamilton 1969).

The city of Gisborne overlies young, soft unconsolidated sediments of Holocene age, built up of alluvial and coastal deposits by successive flooding and fluctuating sea level. The topography of the underlying Neogene basement siltstones and mudstones is variable and buried by up to 40 m of sediment. Studies by Borcherdt (1985) and Hough et. al. (1990) have shown that the sediment through which seismic waves pass can affect the velocity and amplitude of the waves, particularly for areas of young unconsolidated sediments such as those underlying Gisborne.

The extent of damage in the magnitude 6.3 10 August 1993 Ormond earthquake to the city of Gisborne and subsequent felt intensity surveys (MM V-VI) have confirmed that the pattern of damage and shaking was not uniform. It was evident that shaking was much greater in the northern suburbs of Mangapapa and Whataupoko.

2. EARTHQUAKES IN THE GISBORNE REGION

2.1 Return Periods

Earthquake hazard is usually evaluated in terms of Return Period, which is the average time between occurrences for a shock of some particular magnitude or intensity. Table 1 summarises mean return periods for various Modified Mercalli (MM) intensities for the Gisborne Region.

The actual felt intensity is dependent upon the magnitude and characteristics of the source event, distance from source, and the materials through which the waves travel. The calculated return periods take into account the effect of the regional geology or average ground conditions, but do not account for local site conditions. Unfavourable site conditions such as young alluvial deposits can cause an increase in the intensity by 1 or 2 units on the Modified Mercalli (MM) scale and a decrease in return periods (Smith 1990).

MM Intensity	Return Period (Years)
> VI	10
> VII	50
> VIII	200
> IX	1000

Table 1: Mean Return Periods for Earthquakes in the Gisborne Region (adapted from Smith and Berryman 1986)

Felt intensities as high as MM VII have occurred in Gisborne this century. These intensities were felt in the 1931 magnitude 7.9 Napier earthquake, the 1932 magnitude 6.8 Wairoa earthquake, the 1966 magnitude 6.2 Gisborne Earthquake and the magnitude 6.3 1993 Ormond earthquake. Other notable earthquakes which have caused MM intensities of VI occurred in 1914, 1931, 1947 and 1960.

2.2 1993 Ormond Earthquake

The Ormond earthquake epicentre occurred 25 km northwest of Gisborne at approximately 2150 hours on August 10 1993. The event was a magnitude M_L 6.3 event with its focal depth at 48 km and its epicentre located at 38.52°S 177.93°E between Ormond and Waimata (Figure 1). A swarm of aftershocks occurred some 10 km further west of the earthquake epicentre at a focal depth of 36 km (Read and Cousins 1994).

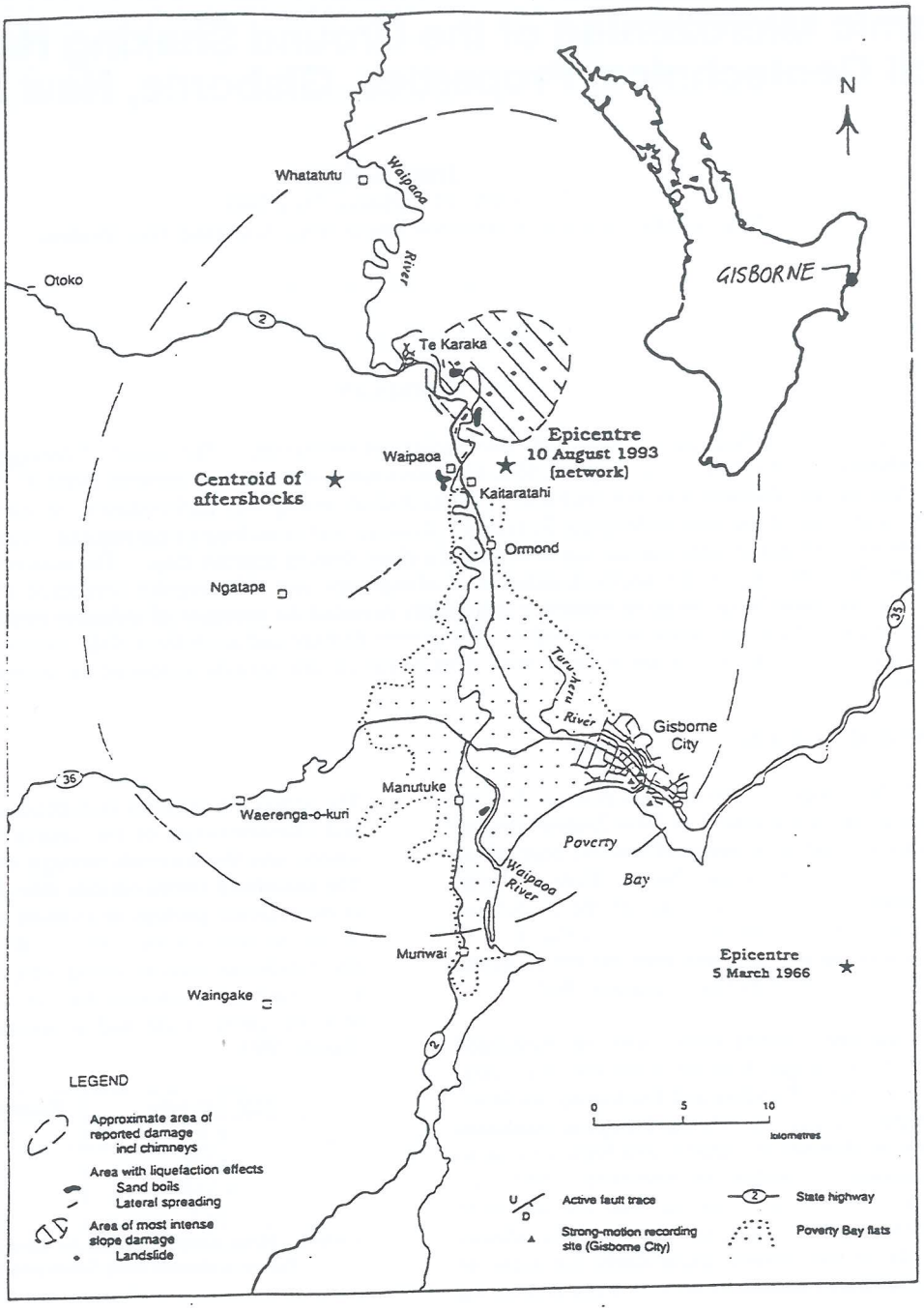

Figure 1: Location Map and Map of Ground Damage Features for the August 1993 Ormond Earthquake

There were reports of strong to moderate shaking over more than 1000 km^2 in the Gisborne region and lesser shaking in Tolaga Bay, Wairoa and Napier (Read and Cousins 1994). Newspaper and Seismological Observatory surveys reported MM intensities of VII, felt in an area of approximately 600 km^2 (Figure 1) and were centred around the epicentre of the aftershocks (Read and Cousins 1994). Maximum peak ground accelerations of 0.24g were recorded in Gisborne City.

2.3 Damage to Gisborne City

Within the city itself, intensities ranging between MM V and MM VI were recorded with the differing intensities felt throughout the city suggesting some variability in ground motion. Higher intensities of MM VI were more prevalent north of the city centre in the suburbs of Whataupoko and Mangapapa, with minor pockets of MM VII (Read and Cousins 1994). Wells (1994) also reported definite microzoning effects around Perry St in the suburb of Mangapapa. Lesser intensities of MM V were more common southwest of the Taruheru River and northeast of the city centre in the suburb of Kaiti.

Strong motion data recorded in Gisborne was higher than expected for MM V-VI intensity shaking based on the attenuation relationship developed by Dowrick (1992). However, shaking in the Ormond earthquake was generally less severe in Gisborne than that produced by the shallower 1966 M_L 6.2 earthquake which produced MM intensities of VI-VII and peak ground accelerations of 0.28g.

3. GEOTECHNICAL INVESTIGATION

3.1 Geotechnical Testing

The geotechnical properties of Gisborne soils were investigated by Cone Penetrometer Testing at 19 sites in May 1995. The locations are shown in Figure 2. In addition, 24 shallow test pits were excavated at selected sites across the city to determine soil properties in the upper metre of the soil profile and provide samples for laboratory testing. At each CPT site the soil profile was characterised by soil types assigned using Robertson and Campanella (1983).

Shear modulus (G), Young's modulus (E) and Poisson's ratio (ν) were then determined for each soil layer from empirical relationships between cone resistance, void ratio and overburden pressure using methods given in Lambe and Whitman (1979) and Mayne and Rix (1993). Further parameters such as shear-wave velocity (V_S) and seismic impedance ratio (a measure of seismic rigidity) were also calculated from relationships with strength modulus, shear wave velocity and bulk density.

For each CPT site a depth weighted mean value was determined for each of the above geotechnical parameters using a method adapted from Fumal and Tinsley (1985) to establish shear-wave velocities for the Los Angeles Region. To determine the depth weighted mean, the thickness of each layer was divided by the mean geotechnical parameter assigned to that layer. This figure was then totalled down the profile and then divided by the total depth of the profile.

Testing of the underlying soils in Gisborne shows they have variable properties both vertically down the profile, and laterally throughout the city. The suburbs of Te Hapara and Elgin are underlain by varying thicknesses of sands, silty sands and sand mixtures, which in turn overlie clays. The sands are generally of loose to medium density, while the clays range from soft to firm in consistency. Gisborne Central is also underlain by these loose to medium dense sands and sand mixtures.

Sands form the upper part of the profile in Mangapapa but thin out towards the east and north, where clays form most of the profile. The density of the sands ranged from loose to medium dense. The clays are generally soft, but are interbedded with stiff clays and silty clays. Soft to very soft clays are dominant in Whataupoko. Some sands overlie and cap these clays in the southern part of the suburb. The soil profile of Kaiti is also dominated by clays, however, the consistency of the clay varies from soft to very stiff. The soft clays generally form the lower part of the profile. Stiff silty clays and silt mixtures are interbedded within the soft clays.

The strength and deformation properties were generally greater for the suburbs of Elgin, Te Hapara and Kaiti, while the soils of Mangapapa and Whataupoko, and the northern part of Gisborne Central were generally weaker. These geotechnical properties are summarised in Table 2.

3.2 Investigation of the Neogene Basement Topography

The subsurface Neogene basement (mudstone) topography was delineated and mapped (Figure 2) with data from a number of sources, including cone penetrometer testing and borelogs from geotechnical investigations around the city. The basement rock also outcrops in several locations in Mangapapa and Whataupoko, as well as around the mouth of the Turanganui River, while basement depths from CPT testing were assumed where cone refusal occurred (q_c>30 MPa).

Depth to basement appears to be greatest beneath Gisborne Central (around 40 metres), with basement depths decreasing towards the hills in Mangapapa, Whataupoko and Kaiti, and increasing out into the Gisborne Plains.

Figure 2 shows there is some variability in the underlying topography of the basement beneath Gisborne. Reports of MM VI and VII in the 1993 Ormond earthquake appear to coincide with sediment thickness of 6 to 10 metres in the suburbs of Whataupoko and Mangapapa. This contour is thought to be the edge of the buried wave-cut platform composed of harder mudstone, buried by softer mud and overlain with sand (Lensen 1969). The position of the 8 and 10 metre contours through these suburbs also approximately coincides with the shearing of service pipes in the 1966 earthquake. Figure 2 also shows reasonable correlation with a map of sediment thickness/depth to basement from a seismic noise study carried out by Hatherton and Orr (1971).

4. GROUND SHAKING HAZARD

Regional ground shaking can be estimated by intensities deduced from calculated return periods, but these statistical values only account for the effects on regional geology and average site conditions. They do not account for unfavourable site conditions which can cause an increase in the intensity by one or two units on the Modified Mercalli scale and a decrease in return periods (Smith 1990). It seems reasonable that this variation in ground shaking might be a consequence of the thickness of the unconsolidated material and the characteristics of the materials themselves.

Suburb	Normalised Cone Resistance q_{c1} MPa	Youngs Modulus E MPa	Shear Modulus G MPa	Shear Wave Velocity V_S m/s	Seismic Impedance Ratio
Te Hapara, Elgin Gisborne Central	1.6-8.6	142-290	47-97	162-225	4.1-7.4
Mangapapa	1.0-4.3	118-211	40-70	149-195	4.8-7.0
Whataupoko	0.9-1.3	87-115	29-38	133-151	7.4-8.6
Kaiti	1.4-3.1	100-201	33-67	141-194	5.7-7.5

Table 2: Summary of strength & deformation properties

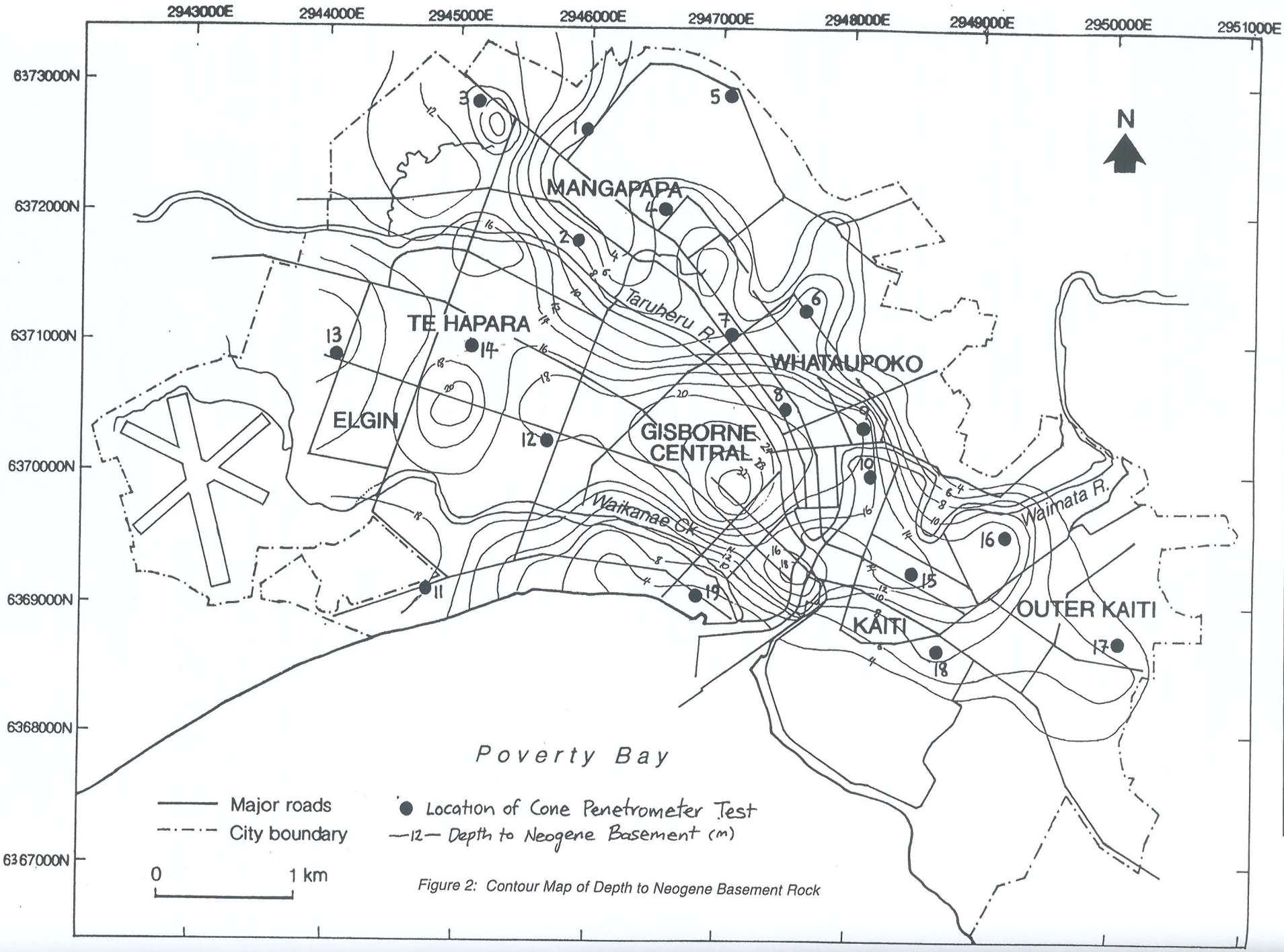

Figure 2: Contour Map of Depth to Neogene Basement Rock

Thus, the composition of near surface materials is also as important as the distance from the earthquake epicentre. Studies (e.g. Rogers et al. 1979, Geli et al. 1988) have also shown that the topography or structure of the basement rock underlying these unconsolidated sediments can also affect the degree of shaking, also causing amplitude enhancement of the seismic waves. The study of these effects and their geographic variation are useful for earthquake microzoning purposes.

4.1 EQC Claim Damage from the 1993 Earthquake

Following the 1993 Ormond earthquake, surveys to assess the degree of shaking intensity and damage to the Gisborne region were undertaken by Civil Defence and IGNS. In addition, the results of the Earthquake Commission (EQC) claims were modelled to assess which areas of Gisborne were more damaged than other areas by the effects of increased ground motion

Around 2800 claims were made to the EQC for damage totalling $4 million, with 797 claims for the city of Gisborne. Claim densities and damage parameters were then calculated from the EQC data set. Claim density (CDen) was calculated as claims per square kilometre (claims/km^2) while a damage factor (DF) was calculated as the ratio of EQC claims per thousand dwellings. Claim density and damage factor are given by:

$$[1] \quad CDen = \frac{n}{area} \qquad \text{where } n = \text{number of claims}$$

$$[2] \quad DF = \frac{n}{1000\ dwellings}$$

EQC claim densities and damage factors given in Table 3 clearly show the suburbs of Mangapapa and especially Whataupoko as having greater claim densities per area and per 1000 dwellings than any other suburbs. The claim density for Whataupoko was around 50% greater than other suburbs to the south and east.

To determine which areas of Gisborne experienced the greatest damage, a contour map of EQC claim density was constructed (Figure 3). In the absence of detailed MM intensity data, contouring EQC claim densities allowed determination of areas of high or anomalous claim density, and thus, delineation of areas of greater ground shaking. Claim densities from the EQC data set in Figure 3 are presented as number of claims per two hundred square metres (claims/200m^2), with the smaller area allowing the pattern of damage to be studied more closely.

The contour map shows two definite anomalous claim density highs of up to 36 claims/200m^2 in Mangapapa and Whataupoko - one around Walsh St in Mangapapa and the other near Whitaker St in Whataupoko. Walsh St is approximately 200 metres from Perry St, reported by Wells (1994) as an area of definite microzoning effects in the 1993 earthquake. Structures in these suburbs are predominantly light timber frame residential dwellings of one or two stories. Claim densities over the rest of Gisborne ranged from six to twelve claims/200m^2. In addition, a smaller peak of around 22 claims/200m^2, occurred in Mangapapa near the intersection of Valley Rd and Gordon St.

4.2 Relationship between Geotechnical Properties and Damage

To test if there are relationships between the damage pattern and geotechnical properties, the data was analysed using simple linear regression and fitting a straight line through the data using the least squares method. An arbitrary value of $r \geq 0.7$ ($r^2 \geq 0.5$) was used to delineate between significant and insignificant correlations. The geotechnical properties (depth weighted mean values from CPT testing) have been used as the independent variable and the claim density (claims/200m^2) at each test site as the dependent variable. Claim density values were derived from the EQC data contoured in Figure 3. Results of the analysis are given in Table 4.

In general, the geotechnical properties of Gisbornes soils determined by cone penetrometer testing, relate well with claim density. Claim densities were lower on soils with greater (stronger) geotechnical properties or lower impedance ratio. Thus, the stronger the soil the less damage that would be expected in an earthquake due to ground shaking. However, this analysis did not explain the anomalous claim density highs, nor their locations.

4.3 Shear-Wave Velocity and Impedance Differences

Studies in the Los Angeles region have indicated that shear-wave velocity is a critical factor in determining the amplitude of ground motion (Fumal and Tinsley 1985). Shear-wave velocity is also an important element in parameters such as the seismic impedance ratio and attenuation.

Good correlations with claim density, allows shear-wave velocity to be used as a means of approximating the response of a deposit to seismic shaking. Shear-wave velocity is also a useful index of the stiffness (an indicator of strength), relative density and consistency of a sediment (Tinsley and Fumal 1985). Studies have also found an inverse relationship between average shear-wave velocities and MM intensities (Borcherdt et al. 1979). Bevin (1995) constructed a contour map of mean shear-wave velocities for Gisborne which showed good correlations with reported MM intensities in the 1993 Ormond earthquake, and with the EQC claim densities in Figure 3. Shear-wave velocities were generally lower in Whataupoko and Mangapapa than the other suburbs. Lower claim densities (<10 claims/200m^2) were also located in areas of higher shear-wave velocity (e.g. Elgin, Te Hapara and Kaiti).

Previous studies have also shown shaking response is greatest where impedance contrasts between surficial and subjacent layers is greatest (Tinsley and Fumal 1985). Thus, at sites of large impedance differences, as the seismic waves propagate upwards, they pass into layers of lower impedance. The resistance to particle motion decreases and the amplitude of the seismic wave increases (Reiter 1990), resulting in greater shaking. Therefore, areas of weaker material overlying stronger material such as very stiff clays or basement rock would expect greater shaking. The largest impedance ratios (7.4 to 8.6) generally occurred in the suburb of Whataupoko, where MM intensities of at least VI were felt.

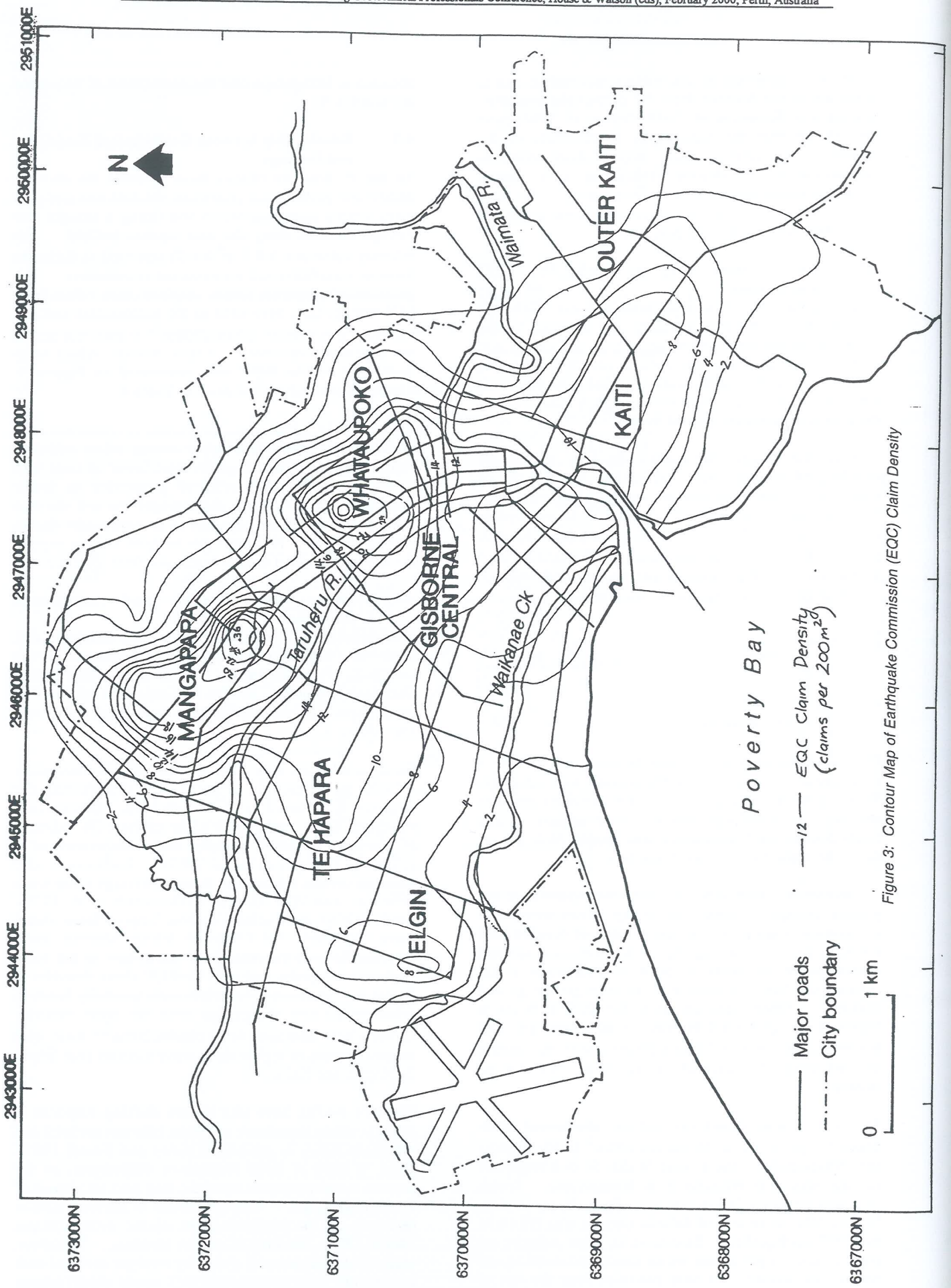

Figure 3: Contour Map of Earthquake Commission (EQC) Claim Density

	Mangapapa	Whataupoko	Kaiti	Gisborne Central	Te Hapara	Elgin
No. Claims (Cl)	220	200	143	107	81	46
% Claims of Total	27.6	25.1	7.9	13.4	10.2	5.8
Total Cost ($)	$556,318	$481,432	$332,307	$307,629	$153,599	$76,320
Mean Cost ($)	$2,564	$2,350	$2,324	$2,902	$1,896	$1,659
Population (1991)	5436	3477	7509	3393	4212	2838
Approx. Area (km^2)	5.78	3.39	6.36	4.02	3.26	3.50
Claim Density Cl/km^2)	38.1	59.0	22.5	26.2	24.8	13.1
Damage Factor Cl/1000 dwellings)	122	153	61	86	52	49

Table 3: Summary and Breakdown of EQC Claims by Suburb for the 1993 Ormond Earthquake

4.4 Resonance, Site Amplification, Response Spectra and Damage

The greatest damage occurred in the Suburbs of Mangapapa and Whataupoko, where the sediment thickness (depth to basement) is 6-16 m (Figure 2). Overlaying Figures 2 and 3 shows that the location of the two anomalous claim density highs appear to overlie sediment infilled Neogene valleys with depths to basement in the base of these valleys also ranging from 6 to 12 metres. The location of these highs also approximately corresponds to the edge of the wave-cut platform shown in Hamilton (1969).

Seismic waves entering these sediment infilled valleys may become trapped and begin to reverberate, giving rise to resonance effects, with the configuration of the underlying topography affecting the amplitude of the seismic waves. A sediment layer is expected to give rise to resonance with frequency given by the relationship:

$$[3] \quad f_1 = \frac{V_s}{4H}$$

where V_S is the shear-wave velocity, H is the layer thickness and f_1 is the resonant frequency (Hz) of the fundamental mode (Hough et al. 1990). The Neogene valleys have shear-wave velocities of approximately 130m/s (mean of CPT sites 6, 7 and 8) and sediment thickness ranging between 6 and 12 metres. From Equation 3, a sediment thickness of 12 metres would imply a resonant frequency (fundamental site period) of 2.7 H_Z (T = 0.37s). Response is at its maximum when the reverberating waves are in phase which each other and is a frequency-dependent phenomena.

Response spectra from the 1993 Ormond earthquake is available for three sites in Gisborne (Read and Cousins 1994). Two of these sites, the CPO and 2ZG sites (in central Gisborne), are soft soil sites with basement depths of up to 35 to 40m. Maximum amplification of peak surface motions here occurred at periods of 0.35 and 0.40s (2.86 and 2.50H_Z). The natural period of these two sites (given by equation 3) is 1.0 to 1.1s respectively (Zhao et al. 1995), so site amplification from resonance effects is unlikely as the natural period of the site and the period at which peak surface motions occurred do not match.

However, for the sediment infilled valleys these peak surface motions of 0.35 to 0.40s are very close to natural site periods, so the greater damage and anomalous claim density highs may have been caused by ground motion amplification at these frequencies. These site amplification effects are considered to be one of the major causes of damage to buildings as a result of earthquakes (Hough et al. 1990), especially in the short period band of 0.3-0.5s (2.0-3.3 Hz). Ground motion characterised by these fundamental periods is of greatest significance to buildings of less than four stories (Rogers et al. 1985), the case for much of Gisborne.

Sediment in the Neogene valleys gives rise to resonant frequencies in phase with one quarter of the expected wavelength. Thus, seismic waves entering these Neogene valleys will reverberate causing amplification of ground motion because the fundamental site period (and frequency) is in the vulnerable range. Response spectra for sites of thicker sediment in Gisborne (CPO and 2ZG sites) have peaks close to that required for resonance behaviour in the Neogene valleys. Marks and Larkin (1995) have also demonstrated amplification of peak ground motion at periods of T =0.4 to 0.5s for modelled infilled valleys similar to the Neogene valleys in Gisborne. Thus, it seems reasonable that this could be applicable for the infilled Neogene valleys and the anomalous claim densities underlying Mangapapa and Whataupoko.

Further study is required to confirm this hypothesis. Detailed seismic cone penetrometer testing would confirm shear-wave velocities through the sediment infilled valleys and delineate the underlying Neogene topography. A seismograph network could also be located in this area, on sites overlying the Neogene valleys, sites overlying the wave-cut platform and sites where the Neogene basement outcrops at the surface. Recordings of response spectra in smaller, more frequent earthquakes would help to confirm calculated wave amplitudes and site periods.

5 CONCLUSIONS

Geotechnical testing of the soils underlying Gisborne has shown they have variable properties both vertically down the profile, and laterally throughout the city. The geotechnical properties reflecting strength and deformation (moduli) were greatest for the suburbs of Elgin, Te Hapara and Kaiti while the soils of Mangapapa

and Whataupoko, and the northern part of Gisborne Central are generally weaker.

Analysis and modelling of EQC claim damage from the 1993 Ormond earthquake has allowed determination of claim densities and the construction of a claim density contour map. Claim densities reveal two anomalous areas of very high claim density compared to the rest of the city. Claim densities were much greater in Mangapapa and Whataupoko, which correlated well with MM intensities from the earthquake. Construction of the claim density contour map allowed the location of these anomalous claim density highs to be determined, and to investigate the cause of these anomalies. Analysis of geotechnical testing by CPT and claim density showed good correlation, but did not completely explain the location of the anomalies.

Investigation of the underlying Neogene basement topography has shown the presence of sediment infilled valleys. Resonance effects are a strong argument for these high claim densities. The two anomalies plot very close to two Neogene valleys, which are infilled by 6 to 12 metres of sediment. Seismic waves with frequencies close to the natural site period could have caused site amplification effects, leading to greater shaking and felt intensity in the 1993 earthquake. This hypothesis is supported by research on site response of sediment infilled alluvial basins. Amplification of up to 0.8g can occur at periods of 0.4 to 0.5s. This is very close to natural site periods for the areas of the anomalous claim density.

Recent major earthquakes such as the Northridge earthquake (California 1994), Kobe (Japan 1995) and Taiwan (1999) are constant reminders of the destruction and loss of life earthquakes can cause, even in developed countries with strict building codes, disaster preparedness and earthquake response planning. So defining earthquake hazards in towns and cities, is an important planning tool.

6 ACKNOWLEDGEMENTS

The author would like to thank Dr Tam Larkin (University of Auckland) for review of this paper and assistance provided by the Earthquake Commission (EQC)

Linear Regression Parameter	Youngs Modulus E MPa	Shear Modulus G MPa	Shear Wave Velocity , Vs m/s	Seismic Impedance Ratio
n	19	19	19	19
M	-0.08	-0.24	-0.18	2.97
B	21.8	21.9	39.6	-7.9
r	0.75	0.76	0.75	0.70
where n is the number of data points; M, B are the slope and the intercept respectively for the regression CDen = M * X + B, where X is the geotechnical property, for which the correlation coefficient is r.				

Table 4: Regression Analysis of Claim Damage and geotechnical properties at each CPT site.

8. REFERENCES

[1] Hamilton, R. M. (1969): Seismological studies of the Gisborne Earthquake sequence, 1966. In: Hamilton, R. M., Lensen, G. J., Skinner, R. I., Hall, O.J., Andrews, A. L., Strachan, C. M., and Glogau, O. M. Gisborne Earthquake, New Zealand, March 1966. DSIR Bulletin, 194.

[2] Borcherdt, R. D. (1985): Predicting earthquake ground motion: an introduction. In: Ziony (ed.): Evaluating Earthquake Hazards in the Los Angeles Region - An Earth Science Perspective. US Govt Printing Office, Washington. United States Geological Survey Professional Paper 1360: 93-99.

[3] Hough, S. E., Friberg, P. A., Busby, R., Field, E. F., Jacob, K. H., and Borcherdt, R. D. (1990): Sediment-induced amplification and the collapse of the Nimitz Freeway. Nature. 344. 853-855.

[4] Smith, W. D., and Berryman, K. R. (1986): Earthquake hazard in New Zealand: inferences from seismology and geology. Roy. Soc. NZ Bull. 24: 223-243.

[5] Smith, W. D. (1990): Predicting Earthquakes in New Zealand. Search. 21 (7). 223-226.

[6] Read, S. A. L., and Cousins, W. J (1994): The Ormond Earthquake of 10 August 1993: an overview of ground damage effects and strong motions. Technical Conference and Annual Meeting of the New Zealand National Society for Earthquake Engineering, 18-20 March 1994.

[7] Wells, J. D. (1994): Earthquake risk (prone) buildings, effects and damage in Gisborne City due to the Ormond earthquake of 10 August 1993. Technical Conference and Annual Meeting of the New Zealand National Society for Earthquake Engineering, 18-20 March 1994.

[8] Dowrick, D. J. (1992): Attenuation of Modified Mercalli Intensity in New Zealand Earthquakes. Earthquake Engineering and Structural Dynamics. 21. 181-196.

[9] Robertson, P. K., and Campanella, R. G. (1983): Interpretation of Cone Penetration Tests. Part I and II. Canadian Geotechnical Journal. 20 (4). 718-745.

[10] Lambe, T. W., and Whitman, R. V. (1974): Soil Mechanics, SI Version. John Wiley and Sons. New York.

[11] Mayne, P. W., and Rix, G. J. (1993): Gmax-qc relationships for clays. Journal of Geotechnical Testing. 16 (1). 54-60.

[12] Bevin, J.E. (1995): Seismic Microzoning of some Earthquake Hazards from Soil Geotechnical Properties of Gisborne City. Unpublished M.Sc. Thesis. University of Waikato. 166pp.

[13] Fumal, T. E., and Tinsley, J. C. (1985): Mapping shear-wave velocities of near-surface geologic materials. In: Ziony (ed.): Evaluating Earthquake Hazards in the Los

Angeles Region - An Earth Science Perspective. US Govt Printing Office, Washington. United States Geological Survey Professional Paper 1360: 127-150.

[14] Hatherton, T and Orr, R. H. (1971): Seismic noise survey of Gisborne City. DSIR Geophysics Division Report No. 63.

[15] Lensen, G. J. (1969): Geological aspects of the Gisborne earthquake 1966. In: Hamilton, R. M., Lensen, G. J., Skinner, R. I., Hall, O. J., Andrews, A. L., Strachan, C. M., and Glogau, O. M. Gisborne Earthquake, New Zealand, March 1966. DSIR Bulletin, 194.

[16] Zhao, J.X., Davenport, P.N. and McVerry, G.H. (1999): Modelling and Earthquake Response of Gisborne Post Office site, New Zealand. Bulletin of the New Zealand Society for Earthquake Engineering. 32 (3) . 146-169.

[17] Rogers, A. M., Tinsley, J. C., Hays, W. W., and King, K. W. (1979): Evaluation of the Relation between near-surface geological units and ground response in the vicinity of Long Beach, California. Bulletin of the Seismological Society of America. 61. 1603-1622.

[18] Geli, l., Gard, Y. P., and Jullien, B. (1988): The effect of topography on earthquake ground motion: A review and new results. Bulletin of the Seismological Society of America. 78 (1). 42-63.

[19] Tinsley, J. C., and Fumal, T. E. (1985): Mapping Quaternary Sedimentary Deposits for Areal Variations in Shaking Response. In: Ziony (ed.): Evaluating Earthquake Hazards in the Los Angeles Region - An Earth Science Perspective. US Govt Printing Office, Washington. United States Geological Survey Professional Paper 1360: 101-126.

[20] Borcherdt, R. D., Gibbs, J. F., and Fumal, J. T. (1979): Progress on ground motion predictions for the San Francisco Bay region. In: Brabb, E. E. (Ed): Progress on seismic zonation of the San Francisco Bay region: U. S. Geological Survey Circular 807. 13-25.

[21] Reiter, L. (1990): Earthquake Hazard Analysis: issues and insights. Columbia University Press. New York.

[22] Rogers, A. M., Tinsley, J. C., and Borcherdt, R. D. (1985): Predicting Relative Ground Response. In: Ziony (ed.): Evaluating Earthquake Hazards in the Los Angeles Region - An Earth Science Perspective. US Govt Printing Office, Washington. United States Geological Survey Professional Paper 1360: 221-248.

[23] Zhao, J.X., McVerry, G.H. and Cousins, W.J. (1995): Horizontal responses of Gisborne Post Office Building in two earthquakes. Technical Conference and Annual Meeting of the New Zealand National Society for Earthquake Engineering. 31 March-2 April 1995. 69-76.

[24] Marks, S. and Larkin, T. J. (1995): The influence of dimension and earthquake magnitude in numerical site response studies. Technical Conference and Annual Meeting of the New Zealand National Society for Earthquake Engineering. 31 March-2 April 1995. 149-153.

DESIGN OF SHALLOW FOUNDATIONS IN CALCAREOUS SOIL – A CASE STUDY "FREMANTLE ICE WORKS, STAGE 3 DEVELOPMENT"

P.A. BIERMA, BE
Airey Ryan and Hill Consulting Engineers, West Perth, W.A., Australia

Summary

The choice of a structural foundation system depends upon the soil parameters determined from geotechnical site investigation. Recent experience on projects located in Fremantle, approximately 17km from Perth, WA, where the coastal site soils primarily comprise calcareous sand, has demonstrated a lack of correlation between foundation design parameters, determined by traditional geotechnical site investigation techniques, and actual performance. The correlations and methods generally adopted for the determination of foundation design parameters appear to be those used to evaluate siliceous sands. This approach can offer a fair degree of accuracy for silicious sands but does not appear to accurately model calcareous sands. The field investigative techniques, and subsequent interpretation adopted may not always accurately model the degree of cementation present in calcareous soils. When neglected, this can lead to grossly conservative results. A high level of conservatism can result in significant structural foundation costs over and above those which would apply had a more accurate determination of the site soil parameters been made.

On the Fremantle Ice Works Stage 3 site, from the results of Cone Penetrometer Testing (CPT) and inferred soil parameters, the initial recommendation from the investigating geotechnical consulting firm was to install piles on the boundary to accommodate eccentric loading. It was also suggested that consideration be given to piling the entire site to alleviate concerns of liquefaction of the underlying calcareous soils under earthquake loading. Concern was also expressed regarding potential extreme differential settlements of shallow spread footings. Airey Ryan and Hill adopted a raft foundation design unassisted by piles. The modelling of this raft foundation incorporated soil parameters inferred from the initial CPT testing. Subsequent deflection monitoring of the installed raft foundation, during construction, revealed deflections of the order of 2 % of those predicted by Finite Element Analysis and by semi-elastic analysis. This indicates that the inferred design parameters used for modelling the soil strata, particularly the stiffness of the underlying layers, were grossly underestimated. This appears to be due to a serious inability to accurately predict stiffness parameters of calcareous soils using an investigative technique, and parameter inference models, appropriate to other soil types. This is conceivably due to a lack of established local correlations for calcareous soil sites, time and cost constraints associated with the geotechnical investigation, and due consideration given to the highly variable and collapsible nature of calcareous soils.

The adoption of a raft foundation, instead of piles and pile caps, resulted in significant savings for the developer. Given the outstanding performance of the raft foundation, compared to that predicted, the installation of the raft appears with hindsight to also be very conservative. The highly variable nature of calcareous soils, difficulty in accurate modelling of behaviour, and the dire consequences of failure under excess load, typically result in conservative estimates of soil design parameters. This naturally results in conservative foundation design. If a high level of conservatism is adopted by both the investigating geotechnical engineers and the structural engineer responsible for foundation design, the cumulative effect on the cost of foundations can be prohibitive for onshore developments. There is a clear need for cost effective field investigative techniques which can determine calcareous soil design parameters to a reasonable degree of precision. The resultant benefits of cost effective and appropriate foundation design can then be passed onto the developer, and ultimately the consumer.

1 INTRODUCTION

Calcareous sands behave significantly differently to "normal" siliceous sands of similar grain size distribution, and have proven to be troublesome for foundation design, both offshore and onshore. Extensive research of calcareous soils has been performed recently at the University of Western Australia, with particular emphasis on foundation systems for offshore structures. However, comparatively little information exists which is specific to the design and performance of onshore shallow foundations on calcareous soils.

The degree of cementation of calcareous soils impacts significantly on its load bearing capacity. The highly variable degree of cementation of a calcareous soil can vary the soil response to load from, virtually that of a solid rock, to that of a very weak, collapsible, unstable soil.

The common existence of cemented layers of calcareous soil at the surface, with weak underlying layers, has often led to concern of liquefaction of the soil under foundations subjected to cyclic earthquake loads, and the possibility of resultant excessive shallow foundation settlement. In the case of the Fremantle Ice Works Stage 3 development, it has been demonstrated that the CPT testing performed underestimated the stiffness and strength of both the cemented layer near the surface and the underlying weaker material. The bearing pressures applied by a medium sized development are relatively "light" when compared to the bearing pressures likely to be exerted by piles or large storage tanks.

This paper presents a case study of the Fremantle Iceworks Stage 3 development. The gross differences between the calculated foundation deflection based upon parameters inferred from the site investigation work, and the deflection that occurred (which was monitored throughout construction) clearly indicate erroneous soil stiffness values derived from the initial site investigation. The soil stiffness parameters derived from the site soil stratigraphy have been demonstrated to grossly underestimate the degree of cementation of the calcareous site soils and the stiffness of the underlying less well cemented layers.

2 GEOTECHNICAL SITE EVALUATION

The "Iceworks" Stage 3 Development consists of a four storey apartment block on a 30m x 22m site within a kilometre of the coast in Fremantle, WA. The adjoining sites comprise a 3 storey building to the east, a 1 storey car deck to the south and a 2 storey building to the west.

The soil profile typically found below the Fremantle area comprises layers of sand, derived from Tamala Limestone, and/or layers of calcareous soil derived from the Safety Bay geological unit, with varying degrees of cementation, overlying weathered limestone rock at depth.

2.1 Fieldwork

The fieldwork for the geotechnical investigation consisted of 3 CPT tests and water level and height level surveys at each CPT test location.

The investigating geotechnical firm reported that, in general, the results of the CPT tests performed indicated soil of lesser strength than that inferred at other nearby sites in the Fremantle region.

The water table was reported to exist at a depth of between 1.05m and 1.25m below the natural ground level.

The CPT tests typically met refusal at 15 to 16m depth, indicating an underlying layer of very strongly cemented calcareous soil or weathered limestone cap rock.

2.2 Inferred Soil Strata & Parameters

Based on the Geological Map of Western Australia, Fremantle Sheet, and the results of the CPT tests, a generalised subsurface soil profile was prepared including an estimate of the Elastic Modulus (E) for each soil layer.

The CPT test cone resistances recorded appeared to indicate particularly low strength soil layers between depths of approximately 3 to 4m and again at 10 to 15m below the existing ground surface. The tip resistances recorded were of the order of 1.25 MPa and 0.5 MPa respectively.

The relationship between EFCP tip resistance (qc) and Elastic Modulus (E) is typically given by :

$$E = \alpha\, qc \qquad (1)$$

where :

E = Estimated soil layer elastic modulus (MPa)
q_c = EFCP tip resistance (MPa)
α = Constant

The empirical constant (α) relating the soil layer stiffness and EFCP tip resistance is generally dependent on the relative density, effective vertical stress and degree of overconsolidation of soil strata being considered and local experience. For the Iceworks Stage 3 site, the weak layers were assigned a constant of 4.0, and for the other layers the constant was approximately 2.7. The inferred geotechnical model for the Iceworks, Stage 3 site is as per Figure 1 below.

Layer	Depth Range (m)	Consistency	Elastic Mod. (MPa)	Description
1	0 - 3	Medium Dense	20	Sand
2	3 - 4	Loose	5	Sandy Silt
3	4 - 8	Loose/Med. Dense	16	Silty Sand
4	8 - 10	Loose	10	Sandy Silt
5	10 - 15	Very Loose/Soft	1	Clayey Silt
6	> 15	Cemented	200+	Limestone

Figure 1: Inferred geotechnical model.

2.3 Recommended Structural Response

Based on the inferred geotechnical model described in Figure 1, estimates of allowable bearing pressure and settlement for different sized shallow spread footings were given by the investigating geotechnical firm. For strip footings, and 150kPa design pressure, the calculated elastic deflection was in the range 45 to 90mm and for pad footings was 15 to 40 mm. As the footing size increased, the calculated deflection also increased for the same bearing pressure. It was noted, in the geotechnical report, that the calculated footing deflections were elastic only and that creep settlement could add up to further 50% deflection and interaction with adjacent footings a possible additional 15 to 30%.

Due to the close proximity of the external walls to the boundaries, it was anticipated that piles would be required to accommodate the eccentric loading on the boundary footings. If the boundary footings were to be piled, the estimated pile settlement would be of the order of 5mm. Concern over differential settlement between the piled boundary footings and internal footings led to the recommendation that consideration be given to supporting the entire building on piles if the structure couldn't be designed to accommodate the anticipated differential settlements.

The proposed piled footing system could utilise cast in-situ grout injected piles toed into the limestone approximately 15m below the existing ground surface. The allowable design pile end bearing pressure and skin friction was recommended as 2 MPa and 5kPa respectively.

Adopting the pile design figures quoted above, a 350mm diameter pile would have a theoretical working capacity in the order of 275kN, and a 450mm diameter pile approximately 42kN.

Based upon the estimated building load, in excess of 40 piles, on a 3.85m square grid, drilled to a depth of 15m, would be required to support the four storey structure. Due to the relatively close spacing of the piles, a continuous raft would be desirable for construction purposes, rather than individual pile caps which would essentially cover the majority of the site area in any case.

Another supporting argument presented for the adoption of a piled foundation system, was concern that the potential for liquefaction of the low strength subsurface soils under cyclic earthquake loads existed. Based on a simplified procedure by Tosho Iwasaki for saturated uncemented sandy soils, the site was classified as having a "high" risk of liquefaction if shallow spread footings were adopted.

3 ALTERNATIVE STRUCTURAL RESPONSE

3.1 Supporting Arguments

The high commercial impact of a piling scheme versus a non-pile assisted footing, warranted the investigation of an alternative foundation design despite the liquefaction concern raised by the investigating consulting geotechnical firm.

Settlement of foundations, and resistance to shear failure, for silica sands depends on both the size and shape of foundation and on its depth below the surface and the degree of compaction of the sand (relative density).

Shallow spread footings such as strip and pad footings are suitable for soil where a stratum of high relative density and adequate thickness exists near the surface. In the case of calcareous soils, shallow footings may be suitable if a cemented layer exists at or near the surface, capable of supporting the imposed loads.

These foundations offer little resistance to differential movements, which must be limited to sufficiently low levels, or allowance made for movement joints in the design of the superstructure. Footings of this type are normally utilised only where the site soils possess low compressibility, or they are proportioned to limit design bearing pressures (and settlements) to low levels.

For the Fremantle Iceworks Stage 3 development, Airey Ryan and Hill adopted a raft foundation which was unassisted by piles. This resulted in a saving of the order of $70,000 or approximately 55% of the cost of the piled option.

In appropriate circumstances, a raft footing bridges over soil irregularities, and the average settlement does not approach the extreme values of spread footings. A raft foundation will also greatly restrict differential settlements, and at the boundary will act as a continuous strap footing, reducing the soil bearing pressures on the boundary to acceptable levels. This can negate any requirement for piling to accommodate eccentric loading.

If piles were to be used at close centres, then pile caps would cover the majority of the building footprint, and so a raft would not increase material requirements or site preparation excessively. In addition, adaptation of the raft foundation to function as the ground slab for the development was possible, providing further cost savings.

The raft foundation is able to spread the building loads over the largest possible area, and reduce the design bearing pressures on the subsoil strata. A raft foundation appeared appropriate, provided total and differential deflections could be limited to acceptable levels, and the issue of liquefaction of the underlying weaker soil strata under earthquake loading could be addressed.

3.2 Background Information

For normal silica sands the ultimate bearing capacity is dependent on the soil unit weight and angle of internal friction which varies primarily with the relative density of the soil. In some circumstances the soil bearing capacity of a raft foundation is also increased due to the larger foundation size and greater founding depth. Terzaghi and Peck (1948) indicate that an increase in allowable bearing pressure of up to 100% is possible for silica sands.

This situation is however, not directly applicable to calcareous soils which differ significantly from silica sands in geological formation, chemistry, physical properties and

performance under load. Calcareous sands generally exist in a very open structure, with an immense scope for variation in properties which are influenced by CaCo3 content, grain size distribution, in situ density and the degree of cementation.

For shallow footings on uncemented calcareous soils the bearing capacity depends primarily on the compressibility of the soil and is largely independent of footing size. This has been demonstrated by centrifuge testing performed at the University of Western Australia by Finnie and Randolph (1) which has shown that the relationship between applied pressure and displacement is almost linear, and that there is no well defined yield point or "ultimate bearing pressure". Instead it is proposed that the 'bearing capacity' of the soil be measured as that which results in acceptable footing settlement for the superstructure being considered. The mode of deformation of the soil is that of localised shearing of the soil particles at the perimeter of the footing. Finnie and Randolph (1) report that previous studies of punching shear failure of un-cemented calcareous soil reveals the lack of a rational approach to predicting the bearing capacity.

Odometer tests, on offshore and onshore uncemented calcareous soils, performed by Joer et.al. (2) indicate that for the onshore deposit, which consists primarily of uniform coarse rounded particles or pellets, there is a quasi linear increase in soil stiffness with controlled displacement. Tests performed on samples with different initial voids ratio indicate a convergence of settlement versus bearing pressure irrespective of the initial voids ratio. This, however, is limited to very high bearing pressures, such as those typical for driven piles, and not those appropriate for shallow foundations. Acceptable settlement limits for shallow foundations correspond to 'low' bearing pressures, and are largely influenced by the initial voids ratio. The work performed by Joer et.al. (2) is confirmed by Finnie and Randolph (1), which indicates that under drained conditions, the major contributing factor towards foundation settlement is compression of the soil directly below the foundation, which is largely independent of foundation size. The primary mode of settlement is compression of the open structure calcareous soil, which is not accompanied by soil yield and displacement that might be expected for denser silica sands.

Soil improvement techniques, such as vibro-compaction can improve calcareous soils to be subjected to 'high' loads likely to break any cementation of soil particles, if present. However, for most onshore sites, where there is some cementation present however weak, application of vibro-compaction will break any cementation between particles, which may not have been broken under 'low' loads. This could result in a reduction in the soil stiffness compared to that available had the bonds between grains not been broken. All that may be achieved is a uniformity in soil stiffness across a particular site which aids design for differential settlement. Vibro techniques for onshore developments, in close proximity to one another, are also not suitable due to possible increased settlement of adjacent structures at the boundary due to a reduction in soil stiffness. In addition damage to adjacent structures can occur due to vibration and compaction of the underlying soil strata.

Where 'low' loads are likely to be imposed on a weakly cemented calcareous soil site it is critical to determine if the imposed bearing pressures are likely to destroy any cementation present, or whether the degree of cementation is likely to reduce in the future, resulting in foundation settlement beyond that anticipated.

A common situation for both onshore and offshore calcareous soil, is that a cemented layer of calcareous soil exists at or near the surface, with weaker layers of un-cemented or variably cemented layers underneath. This is clearly indicated by the CPT test logs for the Fremantle Iceworks site, and is also evident for several other sites in the Fremantle region.

The cemented crust acts to spread the applied shallow foundation loads over a larger region. The crust can in some situations span over weaker subsurface material, shielding it from both overburden pressure and applied load.

Exceeding the strength of the upper cemented crust can lead to a sudden punch through failure accompanied by uncontrolled settlement. Finnie and Randolph (3) observed that the failure mechanism, and resultant settlement, was dependent on both the ratio of the crust thickness to foundation size, and the relative stiffness of the underlying material.

For a 'thin' crust where the thickness ratio of the depth of cemented crust to the foundation size is less than 0.4, the crust acts like a spreader beam and deflects in a bending mode. With increasing load, the flexural tensile capacity of the cemented layer is eventually exceeded and tension cracks initiate at points beneath the perimeter of the foundation and propagate upwards through the crust. Refer to Figure 2 below reproduced from Finnie and Randolph (3).

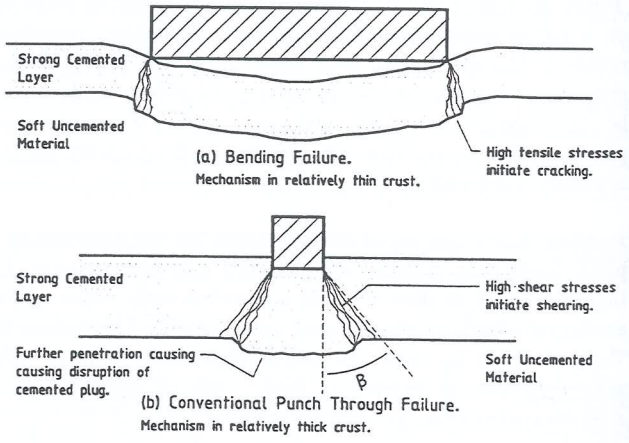

Figure 2: Failure modes for penetration of cemented crust overlying uncemented material.

The degree of settlement is governed by the stiffness of the underlying material and the laboratory results of Finnie and Randolph (3) indicate the bearing modulus is within a factor of 2 of the bearing modulus for the underlying material had no crust been present. This is thought to be due to 'load spread' by the upper cemented layer for small settlements.

Finnie and Randolph (3) claim the degree of load spread is approximately over an area 50% larger than the foundation area which accounts for a bearing modulus of the order of two times greater than had no crust been present.

If the underlying material is uncemented calcareous sand, the bearing modulus is largely independent of foundation size and primarily dependent on the compressibility of the calcareous sand. No strain softening was observed during the testing by Finnie and Randolph (3), with a monotonic increase in bearing capacity with foundation settlement.

For a 'thick' upper crust with a thickness to foundation size ratio in excess of 0.4, the failure mechanism was observed, by Finnie and Randolph (3), to be a punching shear failure through the upper crust in a conical shape approximately 40 degrees to the vertical (refer to Figure 2). The central sheared plug was likened to a stubby pile with crushing of the sheared crust below the foundation possible prior to shearing through to the underlying weaker material with increasing load. For the case where the underlying material was silt, significant strain softening was observed, which could be classified as a sudden punch-through failure with uncontrolled settlement. Where the underlying material was calcareous sand, crushing of the sheared crust 'plug' was also observed but there was no strain softening with punch through to the underlying material.

3.3 Raft Foundation Modelling & Design

Both Finite Element Analysis (FEA) performed by Soil and Rock Engineering using the FEAR program, and a simplified elastic analysis performed by the Author using SpaceGass, were used to predict the settlement of the Iceworks raft foundation. Both analyses assumed the elastic modulus of the soil layers as given in Figure 1 (inferred from the CPT testing), and the same design loading.

3.3.1 Finite Element Analysis

In the case of the FEA performed by an independent geotechnical consulting firm using the FEAR program, the resultant raft curvature could be used to predict the bending moments induced in the raft for reinforcement design. This analysis assumed a uniform loading over the entire surface of the raft and indicated 'dishing' of the raft in the centre. The maximum curvature of the raft was in the short axis direction through the centre of the raft. This indicated a peak ultimate raft bending moment of 130 kNm/m. This is comparable to the moments in the raft calculated assuming an upward uniform bearing pressure exerted by the soil on the base of the raft.

3.3.2 Simplified Elastic Method

Three simplified elastic analyses of the raft were performed by the author. The first comprised a one dimensional model of the estimated wall loads on the 400mm thick concrete raft down the long axis, with the raft supported on springs at 500mm centres. The spring stiffness adopted corresponded to the equivalent soil subgrade modulus taken over the full 15m of soil strata. This analysis indicated an almost uniform soil bearing pressure due to the high stiffness of the raft foundation with respect to the soil strata. This one dimensional analysis indicated maximum settlement at the edges of the raft with hogging between the extreme external walls. This analysis does not model the distortion of the soil surrounding the raft, and is in direct contrast with the 'dishing' indicated by the Finite Element Analysis which also accounts for the two dimensional nature of the raft foundation.

The second two simplified elastic analyses assumed that load spread, due to the stiff upper 3m of soil strata, was occurring as investigated by Finnie and Randolph (3). The Iceworks Stage 3 raft foundation being approximately 20m wide gives a thickness ratio of 0.15 to the 3m stiff crust identified in the CPT test logs. The cone tip resistance for this layer lay in the range from 5 to 15 MPa. A thickness ratio of less than 0.4 indicates a 'bending' type response of the upper layer with load spread at approximately 40 degrees from vertical through the layer. Finnie and Randolph (3) estimated that, based upon CPT tests of prototype foundations on artificially cemented layers subjected to centrifuge testing, cone resistances in the order of 6-10 MPa corresponded to a weakly cemented layer, 10-16 MPa for a medium strength cemented layer and 30-45 MPa for a strongly cemented layer. For the purpose of analysis, the 3.0m stiff layer was assumed to be 'strongly cemented' with a Young's modulus, E of 200MPa and a beam tensile strength of 1.2MPa.

The effect of the loading of the raft foundation on the 3.0m thick upper 'crust', and the spread loading of the raft on the underlying 12m of weaker soil strata was modelled separately. Refer to Figure 3.

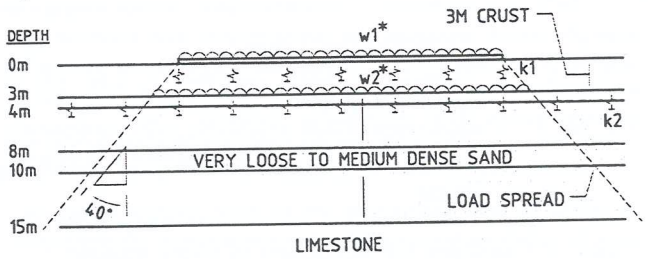

$w2^* < w1^*$ (Approx 70%)
E2 (12m SOIL STRATA) = 3.8 MPa < E1 (3m CRUST) = 20 MPa
k2 < k1 (Approx 4.7%) 3m CRUST VERSUS 12m SOIL STRATA.
S.E. No.1-30m X 22m RAFT LOAD $w1^*$ ON 3m CEMENTED CRUST MODELLED BY SPRINGS (k1) AT 500mm CRS.
S.E. No.2-REDUCED RAFT LOAD $w2^*$ OVER 150m x 150m OF 12m DEEP SOIL STRATA MODELLED BY 3M DEEP 'SOIL' BEAMS ON SPRINGS (k2) AT 5m CRS.

Figure 3: Simplified elastic analysis model.

The first analysis modelled the raft as being supported by a beam grillage with beams at 5m centres over an area of 150m by 150m in plan. The soil surrounding the raft was modelled as 3m deep by 5m wide 'soil' beams with a Young's Modulus of 200MPa. The raft was similarly modelled as concrete beams 400mm deep at 5m centres with a Young's Modulus of 28,600MPa corresponding to the 25MPa concrete to be used for the foundation. The 'soil' beams and raft were supported by springs of 20MPa stiffness equal to the inferred modulus of the 3m thick upper cemented layer.

The second analysis allowed for load spread through the upper 3m deep layer, and modelled the effect of the reduced

raft load on the underlying 12m strata of soil. Again a 'soil' beam grillage was adopted to model the load spread of the upper cemented layer with spring supports of 3.8 Mpa stiffness equal to the equivalent soil modulus for the underlying 12m of soil. The analysis also indicated the greatest curvature of the soil (and raft) through the short axis of the raft through the raft centre. This maximum curvature corresponds to an ultimate (factored) positive bending moment in the 5m wide by 3m deep 'soil' beam of 1439kNm under the centre of the raft, and an ultimate peak negative moment of 823kNm approximately 10m distant from the long axis raft edge.

3.3.3 Theoretical Calculated Deflections

The calculated raft settlements for the different analyses performed are summarised in Figure 4. It is relevant to note that the total raft settlement, for the Simplified Elastic analysis, would be the summation of that calculated for compression of the upper crust (S.E. No.1) and compression of the underlying 12m of soil strata (S.E. No.2).

Raft Deflection (mm)			
Position	F.E.A.	S.E. No.1	S.E. No.2
Centre	45	3	47
Corner	12	2	23
Midway Long Axis Edge	25	3	35
Midway Short Axis Edge	25	3	30

F.E.A – Finite Element Analysis
S.E. No.1 – Simplified Elastic Analysis of Raft on 3m cemented crust.
S.E. No.2 – Simplified Elastic Analysis of spread Raft load on 3m cemented crust acting on underlying strata.

Figure 4: Calculated raft settlements by Finite Element Analysis and Simplified Elastic Analysis

The typical deflected shape of the 'soil' beam grillage is illustrated by Figure 5. The raft loading, reduced by load spread through the upper 3m crust, is also indicated.

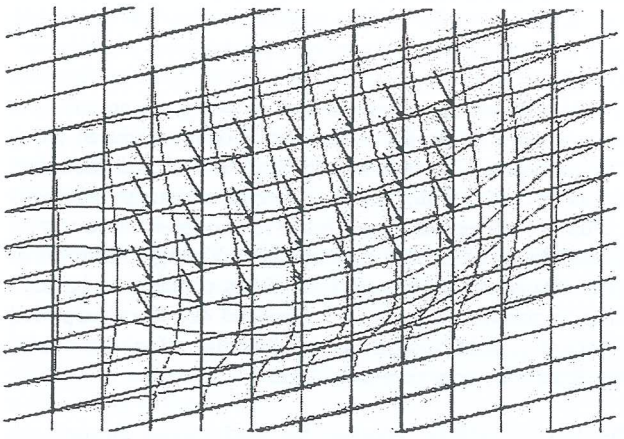

Figure 5: Modelled soil strata deflection

Note that the zone of influence of the raft loading on the underlying soil strata does not extend far beyond the spread raft footprint at the bottom level of the upper crust.

3.3.4 Theoretical Calculated Crust Strength

Based upon the beam flexural tensile strengths quoted in Finnie and Randolph (3) for a 'weak', 'medium' and 'strong' cemented layer pertaining to laboratory prepared cemented crusts, the design moment capacity (unfactored) for a 3m deep by 5m wide soil 'beam' would be 750 kNm, 2250 kNm and 9000 kNm respectively. These capacities indicate a factor of safety against failure of the crust due to the raft load of 1.56 and 6.25 for the 'medium' and 'strong' layers respectively. The crust tensile strengths quoted are however, those of prepared laboratory specimens which have been estimated to correspond to cone resistances of 6–10 MPa for the weakly cemented layer, 10–16 MPa for the medium strength layer and 30–45 MPa for the strongest layer tested. Considering the cone resistance of the upper 3m strata of soil at the Iceworks site is in the order of 5–15 MPa, the theoretical crust flexural capacity is in the order of 1500 kNm. This is within 5% of the calculated ultimate factored design moment acting on the 3m x 5m wide soil 'beam'. More information on the strength and stiffness properties of any such crust at the Iceworks Stage 3 site is required to better determine the crust yield point if in fact a cemented crust exists.

4 FIELD MONITORING VERSUS MODEL

4.1 Raft Deflections

An initial level survey, of the top surface of the raft foundation, was performed on the 1st April, 1998 from a bench mark established at completion of construction of the raft, and far enough away to be outside the raft zone of influence. Further level surveys, performed from the same benchmark, were performed at completion of construction of the first floor, second floor and also several months after project completion. The final set of levels taken on the 2nd December, 1999 indicate a maximum raft settlement of 3mm in the centre, 3mm along the north and south short boundaries, and 1mm midway along both east and west boundary edges. These levels indicate the final raft deflection is of the order of 7% or less than the settlement predicted by both the Finite Element and Simplified Elastic analyses performed on the raft using the soil stiffness moduli inferred from the CPT testing.

4.2 Implications on Assumed Design Parameters

As can be seen, from the raft deflections calculated by the Simplified Elastic analysis, the primary contribution to the total raft settlement is that due to compression of the underlying soil strata, and not compression of the upper cemented crust. The gross differences between the actual raft deflection and that predicted is directly attributable to the inferred soil stiffness modulus quoted for the underlying weaker material.

4.3 Possible Sources of Error

A possible source of error in calculation of the raft settlement may be the lack of modelling of the high degree of confinement due to the adjacent developments to the Iceworks Stage 3 site.

The higher friction ratios of the CPT logs, and drop off in tip resistance just below 2m depth and at 10m depth indicate un-cemented calcareous sand. This approximately relates to the weaker layers, inferred between 3 and 4m depth and between 10 and 15m depth by the investigating geotechnical firm. For the remainder of the logs the friction ratio is relatively low, in the order of 1%, which is characteristic of 'normal' silica sand. The simplified elastic analysis conducted assumes that the settlement or compression of each spring in the model is totally independent to that in adjacent springs. This assumption is valid for calcareous soils where the primary mode of deformation is compression. This is however, not valid for silica sand where the resistance to shear stress and subsequent soil deformation is affected by footing shape, depth and size. Therefore, if a significant portion of the soil strata at the Iceworks Stage 3 site is silica sand, these factors will greatly influence the analysis.

The presence of weak layers in the inferred soil stratigraphy greatly affect the calculated raft settlement due the low E values quoted. Correlations between cone tip resistance (q_c) and Young's Modulus can be misleading for calcareous soils due to the "pressure bulb" created in the soil by the cone during penetration. This pressure bulb can possibly fracture any cementation present in the soil leading to uncharacteristically low tip resistances and hence inferred soil stiffness much lower than that which exists in the undisturbed insitu soil.

Established correlations are generally based on laboratory measured moduli using unaged and reconstituted silica sand samples. This approach does not account for cementation, or past stress or strain history, which can result in significantly higher soil stiffness insitu than anticipated.

5.0 DISCUSSION

5.1 Fieldwork & Soil Design Parameters

The design of shallow foundation systems on sands, particularly calcareous sand sites is generally governed by settlement rather than strength except for unusually high loads or narrow footings.

The cone penetration resistance recorded in the logs is a complex function of both strength and deformation properties of the sand being tested. As no generally applicable analytical solution for soil deformation modulus, as a function of cone tip resistance exists, reliance on established empirical correlations appears to be common practice. However, to the author's knowledge, no such established correlations exist for calcareous soils. This raises the issue of the appropriateness of reliance on silica sand correlations for estimates of soil stiffness for soils anticipated to have a large calcareous sand content. The inference of soil stiffness from CPT test logs is prone to huge variation, even when using well established correlations, and as such relies heavily on local knowledge of site geology. Therefore, in the case of calcareous soil sites, additional testing over CPT testing appears to be required if design parameters are to be determined with any level of accuracy, or good correlations on field data need to be developed.

Insitu tests are preferable, but not always practicable. SPT testing can be useful, due to the well established correlations for number of blows and relative density of soil, or bearing capacity (for silica sands), which may be used for comparison purposes where calcareous soil deposits are suspected. The concept of relative density calcareous soils is not really appropriate due to their high compressibility and crushability of grains. Also, SPT testing can give erroneous results in fine or silty sands of low permeability where there is a drop in pore pressure at the base of the spoon which leads to an increase in effective stress and high blow count readings.

The use of a self boring pressuremeter may be an accurate way of measuring soil stiffness as direct measurements of horizontal displacement versus applied pressure can be made.

Seismic cone testing can be used to verify the stratigraphy highlighted by CPT testing. The speed of shear waves through the soil can be used to estimate the insitu soil elastic modulus without the test destroying any cementation that may be present. Seismic cone tests can also give a good indication of liquefaction potential of calcareous soil sites.
Plate loading tests can be used to give good indications of soil stiffness. These tests are only really appropriate for cemented calcareous soil sites if the plate size and loads are comparable to those to be implemented. Small scale loads and deformations will not indicate any potential punch through failure of a surface cemented crust. Plate loading tests undertaken below the water table can be valuable in measuring pore pressure generation and dissipation for liquefaction analysis.

Laboratory testing, such as the oedometer test, is useful for measuring the one dimensional deformation modulus of silica sands. It is questionable however, whether it is possible to obtain an 'undisturbed' insitu sample of calcareous soil for testing purposes.

The gross difference between the calculated raft settlement and that which actually occurred highlights the need for :

1. The use of supplementary field investigative techniques to confirm / deny the presence of collapsible calcareous soil layers indicated by CPT testing. The use of supplementary field tests, and/or laboratory testing to provide independent estimates of foundation design parameters to those inferred from CPT logs.

2. An industry awareness that use of soil classification charts, and application of high levels of conservatism to correlations applicable to silica sands for calcareous soil deposits, results in safe, but in some instances grossly conservative foundation designs which can be excessively costly to development.

3. Establishment of a database of local experience and correlations for coastal calcareous soil deposits to aid design.

4. A means of determining the presence and properties (Young's Modulus, flexural tensile strength) of any cemented layers of calcareous soil which can be modelled to spread foundation loads and shield weaker underlying layers from imposed loads.

5.2 Liquefaction Potential

The evaluation of the likelihood of soil liquefaction during earthquake loading involves firstly estimating the average cyclic stress ratio likely to be imposed by a design seismic event, and, secondly comparison with the average cyclic stress ratio likely to cause liquefaction of the soil. The current practice in North America, for determination of the cyclic stress ratio to cause liquefaction, is either insitu soil testing and use of field correlations, or laboratory testing on representative soil samples. Because of the difficulty in obtaining undisturbed soil samples, the insitu testing and field correlation approach is generally preferred.

Empiracle correlation charts exist for uncemented sands and silty sands, of cyclic stress ratio versus modified cone tip resistance (from insitu CPT testing) from which the possibility of liquefaction can be evaluated. These are generally applicable to silica sands, in either a fully drained or undrained condition, and must be used in conjunction with local experience.

It has been established that sensitive uncemented fine grained soils of low cone tip resistance and low friction ratio have a high liquefaction potential or liquidity index. For calcareous sands, the high compressibility results in low cone tip resistance, but increased friction ratio. These have a higher resistance to cyclic loading but, the size of the earthquake loading will control their final susceptibility to liquefaction.

Finnie and Randolph (3) have demonstrated that for model tests of shallow foundations on uncemented silt, liquefaction can occur at cyclic load levels as low as 4% of the applied bearing pressure which was 75 kPa. The performance of the soil under cyclic loading was shown to be very sensitive to the local density of the material, with densification of the soil due to preloading by a factor of two, increasing the required liquefaction failure cyclic load level to 10% of the applied bearing pressure.

The earthquake acceleration coefficient for Perth is 0.09, and for Fremantle, WA slightly lower. A site factor of 1.5 (as defined in AS1170.4-1993) would also be appropriate which would give a design earthquake base shear cyclic loading of the order of 10 to 15% of the foundation design bearing pressure. This exceeds the cyclic load levels observed to cause liquefaction of saturated, uncemented calcareous silt under model foundations during centrifuge tests conducted by Finnie and Randolph (3). However, liquefaction of the model shallow circular foundations tested occurred after up to 200 cycles at 48 seconds per cycle which is a far greater duration of load than that of a seismic event.

For the Fremantle Iceworks site, the raft foundation reduced design bearing pressures on the soil stratigraphy significantly below those which would have been applied if pad and strip footings had been used, as assumed by the investigating geotechnical firm in their liquefaction assessment. The testing done by Finnie and Randolph (3), and the existing correlations relating cone tip resistance and liquefaction failure cyclic stress ratio do not account for any cementation of the soil. The upper, stiffer soil strata inferred to be 3.0m deep may effectively shield the weaker underlying material from load. If load spread is assumed, through the stiff soil layer, then the raft foundation load at the interface of the uppermost 'weak' layer identified represents an increase in overburden pressure in the order of 45%. This does not correspond to a large increase in load.

A valuable indicator of liquefaction potential is the measure of pore pressure dissipation. This can give a good indication of relative permeability, and volume change characteristics of the soil, which are very important for evaluation of liquefaction resistance. Pore pressure measurement can indicate whether the soil is free draining with a high permeability, not free draining with a low permeability, or a medium between the two extremes. This greatly influences liquefaction potential. However, no established correlations currently exist between the measured CPTU pore pressure response and liquefaction resistance. As the cone penetrometer used at the Iceworks Stage 3 site was not equipped with a piezometer, such data was not available for evaluation.

The 'low' loads applied to the soil strata by the Iceworks Stage 3 raft foundation, the lack of local correlations for CPT test results, and the absence of pore pressure dissipation information, make liquefaction potential of the soil stratigraphy very difficult to assess. The high cost of adopting piling, as a conservative response to concern of the potential for liquefaction, compared to the costs of a more detailed site investigation, clearly highlight the potential benefit of supplementary testing in addition to the three CPT tests conducted.

6 CONCLUSION

The Fremantle Iceworks project indicates a clear need for :

- Detailed geotechnical site investigative techniques, to determine foundation design parameters to a greater degree of accuracy where calcareous soils are anticipated. This is particularly true where ground improvement techniques are not appropriate, or where the insitu undisturbed soil is likely to have greater strength and stiffness than that when treated.

- The use of several different techniques to firstly provide confidence in foundation design parameters inferred from test data, and also to discourage adoption of grossly conservative design parameters due to lack of information.

- Emphasis to Clients and Developers of possible enormous project cost savings if foundation design parameters accounting for cementation can be determined within an acceptable level of accuracy. The need for additional testing to determine the presence of soil cementation, and analysis to

accurately model such increase in soil stiffness for foundation design needs to be stressed.

- The development of an accessible database of local experience, and correlations for onshore calcareous sites, in order that this experience can benefit the engineering of appropriate foundation systems, and ultimately the greater community.

7 ACKNOWLEDGEMENTS

The author would like to acknowledge the input from Ian M.S. Finnie of Advanced Geomechanics, Nedlands, W.A., Australia and the cooperation of Benchmark Project Builders Pty Ltd, the Builder of the "Iceworks", Stage 3 Development.

8 REFERENCES

1. FINNIE I.M.S, RANDOLPH M.F., "Bearing response of shallow foundations in uncemented calcareous soil", Centrifuge 94, Leung, Lee & Tan, Rotterdam: Balkema, 1994, 535-540
2. RANDOLPH M.F., ISMAIL M., JOER H.A, "Compressibility and crushability of calcareous soils", February 1997, 1-5
3. FINNIE I.M.S, RANDOLPH M.F., "Punch-through and liquefaction induced failure of shallow foundations on calcareous sediments", February 1994, 1-11
4. JEWELL R.J., "An introduction to calcareous sediments", June 1993, 1-15
5. FAHEY M., "Selection of parameters for foundation design in calcareous soil", June 1993, 3-14, 20-24, 32
6. CAMPANELLA R.G., "Guidelines for geotechnical design using the cone penetrometer test and CPT with pore pressure measurement", September, 1995, 44-101, 131-141

8 LIST OF FIGURES

Correlations Between Cone Penetration Resistance and Standard Penetration of some New Zealand Volcanic and Alluvial Deposits

Alaa S Ahmed-Zeki and Peter B C Bosselmann
Foundation Engineering, Auckland, New Zealand

Summary: The results of cone and standard penetration tests carried out in Tauranga volcanic soils and in Whangarei alluvial soils are graphically correlated using normal arithmetic plots. The linear least square equation relating the cone tip resistance, q_c, and the standard penetration N value is in the form $q_c = k * N$, where k is a constant. The ratio q_c/N is then used to establish correlations with the type of soil and the results are compared to international findings.

1 INTRODUCTION

CPT-SPT correlations are useful for the conversion of available field test data into the form appropriate for various foundation analyses and design. It is attempted here to prepare correlations on local materials which should lead to better results than others based on internationally collected data. It has frequently been emphasised that it is imperative to rely on locally prepared correlations (eg. Pender, 1998). A new evidence on the significance of deriving correlations on local soils comes from the finding that cone penetration resistance of pumiceous sand is not an indicator of relative density (Wesley *et al.*, 1998). Additionally interesting is the conclusion arrived at by Marks and Larkin (1998) that the low strain shear modulus of the pumice sand is significantly lower than that of quartz sand at similar relative densities and confining pressures. Pranjoto and Larkin (1995) have suggested the grain softness of pumice sand and the high void ratio as being substantially responsible for its different behaviour in comparison to quartz sand. Nonetheless, it is worthwhile mentioning that Takesue *et al.* (1995) have shown that CPT-SPT correlations as well as pile design values for a volcanic soil distributed in southern Kyushu-Japan and locally known as Shirasu) were consistent with quartz sand values.

2 GEOLOGY

Tauranga Basin where the field tests covered by this study were undertaken, is a Pleistocene, predominantly fluvial/estuarine basin which was partially infilled during a period of rapid subsidence after the eruption of the Waiteariki Ignimbrite (Briggs *et al.*, 1996). The infill in the basin is comprised of terrestrial and estuarine volcaniclastic sediments and non-welded or partially welded distal ignimbrites and airfall tephras (Pahoia Tephras), generally covered by a sequence of younger airfall tephra (eg. Hamilton Ash and Rotoehu Ash). These were reworked via fluvial, lacustrine and estuarine processes (Matua Subgroup), and re-deposited in sequences interbedded with the primary volcanic units.

In Whangarei, the field tests were carried out in a low lying area consisting of undifferentiated riverbed and flood plain alluvium (Thompson, 1961; Markham, 1981). These soils typically consist of thinly to very thinly bedded, very loose to loose, unconsolidated sands, gravels, clays and silts with occasional lenses of black humus rich peat.

3 FIELD TEST PROCEDURES

3.1 Standard Penetration Test

SPTs consist of driving a 50mm outer diameter split spoon sampler into the soil using 64 kg hammer free falling through 0.75 metres. The number of blows required to drive the split spoon sampler a distance of 300mm, after an initial penetration of 150mm is referred to as the SPT "N" value. The test is used mainly to assess the density of non-cohesive soils, but may also give an indication of the relative strengths of cohesive soils. It has the advantages of being simple and rapid, allowing a large number of tests to be undertaken at a relatively low cost, supplemented by a large database. It is a common practice not to record a blow count exceeding 50.

Patterson-Kan and North (1986) stated that due to the fact that mechanical drop hammers as used in New Zealand deliver a much greater energy per blow than the American rope and capstan method, the locally performed tests consequently give numerically lower SPT values. Therefore they suggested that the SPT results may be factored up to 20 to 25% before application to the correlation charts prepared in North America. However, the writers of this article are unaware of anybody applying this procedure in New Zealand.

3.2 Cone Penetration Test

In these tests, a 35mm diameter rod with a cone tipped end is pushed continuously into the soil at a rate of approximately 20mm/second by a hydraulic jacking system.

Measurements are made of the end bearing resistance on the cone (the actual end bearing force divided by the cross-sectional area) and friction resistance on a separate 130mm long sleeve (the frictional force on the sleeve divided by its surface area), immediately behind the cone. A 200 kN load cell was used in Tauranga soils tests while the capacity of the load cell in Whangarei alluvials was 100 kN. As penetration occurs the information is recorded digitally, processed and plotted once testing is finished.

4 ANALYSIS AND DISCUSSION

The depths to the recorded SPT N values were considered to be at the mid points of the 300mm penetration of the sampler. At these depths the corresponding q_c values were recorded. An alternative procedure would have been to calculate average values of N and q_c along the 300mm penetration of the SPT sampler. No correction for overburden pressure was applied. The correlations were carried out for every two adjacent CPT and SPT at the sites. At one location within the volcanic soils, two CPTs were performed adjacent to an SPT location; here the q_c values were averaged at the assigned depths.

A direct q_c versus N relationship was established in the form of;

$$q_c = k * N$$

where k is a constant. The results are presented in Figures 1 and 2 which show that the correlations within the volcanic soils demonstrate a much larger scatter. In Figure 2, setting the trendline's intercept on the vertical axis to zero resulted in a negative value for correlation coefficient, so the dashed trendline representing a non-restricted linear best fit relationship is plotted to demonstrate the close comparison in magnitude for the q_c versus N values under consideration.

Power (1982) reported values for k of 0.3, 0.5 and 0.7 for a range of Chalk types, while Chang (1988) observed values of 0.18, 0.2 and 0.23 for Singapore residual soils with a well-defined correlation.

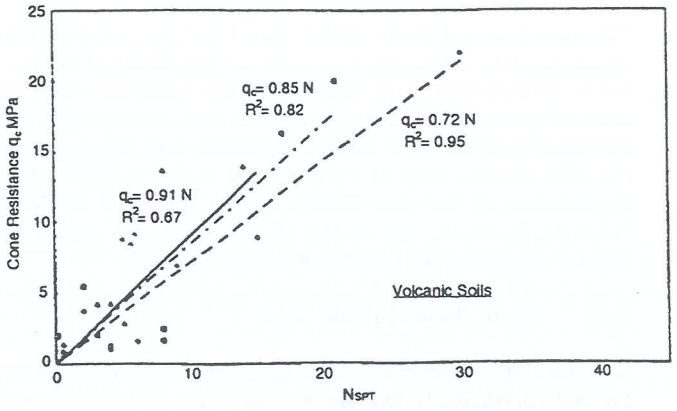

Figure 1 CPT-SPT correlations for volcanic soils. Different symbols denote pairs of CPT-SPTs at different locations of the site.

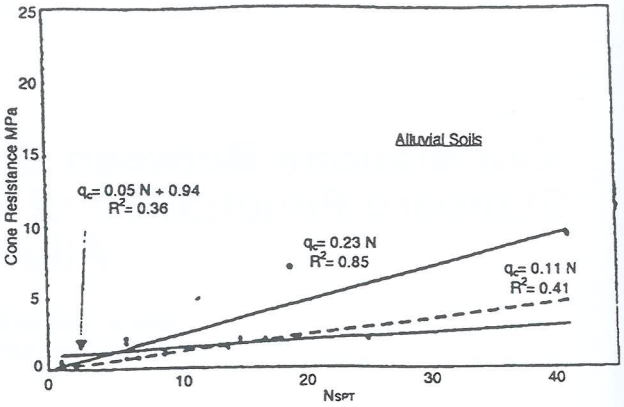

Figure 2 CPT-SPT correlations for alluvial soils. Different symbols denote pairs of CPT-SPTs at different locations of the site

To correlate the findings of these field tests with the type of soil penetrated, Figures 3 and 4 were plotted on normal scales. No grain size analyses were available for incorporation into the current work, so the soil descriptions presented in the borehole records were used. As can be seen, the plots for the volcanic soils show a very significant scatter. Figure 4 for the alluvial soils, however, shows a somewhat better relationship for the two parameters and the q_c/N values here range between 80 and 500 for the adopted units.

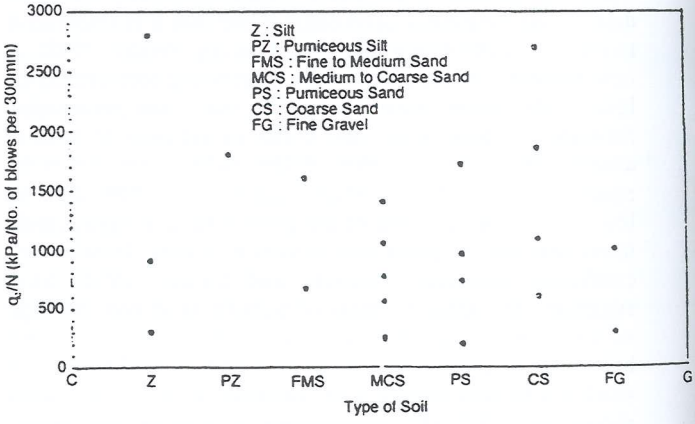

Figure 3 Correlation of q_c/N ratio versus soil type (volcanic soils)

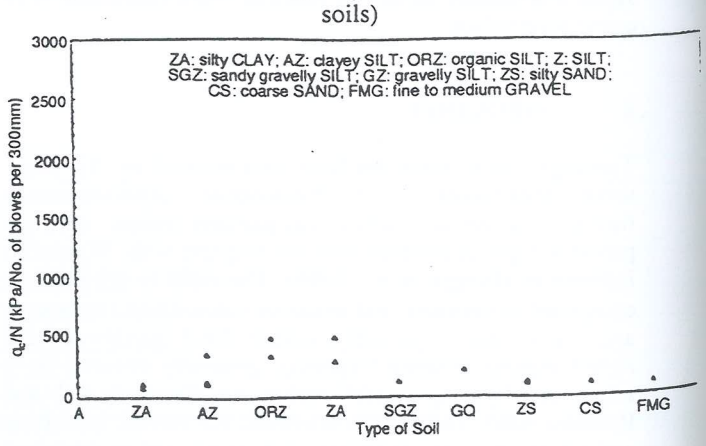

Figure 4 Correlation of q_c/N ratio versus soil type (alluvial soils)

In an attempt to compare parameters from local soils to those published in geotechnical literature overseas, the q_c/N ratio against soil type was plotted as shown in Figure 5 (a) and (b). Extremely high values, which are believed to be due to the sensitivity of the materials to disturbance where SPT N values approach zero, were discarded. The limitation on using the bore log description still applies for these figure, albeit it can be observed that finer tuning to plot the points within any soil group does not seem to alter the general picture.

It is clear on Figure 5 (a) that points of q_c/N ratio versus soil type for the volcanic soils fall far beyond the outer limits observed by Burland and Burbidge (1985) or Robertson *et al.* (1983), regardless of the soil's particle size distribution. The corresponding relationship for the alluvial soils as shown in Figure 5 (b) compares reasonably closely to the published relationships in the fine-grain region, but significantly lower for the sand and gravel sized soils and so it does not show dependence on the grain size distribution. For both volcanic and alluvial soils, the increasing trend of the q_c/N ratio is not visible.

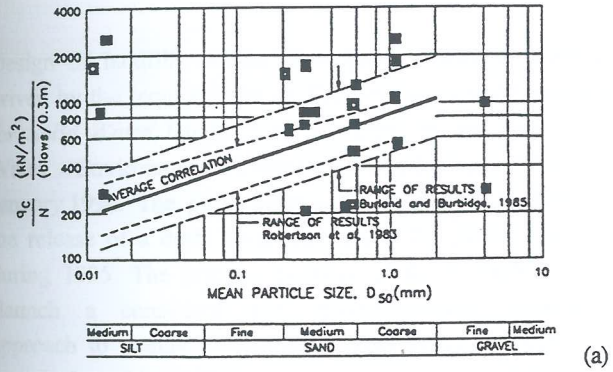

(a)

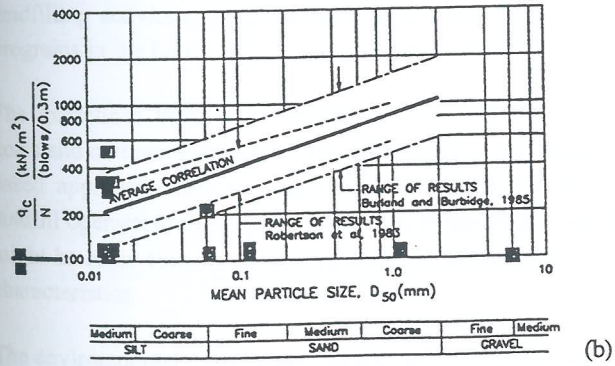

(b)

Figure 5 Relative locations of q_c/N ratio versus "as-logged" soil type points for (a) volcanic soils and (b) alluvial soils, plotted on a pre-prepared figure of the variation of q_c/N ratio with the mean grain size of soil. The dashed lines show the upper and lower limits of observations by the relevant researchers.

(Figure originally printed in the Canadian Foundation Engineering Manual, 3rd edition, 1992, page 52, and is reprinted with the permission of the Canadian Geotechnical Society)

5 CONCLUSION

This study was an attempt to make use of some available data in formalising corrections for the cone resistance and standard penetration in local geological formations. No doubt, more data should improve the results and refine the observations.

Linear least square equations have been presented relating CPT cone resistance, q_c and the standard penetration N value for volcanic and alluvial deposits found at two sites in Tauranga and Whangarei respectively.

However, rather than succeeding in observing well pronounced relationships, a substantial data scatter was observed, especially with the volcanic soils, when plotting q_c/N values against the type of soil. This could indicate either that correlation relationships are difficult to obtain because of inherent variabilities in the two types of field tests, or that the effect of a soil property other than grain size distribution is influential.

In comparison to the observations published overseas, the trend of increasing q_c/N values against increasing soil particle size was absent in this study. Certainly, this study has presented new evidence for the inappropriateness of the direct application of imported correlations for design purposes.

6 ACKNOWLEDGMENTS

The writers are grateful to Prof. Michael J. Pender and Dr. Laurence D. Wesley for reviewing and commenting on this article. The assistance of Mr. Rodney Melville-Smith, Managing Director of Foundation Engineering Consultants in providing access to the company's database is highly appreciated. Also due thanks are forwarded to Mr. Barry Coker, Foundation Engineering Consultants for the valuable discussions on computer spreadsheeting.

7 REFERENCES

Briggs, R. M., Hall, G. K., Harmsworth, G. R., Hollis, A. G., Houghton, F., Hughes, G. R., Morgan, M. D., Whitbread-Edwards, A. R. (1996): *Geology of the Tauranga Area,* Dept. of Earth Sciences Occasional report no. 22, University of Waikato, Hamilton, published in collaboration with Environmental B.O.P & Institute of Geological and Nuclear Sciences Limited.

Burland, J. B. & Burbidge, M.C. (1985) *Settlement of foundations on Sand and Gravel,* Proc. Instn. Civil Engrs. December, 1985, 78 (part 1) pp. 1325-1381.

Canadian Foundation Engineering Manual (1992), 3rd edition, Canadian Geotechnical Society, Technical Committee on Foundations.

Chang, M.F. (1988) *Insitu Testing of Residual Soils in Singapore.* Proc. of the 2nd Intern. Conf, on Geomechanics in Tropical Soils, Singapore 2, 97-108, Balkema Pub., Rotterdam.

Markham, G. S. (1981) Hukerenui-Whangarei sheet Q06/07, 1:100,000, New Zealand Inventory Series, Rocktypes. Dept. of Lands and Survey, Wellington

Marks, S. & Larking, T.J. (1998) *The Seismic Properties of a New Zealand Sand,* 3rd Young Geotechnical Professionals Conference, Melbourne/Australia, Feb. 1998, pp. 83-88.

Patterson-Kane, K.J. & North, P.J. (1986) *Bored Piles in Weak Soils*, Piled Foundations for Engineering Structures, Symposium Proceedings, Hamilton, NZ Geomechanics Society, Vol. 12, Issue 1 (G), September 1986.

Pender, M. J (1998) *Judgement in Geotechnical Engineering-Design Parameter Values,* NZ Geomechanics News No. 55, June 1998, NZ Geotechnical Society, pp. 21-23.

Power, P.T. (1982) *The Use of Electric Cone Penetrometer in the Determination of the Engineering Properties of Chalk.* Proc. of the 2nd Europ. Symp. on Penetration Testing, ESPOT-II, Amsterdam, 2, 769-74, Balkema Pub., Rotterdam.

Pranjoto, S. & Larking, T. (1995) *Some Propert Volcanic Sand,* 2nd ANZ Young Geotechnical Prof Conference, Auckland, November 1995.

Robertson, P.K. & Campanella, R.G (1983) *Interp of Cone Penetration Tests,* Canadian Geotechnical Vol. 20, No. 4, pp. 718-745.

Takesui, K., Sasao, H. and Makihara, Y. (199 *Penetration Testing in Volcanic Soil Deposits,* Proce the International Conference on Advances Investigation Practice, 452-463, Thomas Telford, Lo

Thompson, B.N. (1961) Geological Map of New sheet 2A-Whangarei, 1:250,000, D.S.I.R., Wellingt

Wesley, L.D., Meyer, V. & Pender, M.J. (199 *Penetration Tests in Pumice Sand,* Geomechanics 55, June 1998, NZ Geotechnical Society, pp. 57-61

Geotechnical Considerations of Landfill Design and Construction

Kevin Brennan and Ashton Hincksman, PPK Environment & Infrastructure Pty Ltd

Summary: ***The Environmental Guidelines for Solid Waste Landfills as published by the New South Wales Environmental Protection Authority (EPA) provides a list of 39 so-called "benchmark" techniques. A number of the benchmarks relate directly to the geotechnical characteristics of a landfill site and proposed construction materials. These geotechnical related benchmarks are outlined in the paper.***

To illustrate the requirements of these benchmarks, the methodology and results of a preliminary geotechnical investigation for a proposed landfill site concept plan is presented. Alternatives to the benchmark techniques which have been adopted, or are proposed to be implemented at an operation landfill are provided.

1. INTRODUCTION

Design of landfills within New South Wales is primarily driven by the requirements of *The Environmental Guidelines for Solid Waste Landfills* as published by the New South Wales Environment Protection Authority (EPA) in January 1996. The publication of these guidelines followed the release of a draft document issued for public comment during 1995. The primary purpose of the Guidelines is to 'launch a consistent and environmentally responsible approach to managing landfills across NSW'. In turn it is hoped that this will increase community confidence in landfilling activities and avoid extremely costly remediation programs in the future.

The guidelines themselves include a set of environmental goals and outcomes that are to be achieved via a performance based approach. This method has been adopted to enable landfill operators to develop an approach to landfilling which might be more suitable for the subject site and its individual characteristics.

The environmental goals of the guidelines are included within the document through the provision of a list of 39 so-called 'benchmark techniques' which are based on worlds best practice. The appropriate selection of relevant solutions to each environmental goal should be based on four key points:

1. The site location and proposed waste types need to be determined;
2. That there is no impediment to rejecting some techniques in relation to a given facility;
3. A combination of design and construction, operations management, monitoring, remediation and post closure management measures will generally be required to deal with the range of potential environmental impacts for a given site ie:
    - Geological information;
    - Hydrology
    - Landfill operation
    - Nature of wastes and quantity
    - Meteorology
    - Elevation
    - Quality of groundwater
    - Leachate detection and controls
4. There is no impediment to using operational or design techniques not listed in the benchmark techniques. Alternative methods may be adopted providing justification that the environmental goal will be met.

There are a number of these environmental benchmarks that relate directly to the geotechnical characteristics of the landfill site and proposed construction materials to be used. These design aspects include, but are not limited to:

- Leachate Barrier System
- Leachate Collection System
- Covering of Waste
- Landfill Gas Containment
- Extraction and Disposal of Landfill Gas
- Site Capping and Revegetation

The benchmark requirements have lead to the development of a more detailed geotechnical scope of works being implemented for landfill site investigation and design. To demonstrate the practical application of geotechnical aspects of landfill investigation and development of design alternatives, experience at a proposed putrescible landfill site and existing non-putrescible landfill have been presented.

2. GEOTECHNICAL INVESTIGATION FOR A PROPOSED LANDFILL

To illustrate the requirements and the scope of works of a geotechnical investigation for the concept design of a landfill the following example is presented.

An Environmental Impact Statement (EIS) was recently carried out for the proposed construction and operation of a Class 1 solid waste landfill. The potential site for the landfill was in an existing open cut coalmine, located in the Hunter Valley of New South Wales. At the time of investigation the operation of the mine was nearing completion, with the majority of the site having been reshaped to its original landform. The reshaping used the overburden material resulting from the mining, which comprised a mixture of blasted and excavated siltstones, sandstones and minor carbonaceous materials in a sandy clay/clayey sand matrix. Construction of the proposed landfill cells would require excavation from the existing ground surface level to depths ranging between 5 m and 28 m. The depth of mine overburden remaining in place under the landfill cells would range from 0 m (ie landfill founded on bedrock) to approximately 45 m.

2.1 CONCEPT PLAN

The EIS required a preliminary geotechnical investigation of the site be carried out, with the results to be utilised in the development of a concept plan for the proposed landfill. The concept plan was to comply with EPA Solid Waste Landfills Guidelines for the construction of such facilities. Therefore following excavation to the base of the proposed landfill, the concept plan proposed a liner system that would collect and recirculate leachate. The proposed liner comprised the following arrangement:

- ***Leachate Collection layer***; a minimum 300 mm thick gravel drainage layer, over
- ***Protective Geotextile Layer***; over
- ***Liner***; Compacted Clay Layer (CCL) or a composite liner comprising a High Density Polyethylene (HDPE) geomembrane overlying a Geosynthetic Clay Liner (GCL), over
- ***Cell Base Layer***; a minimum 900 mm of compacted soil.

Waste would be placed within each of the landfill c to a maximum stage height of approximately 15 would be unloaded from trucks at the working shaped by the on site plant.

The concept plan proposed that when the landfill waste would be covered with an engineered cappin The aim of the capping layer is to reduce leachate g by minimising stormwater infiltration, prevent er soil loss by vegetating the cover and to minimise la migration. The proposed cover would comprise the f

- ***Revegetation Layer***; a minimum 1000 mm thicl
- ***Infiltration Drainage Layer***; a minimum 300 sand or gravel drainage layer, over
- ***Sealing Layer***; Compacted Clay layer or a geo over
- ***Gas Drainage Layer***; a minimum 300 mm co over
- ***Seal Bearing Surface***; soil layer covering lan material.

2.2 GEOTECHNICAL ISSUES

In order to comply with the EPA benchmark techn to determine the feasibility of the site for the cons the landfill, the primary tasks/issues of the p geotechnical investigation were as follows:

2.2.1 Settlement

Following the construction of the landfill, assess th settlement of the foundation material (mi overburden) and the resulting possible affects such of the liner.

2.2.2 Mine Subsidence

Consider the effects to the landfill liner and the fi of the leachate collector drains if underground mir subsided as a result of the applied landfill loads.

2.2.3 Slope Stability

Assess the slope stability of the site during an construction and filling of the landfill, consi interfaces, subsurface water, seismic loads a surcharge.

2.2.4 Assessment of Source Materials

Investigate potential on site sources of material with the EPA benchmark techniques (eg permeab construction of the landfill liner and capping laye

2.3 INVESTIGATION SCOPE OF WORKS

The preliminary geotechnical investigation for the EIS comprised a desk study, walk over survey of the site, test pit investigation, limited borehole investigation, laboratory testing and analysis of all results.

2.3.1 Desk study

The desk study reviewed all available material including:

- aerial photographs;
- maps (topography, geological, contour);
- review of past geotechnical investigations;
- review of the mining company records; and
- information obtained from the Mine Subsidence Board.

2.3.2 Walk over survey

The purpose of the walk over survey was to become familiar with ground conditions at the site and to identify/examine features observed on aerial photographs. Features that were highlighted included:

- outcrops of bedrock and exposures of soil profiles;
- evidence of major geological structures such as faults, dykes, jointing, dip of strata;
- signs of slope instability such as fresh rock faces, rubble at the top of slopes, hummocky or scarp topography;
- filled ground; and
- groundwater, boggy ground, watercourses, springs.

In addition, sites for the test pit and borehole investigations were selected during the walk over survey; with particular attention given to vehicle access, services and boundaries of the proposed landfill.

2.3.3 Test Pit Investigation

Test pits were excavated using a Hyundai 290 excavator, fitted with a 1.5 m wide bucket. The test pits were located in areas both disturbed by past mining operations and undisturbed area that would be mined in the near future. The test pits were excavated to the maximum reach of the machine – averaging a depth of 5.5 m below existing ground surface level. The test pits were logged and representative samples of the subsurface materials were recovered by the supervising geotechnical engineer.

2.3.4 Borehole investigation

Boreholes were drilled at representative locations across the site using a truck mounted Mobile B80 drill rig. The boreholes were drilled through the mine waste overburden using a Sim-cas eccentric under-reaming hammer bit which advanced the casing to the base of the overburden. At selected depths the hammer bit was removed and the strength/compaction of the mine waste overburden soil profile was determined from Standard Penetration Tests (SPT) 'N' values augmented with hand penetrometer readings on cohesive samples recovered in the SPT split spoon. The underlying bedrock was drilled using a standard down the hole air percussion hammer. The boreholes were logged and representative samples of the subsurface materials were recovered by the supervising geotechnical engineer.

2.3.5 Laboratory

Selected subsurface materials sampled from the test pits and the boreholes were tested in NATA registered laboratories to assess the feasibility of reusing the mine waste overburden (disturbed areas) and the natural clay deposits (from undisturbed areas) for clay lining or capping of the landfill. Samples taken from the mine overburden waste profiles included gravel and cobble size material. For laboratory testing purposes the samples were manually sorted on site to be predominantly free from material greater than 75 mm maximum dimension.

Laboratory testing included field moisture content, Atterberg limits, particle size distribution, Emerson dispersion and constant head permeability.

2.4 RESULTS

In general terms the test pits and boreholes located in disturbed areas encountered a surface layer of topsoil overlying mine overburden waste material (ranging in thickness from approximately 25 m to 37 m) and then sedimentary bedrock. Difficult drilling and test pitting conditions were experienced at some locations due to some of the sandstone boulders encountered being greater than 2 m thick. Some voids or zones of low air return were encountered when the boreholes encountered cobbles or boulders. SPT 'N' values ranged from 7 to 23, with an average 'N' value of 16; it was noted that gravel inclusions in the fill may have elevated the recorded 'N' values. In general the mine overburden waste material appeared to be moderately to well compacted.

The test pits located in mine's undisturbed areas (at the time of investigation) encountered a relatively thin layer of topsoil overlying natural clayey and sandy soils and then relatively shallow sedimentary bedrock at depths ranging from 0.7 m to 2.8 m. The natural clays and silts encountered in the test pits were of medium to high plasticity and ranged in strength from very stiff to hard.

No groundwater was observed in the test pits predominantly due to pumps re-diverting groundwater flows around the open cut mine operations (in order to keep the mine dry). During drilling of the boreholes a slight flow of groundwater was observed at the interface of the mine overburden waste fill and the sedimentary bedrock. In one of the boreholes a stronger flow was also observed from the interface of a coal layer in the bedrock.

The laboratory tests indicated the tested clays from the mine overburden waste material ranged from low to medium plasticity and had a slight to moderate tendency to disperse when immersed in water. The tested natural clays from the undisturbed areas (at the time of investigation) were of medium to high plasticity with a slight tendency to disperse when immersed in water.

Permeability tests were undertaken on both samples of mine waste overburden materials and samples of the natural clays from areas that were to be mined. The samples were recompacted to 98% Standard Maximum Dry Density prior to testing. The permeability of the tested samples ranged from 7.0×10^{-11} m/sec to 7.6×10^{-9} m/sec indicating a low to medium level of permeability. It should be noted that the permeability tests were undertaken on test samples with particle sizes less than 19 mm. The grading tests identified a high gravel percentage in the samples prior to sorting, therefore an increase in the field permeability of the material would be expected. Field permeability tests in trial pads of compacted material would be necessary to gain a more representative design permeability.

2.5 ANALYSIS

2.5.1 Settlement

Based on the proposed concept plan and the results of the preliminary geotechnical investigation, the majority of the proposed landfill would generally be founded on mine waste overburden which was variable in particle size, compaction and appeared to have been placed in an uncontrolled manner; a small portion of the landfill would however be founded on bedrock. As stated previously the depth of overburden material to be removed to construct the landfill would range from approximately 5 m to 28 m. Some of this material had been placed over 25 years prior to the investigation and therefore was considered to have provided a surcharge effect on the mine overburden waste material that would remain beneath the landfill (note depth of remaining material ranged from 0 m - ie landfill founded on bedrock - to approximately 45 m).

EPA guidelines indicate waste compaction goals in the range of 0.65 tonnes/m^3 to 0.85 tonnes/m^3 depending on the receival rates per annum. Thom and Pym[iii] indicate a density range of 0.3 tonnes/m^3 for green waste and up to 1.3 tonnes/m^3 for demolition rubble. Using these values and with the results of the preliminary geotechnical investigation in mind, the settlement analysis at the proposed landfill adopted a conservative value of 1.1 tonnes/m^3 for the landfill waste material, and 1.9 tonnes/m^3 for the mine overburden waste material. Generally Elastic Modulus 'E' values for the soil profile adopted a value of 2N where 'N' equalled the SPT value; however consideration was also given to the potential for voids between overlapping cobbles and boulders within the mine overburden.

Estimates of settlement were dependent on the quality and thickness of overburden underlying the landfill. As the composition of the mine overburden waste material was predominantly dry sands, gravels and cobbles, the anticipated settlements would occur predominantly instantaneously. Minimal long term consolidation was expected due to a reduction in pore water pressures in clayey soils.

Worst case settlement values (ie large values) were recorded in proposed landfill areas where minimal overburden was removed and the depth of overburden remaining was great. Conversely best settlement values (ie minimal values) were calculated where the depth to bedrock was minimal. Settlements ranged from 0 mm to approximately 660 mm with typical settlements in the order of 300 mm. It was noted that these settlement values were expected to occur over relatively localised areas and not over the entire landfill base.

Differential settlements were also considered in the transition zone where the foundation of the landfill changed from bedrock to the mine overburden waste material. The magnitude of possible worst case differential settlements was analysed to be in the order of approximately 660 mm. It is unlikely that such sharp changes in settlement would occur; rather it was expected settlements would occur in the form of the traditional bowl shape, extending over distances greater than 5 m.

The calculated settlement values based on the results of the preliminary geotechnical investigation were used in the concept design of the proposed landfill leachate barrier system. The barrier system had to be able to accommodate the strains induced by settlement and differential settlement of the mine overburden waste remaining underneath the proposed landfill.

For strains to reach a value that could cause risk to the integrity of the liner, large settlements over short distances (such as potholes) would be required. Based on the results of the preliminary investigation, the risk of pothole formations via the collapse of voids in the mine overburden waste material were minimal.

The calculations indicated strains of up to approximately 4% were possible if the landfill was founded on the mine overburden waste material, in its present condition. These strains would be reduced if the subgrade was improved by say impact proof rolling or by placement of geogrid forming a "bridging" layer.

Normal compacted clay materials cannot withstand tensil strains resulting from settlement/differential settlement greater than 0.85% without distress such as cracking occurring[iv]. The ability for a CCL to bridge a pothole/void between say boulders in the mine overburden waste was questionable given clay has a relatively low tensile strength; the incorporation of a geogrid or similar would assist in bridging pothole/voids formed from settlement of the mine overburden waste.

Alternatively a composite liner system comprising a HDPE geomembrane overlying a GCL would be able to accommodate 10 to 15% strain with negligible increase in permeability. Should settlement of the mine overburden waste material induce a strain greater than 10 to 15% in the geosynthetics, an increase in the permeability of the liner system could be expected.

2.5.2 Mine subsidence

Mine Subsidence Board guidelines indicate that where underground mine workings are greater than 20 m below the surface level, the risk of pot hole subsidence at that surface level is low and the area would not be considered to be at risk of pot hole subsidence.

For the proposed landfill site in the Hunter Valley, NSW, no underground mining had occurred beneath the site, therefore there was no immediate risk of mine subsidence and/or pot holing to the landfill structure. Furthermore it was understood that both the colliery and the Department of Mineral Resources considered that the extraction of coal seams known to be beneath the proposed landfill site was not presently, nor considered in the future to be economically feasible (thin coal seams, poor quality and high stripping ratio).

2.5.3 Slope Stability

A computer aided slope stability analysis of the proposed 1 vertical to 3 horizontal construction slopes was carried out using soil parameters derived from the subsurface preliminary investigations, seismic loads (adopted from the Australian Standard AS 1170.4 (1993) Minimum Design Loads on Structures Part 4: Earthquake Loads) and a range of groundwater levels (to accommodate the change in groundwater levels following the completion of mining operations and the decommissioning of groundwater pumps).

The slope stability analysis of the subsurface soil and rock profile forming the sidewalls of the landfill, indicated that for ground water levels below or up to the proposed base of the landfill, and with seismic loads applied, the minimum factors of safety for various landfill cross sections were greater than 1.5.

Therefore it would appear that the proposed construction slopes of 1 vertical to 3 horizontal would be adequate to provide stability of the landfill at all stages provided appropriate construction sequencing and earthworks standards are adhered to and landfilling occurred from the toe of the slope upwards.

2.6 CONCEPT PLAN BASED ON INVESTIGATION RESULTS/ANALYSIS

2.6.1 Landfill liner and Leachate Collection System

Following excavation to the base of the proposed landfill, the concept plan of the proposed liner system to be constructed directly over the remaining mine overburden waste material comprised the following layers (reference to the attached Figure 2.1):

2.6.1.1 Compacted base

The purpose of the compacted base layer was to provide a uniform base and working platform for construction of the landfill liner. The base layer would also provide an additional but limited bridging mechanism over the remaining mine overburden waste material. The base layer was designed to have a minimum thickness of 0.8 m (4 lifts at 200 mm compacted layers). The sub-base layer was designed to be compacted to a minimum density of 98% relative to SMDD and to within ± 2% of OMC.

Mine overburden waste materials were expected to be suitable after sorting/sieving for use in construction of the compacted base layer under the composite liner, whilst also providing some attenuation to leachate. This material would also be able to be used for the daily landfill cover.

Due to the high quantity of cobbles and boulders encountered in the preliminary investigation test pits and boreholes, supervision by an experienced earthworks contractor or a geotechnical engineer during excavation was recommended in order to provide visual identification of materials likely to be most suitable for use in the landfill construction/operation.

Materials in the compacted base layer were to have a maximum particle size of 75 mm. The material used in the top layer of the base, directly under the geosynthetic composite layer, had to be free from objects that could damage the liner, such as stones and rocks.

2.6.1.2 Liner

Mine overburden waste materials and natural clays sampled from the site were tested and assessed for suitability in meeting the clay liner specification. The materials selected for laboratory testing were considered to be representative of the more clayey materials encountered at investigation locations in terms of having potential to meet the specification for a clay liner (such as EPA requirement of a permeability less than 1×10^{-9} m/sec).

The laboratory test results indicated that the mine waste materials had a slight to moderate potential for dispersion and a low to medium level of permeability. However as stated previously to carry out the laboratory permeability testing, all material greater than 19 mm diameter were removed from the samples. Therefore, unless acceptable in situ permeability test results were recorded, on site sorting, sieving, screening and removal of gravel, cobble and boulder inclusions from the mine overburden waste material would be required prior to it being considered for use as a CCL.

The natural clays generally had a lower tendency to disperse, had lower permeability values and had negligible gravel content compared to the mine overburden waste material. The preliminary geotechnical investigation encountered an average in situ clay layer thickness of 0.9 m underlying the areas that were undisturbed at the time of investigation. Based on this thickness, the estimated volume of clay deposits was sufficient for the construction of a CCL for the proposed landfill. However it was noted that the preliminary investigation test locations covered only a small section of the undisturbed areas (due to access availability) and encountered a clay subsurface profile that varied in thickness from 0.2 m to 1.8 m. To determine the actual available volume of clay, further investigation of the entire undisturbed areas was required prior to considering sourcing the on site clay deposits. It is noted that changes to the mining operations were also required to allow selective sourcing of clay deposits and stockpiling until required for the construction of the landfill.

As stated previously, when strain levels in a CCL (resulting from settlement of the underling materials) exceed 0.8 to 1.0 per cent, cracking and an associated increased permeability would occur. Based on the results of the preliminary geotechnical investigation, the calculations indicated strains of up to 4 per cent were possible. A CCL was therefore determined to be not feasible due to the potential increase in permeability, and also due to the difficulties associated with changing the method of mining to allow sourcing of the clay.

As an alternative to the clay liner a decision to adopt a HDPE geomembrane overlying a GCL was made. The GCL and HDPE components of the liner system were able to accommodate 10 to 15% strains with negligible increase in permeability. The GCL and the HDPE layers work as a composite liner system in providing a low permeability barrier system against leachate migration from the landfill. A flexible 1.5 mm thick HDPE with a permeability of 8.1×10^{-15} m/sec was selected. The selected GCL would comprise sodium bentonite sandwiched between 2 layers of non-woven polypropylene geotextile that had a permeability of 3×10^{-11} m/sec. The overall in situ co-efficient of permeability was less than 1×10^{-9} m/sec as specified for a clay liner by the EPA.

2.6.1.3 Protective Geotextile Layer

A geotextile was provided over the HDPE to protect it from puncture from the overlying gravel drainage layer. The geotextile was sized based on the type of gravel proposed for use and the thickness of the drainage/operations layer. If the gravel was relatively angular, or large, a heavier geotextile was required. For smaller, rounded gravel, a lighter grade geotextile could have been considered. The protective geotextile layer had to be of sufficient strength to accommodate the operations of the landfill earth moving equipment. It was noted that considerable care was to be taken during construction not to damage the HDPE when placing the gravel drainage layer over the geotextile.

2.6.1.4 Leachate Collection

Overlying the protective geotextile layer was a leachate drainage layer comprising a 300 mm minimum thickness layer of drainage gravel (typically 20 mm rounded gravel). The gravel drainage layer provided a path for leachate collection and drainage, with the aim of reducing leachate heads on the liner, while providing a protective operations layer between the waste and the liner system.

At the lowest point of each cell of the landfill a Leachate Collection Sump was to be constructed by forming a local depression in the liner system and filling the depression with gravel. Leachate would be pumped from the sump via a network of HDPE pipes to a Leachate Transfer Pumping Station.

The waste compactor and associated equipment were recommended to be kept well away from the geosynthetic liner. The compactors were not to operate directly on the drainage layer, but on a layer of select waste placed above and in front of the compactor's operation. The first lift of waste had to be free of large or long objects that could be forced through the drainage layer into the barrier system.

2.6.1.5 Lining the 1 Vertical to 3 Horizontal Landfill Side Slopes

On the 1 vertical to 3 horizontal side slopes, the same liner system as proposed for the base was recommended except that the smooth HDPE geomembrane was replaced with textured geomembrane. The textured surface of the HDPE geomembrane provided increased friction against the underlying GCL and overlying geotextile. The need for textured geomembrane depends on the length of slope and landfill operations.

The GCL selected had sufficient internal shear strength to prevent side slope failure in the plane of the geosynthetics (through the bentonite). The shear strength for the GCL in the barrier depended on the construction sequencing and filling operations in the cell. If the leachate drainage layer was placed over a long length of the 1 in 3 side slope above the landfill base, large shear forces would occur within the lining system, with the critical slip plane occurring within the bentonite of the GCL. If the drainage layer was placed up the slope progressively as the waste progressively filled up the batter, the shear forces would be less and therefore the required internal shear strength of the GCL would not be as critical. Calculations indicate that the leachate drainage layer was not to be placed more than 10 to 15 m up the slope ahead of the waste filling. Placing the layer higher put the geosynthetics at risk of tearing from the weight of the gravel plus dynamic load of the equipment placing it. It was recommended that the leachate gravel drainage layer be placed by construction equipment from the layer of waste; that is no construction equipment was to traffic on the liner.

The side wall liner typically extended past the toe of the batter onto the landfill floor for at least 3 m. To hold the liner on the side walls of the landfill, the liner was extend over the crest of the batter for a short distance, and terminated in a vertical "anchor trench". Anchor trenches are typically excavated with a backhoe; therefore the liner was to be draped into the trench which was to be then backfilled with the excavated soil. The backfill would be compacted in layers as the backfilling proceeds.

2.6.2 Landfill Cell Capping

For the proposed Hunter Valley landfill, the concept plan made reference to the EPA Solid Waste Landfill guidelines for future site capping. The recommendations for the proposed landfill were as follows (from bottom of capping system to top):

2.6.2.1 Seal Bearing Surface

An intermediate cover layer which provided the subgrade for the capping system and produced the finished profile for the final landform. This layer was essentially the daily cover layer, thickened to 500 or 600 mm thick to minimise exposure of waste during the extended period between finishing of landfilling in an area and placing the capping system. This layer provided the bearing surface for the next layer.

2.6.2.2 Gas Drainage Layer

A gas collection/relief layer made up of 300 mm of coarse sand with a minimum permeability of 1×10^{-4} m/sec as specified by the EPA. This layer would minimise the potential for uncontrolled gas emissions through the cap should a gas management system be installed.

2.6.2.3 Sealing Layer

From the preliminary geotechnical investigation, it was determined that there was likely to be insufficient quantities of readily available clay materials on site to construct a 500 mm CCL with the hydraulic conductivity required by the NSW EPA guidelines (permeability of less than 10^{-8} m/sec).

Therefore a geosynthetic layer was adopted instead of the 500 mm thick clay sealing layer. Either a polyethylene geomembranes or GCL, or both in combination producing a

composite liner was to be adopted. The GCL had to be suitable for the slopes to which the final landform would be constructed.

2.6.2.4 Infiltration Drainage Layer

A 300 mm thick layer of coarse sand or medium gravel (20 mm rounded) was recommended for the capping drainage layer, possessing a minimum hydraulic conductivity of 1×10^{-4} m/sec in accordance with EPA guidelines.

2.6.2.4 Revegetation Layer

A minimum 1000 mm thick vegetation layer. It was recommended that the vegetation chosen had to have a root system would not penetrate the sealing layer.

3. ALTERNATIVE BENCHMARK TECHNIQUES

The EPA benchmark techniques are sensitive to the location of the landfill site and the type and quantity of waste received. These benchmark techniques are used as reference points only, and alternative design techniques are feasible, provided that justification is made available. Depending upon the individual circumstances, variation to the benchmark techniques may provide economic and environmental benefits, providing the appropriate preliminary assessment/site investigation and analysis are undertaken.

To demonstrate the assessment process, brief examples of four alternative techniques which have been adopted, or are proposed to be implemented, at Pacific Waste Management's Elizabeth Drive Landfill are presented. Assessments of alternative cover material, leachate drainage media, leachate collection pipe spacing and soil liner material have been undertaken. Elizabeth Drive is a state of the art Class 2 solid waste landfill situated in Sydney's west. It has been excavated within shale and laminite bedrock and is lined with a CCL.

3.1 ASSESSMENT OF ALTERNATIVE LEACHATE DRAINAGE MATERIAL

An assessment was undertaken on a sample of blast furnace slag (BFS) material proposed to be used as an alternative leachate drainage material at Elizabeth Drive Landfill. The landfill previously used rounded river gravel for leachate drainage requirements.

The purpose of the assessment was to make comments on the suitability of the material with regards to its physical characteristics for its intended use as a leachate drainage material.

To meet the EPA Guidelines for Solid Waste Landfills (January 1996), the drainage material should exhibit a coefficient of permeability $k>1 \times 10^{-3}$ m/s and ideally should be:

- rounded;
- of grain size greater than 20 mm;
- smooth surfaced;
- non-reactive in mildly acidic conditions;
- relatively uniform in grain size; and
- free of carbonates that could form encrustations around the collector pipes.

It was considered that by undertaking an assessment of the material characteristics (approximate permeability, laboratory calcium carbonate testing, TCLP testing and organic content) an indication of the suitability of the material to meet the objectives of the EPA drainage material requirements could be made.

3.1.1 Permeability

Hazen's formula was used to provide an approximation of the materials coefficient of hydraulic conductivity. Due to the relatively large particle size of the material is was determined that laboratory permeability testing would not be representative. The grading results for the BFS material indicated that the sieve size through which 10% of the material passed was approximately 2.5 cm. This equated to a k value of approximately 6 m/sec, indicating compliance with the guideline requirements.

3.1.2 Physical Characteristics

The particle size of the BFS was generally larger that 20 mm (<5% passing the 19 m sieve). Material was generally subrounded due to the nature in which the material was produced. Although the particles were not rounded, it was not anticipated that this would cause any detrimental impact on the performance of the slag when acting as a leachate drainage material due to the relatively low proportion of fines existing within the material.

3.1.3 Chemical Characteristics

When subjected to acidic conditions the material appeared to be non-reactive with TCLP results indicating a reduction in pH and no metals detected above inert levels.

Calcium carbonate laboratory test results (by weight) of 21.9% indicated a larger percentage present than currently considered 'ideal' by the EPA Guidelines. However, recent studies have been undertaken in the United States on the

effects of calcium carbonate content in relation to leachate drainage systems:

- Study by Waste Management International/RUST on suitability of carbonate aggregate for landfill leachate collection systems based on research performed at University of Missouri-Rolla[i].
- A progress report on the WMI Research and Development project on carbonate compatibility for landfill leachate collection systems being performed at the Illinois Institute of Technology[ii]
- RUST experience in use of slag material as a leachate drainage media in Wheeler Landfill, Indiana

Results of leachate testing undertaken at the Elizabeth Drive Landfill as part of the environmental monitoring over the last 4 years indicate a relatively neutral pH. Results from the Elizabeth Drive Landfill indicated that between 1995 and 1999, pH levels were generally between 6.62 and 7.97. These results were consistent with the findings of the US studies which details leachate results from a large number of landfills.

Based on the comments and recommendations from the previous studies and past experience, it was determined that the calcium carbonate content measured within the slag material would not pose a problem in its intended use as a leachate drainage collection material providing the characteristics of the leachate do not become substantially more acidic. This finding was in conflict with the Guideline requirement and therefore further discussion was entered into with the appropriate NSW EPA representatives.

3.1.4 Comments and Recommendations

Correspondence with the EPA indicated that providing it was demonstrated that no detrimental environmental effect would occur from use of the slag, the enterprise's endeavour of seeking to apply a beneficial re-use of a waste product within the leachate collection system would be fully supported. The EPA concurred that the elevated levels of calcium carbonate would not be detrimental to the system provided that the waste stream remained non-putrescible and low pH wastes were excluded. It was deemed essential that a rigorous protocol be adopted to ensure the materials quality is maintained.

The preliminary sampling and laboratory results indicated that the material was suitable for use as a leachate drainage layer. The blast furnace slag was therefore adopted for use within the leachate collection system. Significant cost savings were realised when compared with the previously used single size rounded river gravel. A comprehensive periodical conformance testing program was implemented to provide evidence that the imported slag material continued to meet the requirements and did not deviate from the tested specimen.

3.2 ASSESSMENT OF ALTERNATIVE DAILY COVER MATERIAL

The purpose of the analysis was made of a material proposed to be used as an alternative daily cover material to the clays and weather shale currently in use at the Elizabeth Drive Landfill. An assessment was made to characterise the material within the Unified Soil Classification system. Additional laboratory testing was also undertaken with respect to a range of potential contaminants.

The NSW EPA Guidelines identify the objectives of daily cover as being:

- Limiting run-on and infiltration of water;
- Controlling and minimising the risk of fire;
- Minimising the emission of landfill gas;
- Suppressing site odour;
- Reducing fly propagation and rodent attraction; and
- Decreasing litter generation

3.2.1 Proposed Material

The proposed cover material consisted of recycled demolition waste. Originating at a number of sources, the material is transported to the recycler's yard and processed through a crusher and screens. Through the screening process the material is separated into two stockpiles – one of coarse (approximately 70% of the waste), and one of fine. A ready market is available for the coarse material, however the fine material is not in great demand. It is this excess material that was proposed for use as daily cover material

Two composite samples of the proposed material were taken from a number of stockpiles. Particle size distribution tests, including hydrometer analysis were carried out on each of the two samples. Chemical laboratory tests were also undertaken on a separate single composite sample and two subsequent samples. The tests included total metals, PAH, TPH, BTEX, OCP and TCLP.

3.2.2 Physical Properties

Based on the grading results obtained, the material may be classified as SW – well graded gravelly sand with clay and silt. The two gradings indicate that the manner in which the material is crushed during processing generates a relatively homogeneous material below the 4.75 mm sieve, varying only in the proportion of crushed construction rubble in the gravel

fraction. A visual assessment of the material identified the composition as crushed concrete and brick fragments.

Again, through the application of Hazen's formula, an approximation of the coefficient of permeability was obtained of between 4.0×10^{-4} cm/sec and 3.6×10^{-3} cm/sec. These results, when compared with those of cover material currently in use (weathered shale and clay) indicate that there may be a potential reduction in run-off and resulting marginal increase in leachate generation through infiltration. However, due to the relatively short period of time in which the daily cover material is exposed to the elements, and the current practice of compacting the daily cover, it was not deemed to be a significant issue. Should areas of daily cover be exposed for prolonged periods it was recommended that intermediate cover consisting of the existing stockpile of residual clay be used.

3.2.3 Chemical Properties

Chemical testing was undertaken to assess the potential of introducing contaminants into the surface water collection system from run-off across the proposed cover material. The results indicated that concentrations of the selected analytes within the three samples did not exceed the relevant NSW EPA criteria for disposal as inert waste, and as such would not pose a threat to the stormwater system.

It was noted that although the concentrations measured did not exceed the EPA criteria, the concentrations of TPH compound, metals, pesticides and PAHs were above background levels. This indicated that the material had potentially been sourced from a location where the previous site activities had impacted on its characteristics. Additionally, the presence of these levels indicated the potential for higher concentrations to exist within the material.

3.2.4 Comments and Recommendations

As the material is sourced from a number of locations prior to being processed at the recycler's facilities it is likely that the existence of chemical compounds may vary between individual loads. It was recommended that should large quantities of the proposed material be delivered to site for use as daily cover material, that a regular sampling and testing program be implemented. In general the material was suitable for use, providing the appropriate precautions were undertaken prior to its use.

3.3 LEACHATE COLLECTION PIPES

The evaluation was undertaken to assess the performance of a proposed leachate drainage system comprising of a 300 mm thick gravel drainage blanket over a CCL. The existing liner was designed to slope towards the north at 3.5% and to the west at 1%. Perforated HDPE leachate collector drainage pipes within trenches run in the gravel drainage blanket layer in an east/west orientation at 120 m centres and north/south at 50 m centres.

The proposed leachate collection system removed from the existing design the north/south collection trenches and pipes. A significant economic saving both in labour and materials would result if the proposed system was adopted.

The current EPA Guideline Benchmark requires leachate pipe separation to be a maximum of 50 m, to achieve a goal of no more than 300 mm of leachate head on the barrier liner layer.

3.3.1 Model Preparation

To model the flow of leachate through the proposed collection system, the Hydrologic Evaluation of Leachate Performance (HELP) computer program, version 3.04 was used.

A HELP program model is generated through the detailing of the landfill's geometry, leachate collection system and material properties. Meteorological data is then input into the program to model leachate flow quantities and resulting leachate head.

3.3.1.1 Weather Data

For the purposes of this assessment, precipitation data of 50 years was obtained from a Bureau of Meteorology weather station located near the landfill site. Additional climatic information, including temperature, solar radiation and evapotranspiration data was also obtained where available.

3.3.1.2 Landfill Geometry

The following assumptions were adopted for the surface profile parameters of the landfill:

- The landfill will be covered with topsoil and a fair stand of grass;
- No capping layers have been constructed;
- The covered surface of the landfill is graded to a slope of 1%
- The surface length over which run-off would travel is 120 m; and
- The fraction of area allowing run-off is 0%.

It should be noted that the model parameters were adopted to provide a 'worst-case' scenario, allowing maximum infiltration of rainfall. Such a landfill profile would determine the potential maximum output of leachate.

Three subsurface landfill profile cases were chosen to be evaluated by the HELP model. All cases included a compacted clay liner of 1000 mm thickness, overlain by a 300mm thick drainage blanket, waste layer and 500 mm cover layer. The three cases varied in waste thickness only. Waste thickness of 11 m, 20 m and 58 m were adopted for proposed minimum, average and maximum waste thickness respectively for Cases 1, 2 and 3.

3.3.1.3 Leachate Flow Path

Once reaching the collection drainage blanket, the maximum distance leachate would need to travel before reaching a collection pipe and drain, would be 130 m. This is based on the 3.5% north/south and 1% east/west grade, and a 120 m drain spacing running east/west.

3.3.2 Results

A summary of the results is included below:

Case	Average Leachate (m^3/year)	Maximum Leachate Head (mm)
1	1738	187
2	1734	145
3	1731	117

The results indicate that the proposed leachate drainage system would limit the maximum head on the CCL to a 'worst-case' of approximately 187 mm, which is below the EPA Guideline goal requirement of 300 mm.

It should be noted that the head of leachate on the liner decreases with increasing waste thickness. This is due to a larger proportion of the precipitation infiltrating through the cover layer being suspended/absorbed within the waste layer.

Actual recorded leachate quantities generated at the landfill indicate approximately 1095 m^3/year is produced and recirculated back into the waste mass. The volumes estimated by the HELP models are significantly greater, as expected, indicating the conservative nature of the parameters adopted.

3.3.3 Comments and Recommendations

On the basis of the results obtained, it appeared that the proposed leachate drainage system was feasible and would satisfy the EPA goal of less than 300 mm leachate head on the barrier liner layer. Based on these results it was suggested that in the circumstances at Elizabeth Drive, the north/south leachate drains at 50 m centres were not warranted.

A case is currently being put forward to the EPA to amend the current landfill design and implement the proposed system.

3.4 EFFECTS OF INCREASED GRAVEL CONTENT ON CLAY LINER PERMEABILITY

An assessment was undertaken on two types of gravelly clay material to assess its suitability in meeting the EPA benchmark techniques.

The EPA requires that the leachate barrier system be designed to contain leachate over the period of time that the waste poses a potential threat to the environment and should be designed and installed in accordance with an approved construction quality assurance program. Should a recompacted or modified soil liner be adopted, the guidelines identify a suitable liner material as having a compacted thickness of at least 900 mm and an insitu coefficient of permeability of less than 10^{-9} m/s.

Currently at Elizabeth Drive Landfill a recompacted soil liner is installed to a thickness of 1000 mm, with the coefficient of permeability exceeding the EPA requirements. This material has been previously validated through extensive laboratory testing, including triaxial cell permeability testing. The construction specification adopted to date for the installation of this material limits the gravel content to 10%. This upper limit was implemented as it is generally difficult to simulate the effects of macro defects, such as potential effects of gravel, on permeability within the limits of laboratory testing techniques.

3.4.1 Proposed Material

Large stockpiles of clay with gravel contents ranging between 10 and 30% have resulted from the selective stockpiling of material on the site during the cell excavation process. In order to validate the suitability of this material for use as a liner material, two representative sources of material were selected. Gravel contents for each material selected were 15% (Area A) and 25% (Area B).

3.4.2 Test Method

In order to accurately measure the performance of the proposed clay liner, the use of insitu Sealed Double Ring Infiltrometers (SDRI) was adopted. One testpad for each material selected was constructed under quality assurance procedures and conditions currently used for all clay liner installation at the site. The pads were placed to a compacted

thickness of 1000 mm at a location adjacent to the active landfill cell. The pads were constructed over a subgrade of compacted blast furnace slag covered with geotextile.

One SDRI apparatus was installed within each of the two testpads. Each SDRI apparatus consisted of a 1.5 m diameter internal and 2.5 m diameter external ring. The rings were sealed into each pad using a mix of bentonite and concrete. Clay and sand was placed around the outer circumference of the external ring to minimise potential desiccation.

The inner rings were fitted with an external valve and flexible bladder at a height of 500 mm to allow measurement of the water displaced within the inner ring. The Area A rings (inner and outer) were filled with water to a height of 600 mm. The Area B rings were filled to a height of 1000 mm. Throughout the test the head of water within the outer rings was maintained at 600 mm and 1000 mm respectively by filling from an external source.

To minimise the potential influence of evaporation and direct rainfall, both sets of rings were covered with 15 mm plywood and covered with tarpaulins. To allow estimation of the potential effect of evaporation, a '44' gallon drum was filled to a height of 800 mm and placed beneath the covers of one of the tanks.

Falling head permeability laboratory tests were undertaken in 2 litre moulds to provide a comparison with field testing.

3.4.3 Measurement

To estimate the seepage water into the testpads within the internal ring, weighing of the flexible bladder was undertaken. The valve was sealed and the bag weight determined using electronic scales. The bag was then refilled and reconnected to the valve. Measurement was undertaken initially on a daily basis to ensure that sufficient quantity of water was available within the flexible bladder should high flowrates eventuate. Based on these initial results, it was deemed sufficient to undertake readings every three to four days apart. The tests have been undertaken for approximately 5 months.

It is expected to decommission both infiltrometers once the tests have run for a period of 6 months. This will enable a measurement of the actual wetting front to be undertaken and an accurate indication of permeability made. Ideally the test would run until failure of the apparatus or penetration of the entire liner thickness, however the material requires validation to be used in the current cell construction works.

3.4.4 Draft Results

Laboratory results undertaken on the clay samples have indicated that both materials performed above the EPA benchmark requirements with results in the order of 1×10^{-10} m/s.

Preliminary calculations based on the field results have shown that although the material initially appears to have a marginally higher permeability than recommended, once the initial uptake has occurred, and the wetting front has been established, the seepage reduces. This point occurs after approximately 60 days of measurement for Area A, with no appreciable change for Area B. The coefficient of permeability for Area A appears to stabilise at approximately 1×10^{-9} m/s. The Area B material has a marginally higher permeability coefficient of approximately 5×10^{-9} m/s.

Some reduction in total seepage may need to be made to compensate for evaporation in determination of the final results, although draft results indicate that this may be relatively insignificant.

3.4.5 Discussion

Actual permeability of the material will not be able to be calculated until an accurate measurement of the wetting front is made during the decommissioning phase. However, the results obtained to date indicate that the material used within Area A is generally suitable for use a liner material according to EPA requirements. Area B, with a greater gravel content, appears to have a permeability coefficient marginally above the EPA requirement. As a result it would generally be recommended that the current specification gravel specification limitation be increased from 10% to 20%.

Providing selective sourcing of material and gradings are undertaken, it would be possible to make use of large portions of the stockpiles material for liner construction. Material not meeting the specification requirements should be used for daily cover requirements. An appropriate conformance testing program would need to be implemented to ensure gravel content did not exceed the limits set.

4. DISCUSSION

The purpose of geotechnical investigations, at proposed or current landfill sites, is to assist in the development of landfills in accordance with the NSW EPA Solid Waste Landfill Guidelines. Through interpretation and analysis of the geotechnical investigation results, assessment of the potential to adopt alternative benchmark techniques can be made. Provided that appropriate investigations and analysis

are undertaken, cost effective and environmentally sound solutions to landfill design problems can be developed.

REFERENCES

i *Suitability of Carbonate Aggregate in Landfill Collection Systems*, C. Rubak (PE), J. Stark (PE), W. Upman (PG), M. Stevens (PhD), Waste Management Inc, University of Missouri-Rolla, 25 September 1996

ii *Carbonate Compatibility Study, Progress Report 1* (3 April, 1996) and *Progress Report 2* (16 April, 1997), J.Budiman, S. Farhan, Department of Civil and Structural Architectural Engineering, Illinois Institute of Technology, Chicago, IL

iii *The Long Term Settlement Behaviour of Waste and its Effects on Future Development* M. J. Thom and J Pym 3rd National Hazardous & Solid Waste Convention, Sydney (1996)

iv A suggested methodology for assessing the technical equivalency of GCLs to CCLs, R.M. Koerner and D.E. Daniel, Proceedings International Symposium on Geosynthetic Clay Liners, Nurnberg 1998.

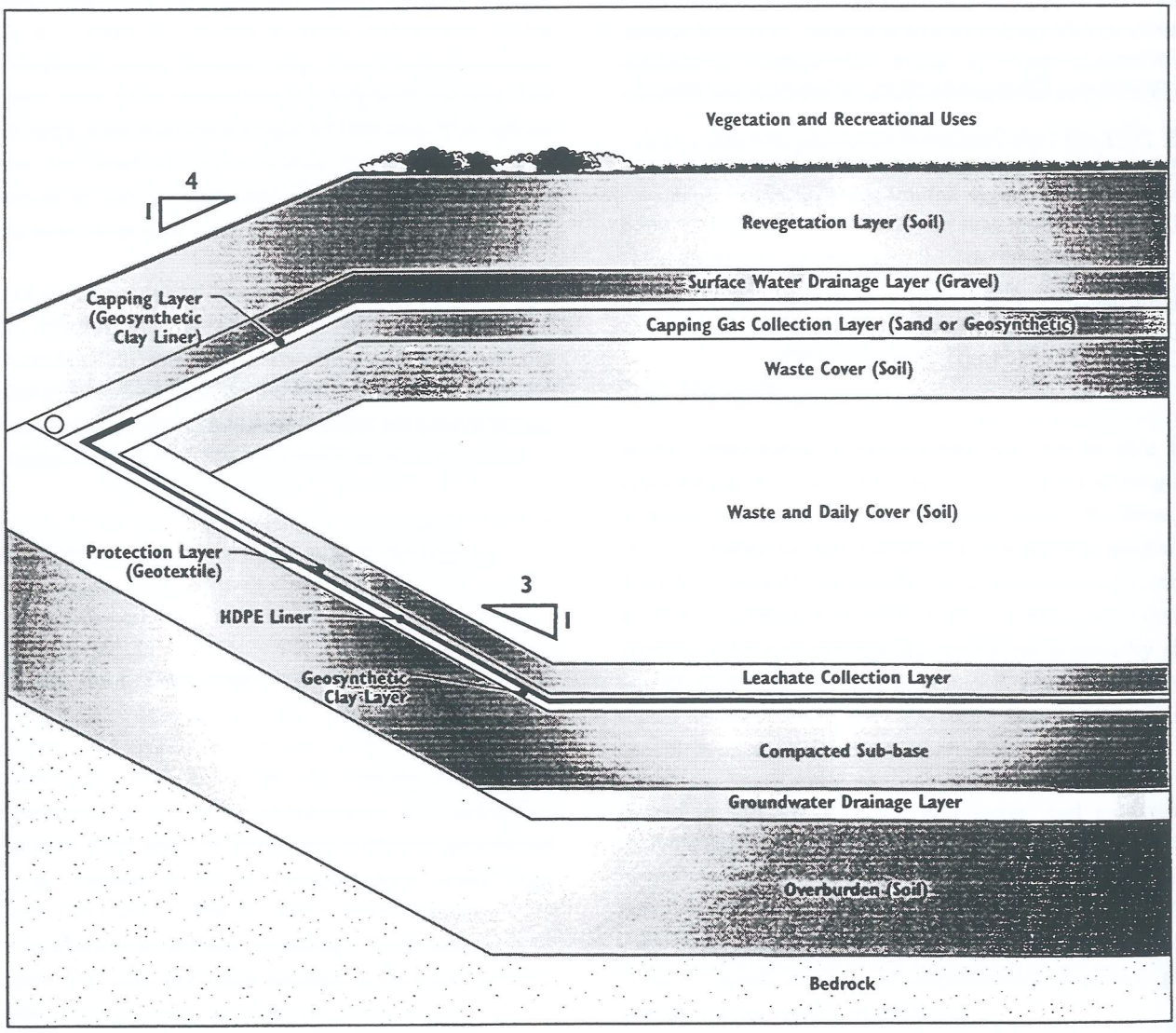

Figure 2.1 Concept Plan for Proposed Landfill

Geotechnical Considerations in Well Casing Design

Eloise Browne-Cooper, Advanced Geomechanics, 4 Leura Street, Nedlands Western Australia, 6009

Summary Offshore well casing must be designed to be not only structurally, but also geotechnically stable in accordance with API or other similar standards. Understanding the interaction of well components with the surrounding sediments is imperative, as it is these sediments that provide the resistance to applied vertical, lateral and torsional loading during both installation and operation of the well. At each stage of construction, from the placing of the temporary guide base to the completion of the well, the surrounding sediments need to resist the loads applied by the self weight of each well component and possible live loadings caused by snagging of any exposed well components or flow lines. The stages of component installation and, most importantly, the geotechnical properties of the surrounding sediments must be fully understood before any loading can be considered.

It has been found that the well and flow line layout also has a significant effect on the governing load combination and careful consideration must be given to possible snag load locations. This paper will outline the different types of geotechnical analyses that must be undertaken for the verification of offshore wells.

1 INTRODUCTION

Offshore well casing is usually completely designed before it is checked for geotechnical stability. Significant changes in the design after this stage would be expensive, so geotechnical stability issues are usually overcome by extending the existing structure (ie. increasing the initial grouted casing length or adding more high torque connectors).

The following geotechnical verifications should be conducted before the well casing design is finalised, and are outlined in this paper.

- Temporary guide base (TGB) stability
- Open hole stability
- Lateral capacity
- Bending induced cracking
- Axial capacity
- Torsional capacity
- Effects of drilling mud

These types of analyses are also relevant for drilled and grouted piles, which are often constructed using well casing in offshore scenarios.

2 WELL CASING INSTALLATION SEQUENCE

Well casing installation consists of several key stages. At each stage, the well components must be supported by the surrounding sediments though the mudmat (or TGB) or the grouted casing (ie. no support is provided by the installation vessel after each component is installed).

A typical well casing installation sequence is outlined (typical casing and drill hole dimensions have been used):

1. Place temporary guide base (TGB).
2. Drill 36" Internal Diameter (ID) hole to a depth of 48 m.
3. Insert 48 m long 30" Outer Diameter (OD) casing and suspend it from TGB.
4. Grout 30" OD casing in the 36" ID hole.
5. Drill a 17½" ID hole through the 30" OD casing to 470 m below mudline.
6. Insert 468 m long $13^3/_8$" OD casing.
7. Grout $13^3/_8$" OD casing in 17½" ID hole.
8. Mount blow-out preventer (BOP).
9. Drill a 12¼" ID hole through the $13^3/_8$" OD casing to an approximate depth below mudline of 2500 m.
10. Insert 2500 m long $9^5/_8$" OD casing.
11. Grout $9^5/_8$" OD casing in 12¼" ID hole.
12. Drill a 8½" ID hole through the $9^5/_8$" OD casing to an approximate depth below mudline of 3400 m.
13. Insert approximately 900 m long 7" OD liner into reservoir.
14. Complete the wellhead.

The geotechnical design of well casing is principally concerned with stages 1 to 7 listed above. A typical installation sequence showing installation stages 1 to 7 is presented on Figure 1.

3 LOADING COMBINATIONS

The loads applied to the well casing change during

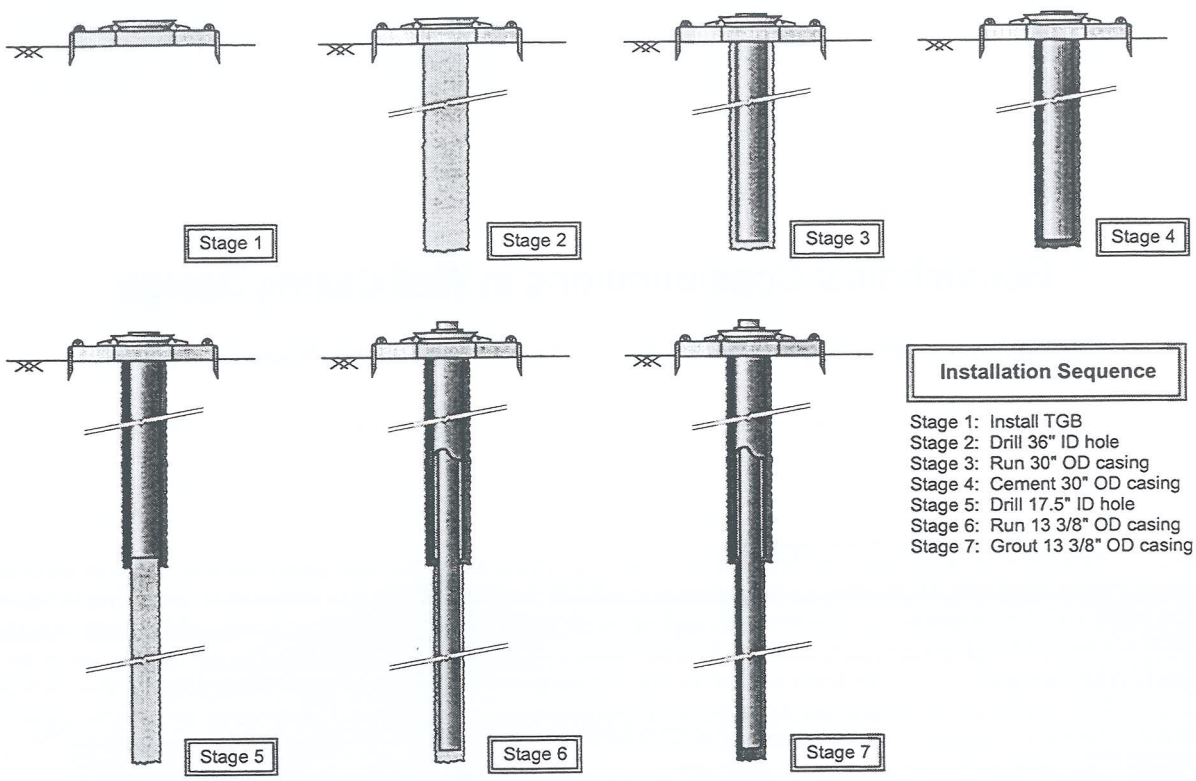

Figure 1: Well casing installation stages

installation and operation. At each stage of installation, the well must support the self weight of its components. Once installed, the well must support its self weight and any possible snag loading.

The loads acting on the well casing are assumed to be static, cyclic loading of the casing is not expected and thus only static loading is usually analysed.

3.1 Axial Loading

The axial loading on the well casing consists of the self weight of the well casing components. During installation this axial load changes, the most critical stages are:

(i) when the hole is initially drilled through the TGB (Stage 2);
(ii) when the TGB supports the ungrouted first casing (Stage 3);
(iii) when the grouted first casing supports the ungrouted second casing (Stage 7); and
(iv) when the grouted second casing supports the rest of the well casing string (Stage 10).

3.2 Snag Loading

Well casings must be designed to withstand an applied snag load, to cover the scenario of a boat anchor or trawling net catching on a well component and the load is often considered to be in the range of 100-200 kN. Snag loading is assumed to be applied as a temporary horizontal load acting at any point of the well-head structure and surrounding flow lines that can be snagged. Usually the worst lateral and torsional loading positions are checked.

3.2.1 Lateral loading

Snag loading of the well head or surrounding flow lines can induce a lateral load and/or a moment acting at the well casing head which must be resisted by the surrounding sediments.

3.2.2 Torsional Loading

Snag loading applied to the well head or surrounding flow lines can cause torsional loading on the well casing that must be resisted by the surrounding sediments. The ability of the flow lines to sustain a snag load needs to be considered. The amount of torsion that can be transferred from the flow line to the well casing depends on the ability of the flow line to transfer torsional loading without yielding.

4 TEMPORARY GUIDE BASE

In well construction, the first sections of casing are suspended from a temporary guide base (TGB). The TGB is usually in the form of a mudmat with a central hole through which the casing is installed. Only axial loads, in the form of the self weight of the TGB and first casing, act on the TGB during installation. Once the first casing is grouted, it supports all further applied loads.

The TGB settlement should be calculated for both touchdown and the stage where the first casing is hung from it (Stage 3). The stability of the TGB sitting over the open drill hole (Stage 2) should also be calculated.

4.1 Geotechnical Parameters for TGB Settlement and Stability

To calculate the TGB settlement and stability with any degree of accuracy, the strength profile of the soil over the top 5 m should be established. The following soil parameters are required for axial load and settlement analysis and TGB stability:

- Effective unit weight.
- Undrained shear strength (cohesive soils), or earth pressure coefficient at rest and interface friction angle (sands) (for calculation of stability at Stage 2).
- Small strain shear modulus.

4.2 Settlement at Touchdown

The touchdown settlement of the TGB is a function of the underlying sediments strength and deformability. The bearing capacity of the TGB must be checked and the associated settlements calculated.

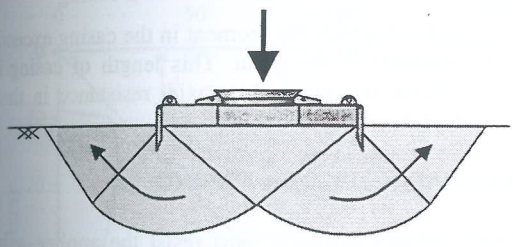

Figure 2: Bearing failure of TGB

4.3 Stability at Stage 2 - Unsupported hole collapse

Before the first segment of casing is installed, the TGB is sitting on an open hole. At this stage, an unsupported hole could collapse due to the weight of the TGB, illustrated in Figure 3. This is of particular importance in uncemented and cohesionless sediments or very soft cohesive sediments.

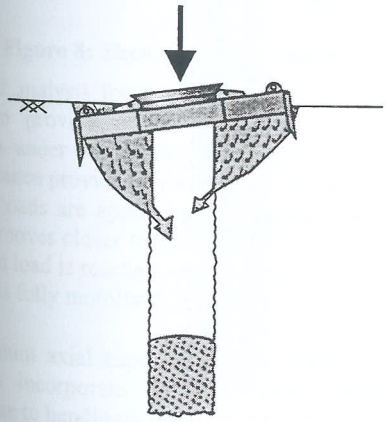

Figure 3: Unsupported hole collapse

When the hole is first drilled, the surrounding soil will respond in an undrained manner, pore water suctions are generated within the soil in response to changes in boundary conditions, such as drilling a hole or applying an external load. While these pore suctions remain, the soil may remain stable. With the passage of time, these may dissipate and hole collapse may occur.

The risk of hole collapse can be minimised by ensuring the time between drilling the hole and installing and grouting the casing is kept to a minimum.

Drilling fluid smeared on the sides of the hole provides a seal between the water and sediment. This assists the sediment by forming suction pressures that remain stable by reducing the pressure differential between the soil and the water in the open hole. The extent of the support, provided by the drilling fluid, is not considered to be reliable under the conditions present in the near surface sediments.

4.4 Stability at Stage 3 - Ungrouted First Casing

After the first casing is installed (before grouting), the TGB must support the casing self weight, and at this stage further settlement of the TGB is anticipated. The empty annulus between the casing and the hole is also susceptible to hole collapse, with the sediments collapsing into the annulus. This type of collapse is not serious as the grout pressures are usually high enough to push the collapsed sediments back into place, but it could lead to larger settlement of the TGB.

5 LATERAL CAPACITY OF A CASING

The capacity of the casing to resist lateral loads is dependent on the lateral resistance provided by the near surface sediments, shown schematically in Figure 4. The casing resistance to the lateral loading typically affects only the top 20 diameters of casing, whereas the first casing string is usually over 45 diameters long. This depends on the load size and the lateral resistance provided by the sediment.

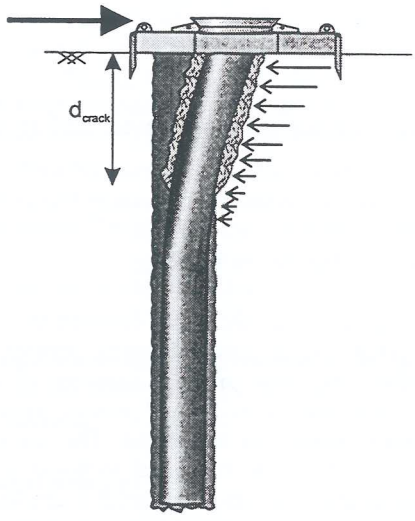

Figure 4: Lateral load on casing

5.1 Geotechnical Parameters for Lateral Analysis

The accuracy of the analysis depends on the definition of the ultimate lateral soil resistance, p_{ult}, and the shape of the p-y curves. The following soil parameters are required for lateral analysis:

- Effective unit weight.
- Undrained shear strength (cohesive soils), or earth pressure coefficient at rest and interface friction angle (sands).
- Shear modulus.
- The strain corresponding to one half the maximum principal stress difference in a laboratory compression test.

5.2 Lateral Analysis

The ability of the well casing assembly to resist a horizontal snag load can be analysed using a computer program such as LPILE[1]. This program allows for differential rotation and lateral displacement of the grouted casing along its length, and includes appropriate modelling of the sediment behaviour using lateral load/displacement (p-y) curves.

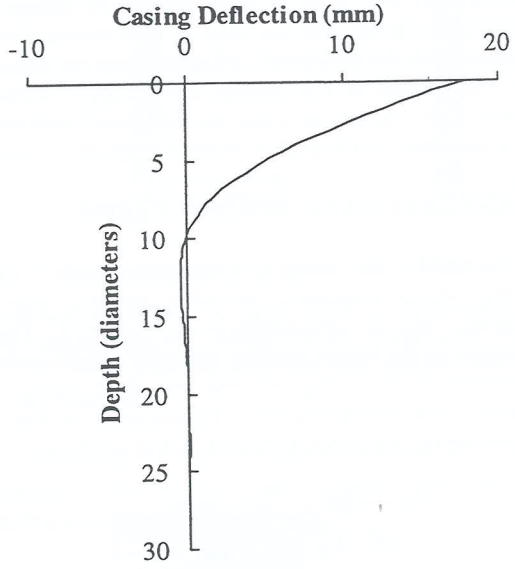

Figure 5: Casing deflection under lateral loading

A typical casing-head deflection curve for well casing in a low strength cohesive sediment is shown in Figure 5.

5.3 Grout cracking due to bending

Lateral loading can cause the grout between the casing and the soil to crack due to tensile bending stresses. This can adversely affect the shear transfer capacity of the casing (axially and torsionally) over this section, resulting in a reduced overall capacity of the casing. The cracking of the grout is accounted for in axial and torsional analyses by assuming the length over which the grout is cracked has zero shear transfer capacity in axial and torsional analysis.

The depth to which grout cracking may occur due to bending, caused by lateral loading of the casing, can be calculated by determining the curvature at which the tensile cracking strain exceeds the tensile cracking strain of the grout.

Figure 6 shows the distribution of moment down the casing under an applied snag load and the maximum cracking moment of the grout. The grout is assumed to be cracked over

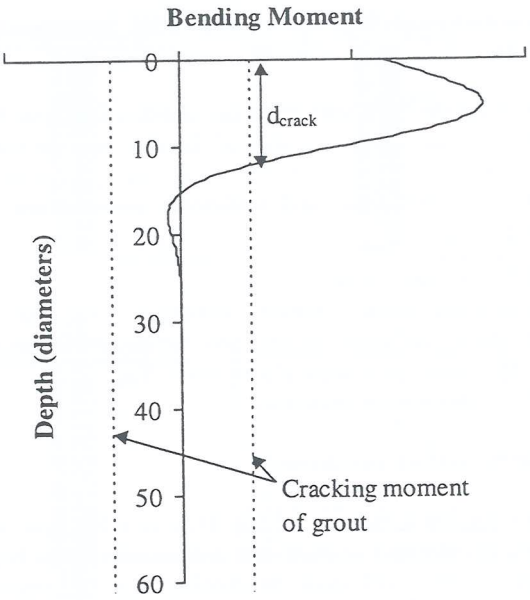

Figure 6: Distribution of moments down casing

a length d_{crack}, above which the moment in the casing exceeds the cracking moment of the grout. This length of casing is assumed to provide no torsional or axial resistance in their respective analyses.

6 AXIAL CAPACITY OF A CASING

The casing/grout-soil interface must resist the applied axial load by transferring the load from the casing to the soil, shown schematically in Figure 7.

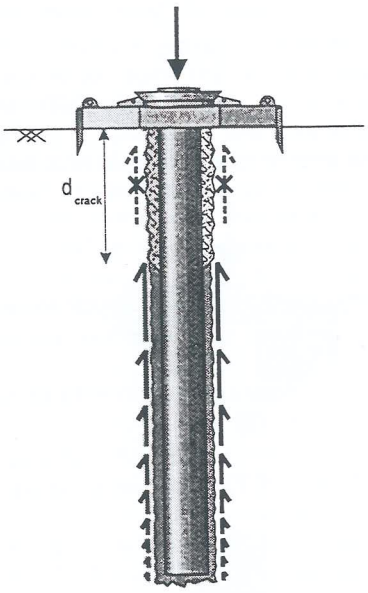

Figure 7: Axial loading on casing

6.1 Geotechnical Parameters for Axial Analysis

The geotechnical parameters required for axial analysis are:

- Undrained shear strength (cohesive soils), or coefficient earth pressure at rest and interface friction angle (sands).
- Peak shaft friction.
- Small strain shear modulus.

- Residual shear stress.
- Displacement to residual shear stress.

These parameters define the axial response of the soil-casing interface.

6.2 Axial Analysis

The axial resistance to each axial loading stage can be estimated using a non-linear, axial load transfer program such as RATZ[2]. This program treats the casing as an elastic bar, with properties that may vary along the length. Interaction with the soil is characterised by discrete, non-linear springs that are distributed at regular intervals along the embedded section of the casing. The t-z curve is a function that relates the local shaft friction at the casing-soil interface to the current casing displacement, taking account of the previous displacement history. The shape of this curve strongly depends on the geotechnical parameters input into the analysis.

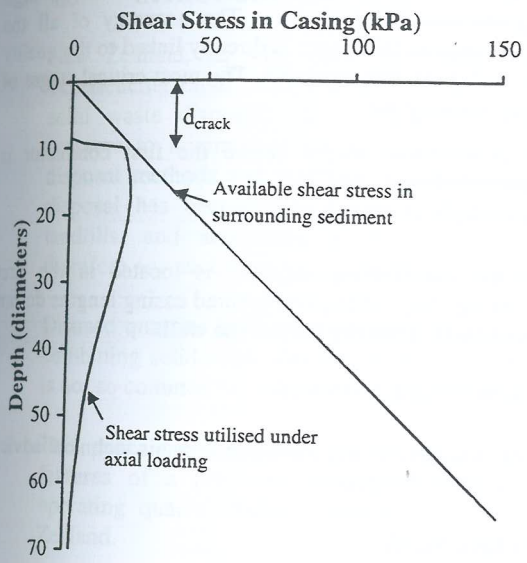

Figure 8: Shear Stress in casing

In the axial analysis for the well casing, the length d_{crack}, is assumed to provide no axial resistance. A shear stress distribution under an applied axial load, and the available shear resistance provided by the soil, is presented in Figure 8. As higher loads are applied to the casing, the utilised shear stress line moves closer to the available shear stress line until a maximum load is reached where the available shear strength of the soil is fully mobilised.

The maximum axial capacity of the casing should be high enough to incorporate the detrimental effects of grout cracking due to bending/torsion (Section 5.3) and the possible reduction of axial capacity due to the type of drilling mud used (Section 9).

6.3 Casing-Grout Shear Transfer

Shear transfer keys or weld beads may be required to transfer the axial load from the steel casing to the surrounding grout. Shear transfer keys are required in the regions of the casing where the shear stress distribution induced by the applied axial load exceeds the shear transfer capacity of the steel-grout bond.

7 TORSIONAL CAPACITY OF A CASING

The torsional response of the casing is analysed by considering the remaining shaft friction available for mobilisation after allowance is made for the shaft friction, which has already been mobilised under axial loading, shown schematically in Figure 9.

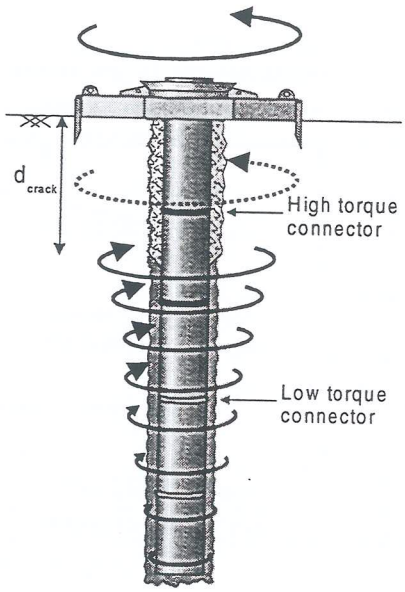

Figure 9: Torsional load on casing

The connectors used to join the lengths of casing can be normal "low torque" connectors (not capable of transferring significant torque) or "high torque" connectors (that are capable of transferring torque to the next length of casing). These high torque connectors are relatively expensive and it is preferential to use the minimum number of connectors possible in well design.

7.1 Geotechnical Parameters for Torsional Analysis

The following soil parameters are required for the torsional analysis:

- Undrained shear strength (cohesive soils), or coefficient earth pressure at rest and interface friction angle (sands).
- Shear modulus.

7.2 Torsional Analysis

Torsion applied to the casing at the seabed is transmitted down the casing, gradually decreasing with depth, as the torsion is dissipated into the soil by circumferential shear stresses resisting the casing motion. Any torsional transfer capacity of the grout, surrounding the casing, is considered to be minimal and is ignored in the torsional analysis.

The torsional resistance of the casing-soil interface can be analysed using a non-linear torsional load transfer computer program. The axial load transfer computer program RATZ[2]

can also be used to analyse torsionally loaded piles by using an equivalent set of torsional parameters in place of the standard axial parameters (this approach has been validated by the author of RATZ[2]).

Figure 10 shows the distribution of torque down a typical casing in weak, cohesive sediment. The torsional transfer capacity of a normal "low-torque" connector is shown, and in this case, high torque connectors between casing segments are required to a depth of about 20 diameters. Casing segments are typically 9-12 m long, and under the applied load, the casing would require 1-2 high torque connectors.

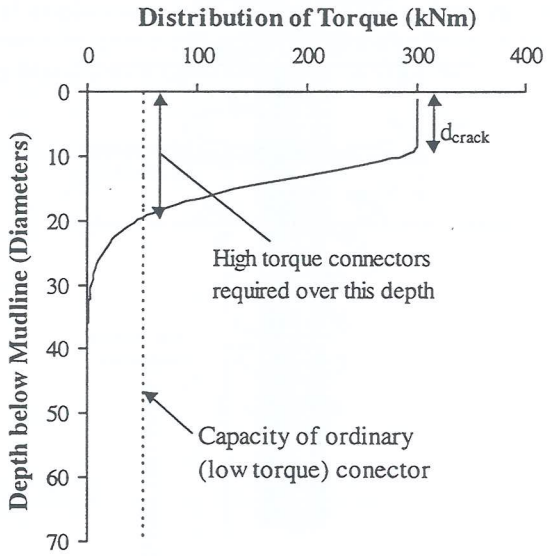

Figure10: Distribution of torsion down pile

8 THERMAL LOADING ON CASING DUE TO GROUT SETTING

As the grout around the casing sets, the temperature in the grout and the casing will rise. During this time, the steel casing will expand. As the grout cools to the ambient temperature, the casing will contract again. This expansion and contraction of the steel casing is known as thermal straining. These thermal strains can lock in residual stresses at the casing-soil interface, which should be incorporated into casing capacity analyses.

Thermal strain can be incorporated into the axial analysis as a loading cycle that is applied before the static axial load (ie. the dead weight of the next casing). Typical temperature changes of approximately 35°C can be expected in the casing due to grout setting.

9 EFFECTS OF DRILLING MUD

The type of drilling fluid (drilling mud) used in the creation of the hole for the casing can affect the shaft friction on the grout/soil interface. Drilling mud smears along the sides of the hole wall during the course of drilling, and even flushing the hole with water cannot guarantee removal of all mud.

Eide and Aas[3] suggest bentonite drilling mud can reduce the effective shaft friction between a grout and sediment by up to 25%. This can be accounted for conservatively by decreasing the peak axial capacity of the casing by 25% if bentonite drilling mud is used in the well construction.

10 GROUT COVERAGE

The consistency of the grout is relatively liquid to assist with workability. Excess grout is pumped into the annulus between the soil and casing until grout return is observed at the top of the casing. The effect of hole collapse around the casing may inhibit some grout coverage over the top section of the casing. This section is usually assumed to have no load transfer capacity due to cracking under lateral loading, and therefore the extent of grout coverage over this section is not considered critical.

11 CONCLUSION

Optimisation of well casing design is dependent on high quality geotechnical information. The accuracy of all the analyses outlined in this paper is directly linked to the quality of the geotechnical data available. The most critical stages of well casing stability are:

- The construction stages before the first conductor is grouted; and
- The application of snag loading.

Most of the load-bearing capacity is located in the first grouted casing. Any subsequent grouted casing lengths do not significantly add to the capacity of the well.

12 ACKNOWLEDGMENTS

Ian Finnie is gratefully acknowledged for his technical advice in the creation of this paper.

13 REFERENCES

1. Ensoft Inc, "LPILE for Windows", 1994.

2. RANDOLPH, M.F., "RATZ User Manual", 1994.

3. Aas, G. and Eide, O. "Special Application of Cast-in-place Walls for Tunnels in Soft Clay in Oslo", Proc. 5th European Conference on Soil Mechanics and Foundation Engineering. Madrid, 1972, pp 63-74.

Geotechnical Features of Tirohia Quarry Landfill

TONY DAVIES
Worley Consultants Ltd.
Auckland, New Zealand

Summary

At Tirohia Quarry, seven kilometers south of Paeroa, New Zealand, andesite rock is quarried for commercial aggregate use. The quarry owner proposes to construct a modern sanitary landfill at the site, filling the pit with 800,000 tonnes of municipal refuse while quarrying continues. The main issues considered while investigating the suitability of converting the quarry to a landfill included the effect of quarrying on the landfill liner (potential blasting/vibration effects), and the effect of leachate escape on the regional groundwater system.

1.0 INTRODUCTION

New Zealand, as with most developed countries, is experiencing rapid change in the business of municipal solid waste disposal. In a climate of considerable pressure to minimise waste and develop non–polluting disposal methods and facilities, waste management and disposal has become big business. Sites suitable for landfills, and acceptable to the public, are scarce, therefore any such sites are a valuable economic resource.

Disused quarries have a long history of use as landfills: combining solid waste disposal with an operating quarry is not so common but has obvious commercial benefits.

This paper presents some geological and geotechnical features of a proposed municipal landfill site at an operating quarry, 100km southeast of Auckland, New Zealand.

It is proposed to fill the existing quarry pit with non-hazardous municipal solid waste (approximately 800,000 tonnes of refuse) whilst quarrying continues.

The design of the landfill is based on best practice standards currently accepted in New Zealand and overseas as appropriate for municipal solid waste disposal.

2.0 SITE DESCRIPTION

Tirohia Quarry is situated on the north western end of a prominant spur protruding into the Hauraki Plains from the western side of the Coromandel-Kaimai Range (Figure 1). This spur has steep sides and a relief of approximately 300m.

The geological map of the area indicates that development of the spur most likely resulted from movement on faults that bound the spur along its northern and western margins.

Quarrying has resulted in the formation of a narrow valley, opening to the north, that is bounded by (i) the currently operating 70m high eastern highwall, (ii) a steep, benched slope at the head (southern end) of the valley, (iii) a remnant ridge to the west. The remnant ridge forms a barrier between the quarry and the terrace flats and Hauraki Plains to the west.

The western slope of the ridge is moderately steep and is covered by quarry waste (strippings) placed during the early stages of quarrying. The toe of the slope merges with the very gently sloping terrace flats, which in turn merge westward with the Hauraki Plains.

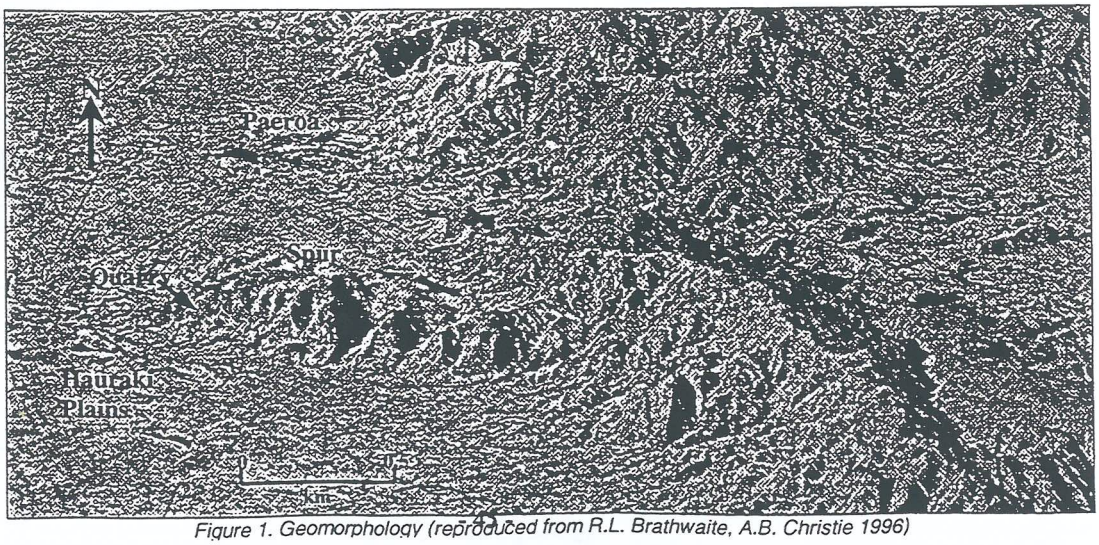

Figure 1. Geomorphology (reproduced from R.L. Brathwaite, A.B. Christie 1996)

2.1 Geology

The quarry is situated in complex volcanic terrain of Late Miocene and Pliocene age (i.e. 5 to 8 million years). The Hauraki Plains to the west of the ranges are underlain by Quaternary age, volcanic-derived fluvial sediments, peat, and primary volcanic deposits (pyroclastic flows and airfall ash) which infill the active Hauraki rift. The Waihi Basin to the east of the site contains deposits of Pliocene to early Pleistocene pyroclastics (e.g. ignimbrite) and fluvial (river) and lacustrine (lake) sediments.

Brathwaite and Christie (1996) map the andesite lava flows exposed at the quarry as Tirohia andesite, an informal member of the Kapukapu Andesite formation of mid-Miocene age (7 million years). Kapukapu Andesite consists predominantly of tuff breccias, tuff and andesite flows, estimated to be in the order of 800m in thickness.

The Tirohia andesite member is reported to be not generally hydrothermally altered and is interpreted as mostly intrusive, forming domes (Brathwaite and Christie 1996).

The Pleistocene age alluvial sediments underlying the western terrace consist mainly of undifferentiated, volcanic-derived sediments.

The western terrace and ridges surrounding the quarry have a variable cover of weathered andesitic and rhyolitic volcanic ash. The ash is thought to be an accumulation of many separate eruptive events originating in the Taupo Volcanic Zone.

2.2 Subsurface Conditions

The geology of the site is dominated by a considerable thickness of jointed, andesite lava flow underlain by a dome-shaped body of andesitic breccia that is also interpreted to be of considerable thickness (Figure 2). An upper breccia unit identified in drillholes overlies the andesite lava flow to the east of the quarry. The upper breccia is overlain by tuff breccia and, in places by thin andesite flows.

The andesite lava is fresh to slightly weathered, moderately strong, jointed rock. The andesite is the rock quarried for construction aggregates. The andesite forms a distinctive columnar jointing pattern as it cools from the molten lava state. Jointing is pervasive and is the rockmass property that to a large degree determines its bulk permeability.

The joints in the andesite form two prominent sets:

- Sub-vertical set that forms near vertical columns up to 20m long
- Sub-horizontal set forming flat plates between the sub-vertical joints.

At the southern end of the quarry, joint patterns are less regular, with convoluted and radiating columns indicating a possible sub aerial extrusion.

The breccia is a weak rock comprising andesite and rhyolite fragments to one metre diameter set in a poorly welded, coarse grained glassy matrix. Jointing is not common although closely spaced fractures were observed in zones up to 1m in thickness. The degree of welding in the matrix is variable, ranging from weakly welded to strongly welded.

Contact between the andesite lava and the underlying breccia dome is marked by a zone of alteration in the breccia between 1m and 4m in thickness. The zone is interpreted to result from heating of the breccia on contact with intruding lava. The zone is characterised by an increased degree of welding and a resulting decrease in permeability, compared to the unaltered breccia.

3.0 HYDROGEOLOGY

3.1 General Setting

Groundwater recharge and movement is controlled to a significant extent by the spur. Regional surface and groundwater flow is from the range westward to the plains, the latter being a major groundwater discharge zone characterised by swamps and peat growth. The regional westward flow pattern is affected locally by topographic features such as hills and valleys.

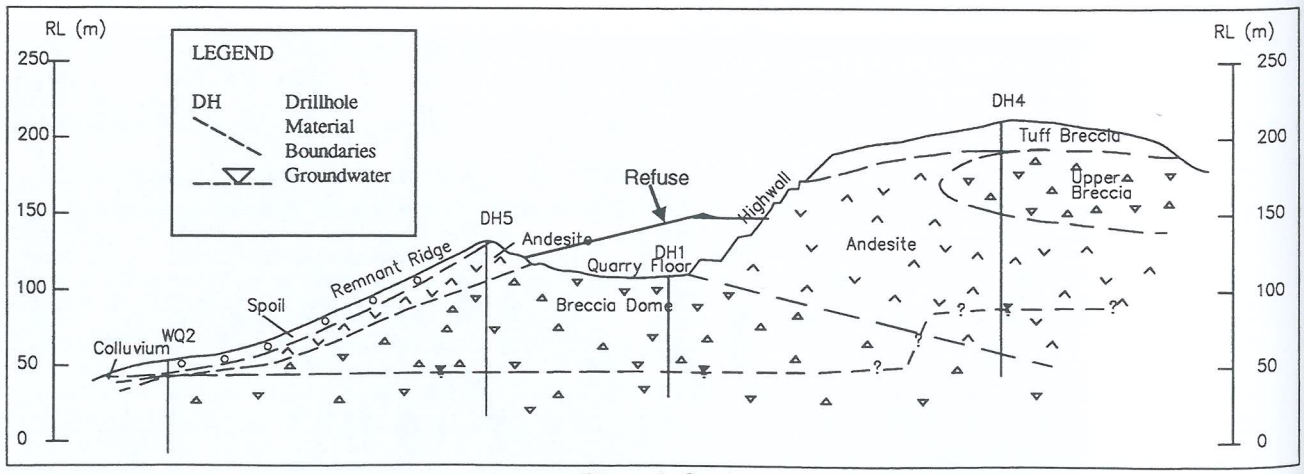

Figure 2. Section

In the vicinity of the landfill site shallow and moderately deep groundwater is likely to derive from rainfall on the spur while water at greater depth may include a small contribution from regional flow originating on the range.

Surface drainage off the spur is mainly via entrenched, steep-sided, ephemeral streams that flow to the north and south around the quarry. The streams have steep gradients and include waterfalls. Permanent flow in the Owhakatina Stream is recorded only near the western side of the quarry where it encounters the low land of the terrace flats west of the remnant ridge. The flow in the shallowly incised streams that rise on the terrace flats is likely to be dominated by discharging groundwater.

3.2 Water Level Measurements

Static water level data indicate that groundwater level is approximately 60m below the floor of the quarry and that groundwater flow direction is towards the northwest (Figure 3). The water table nears ground surface along the toe of the western flank of the remnant ridge, i.e. in the transition zone to the terrace flat. The shallowly incised, ephemeral streams on the terrace also rise in that area, suggesting groundwater close to the surface.

The data indicate that the streams that drain the high ground east of the quarry are ephemeral. The stream beds are essentially 'perched' above groundwater level for much of their length.

3.3 Hydraulic Conductivity of Main Lithological Units

The hydraulic conductivity of materials is an important parameter in landfill liner and cover design as it defines the rate at which fluid moves through the material.

The hydraulic conductivity (K) is dependent on the nature of both the material and the fluid passing through it. A high hydraulic conductivity (e.g. those of sand/gravel and fractured rock) implies high flow rates while low values (e.g. those of clay and solid rock) indicate low rates.

3.4 Breccia.

The landfill site is underlain in part by a dome-shaped breccia layer in excess of 80m in thickness. The breccia has a hydraulic conductivity that is assessed to be greater (i.e. allows water to flow through it more easily) than the surrounding andesite.

The breccia generally has few fractures (joints) but at depth contains narrow fractured zones and sections where the matrix is poorly welded. The measured laboratory permeability of a section of drill core is 1.1×10^{-6} m/s.

While drilling through the andesite (i.e. DH5) it was observed that as drillholes were advanced, relatively static drilling fluid levels were recorded.

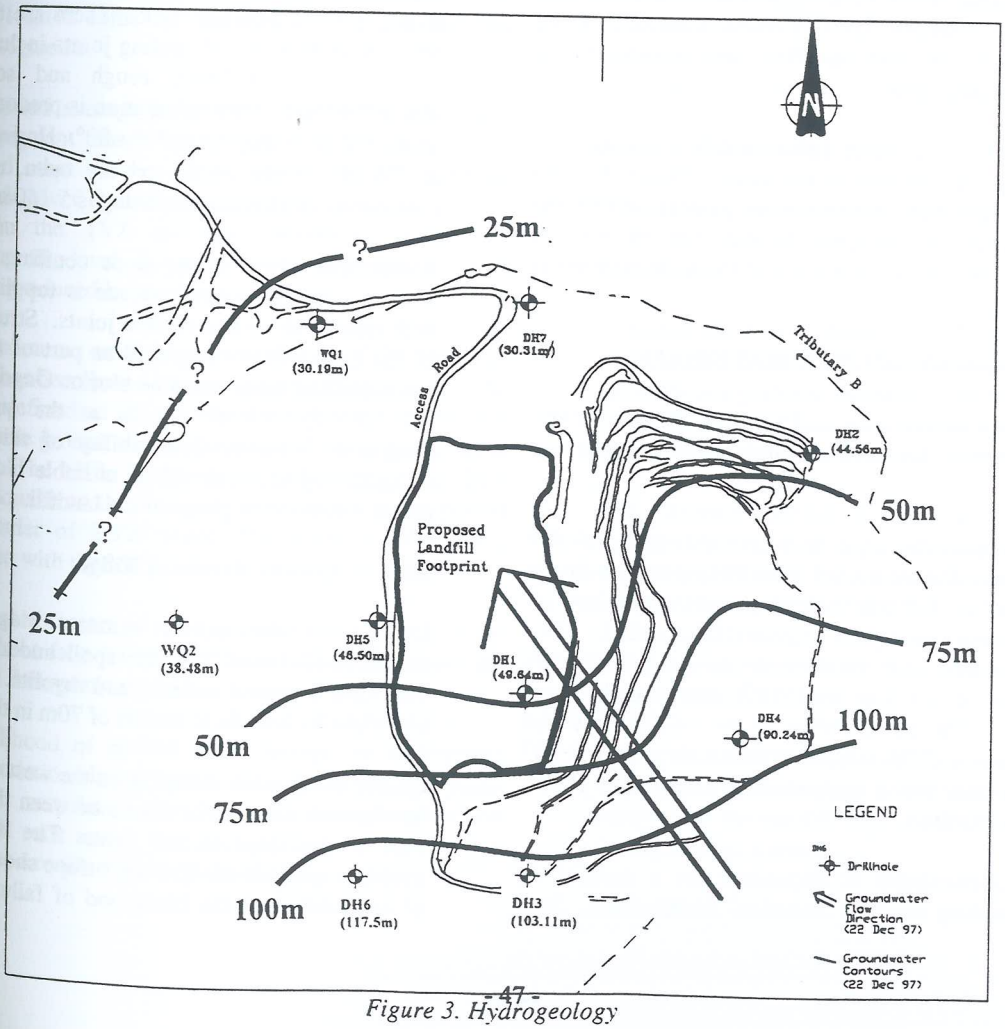

Figure 3. Hydrogeology

However, once the breccia was encountered, and the upper altered crust of the breccia penetrated, drilling fluids quickly drained and static levels did not occur again until deep groundwater was encountered. Shallow piezometers installed to intersect groundwater above the breccia remained dry after installation.

Falling head field tests in the unaltered breccia indicate a hydraulic conductivity of 1 X 10^{-6} m/s. Testing in the altered andesite/breccia contact zone indictae a much lower hydraulic conductivity of 8 X 10^{-9} m/s.

3.5 Andesite

The andesite is blocky with fractures (joints) both sub-vertically and sub-horizontally. The sub-horizontal fractures appear to be tight and therefore are considered to provide minimal permeability. Falling head field tests in the andesite range from 2 x 10^{-8} to 8 x 10^{-10} m/s.

3.6 Groundwater Flow

An understanding of groundwater flow direction assists in assessing potential effects that may arise in the event of seepage from the landfill site.

There are no groundwater users within 2km of the quarry at present, although groundwater may be utilised at some future time. Any leachate which seeps through the landfill liner system will move with groundwater in a north/north-westerly direction towards the installed monitoring wells (Figure 3). The assessed seepage rate of leachate is minimal and its effect on groundwater is expected to be negligible.

Groundwater levels indicate a steep gradient between the southern ridge and the base of the quarry (Figure 4). The steepening of gradients appears to be associated with the transition from the andesite to the breccia and in particular, to the zone of alteration at the andesite/breccia contact.

4.0 LINER AND COVER MATERIALS

The suitability of the near surface deposits of volcanic ash and colluvium for liner and daily cover material was investigated.

Testing indicated the colluvium was the most suitable liner material. The measured laboratory permeability of the colluvium is 10^{-10} m/s using deionised water, and 10^{-8} m/s using leachate from a municipal landfill. This compares to liner and final cover design permeability requirements of not less than 10^{-9} m/s and 10^{-7} m/s respectively. The permeability of the colluvium tested using leachate, and the ash using water, do not meet 10^{-9} m/s requirement and a supplementary synthetic HDPE liner will be required.

Soil liner permeability is dependent on a number of factors including leachate chemical composition, liner soil fabric and liner protection during landfill construction and operation.

Leachate chemicals can affect permeability by solutioning and precipitating soil minerals and by clay particle flocculation, dispersion and swelling. Testing completed for this assessment classified the colluvium as non-dispersive. The chemical composition of the leachate was not determined, however a published study (Qasim and Chaing 1994) indicates that acids can cause dissolution of kaolinite which is abundant in the colluvium (IGNS, 1997).

5.0 SLOPE STABILITY

The long-term security of the landfill requires that the landfill site and surrounding slopes are stable. The assessment of landfill slopes is based on an analytical approach, which considers both static and seismic load conditions.

5.1 Quarry Highwall

Between 20m and 40m of tuff breccia overlies andesite in the quarry highwall. Existing vertical cut slopes up to 10m high show minor spall type failures. Spall debris is contained on benches at the base of slopes and does not present a significant hazard. The ongoing use of benches is proposed to mitigate this type of instability.

The lower half of the quarry highwall comprises very strong, jointed andesite rock. There are two main joint sets. A vertical set of cooling joints includes joints that are continuous (20m+), rough and some are iron stained/infilled. Joint orientation is predominantly to the south and west dipping at 70° - 80°. Horizontal joints dip at 5°- 10° to the north and are open, tight, irregular, continuous (5-10m), and spacing is 5 - 50 mm.

Assessment of the lower slope confirms that the most likely instability in the andesite is toppling-type failure with release along the vertical joints. Structural mapping of the quarry face completed as part of this assessment has identified some unstable blocks. Ongoing observation will identify unstable blocks as the quarry operation progresses. Potential instability of this type will be mitigated by the removal of unstable blocks during the initial construction phase of the landfill.

5.2 Quarry Remnant Ridge

Drilling in the quarry remnant ridge (west side) encountered 5m of andesite spoil underlain by 35m of very hard fractured andesite and rhyolite. The andesite is underlain by breccia in excess of 70m in thickness.

Quarry overburden dumping on the west side of the ridge has formed a wedge of debris between the ridge and the base of the slope to the west. The debris comprises boulders and gravel. The west slope showed no evidence of instability and the likelihood of failure is considered

very low. In the unlikely event that instability did occur it would have no effect on the stability of the landfill.

The remainder of the ridge, including the east side, comprises competent andesitic rock which will contain the landfill. Instability in this material is not expected.

5.3 Quarry Floor

The quarry floor steps down from south to north in floors approximately 10m (vertical) apart and is underlain by very strong andesitic lava and welded breccia. These materials represent competent bedrock. No existing or potential instability has been identified in the quarry floor.

6.0 Earthquake Effects

The site is distinct from the main seismic region of New Zealand in an area of relatively low seismicity. It is situated on the western side of the Coromandel Volcanic Zone (CVZ). There is no evidence of active faulting in the CVZ that would have a significant effect on the site. Immediately to the west is the Hauraki Rift, which extends from Whangarei, through the Hauraki Gulf and the Hauraki depression into the Taupo Volcanic Zone (TVZ). The rift consists of a set of fault-angle depressions.

The most significant known fault associated with the rift is the Kerepehi Fault, which is known to be active. The fault is located some 5.5 km west of the site and has several segments.

The assessed average recurrence interval for movement on the segment closest to the site is 2,500 years. It is estimated that such a movement could generate magnitude Mw 6.9 earthquakes (Figure 7).
Faults in the TVZ are not considered capable of producing the level of ground shaking at the site that could be produced by the Kerepehi Fault.

The maximum credible earthquake (MCE) level of shaking has been based on a deterministic approach. The MCE is defined as the earthquake that would cause the most severe ground shaking capable of being produced at the site. The MCE is associated with a magnitude Mw 6.9 earthquake on the Kerepehi Fault with a return period of the order of 2,500 years. The duration of shaking associated with the MCE is in the order of 20 seconds.

The assessed factors of safety against slope failure of the landfill front face for the 450 year and MCE events are 1.2 and 1.0 respectively.

The likelihood of landfill liner damage by differential liner foundation displacement as a result of earthquake faulting is very low. The liner will be constructed on competent rock and is therefore unlikely to sustain any damage as a result of earthquake shaking.

6.1 Blasting Effects

It is proposed to continue quarry activities while operating the proposed Tirohia landfill. Quarry blasting activities will be within 150m to 200m of the landfill operation and will induce ground vibrations.

Vibrations induced by blasting are different to those associated with earthquakes. The most significant difference is the duration of shaking. The duration of strong shaking associated with blasting vibrations is about 1 second and compares to the duration of strong shaking associated with the site MCE of 20 to 30 seconds. Consequently, the potential effects of blasting are considerably less than those associated with earthquakes.

The assessment indicates critical peak particle velocities of 83mm/s and 44mm/s for the quarry east and south faces respectively and 55mm/s for the landfill front face. All but one of the peak particle velocities actually measured while blasting at the site were less than the assessed critical peak velocity values. The exception was for a blast measured at a distance of 50m. Future quarry blasting is estimated to occur at a distance of 150m to 200m from the landfill and at this distance the peak particle velocities are likely to be less than 20mm/s (i.e. much less than the critical values).

The effect of blasting on the landfill liner is not expected to be significant. The only mechanism by which the liner could be damaged is if differential movements were induced in the underlying rock mass. This is not expected to occur since the liner will be constructed on competent rock and is confined by the overlying landfill mass.

7.0 CONCLUSIONS

The existing quarry site is underlain by a sequence of andesitic volcanic materials comprising breccia, tuff and lava flows.

Groundwater flow is from the high ground of the spur to the Hauraki Plains. In the vicinity of the quarry the groundwater gradient increases from the low permeability andesite lava to the higher permeability materials of the lower part of the breccia dome.

Site colluvium and ash materials as tested do not satisfy the maximum allowable permeability design requirement for the landfill liner and a supplementary synthetic HDPE liner will be required. Colluvium and ash materials tested are of suitable quality and present in sufficient quantity to satisfy the requirement for final cover and daily cover for the proposed landfill.

Quarry and landfill slope stability under static and seismic (earthquake and blasting) conditions is acceptable. The integrity of the landfill liner is expected to be maintained during seismic events.

The geological, hydrogeological, geotechnical and seismic investigations indicate that the Tirohia Quarry site is suitable for the development and operation of the proposed sanitary landfill.

REFERENCES

Engineering Geology 1998, Tirohia Landfill, Seismic Hazard and Blasting Vibrations.

Adams, R.D., Muir, M.G., Kean, R.J., 1972: "Te Aroha Earthquake, 9th January, 1972." Bulletin of the NZ National Society for Earthquake Engineering 5: pp54-58

Institute of Geological and Nuclear Sciences Ltd, 1998 XRD analysis of Tirohia Clays

Qasim, S.R. and Chaing, W., 1994: "Sanitory Leachate - Generation, Control and Treatment", Techtonic Publishing Co. Inc USA

R.L. Brathwaite, A.B. Christie (1996). Geology of the Waihi Area. IGNS Geological Map 21.

Worley 1998, Assessment of Environmental Effects, Proposed Tirohia Landfill.

Uplift Capacity of Suction Caissons

Weimin Deng BE MIEAust CPEng
Centre for Geotechnical Research, The University of Sydney

Summary: Prediction of the uplift capacity of suction caissons is a critical issue facing design engineers and rational methods are required in order to produce reliable designs. Extensive theoretical investigations have been carried out of suction caissons subjected to vertical or inclined uplift loading for cases where the behaviour of the seabed soil is undrained, partially drained or drained. A brief literature review on foundations subjected to combined loading is included. Different analytical design models are discussed. Simplified methods for the estimation of the uplift capacity are described, based on the results of the finite element study. The simplified methods are then validated by upper bound theoretical solutions and experiment results. The expressions developed in this paper take into account the influence of the aspect ratio of the caisson, the point of application and angle of inclination of the loading, the undrained shear strength of the soil, the soil permeability and load rate.

1 INTRODUCTION

Compliant offshore structures, like mooring systems and tension leg platforms (TLPs), are usually subjected to considerable uplift forces. These structures require foundations that can anchor them to competent strata and it has been common in the past to use piles to provide such a foundation. However, there are some construction difficulties associated with the installation of the long piles usually necessary, particularly in large depths of water and in some soil type. Largely because of these difficulties a new type of foundation, the suction caisson, has been developed and used to provide uplift resistance, depending on the in situ conditions. A suction caisson, open at the bottom and closed at the top, is designed to penetrate to the sea floor by its own weight and sometimes by also creating an inside under-pressure relative to the outside water pressure. The latter is known as the active suction installation method. As soon as there is any tendency to pullout movement, the suction caisson mobilises significant pullout capacity through the development of negative pore water pressure inside the soil plug and at the bottom of the caisson. This is known as the passive suction condition. The main advantages of suction caissons over tension piles are: the ease of installation of the caissons with the active suction arrangement; the mobilization of passive suction forces at the caisson's bottom during uplift; and the possibility of placing additional ballast on the large diameter sealed top to provide increased pullout capacity. To date, the geometry of suction caissons has tended to involve relatively low aspect ratios, with length less than 3 times the diameter.

The main focus of this paper is on a) suction caissons subjected to vertical uplift loading for cases where the behaviour of the seabed soil is undrained, partially drained or drained, and b) suction caissons subjected to inclined uplift loading for cases where the behaviour of the seabed soil is undrained. The two cases are illustrated in Fig.1. The soil types assumed in this investigation are normally consolidated to lightly over-consolidated cohesive soils.

The theoretical investigations described in this paper have been carried out using a 3-D semi-analytical finite element approach (Taiebat, 1999) incorporated in the software package AFENA (Carter et al., 1995). Simplified prediction methods were developed based on the finite element results. Predictions of the ultimate capacity by the simplified methods have been compared to those obtained independently from upper bound techniques (Randolph et al, 1998) and experimental measurements in 76 individual tests from 12 independent studies. The solutions developed in this study are both for quasi-horizontal and quasi-vertical loading. The developed expressions have also taken into account the influence of the aspect ratio of the caisson, the point of application and angle of inclination of the loading, the undrained shear strength of the soil, the soil permeability and the loading rate.

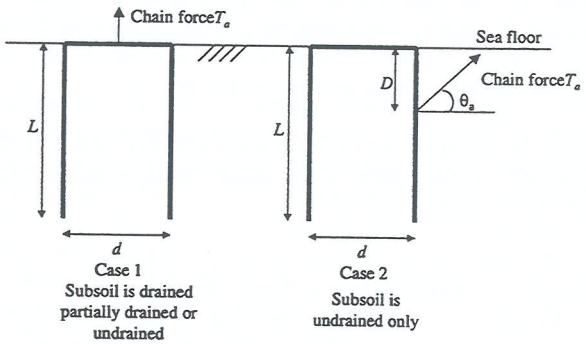

Figure 1 Study cases

2 FOUNDATIONS SUBJECTED TO COMBINED LOADING

The response of a foundation system subjected to combined loading has been a topic of much interest to geotechnical researchers and practitioners, particularly over the last decade. Research in this area has mainly involved investigation of bearing capacity problems. The bearing capacity failure locus for rigid shallow foundations subjected to combined loading has been derived on the basis of experimental results using curve fitting. For example, Butterfield and Gottardi (1995) investigated the behaviour of footings on sand under fully drained or partially drained conditions. Martin (1994) investigated the behaviour of a spudcan footing in undrained

clay. In these cases, the footings either had a flat base or a spudcan shape and no consideration was given to the resistance to uplift loading. For these cases, it was found that maximum moments and horizontal loads are sustained in the presence of some vertical compressive load, i.e. typically when $V/V_o \approx 0.4$ to 0.5, where, V is the vertical component of the ultimate load and V_o is the ultimate load for cases of purely vertical loading.

It is evident from many of the previous studies of combined loading that a yield or failure locus relating the vertical (V), moment (M) and horizontal (H) loads at the ultimate condition can often be expressed in the form:

$$f\left(\frac{V}{As_u}, \frac{M}{Ads_u}, \frac{H}{As_u}\right) = 0 \qquad (1)$$

where, A is the plan area of the foundation, d is the diameter of the foundation, s_u is the undrained shear strength of the soil at the base of the foundation. It is usually assumed that associated plasticity provides a reasonable description of undrained failure in the soil, so that this yield surface also describes a plastic potential defining the relative magnitudes of the incremental deformation during elasto-plastic yielding. To apply the normality relationships on the yield surface, the load and displacement definitions must form work conjugate pairs so that the normalised total system work, W, is written as:

$$\frac{W}{Ads_u} = \left(\frac{V}{As_u}\right)\frac{\delta v}{d} + \left(\frac{M}{Ads_u}\right)\delta\theta + \left(\frac{H}{As_u}\right)\frac{\delta h}{d} \qquad (2)$$

where δv, δh and $\delta\theta$ are the incremental vertical and horizontal caisson displacements and its rotation at failure. These incremental displacements are measured at the same point at which the loads are assumed to act.

In a study of multi-footing foundation systems, Murff (1994) suggested a general form of the failure locus, which included some uplift capacity, given as:

$$f = \sqrt{\left(\frac{M}{d}\right)^2 + \Lambda_1 H^2} + \Lambda_2\left[\left(\frac{v}{v_c}\right)^2 - \left(1 + \frac{V_t}{V_c}\right)V + V_t\right] = 0 \qquad (3)$$

in which V_t V_c are the ultimate vertical compression and tension capacities, Λ_1, Λ_2 are constants and d is the footing diameter. It was assumed that this is a form of associated yield or failure surface. However, as indicated by Bransby and Randolph (1997), the locus described by equation (3) gives very poor agreement with numerical predictions of the collapse loads for strip footings when $M = 0$.

The response of a suction caisson (skirted foundation) to combined vertical (V), moment (M) and horizontal (H) loading has been studied for bearing problems by Bransby and Randolph (1997) using a two-dimensional finite element analysis. In this study, the caisson was considered as a long strip footing and one value of the aspect ratio, $L/d = 0.167$, was investigated in detail. On the basis of the plane-strain finite element predictions, they suggested a yield locus as:

$$f = \left(\frac{V}{V_0}\right)^{2.5} - \left(1 - \frac{H}{H_0}\right)^{1/5}\left(1 - \frac{M}{M_0}\right) + \frac{1}{2}\left(\frac{M}{M_0}\right)\left(\frac{H}{H_0}\right)^5 \qquad (4)$$

However, in practice suction caissons are often circular in plan. To obtain a more precise understanding of the behaviour of a circular foundation under vertical, moment and horizontal loading, a three-dimensional analysis is required. Further, the study by Bransby and Randolph (1997) produced a yield locus for problems involving only bearing (compressive) loads. No consideration of the resistance to uplift loading was included.

3 ANALYTICAL DESIGN MODELS

3.1 Bottom Resistance Failure

When a suction caisson is pulled out at a rapid rate and when large deformation takes place, it may be completely pullout out with the soil plug inside. In this case, the bottom resistance (passive suction) and whatever tensile strength of the clay may have are fully mobilized at the bottom of the caisson. The pullout capacity in this case is given by the frictional resistance and the weight of suction caisson, plus the resistance at the bottom of the suction caisson (passive suction) (Fig.2). In this case the ultimate pullout force is given by:

$$P_u = F_s + W + R_b \qquad (5)$$

where, Fs is the skin friction on the wall, W is the underwater weight of the foundation which includes the soil plug, and R_b is the bottom resistance (passive suction).

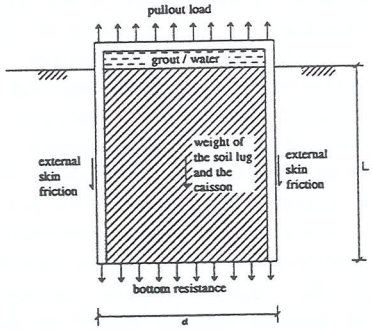

Figure 2 Bottom resistance failure

3.2 Reversed Bearing Capacity Failure

Considering the failure in uplift as a reversed bearing capacity problem is a widely used approach for estimating the pullout capacity of suction caissons. This approach was firstly introduced by Finn & Byrne (1972) after performing laboratory model tests to understand the factors governing the pullout capacity of suction caissons. This idea was then further verified and enhanced by other researchers (e.g., Andersen *et al*, 1993). The failure mechanism of this model is shown in Fig.3.

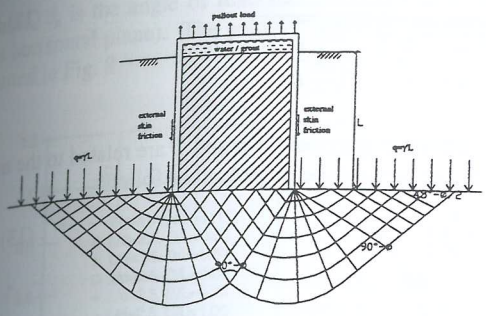

Figure 3 Reversed bearing capacity failure

In this case, the pullout capacity of circular suction caissons under vertical and static loads may be estimated by the following formula:

$$P_u = 1.2AN_c s_u d_c + F_{ts} \qquad (6)$$

Where, N_c is the bearing capacity factor with respect to cohesion s_u of the soil. For $\varphi = 0°$ the theoretical value is 5.14 for N_c. d_c is the embedment factor. A is the section area of the caisson. F_{ts} is the friction between the external surface of the caisson wall and the soil.

3.3 Sliding Failure

When a suction caisson is pulled out at an very slow rate, the pullout capacity can be given by the frictional resistance and the weight of suction caisson (Fig.4), such as:

$$P_u = F_s + W_f \qquad (7)$$

Where, F_s is the skin friction on the wall, W_f is the submerged weight of the foundation. This failure mode assumes negligible bottom resistance and is more likely to occur under fully drained conditions.

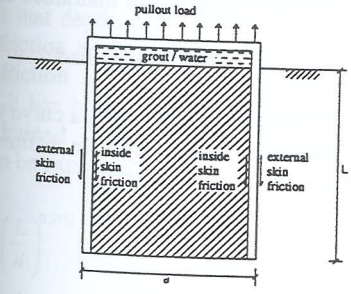

Figure 2 Sliding failure

3.4 Conical Wedge Failure

A possible failure mechanism for suction caisson subjected to inclined uplift loading is illustrated in Fig. 5. r_0 is the radius of the caisson (d is the diameter of the caisson), R is the radius of the deforming wedge, Z_0 is the depth of deforming wedge, h is the depth of the centre of the rotation of the caisson, D is the lug depth, and L is the length of the caisson. Near the surface, a deforming conical wedge forms and is pushed laterally and upwards by the translating and possibly rotating caisson. Below the wedge, the soil is assumed to flow horizontally around the caisson. To accommodate this mechanism, the soil wedge must conform to the caisson at the caisson-soil surface, and must move tangentially to the right soil-caisson interface.

This failure mechanism was firstly developed by Murff & Hamilton (1993) for laterally loaded piles and was then used by Randolph et al (1998) for suction caissons subjected to inclined uplift loading. Similar mechanisms have also been detected in the finite element modelling.

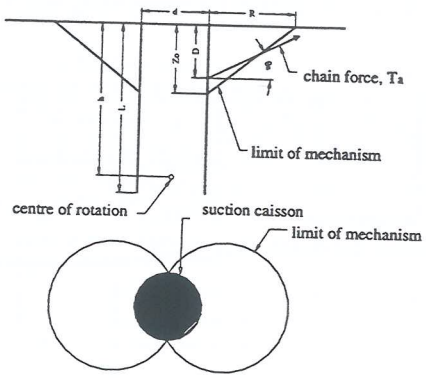

Figure 3 Conical wedge failure

4 THEORETICAL SOLUTIONS

Studies by 2-D and 3-D finite element modelling have been carried out for different aspect ratios of the caissons, different soil strength profiles, different soil permeability and different loading rate. The simplified expressions for the estimation of uplift capacity of suction caisson were then developed by curve fitting the finite element predictions. Details of the finite element study and the detailed derivation of the theoretical solutions have been presented elsewhere in Deng & Carter (1999a) and Deng & Carter (1999b).

4.1 Vertical Uplift Capacity - Undrained

The vertical uplift capacity can be estimated by a modified form of the equations governing the reversed bearing capacity problem. The ultimate uplift capacity can be expressed as the ultimate value of the average uplift traction, p_u, applied at the top over the caisson area, $A = \pi d^2/4$. In this case p_u will be the sum of two terms, one representing the effective overburden pressure at the level of the caisson tip, and the other depending on the undrained shearing resistance of the soil, i.e.,

$$p_u = 1.2N_p d_c s_{u(tip)} \qquad (8)$$

where L is the embedded length of the caisson and d is its diameter. $s_{u(tip)}$ is the undrained shear strength of the soil at the depth of tip of the caisson.

The uplift capacity factor, N_p, which has taken account of the effects of the bottom resistance and the soil-wall friction, may be expressed as: (Deng & Carter, 1999a)

$$N_p = 7.9\left(\frac{L}{d}\right)^{-0.18} \quad (9)$$

where L/d is the aspect ratio. In equation (8), d_c is the usual embedment factor for undrained bearing capacity, given by $1+0.4(L/d)$. The theoretical relationship between N_p and L/d (or s_{uip}/kd, where k is the undrained strength gradient with the depth) has been plotted in Fig. 6, together with the lower bound solutions for bearing capacity factor N_c suggested by Houlsby and Wroth (1983). There is good agreement between the two analytical estimates of N_p and N_c.

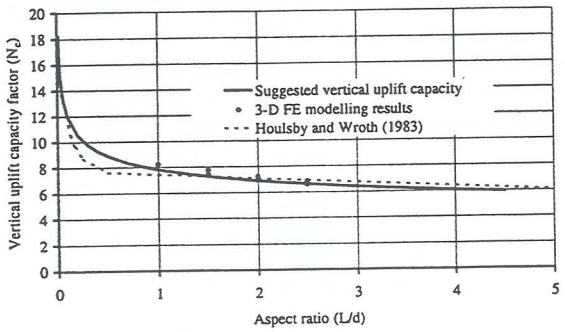

Figure 4 Vertical uplift capacity ratio

Clearly, the ultimate vertical uplift load can be expressed simply as:

$$V_u = p_u A \quad (10)$$

4.2 Lateral Capacity – Undrained

Previous investigators (e.g., Randolph and Houlsby, 1984; Murff and Hamilton, 1993) have carried out studies of the ultimate behaviour of piles in clays under lateral loading. These studies were of pile segments or complete piles subjected to lateral loading applied at the top of the pile, and hence the solutions do not take into account the influence of the relative depth to the loading point, D/L (where D is the depth of the load application point from the soil surface).

Studies by Deng and Carter (1999b) have shown that a good approximation for the ultimate horizontal load that may be applied to a suction caisson, H_u, can be expressed approximately as:

$$H_u = N_h A s_{u(2/3L)} \quad (11)$$

where, $s_{u(2/3L)}$ denotes the undrained shear strength at a depth equivalent to 2/3 of the caisson length. It was also found that N_h could be described by an expression of the form

$$N_h = \frac{\alpha}{\sqrt[4]{\left(\frac{\alpha}{6.3}-\frac{D}{L}\right)^4+\left(\beta\frac{D}{L}\right)^4}} \quad (12)$$

The dimensionless parameters α and β are related to the aspect ratio, L/d, and they can be expressed as follows

$$\alpha = 7.02\left(\frac{L}{d}\right)^{-0.3785} \quad (13)$$

and

$$\beta = 1.58e^{-0.775\left(\frac{L}{d}\right)} \quad (14)$$

The above solutions are applicable to the case of soil strength increasing linearly with depth (e.g., normally consolidated soils). The method may also be applied to cases where foundations are embedded in overconsolidated soils. In the latter case, the soil strength $s_{u(2/3L)}$ appearing in expression (11) should be replaced by the strength of the soil at the depth at which only horizontal displacement occurs when horizontal load is applied.

The above solutions are plotted in Fig. 7 for cases where the aspect ratio, L/d, is 1.0, 1.5, 2.0 and 2.5.

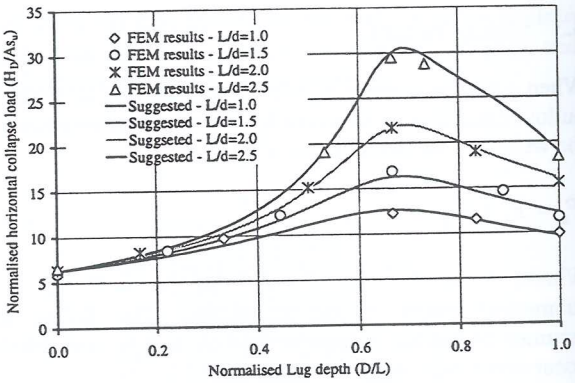

Figure 5 Lateral capacity factor for undrained conditions

4.3 Inclined Uplift Capacity – Undrained

Deng and Carter (1999b) found by fitting a curve to the results of finite element analyses that the ultimate inclined uplift load can be expressed to sufficient accuracy as:

$$\frac{V}{V_u}+\left(\sqrt{1-\left(\frac{H}{H_u}\right)^2}-1\right)^2-1=0 \quad (15)$$

in which V_u is the ultimate value for purely vertical load, given by equation (10), and H_u is the ultimate lateral resistance for purely horizontal load applied at a lug depth, D. The value of H_u is given by equation (11). V and H are the vertical and horizontal components of the ultimate inclined load applied to the axis of the caisson, and obviously,

$$\frac{V}{H} = \tan\theta_a \quad (16)$$

where, θ_a is the angle of load inclination (with reference to the horizontal plane). The solution given by equation (15) is plotted in Fig. 8.

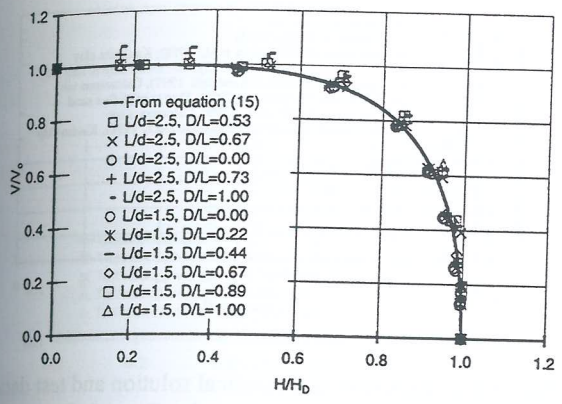

Figure 6 Inclined uplift capacity (undrained)

In practice, load is usually applied to anchor caissons by the attachment of a chain to a lug fixed to the sidewall of the caisson. A load applied directly to the caisson wall at a depth D is statically equivalent to the case of the same load applied at the centre line, at a depth of $D+(d/2)\tan\theta_a$. Therefore, the failure load for the more usual case of sidewall attachment can be obtained from equation (15), after making appropriate allowance for the location of the fixing point.

4.4 Vertical Uplift Capacity – Fully Drained

In cases where the subsoil is fully drained, the pullout capacity of the caisson is equal to the total friction developed between the soil and the caisson wall. At any depth h, the friction between the soil and the caisson wall, f_s, can be expressed as:

$$f_s = \sigma_h' \tan\delta \qquad (17)$$

where, σ'_h is the effective horizontal stress acting on the soil element at that depth, δ is the interface friction angle. The interface friction angle may be influenced by the soil type (internal friction angle and OCR) and the aspect ratio. Therefore it has been suggested (Deng and Carter, 1999a) that the drained vertical uplift capacity of a cylindrical caisson can be expressed as:

$$p_{u(net)} = 9.1\left(\frac{L}{d}\right)^{0.5372}(1-\sin\phi')(OCR)^{\sin\phi'}\tan\phi'\sigma'_{v(bottom)} \qquad (18)$$

where, γ' is the effective unit weight of soil, ϕ' is the effective friction angle, OCR is the over-consolidation ratio, and $\sigma'_{v(bottom)}$ is the vertical effective stress at the location of bottom of the caisson.

Equation (18) has considered the friction along both the external and the internal caisson wall. The effects of the the relationship between the interface friction angle, δ, and the soil friction angle, ϕ' and the correlation of horizontal effective stress in the soil to the original in situ effect stress have also been reflected on.

4.5 Vertical Uplift Capacity – Partially Drained

The pullout capacity of suction caissons subjected to uplift loading under partially drained conditions can be estimated by the following formula (Deng & Carter, 1999a):

$$p_{u(net)} = N_f\, p_{u(drained)} + N_b\, s_{u(tip)} \qquad (19)$$

where

$$N_b = [0.13 - 0.446\ln(T_k)]1.6^{\frac{L}{d}} \qquad (20)$$

$$N_f = 0.632 - 0.091\ln\left(\frac{L}{d}\right) \qquad (21)$$

In expression (19), the first component is the friction resistance developed along the caisson wall and the second component is the resistance developed at the bottom of the caisson. Therefore N_f is called the friction factor and N_b is the bottom breakout resistance factor. $p_{u(drained)}$ is the drained pullout capacity and $s_{u(tip)}$ is the initial undrained strength at the tip of the caisson. T_k is a non-dimensional load rate parameter that can be defined as:

$$T_k = \frac{C_v}{vd} \qquad (22)$$

where, C_v is the coefficient of consolidation of the soil and v is the load rate (steady velocity) at which the caisson is pulled from the ground.

It was found that when $T_k > 0.6$, the pullout behaviour is effectively fully drained, so $N_b = 0$. When $T_k < 0.002$, the pullout behaviour can be considered as effectively undrained. The upper limit of N_b is determined by the undrained condition. Hence, equations (19) to (21) are applicable whenever $0.002 < T_k < 0.6$.

4.6 Lateral capacity – fully drained

Broms (1964) developed a simple but reliable method for the estimation of lateral capacity for suction caissons in sands. Broms' expression for the ultimate lateral capacity of a caisson embedded in saturated sand can be expressed as:

$$Q_u = \frac{\gamma' dL^3 \tan^2(45^\circ + \frac{\phi}{2})}{2(D+L)} \qquad (23)$$

where Q_u is the ultimate lateral load, ϕ is the angle of internal friction of the sand, γ' is the submerged unit weight of the sand, L is the embedded depth of the caisson, d is its diameter, and D is the distance from the point of application of the lateral force to the sand surface.

5 EVALUATION OF THEORETICAL SOLUTIONS

The theoretical solution for inclined uplift capacity can be verified by the solutions obtained by an upper bound technique using the theory of soil plasticity (Randolph et al, 1998). The theoretical solutions discussed above can also be examined in the light of available experiment data. The published

experimental data include laboratory model-scale and centrifuge results, as well as some field test results. The test results include 76 individual tests from 12 independent studies, which are detailed in Deng & Carter (1999c).

5.1 Evaluation By Upper Bound Techniques

A three-dimensional upper bound technique was developed by Randolph et al (1998), based on the flow mechanism proposed by Murff & Hamilton (1993). This technique is focused on the capacity of suction caissons subjected to quasi-horizontal loading form a mooring chain. This method was extended to include quasi-vertical loading of suction caissons for TLP anchorages by Deng & Carter (1999b) by adopting the uplift capacity factor, as shown in expression (9), when considering the energy dissipation at the caisson tip due to soil movement in the vertical direction. Detailed comparison between the theoretical solution for inclined uplift capacity and the upper bound techniques can be found in Deng & Carter (1999b).

It was found that the differences between the theoretical solutions and the upper bound solutions for cases where the load is applied vertically along the sidewall are less than 5% for most aspect ratios. While for cases where purely horizontal load is applied the differences are 1% to 20%. A detailed comparison for inclined load cases is given in Fig.9.

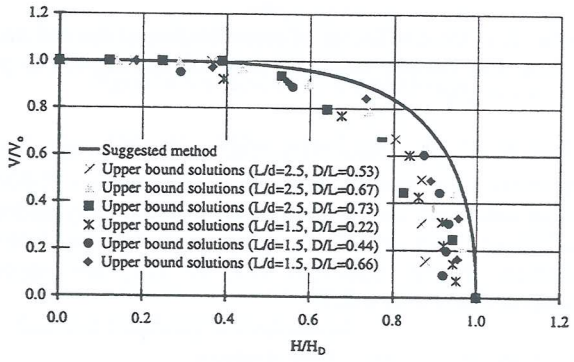

Figure 7 Comparison of theoretical solutions and upper bound solutions

As shown in Fig.9, the upper bound solutions for the ultimate loads are generally lower than the theoretical solutions. The reasons for this are likely due to:

- The theoretical solutions were derived from the finite element predictions. Generally finite element results tend to be over-estimates and it was also assumed in the finite element analysis that the interface between the soil and the caisson is perfectly bonded.
- The upper bound method is not entirely rigorous and has some limitations. One of the limitations is that this upper bound solution is not kinematically complete, since it ignores interaction between the top and the bottom of the 'flow' region (below the conical wedge) and the adjacent soil.

5.2 Evaluation By Test Data

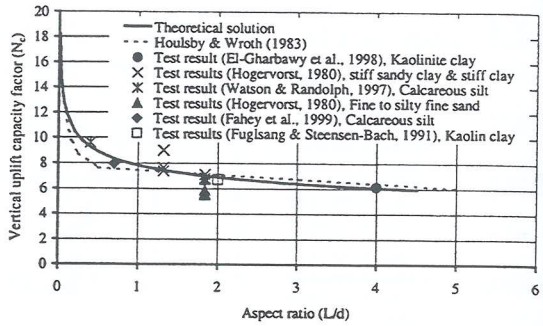

Figure 8 Comparison of theoretical solution and test data for undrained vertical uplift capacity (after Deng & Carter, 1999c)

Detailed evaluation can be found in Deng & Carter (1999c). Figures 10, 11, 12 and 13 show comparisons of the test results and the theoretical solutions for vertical uplift capacity (undrained), lateral capacity (undrained), inclined uplift capacity (undrained) and vertical uplift capacity (drained) respectively. From the comparisons, the following conclusions can be drawn.

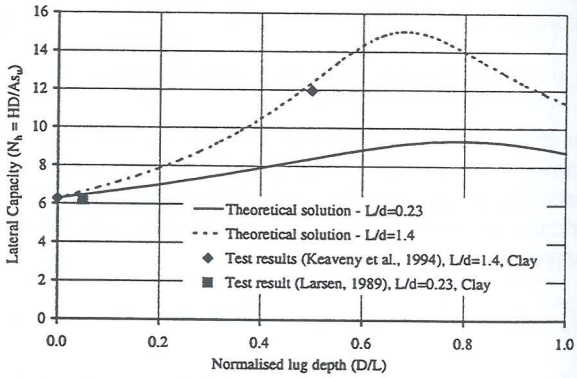

Figure 9 Comparison of theoretical solution and test data for undrained lateral capacity (after Deng & Carter, 1999c)

- The suggested theoretical method for estimating the undrained vertical capacity of suction caissons seems to apply reasonably well to a wide range of soils, including stiff clay, kaolinitic clay, sandy clay, calcareous silt, fine sand, and silty fine sand.

For estimation of the lateral capacity of suction caissons, the suggested theoretical solution is reasonable for cases where the subsoil is clay or has significant cohesion and deforms under undrained conditions.

- The suggested theoretical method for the estimation of the inclined uplift capacity of suction caissons under undrained conditions appears to be reasonably accurate for design purposes.

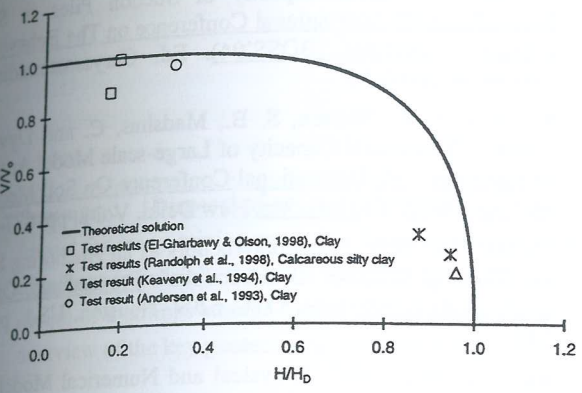

Figure 10 Comparison of theoretical solution and test data for undrained inclined uplift capacity (after Deng & Carter, 1999c)

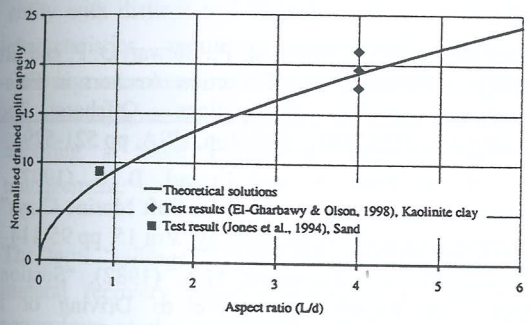

Figure 11 Comparison of theoretical solution and test data for drained vertical uplift capacity (after Deng & Carter, 1999c)

Six tests included measurement of the drained lateral capacity. The comparison shows that the differences between the prediction of Broms' formula and the measured lateral capacity are between 0.0 ~ 21.7%, which indicates that Broms' formula appears to be reliable for cases where the subsoil is sand or noncohesive soil. Twenty-three individual test results were recorded for vertical uplift capacity (partially drained). The differences between test results and estimation by expression (19) are 2.3 ~ 23.3% for aspect ratio L/d = 0.75, 4.5 ~ 10.8% for L/d = 1.0, 4.3 ~ 24.7% for L/d = 1.5, 10.7 ~ 47.7% for L/d = 2.0 and 114.6% for L/d = 4.0. It may be seen that for aspect ratios less than 2, the test results agree reasonably well with the theoretical solutions. It is also noted that the theoretical solutions generally overestimate the measured capacities. However, for those tests with an aspect ratio larger than 2, the theoretical solutions generally significantly overestimate the measured responses. Use of the suggested formula (19) in design together with an appropriate factor of safety is therefore recommended for aspect ratio less than 2 only.

6 CONCLUSIONS

In this paper, theoretical solutions for estimation of the uplift capacity of suction caissons, for cases where the subsoil is drained, partially drained or undrained and the load is applied horizontally, vertically or inclined, have been presented. These methods have been verified by the results from a relatively large number of laboratory and field tests and solutions obtained from an upper bound technique using the theory of soil plasticity. The following conclusions were reached.

- Different failure mechanisms will be developed when the point of load application, the angle of load application or the subsoil's drainage condition is different.
- The suggested theoretical method for estimating the undrained vertical capacity of suction caissons, equations (8) and (9), seems to apply reasonably well to a wide range of soils, including stiff clay, kaolinitic clay, sandy clay, calcareous silt, fine sand, and silty fine sand.
- For estimation of the lateral capacity of suction caissons, the use of equation (13) and (14) is suggested for cases where the subsoil is clay or has significant cohesion and deforms under undrained conditions. The use of Broms' formula, equation (25), is suggested for cases where the subsoil is sand or is non-cohesive and deforms in a fully drained manner.
- The suggested theoretical method for the estimation of the inclined uplift capacity of suction caissons under undrained conditions, equations (17) and (18), appears to be reasonably accurate for design purposes.
- The suggested formula for the estimation of drained vertical uplift capacity, equation (20), can be used for a wide range of aspect ratios and for various kinds of soils.
- The suggested formulae for estimating the vertical uplift capacity for partially drained conditions, equations (21) to (23), appear to be reasonably accurate only for those cases where the aspect ratio of the caisson is less than 2.
- It should also be noted that the theoretical methods for the estimation of uplift capacity of suction caissons presented in this paper consider only two-sided (anti-symmetric) failure mechanisms.

ACKNOWLEDGEMENTS

The work described in this paper forms part of the research program of the Special Research Centre for Offshore Foundation Systems, established and supported under the Australian Research Council's Research Centres Program. The author would also like to thank his supervisor, Challis Professor John P. Carter, Head of the Department of Civil

Engineering at The University of Sydney for his invaluable guidance throughout this work.

REFERENCES

Andersen, K. H., Dyvik, R. etc. (1993). "Field Tests of Anchors in Clay. II: Predictions and Interpretation". Journal of Geotechnical Engineering, ASCE, Vol. 119 (10), pp 1532 - 1549

Bransby, M.F., Randolph, M. F. (1997). "Shallow foundations subjected to combined loadings". Proceedings, The 9th Int. Conf. On Computer Methods and Advances in Geomechanics, Wuhan, China, Vol. 2, pp. 1947-1952

Broms, B. B. (1964) "Lateral Resistance of Piles in Cohesiveness Soils". Journal of the Soil Mechanics and Foundations Division, ASCE, Vol. 90, SM2, pp. 27-63.

Butterfield, R. and Gottardi, G. (1995). "Simplifying Transformations for the Analysis of Shallow Foundations on Sand". Proceedings, The 5th International Society of Offshore and Polar Engineers Conference, The Hague, USA. pp 534-538.

Carter, J.P. and Balaam, N.P. (1995). "AFENA – A Finite Element Numerical Algorithm – Users' Manual", Centre for Geotechnical Research, The University of Sydney.

Deng, W. and Carter J. P. (1999a). "Vertical Pullout Behaviour of Suction Caissons". Research Report, Centre for Geotechnical Research, The University of Sydney.

Deng, W. and Carter J. P. (1999b). "Analysis of Suction Caissons Subjected to Inclined Uplift Loading". Research Report, Centre for Geotechnical Research, The University of Sydney. .

Deng, W. and Carter J. P. (1999c). "Evaluation of Methods to Predict the Uplift Capacity of Suction Caissons". Research Report, Centre for Geotechnical Research, The University of Sydney.

El-Gharbawy and Olson (1998). "Pullout Capacity of Suction Caisson Foundation for Tension Leg Platforms". Proceedings of the Eighth (1998) International Offshore and Polar Engineering Conference. ISOPE, Golden, CO, USA. pp 531-536

Fahey Watson, P. G. and Tremain, T. (1999) "Vertical-Horizontal Loading of Skirted Foundations Compared With Vertical-Torsional Loading". Proceedings of the Ninth (1999) International Offshore and Polar Engineering Conference. ISOPE, Brest, France. pp 31-38

Finn, W. D. L. and Byrne, P. M (1972). "The Evaluation of the Breakout Force for a Submerged Ocean Platform". Proceedings, Offshore Technology Conference, Houston, Texas, OTC 1604.

Fuglsang, L. D. and Steensen-Bach, J. O. (1991). "Breakout Resistance of Suction Piles in Clay". Proceedings of the International Conference: Centrifuge 91. H. Y. Ko and F. G. Mclean eds., A. A. Balkema, Rotterdam, The Netherlands, pp. 153-159.

Hogervorst, J. R. (1980). "Field Trials With Large Diameter Suction Piles". Proceedings, Offshore Technology Conference, OTC 3817. Houston, USA, pp. 217-222

Houlsby, G. T., Wroth, C. P., (1983). "Calculation of Stress on Shallow Penetrometers and Footings". Symposium on Seabed Mechanics, Newcastle, UK, September 1983, pp. 107-112.

Jones, W. C., Iskander, M. G., Olson, R. E. and Goldberg, A. D. (1994). "Axial Capacity of Suction Piles in Sand". Proceedings 7th International Conference on The Behaviour of Offshore Structures (BOSS'94). Ed. Chryssostomidis, C., Pergamon. pp 63-75.

Keaveny, J. V., Hansen, S. B., Madshus, C. and Dyvik, R. (1994). "Horizontal Capacity of Large-scale Model Anchors". Proceedings 13th International Conference On Soil Mechanics and Foundation Engineering, New Delhi, Vol 2, pp. 677-680.

Larsen, P. (1989). "Suction Anchors as an Anchoring System for Floating Offshore Constructions". Proceedings, Offshore Technology Conference, OTC 6209. Houston, USA. pp 535-540.

Matin, C. M., (1994). "Physical and Numerical Modelling of Offshore foundations under Combined Loads". D. Phil Thesis, University of Oxford.

Murff and Hamilton (1993). "P-Ultimate for Undrained Analysis of Laterally Loaded Piles". Journal of Geotechnical Engineering, ASCE, Vol. 119(1), pp. 91-107.

Murff, J. D. (1994). Limit Analysis of Multi-footing Foundation Systems. Proc. Of the 8th Int. Conf. On Computer Methods and Advances in Geomechanics, Morgantown, pp. 223-244.

Randolph, M. F., O'Neill, M. P., Stewart D. P. and Erbrich, C. (1998). "Performance of Suction Anchors in Fine-Grained Calcareous Soils". Proceedings, Offshore Technology Conference, OTC 8831. Houston, USA, pp 521-529.

Rao, S. N., Ravi, R. and Prasad, B. S. (1997). "Pullout Behaviour of Suction Anchors in Soft Marine Clays". Marine Georesources and Geotechnology. Vol 15. pp 95-114

Senpere, D. and Auvergne, G.A. (1982). "Suction Anchor Piles - A Proven Alternative to Driving or Drilling". Proceedings, Offshore Technology Conference, OTC 4206. Houston, USA. pp. 483-489

Singh, B., Datta, M. and Gulhati, S. K. (1996). "Pullout Behaviour of Superpile Anchors in Soft Clay under Static Loading". Marine Georesources and Geotechnology, Vol 14, pp. 217-236.

Taiebat, H. (1999). "Behaviour of Offshore Foundations Subjected to Cyclic Loading", PhD Thesis, The University of Sydney.

Watson, P. G. and Randolph, M. F. (1997). "Vertical Capacity of Caisson Foundations in Calcareous Sediments". Proceedings International Society of Offshore and Polar Engineers Conference, Hawaii, USA. pp 152-159.

Geotechnical Considerations in Designing Tailings Storage Facilities to Minimise Environmental Impact

Joseph M. Dwyer
Senior Geotechnical Engineer, Dames & Moore Pty Ltd, Western Australia

Summary: Disposal of tailings is commonly considered to be the single most important source of potential environmental impact for many mining projects. Increased public awareness and regulatory involvement have meant that the management of tailings is possibly the most sensitive environmental issue confronting the mining industry at present. Consequently, the design of a tailings storage facility has evolved into a critical aspect for all mining operations. This paper provides a broad overview of the key geotechnical considerations associated with environmentally responsible tailings storage facility design.

1. INTRODUCTION

The primary objective of mining is the economic recovery of mineral commodities from the parent ore. In as much as tailings are a waste byproduct of the recovery process, traditionally they were not distinguished as a separate entity with distinct and complex physical and chemical characteristics requiring experienced management. Growing awareness of mining impacts over the last decade has, however, pressured the mining industry into adopting a more responsible approach to tailings management.

The term "tailings" is derived from the fact that the mineral recovery process generates a product called concentrate at the top (or "head") and a waste called tailings at the end (or "tail"). The tailings contain crushed gangue minerals, spent process water and varying amounts of chemical reagents added during the process to enhance the recovery of the product mineral from the ore. The tailings are typically discharged as a low-density, free-flowing liquid to storage areas termed "tailings storage facilities" (TSFs).

In the past, tailings storage facilities were all called "tailings dams", as they acted as permanent hydraulic structures. The current trend in tailings management is to try and minimise the potential for environmental impact by minimising the water content in the contained tailings. Hence the preferred reference to a "tailings storage facility" rather than a "dam". A variety of tailings storage methods is available to the geotechnical designer. This paper focuses on the geotechnical design considerations for the storage of tailings behind TSFs utilising earthfill embankments.

2. ENVIRONMENTAL ISSUES

Some of the most significant, and certainly most visible, environmental impacts arising from mining are associated with the construction, operation and long-term performance of TSFs. The potential for environmental impact can, however, be mitigated with careful consideration of the following issues during the TSF design and operation stages.

- **Land Degradation** - an area of land, possibly up to several hundred hectares, will be disturbed to construct an aboveground TSF.

- **Water Pollution** - seepage of process liquor from impounded tailings can result in:
  - rising groundwater levels, possibly into the vegetation root zone;
  - contamination of groundwaters from mobilised heavy metals and/or other contaminants; and
  - acid mine drainage from the oxidation of sulphidic tailings.

- **Surface Water Impact** - the siting of an aboveground TSF will alter the hydrological regime of the area, which may affect the downstream environment.

- **Remnant Process Chemicals** - the tailings' may contain remnant traces of chemicals used in the recovery process that may be environmentally hazardous.

- **Release of Tailings** - the path of tailings from an embankment breach can extend hundreds of metres downstream, contaminating large areas.

- **Visual Impact** - the siting of a TSF will impact the surrounding landscape, particularly at closure when at full height.

- **Air Quality** - fine grained tailings can be easily eroded when dry, and when windblown may cause a dust hazard.

- **Social Impacts** - the siting of a TSF may affect the cultural, archaeological and socio-economic environment.

3. HOW SAFE ARE TSFs?

Comparisons between TSF failures and incidents at hydroelectric and water-retaining structures were documented by the International Commission of Large Dams (ICOLD, 1995). ICOLD plotted the total number of failures reported worldwide in 10-year increments for TSFs and water supply dams. The results are shown in Figure 1.

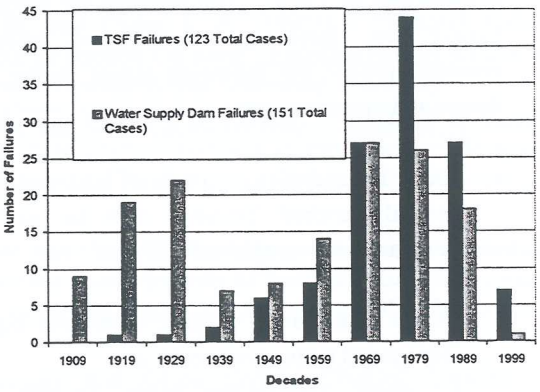

Figure 1 - Water Supply Dam and TSF Failures (ICOLD, 1995)

Even though the database is not complete, the overall behaviour of the two structure types is observed to be very similar and identifies some convincing trends. The increase in the frequency of TSF failures relative to water supply dam failures may be due to increased regulatory involvement and community awareness and hence their reporting.

4. TSF DESIGN GUIDELINES

The aim of modern tailings management is to apply sound engineering principles from a variety of disciplines related to dam, geotechnical and environmental engineering in order to store tailings safely and economically with minimal disturbance to the surrounding environment. Concern over the potential hazards associated with tailings storage has led to an increased involvement by regulatory agencies. As a result, a number of guidelines for tailings management have been developed, some of which are described below.

In Western Australia, legislative controls on tailings storage are mainly the responsibility of the Department of Environmental Protection (DEP) and the Department of Minerals and Energy (DME). To assist the designers, operators and owners of TSFs in Western Australia, the DME has published guidelines on the design, approval and operation of TSFs. Similar guidelines exist in other Australian states and territories. The Australian federal DEP has also published a series of best-practice management handbooks on mining, including TSF design and tailings management.

A number of technical bulletins covering TSF design, operation and closure have been published by the ICOLD tailings sub-committee. Readers of these bulletins, however, should be aware that, to the best of the author's knowledge, there is no international legislation that could force the application of these guidelines to Australian practice.

Whilst these publications provide the designer with guidelines and best-practice principles for sound tailings management, they are by no means prescriptive. The tailings designer must be able to apply the techniques of geotechnical analysis and engineering in association with the documented principles in order to achieve a site-specific environmentally responsible TSF. The tailings designer can apply the principles of soil mechanics to characterise the tailings and their behaviour, however, an appreciation of their difference from most naturally occurring soils is required.

5. KEY GEOTECHNICAL DESIGN CONSIDERATIONS

5.1 Tailings Characterisation

Most tailings are in the form of a fine-grained slurry with a solid fraction that behaves like a soil, however, depending upon the orebody characteristics and process type, they can vary considerably in their physical, chemical and mineralogical characteristics. As the performance of a TSF is largely influenced by the properties and characteristics of the tailings to be stored, it is imperative that the tailings' properties be determined early in the design development, and periodically reviewed during operation to optimise the TSF's performance.

Hard rock ore crushed as part of the mineral recovery process generally produces angular particles in the sand, silt and even clay-size fractions. As a result, these tailings have geotechnical characteristics more common to granular materials than to silts or clays, regardless of their particle size distribution.

Geotechnical property tests performed on small tailings samples provide a basis for comparison with other tailings and soils and enable the extrapolation of laboratory other properties. A typical suite of laboratory tests might include:

- solids content (% by weight);
- specific gravity of solids;
- particle size distribution;
- soil plasticity (Atterberg Limits); and
- liquor pH and salinity.

Results from the above tests are used to define TSF design parameters such as flow characteristics, beach slope, settling rate and storage density. The following more specialised tests can be conducted to refine the design parameters:

- Settling Test – to determine the tailings' rate of water release.
- Triaxial, Shear Box and Vane Shear Tests – to determine strength parameters (friction angle, cohesion, shear strength) for use in stability, bearing capacity and liquefaction potential analyses.
- Shrinkage Limit Test – to determine the maximum density that can be achieved by atmospheric drying alone.
- Consolidation Test – to determine the rate of water release and time dependent deformation under load.
- Permeability Test – to determine the rate at which water will flow through the tailings (used in seepage analyses).
- Compaction Characteristics (maximum dry density and optimum moisture content) – to determine the tailings' suitability for use in TSF raising works.
- Dispersivity – to determine the erodibility of the tailings.
- Mineral and Chemical Composition – to define the mineralogy of the tailings and the nature of any potential contaminants.
- Rheology Tests – to determine the tailings' flow properties.

For operating mines, production tailings are available for testing, however, if the design is for a new mine, then samples must be taken from tailings produced in laboratory scale metallurgical tests. For both cases the critical concern is obtaining a representative sample. Mine process water should be used wherever possible such that laboratory test results are representative of the tailings' behaviour within the TSF.

5.2 Tailings Storage

Surface impoundments are by far the most common tailings storage method, however, changing economic and regulatory conditions now require the consideration of more innovative deposition and storage methods. The available storage methods generally fall within one of the following categories:

- surface impoundments;
- in-pit disposal (disused open pits);
- paste backfill (underground mine stopes);
- deep water (ocean or lake); or
- river disposal.

A brief description of the geotechnical considerations for each of the above storage methods follows.

5.2.1 Surface Impoundments

Surface storage of tailings generally utilise earthfill embankments to retain both the tailings solids and liquor. The impoundment layout is selected to be compatible with the topographic setting of the site and can be either a:

- cross-valley impoundment (single embankment);
- side-hill impoundment (three embankments); or
- paddock or ring-dyke impoundment (four embankments).

Surface impoundments are formed by two general classes of embankment structure:

- water-retention type embankments; or
- raised embankments.

Water-retention type embankments are constructed to their full height prior to commencing tailings discharge, and are best suited to impoundments with high water storage requirements (such as a cross-valley impoundment with a large internal catchment).

Raised embankments are the most common type of surface impoundment structure. They differ from conventional water-retention type embankments in that construction of the embankment is staged over the life of

the facility to limit upfront capital costs before the mine is in production. Raised embankments begin initially with a starter embankment sized to impound often the initial two to three years of tailings output. Subsequent raises of the embankment are scheduled to keep pace with the rising elevation of the tailings. In areas of high net-evaporation an impoundment is typically sized to store tailings at a vertical rate-of-rise of around 2.5 m/annum. The embankment raise height and schedule is determined on the actual tailings rate-of-rise measured during operation.

TSF embankments are raised using a wide range of materials, including natural soils, mine waste or tailings. The method of raising is categorised by the direction of translation of the crest as the raising proceeds. In order of increasing cost, the raise methods are:

- upstream;
- centreline; and
- downstream.

Cross-sections of the above raise types are illustrated in Figure 2.

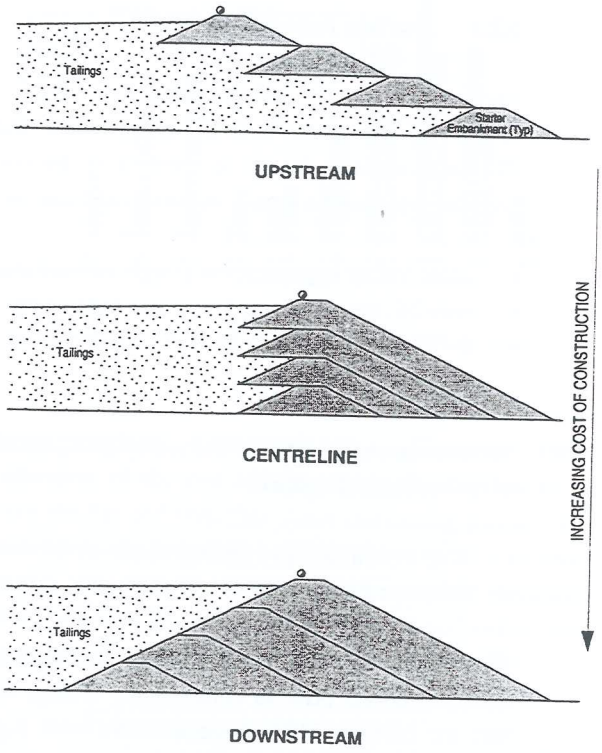

Figure 2 - TSF Raise Methods

The initially low density and strength of the deposited tailings, and their relatively slow strength increase with time, are important geotechnical considerations for the design of a TSF. Upstream raising of a TSF can therefore present some interesting geotechnical challenges as construction often utilises tailings as the fill material and the raise embankment is founded on the stored tailings.

5.2.2 In Pit Disposal

Tailings disposal into mined-out pits provides a relatively cost-efficient storage method. This alternative is attractive for many operations as it may reduce the mine owner's environmental liability by filling an otherwise deep void, however, there are a number of geotechnical issues that limit the usefulness of in-pit disposal, including:

- typically about 25% less material than was removed can be placed back into the pit;
- the pit fills at a fast rate due to the small surface area and large depth;
- the rapid rate-of-rise of the tailings results in poor consolidation, resulting in reduced storage capacity and large ongoing settlement;
- rehabilitation may be delayed many years due to the unstable tailings surface;
- there is potential for contaminant migration with hazardous tailings stored below the groundwater table; and
- tailings disposal into the pit precludes the recovery of further mineral from the pit at a future date.

5.2.3 Paste Backfill

In certain circumstances tailings can be mixed with additives (such as cement) to form a paste and discharged underground to provide structural support. Some South African gold mines have used this method since the turn of the century, however, its application in Australia has been limited.

Underground disposal can reduce the site's environmental liability as the volume of tailings to be stored on the surface can be reduced by up to 50%. The method, however, requires tailings with suitable characteristics (generally high permeability and low compressibility) and they need to be inert without potential hazard as they are likely to be stored below the groundwater table.

5.2.4 Deep-Water Disposal

A minority of mining operations discharge tailings in deep water, either into a lake or the ocean. The lack of reliable operating data available for comparison to baseline data has resulted in the public perceiving this

method as "environmentally unacceptable". However, in highly seismic, high rainfall and steep terrain mining areas or where tailings are likely to generate acids due to pyrite and other sulphides in the ore, then deep water disposal may be the only feasible method.

5.2.5 River Disposal

As per deep-water disposal, river disposal may be the only economic alternative in highly seismic, high rainfall and steep terrain areas. The degradation of the downstream environment at a number of operations has resulted in poor public acceptance of this method.

5.3 Tailings Deposition

Tailings is deposited as a slurry at water contents ranging from 40 to 200% (solids content 30-70%). Selection of the most appropriate deposition method generally depends on the tailings' characteristics, process type, site constraints and the local climate. The available deposition methods include:

- **Cyclic Drying** (paddock rotation), where thin layers of tailings are rotated through a system of 'paddocks'. In regions of high net-evaporation this method can provide a dense, stable tailings mass.

- **Subaerial Deposition**, which is a generic term for the deposition of tailings on beaches above the decant pond water level. This method is typically used in cyclic drying systems.

- **Thickened Discharge**, which involves thickening the tailings slurry to a solids content of up to 70% (water content 40%) to take advantage of the natural beach slope formed by sub-aerially deposited tailings, creating a tailings stack with an essentially conical shape. Thickened tailings generally beach at a steeper slope

- **Subaqueous Deposition**, which is the pumping of tailings into a liquor-filled containment. This method is typically used in areas of high net-rainfall or to minimise the acid generating potential of sulphidic tailings.

- **Co-disposal**, where the mixing of coarse and fine tailings streams produces another material with geotechnical properties superior to either of the constituent wastes.

Any of the above deposition methods may be the most appropriate, irrespective of the mineral being mined, and should be considered as part of the design development.

5.4 Site Selection

The principal criteria for TSF site selection are:

- properties of the tailings;
- distance and elevation relative to the plant;
- topography of the available terrain;
- hydrological and hydrogeological regime;
- site geology and geotechnical soil profile;
- location of ore reserves;
- lease areas available;
- regulatory requirements;
- sites of significance; and
- rare or endangered flora and fauna.

The selection of the most appropriate site is essentially a screening process considering the above criteria, commencing with a preliminary evaluation followed by a more detailed investigation and evaluation. The screening process involves the application of various constraints to an initial array of sites, which ultimately results in a much smaller subset of reasonable siting possibilities.

5.5 Geotechnical Site Investigation

A field investigation is undertaken to determine the geotechnical suitability of the proposed site for tailings storage and the suitability of local materials for use in the TSF construction. A typical sequence of events for a geotechnical site investigation would involve a preliminary desk study of aerial photographs, and geological and contour maps, followed by a subsurface exploration with sampling, field tests and laboratory testing of undisturbed and bulk samples.

In addition, for TSF upstream raising a geotechnical investigation of the stored tailings is often conducted to determine the stored tailings strength profile and assess its suitability to found the raise.

5.6 Embankment Design

5.6.1 Slope Stability

Under normal conditions a soundly designed and constructed TSF is expected to perform without excessive deformation or the threat of slope instability. The embankment could become unstable if:

- overtopped by tailings or supernatant liquor;
- high water pressure levels develop within the embankment as a result of a high phreatic surface;
- seepage through the embankment or foundation results in piping of fine-grained materials; or
- the tailings, embankment or foundation liquefy during seismic loading.

It is generally regarded that minimum long-term factors of safety of 1.5 (typically corresponding to a less than 1% probability of failure) and 1.0 (typically 50% probability of failure) represent an acceptable level of safety for TSFs under respective static and seismic loading conditions. The geotechnical factors influencing the TSF embankment stability are the:

- embankment height and slope;
- phreatic surface position;
- nature and strength of the embankment fill and foundation materials; and
- time duration of loading (undrained versus drained behaviour).

As the embankment profile and storage properties changes during the life of the TSF, the embankment stability should be regularly reviewed during operation. Sensitivity analyses for a range of soil properties and phreatic surface levels are recommended as part of the embankment stability assessment.

5.6.2 Seismicity

To be stable under earthquake loading the geotechnical design needs to take into consideration:

- the level of seismic activity (historic and predicted) at the site;
- the ability of the TSF and its foundations to survive seismic shaking;
- the potential for liquefaction of the stored tailings, embankment fill or foundations due to a seismic event; and
- the TSF siting relative to areas of habitation and infrastructure.

The following two earthquake levels are generally considered during the geotechnical design:

- the Operating Basis Earthquake (OBE) for normal operations; and
- the Maximum Credible Earthquake (MCE) for extreme conditions.

The OBE is the earthquake that is liable to occur at least once during the expected life of the structure and is often chosen as the earthquake that has a 10% probability of exceedance in a 50-year period, which is equivalent to an annual probability of exceedance of 1 in 475 (Fell *et al.*, 1992). A TSF is expected to function in a normal manner after the passage of the OBE.

For TSFs located in highly seismic areas or where failure could result in large loss of life or extensive property damage, the seismic analysis is usually based on the MCE. After the passage of the MCE, damage to the TSF is acceptable as long as the integrity and stability is maintained and the release of impounded tailings and liquor is prevented. The MCE is defined as the maximum hypothetical earthquake that could be expected from the regional and local potential sources for seismic events that would produce the severest vibratory ground motion at the site (Fell *et al.*, 1992).

Loose, saturated sands of the gradation normally produced from most mine tailings are highly susceptible to liquefaction. Tailings liquefaction results in a sudden strength loss that can have catastrophic effects should the embankment fail. Liquefaction is an important consideration for TSFs raised using the upstream technique as the raises are founded on the stored tailings. The risk of liquefaction can be minimised by maintaining the decant pond level away from the embankment during operation such that these tailings are not saturated.

5.6.3 Hydrological Considerations

Historically overtopping has been the most frequent cause of TSF failure, often a result of mis-management rather than poor design. Overtopping can severely erode the embankment downstream slope, either reducing the freeboard or compromising the stability until stored tailings and liquor are released to the downstream environment. Therefore, experienced determination of the design flood is essential. The design of a major TSF, where failure could result in loss of life or extensive property damage, should be based on the probable maximum flood (PMF).

Although the discharge of toxic liquor is to be avoided if at all possible, controlled discharge is preferable to having the embankment overtopped which could result in a catastrophic failure with the release of huge volumes of tailings and liquor.

5.6.4 Erosion Control

Erosion of the TSF embankment surface can occur due to the action of wind or water. Uncontrolled erosion can adversely affect TSF stability, either directly by modification of the embankment geometry, or indirectly as a result of the eroded material blocking drains.

Some embankment materials, such as sands, silts and dispersive clays, are more susceptible to erosion than others. Materials of this type should not be left exposed on the embankment crest or downstream slope. Tailings themselves are generally highly erodible and should be covered with a layer of waste rock if they are used in TSF raise construction. Sulphidic tailings used to upstream raise a TSF will need to be covered with a suitable barrier on the downstream batter to prevent acid mine drainage.

Internal erosion of material from the embankment resulting from seepage (commonly termed 'piping') can become a serious issue. Piping can occur when drainage measures provided to control the seepage are inadequate or when defects occur within the embankment, such as settlement cracking or poor fill compaction. Internal erosion is best managed by correct selection of construction materials, correct filter design and experienced construction supervision.

5.7 Seepage

The notion of a "water-tight" TSF is a false one, all TSFs leak. Seepage can be separated into the following two categories:

- seepage through the storage embankment or embankment foundations; and
- seepage to the groundwater mass.

Seepage of the former will in most cases 'daylight' on the embankment slope or downstream of the embankment. This can compromise the embankment stability if the internal embankment drains are inadequate. Seepage of the latter type may express itself downstream of the TSF, but is generally confined to the issues of rising groundwater table and groundwater contamination.

TSF seepage control is site-specific and should be evaluated during the design development according to the following three general categories:

- seepage barriers;
- seepage recovery systems; or
- liners.

5.8 Instrumentation

The purpose of instrumentation is to measure phenomena crucial to the behaviour of a TSF. Geotechnical instrumentation utilised as part of the TSF design may include:

- bores to measure standing water levels and to sample groundwater for chemical analysis;
- piezometers (standpipe, pneumatic, hydraulic or vibrating wire) to monitor pore pressures for stability analyses;
- flow measuring devices (V-notch, rectangular or trapezoidal weirs) to measure seepage discharge;
- settlement plates and inclinometers to measure embankment deformation;
- survey control network to accurately measure TSF movement; and
- motion accelerographs (seismographs) to record the TSF's behaviour during seismic events.

6. CONCLUSION

The long-term storage of tailings poses a significant risk to the environment surrounding a tailings storage facility. Increased awareness of the potential hazards associated with tailings storage over the last decade has led to stricter control by government authorities and increased responsibility by mine owners. As a result, the geotechnical assessment and design of tailings storage facilities has evolved into a critical aspect of mining operation. The challenge to miners and their geotechnical advisors is to use the principles of soil mechanics and geotechnical engineering in association with an appreciation of the complex behaviour of tailings to design, construct and operate a tailings storage facility in such a way that it remains safe and stable for perpetuity and results in minimal impact to the surrounding environment.

7. ACKNOWLEDGEMENTS

The author wishes to thank Dr Elio Novello (Dames & Moore) for his assistance with the review of this paper and Mrs Sharmalie Ranjithkumar for formatting and typing the manuscript.

8. REFERENCES

1. Department of Minerals and Energy (DME) WA, 1999; Guidelines on the Safe Design and Operating Standards for Tailings Storage, May 1999.

2. Department of Minerals and Energy (DME) WA, 1998; Guidelines on the Development of an Operating Manual for Tailings Storage, October 1998.

3. Environmental Protection Agency (EPA), 1995; Tailings Containment, Best Practice Environmental Management in Mining, June 1995.

4. Fell, R., MacGregor, P. and Stapledon, D., 1992; Geotechnical Engineering of Embankment Dams, A. A. Balkema Publishers.

5. International Commission of Large Dams (ICOLD), 1995; Dam Failures Statistical Analysis, Bulletin 99.

6. International Commission of Large Dams (ICOLD), 1996; A Guide to Tailings Dams and Impoundments – Design, Construction, Use and Rehabilitation, Bulletin 106.

7. International Commission of Large Dams (ICOLD), 1996; Monitoring of Tailings Dams – Review and Recommendations, Bulletin 104.

8. International Commission of Large Dams (ICOLD), 1996; Tailings Dams and Environment – Review and Recommendations, Bulletin 103.

9. International Commission of Large Dams (ICOLD), 1989; Tailings Dam Safety – Guidelines, Bulletin 74.

10. Jewell, R.J., 1998; An Introduction to Tailings. Case Studies on Tailings Management, International Council on Metals and the Environment, November 1998.

11. Phillips, J., 1997; International Dam Standards. Proceedings of the International Workshop on Managing the Risks of Tailings Disposal, Stockholm, Sweden, May 1997.

12. Vick, S.G.; 1983; Planning, Design and Analysis of Tailings Dams; John Wiley & Sons Inc., 1983.

Finite Element Analysis of Deeply Buried Flexible Pipes

Sarah Elkhatib
GHD Pty Ltd, Perth, Western Australia

Summary Residue underdrains in tailings storage facilities are commonly buried under high fills. Flexible plastic pipes are normally used, the material being either PVC or HDPE. The performance of flexible pipes under large heights of tailings is relatively unknown. Guidelines for the design of buried flexible pipelines are presented in Australian Standard 2566.1. However, these are mainly for shallow burial of pipes. The main limitation of existing design methods is that the effect of arching is ignored. Many pipe designers use the prism load routinely even when considerable arching occurs. This often leads to conservative designs which are not cost-effective. A new bauxite residue disposal area to be developed at Worsley in Western Australia was used as a case study. The residue underdrains will be buried under 70 m of tailings and therefore subjected to very high overburden pressures. Due to the limitations of existing design methods, finite element analysis (FEA) was used to model the pipes. FEA can simulate the complex interaction between the pipe and soil more accurately than other methods. Several factors which influence the structural performance of flexible pipes were examined and the results are presented in this paper. The advantages of using FEA over conventional design methods are discussed.

1. INTRODUCTION

A network of slotted pipes is generally required for the collection and removal of liquor from residue storage facilities. The residue underdrains are commonly flexible pipes buried under high fills.

Buried flexible pipelines can be designed using various methods available in the literature. However, most of the conventional design methods have limitations. They are primarily for shallow burial of pipes, and so are inappropriate for residue storage applications. A more appropriate procedure for simulating the complex interaction between the pipe and soil is finite element analysis (FEA).

A new bauxite residue storage facility at Worsley in Western Australia was used as a case study. The residue underdrains, which will ultimately be buried under 70 m of tailings, were designed using FEA.

This paper presents the results of the modelling carried out and discusses the influence of several factors on the structural performance of the deeply buried pipes. The results from FEA are compared to ones calculated using conventional design methods and a discussion of their limitations is provided.

2. OVERVIEW OF WORSLEY ALUMINA

The Worsley Project lies in the Darling Ranges in the south-west of Western Australia. It is located 200 km south of Perth and 50 km east of Bunbury on the headwaters of the Augustus River. The production of alumina at Worsley is expected to double from 1999 to 2000. Consequently, this will lead to an increase in residue production that will exceed the storage capacities of the existing disposal areas. This identified the need to develop another facility to store the residue.

The two general areas used for the disposal of residue are the Northern Valley and the Southern Valley. The Northern Valley contains the existing five bauxite residue disposal areas (BRDA 1, 2, 3, 4, and 4X), as shown in Figure 1. The new residue disposal area, named BRDA 5, is located in the Southern Valley.

BRDA 5 will be the largest of all the residue disposal areas when developed to its ultimate stage. It will be approximately 70 m in depth, occupy an area of 450 hectares and store 185 million m^3 of residue.

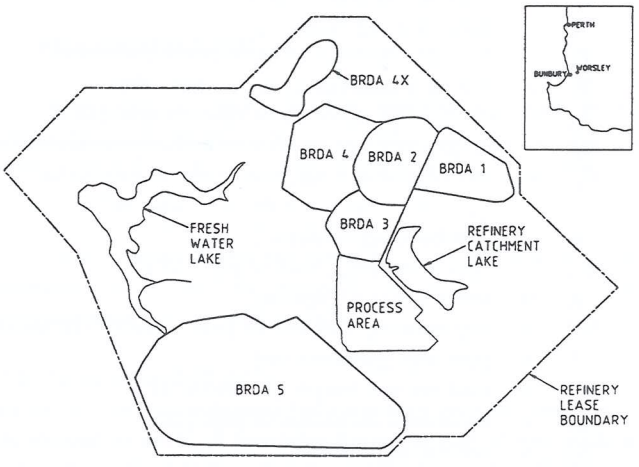

Figure 1: Site plan of the Worsley Alumina Refinery

The underdrainage blanket on the floor of BRDA 5 consists of the layers illustrated in Figure 2. A clay blanket of low permeability overlies the foundation and is designed to prevent seepage of contaminated liquor into the groundwater stream. The clay blanket is overlain by a highly permeable gravel blanket and a network of residue underdrains. At ultimate development, the underdrains will total approximately 75 km in length. The pipes are designed to collect and remove liquor, thereby increasing residue strengths, and reducing the pressure head across the clay liner, and hence minimising contaminant leakage. The pipes are surrounded by a gravelly backfill. The trench backfill and the clay fill are referred to as the embedment and native soils respectively.

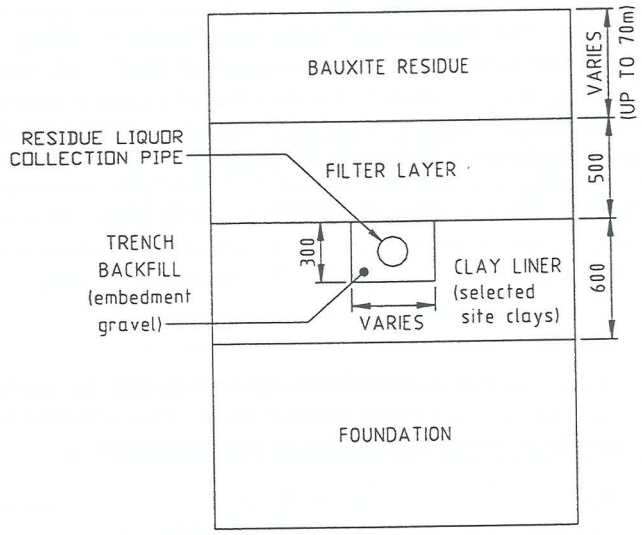

Figure 2: Illustration of underdrainage system of BRDA 5

3. NOTATION AND UNITS

The following symbols are used in this paper.

B	=	trench width [m]
C'	=	soil cohesion [kPa]
D	=	Mean diameter of pipe [m]
D_e	=	external diameter of pipe [m]
D_L	=	deflection lag factor [-]
E_e	=	Young's modulus of embedment soil [kPa]
E_n	=	Young's modulus of native soil [kPa]
E_p	=	modulus of elasticity of pipe material [kPa]
E_e'	=	modulus of soil reaction of embedment soil [kPa]
E_n'	=	modulus of soil reaction of native soil [kPa]
I	=	moment of inertia of the pipe wall [m^4/m]
K	=	pipe bedding constant [-]
P_{cr}	=	critical buckling load of pipe [kPa]
R	=	mean radius of pipe [m]
SN	=	ring-bending stiffness of pipe (= EI/D^3) [kN/m/m]
T	=	pipe wall thickness [m]
W	=	load per unit length of pipe [kPa]
Δx	=	horizontal deflection of pipe [m]
Δy	=	vertical deflection of pipe [m]
ϕ	=	soil friction angle [degrees]
γ	=	unit weight of soil [kN/m^3]
ν	=	Poisson's ratio [-]

4. DESIGN CRITERIA

For buried flexible pipes, the main failure modes which need to be considered are excessive deflection, circumferential bending strain and wall buckling (Moser, (1)).

4.1 Deflection

Deflections caused by the weight of the overlying fill can be the governing criterion in the design of buried pipelines. Longitudinal deflection is usually not of concern. With careful placement of the bedding, the pipe does not sag. Ring deflection, however, is of great concern as it can lead to reversal of curvature of the pipe. It can cause leaks, reduce flow and also contribute to incipient collapse of the ring. Deflection limits vary for different pipe materials. For high-density polyethylene (HDPE) pipes, the recommended limit is 7.5%.

4.2 Bending Strain

When a pipe deflects under load, bending strains are induced in the pipe wall. Strain is related to deflection and so most pipe manufacturers specify installation techniques which will limit deflection and thus limit the strain. Poor installation can lead to localised deformations, which can influence the performance of the pipe. The recommended strain limit for HDPE pipes is 4%.

4.3 Buckling

Buckling may govern the design of pipes which have low stiffness and are subjected to high soil pressures. The actual pressure on the pipe can be compared with the allowable buckling pressure to obtain a factor of safety against buckling. Australian Standard 2566.1 (2) recommends a factor of safety of 2.5 be adopted against buckling.

The above parameters indicate that deflections and loads on pipes are of most importance. Limiting deflections can often limit strains and limiting the load on a pipe increases the factor of safety against buckling. As a result, these two parameters were the main ones investigated.

5. EXISTING DESIGN METHODS

One of the most important properties of flexible pipes is their ability to induce arching. Arching is the load redistribution which occurs when the pipe stiffness is different to that of the soil. The stiffness of most flexible pipes is less than the soil stiffness and so the overburden load (or prism load) is redistributed away from the pipe and into the adjacent soil. Theoretically, the load on a pipe will only be equal to the prism load if the pipe and soil have the same stiffness.

Several methods exist for the design of buried pipes, as discussed below. One of the major limitations in these conventional methods is the neglect of arching.

5.1 Spangler's Iowa State Formula

The Iowa State Formula was developed by Spangler (3) in 1941. Spangler incorporated the effects of the surrounding soil on the pipe's deflection. He modelled the vertical pressure on the pipe as a uniform distribution and the lateral

pressures as parabolic distributions. Through analysis he derived the following formula:

$$\Delta x = \frac{D_L K W r^3}{E_p I + 0.061 E_e' r^3} \quad (1)$$

The deflection lag factor, D_L, accounts for the fact that as a result of soil consolidation at the sides of the pipe, additional load may be expected on the pipe with time. A value ranging from 1.5 to 2.5 for D_L was originally proposed. However, due to the inherent conservatism in the formula, Moore (4) suggested that a value of 1.0 be used, but with the prism load rather than a load reduced because of arching. The bedding constant, K, varies with the bedding angle. However, a value of 0.1 is often assumed in the calculation.

Spangler did not go beyond the determination of the horizontal deflection. He assumed that the vertical deflection was always equal to the horizontal one. However, contrary to Spangler's assumption, in the case of very flexible pipes, the vertical deflection departs considerably from the horizontal one (Prevost and Kienow, (5)). Spangler's original work involved steel pipes with stiffness values significantly higher than that of HDPE. Therefore, use of Spangler's equation to predict Δx of HDPE pipes would yield unrealistic results (Jeyapalan and Abdelmagid, (6)).

The other inaccuracy in the Iowa state formula is the modulus of soil reaction, E_e'. This is a semi-empirical parameter required for input into the formula. Unfortunately, E_e' is not a true soil parameter and cannot be measured either in a laboratory or in the field. Efforts to develop tests to evaluate it have been largely unsuccessful. The most widely used E_e' values were developed by Howard (7) in 1977. Howard used Spangler's formula for back-calculating E_e' from field data. However, his values do not reflect the change in soil stiffness that occurs with increasing depth of fill.

5.2 Critical Buckling Loads

The use of Luscher (8) buckling theory is common in the design of buried plastic pipes. This approach used the modulus of soil reaction to characterise the soil support. The uncertainties associated in using this modulus are as discussed above. Luscher's buckling theory is a simplified analysis of the soil-pipe system as it ignores shear deformations in the soil.

A more rigorous approach considers the soil to behave as a continuum (Moore and Selig, (9)). For a flexible pipe supported by uniform ground of modulus, E_n, continuum buckling theory suggests that the critical buckling load can be calculated using the following formula:

$$P_{cr} = \frac{(E_p I)^{1/3} (E_n)^{2/3}}{D} \quad (2)$$

In contrast to the spring model, continuum theory employs modulus parameters with real physical meaning.

5.3 Australian Standard 2566.1

AS 2566.1 outlines guidelines for the design of buried flexible pipelines. The calculation of deflections is based on the Iowa formula. However, E_e' in the Iowa formula is replaced by an effective combined modulus which accounts for both the embedment and native soils.

Other limitations include the use of the empirical parameter E_e' and the assumption that Δx and Δy are equal, as discussed for the Iowa formula.

The calculation of the allowable buckling pressure using AS2566.1 is based on continuum buckling theory. However, the soil modulus, E_n, is replaced by an effective combined modulus.

5.4 Finite Element Analysis

FEA has been developed as a numerical method to solve complex problems in continuum mechanics. It permits a reasonably accurate treatment of the soil-pipe interaction problem. The soil mass around a pipe is set up as a mesh of soil elements and each element can be assigned different properties. Various loading conditions, sub-surface conditions and structural properties can be modelled mathematically, which is an advantage over physical testing of such structures.

Soil stiffness is defined using Young's modulus and Poisson's ratio, both which can be readily obtained using laboratory testing. The three design criteria that need to be checked can generally be obtained directly from FEA programs, eliminating the need to use inappropriate formulae. FEA also incorporates the effects of arching, yielding more realistic results regarding the interaction of the pipe and soil system.

6. DESIGN OPTIONS

Several design options were considered to obtain the most optimal design. The main variables were:

- the trench width;
- the embedment soil stiffness; and
- the pipe stiffness.

7. FEA MODELLING

The large array of pipes at Worsley and the magnitude of the loads they will be subjected to justifies the use of rigorous design procedures to ensure an adequate design is adopted.

Due to its advantages over conventional pipe design methods, FEA was used to model the complex soil-pipe system. The software used for the analysis is called FLAC (Fast Lagrangian Analysis of Continua).

7.1 Overview of FLAC

FLAC is a two-dimensional finite element program which was developed in 1986. It simulates the behaviour of soil, rock or other materials that may undergo plastic flow when their yield limits are reached. Materials are represented by elements which form a grid. Each element behaves according to a

prescribed linear or non-linear stress/strain law in response to the applied forces or boundary conditions.

7.2 FLAC Model

7.2.1 Geometry

Figure 3 shows the finite element mesh used in the analysis. Only one-half of the pipe was modelled due to symmetry.

FLAC is limited by a maximum mesh size. Accordingly, the vertical and lateral extents of the model are limited, and so the mesh size should be selected carefully in order to keep it within FLAC's capability without compromising the accuracy of the results. Therefore, the vertical depth of up to 70 m was simulated by assuming an appropriate residue height above the pipe and by substituting the remainder of the residue by an equivalent uniform surcharge load. The height above the pipe was large enough to ensure that the equivalent surcharge above this height has the same effect as the actual residue. The lateral extent of the mesh away from the pipe was also chosen such that the vertical boundary does not interfere with the stress conditions close to the pipe.

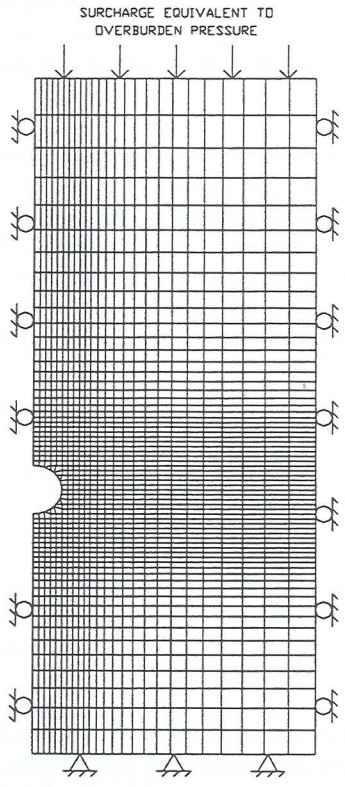

Figure 3: FEA mesh and applied boundary conditions used in the analysis

7.2.2 Soil Properties

Soil properties required for input into FLAC include the unit weight, cohesion, friction angle and bulk and shear moduli. The bulk and shear moduli were calculated from Young's modulus and Poisson's ratio. Table 1 shows the properties used for the analysis. When a different trench backfill was to be examined, only Young's modulus was varied. The remaining properties do not vary significantly for the materials considered. Also, they do not have a significant influence on the pipe's performance criteria and so were kept constant for simplicity.

Table 1: Soil parameters used in the analysis

Zone	γ (kN/m^3)	c' (kPa)	ϕ' (°)	E (MPa)	ν
Residue (unconsolidated)	20	0	35	20	0.3
Filter	20	0	35	20	0.25
Trench Backfill (embedment soil)	20	0	35	Varies (10-60)	0.25
Clay Liner (native soil)	17	5	32	60	0.3
Foundation	14.5	25	30	40	0.3

The primary materials considered for the trench backfill included lateritic gravel (E_e = 20–30 MPa) and crushed basalt (E_e = 60 MPa). Intermediate values were used in the analysis to account for slightly different materials that may be available on site and to establish relationships between soil stiffness and pipe performance criteria.

7.2.3 Pipe Properties

The pipe was modelled as a series of structural beam elements which were assumed to behave in a linear elastic manner. The parameters required for establishing the stiffness matrix of the pipe were Young's modulus, moment of inertia through the pipe wall and the cross-sectional area of the pipe wall.

Several pipe diameters were examined depending on the area that the pipe is servicing. The trends observed were consistent and so only results from the HDPE pipes with an external diameter of 100 mm are presented. Several pipe stiffnesses were considered and these are presented in Table 2. For all the pipes, E_p = 337 MPa.

Table 2: Properties of pipes used in the analysis

Pipe No.	t (mm)	I (m^4/m)	SN (kN/m/m)
1	2.5	1.3×10^{-9}	0.47
2	2.9	2.0×10^{-9}	0.72
3	3.3	3.0×10^{-9}	1.12
4	4.0	5.3×10^{-9}	2.03
5	5.0	1.0×10^{-8}	4.09
6	6.6	2.4×10^{-8}	9.91
7	10.0	8.3×10^{-8}	38.52

Note that whilst it was apparent that some of these pipes were too thin-walled to withstand high loads, they were included in the analysis to establish a relationship between the pipe/soil stiffness ratio and the pipe's structural performance.

7.2.4 Boundary Conditions

The boundary conditions specified are illustrated in Figure 3. Nodes lying on the bottom horizontal boundary were restricted from movement in both the horizontal and vertical directions. Symmetry is simulated by allowing only vertical movement of the nodes lying on the pipe centre-line. The nodes on the right vertical boundary were restricted from horizontal movement.

8. RESULTS AND DISCUSSION

8.1 Trench Installations

The installation of pipes in trenches can have a significant influence on the design of a buried pipe. Several factors need to be considered for pipes installed in trenches. These include the width of the trench and the stiffness of the trench backfill.

The effects were examined by modelling various trench widths, ranging from 1.6 pipe diameters to 4 pipe diameters. The soil embedment modulus, E_e, was also varied between 10 MPa and 60 MPa. Note that when $E_e = 60$ MPa, the model is effectively without a trench as $E_n = 60$ MPa also. This simulates an embankment type installation. The same pipe was used in all the models. This was a 100 mm HDPE pipe with a stiffness of 9.9 kN/m/m.

8.1.1 Deflections Using FLAC

Figure 4 illustrates the relationship between the trench widths and vertical deflections of the pipe for various embedment soil moduli. It shows that deflections are sensitive to both criteria, especially at lower values of soil modulus. A soft backfill does not provide as much support for the pipe enabling the pipe to deflect more vertically and laterally. This emphasises the importance of careful selection of the trench backfill material and the compaction effort.

The vertical deflections also increase as the trench width increases. The trench walls, where an increase in soil stiffness is encountered (from the embedment to the native soils), are further away from the pipe and so the influence of the stiffer native soil in supporting the pipe is reduced.

Note that except for $E_e = 10$ MPa, all the cases considered resulted in deflections less than 7.5%.

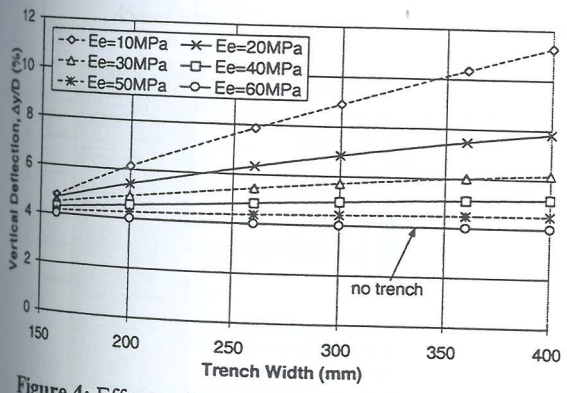

Figure 4: Effects of trench width and backfill on vertical deflections

The horizontal deflections were also calculated and they showed that deflection ratios (ie $\Delta y/\Delta x$) were always greater than unity for the soil and pipe combinations considered. For stiffer embedment materials, the deflection ratio was found to be higher than for softer materials. The ratios ranged from 1.5 (for $E_e = 10$ MPa and $B = 4D_e$) up to 5 (for $E_e = 50$ MPa and $B = 1.6D_e$). This confirms that the Iowa formula for calculating deflections is not adequate, as it assumes that the vertical and horizontal deflections are equal.

Note that the trends observed are only for cases where the native soil is stiffer than the embedment soil. If the embedment material were stiffer, then a wider trench would result in smaller deflections. Such cases were considered in the analysis to account for the variability of the soils on site. However, those results are not presented.

8.1.2 Deflections Using Conventional Methods

The vertical deflections obtained from FLAC were compared to those calculated using both Spangler's formula and AS2566.1. The results are illustrated in Figure 5. The results are shown for a soft backfill ($E_e = 10$ MPa) and a stiff backfill ($E_e = 50$ MPa).

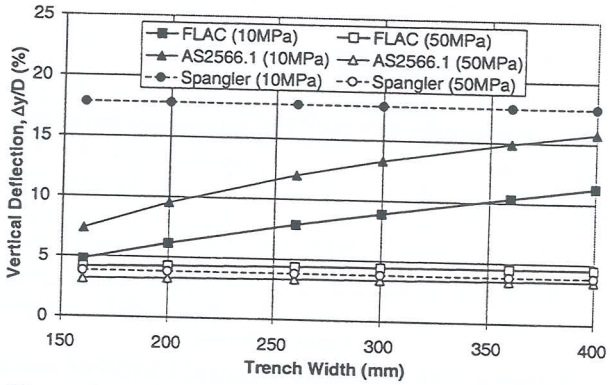

Figure 5: Comparison of FLAC with conventional methods

For a soft backfill, Spangler's equation significantly overestimates deflections as it does not account for the support provided by the stiff native soil. AS2566.1 appears to follow the same trend as FLAC, however, the deflections are still overestimated for the soft backfill case. Note that Spangler's equation gives a constant value regardless of the trench width. The results from FLAC and AS2566.1 appear to converge with Spangler's results as the trench width increases. This is a result of the native soil having less influence on the behaviour of the pipe as the trench width increases. Note that for $E_e = 10$ MPa, even the narrowest trench does not satisfy the deflection constraints when calculated using conventional methods.

For a stiff backfill, both Spangler's equation and AS2566.1 underestimate deflections. However, the difference is not as significant as for the soft backfill, and they were all less than 7.5%.

8.1.3 Strains

Bending strains were calculated for each of the cases considered. Trends observed indicate that strains increase as the embedment soil stiffness decreases. However, the strains were always less than 4%. HDPE pipe can tolerate high strains resulting from its deformation because of its ductility, and so pipe strain was not the governing criterion in the design of the pipes.

8.1.4 Buckling

Whilst Figure 4 indicates that with respect to deflections, ideally a narrow trench with stiff backfill is the best combination for design (only if the native soils are stiffer than

the embedment soils), this has to be compromised with the buckling criteria of the pipe. Figure 6 illustrates the relationship between the vertical load on the pipe and trench widths for various embedment moduli.

As the flexible pipe undergoes vertical deflection, the soil above it tries to follow the pipe downwards. However, the soil's movement is resisted by shear resistances along the trench walls. Movement along these slippage surfaces is resisted by the soil's shear resistance, which brings about an active state in the soil above the pipe. Through this action, part of the weight of the backfill is carried over into the trench walls.

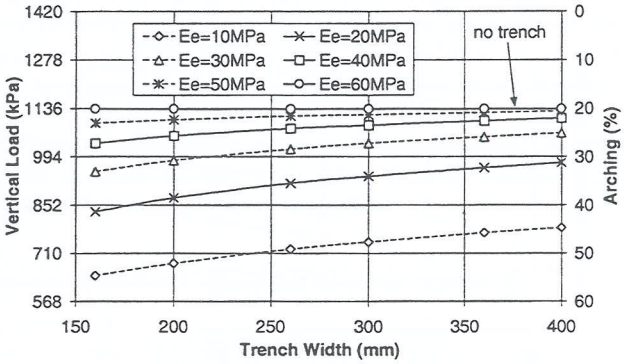

Figure 6: Effects of trench width and backfill on arching

Figure 6 indicates that the embedment soil stiffness significantly influences the load on the pipe. As the soil stiffness decreases, more load is redistributed away from the pipe. A softer soil results in higher pipe deflections and more soil compression. This mobilises an active state in the backfill and load is shed to the stiffer soils.

Arching in excess of 50% was observed. The critical buckling loads were calculated using continuum buckling theory and then compared to the reduced loads on the pipe to obtain factors of safety against buckling. The cases with soft backfill (ie 10 MPa and 20 MPa) failed the buckling criteria. Cases with a trench width greater than $3.5D_e$ also failed.

Factors of safety calculated using the prism load rather than the reduced load, were generally always less than 2.5, and so failed the buckling performance criteria. Note that using the prism load will always result in lower factors of safety, and hence, AS2566.1 will lead to conservative designs.

8.1.5 Stress and Displacement Contours

Figures 7(a) and 7(b) show the vertical stress distributions and vertical displacement contours for the two different pipe installations: one in a trench (E_e = 20 MPa and 200 mm trench width) and the other without a trench (E_e = 60 MPa).

Figure 7(a) illustrates how load is distributed to the stiffer native soil. The lowest stresses occur at the pipe crown where the greatest displacements occur. Soil compression is significant above the pipe, also assisting in load redistribution.

Figure 7(b) illustrates the case without a trench. Minimum stresses occur at the pipe invert and crown. However, a significant load increase is observed in the soil directly adjacent to the pipe. Note also that vertical displacements of the soil are almost uniform across the model.

8.1.6 Vertical Loads on Pipe

Figure 8 shows the vertical stresses in the soil across a plane above the pipe for a few of the cases with trenches and the case without a trench. The minimum stresses occur at the pipe crown. Also shown is the prism load at approximately 1420 kPa (equivalent to 71 m of overburden height). The stress at the crown of the pipe is approximately 600 kPa, indicating that arching in excess of 50% occurs. A local maximum occurs at the pipe springline. This varies for the different trench widths. Away from the pipe, the stresses then reduce until the trench wall is encountered. A significant increase is observed due to the sudden increase in soil stiffness. The increase exceeds the prism load to counteract the load reductions above the pipe. The stresses then decrease gradually and approach the prism load further away from the pipe.

Note that Spangler's assumption of uniform vertical pressures on the pipe is incorrect.

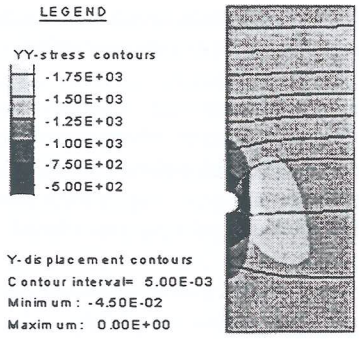

(a) Pipe in 200 mm trench

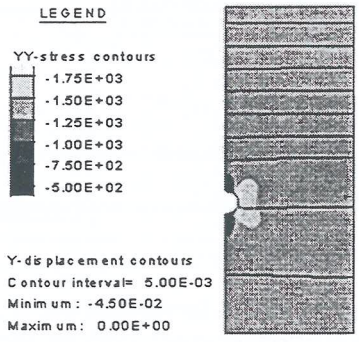

(b) Pipe without trench

Figure 7: Stress and displacement contours for different pipe installations

The case without the trench exhibits different trends. Whilst the stress above the pipe crown is also at approximately 600 kPa, it increases significantly over the radius of the pipe, and reaches a maximum (in excess of the prism load) at the pipe springline. The stresses then gradually decrease until the prism load is reached.

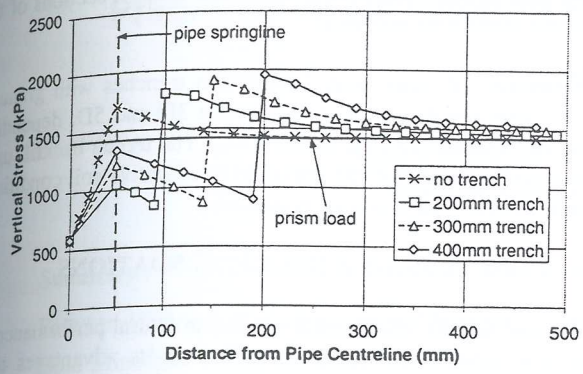

Figure 8: Vertical stresses acting on a plane above the pipe

8.2 Pipe and Soil Stiffness

The stiffness of a pipe and soil system plays an important role in the design of flexible pipes and is the main variable influencing arching around a pipe.

Several pipe stiffnesses were considered in the design of the residue underdrains. The embedment soil was also varied to determine the best combination of pipe and trench backfill for the underdrainage system. The trench width used for this study was kept constant at 200 mm.

8.2.1 Deflections Using FLAC

Figure 9 illustrates the relationship between pipe stiffness and deflections for various soil moduli. As would be expected, an increase in pipe stiffness results in smaller vertical deflections of the pipe. Also, an increase in the embedment soil modulus results in smaller deflections.

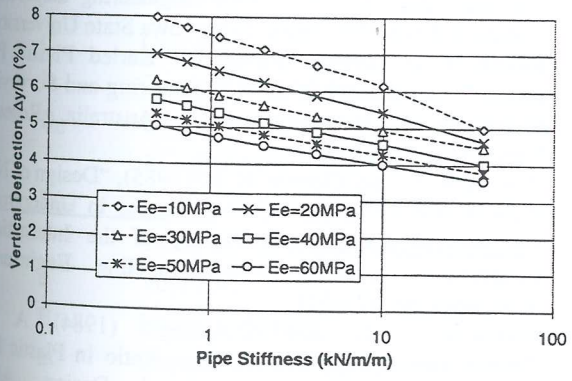

Figure 9: Effects of pipe and soil stiffness on deflections

Horizontal deflections were also calculated for all the cases. The ratio of vertical to horizontal deflection of the pipe increases significantly with the decrease in pipe stiffness and increase in soil stiffness. Again, the deflection ratios were greater than unity for all the cases considered.

8.2.2 Deflections Using Conventional Methods

The vertical deflections calculated by FLAC were compared to those calculated using conventional methods. The results are illustrated in Figure 10. The same trends were observed as for the previous case. For soft backfills, both the conventional methods overestimate deflections significantly, resulting in deflection in excess of 7.5%. For stiff backfills, both methods underestimate deflections, but not significantly.

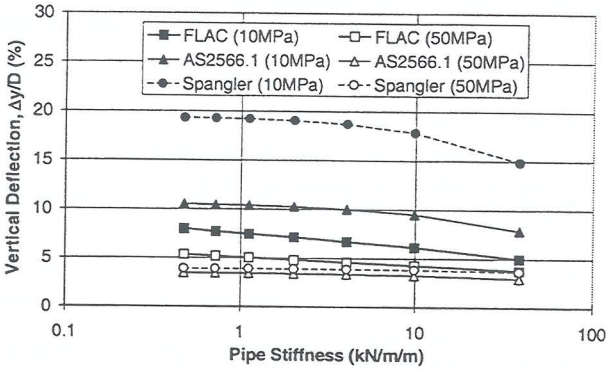

Figure 10: Comparison of FLAC with conventional methods

8.2.3 Strains

The strains were calculated for all the cases modelled and they were always less than the recommended limit of 4% for HDPE pipes, and so this was not a governing factor in the selection of the pipes.

8.2.4 Buckling

Figure 11 illustrates the relationship between arching and pipe stiffness for various soil moduli. As the pipe stiffness increases the pipe attracts more load. This is a result of the smaller deflections of the pipe. When a pipe deflects, the soil directly above it is mobilised. As the stiffness of a pipe increases, it deflects less and consequently, less backfill is mobilised, resulting in more load on the pipe.

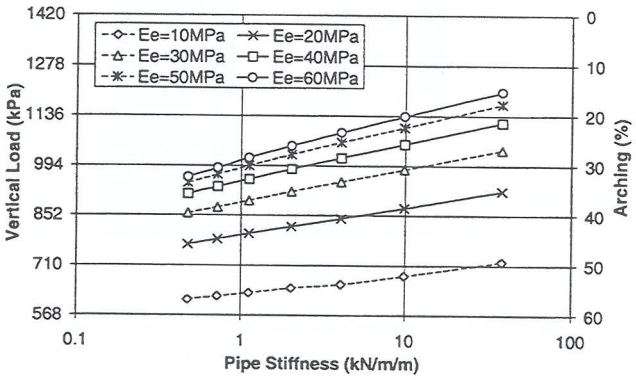

Figure 11: Effects of pipe and soil stiffness on arching

For low values of soil modulus (ie 10 MPa), arching in excess of 50% was observed. Figure 11 indicates that arching is more dependent on the surrounding soil than the pipe stiffness.

Based on the loads shown in Figure 11, the factors of safety against buckling were calculated. The thin-walled pipes, although subjected to lesser loads, generally failed the buckling criteria because their critical buckling pressures were too low. However, the three stiffest pipes were capable of

withstanding the loads imposed on them.

Calculating factors of safety using the prism load, rather than the reduced load, resulted in almost all the pipes failing the buckling criteria. This indicates that AS2566.1 would require stiffer pipes to be specified, leading to conservative designs.

8.2.5 Stress and Displacement Contours

Figures 12(a) and 12(b) show the vertical stress contours in the soil elements and their displacements. The figures illustrate the effects of increasing the pipe stiffness. All other properties were kept constant.

The stress contours show the load redistribution away from the pipe. Whilst most of the displacement contours appear to be the same, the one directly above the pipe is different. The stiffer pipe prevents the soil from settling as much and hence load transferral to the native soil is not as significant.

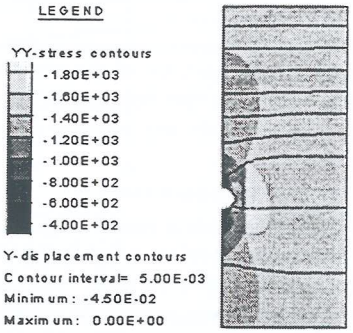

(a) Pipe stiffness = 0.47 kN/m/m

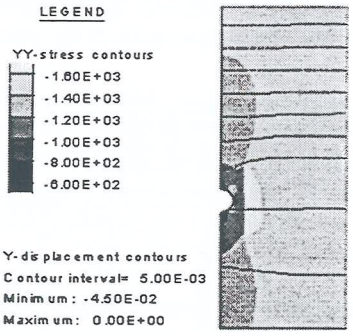

(b) Pipe stiffness = 10.0 kN/m/m

Figure 12: Stress and displacement contours for different stiffness pipes

It is important to recognise that the pipe stiffness plays a vital role in the successful design of flexible pipe-soil interaction systems. The field performance of a pipe would depend heavily on its ability to carry a portion of the load and encourage positive arching.

8.3 Adopted Design at BRDA 5

The detailed design adopted for BRDA 5 is not presented here due to its complexity. Pipes with different diameters were used depending on the area they are servicing. The pipe stiffness and material also vary depending on the location of the pipe in the valley. Obviously, the deepest sections of the valley require stiffer pipes.

Generally, all pipes were installed in trenches with granular fill. The trench widths vary between 3D and 5D, depending on the conditions of the native soils. The trench backfill used was well-graded lateritic gravel in good native soil conditions and crushed basalt in poor conditions.

9. CONCLUSIONS & RECOMMENDATIONS

Various factors which influence the structural performance of HDPE pipes were examined. Due to its advantages over conventional design methods, FEA was used for the analysis. The general trends observed indicate that the design of pipes is not simple. Several factors need to be considered. Whilst one variable may have a positive influence on pipe deflections, it may have a negative influence on wall buckling. All the criteria need to be considered for an optimal design to be reached.

Conventional design methods do not have sufficient variables to account for the complex interaction between the pipe, the granular backfill and the in-situ soil, and so can only provide a crude approximation of a pipe's performance. Such methods should only be used within the limits set by the assumptions made in their development.

10. REFERENCES

1. Moser, A. P. (1990), "Buried Pipe Design", McGraw-Hill.
2. AS/NZS 2566.1:1998, "Buried Flexible Pipelines - Part 1: Structural Design, Australian/New Zealand Standard.
3. Spangler, M. G. (1941), "The Structural Design of Flexible Pipe Culverts", Iowa Engineering Experiment Station Bulletin 153, Ames, Iowa: Iowa State University.
4. Moore, I. D. (1989), "Review of Buried Plastic Pipe Design", Department of Civil Engineering and Surveying, University of Newcastle, NSW, Australia, Research Report No. 039.05.89.
5. Prevost, R. C. and Kienow, K. K. (1985), "Design of Non-Pressure Very Flexible Pipe", Advances in Underground Pipeline Engineering, Proceedings of the International Conference on Underground Pipeline Engineering, Wisconsin, pp. 527-541.
6. Jeyapalan, J. K. and Abdelmagid (1984), A. M., "Importance of Pipe Soil Stiffness Ratio in Plastic Pipe Design", Pipeline Materials and Design, ASCE Convention, San Francisco, California, pp. 48-66.
7. Howard, A. K. (1977), "Modulus of Soil Reaction Values for Buried Flexible Pipe", Journal of the Geotechnical Engineering Division, ASCE, Vol. 103, GTI.
8. Luscher, U. (1966), "Buckling of Soil-Surrounded Tubes", Journal of Soil Mechanics and Foundation Engineering, ASCE, Vol. 192, No. 6, pp. 211-228.
9. Moore, I. D. and Selig, E. T. (1990), "Use of Continuum Buckling Theory for Evaluation of Buried Plastic Pipe Stability", Buried Plastic Pipe Technology, ASTM STP 1093, pp. 344-359.

Prediction of Dewatering Related Settlement in Waihi Township, New Zealand

Anthony Fairclough, M.IPENZ, NZGS, IAEG, ISSMGE, ISRM.
Geotechnical Engineer, URS Greiner / Woodward-Clyde.

Summary :

Between 1995 and 1998, Woodward-Clyde (NZ) Limited (WCNZ) conducted a settlement and rebound study of the Martha Gold Mine and Waihi township. The objective of this study was to support a resource consent application to extend the Martha pit.

Dewatering of the Martha pit has caused the groundwater level in most of the soil and rock layers immediately adjacent to the Martha pit to fall. Lowering of the general groundwater level has resulted in an increase in the level of effective stress within these soil and rock deposits. This increase in effective stress, and four other unrelated factors, has caused some of the soil and rock layers around the pit to consolidate resulting in settlement of the ground surface.

In order to estimate the magnitude of settlement and rebound that is likely to occur in Waihi due to operating and decommissioning the Martha pit, WCNZ completed an extensive program of research, investigation, laboratory testing and modelling. This paper summarises the methodology and results of this work.

While there has been a change in effective stress leading to some consolidation of the ground surface, dewatering of the Martha Pit has not caused any structural distress in the township, and engineering predictions indicate that no distress due to this cause is likely in the future. The magnitude of dewatering related settlement measured in Waihi Township is low compared to that measured in New Zealand and the United States at sites which have been affected by fluid extraction.

1.0 Notation

C	Cohesion.
D	Constrained modulus.
D_C	Constrained modulus of a soil or rock layer during initial consolidation.
D_{UR}	Constrained modulus of a soil or rock layer during unload and reload cycles.
e	Void Ratio.
E	Young's Modulus.
m_v	Coefficient of Compressibility.
s	Estimated settlement
t	Layer thickness
$\Delta \sigma'_v$	Change in effective stress at the centre of a soil or rock layer.
μ	Possions ratio
ρ_B	Bulk Density
$\varnothing$	Angle of friction.

Note: $D = 1 / m_v$ *

$D = E (1 - \mu) / \{ (1 + \mu) (1 - 2\mu) \}$ *

* After Lambe and Whitman (1979).

2.0 Introduction

Settlement of the ground surface due to the extraction of fluids such as groundwater, oil, gas, and geothermal water has been documented at numerous sites throughout the world.

The extraction of water from the ground, for either water supply or dewatering purposes, has resulted in ground settlement of more than 6 metres in Mexico City (Rivera *et al* 1991) and around 9 metres in the San Joaquin Valley, California (Johnson 1991).

Mine dewatering related settlement has been documented in New Zealand at the Huntly East Coal Mine. During 1983, an area of approximately 7 hectares experienced settlement of up to 800mm (Kelsey, 1985).

Historically, underground mining occurred at the Martha Mine from the late 1880's through to the early 1950's. Old mine records indicate that the underground workings extend to 457m below sea level (BSL). Dewatering of the old mine occurred to the maximum depth of the workings (McAra, 1988).

The Waihi Gold Mining Company Limited (WGC) has operated an open pit mine at the Martha Mine site in Waihi since 1989. Originally Martha Hill outcropped at 160m above sea level (ASL). Resource consents have recently been granted allowing the Martha pit to extend to a depth of 95m below sea level (BSL). The location of the Martha pit is shown on Figure 1.

The Martha pit has been progressively excavated and dewatered over the last ten years and, as at June 1999, the pit excavation extended to a level 10m ASL. Since 1989, the groundwater level has been held at a level 5 to 20 metres below the base of the pit excavation by pumping. This has caused the groundwater level in most of the soil and rock layers adjacent to the pit excavation to fall.

Lowering of the general groundwater level around the pit has increased the magnitude of effective stress within the dewatered zones. This has caused some of the soil and rock layers adjacent to the Martha Pit to consolidate. Monitoring has shown that dewatering of the Martha Pit has not adversely affected buildings or services within Waihi Township. Engineering predictions also indicate that buildings or services are unlikely to be damaged as a result of mine dewatering.

In addition to mine related settlement, four other causes of settlement were identified in Waihi Township:

i) Natural consolidation settlement of fill and the underlying natural soils;

ii) Cyclical shrinkage and swelling, of the near surface soils, due to rainfall and changing soil moisture levels;

iii) Movement or collapse of historic mine workings; and;

iv) Consolidation of upper soil layers due to reduced water infiltration.

Considerable work was undertaken to evaluate these, and separate their effects from the mine related settlement.

A percentage of the settlement due to mine dewatering is recoverable if the groundwater level is allowed to recover after the pit is decommissioned. As the groundwater level rises, the effective stress levels will decrease, and a proportion of the settlement will be recovered through rebound.

3.0 Study Approach

The settlement and rebound study was conducted in eight stages.

The first stage of the study was a review and analysis of all the available data. This included a review of published and unpublished maps, reports, aerial photographs, historical records and survey data.

The second stage of the study was the development of plans summarising the settlement measured in Waihi Township, and preliminary two dimensional geological, geotechnical and hydrogeological models. During this stage of the study, areas of insufficient data and areas of high or unusual settlement were identified.

The third stage of the study comprised field investigations and laboratory tests targeted to address information gaps.

The fourth stage of the study was the generation of detailed two dimensional geological, geotechnical and hydro-geologic models, and a detailed analysis of these models in conjunction with the measured settlement and rainfall data. During this stage, a preliminary estimate of the potential settlement and an interim report was completed.

The fifth stage comprised additional field investigations targeted to confirm the extent of the potentially compressible layers, confirm the geotechnical characteristics of key units, and clarify issues identified during stage four of the study.

The sixth stage of the study was the development and refinement of simple one-dimensional geotechnical models. These models were constructed using records of drillholes, readings from groundwater piezometers installed within these drillholes, and laboratory data. The stiffness properties of the different geologic units were refined using the one-dimensional models by comparing predictions of surface settlement made by the models to measured survey data.

The seventh stage of the study was the development of a finite element model along a section through the Martha Mine and Waihi Township. This was achieved using the computer program "Plaxis" (Version 6), the geological, geotechnical and hydrogeologic cross-sections, and geotechnical data from the refined one-dimensional models. Where possible, measured groundwater profiles were used in the finite element models, however, the

maximum number of layers able to be modelled by Plaxis version 6 is ten. Because of this, adjacent geologic units with similar geotechnical properties were modelled as a single layer. The groundwater profiles in these combined layers were initially estimated using field measurements, and then refined by comparing predictions of surface settlement with survey data.

Finally, the refined one dimensional and finite element models were used to predict settlement and rebound due to operating and decommissioning the Martha Mine. By subtracting the predicted rebound from the predicted settlement, an estimate of the permanent ground surface settlement was made.

4.0 Geologic Summary

The near vertical ore-bearing vein systems that originally outcropped on Martha Hill are located within andesite. The andesite is overlain to the east, south and west of the Martha pit by younger ignimbrite, ash, tuff, and alluvial deposits which, in places, are overlain by fill.

For the purposes of the settlement and rebound study, the geological units present at Waihi were grouped into three main deposits according to their geological and geotechnical characteristics. These units were :

i) Older deposits comprising andesite and altered andesite,

ii) Younger Deposits comprising ignimbrite, ash, tuff and alluvial deposits, and,

iii) Man-made Deposits comprising fill.

Figure 2 shows a typical subsurface distribution of the geological units under Waihi Township. Several cross-sections were developed using published maps, field observations and machine drillhole information.

The overall strength of the older deposits is relatively high, and this, together with the fact that they have previously been dewatered, means that they are relatively incompressible.

The overall strength of the younger deposits is highly variable and the unconfined compressive strength of these deposits range from >100 MPa (welded ignimbrite) to <0.1 MPa (alluvium). Most of the younger deposits comprise materials which will consolidate if dewatered or depressurised.

In many locations within Waihi Township, particularly adjacent to historic mine workings and railways, there are man-made deposits of unconsolidated to poorly consolidated fill. In addition, many old swamps have been drained or filled, and the land used for residential development. Most of the man-made deposits are still undergoing post depositional consolidation, or are causing the consolidation of underlying natural deposits independently of the current mine workings.

5.0 Hydrogeologic Summary

The permeability of the materials encountered at Waihi appear to be largely dependant on defect and fracture frequency in the case of welded materials or rock, and on porosity in the case of a soil. For the purposes of the settlement models, the geological units were broken into three groups of comparable permeability :

i) Highly to moderately permeable. Unaltered andesite and welded ignimbrite fall in to this group. The fractures in these units were generally open and moderately widely to widely spaced in the andesite, and closely spaced in the welded ignimbrite. The boulder alluvium is also highly permeable. This unit comprises cobbles and boulders in a silt, sand and gravel matrix.

ii) Moderate to low permeability. The geological units that fall into this group are the unwelded to moderately welded ignimbrite, ash and tuff deposits. The fractures in these units are very widely spaced, tight, and poorly interconnected. Some of the silty and sandy alluvial layers had a low to medium permeability and are also included in this group.

iii) Low permeability. The units in this group include the altered andesite and clay alluvium layers.

Under Waihi township, the presence of an almost continuous layer of low permeability altered andesite, on the surface of the older deposits, separates the older and younger deposits into separate groundwater regimes.

Historic underground mining dewatered the andesite rocks under Martha Hill and Waihi Town via a system of stopes, shafts and drives. This dewatering only drained those overlying younger deposits able to drain through the altered andesite cap into the andesite. Drainage of the younger deposits was, therefore, mainly limited to areas

immediately around the shafts and drives that penetrated the younger deposits.

When historic mining ceased in 1952, pumping stopped and the groundwater levels returned to an elevation close to the ground surface. Re-establishment of the groundwater level within the dewatered younger deposits almost certainly resulted in a partial rebound of the ground surface.

Data from piezometers, installed prior to mine dewatering recommenced in 1989, shows that the groundwater level in 1988 was close to the ground surface in all layers.

Piezometric and survey data indicates that the present day limit of groundwater draw-down (and mine related settlement) is approximately 700 metres north, 2000 metres east, 1200 metres south and 400 metres west of the Martha pit. Within the andesite, these limits appear to correspond with the location of major structural faults.

Piezometric data indicates that the water level in the andesite rock immediately adjacent to the Martha pit has been drawn down to a level similar to the dewatering pump intake in the old Waihi No.7 shaft. The groundwater level measured in piezometers within andesite layers generally rises as the distance from the pit increases. Piezometers installed within altered andesite indicate that the piezometric pressure within this unit is variable and the unit is only locally drained via the historic underground workings.

Piezometers within the ignimbrite, ash, tuff and alluvial layers indicate that the groundwater level within the younger and man-made deposits follow a separate regime to the underlying older deposits.

The welded ignimbrite layer appears to have been dewatered to a level which is controlled by the units exposure in the Martha pit wall. Some recharge of this unit appears to occur via infiltration from overlying layers, and through outcrops of welded ignimbrite in the beds of streams.

Piezometers in the pumiceous ignimbrites, ash and tuff layers, that underlie the welded ignimbrite, indicate that the groundwater levels within these units are variable and are only drained locally.

Piezometers in the fill, alluvium and boulder alluvium layers, analysed in conjunction with rainfall data and six-monthly survey data, indicate that the groundwater level in these layers is controlled by :

i) the lowest level of the unit concerned exposed in the Martha pit wall,

ii) rainfall recharge, and,

iii) under-draining of the surface boulder alluvium by the welded ignimbrite layer.

6.0 Geotechnical Summary

Review and analysis of historic, survey, rainfall, geological and geotechnical data identified five physical processes that produce settlement of the ground surface within Waihi Township. In most areas at least three of these causes of settlement occur simultaneously. The five settlement processes which were identified are :

i) Natural consolidation settlement of fill and the underlying natural soils;

ii) Cyclical shrinkage and swelling, of the near surface soils, due to rainfall and changing soil moisture levels. At some locations, seasonal shrink and swell of ±20mm has been measured;

iii) Movement or collapse of historic mine workings such as the Milking Cow block cave;

iv) Consolidation of upper soil layers due to reduced water infiltration. This reduced infiltration is due to a combination of :
   - El Nino weather patterns and a lower than average rainfall over the five or six years prior to the study;
   - the installation of sewage and storm water reticulation systems in Waihi township since the mid 1980's;
   - the clearing or modification of streams; and;
   - the local removal of vegetation.

v) Dewatering of the present day Martha Mine.

Settlement caused by i, ii and iii frequently results in differential settlement and damage to settlement intolerant structures. The consequences of settlement causes iv and v are usually regional, more subtle in nature, and therefore less destructive.

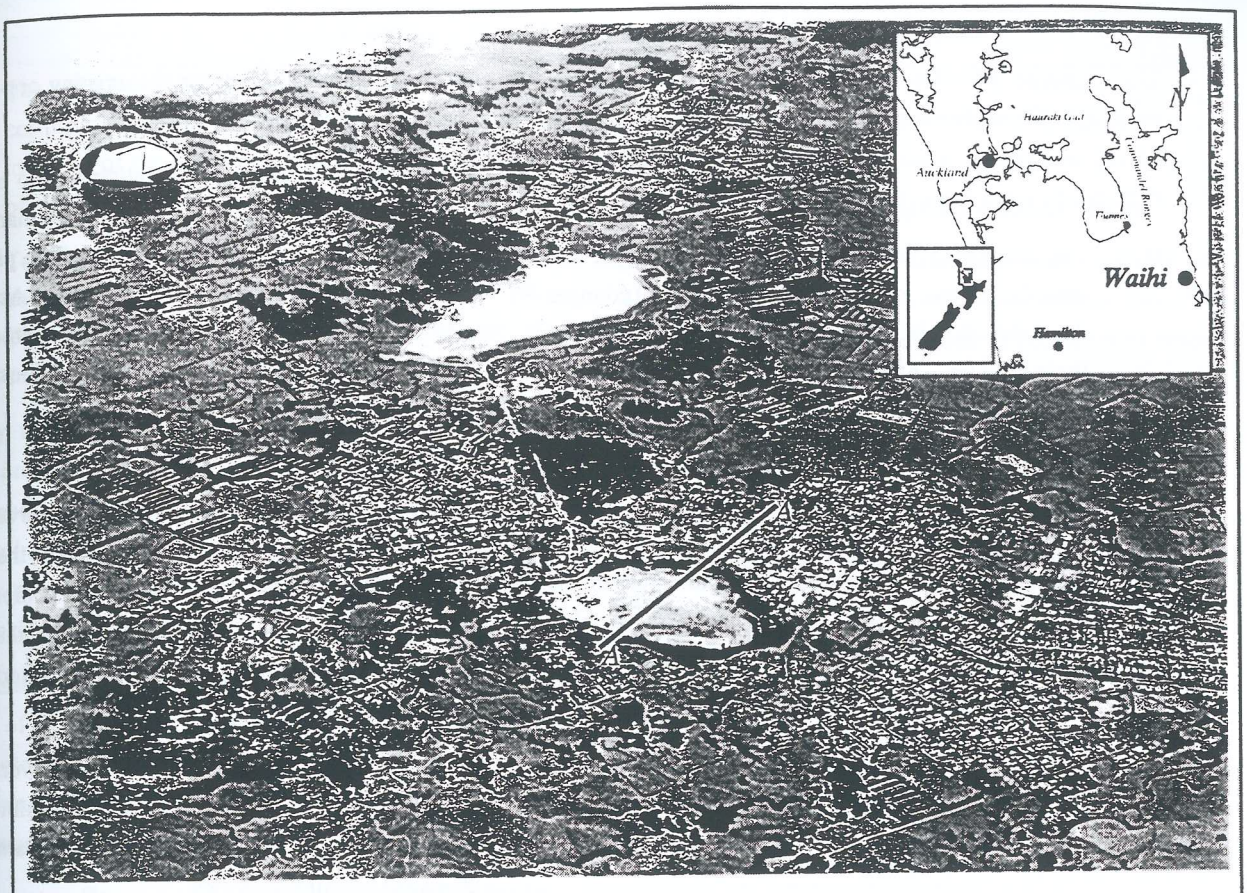

FIGURE 1
Location Plan

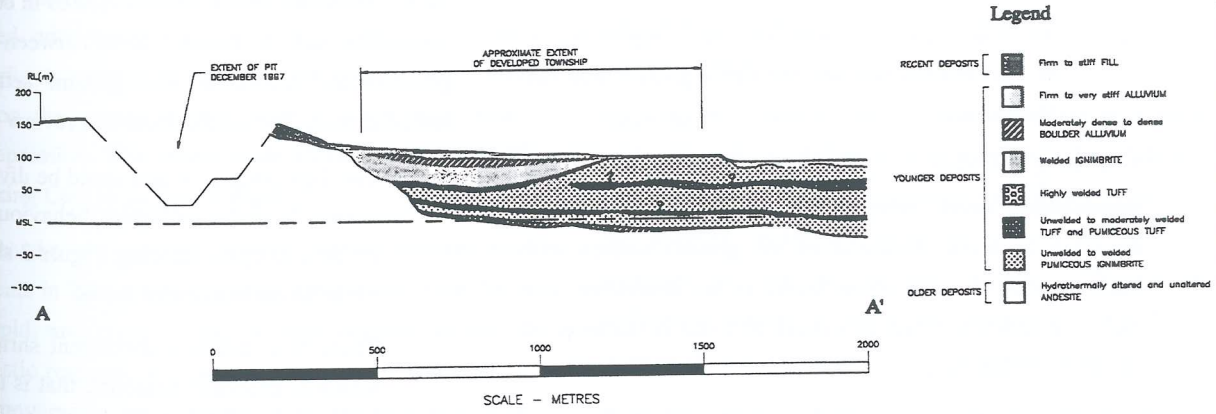

FIGURE 2
Typical Geological Cross Section A-A'
(Refer to Figure 1 for location)

The results of the geological and geotechnical investigations, observation of laboratory tests, analysis of survey monitoring results, and the analysis of laboratory tests results are summarised below :

i) The calculated pre-consolidation pressures of the ignimbrite, tuff, ash, and alluvial layers (younger deposits) underlying Waihi Township suggest that these layers had not undergone significant consolidation during historic dewatering.

ii) Many of the unwelded to poorly welded ignimbrite samples tested in the laboratory exhibited low to moderate consolidation characteristics up to a critical pressure. Once this critical pressure is exceeded the samples exhibit moderate to high consolidation characteristics. Observations of laboratory tests indicate that this critical pressure appears to reflect the collapse strength of pumice within the material, and welding of the material, rather than preconsolidation of the material;

iii) The pumiceous ignimbrite and tuff layers are brittle and compressible once critical pressures are exceeded;

iv) Some of the welded ash layers are brittle and moderately compressible once critical pressures are exceeded;

v) In places, the alluvium and fill layers are highly compressible;

vi) Most of the near surface cohesive alluvial soils are susceptible to cyclical shrink and swell;

vii) The consolidation coefficient of compressibility (m_v) is between two and ten times greater than the rebound m_v.

Following the eventual pit closure, and recovery of the groundwater level, rebound of the ground surface is expected to occur. Rebound of the ground surface will occur as the effective stress levels in the dewatered soil and rock layers decrease as a result of a rise in the level of the groundwater table.

Settlement developed during operation of the Martha pit is unlikely to be fully recovered for two reasons :

a) Most of the younger alluvial and man-made deposits are normally consolidated. Soil stresses, as a result of dewatering the Martha pit, are anticipated to exceed the existing pre-consolidation pressure in some locations.

b) The final lake level is anticipated to be around RL 104 m ASL. This represents a permanent lowering of the groundwater table around the pit and Martha Hill by between 0 and 30 metres. As a result, the original effective stresses in the ground will not fully recover to pre-existing conditions.

7.0 Settlement Monitoring Data

WGC has measured a network of 180 survey pins, on a six-monthly basis, since dewatering of the Martha pit commenced in 1989. This network comprises surface settlement marks which were installed throughout the township before major excavation or dewatering of the pit commenced.

In addition, several close order survey networks have been established around buildings which exhibit cracks, or properties whose occupants or owners claim have been damaged by mine activities.

The close order survey networks comprised a combination of piezometers and closely spaced survey pins. Survey pins were installed at a spacing less than 50 metres across properties and around buildings. Deep seated and near surface survey pins were installed to separate mine related settlement from the other causes of settlement which were known to be present in Waihi.

Six-monthly pit contour plans, and the corresponding survey monitoring data, were reviewed in conjunction with piezometer data to identify links between pit operations, groundwater movement and ground settlement in the township area. The results from this review indicated that:

i) The Township of Waihi could be divided into seven zones of similar settlement behaviour demonstrated by the survey monitoring. Figure 3 shows the extent of the seven settlement zones

ii) There is a moisture dependent shrink-swell cycle, which is generally seasonal, that is unrelated to the mining operations;

iii) It was observed that ground movements occur rapidly, and many of the younger deposits exhibit a near-elastic response to changes in the groundwater level.

iv) The periods of greatest settlement usually correspond with pit wall cutbacks that result in a lowering of the exposure of younger deposits in the pit wall.

v) To date, the measured settlement has not been consistent, or symmetrical, around the Martha pit. The complex geology surrounding the pit is considered to be the main reason for this.

Survey results indicated that settlement Zones 1 and 2 were probably unaffected by mine dewatering related settlement. In Zones 1, 2 and 3, settlements appear to be predominantly controlled by cyclic variation of the soil water content, with some settlement due to mine dewatering in Zone 3.

Settlement within Zones 3 to 7 is due to a combination of any 5 of the causes of settlement previously discussed in the geotechnical summary. Of Zones 3 to 7, Zone 3 is the zone least affected by mine dewatering and Zone 7 is the zone most affected by mine dewatering.

Settlement in Zones 4 to 7 appears to be primarily due to changes in the groundwater level caused by present day mining activities. Survey data indicates that considerable seasonal fluctuations are also present in these zones. The settlement in Zone 7 is primarily due to the combined effects of mine dewatering and stress redistribution within the Milking Cow block cave.

The Milking Cow is an historic block cave feature. Old mine records indicate that this underground excavation is over 300 metres deep, and was extensively mined and backfilled with waste soil and rock between 1910 and 1945. Prior to present day mining, the Milking Cave was visible on the ground surface as a 20 metre deep water filled depression. The approximate location and extent of the Milking Cow is shown on Figure 3

To date, the six-monthly survey results indicate that settlements in Zones 4 to 7, due to mine dewatering, have been rapid, and many of the younger deposits exhibit a near-elastic response to changes in the groundwater level. These movements are expected to be partially recovered when the pit is decommissioned and the pit-lake reaches its final level.

In all settlement zones, differential settlement, unrelated to mine dewatering, can be expected due to the local occurrence of unconsolidated alluvium, fill or rock outcrops, which respond differently to changes in load, rainfall recharge and surface water conditions.

8.0 One Dimensional Geotechnical Models

Once the soil property data had been collated and analysed, and the soil and rock characteristics identified, work focused on the development of geotechnical models which could be used to estimate settlement and rebound of the ground surface due to operating and decommissioning the Martha pit.

Preliminary one dimensional geotechnical (POD) models were initially constructed for several drillhole locations using :

a) borehole logs;

b) geotechnical laboratory data; and

c) measured piezometric levels.

For all one-dimensional models, the following equation, originally developed by Terzaghi during the 1930's, was used to estimate the settlement of each layer :

$$s = m_v \times t \times \Delta\sigma'_v \quad \text{(Lambe \& Whitman, 1979)}$$

The estimated settlements, for all the layers encountered in a drillhole, were summated to provide an estimate of the ground surface settlement.

The values of m_v used in the POD models were selected based on the layer material types, and the mid-layer effective stress, both before and after dewatering. Estimates of the material properties were obtained from the results of laboratory tests.

Once the POD models had been constructed, an estimate of settlement was made using piezometric readings taken in December 1995. These predictions were then compared to the average settlement measured around the drillhole locations by the six monthly surveys. The average difference between the actual and estimated settlement due to mine dewatering was found to be approximately 30%.

Next, the values of material stiffness (m_v) used in the POD models were refined so that the difference between the measured and estimated settlement was less than 10%.

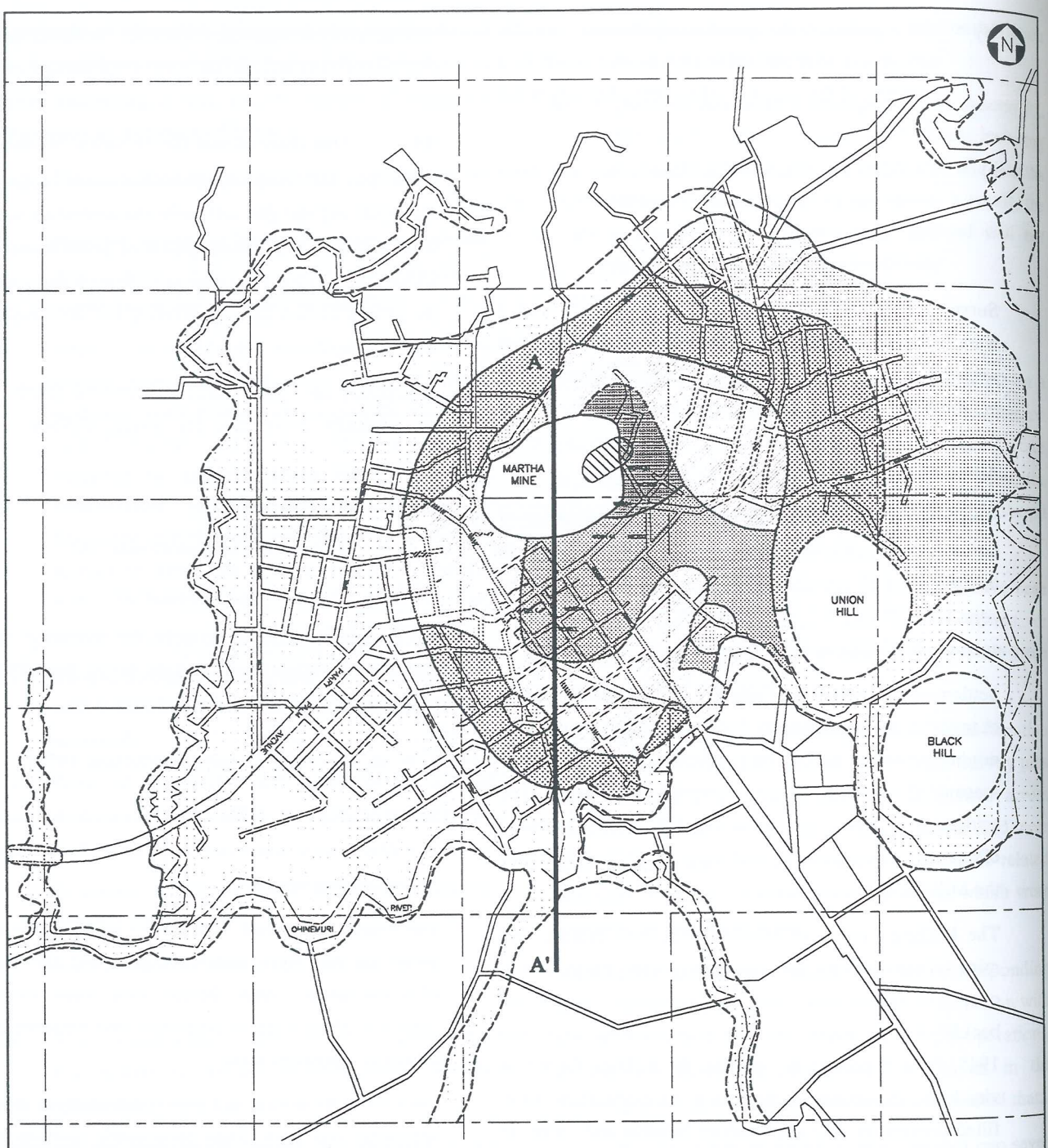

ZONE	AVERAGE MEASURED CONSOLIDATION SETTLEMENT (mm) FROM DECEMBER 1988 TO DECEMBER 1996.	AVERAGE OBSERVED FLUCTUATION IN GROUND SURFACE (mm)	LIKELY CAUSES OF OBSERVED SETTLEMENT (REFER TO SECTION 6)
1	6	±3	i, ii, iii, iv
2	0	±10	i, ii, iii, iv
3	11	±5	i, ii, iii, iv,v
4	24	±8	i, ii, iii, iv,v
5	46	±9	i, ii, iii, iv,v
6	63	±8	i, ii, iii, iv,v
7	106	±9	i, ii, iii, iv,v

FIGURE 3
Plan of Settlement Zones
(As at December 1996)

Refinement of material stiffness, in general, was limited to an adjustment of ± 20% and concentrated on those layers that most significantly influenced the total settlement. The exception to this was when laboratory data from adjacent drillholes indicated that a sample anomaly had occurred. The refined models were known as the refined one-dimensional (ROD) models.

A second calibration was undertaken using the ROD models and additional survey and piezometric data measured in May 1996. The May 1996 piezometric data was keyed into the ROD models to obtain an estimate of settlement. These predictions were then compared to the measured settlement. Differences between the estimated and measured settlements were less than 10%, indicating that reliable models had been constructed. A summary of the material stiffnesses used in the one dimensional settlement models is presented in Table 1.

Table 1

Summary of Material Compressibility.

Material Type	m_v, (m^2/ MN) Calculated from Consolidation Test Results.	m_v, (m^2/ MN) Calculated from Triaxial test Results.
Fill	0.02 to 0.27	---
Alluvium	0.02 to 7.65	0.01 to 0.23
Boulder Alluvium Matrix	0.01 to 0.08	0.02 to 0.22
Weathered Welded Ignimbrite	0.01 to 0.05	---
Welded Ignimbrite	---	0.00005 to 0.00017
Moderately Welded Pumiceous Ignimbrite	0.005 to 0.10	0.0002 to 0.0085
Unwelded Pumiceous Ignimbrite	0.006 to 0.035	0.002 to 0.013
Moderately Welded Tuff	---	0.0006 to 0.0054
Slightly Welded Tuff / Ash	0.012 to 0.24	0.0014 to 0.019
Unwelded Tuff / Ash	0.01 to 0.25	0.0006 to 0.065
Altered Andesite	---	0.0003 to 0.057

The ROD models were used to predict settlement and rebound of the ground surface at the drillhole locations due to operating and decommissioning the Martha pit. These predictions were made by feeding an estimate of the appropriate groundwater levels and rebound stiffness into the ROD models. The reload stiffnesses were estimated from the laboratory test results and are summarised in Table 2 in the form of Reload Compressibility Ratios.

Table 2

Summary of Virgin / Unload : Reload Compressibility Ratios

Material	Compressibility Ratio (Virgin m_v / Unload : Reload m_v)
Fill	3 to 9
Alluvium	3 to 7
Boulder Alluvium	3 to 6
Welded Ignimbrite	1
Ash and Tuff	3 to 5
Pumiceous Ignimbrite	3 to 5
Altered Andesite and Andesite	1

9.0 Finite Element Models

A preliminary finite element model (PFE model) of a section through Martha pit and Waihi township was initially constructed using Plaxis and :

i) Geological cross-section A-A (refer to Figure 2);

ii) Material data from the refined one dimensional geotechnical models; and

iii) The groundwater draw-down cones for May 1996.

The selection of the material stiffness, to be used in the finite element models, was very difficult due to the variation in geotechnical properties between adjacent drillholes.

Initially, the average layer stiffness was calculated using all the one-dimensional settlement models. Estimating material stiffness using this method resulted in finite element models which gave an estimate of settlement which was within 40% of the survey results.

A second value of the material stiffness was based on the one-dimensional settlement models of drillholes WC202 and WC206 only. This method gave an estimate of settlement which was generally within 20% of that measured by survey methods.

Table 3 summarises the finite element model material input parameters. For the purposes of the PFE model, a

Mohr-Coulomb type model was selected to represent the behaviour of all material types.

The complex sequence of inter-bedded tuff, ash and pumiceous ignimbrite units; that underlie the welded ignimbrite, is modelled by two layers in the finite element model. This simplification was possible because these units have similar geotechnical and hydrogeologic properties, and appear to have a compatible level of dewatering.

A simplification of the geology was unavoidable, as the maximum number of different layers able to be analysed by Plaxis version 6.31, is ten.

Predictions of settlement made by the PFE model were compared to the settlements measured during May 1996. In general, the difference between the predicted and measured settlement was less than 20%.

Table 3

Material Properties Used in the Refined Finite Element Models

Layer Name	C (kPa)	∅ (^{0})	ρ_B (t/m^3)	D_C (MPa)
Andesite	80,000	50	24.0	38,000
Altered Andesite	3,000	42	22.0	300
Moderately Welded Pumiceous Ignimbrite, Ash & Tuff	300	42	16.0	2500
Unwelded to moderately welded Ash & Tuff	200	34	17.0	150
Highly Welded Ignimbrite	120,000	46	22.5	10,000
Boulder Alluvium	10	34	20.0	800
Alluvium	10	28	16.5	20
Fill	10	28	15.0	4.5

Using the PFE model as a base, the two-dimensional groundwater level within the altered andesite, pumiceous ignimbrite and ash layers (initially estimated / interpreted and considered the most variable set of input data) was adjusted to reduce the difference between predicted and measured settlement. This model is referred to as the Refined Mohr-Coulomb Finite Element Model (RM-CFE model).

The RM-CFE model predicted settlements that were generally within 8mm (approximately 10%) of that actually measured.

Finally, more sophisticated material models, that have the ability to model inelastic consolidation and rebound of soil and rock, were constructed. Using the RM-CFE model as the base, a Preliminary Advanced Finite Element model (PAFE model) was developed using advanced mathematical models to model soil and rock behaviour.

Both the RM-CFE model, and the RAFE model, were used to predict maximum settlement due to mine dewatering. This prediction was made by feeding the predicted maximum groundwater draw-down profiles into the finite element models. In general, the magnitude and pattern of settlement predicted by the two models was very similar.

The main difference between the two finite element models was the prediction of settlement within 100 metres of the pit crest. The RM-CFE model predicted approximately 300mm of movement at the pit crest while the RAFE model predicted approximately 150mm. Within Waihi Township, both models predicted approximately 100mm of settlement at a distance 150 metres from the pit crest reducing to 10mm at a distance 1100 metres from the crest of the pit. The results of the finite element modelling are summarised in Table 4.

A prediction of ground surface rebound due to future recovery of the groundwater levels was made using the RAFE model. The RAFE model was used to predict rebound as the RM-CFE model does not have the ability to directly model inelastic rebound.

An estimate of the nett long-term ground surface settlement was made by subtracting the predicted rebound from the maximum settlement.

Due to a lack of survey data near the pit crest, and variability of the fill layer, a detailed knowledge of the site, and engineering judgement, was relied upon to select the finite element model which gave the best prediction of settlement near the pit crest.

Discussions with the WGM surveyors suggested that the predictions made by the RM-CFE model were probably more realistic than those made by the RAFE model. For this reason, the predictions of long-term settlement presented in Table 4, are made using the RM-CFE model.

Upon completion of the geotechnical modelling, a comparison of the predictions made by the ROD, RAFE and RM-CFM models was made.

Table 4

Predicted Settlement and Rebound.

Node Number	Distance Between the Node & Pit Crest (m)	Estimate of Maximum Settlement using the RM-CFE Model (mm)	Estimate of Maximum Settlement using the RAFE Model (mm)	Estimate of Rebound using the RAFE Model (mm)	Estimated Long Term Settlement of the Ground Surface (mm)
629	0	301	153	34	267
663	50	196	122	8	188
697	100	182	114	12	170
731	150	105	95	18	87
765	200	88	81	25	63
799	220	82	79	27	55
833	260	85	86	38	47
867	320	86	81	47	39
901	330	92	84	51	41
935	450	80	72	37	43
969	480	75	68	32	43
1003	520	67	62	27	40
1037	700	37	40	20	17
1071	800	28	31	14	14
1105	825	27	30	13	14
1139	975	17	23	4	13
1137	1075	10	11	4	6
1207	1125	2	2	0	2
1241	1313	>1	>1	0	>1
1275	1500	>1	>1	0	>1
1309	1600	0	0	0	0
1343	1700	0	0	0	0
1377	1800	0	0	0	0
1411	1900	0	0	0	0
1445	2000	0	0	0	0

Predictions made using the refined finite element and one dimensional models were of the same order, and were generally within 20% of each other. The finite element models usually predicted less movement of the ground surface than the one dimensional models.

10.0 Conclusions

1) The magnitude of dewatering related settlement is low compared to that measured at other sites in New Zealand and the United States. Monitoring has shown that dewatering of the Martha Pit has not adversely affected buildings or services within Waihi Township.

2) The geology and hydrogeology of Martha Mine and Waihi Township is extremely complex with closely inter-bedded layers, confined hydrogeologic systems and perched water tables.

3) The measured settlement, to date, has not been consistent, or symmetrical, around the Martha pit. The complex geology surrounding the pit is considered to be the main reason for this.

4) Settlements, in each of the seven settlement zones identified to date, are attributed to a combination of five processes of consolidation. Only one of the five processes of consolidation is directly related to current mine dewatering.

5) Graphs showing actual settlement against time indicate a progressive, staged settlement that occurs as the pit geometry is altered, exposing the younger geologic deposits in the Martha pit wall at a lower elevation. This allows dewatering of the younger deposits to develop to the level of the units exposure in the pit wall.

6) To date, settlements have occurred rapidly, and many of the younger deposits exhibit a near-elastic response to changes in the groundwater level. These movements are expected to be partially recovered, due to rebound, as the pit-lake reaches final level. Full recovery of settlement is not expected due to the altered groundwater regime and unrecoverable consolidation of the affected geologic units.

7) Acceptable levels of differential settlement and tilt are predicted by the finite element models.

8) Understanding of the following was essential for the successful prediction of settlement at Waihi:
   - Identification and quantification of all the causes of settlement present in Waihi.
   - Thorough research of historic mine features, both above and below the ground surface, and property use histories.
   - Detailed understanding of the geology and hydrogeology of Waihi.
   - Detailed understanding of the soil and rock geotechnical characteristics.
   - Excavation and dewatering history of the Martha Pit.
   - A summary of the measured settlements.
   - Historic Rainfall and weather patterns for Waihi Township.
   - Most importantly, how all the above were related, or connected, to each other.

9) Due to the complexity of the issues, it was imperative that thorough field observations and note keeping was undertaken. An understanding of the problem took several months to develop, and seemingly unimportant details were often later found to be a crucial component of the problem.

10) Finite element modelling proved essential when estimating differential settlement and tilt.

11) Engineering models are only as reliable as their input data.

REFERENCES

Johnson. A.I., 1991, Preface, *Proceedings of the Fourth International Symposium on Land Subsidence, Houston, Texas, May 1991.*

Kesley, P. I., 1985, An Engineering Geological Investigation of Ground Subsidence Above the Huntly East Mine Area. *Geological Society of New Zealand Miscellaneous Publication 32A, Christchurch Conference December 1985.*

Lambe, T.W. and Whitman, R.V., 1979, Soil Mechanics, *John Wiley and Sons.*

McAra, J.B., 1988, Gold Mining at Waihi, 1878 to 1952, *Martha Press.*

Rivera. A, Ledoux. E and De Marsily. G, 1991, Non-linear Modelling of Groundwater Flow and Total Subsidence of the Mexico City Aquifer-Aquitard System. *Proceedings of the Fourth International Symposium on Land Subsidence, Houston, Texas, May 1991.*

ACKNOWLEDGEMENTS

The author would like to thank The Waihi Gold Mining Company Limited and Normandy Mining Limited for their co-operation and permission to publish this paper.

INVESTIGATION OF SLOPE MOVEMENTS IN A COASTAL SAND DUNE IN SOUTH-EAST QUEENSLAND

S.R. Fidler
Golder Associates, Brisbane

Summary This paper presents the results of monitoring and investigation of slope movements which occurred in a coastal sand dune in South East Queensland, at a time of elevated groundwater levels. The magnitude and pattern of displacement suggest that a Factor of Safety of very close to 1 developed as a result of the rise in groundwater levels. Subsurface investigations identified the presence of a layer of former swamp deposits (sandy clay and clayey sand) beneath the dune, which has been interpreted as the layer in which shear displacement was concentrated. Finite element and limit equilibrium analyses using a Mohr-Coulomb constitutive model yield consistent results, and indicate that an angle of friction of 11° is required for a Factor of Safety of 1 for a failure mechanism which passes through the former swamp deposits. Such a low friction angle is inconsistent with limited laboratory testing on the material. Further work is being undertaken to better understand the mechanisms which led to the development of large scale movements, in order to better predict the potential future development of such movements.

1 INTRODUCTION

Results of monitoring and analyses carried out in relation to slope movements which occurred in a coastal sand dune in South East Queensland are presented in this paper. The sand dune is a relatively young dune, which extends over older swamp deposits. The crest of the dune is approximately 80 m above the toe, and the slope of the dune is 23° on average with steeper sections of up to 40° in places. A contour plan for the dune is illustrated in Figure 1, and a cross-section through the dune is illustrated in Figure 2. In late 1998, a downward displacement of 3.3 m developed near the crest over a period of approximately 17 days. The downward displacement at the crest was accompanied by the development of a 2.7 m scarp mid-way down the dune, and an upwards movement of 4.3 m at the toe of the dune, indicating horizontal movement of a lower wedge of sand and downward movement of an upper wedge.

2 DESCRIPTION OF DUNE MOVEMENTS

The slope movements developed at a time when dredging associated with a sand mining operation was being carried out at a distance of 400m behind the toe of the dune, in a dredge pond with a water level at 35m above the toe. The location and level of the dredge pond were within the normal operational guidelines for the mine.

For several days preceding the first observed formation of cracks in the slope, loud rumbling noises were heard emanating from the dune. Such behaviour has been previously observed to precede large slope movements in similar terrain in the area. Four days after the first rumbling sounds were heard, a crack was observed in the ground along the crest of the north-west dune, and crude measurements of slope movement were instituted at that time (measurement using a tape measure between two stakes). More detailed monitoring using surveying equipment was established shortly thereafter, and measurements of the vertical displacement at the crest were made every fifteen minutes initially.

The cumulative displacement measured at the crest is illustrated in Figure 3. More than 1 m of vertical movement developed at the crest over the first 48 hours of movement. A total movement of approximately 3.3 m developed over a period of approximately 17 days, after which time the movement slowed to less than 0.5 mm/hour. The slope has remained stable since that time. Detailed information regarding the rates of displacement in the first seven days of movement are illustrated in Figure 4, with information on tidal water levels close to the toe of the dune. It can be seen that the rate of movement is closely tied to tidal fluctuations, and that peaks rates of movement occur approximately 1.5 hours after tide peaks. The mechanism of tidal influence is yet to be considered in detail.

In addition to the movement at the crest, a mid-slope scarp developed (which was first observed the day after the first observation of the upper crack). At the completion of monitoring, a relative displacement of 2.7m had developed at the mid-slope scarp. The location of the upper and mid-slope scarps and the recorded movement for these features are illustrated in Figures 1 and 2 (the cross-section illustrated in Figure 2 is for the section on which the largest slope

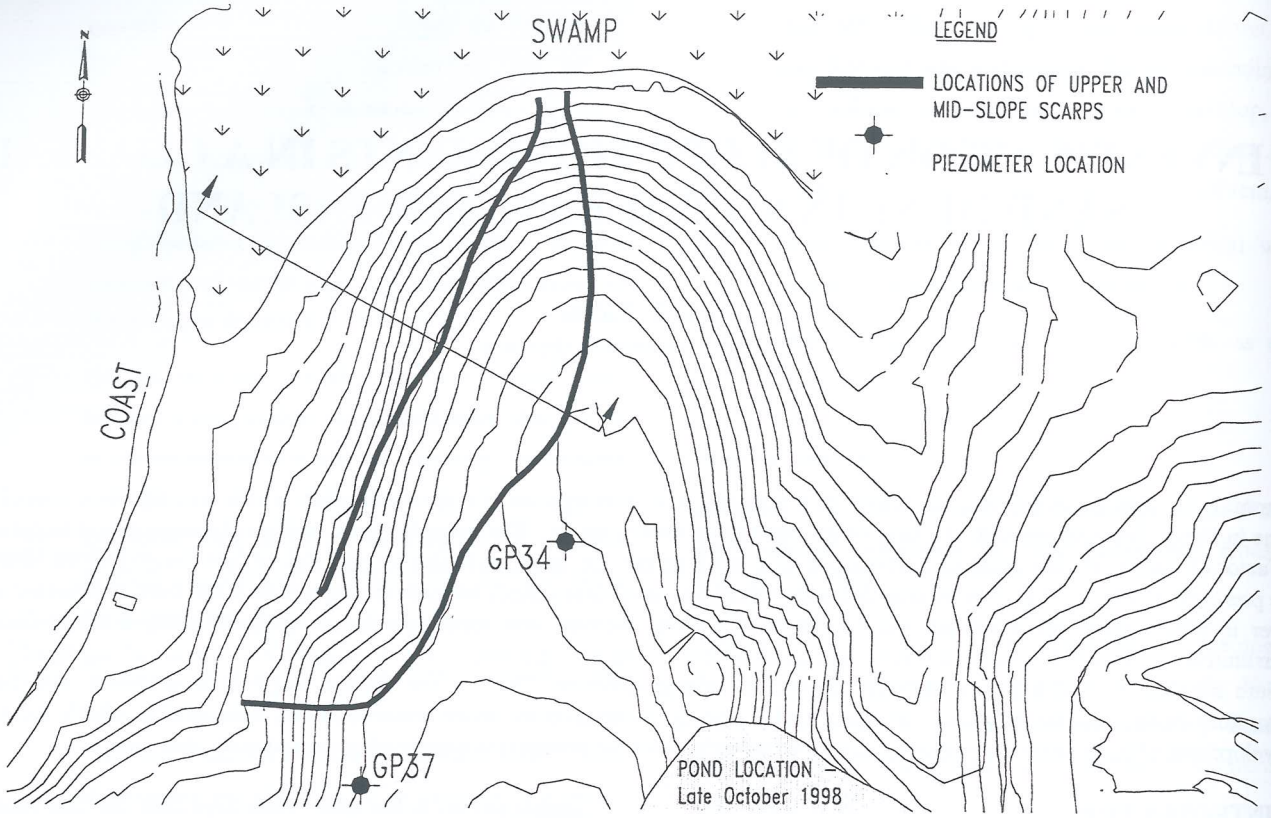

Figure 1 Plan of sand dune

movements were measured). Apart from some leaning trees near the toe, there was no readily apparent evidence of mounding in this area. However, significant displacements developed in this area, as indicated by surveying carried out prior to and following the movements (refer to Figure 2).

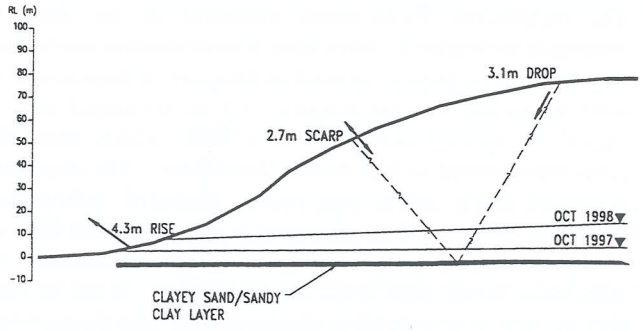

Figure 2 Cross-section through dune indicating measured displacements

3 GROUNDWATER CONDITIONS

The water table within the dune rose over a period of approximately 8 months preceding the slope movements, in response to seepage from the mine dredge pond. The pond moved towards the dune from the east, and on 30 October 1998 was located as shown in Figure 1.

The results of water level monitoring at two piezometers in the vicinity of the dune are illustrated in Figure 5. The locations of these piezometers are shown in Figure 1. It can be seen that the water table at the rear of the dune was at an elevation of approximately 7 m AHD in the period prior to direct influence from the dredge pond, and that peak levels in excess of 18 m AHD were recorded on 6 November 1998. Water levels dropped relatively rapidly following 6 November, as the dredge pond was moved away from the area of slope movements. The results also indicate that similar groundwater levels were present along the length of dune where movements were observed.

4 SUBSURFACE INVESTIGATIONS AND LABORATORY TESTING

Drilling and cone penetrometer testing was carried out at a number of locations along the toe of the dune, and at three locations near the crest of the dune, to assess the nature of materials beneath the dune, and to assess the extent of the suspected swamp deposits beneath the dune. As indicated in Figure 1, swamp deposits were present around the base of the dune to the north and west, and the shape of the dune indicated that it had been blown out over pre-existing swamp deposits.

Drilling and cone testing results identified the presence of a layer of variably sandy clay/clayey sand beneath the dune, with a variable percentage of organic material (refer to Figure 2). Some samples of this material were essentially peat. The

layer extended along the majority of the toe of the dune, and was present in the boreholes drilled from the crest of the dune. Samples of clayey material from beneath the crest of the dune were very stiff to hard (as would be expected for clay normally consolidated beneath an 80 m high dune), and samples from beneath the toe were generally firm. It appears that the layer of sandy clay/clayey sand was deposited in a lake, over a previously deposited, relatively deep layer of weathered sand. The investigation did not identify the presence of any other layers on which movements could have potentially developed, and it has been assumed that shear displacement was concentrated in this layer.

Shear box testing on a sample of clayey sand from this layer yielded an angle of friction of 27°. Additional laboratory testing on further samples recently obtained is currently underway.

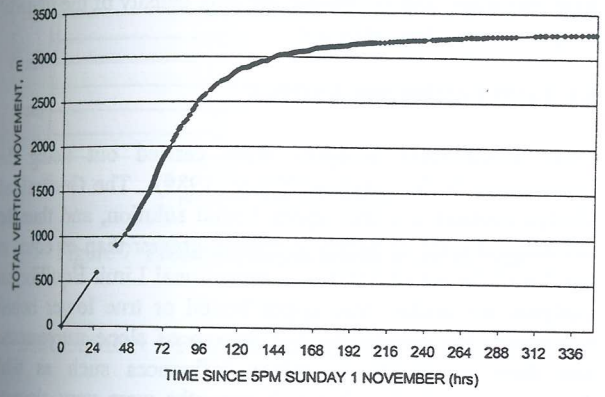

Figure 3 Cumulative displacement measured at crest

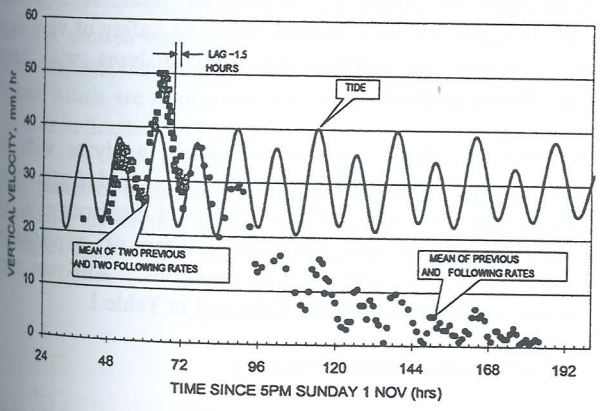

Figure 4 Rates of displacement at crest

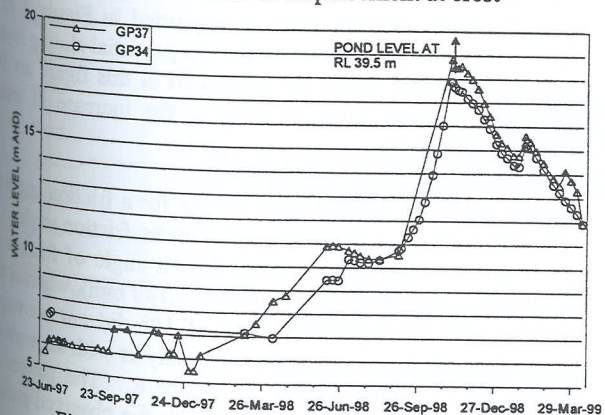

Figure 5 Measured groundwater levels at crest of dune

BACK-ANALYSIS OF MOVEMENTS

5.1 General

Back-analyses to assess the conditions which led to the development of the slope movements described above have been undertaken using two approaches:

- non-linear stress-strain analysis using the finite element technique
- Limit Equilibrium methods

Finite element analyses have the advantage that they do not make a priori assumptions regarding stress distributions or locations of limiting soil stresses, and stresses and displacements are therefore determined by considerations of equilibrium, strain compatibility, and soil strength. Limit equilibrium methods, which are widely available and are relatively easy to use were also used for back-analysis, since such methods would ideally be used in any analysis of future potential problems of a similar nature.

Prior to commencement of the back-analyses, it was necessary to consider the choice between drained and undrained analyses. Loading of the slope took place over a period of approximately 8 months as the water table in the dune rose and increased the weight of sand above the potential sliding layer. In addition to the increase in total stress due to increased bulk density (possibly with consequent pore pressure increases depending on the rate of loading), pore pressure increases develop as a result of equilibration with the raised water table. In the extreme case of rapid increase in water level, the pore pressure increase in the lower permeability potential sliding layer would initially depend on total stress changes and the A and B pore pressure parameters. For typical values of A and B, the pore pressure changes which would accompany such an undrained loading would be less than the pore pressure changes which would develop as a result of equilibration with the raised position of the water table. Thus, in this case, drained conditions should be more critical than undrained conditions. Analyses for this study have therefore been carried out as drained analyses, with pore pressures that correspond directly to the rising level of the water table in the sand dune. It is possible that the dune movements developed prior to the full equilibration of pore pressures, in which case the actual soil strengths would be somewhat less than indicated by the back analysis.

5.2 Finite Element Modelling

In the finite element modelling carried out for this study, soil behaviour was described using an elastic, perfectly plastic constitutive law, with a limiting shear strength condition defined in terms of the Mohr-Coulomb failure criterion.

The finite element mesh used for analyses is illustrated in Figure 6. The lateral boundaries of the model were specified as zero horizontal displacement boundaries, and the basal boundary was specified as a zero displacement boundary. The lateral boundaries were chosen to lie outside the limits of observed slope movements. The formulation of the finite element model is for plane strain conditions, and therefore

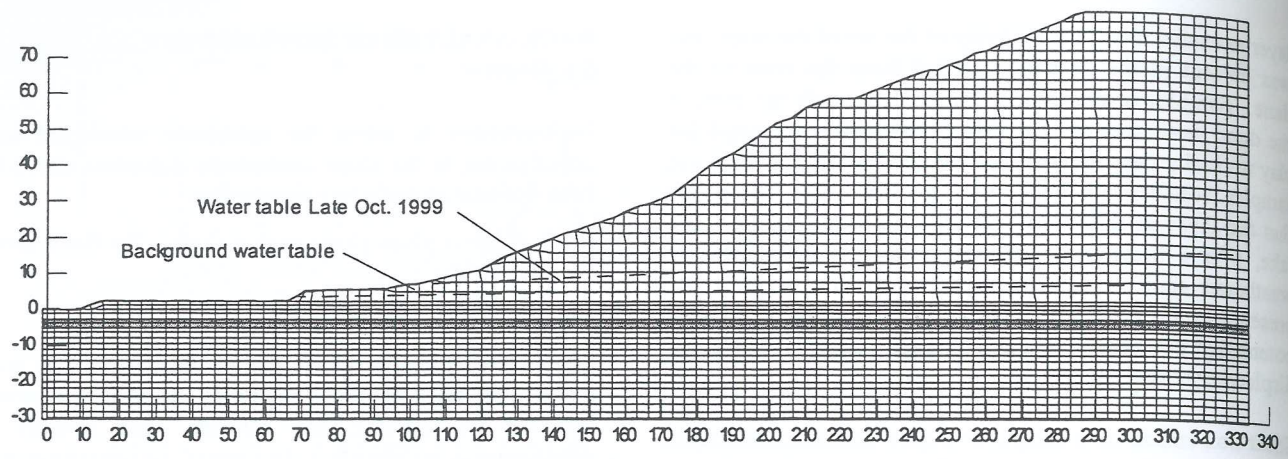

Figure 6 Finite Element Mesh

represents a slope which is infinitely long and of uniform cross section in the direction perpendicular to the section which was analysed. The cross-sectional geometry adopted for the model is that of the cross section on which maximal slope movements occurred. The implications of the assumption of plane strain conditions are discussed further in the following.

Properties adopted for the various slope materials are summarised in Table 1. Properties for the dune sand were based on previous testing. Variable strengths were adopted for the material in the clayey sand/sandy clay layer, in order to determine the angle of friction for which large slope movements were initiated in the model.

Table 1– Material Properties Adopted in the Finite Element Model

Material	Strength Properties	Density
Dune sand	$\phi' = 32°$	γ =19 kN/m3 below water table γ =16 kN/m3 above water table
Sliding layer	ϕ' = variable	γ =18 kN/m3
Underlying sand	$\phi' = 35°$	γ =19 kN/m3

Analyses were carried out for two water table elevations, as illustrated in Figure 1. The two water table conditions are based on the water table profiles for steady state conditions prior to the water table rise, and for the conditions at the end of October following a water table rise over the previous 8 months. At this stage, no attempt has been made to consider the effects of tidal fluctuations.

The stress history of the slope was imitated by commencing modelling with an approximately horizontal ground surface, and then sequentially adding layers of material to the model to simulate accretion of the dune over a period of time. Stress conditions in the slope were calculated in this manner for the case of steady state water table conditions, and changes from this condition were then calculated by increasing the water table elevation, and increasing the bulk density of the material in the zone of water table rise.

5.1 Limit Equilibrium Analyses

Limit Equilibrium analyses were carried out using the Generalised Wedge Method (Giam, 1989). The Generalised Wedge Method is a true upper bound solution, and thus the calculated Factor of Safety is strictly greater than or equal to the "true" Factor of Safety. Conventional Limit Equilibrium analyses are neither true upper bound or true lower bound analyses. The magnitude and pattern of slope movements, and their sensitivity to minor influences such as tidal fluctuations, indicates that soil strengths were very close to fully mobilised along a kinematically admissible surface. This suggests that an effective Factor of Safety of very close to 1 should be adopted for back-analyses with Limit Equilibrium methods.

As discussed further in the following, analyses with the Generalised Wedge Method were based on wedge geometries which were consistent with the observed displacements, and which were consistent with the pattern of displacement indicated by the finite element analyses. Analyses were carried our using parameters indicated in Table 1.

6 BACK ANALYSIS RESULTS

Horizontal displacement, calculated at the toe of the dune using the finite element method, is plotted in Figure 7 as a function of the angle of friction for the potential sliding layer. The displacements which are illustrated in this figure are for the load increment corresponding to the increase in water table.

Limited plasticity developed at the toe for a friction angle of 15°, with increasing displacement at lower friction angles. A converged solution was obtained for an angle of friction of 11° (with displacements of the order of 140 mm), whereas the analysis with an angle of friction of 10° did not converge. The pattern of displacement for the analysis with an angle of friction of 11° is illustrated in Figure 8. The pattern of displacement is roughly consistent with the observed pattern

of displacement. However observations of the displacement at the upper scarp suggest displacement developed on a plane at a much steeper angle than that indicated by the finite element analysis. Similarly, the finite element analysis indicates the likely formation of a mid-slope scarp at a lower elevation and on a steeper plane than that observed.

Analysis using the Generalised Wedge Method was carried out using the wedge geometries indicated in Figure 8, and a friction angle of 11°. The calculated Factor of Safety for this case was 0.98.

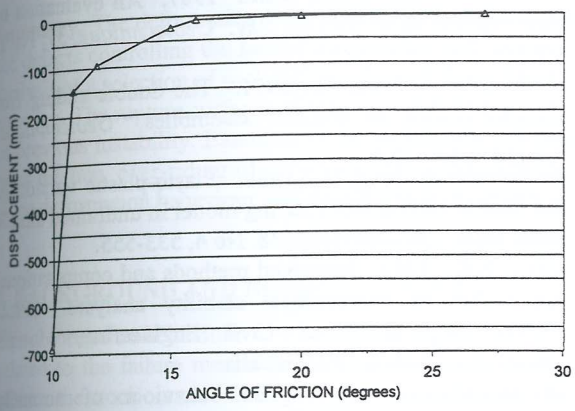

Figure 7 Predicted displacement at toe of dune

7 DISCUSSION OF BACK ANALYSIS RESULTS

The back analysis results indicate that an angle of friction of 11° would be necessary for large slope movements to develop, such as were observed. An angle of friction this low is inconsistent with the results of laboratory testing, and with values which are conventionally adopted for similar swamp deposits in South-East Queensland.

One possible explanation is that large movements have previously developed at this site, and have caused residual strength to develop along the pre-existing slip surface. It should be noted, however, that laboratory testing carried out to date has not indicated that residual shear strength is substantially less than peak shear strength for the sandy clay/clayey sand layer beneath the dune.

The mechanisms for the development of a pre-existing slip surface are not evident. For a previous slip to have caused residual strength to develop on a discrete failure surface, it would be necessary for it to have developed after consolidation of the pre-existing swamp deposits beneath the dune (since failure on a discrete plane would not generally develop in a soft clay). A possible trigger for previous movements could be an earthquake.

It is worth noting that even for friction angles as high as 27°, the finite element analyses indicated the full development of plasticity in the clayey sand/sandy clayey layer, in almost the entire length from beneath the crest to the toe. Full development of plasticity was predicted in limited areas for the conditions preceding the water table rise, and the area of plasticity extended towards the toe as a consequence of the water table rise.

Although the full development of plasticity was predicted locally by the finite element analyses, large-scale displacements did not develop in the model since the local conjugate failure directions were not aligned horizontally. Relationships between local shearing on conjugate planes and overall shear displacements have been discussed extensively in the literature (for example, de Josselin de Jong (1971, 1988), Airey and Wood (1987), and Wroth (1987)). It has been postulated that, for example, displacements in a shear box test develop on vertical surfaces, and that overall horizontal displacements are made up of a combination of shearing on vertical surfaces and rigid body rotations (de Josselin de Jong, 1971). The references cited above indicate that shearing which develops as a result of such a mechanism provides less resistance than would be indicated by the angle of friction and the stress normal to the overall direction of shear displacement.

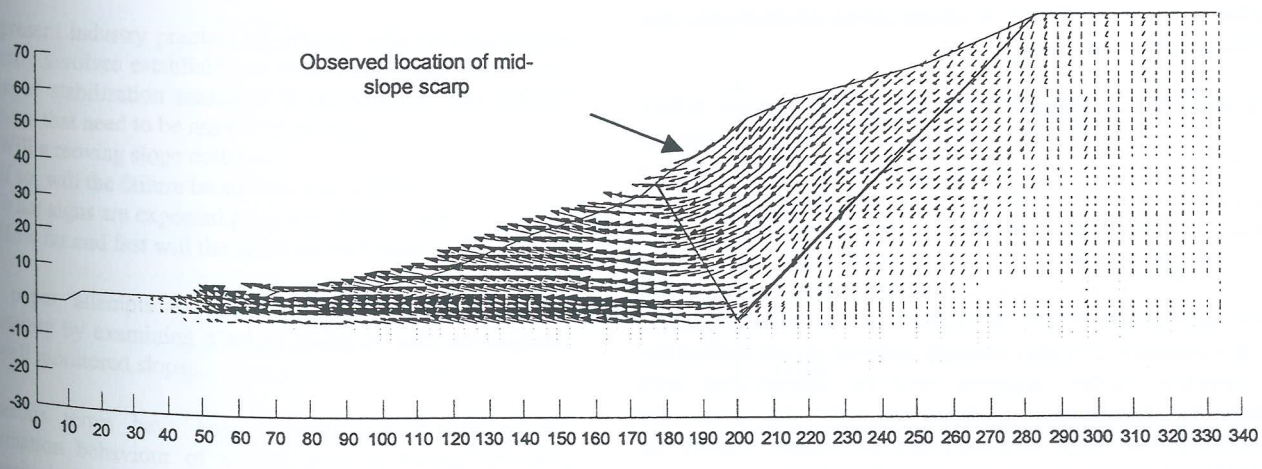

Figure 8 Pattern of displacement predicted by finite element analysis

It appears possible that displacement at the toe may have been initiated by such a mechanism, leading to progressive development of movement through the remainder of the layer already at limiting conditions. The observed rumbling from the dune for a period of several days prior to the development of movement at the crest indicates a progressive development of movement commencing at the toe. Further analysis using alternative constitutive models (for example the constitutive models developed by de Josselin de Jong (1971, 1988)) may provide additional insight into the conditions which led to movement.

8 CONCLUSIONS

Large displacements which have developed in a coastal sand dune overlying former swamp deposits have been analysed using finite element and limit equilibrium techniques, in an attempt to understand the factors which led to the development of movement. Understanding the mechanisms which led to the movement is important, since future mine paths will pass within a similar distance of coastal dunes which are similarly located over former swamps.

The analyses yielded consistent results which indicate that for a Factor of Safety of 1 to develop as a result of an observed water table rise, an angle of friction of 11° is required for a layer of organic sandy clay and clayey sand which was encountered beneath the dune. The failure mechanism predicted by the analyses is similar to that observed in the field.

Laboratory testing on a sample of clayey sand collected from the likely sliding layer beneath the dune has indicated an angle of friction of 27°, which is consistent with values typically adopted for swamp deposits in the area. Mechanisms for the development of a plane of weakness with a friction angle of 11° are speculative only, but might include the prior development of plane with residual shear strength due to large scale movements caused by an earthquake. Geomorphological evidence of previous large scale movements would be difficult to discern, and evidence for the presence of a plane of weakness with very low angle of friction may be difficult to obtain from conventional site investigation techniques.

It is possible that analyses based on a Mohr-Coulomb failure criteria has led to under-prediction of the friction angle for the former swamp deposits beneath the dune, since such a model requires one of the conjugate failure directions to align horizontally for failure to develop. However, it is not clear that this requirement would necessarily hold in a system where soil plasticity is fully developed on inclined planes, but movement is essentially constrained to the horizontal plane by the presence of higher strength material above and below. If possible, further analyses will be carried out with alternative constitutive models, in order to assess the possibility that large displacements developed without the presence of a plane of very low strength material.

Further analyses will also be carried out in relation to similar large scale movements, which have previously developed at the mine in the batters of the dredge pond. Analysis of similar movements will hopefully assist in the assessment of whether such movements require the presence of very low shear strength materials.

9 REFERENCES

1. Airey, D.W. and Wood, D.M.. 1987. An evaluation of direct simple shear tests on clay. *Geotechnique*, 37, No 1, 25-35.
2. de Josselin de Jong, G. 1971. The double sliding free rotating model for granular assemblies. *Geotechnique*, 21, No 2, 155-163.
3. de Josselin de Jong, G. 1988. Elasto-plastic version of the double sliding free rotating model in undrained simple shear tests. *Geotechnique*, 38, No 4, 533-555.
4. Giam, S.K. 1989. Improved methods and computational approaches to geotechnical stability analyses. Ph.D Thesis, Department of Civil Engineering, Monash University, Melbourne, Australia.
5. Wroth, C.P. 1987. The behaviour of normally consolidated clay as observed in direct shear tests. *Geotechnique*, 37, No 1, 37-43.

Deformation Behaviour of Rock Slopes on Pre-Existing Shear Surfaces

James Glastonbury
School of Civil and Environmental Engineering, The University of New South Wales

Summary: The deformation behaviour of a rock slope prior to collapse is inherently related to the failure mechanism, strength of the defects controlling the failure mechanism, and in some cases is related to the rock mass strength. This paper presents results of analysis of a selection of rock slopes whose deformation behaviour has been influenced by defects that have experienced significant shearing. The rupture surfaces of these slope failures have experienced large deformation due to either regional folding, stress relief or previous instability. Examination is made of the relationship between normal effective stress acting on the rupture surface, rock mass dilation, over-riding of defect asperities and shearing or crushing of asperities. These factors are considered in the context of slope deformation behaviour and discussion is presented on their influence.

1 BACKGROUND AND NOMENCLATURE

The deformation behaviour of a rock mass prior to collapse is related to the failure mechanism and the strength of defects within the rock mass. Skempton and Hutchinson (1969) presented the terms "first-time slides" and "slides on pre-existing slip surfaces" to distinguish between slides in unsheared ground and slides on surfaces that have experienced significant shearing. Hutchinson (1988) suggested that slides on pre-existing slip surfaces can be further sub-divided into two distinct categories:

1. Failures on surfaces which have been pre-sheared due to geological processes other than landsliding; and
2. Failures on surfaces that have been pre-sheared by previous landsliding episodes (reactivated sliding).

Geological processes responsible for causing shear along defects include rebound/stress relief, regional faulting and folding under tectonic stresses and glaciotectonic influences. This paper discusses the nature of landslides on pre-existing shear surfaces and the influence this shearing can have on the pre-collapse behaviour of a rock slope.

The present industry practice of dealing with moving slopes generally involves establishment of a monitoring system and design of stabilisation measures if appropriate. The critical questions that need to be answered include:

- Will a moving slope collapse?
- If so, will the failure be sudden and brittle?
- What signs are expected prior to collapse? and
- How far and fast will the slope move before collapse?

This paper attempts to address some of these areas of uncertainty by examining a select group of well investigated and well monitored slopes.

Numerous terms have been adopted for describing the deformation behaviour of a rock mass including rebound, regressive/progressive movement, elastic deformation and creep. No two rock slopes will behave in the same manner in terms of deformation, due to the variability in rock mass characteristics. However, the deformation behaviour of a rock slope can be shown to exhibit certain typical stages, such as decreasing displacement rate, constant displacement rate or accelerating displacement rate.

The cases presented in this study are all natural slopes and no assessment of their elastic response to load variation has been made or measured. Following the initial elastic response, plastic deformation associated with stress relief may occur. In most cases this is observed as shearing along defects and may occur as steady movement over protracted periods or as episodic (stick-slip) movement. The rock mass response to stress relief and other external changes (such as increasing groundwater level) may be short-lived and rates of displacement may reduce with time or the response may be ongoing leading to accelerating rates of displacement and eventual collapse. The term creep has been adopted in this study to describe the time-dependent "slow, more or less continuous deformation or flow of natural and excavated slopes" (Emery, 1978). Creep is generally recognised to have three main divisions, as indicated in Figure 1. These terms will be used to describe the case studies presented in the following sections of this paper.

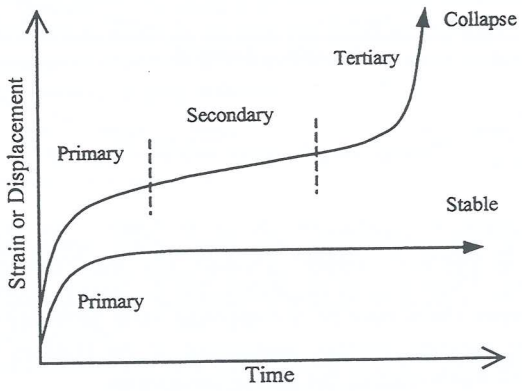

Figure 1: Diagrammatic representation of creep curves for moving slopes

2 DESCRIPTION OF CASE STUDY DATA

2.1 Classification

Ten cases of rock slides on previously sheared surfaces were examined in this study and their characteristics are summarised in Table 1. They were categorised according to whether they were first time slides on pre-sheared surfaces or reactivated slides. They were also sorted in terms of geological environment, failure mechanism and displacement-time behaviour, with comment provided in Table 1.

In all cases, the failure mechanism is broadly described as translational sliding, using Hutchinsons (1988) classification system. On a detailed level, cases represent wedge sliding or block sliding on planar or curved failure surfaces. Diagrammatic illustration of slide geometry is presented in Table 2. Information on the cases was obtained from published literature and unpublished reports. In all cases displacement monitoring commenced after the slope started moving. Comparison of data is not straightforward due to variations in length of monitoring period and intervals between readings. Eight of the slopes presented in the database were monitored using surface survey prisms.

Table 2: Diagrammatic Illustration of Slide Geometry.

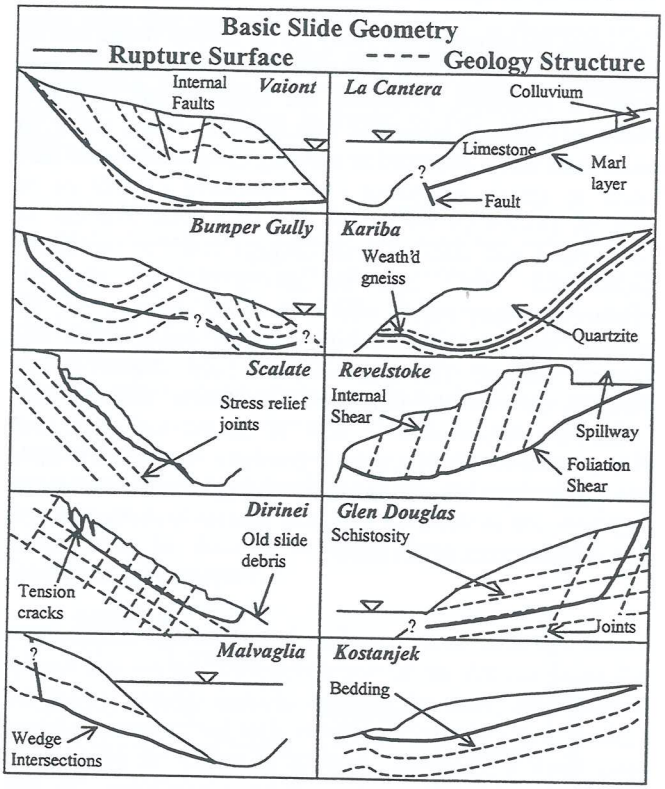

The interpreted mechanism shown in Table 2 for Bumper Gully is based on surface geology and geomorphological mapping. There is some suggestion that the failure mechanism at Bumper Gully may be a compound slide involving some internal shearing. Further assessment of the Bumper Gully case will likely confirm the failure mechanism.

Comparison of total measured displacements is difficult due to variations in size of the slope failures. It is expected that, all other things being equal, a larger rock mass will exhibit greater displacement than a small rock mass. It is suggested that failure limits in terms of strain may be more relevant than total displacements. Therefore, for the purpose of comparison, total displacements for each case have been normalised against the down-slope length of the failed mass, to give an indication of strain of the rock mass. It is considered that the down-slope length is the most appropriate parameter for normalising, as vector deformation of these sliding failures is generally in a direction parallel to the slope face.

2.2 Case Study Commentary

Two of the ten cases examined (Vaiont and Scalate) progressed through to collapse. The remaining eight cases exhibited movement of varying extent and may be considered to have failed in terms of serviceability criteria but they did not show sudden catastrophic collapse.

The mechanism of previous shearing on the rupture surface of each of the slides was examined, and is indicated in Table 1. Causes of previous shearing include regional tectonic folding of strata, stress relief due to unloading and earlier periods of sliding. Five cases had previously sheared basal rupture surfaces associated with both regional folding and earlier sliding. Two cases had previously sheared rupture surfaces derived from both stress relief and earlier sliding activity. Two cases showed no signs of folding or stress relief but were reactivated landslides and one case was likely a first-time slide on a surface previously sheared by regional folding.

There were essentially two geological categories within the ten cases examined. Four cases involved sliding in sedimentary environments (limestone, marl, sandstone and siltstone), with rupture surfaces defined by bedding. The other six cases were from metamorphic terrains (schist, gneiss and quartzite) with rupture surfaces defined by jointing or schistosity. All failures were predominantly defect controlled.

3 ANALYSIS OF DEFORMATION BEHAVIOUR

3.1 How Do Slides on Pre-existing Shears Behave?

3.1.1 General

All ten slides respond in different ways to load changes, such as groundwater rise or stabilisation works. Slides with a larger normal effective stress (on the rupture surface) generally show a more regular displacement-time response under periods of constant loading. Slides at low normal stress levels tend to show more erratic behaviour at constant loading. Many of the slides exhibited sensitivity to rainfall events, with larger slides generally showing a more delayed reaction time.

Geomorphological features on a number of the slides suggest significant movement. This movement combined with irregular rupture surfaces has resulted in disaggregation of slide masses. Vaiont and Kariba show disrupted slide masses overlying a rupture surface of complex geometry. Bumper Gully shows a highly to moderately disturbed slide mass, over what is likely to be an undulose and curved slide surface. La Cantera slide is described as highly fractured yet the rupture surface is understood to be relatively planar. The large total

movement (50m+) of this slide may explain the high degree of fracturing.

Movement rates for nine of the slides were typically between 0.05 and 0.5mm/day. Vaiont had monitored rates generally above 1mm/day, with occasional peaks at about 20-40mm/day and a final displacement rate immediately prior to collapse assessed to be about 200mm/day. Distinct primary, secondary and sometimes tertiary creep stages are visible in the monitoring data for most cases, with Vaiont showing particularly distinct phases (refer to Figure 2). Many of the slides were stabilised so complete tertiary creep sequences are often not available and may in some cases not have developed.

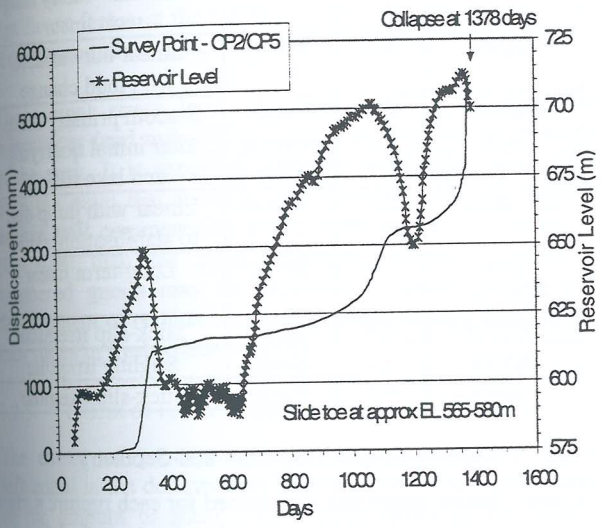

Figure 2: Displacement data for Vaiont slide showing relationship with reservoir level (Hendron and Patton, 1985).

3.1.2 Stick-Slip Displacement Behaviour

Stick-slip motion is the term used to describe sequential episodes of rapid displacement followed by periods of low displacement rate. It is associated with the sudden over-riding of asperities on the rupture surface. In many slopes this type of behaviour may be observed in association with peaks in rainfall or snowmelt. In examination of these cases, focus was on stick-slip displacement behaviour during periods of relatively consistent stress levels. Consideration also needs to be given to intensity of monitoring. If readings are made at long intervals then a smoother displacement-time curve will be produced and stick-slip motion may be unrecorded. The displacement-time data for Revelstoke slide, presented in Figure 3, suggests some stick-slip type behaviour at very low normal stress levels. This slide was described as reactivated (with some regional folding) but the extent of previous shearing is unknown. Clay gouge and breccia are known to occur along at least part of the rupture surface and the normal stress level is very low. It is possible that the slide surface is not at residual strength and this combined with the presence of breccia may cause some brittle response to shearing (and hence a possibility for stick-slip motion).

Most other slides examined in this study show more uniform displacement-time behaviour at higher normal stress levels. This is attributed to the fact that destruction of asperities has taken place to a greater extent on these other slides. The data also suggests that slides that have undergone large shear displacements exhibit a reduced stick-slip tendency.

Cases such as Kostanjek, Vaiont and La Cantera involve sliding on clay coated rupture surfaces that have experienced significant shearing during previous sliding episodes and/or regional folding. The normal stress levels on these rupture surfaces were high and significant crushing and shearing of asperities is expected to have occurred. These three slides do not exhibit any apparent stick-slip tendencies and tend to show more gradual changes in displacement-time behaviour.

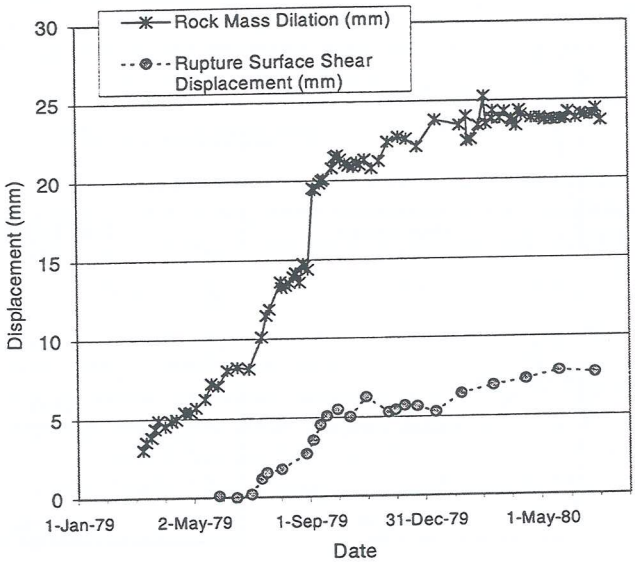

Figure 3: Displacement data for Revelstoke slide showing irregular (stick-slip) behaviour (Martin & Kaiser, 1984)

3.1.3 Radial Displacement Behaviour

Radial displacement behaviour was observed in a number of the cases examined. In all cases, it appeared that extent of radial change in displacement behaviour was related to the extent of fracturing of the slide mass. In the case of Bumper Gully, the slide mass was recognised to be very disturbed, with average RQD's of the order of 15-50%. Highest rates and greatest magnitudes of movement were observed towards the centre and front of the slide. Rates and magnitudes of movement appear to show a general decrease with increasing radial distance towards the rear and sides of the slide. Similar patterns were observed in Dirinei and Malvaglia slides, which were described as highly fractured.

3.2 Reasons Behind Deformation Behaviour

3.2.1 Overview

Translational slides may be considered analogous to laboratory direct shear tests on defects. The critical factors that determine the behaviour of a slide mass on a pre-sheared surface include:

1. the effective normal stress acting on the rupture surface;
2. rupture surface properties and geometry;
3. rock mass properties of the overlying slide mass; and
4. extent of previous shearing.

3.2.2 Normal Stress

Analysis of test data for rock defects highlights the relationships between defect roughness, normal stress and shear strength. At all but very low normal stress levels, the shear strength of a defect decreases with progressive shear strain, until residual friction angle is attained. At low normal stresses dilation of the defect and over-riding of asperities is dominant while at high stress levels shearing and/or crushing of asperities is dominant. At high normal stress levels a more rapid reduction in shearing resistance is expected (ie: the strain required to reach residual strength is expected to be lower). This is schematically illustrated in Figure 4.

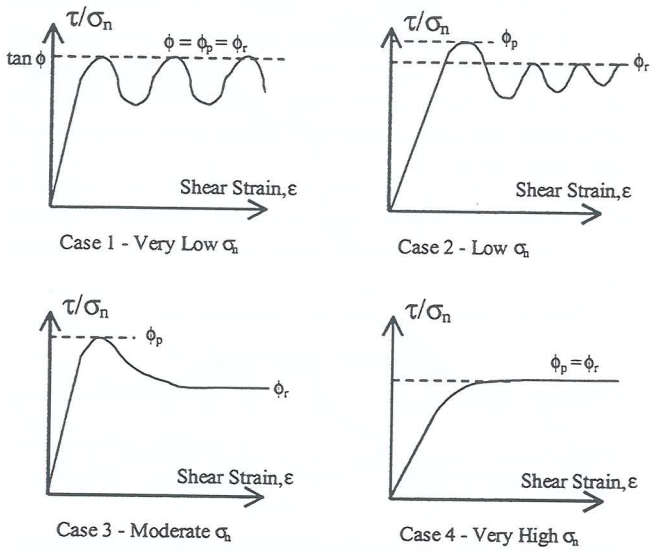

Figure 4: Diagrammatic stress-strain curves for defects at various levels of normal stress (Xu & de Freitas, 1990).

Shearing and/or crushing of asperities is likely to have taken place to some extent in all of the ten cases examined. However, some rupture surfaces are still described as rough and irregular, such as Dirinei and Scalate at low normal stress levels (following Case 2 type behaviour, Figure 4). Other slides have rupture surfaces coated with clay gouge or breccia, such as Vaiont, La Cantera and possibly Bumper Gully at relatively high normal stress levels (Case 3 or 4 type behaviour). Table 3 contains details of average normal stress levels, rupture surface infill and displacement characteristics for each of the ten slides examined in this study.

The case with the highest normal stress level (Vaiont) has long been recognised to have involved sliding on a rupture surface that was at residual strength. The extent of earlier shearing (from previous sliding and regional folding) and the low UCS of the clayey limestone layers contributed to the destruction of asperities and development of residual strength. It is therefore expected that no further strength loss on the rupture surface would have occurred and further displacement behaviour would have been essentially ductile (Case 4 type behaviour, Figure 4). The suddenness of the Vaiont failure may be attributable to brittle failure within the fractured slide mass rather than along the rupture surface. The geometry of the rupture surface was such that internal deformation was required for the slide to proceed. Hendron and Patton (1985) in fact showed that results of stability analysis were sensitive to values of internal friction angle. They also suggested that there was strong three-dimensional control on the slide, which may have also contributed to the brittle collapse.

Table 3: Normal effective stress, rupture surface infill and general displacement behaviour.

Slide	Avge σ'_n (MPa)	Infill	General Displacement-Time Behaviour
Vaiont	3.4	Clay	Smooth primary-tertiary sequences
Malvaglia	1.1	Rock	Long-term linear
Kostanjek	0.9	Clay	Not clear - likely long-term linear
Kariba	0.8	Rock	Linear but variable with load change
Bumper Gully	0.8	Gouge/ Breccia	Smooth primary creep after initial quarrying and lake filling
La Cantera	0.8	Clay	Linear with jump due to stabilisation works
Glen Douglas	0.6	Rock	Long-term linear
Revelstoke	0.4	Clay	Stick-slip irregular
Dirinei	0.3	Rock	Slightly irregular
Scalate	0.2	Rock	Stick-slip irregular

3.2.3 Rupture Surface Properties and Geometry

A basic friction angle was determined for each rupture surface by examination of direct shear test data (on smooth defects) in published literature (Einstein and Dowding, 1989). The basic friction angle is primarily a function of the rock type but is also sensitive to normal stress levels. Where laboratory direct shear test results on infill material was available these results were adopted for basic friction angle where appropriate.

Many slides in this database have rupture surfaces with large-scale irregularities that affect the overall stability of the slope. An assessment has been made of the relevant field scale asperity from descriptions of the rupture surface geometry or by analysis of the changes in vector displacement direction. This asperity roughness is considered as a dilation angle (i) which adds to the overall frictional resistance, and is presented in Table 1. In the case of large slides with complex rupture surfaces, the asperities seen at laboratory scale testing are of little relevance. McMahon (1985) has suggested that the relevant asperities are those that have a wavelength measured over 2% of the length of the rupture surface. In many cases this value served as a useful guide for assessment of dilation angle. Some behaviour differences were noticed from the data when comparing slides on undulose or irregular surfaces with those on relatively planar surfaces. It was assessed that degree of break-up of the slide mass is significantly influenced by the irregularity of the rupture surface. Vaiont, Dirinei, Malvaglia, Kariba, Glen Douglas and Bumper Gully slides all show significant rock mass disaggregation. These slides all occur on rupture surfaces with higher dilation angle values.

3.2.4 Rock Mass Properties

The extent of disaggregation of a slide mass is seen from the data to be not only a function of rupture surface geometry, but is also influenced by failure mechanism, amount of previous sliding and the rock mass strength. The extent of shearing along the rupture surface as a percentage of rock mass dilation was measured at Revelstoke, and is illustrated in Figure 3. It was observed that basal shear accounted for about 40% of the total observed deformation with rock mass dilation accounting for the remainder. It was also observed in this particular case that rock mass dilation preceded shearing along the rupture surface. It is suggested that dilation may have been required in order to over-ride asperities. The internal friction angle (and hence the rock mass strength) of the slide mass may be a significant factor in the stability of the slope, particularly for slides on complex rupture surfaces (as illustrated by Vaiont).

The normal stress level at which crushing of asperities commences (and over-riding ceases) depends on the strength of the rock. It is expected (although not readily observable from the data) that shearing and crushing along the rupture surface will commence at lower stress levels for sliding on clay marl than for fresh limestone. Similarly, slides in weathered gneiss may be expected to show yielding and development of residual strength at lower normal stress levels than slides in fresh gneiss.

3.2.5 Extent of Previous Shearing

The extent of previous shearing has been shown to be influential in the deformation behaviour of these slides. Based on the amount of shear displacement many of the rupture surfaces examined are at or close to residual strength. Slides that have undergone the greatest total displacement have a tendency for more regular deformation and the degree of stick-slip type behaviour is reduced on these slides. This is again related to progressive destruction of asperities on the rupture surface and development of residual strength.

La Cantera slide illustrates that disaggregation of the slide mass can also occur on relatively planar rupture surfaces. Disaggregation in this case is likely due to the large displacement this slide has experienced.

The type of previous shearing (ie: stress relief, sliding or regional tectonic folding) does not appear to influence the deformation behaviour in any significant manner. It is assessed that the extent of shearing and the normal stress levels at which that shearing occurred are of more influence.

4 CONCLUSIONS

The displacement behaviour of a slide on a pre-sheared surface has been shown to be predominantly controlled by:

- the effective normal stress acting on the rupture surface;
- rupture surface properties and geometry;
- extent of previous shearing; and
- rock mass properties of the overlying slide mass.

The first three factors listed above influence the extent of strength reduction from peak towards residual strength and hence the degree of brittleness remaining on the rupture surface. The fourth factor influences the ability of the slide mass to dilate and over-ride asperities on the rupture surface. The development of residual strength on a rupture surface with progressive shear displacement suggests that the likelihood of sudden brittle failure is reduced. The ten cases examined illustrate that stick-slip type motion is reduced with increased displacement. However, Vaiont illustrates that other factors (such as internal deformation) need to be considered before assessment of brittleness can be made.

In contrast to first-time slides on rupture surfaces that have not experienced shear displacement, slides on pre-sheared surfaces are expected to have a reduced stick-slip tendency. Slides on pre-sheared surfaces often show a high degree of disaggregation and following from this they often show a tendency for radial displacement behaviour.

6 ACKNOWLEDGEMENTS

This work forms part of a research project on the deformation behaviour of rock slopes, being undertaken at The University of New South Wales. It has been carried out with valuable support and contributions provided by NSW Dept. of Land and Water Conservation, SMEC, Goulburn Murray Water, Australian Water Technologies, US Bureau of Reclamation, Dams Safety Committee of NSW, ACTEW Corporation, Qld Dept of Natural Resources, Snowy Mountains Hydro-Electric Authority, SA Water, Pells Sullivan Meynink, RTA, NSW Dept of Public Works and Services, Qld Dept of Main Roads, BCHydro, USGS, Contact Energy and Melbourne Water.

REFERENCES

1. Einstein, H.H. and Dowding, C.H. (1989) Shear resistance and deformability of rock discontinuities. In Y. Touloukian *et al* (eds.) *Physical Properties of Rocks and Minerals*. Chapter 7, pp177-219. Hemisphere Publishing.
2. Emery, J. (1978). Simulation of slope creep. In Voight (ed.), *Rockslides and Avalanches, 1. Natural Phenomena.* Elsevier, Amsterdam.
3. Hendron, A.J. and Patton, F.D. (1985) *The Vaiont Slide, A Geotechnical Analysis Based on New Geologic Observations of the Failure Surface*. US Army Corps of Engineers Technical Report GL-85-5.
4. Hutchinson, J.N. (1988) General Report: Morphological and geotechnical parameters of landslides in relation to geology and hydrogeology. In Bonnard (ed) *Proc. Fifth Int Symp Landslides*, Switzerland. Balkema. 1:3-35.
5. McMahon, B.K. (1985) Some practical considerations for the estimation of shear strength of joints and other discontinuities. In: *Proc. International Symposium on the Fundamentals of Rock Joints*, pp 475-485.
6. Martin, C.D. and Kaiser, P.K. (1984) Analysis of a rock slope with internal dilation. Canadian Geotech. Journal, Vol. 21, pp 605-620.
7. Skempton, A.W. and Hutchinson, J.N. (1969) Stability of natural slopes and embankment foundations - state of the art report. *Proc Seventh Int Conf Soil Mechanics and Foundation Engineering*, Mexico. Vol. 1, pp 291-340.
8. Xu, S. and de Freitas, M.H. (1990) The complete shear stress-vs-shear displacement behaviour of clean and infilled rough joints. In Barton and Stephansson (ed.) *Rock Joints*. Rotterdam, Balkema.

Case Name (Origin)[1]	Geology	Avge σ'_n[2] (MPa)	Rupture Surface Description	Approx UCS Category[3]	Approx ϕ_b (deg)	Approx i[4] (deg)	Total Displ (mm)	Displacement/ Slope Length (%)	Comments on Displacement Behaviour
Valont (R, F)	Lime-stone	3.4	Dip = 24 deg (avge). Defined by bedding partings in monoclinal fold. Rupture surface in clay units within marly limestone. Direct shears: ϕ_r=8-10deg. Small monoclinal folds perp to direction of shearing giving i = 9-10deg.	R2	10	10	5340+ (measured over 42 months)	0.39+ (measured)	Reactivation due to reservoir filling. Planar/curved slide with some rotational movement influenced by internal deformation of slide mass (analysis sensitive to ϕ chosen for internal deformation). Displ closely associated with reservoir level/rain. Three sequences of primary to tertiary creep behaviour. Expect some strain hardening in fractured slide mass
Bumper Gully (R, F)	Sandstone /siltstone	0.8	Dip = 24 deg. Slide base geometry affected by synclines/anticlines – follows bedding partings in most of length with joints controlling remainder of length.	R2	22	6	3800+ (measured over 480 months)	0.78+ (measured)	Reactivation due to reservoir filling. Complex translational and rotational slide. Numerous small surficial slides defined by local folds on surface of larger slide. Highly-moderately disturbed slide mass (RQD=15-50%). Variation in displ. vector behaviour suggests i=6-10deg.
Scalate (SR, R)	Schistose gneiss (weath'd)	0.2	Wedge sliding on joint sets (incl. stress relief joints) – rough & irregular – with intersection plunge=40deg. Expect some staining of joint surfaces.	R3	25	10	290+ (measured over 9 months)	0.36+ (measured)	Stick-slip behaviour seen in early displacement monitoring. Seasonal rainfall has only minor impact on slide behaviour. Slide exhibited primary, secondary and tertiary creep phases before collapse. Vector displ. plunge = 40deg.
Dirinel (SR, R)	Schistose gneiss (weath'd)	0.3	Planar sliding on 33deg dip stress relief joints – rough & irregular - with minor crushing on slide surface.	R3	25	8	1900+ (over 34 months) 5000+ (inferred from geomorph)	5.0+ (inferred)	Reactivation associated with fluvial oversteepening and rain. Sensitive to high intensity rain events. Slide shows overall primary creep trend. Radial displ behaviour observed. Vector trend parallel to rupture surface.
Malvaglia (R)	Schistose gneiss	1.1	Wedge sliding on joint sets and schistosity. No infill. Dip of 21+ deg on rupture surface.	R3	25	6	130 (measured over 65 months)	0.09+ (measured)	Reactivation due to reservoir filling. Radial decrease in displacement rates suggesting dilatant (fractured) rock mass, therefore possibly large historical displacement. Sensitive to seasonal rainfall. Approx. linear displ-time behaviour.
La Cantera (R)	Lime-stone/ dolomite/ clay marl	0.8	Planar slide in 5m thick clay marl layer (following bedding) dipping at 18 deg. Illite/kaolinite coating on rupture surface with ϕ_r=17-18deg. Distinct shear surface in inclinometer readings.	R2	18	0	80+ (over 10 months) 50000+ (inferred from geomorphology)	11.0+ (inferred)	Geomorphological features suggest previous sliding of the order of 50 metres. Rupture surface at residual. Slide mass is highly fractured. Expect low dilation angle on rupture surface due to shearing in clay marl layers. Slide shows near-linear displ-time behaviour with no signs of stick-slip.
Kariba (R, F)	Gneiss/ quartzite	0.8	Rotational slide along rupture surface defined by syncline along weath'd gneiss/quartzite contact. Rupture surface dips at 35-40deg out of slope at head and 20 deg into slope at toe.	R2	23	8	690+ (measured over 432 months)	0.27+ (measured)	Slide reactivated by dam works and reservoir filling. Slide mass highly fractured and sensitive to rain/spray from spillways. Previous sliding known to be significant with numerous tension features at head of slide. Internal deformation of slide mass required for movement of slide.
Revelstoke (R, F)	Quartzite/ gneiss	0.4	Translational sliding along 23deg dip foliation shear. Direct shear ϕ_r=18deg on 20-50mm clay gouge. Undulose surface due to regional folding. Clay gouge & breccia on rupture surface.	R2	18	6	34+ (measured over 18 months)	0.04+ (measured)	Slide mass has numerous steeply dipping internal shears and some fracturing. Dilation of slide mass (measured using extensometers) observed to occur before shearing along rupture surface. Displacement sensitive to rainfall. Rupture surface dilation determined by regional folding.
Glen Douglas (R, F)	Schist/ phyllite (weath'd)	0.6	Planar sliding on schistosity (up to 30 deg dip) with back release on joint set. Slide located within regional fold. Crenulation on schistosity gives large difference between peak and residual ϕ.	R2	21	8	620+ (measured over 228 months)	0.17+ (measured)	Slide mass quite broken suggesting large prehistoric movement. Crenulation on schistosity + regional folding add to frictional resistance. Dilatant rock mass, therefore likely to be more influenced by larger geometrical features on rupture surface. Approx linear long-term displ-time behaviour.
Kostanjek (F)	Dolomitic breccia/ limestone/ marl	0.9	Planar sliding on three levels. Main surface in silty schists and marls. Upper surfaces within clayey marl. Dip=10deg. ϕ_r=9deg on main rupture surface	R1	9	2	6500+ (measured over 372 months)	0.47+ (measured)	Slide activated by quarrying, blasting and high groundwater pressures. Peak shear strength measured as 20-28 deg therefore large drop to residual strength. Likely 1st time slide but previous shearing due to regional folding.

Table 1: Data on slides occurring on previously sheared rupture surfaces.

(1) R = reactivated landslide, F = folding has affected slide surface, SR = stress relief has affected slide surface.

(2) Average normal effective stress acting on rupture surface.

(3) Unconfined compressive strength category as per ISRM.

(4) Assessed relevant field scale dilation angle.

Laboratory Evaluation of the Treatment of Alkaline Leachate with Coal Washery Discard

STUART C. GRAY
Doctoral Student, Department of Civil, Mining and Environmental Engineering, University of Wollongong NSW 2522 Australia
CARL E. MORRIS
Senior Lecturer, Department of Civil, Mining and Environmental Engineering, University of Wollongong NSW 2522 Australia
MUTTUCUMARU SIVAKUMAR
Assoc. Prof., Department of Civil, Mining and Environmental Engineering, University of Wollongong NSW 2522 Australia

Summary This paper presents a laboratory investigation into the utilisation of a New South Wales coal washery discard (CWD) as an inexpensive and readily available material for reducing groundwater alkalinity in situ. It is part of a larger study examining the potential for Australian CWD to be used as a permeable reactive barrier material for the removal of various inorganic and organic contaminant species from groundwater. Batch test results indicate that both fine and coarse CWD can reduce the pH of an alkaline contaminant solution from pH 11-12.5 to pH 8.5. The geochemical equilibrium model MINTEQA2 has been used to assist in the identification of the major attenuation mechanisms. It appears that the kaolinite and siderite within the CWD are dissolving and relatively insoluble secondary minerals (aluminium and iron hydroxides) are being formed. This process is time-dependent, and requires a higher residence time for contaminant solutions with a higher initial pH. Results indicate that CWD has the potential to be an economical and environmentally sustainable groundwater treatment material.

1 INTRODUCTION

Coal washery discard (CWD) is composed of high ash rock that was interbedded with, or was adjacent to, the coal prior to its extraction. It is separated from the coal during the washing stage of coal processing. Approximately 25 million tonnes of CWD were produced within New South Wales, Australia, during 1997-98. Since NSW has 7810 million tonnes of recoverable coal reserves and is currently producing coal at almost 108 million tonnes per year, the production of coal and CWD is likely to continue for many decades.

The primary disposal option for CWD is surface or near-surface emplacement (Wangen and Jones, 1984). This method requires large land areas and has the potential to result in surface water and groundwater contamination. Fluidised-bed combustion is growing in application and is discussed by Duffy and Kable (1984). It is therefore necessary to develop new options for the environmentally sustainable disposal of CWD. This paper is part of a larger study examining the use of Australian CWD as a permeable reactive barrier material for the in situ removal of inorganic and organic contaminants from groundwater. The use of a waste material in reactive barriers is likely to be cost-effective and reduces the demand for emplacement areas.

This paper focuses on a laboratory investigation into the neutralisation of alkaline groundwater at a blast furnace slag (BFS) emplacement using coarse Illawarra CWD. The aim is to quantify the neutralisation process and identify the primary attenuation mechanisms. Geochemical modelling with MINTEQA2, developed at the U.S. Environmental Protection Authority (Allison et al., 1991), has been performed to assist in this investigation.

2 CONTAMINANT SOLUTION

The alkaline contaminant solution has been taken from a BFS emplacement situated south of Wollongong, NSW, Australia. Table 1 gives the chemical characteristics of this groundwater. Column three of Table 1 lists some chemical characteristics of a sample of this groundwater which has been treated with acid to reduce the pH for purposes of this study.

It can be deduced from the data in Table 1 that the groundwater is saturated or nearly saturated (depending upon rainfall levels) with calcium hydroxide ($Ca(OH)_2$). This forms from the dissolution of calcium oxide (CaO) in the BFS. Since the emplacement is within a coastal marine aquifer, halite (NaCl) also dominates the groundwater chemistry.

During high intensity rainfall, this alkaline plume flows into a natural canal at the emplacement site and discharges into a stormwater drain. The drain flows into Lake Illawarra, which is a sensitive estuarine environment. In an attempt to prevent the movement of high pH water into Lake Illawarra, the canal has been filled with 6000 tonnes of local Illawarra coarse CWD to act as a permeable reactive barrier. Refer to Gray et al. (1999) for more detail regarding this CWD reactive barrier.

(2) Average normal effective stress acting on rupture surface.
(3) Unconfined compressive strength category as per ISRM.
(4) Assessed relevant field scale dilation angle.

Table 1. Quality of the BFS groundwater.

Parameter	Groundwater taken from emplacement	Sample treated with acid
pH	12.70	11.14
conductivity (µs/cm)	6870	1684
calcium (Ca)	450	100
magnesium (Mg)	0.93	0.35
sodium (Na)	370	*
potassium (K)	29	*
iron (Fe)	0.2	2.2
aluminium (Al)	0.6	1.3
manganese (Mn)	0.01	*
zinc (Zn)	0.26	*
alkalinity as $CaCO_3$	486	82.5
chloride	300	*
sulphate	24.7	*

(all units mg/L except pH and conductivity)
* not measured

3 COAL WASHERY DISCARD PROPERTIES

The CWD used in these tests came from the South Bulli Colliery, which is part of the NSW Illawarra/Southern coalfield. Coal from this region is extracted from the Illawarra Coal Measures (approximately 200 metres thick on average), which is overlain by sandstones, shales and conglomerates and underlain by basalts, shales and sandstones. The larger study is also investigating the attenuation properties of CWD from the other four coalfields throughout NSW (Newcastle, Hunter, Western/Lithgow and Gunnedah) as well as from coalfields throughout Queensland.

Several tests have been conducted on the Illawarra CWD samples including particle size distribution, mineral content, and leachate composition.

3.1 Particle Size Distribution

CWD is produced as either a coarse rock-like material or as fine slurry (or tailings) depending on the processing mechanism. Coarse reject usually contains particles of size 0.5-127 mm, and fine reject is composed of particles of size <0.5 mm. According to McGlinn (1992), coarse reject can be divided by size into 'medium' (0.5-12.7 mm) and 'coarse' (12.7-127 mm). This study focuses on the attenuation capacity of coarse CWD since it is necessary that the reactive barrier is highly permeable.

At the macroscopic level, coarse Illawarra CWD is composed of carbonaceous shale and mudstone, sandstone fragments, ironstone, sand-sized particles and a small proportion of fines. Typical particle size distributions are given in Figure 1. On average, this CWD is composed of approximately 84% gravel and cobbles, 15.5% sand-sized particles and only 0.5% silt/clay sized particles. Note that both coarse samples contain a small amount of fines (about 4%).

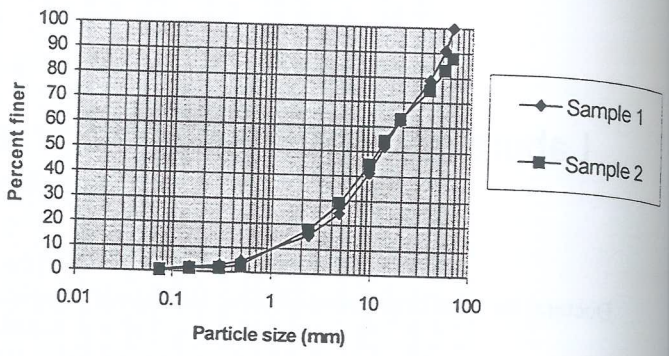

Figure 1. Particle size distribution for coarse Illawarra CWD.

Reactive barriers must be permeable to allow groundwater to pass through them so that contaminants in the water can react with the media within the barrier. However, if the hydraulic conductivity of the barrier is too high, the residence time may be insufficient. Of course, if the hydraulic conductivity is too low, then the groundwater may flow around the barrier. Column testing (described by Shackelford, 1994) will be used to investigate the relationship between contact time and pH reduction.

3.2 Mineral Content

X-ray diffraction analysis was used to identify the mineral phases present in the CWD. Each analysis identified quartz (SiO_2), kaolinite ($Al_2Si_2O_5(OH)_4$), siderite ($FeCO_3$), calcite ($CaCO_3$) and illite ($KAl_2(Si_3AlO_{10})(OH)_2$) as the major mineral components of CWD. As shown by Figure 1, most of these minerals are within gravel-sized particles. Unlike the CWD produced in many other areas of the world, Illawarra CWD contains very small quantities of acid producing pyrite. According to Ward (1980), siderite forms in coals and other organic sediments that do not contain pyrite, due to the lack of sulphur compounds.

Short et al. (1998) has also studied CWD from the South Bulli Colliery, and the mineral composition of CWD according to this study is given in Table 2.

Table 2. Mineralogy of South Bulli CWD (adapted from Short et al., 1998)

Mineral	% by mass
Quartz	25
Clay minerals (kaolinite, illites, chlorites)	35
Siderite	5-10
Calcite	2
Carbon/fine coal	20-30

CWD has the potential to remove various organic and inorganic species from groundwater. Its high carbon content may make it a viable option for the treatment of harmful organic species such as phenol, benzene and toluene. In addition, the clay minerals may remove trace heavy metals

from groundwater via cation exchange processes, while the carbonates provide a neutralisation capacity.

3.3 Leachate Composition

Neutralisation of pH is achieved by the interaction of the contaminant solution with the mineral species present. Several studies have examined the leaching behaviour of CWD, including Ward (1980), Kerth and Wiggering (1990) and McGlinn (1992). In each of these studies, soluble components were extracted from the CWD using an acidic solution.

When Illawarra CWD is subject to a standard leaching test, a leachate of pH 8.5-9.5 is produced. According to McGlinn (1992), calcium and magnesium are the major cations in this alkaline solution. Iron and aluminium are present in lower concentrations. It is most likely that this pH rise is due to partial dissolution of the carbonates calcite ($CaCO_3$) and siderite ($FeCO_3$). Since dolomite ($(Ca,Mg)CO_3$) was not identified from X-ray diffraction, it is most likely that the magnesium present in the leachate is derived from a magnesium-bearing siderite (McGlinn, 1992).

It cannot be assumed that these CWD minerals will behave in the same way under highly alkaline conditions. Indeed, one would expect that most of the minerals would be much less soluble when exposed to the BFS leachate.

4 LABORATORY TESTING

No standard method could be found for measuring the neutralisation capacity of the Illawarra CWD. Hence, the standard method for a short-term batch test, ASTM D 4319-93 (ASTM, 1997), was used. Conventional batch tests are used to establish an adsorption isotherm for a contaminant/soil combination. This method assumes that contaminant attenuation from all other reactions - precipitation and oxidation-reduction - is negligible. In this case, it is reasonable to assume that any pH reduction is due to reactions between the multicontaminant solution and aqueous species leaching from the CWD. Ion exchange and adsorption processes may be taking place, however these are likely to have a smaller impact on solution pH than mineral dissolution.

A sample of coarse Illawarra CWD was first dried in the oven to remove non-structural moisture and then crushed to a maximum particle size of about 10 mm for small-scale laboratory testing purposes. A portion of the crushed coarse CWD was then passed through a 500 μm sieve to obtain a sample of fine reject (<0.5 mm). For both the coarse and fine fractions, 5 g, 10 g, 20 g and 25 g samples were combined with the pH 11.14 multicontaminant BFS groundwater solution (Table 1) in a solution volume (mL) to CWD mass (g) ratio of 4:1. The BFS groundwater was treated with acid so as not to harm the calcium ion selective electrode used for instantaneous calcium monitoring. Each reaction flask was then shaken on a laboratory shaker for 6 hours for every 3 day portion of the contact period. The contact period ranged from 1 day to 13 days. At the end of each contact period, the supernatant was separated from the solid phase and filtered before analysing for pH, conductivity, calcium, magnesium, iron, aluminium, alkalinity and carbonate using the appropriate standard analytical method described in APHA (1985).

In addition, to assist in the identification of the major attenuation mechanisms, 20 g samples of oven-dried quartz sand, oven-dried kaolinite clay, pure calcite and coarse CWD were combined with the pH 12.59 contaminant solution (Table 1). Siderite is not available in pure form, and therefore could not be included in this test. The standard method procedure was used to monitor any pH change over time.

5 BATCH TEST RESULTS

Figure 2 compares the pH reduction over time for the 5 g, 10 g, 20 g and 25 g coarse CWD samples. In each case, the pH reduces to about 8.3 - 8.8 after three days and converges to 8.5 after 13 days. This similar pH reduction pattern is due to the contaminant solution to CWD ratio being the same in each case.

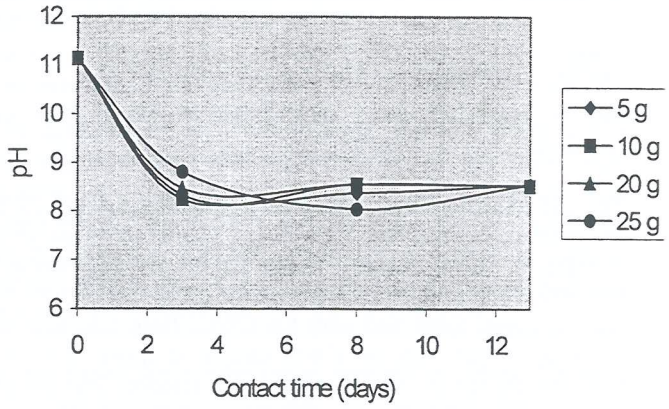

Figure 2. pH reduction for coarse CWD samples.

The pH reduction over time for a 20 g coarse CWD sample and a 20 g fine CWD sample is given in Figure 3. Coarse and fine CWD have a similar pH reduction pattern. Note, however, that the reduction rate is greater for the fine CWD during the first few days. This is most likely due to the greater surface area within the fine sample and the greater initial mineral dissolution. Over time, an equilibrium pH of about 8.5 is reached in each case.

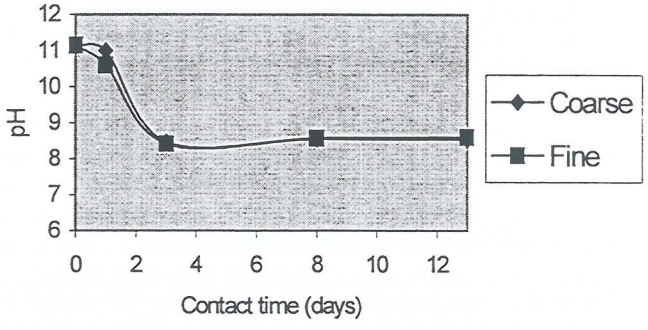

Figure 3. pH reduction for 20 g samples.

Other groundwater quality parameters were monitored in addition to pH (Table 3). Again, it is necessary to show the changes for only one CWD mass.

Table 3. Changes in contaminant solution chemistry for 20 g CWD samples.

Analyte	Initial	Coarse CWD			Fine CWD		
	Level	3 d	8 d	13 d	3 d	8 d	13 d
pH	11.14	8.49	8.55	8.54	8.41	8.57	8.6
cond (µS/cm)	1684	1708	1785	1877	1752	1782	1854
CO_3^{2-}	12.8	-	-	-	-	-	-
HCO_3^-	-	70.14	88.57	102	73.28	94.78	103.3
Ca^{2+}	100	30.43	44.13	29.42	47.61	55.01	66.67
Mg^{2+}	0.35	2.06	2.32	2.13	3.95	4.63	4.96
Fe^{2+}	2.2	1.45	1.77	0.59	0.95	0.33	0.49
Al^{3+}	1.3	1.74	0.74	1.03	2.7	1.33	0.81

(all units mg/L except pH and conductivity)

As shown in Table 3, electrical conductivity increases over time for both the fine and coarse samples. This indicates that minerals within the CWD are gradually dissolving in the alkaline environment. In each case, there is a net increase over time in magnesium, and a net decrease in calcium, iron and aluminium.

The pH reductions resulting from combining the pH 12.59 contaminant solution with individual CWD minerals are given in Figure 4. This data clearly shows that the pH reduction with kaolinite alone is much greater than the pH reduction with the other minerals alone and with the CWD. Note also how the reduction in pH with the CWD sample is slower than that observed for the pH 11.14 contaminant solution. The pH has only reduced to 9.7 after 11 days of contact. These results will be explained in the following section.

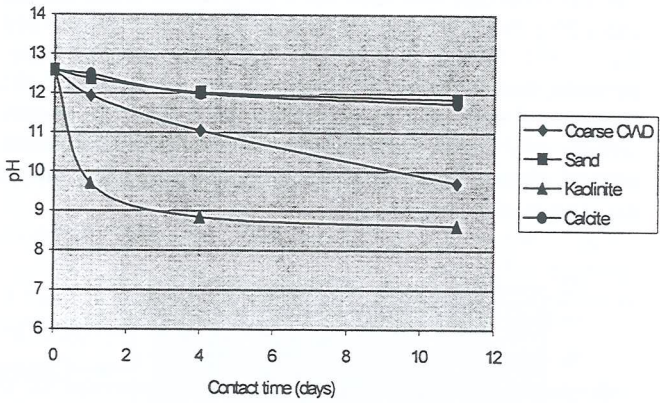

Figure 4. pH reduction for individual minerals.

6 ATTENUATION MECHANISMS

The results from these laboratory batch tests show that CWD can reduce the pH of alkaline groundwater. This pH reduction is caused by the interaction between certain minerals within the CWD and the alkaline species in the BFS groundwater. The equilibrium geochemistry model MINTEQA2 has been used to aid in the identification of the major attenuation mechanisms.

6.1 Hydroxide Formation

The primary mechanism which leads to this pH reduction is most likely to be the dissolution of siderite and kaolinite from the CWD and the formation of secondary minerals: ferrous hydroxide ($Fe(OH)_2$), ferric hydroxide ($Fe(OH)_3$) and aluminium hydroxide ($Al(OH)_3$) precipitates. The formation of the iron precipitates is given by (1) and (2) and the formation of the aluminium precipitate is given by (3) and (4). Ferrous hydroxide is readily oxidised in air to form ferric hydroxide. Unfortunately, ferric hydroxide tends to have a positive total net surface charge and often coats the negatively charged surfaces of many soil particles (Fryar and Schwartz, 1994). This coating may hinder further dissolution of siderite and could also reduce the hydraulic conductivity of a reactive barrier.

$$FeCO_{3(aq)} + Ca(OH)_{2(aq)} \Leftrightarrow Fe(OH)_{2(s)} + Ca^{2+} + CO_3^{2-} \quad (1)$$

$$2FeCO_{3(aq)} + 3Ca(OH)_{2(aq)} \Leftrightarrow 2Fe(OH)_{3(s)} + 2e^- + 3Ca^{2+} + 2CO_3^{2-} \quad (2)$$

$$Al_2Si_2O_5(OH)_{4(s)} + 6H^+ \Leftrightarrow 2Al^{3+} + 2H_4SiO_{4(aq)} + H_2O \quad (3)$$

$$2Al^{3+} + 3Ca(OH)_{2(aq)} \Leftrightarrow 2Al(OH)_{3(s)} + 3Ca^{2+} \quad (4)$$

This attenuation mechanism can also explain the changes in solution chemistry shown in Table 3. The consistent increase in magnesium can be attributed to the dissolution of a magnesium-bearing siderite. Magnesium does not form a hydroxide since $Mg(OH)_2$ is considerably more soluble than the aluminium and iron hydroxides. The level of calcium reduces due to additional carbonate ions entering into solution from the dissolution of siderite and the resulting precipitation of calcite. In addition, there is a net decrease in aluminium and iron due to the formation of the hydroxides. Since the concentrations of most of the measured species are decreasing, the increase in solution conductivity implies that other unmeasured species are entering into solution.

Results from X-ray diffraction analysis confirm that the formation of the aluminium and iron precipitates is the most likely attenuation mechanism. A significant drop in the intensity at 2θ = 12.33 and 24.84 (kaolinite peaks) and 2θ = 32.05 (siderite peak) was observed for the coarse Illawarra CWD after 11 days batch testing. In addition, a significant drop in the intensity at the kaolinite peaks was also observed for the kaolinite clay after 11 days batch testing. This indicates that the kaolinite and siderite are partially dissolving and releasing Al^{3+} and Fe^{2}+ ions that are able to react with the

OH^- ions. It should be noted at this stage that although the dissolution of siderite and kaolinite is favoured by acidic conditions, dissolution at pH 11-12.5 is sufficient to remove most of the hydroxide from solution. Kau et al. (1996) reports that kaolinite dissolution and the release of Al^{3+} ions is least at approximately pH 7 and increases marginally under basic conditions.

This attenuation mechanism has been simulated using MINTEQA2. The model incorporates the initial concentrations of various species within the BFS groundwater and the mineral phases added when the contaminant solution is mixed with the CWD. It was assumed that the CWD is 15% kaolinite and 10% siderite by mass, as given in Table 2. In this way, a 20 g sample in 80 mL of solution contains 0.2 mol/L kaolinite and 0.216 mol/L siderite. The MINTEQA2 output is summarised in Table 4.

Table 4. MINTEQA2 output at equilibrium.

Parameter	MINTEQA2 output
equilibrium pH	8.28
kaolinite	0.1999 mol/L
siderite	0.2016 mol/L
aluminium hydroxides/oxides formed (gibbsite, diaspore)	5.9×10^{-5} mol/L
iron hydroxides/oxides formed (wustite, ferrihydrite)	1.4×10^{-2} mol/L

The predicted pH reduction using MINTEQA2 is reasonably close to the actual reductions measured for the pH 11.14 contaminant solution (Figure 2 and Figure 3). However, it is substantially lower than the pH recorded after 11 days contact between the pH 12.59 contaminant solution and the coarse Illawarra CWD (Figure 4). Since MINTEQA2 is an equilibrium model, it does not incorporate reaction kinetics. Rather, it assumes that all reactions proceed instantaneously. In this case, the dissolution of kaolinite and siderite is slower at higher initial pH, resulting in a slower pH reduction. Although the pH for the CWD sample in Figure 4 will eventually converge to about pH 8.3-8.5, it takes longer than the samples in Figure 2 and Figure 3.

Note also from Table 4 that the dissolution of siderite is greater than the dissolution of kaolinite, and the formation of iron hydroxides is far greater than that for aluminium. Therefore, based on the MINTEQA2 output, the formation of iron hydroxides is the dominant pH reduction mechanism when a sample contains both siderite and kaolinite. This could be explained by the fact that ferric hydroxide is more insoluble than aluminium hydroxide. However, this result seems to contradict the data in Figure 4 that shows how kaolinite alone provides a greater pH reduction than kaolinite and siderite combined. This will require further investigation.

6.2 Silica Dissolution

Another attenuation mechanism that has been considered is silica dissolution. The dissolution of silica is favoured by alkaline conditions, and results in the generation of H^+ as shown by (5).

$$SiO_{2(s)} + 2H_2O \Leftrightarrow H_4SiO_{4(aq)} \qquad (5)$$

Short et al. (1998) believes that the dissolution of silica can have a neutralising effect on alkaline solutions. However, Figure 4 indicates that the process in (5) is very slow and has only a very small impact on solution pH within the first 11 days of contact. MINTEQA2 predicts that the pH will reduce from 12.5 to 10.33 when silica interacts with the alkaline solution. However, recall that MINTEQA2 assumes that all reactions proceed to completion instantaneously. Therefore, although the pH may eventually reach 10.33, this may take weeks or months in the laboratory.

Since the CWD is to be used as a reactive barrier material, contact time is limited and may become particularly low during times of high rainfall. Hence, although silica can theoretically reduce the pH of an alkaline solution in the long term, it would not necessarily be the dominant pH reduction mechanism within a reactive barrier.

7 CONCLUSIONS AND RECOMMENDATIONS

The development of new utilisation options for CWD is a growing area since millions of tonnes of this waste rock material will continue to be produced annually within New South Wales. This paper is part of a larger study investigating the potential for CWD to be used as a permeable reactive barrier material for the in situ removal of various organic and inorganic contaminant species from groundwater.

In this paper, the neutralisation capacity of coarse Illawarra CWD has been examined. Based on a laboratory batch testing programme, it appears that CWD is capable of reducing the pH of highly alkaline groundwater saturated with $Ca(OH)_2$. An equilibrium pH of about 8.5 was reached within about three days for both the fine and coarse CWD samples when the initial contaminant solution pH was 11.14. However, when the CWD was combined with the pH 12.59 contaminant solution, the pH had reduced to only 9.7 after 11 days of contact.

It appears that the primary mechanism reducing the pH is the dissolution of kaolinite and siderite from the CWD and the formation of aluminium and iron hydroxides. X-ray diffraction analyses highlight this gradual dissolution in kaolinite and siderite during batch testing. The MINTEQA2 geochemical model has been used to simulate this process. Based on this model, the equilibrium pH is about 8.2-8.3 regardless of the initial contaminant solution pH. This value is similar to the final pH measured in the laboratory for the pH 11.14 solution since it had already reached equilibrium. However, due to the slower dissolution of kaolinite and siderite in higher pH, the pH of the 12.59 contaminant solution had not reached this equilibrium level after 11 days. This means that the hydraulic conductivity of a CWD reactive barrier must be optimised so that the residence time is sufficient to neutralise the highest pH to be expected in the field.

Silica dissolution was found to be negligible, despite the alkaline conditions. Although silica may theoretically dissolve in the long term to produce an acidic solution, contact times are limited within a reactive barrier. Therefore, the contribution by silica to the total pH reduction would be negligible.

8 ACKNOWLEDGMENTS

The laboratory facilities and field equipment provided by Wollongong City Council is gratefully appreciated. The authors are also thankful to Joanne George (University of Wollongong) for laboratory assistance.

9 REFERENCES

Allison, J.D., Brown, D.S. and Novo-Gradac, K.J. (1991). *MINTEQA2/PRODEFA2: A geochemical assessment model for environmental systems*. EPA/600/3-91/201. US NTIS.

American Public Health Association (1985) *Standard Methods for the Examination of Water and Wastewater*. 16th edition. Washington.

American Society for Testing and Materials (1997). Standard Test Method for Distribution Ratios by the Short-Term Batch Method. *Annual Book of ASTM Standards Vol. 4.08*. ASTM, West Conshohocken. pp. 533-538.

Duffy, G.J. and Kable, J.W. (1984). *The Comparative Environmental Impact of Methods for the Disposal of Coal Washery Tailings with Particular Reference to Fluidised-Bed Combustion*. CSIRO Institute of Energy and Earth Resources, Division of Fossil Fuels, North Ryde.

Fryar, A.E. and Schwartz, F.W. (1994). Modelling the removal of metals from groundwater by a reactive barrier: Experimental results. *Water Resources Research*. Vol. 30, No. 12, pp. 3455-3469.

Gray, S.C., Indraratna, B. and Yassini, I. (1999). Contaminant Transport through a Coal Washery Discard Reactive Wall. *Environmental Engineering 1999*. ASCE, Virginia.

Kau, P.M.H., Smith, D.W. and Binning, P. (1996). *The Dissolution of Kaolin by Acidic Fluoride Wastes*. University of Newcastle, Department of Civil, Surveying and Environmental Engineering, Research Report No. 114.11.1996.

Kerth, M. and Wiggering, H. (1990). The weathering of colliery spoil in the Ruhr - Problems and solutions. *Proceedings of the Third Interational Symposium on the Reclamation, Treatment and Utilisation of Coal Mining Wastes*, Glasgow, pp. 417-424.

McGlinn, P. (1992). *Characterisation and Leaching Behaviour of Coal Washery Tailings*. University of Wollongong, Department of Geology, MSc. Thesis.

Shackelford, C.D. (1994). Critical Concepts for Column Testing. *Journal of Geotechnical Engineering*. Vol. 120, No. 10, pp. 1804-1828.

Short, S.A., Bannigan, D.J. and Nichols, P.S. (1998). pH Management of Waste Waters or Leachates by Exposure to Coal Washery Discard. *Proceedings of the 2nd International Conference on Environmental Management*, Wollongong, Australia, pp. 347-354.

Wangen, L.E. and Jones, M.M. (1984). The Attenuation of Chemical Elements in Acidic Leachates from Coal Mineral Wastes by Soils. *Environ Geol Water Sci*. Vol. 6, No. 3, pp. 161-170.

Ward, C.R. (1980). *Mineralogical Characteristics and Weathering Behaviour of NSW Colliery Waste Materials*. Department of Applied Geology, NSW Institute of Technology.

DETERMINATION OF FIELD STRESS RATIO AND YOUNG'S MODULUS USING THE UNDER EXCAVATION TECHNIQUE

Hole, J.A.; Geotechnical Engineer; Pells Sullivan Meynink Pty Ltd;
Suite 11, 10 East Parade, Eastwood NSW 2122.

ABSTRACT

The under-excavation technique (UET) is a simple method of assessing the Field Stress Ratio (k) and Young's Modulus (E) of a rock mass from its response to an advancing excavation. The key to this method is that a hole in an elastic medium under stress will have a unique convergence signature which can be measured. The advantages of this method are its simplicity, low cost, utility, applicability to excavations of irregular dimensions, is non-invasive and views the rock mass at a suitably large scale. Further, it can be applied to any excavation in relatively homogeneous material , being particularly suited to tunnels and shafts.

This paper (1) outlines the theoretical background for the UET, (2) explains a practical and simple way to apply it, and (3) offers the case study of the Eastern Distributor Tunnel where it has been successfully applied.

1. INTRODUCTION

For thousands of years humans have been developing underground space, largely in the pursuit of minerals. With growing pressure on today's crowed cities, there is an increased push towards the development of underground space for civil engineering applications. This push has resulted in the development of new and the refinement of old design and monitoring tools. The Underground Excavation Technique (UET) is one such tool.

Techniques for analysing a rock mass's response to an advancing excavation are not new (Pells et al, 1981), however until the development of numerical analysis software they were limited to tunnels of regular profile. With increasingly available and simple to use numerical modelling software, it is now relatively simple to estimate the geometric influence an excavation has on sidewall convergence.

From a practical view point, the UET allows the continual assessment of insitu stresses in a rock mass to be during the excavation phase of a project, providing a useful tool to assist in the design of excavation support and an aid to recognise zones of abnormal ground conditions. It also allows a check to be made on insitu stress measurements that may have been made during the investigation phase of a project.

2. THEORETICAL BACKGROUND

In 1898 Kirsch published one of the first closed form solutions describing the relationship between stresses and strains around an excavation in a homogeneous elastic medium. The Kirsch Solution has become the basis for numerous methods for assessing the behaviour of a hole in a media, including the UET.

The mathematical derivation of the Kirsch Solution is beyond the scope of this paper, and no attempt is made to reproduce it here. Rather, this paper limits itself to the principles of the UET. Readers seeking a more complete coverage of the Kirsch Solution are referred to standard texts on the subject - Love (1927) and Jaeger & Cook (1971).

The Kirsch Solution for radial displacements at the surface a circular excavation in an infinite homogeneous isotropic linear elastic medium (plain strain) can be represented as:

$$u = \frac{(1-\nu^2)}{E} dp\left[\tfrac{1}{2}\left(1+\tfrac{1}{k}\right)+\left(1-\tfrac{1}{k}\right)\cos\theta\right] \qquad \text{Eqn 1}$$

where:

u = radial displacement of a point on the perimeter of the hole;
p = field stress at the level of the hole;
d = diameter of circular hole;

E = Young's modulus (elastic parameter);
υ = Poisson's ratio (elastic parameter);
θ = angle from the x axis to the point on the perimeter of the hole being considered; and
k = stress ratio (typically horizontal stress divided by vertical stress).

Figure 1 shows the geometric relationship between the parameters of eqn 1.

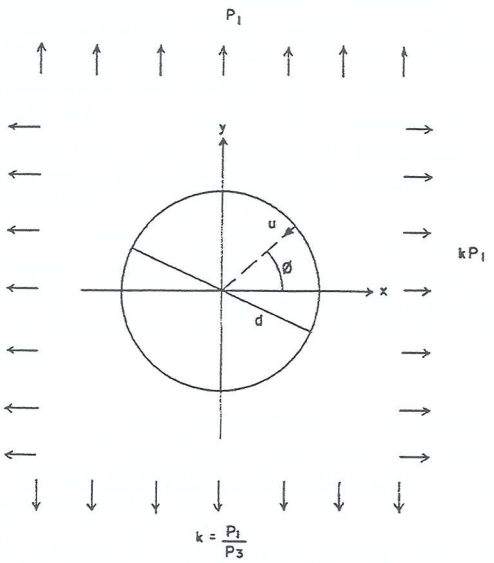

FIG 1: Circular Hole in an Infinite Elastic Medium.

The UET is based on the principle that for each independent displacement vector that can be measured one of the independent material property variables described by the Kirsch Solution can be calculated. The remainder of the variables must either be assessed using testing procedures or estimated. As two displacement vectors in most excavations can be effectively measured (sidewall convergence and crown sag for tunnels and sidewall convergence in two planes for basements and shafts) three parameters must be known. It should also be noted that in some cases displacement vectors can only be measured in one plane, the consequence being that an additional parameter must be determined through testing or assumed.

Of the five parameters presented in the Kirsch Solution, two can be simply accounted for: the geometry of the excavation; and the Poisson's ratio (ν), which can usually be assessed by laboratory testing or estimated from comparison with published values for similar materials. The results of the UET are also relatively insensitive to ν because of its limited range for most rocks (0.15 to 0.3).

For tunnels a third parameter, vertical stress, can be estimated based on the thickness and density of the overburden. This leaves the field stress ratio (k) and Young's modulus (E) to be determined.

If a material property has to be tested for or assumed it is usually E as there are laboratory techniques that can do it, albeit with some difficulty, and there are published ranges of E for most rock types.

The Kirsch Solution in its original form has limited application in civil and mining engineering because of its geometric constraints. However, a simplified form of it referred to as the "Lame Solution" in Pells et al (1981) does. The Lame solution combines the geometric term, presented in the square brackets in eqn 1, into a single "displacement influence factor"(I_δ), giving:

$$\delta = pd\frac{(1-\upsilon^2)}{E}I_\delta \qquad \text{Eqn 2}$$

where: $I_\delta = nk$

The displacement influence factor is unique for each location on the excavation perimeter. Often for tunnels of regular geometry this can be assessed using a closed form solution, however for tunnels of irregular geometry or foundation excavations this is not possible.

Instead, a numerical model is used to estimate I_δ. More specifically, it estimates the change in the convergence under a range of each subject variable. The results of this model can usually be simplified to a linear relationship for each of the monitored axes of convergence, viz:

$$\delta_1 = (a+bk)E \qquad \text{Eqn 3.}$$

$$\delta_2 = (c+dk)E \qquad \text{Eqn 4}$$

Equations 3 and 4 can be solved simultaneously or graphically, with the point of commonality being the unique convergence signature for a particular point on a given excavation. This is perhaps most easily understood by looking at the example in section 5 and its results presented by Figure 7.

In order to apply the above theory to practice a number of simplifying assumptions need to be made. These assumptions can be divided into two groups: general assumptions and model specific assumptions. These assumptions and the errors that they introduce are as follows.

General Assumptions

1. Faulty readings - poor monitoring results may be hard to distinguish from real results.

2. Discontinuity affected readings - where local inelastic displacement has occurred due to discontinuities.

3. Pre-monitoring convergence - convergence occurs prior to the installation of monitoring apparatus. This is considered further in the following section.

4. Numerical modelling - does not produce exact solutions.

5. Isotropy - many rock masses do not behave isotropically.

6. Liner influence - the influence on convergence of liners and supports can be difficult to assess.

7. Temperature - assumed to be constant (minor).

Model Specific Assumptions

1. Homogeneous medium - only a single value for the Young's modulus is accepted.

2. Elastic medium - plastic behaviour is not modelled.

It should be noted that some numerical models can accommodate in-homogeneous and plastic behaviour, UDEC being one example.

3. PRE-MONITORING CORRECTION

A certain amount of displacement occurs prior to the installation of monitoring points. Indeed, some converge occurs in front of the excavation face. As such, a correction must be made to the monitored convergence to account for pre-monitoring convergence. This can be achieved using a Boundary Integral Element Model (BIEM).

The theoretical background for the BIEM is essentially the same as discussed in section 2. A 3-D model is produced of the excavation extending some way into the rock mass. From this model it is possible to estimate the total convergence experienced at any distance back from the face. It should be noted however that this relies on an estimate being made for E, ν and k. The first runs of the BIEM model are likely to be inaccurate because of the assumed parameters, however, these parameters can be improved by using the results of the UET in an iterative manner until such time as the two match. An example of a BIEM model is presented in Section 5.

As a first pass it is reasonable to estimate the pre-monitoring convergence from published solutions, such as those by Brady & Brown (1985). It should be noted that when using these solutions no account is taken of the specific geometry of the tunnel or the material properties of the rock mass. As such, for tunnels of geometry that considerably differs from circular or for highly heterogeneous stress fields, these solutions can be misleading. Figure 2, which was taken from Brady & Brown (1985), shows the radial displacement of a circular tunnel in a hydrostatic stress field.

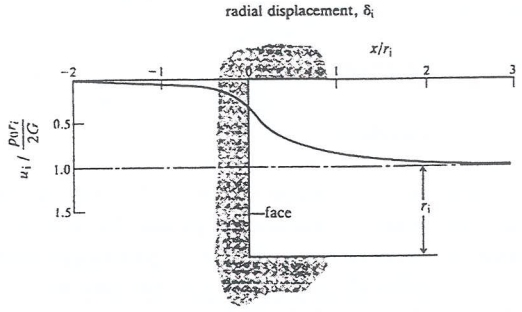

FIG 2: Proportion of Radial Displacement Experienced in Relation to Face Advance (Brady & Brown, 1985)

As shown by Figure 2 and concluded by Hocking (1976) "80% of the vertical elastic displacement of the crown of a tunnel will occur within 0.75 radii from the face". While the amount of convergence within the first radii of a tunnel will vary depending on its profile, the importance of having monitoring records from as close to the face as possible is clear.

4. PRACTICAL APPLICATION

4.1 Fields of Application

Strictly speaking the theory on which the UET is based is only valid for homogeneous isotropic linear elastic mediums, a situation not found in nature. However, in practice it can be applied to any rock environment where either the elastic component of deformation is significantly greater than the plastic component or the amount of plastic deformation is known. The former includes most hard rock environments and thus the UET can be expected to work reasonably well provided significant stress induced fracturing does not occur around the excavation.

The more displacement vectors measured the larger the redundancy in the Kirsch Solution and the greater the confidence in the answers from the UET. As such the UET is best suited to tunnels because convergence can be

measured along two planes, and the magnitude of one of the stresses (vertical stress) can be calculated. This gives two independent convergence signatures which can be used to back-calculate E and k. The UET can still be used for vertical excavations (shafts and foundations), but the magnitude of one of the horizontal stresses or E has to be estimated.

4.2 Numerical Modelling

The role of numerical modelling is to ascertain a suitable I_s and to develop the BIEM. This can be achieved with a variety of numerical techniques. As there are ample examples of easy to use software that can be used for such modelling in the market place today no further discussion is given to it here.

4.3 Instrumentation

4.3.1 Location

A significant advantage of the UET is that it can utilise the same suite of monitoring points that are included in most conventional excavations. Typically in tunnels this includes sidewall convergence monitoring and crown sag monitoring. However, any monitoring arrangement is acceptable, with the better result being achieved the closer the measured displacement vectors are to the principal stress planes.

4.3.2 Type of Monitoring Apparatus

The type of monitoring apparatus required depends on the precision required. The regularly employed convergence measuring equipment can be divided into three categories, viz:

- Borehole extensometers: measure the movements of both the perimeter of the excavation as well as the differential movements of the rock mass surrounding the excavation. Because they can be measured remotely and their accuracy they are the most attractive monitoring option, sadly they are also the most expensive (accuracy ±0.01mm).

- Direct measurements: the distance between two points on the excavation perimeter can be assessed directly using tape convergence measurements. The results of this method are typically accurate enough for the UET, however there can be some difficulty in recording measurements as they must be taken across the face of the excavation (accuracy to ±0.1mm).

- Surveying: total station surveying has limited application in collecting data for the UET because of its relatively poor accuracy (accuracy to ±1.0mm).

5. CASE STUDY - EASTERN DISTRIBUTOR TUNNEL

5.1 General

The Eastern Distributor Tunnel is a double-decker road tunnel in Sydney's eastern suburbs. It forms the backbone of a road link that connects the Sydney Harbour Tunnel in the north with the Kingsford Smith International Airport in the South. The tunnel is approximately 1.7km in length and carries 3 lanes of traffic in each direction and is excavated almost exclusively in slightly weathered Hawkesbury Sandstone (Bertuzzi & Justice, 1999). The tunnel is complicated by a series of on-load/off-load ramps that result in a continually changing profile, with a maximum unsupported span of 22m. The crown of the tunnel is not greater than 35m below the ground surface and the tunnel is typically 12m high.

The Eastern Distributor Tunnel was well suited to the UET for the following reasons:

- the low stress environment meant that the Hawkesbury Sandstone would behave in a pseudo-elastic manner, as has been shown by monitoring of other excavations in Sydney;

- the low insitu stress due to the shallow depth of the tunnel made conventional stress assessment methods (over coring, flat jacking and hydraulic fracturing) unreliable;

- access from both within the tunnel and from the surface for conventional stress measurements was limited;

- the changing ground conditions due to faulting and varying tunnel depths required a large suite of stress measurements to account for the changing ground conditions for which the cost of conventional methods was prohibitive; and

- an extensive array of monitoring stations was installed for tunnel observations as part of the excavation contracts.

An additional advantage for the application of the UET at the Eastern Distributor was that the Young's modulus for Class I/II Hawkesbury Sandstone is generally accepted to be between 1500 and 2500MPa.

5.2 Monitoring Array

The monitoring used for the UET consisted of crown sag and sidewall convergence at 50 to 100m internals.

Figure 3 shows the typical tunnel cross section and monitoring array.

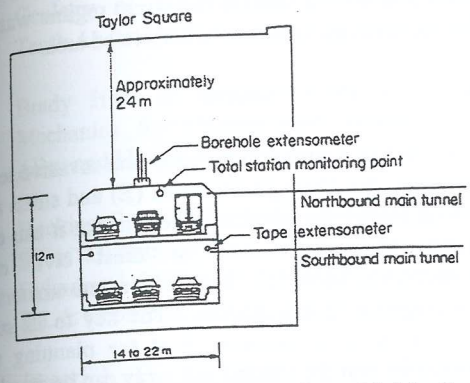

FIG 3: Typical Tunnel Cross Section with Monitoring Array

5.3 I_δ Numerical Model

The numerical model to assess the convergence signature of the tunnel was developed using Phase^2, a finite element package from the Rock Engineering Group, University of Toronto. The model incorporated three stages: (1) balancing of insitu stresses; (2) excavation of the north bound tunnel; and (3) excavation of the south bound tunnel. An eight node finite element mesh was used with node spacing reduced to not greater than 200mm at the perimeter of the tunnel. Figure 4 shows the output of the model after complete tunnel excavation for a 13m span section of the tunnel.

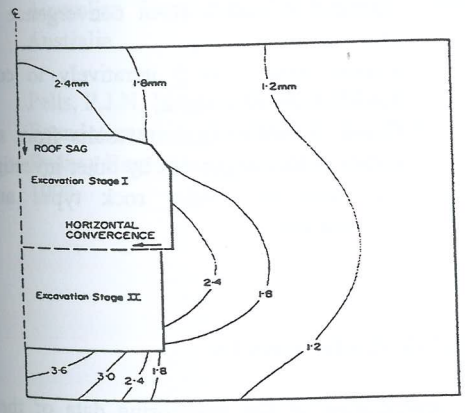

FIG 4: Total Displacement Contours from I_δ Model

The model was run for a series of E and k. The results from which were plotted to obtain a graphical solution for E and k for varying sidewall and crown convergence. An example of this is presented as Figure 7 with the monitoring results plotted onto it.

5.4 BIEM

A three dimensional BIEM was developed to estimate the pre-monitoring convergence, as discussed in Section 3. This was conducted using Examine 3D, a boundary element numerical package from the Rock Engineering Group, University of Toronto. A cross section of the displacement output of the model is presented as Figure 5 and the results are summarised by Figure 6.

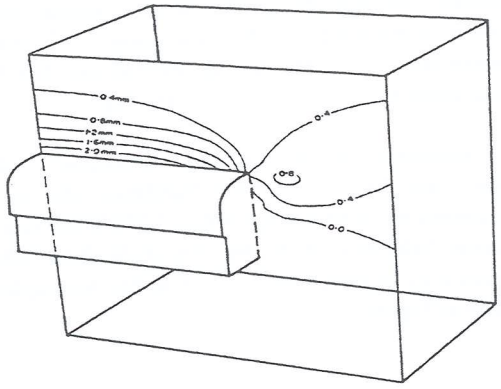

FIG 5: BIEM Model - Assessment of the Convergence Prior to Convergence Monitoring.

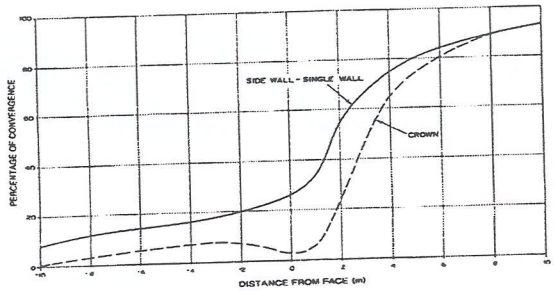

FIG 6: Summary of BIEM Results

5.5 Fault Zone

The 13m span of the tunnel modelled as part of this study passed through the Woolloomolloo Fault Zone (WFZ), as described in Bertuzzi & Justice (1998). The WFZ is a reverse fault with throw of up to about 6m. Significant strike slip movement is though to also be associated with the faulting action; however, there is little evidence to definitively support this postulation.

As part of the investigation phase of the project hydro-fracture testing was conducted in a single borehole that intersected the WFZ. The results of this testing indicated a k of 2 to 6, with the higher values recorded towards that base of the borehole which was approximately at the level of the tunnel crown.

5.6 Results

The sidewall convergence and crown sag results, corrected for pre-monitoring convergence, have been plotted on the graphical solution for E and k which was developed using the numerical model described in section 5.3. This is presented as Figure 7.

The sag results varied from the crown rising by 6mm to it lowering by 7mm. There was no apparent pattern to these results that was discernible by the author through the noise introduced by the inaccuracy of total station surveying. As such, the sag monitoring data had to be discarded for the purposes of assessing k.

To establish k it was necessary to assume a value for E. For Class I/II Hawkesbury Sandstone this is generally accepted to be between 1500 and 2500MPa and typically about 2000MPa (Pells, Mostyn & Walker, 1998). The sensitivity of the prediction of k to this assumption can be seen at Figure 7.

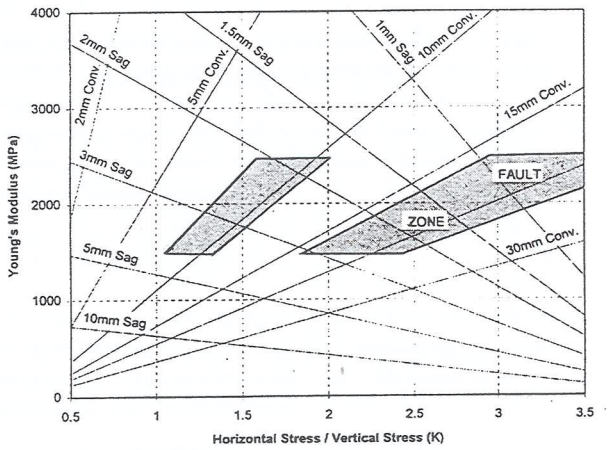

Fig 7 Stress Regime versus Sag and Horizontal Convergence with Monitoring Results

The results for the 12 sidewall convergence monitoring points recognised two discrete stress regimes; one for the general rock mass, and the other for the fault zone. The stress ratios for these two areas are summarised by Table 5.1.

Table 5.1
Summary of Assessed Stress Regime

AREA	STRESS RATIO (k)	
	RANGE	MEAN
General rock mass	1.1 to 2.0	1.6
Fault zones	1.8 to 4.0	2.8

Given the structural complexity associated with faulting, these results compare favourably with those obtained from the hydro-fracture testing which predicted a range of k from 2 to 6. No tests of the stress regime was conducted for the areas outside the fault affected area.

6. CONCLUSIONS

The UET is a simple, low cost, non invasive technique of assessing the Young's Modulus (E) and stress ratio (k) of a rock mass. Its advantage lies in that it can employ the monitoring array used in most civil engineering excavations, including borehole extensometers and tape convergence measurements. The key to its successfully application is to consider it at the planning stage of a project so that the monitoring array can be developed so as to be applicable to it.

The UET has it limitations, as do all insitu stress measurement techniques, however its advantages well outweigh them. There is no doubt that the UET will become an increasingly popular tool for both the design and analysis of civil excavations.

Summary of the UET process:

1. Convergence signature model,
2. BIEM Model to assess pre-monitoring convergence,
3. Install and monitor convergence vectors,
4. Correct convergence results for pre-monitoring convergence using BIEM,
5. Estimate E and k from convergence signature model,
6. Repeat steps 1 to 5 iteratively to correct for model errors in E and k,
7. Check E and k against results from stress test and/or values suggested by other investigations in the same or similar rock types and stress environments.

ACKNOWLEDGMENTS

The contribution of the monitoring data of the Eastern Distributor Tunnel by Maunsell McIntyre Pty Ltd is acknowledged. Additionally, the guidance of Dr Philip Pells, Mr Garry Mostyn and Mr Robert Bertuzzi has been greatly appreciated.

REFERENCES

1. Bertuzzi, R. & Justice, T.R. (1999); The Geology of the Eastern Distributor Tunnel; Tenth Australian Tunnelling Conference 1999.

2. Brady H.G. & Brown E. T. (1985); Rock Mechanics for Underground Mining; George Allen and Unwin, London.

3. Hocking G. (1976); Three-Dimensional Elastic Stress Distribution around the Flat End of a Cylindrical Cavity; Int. Journal Rock Mech. Min. Sci. & Geomech. Vol 13, pp. 331-337.

4. Jaeger J. C. & Cook N. G. W. (1971); Fundamentals of Rock Mechanics; Chapman & Hall; London.

5. Love A. E. H. (1927); Treatise on the Mathematical Theory of Elasticity; Cambridge University Press, Cambridge.

6. Pells, P.J.N, et al (1978); design Loadings for Foundations on Shale and Sandstone in the Sydney Region; Australian Geomechanics Journal.

7. Pells P.J.N., McMahon B.K. & Redman P.G. (1981); Interpretation of Field Stresses and Deformation Moduli from Extensometer Measurements in Rock Tunnels; Fourth Australian Tunnelling Conference, Melbourne, Australia.

8. Pells, P.J.N, Mostyn, G. & Walker, B.F. (1998); Foundations on Sandstone and Shale in the Sydney Region; Australian Geomechanics - Dec 1998.

Use of the Acoustic Scanner for Geotechnical Investigations

Paul Horrey

Riddolls & Grocott Ltd.
Christchurch, New Zealand

SUMMARY

The acoustic scanner (or acoustic televiewer) is a geophysical tool capable of providing oriented acoustic images of a drillhole wall. It is being increasingly used in geotechnical investigations to determine the orientation of rock mass defects. Acoustic scanning was recently carried out at Roxburgh Dam, New Zealand, where two 60 m deep cored holes were drilled in schist rock. The holes were scanned and the data processed using proprietary software. A detailed comparison was made between the drill core and scanner images. The images produced clearly showed the major rock mass defects present, enabling their true dip, azimuth, and approximate thickness to be determined. Acoustic scanning was subsequently used at the site to rapidly and cost effectively determine the presence and orientation of defects in 37 non-cored foundation drainholes.

Acoustic scanning has considerable potential for use on geotechnical projects where defect orientation is a prime objective. It may be used in conjunction with core drilling to provide high quality geotechnical data and with non-core drilling to provide cost effective spatial coverage or data "infill" between cored holes. In some situations the scanner may also be used to estimate in situ stress orientations from analysis of drillhole breakout.

1. INTRODUCTION

Acoustic scanning is a relatively new technique for obtaining *in situ* geotechnical information from acoustic images of a drillhole wall. This paper introduces the technique and presents an example of its use in schist terrain at Roxburgh Dam in New Zealand's South Island. This is followed by a more general discussion of the geotechnical applications and practical limitations of the scanner based on the author's experience at Roxburgh and several other sites.

2. THE ACOUSTIC SCANNER

The acoustic scanner (also known as the acoustic televiewer) is a wireline geophysical tool incorporating a rapidly rotating transducer, which emits short bursts of sound energy[1]. Originally developed for the petroleum industry, the scanner is now used increasingly in geotechnical investigations.

Each acoustic pulse is reflected off the borehole wall and its amplitude and travel time recorded as it returns to the tool. The amplitude (or strength) of the reflected signal provides an indication of the reflective properties of the wall rock, which in turn can be related to the strength and hardness of the rock. Defects containing crushed rock or gouge that is softer than the surrounding rock are thus readily identified, as are boundaries between lithologies of contrasting strength. The acoustic travel time, when suitably corrected for the sonic velocity of the drillhole fluid, provides a measure of the drillhole diameter, thereby allowing open joints, voids, caving and breakout to be determined. As the tool traverses the drillhole a continuous helical scan is formed. The basic operation of the tool is shown in Figure 1.

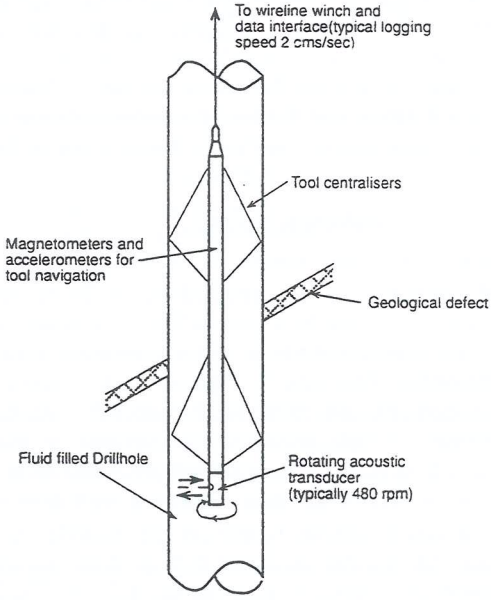

Figure 1: Operation of the acoustic scanner

The three dimensional orientation of the tool is recorded by a series of on-board magnetometers and accelerometers. In this manner the tool always knows exactly where it is in relation to the base of the hole. The amplitude and travel time data may therefore be imaged and presented in their correct orientations for later computer-based interpretation.

Data interpretation is carried out using various proprietary software packages, which allow the orientation (dip, dip direction) to be determined for each identified defect. The amplitude and travel time data are "imaged" using a gradational colour palette.

Interpretation is carried out on "unwrapped" 360° displays of the imaged drillhole wall. Planar features encountered in the drillhole appear as sinusoidal traces. A "best fit" sine curve is manually fitted to each defect trace and the orientation automatically calculated. The interpretation software also allows defect orientations to be exported as ASCII files for tabulation and presentation using stereoplotting software.

3. CASE STUDY– ROXBURGH DAM

3.1 Background

Roxburgh Dam is a concrete gravity structure located on the Clutha River in New Zealand's South Island. The dam has an annual power output of 320 MW from 8 turbines and was completed in 1956. Although comprehensive as-built geological logs of the foundation exposure were made, further information on the engineering geology of the schist rock on which the dam is founded was recently considered desirable. To this end a staged investigation programme including cored drilling, groundwater instrumentation and downhole geophysics was carried out. A feature of the investigation was the use of acoustic scanning to obtain orientated data on rock mass defects from drillholes.

3.2 Geological Setting

Roxburgh Dam is situated in a broad northwest trending belt of the Otago Schist. The schist originates from quartzofeldspathic and volcanogenic sediments of Mesozoic-Paleozoic age, that have been metamorphosed to textural zone IV. At least four phases of deformation are recognised in the region, which remains seismically active. The rock mass in the vicinity of the dam exhibits a well-developed sub horizontal foliation and is moderately to widely jointed. It contains shears both parallel and oblique to foliation. Intact rock strengths of 50 to 200 MPa are typical.

3.3 Field Investigations and Results

Two diamond cored PQ/HQ size (122/95 mm diameter) drilholes were drilled on the left abutment of the dam in mid 1997 to install additional piezometers. The acoustic scanner was trialed in these holes and the results compared with the drill core and conventional density, sonic and caliper logs[2]. A typical section of scanner image from one of these holes is presented in Figure 2. Following data processing, the acoustic images were interpreted to determine the type and orientation of all planar features identified. The trial concluded:

- The scanner clearly identified all the major shears (both sub-horizontal and steeply dipping) present in the core.
- The scanner identified the majority of joints present in the core. Those joints identified in the drill core but not revealed by the scanner may have been tight *in situ* and therefore not differentiable from the adjacent wall rock.
- The orientation of all defects identified could be readily determined during subsequent data processing.
- Due to the geometric considerations the dip angle determined for steeply dipping defects is generally of greater precision than that for shallow dipping features.

Following the success of the trial, 37 foundation drainholes located within the lower dam inspection gallery were scanned during 1998[3]. These holes had originally been drilled during construction by diamond coring, although the cores were not retained.

Immediately prior to scanning, the holes were flushed with high-pressure water jets and several of them reamed and deepened using a small percussive rig. A "dummy" probe of the same dimensions as the scanner was used to determine the "scannable" depth of each hole, allowing an optimum investigation schedule to be developed. The scanning operation took place over 5 days during which 466 m of drillhole were scanned. Data interpretation was carried out on site in tandem with the data acquisition. This had the major advantage of allowing the investigation to be modified as it progressed. Additional holes were scanned in areas where data quality was poor or where features of particular interest were identified. The scanner equipment used for the drainholes was different from that used for the surface holes, primarily due to the headroom restrictions in the dam galleries.

In spite of the holes having been drilled over 40 years previously, a large number of rock defects were identified from the scanner images, and their orientation determined. As with the earlier trial, defect classification from the scanner images was somewhat subjective, and difficulty was occasionally experienced in differentiating open or infilled joints from thin foliation shears and crushed zones on the scanner images (i.e. it was not always possible to determine whether or not shear displacement had occurred along the defect). "Major" shears (i.e. greater than 20 mm thickness) were readily identifiable.

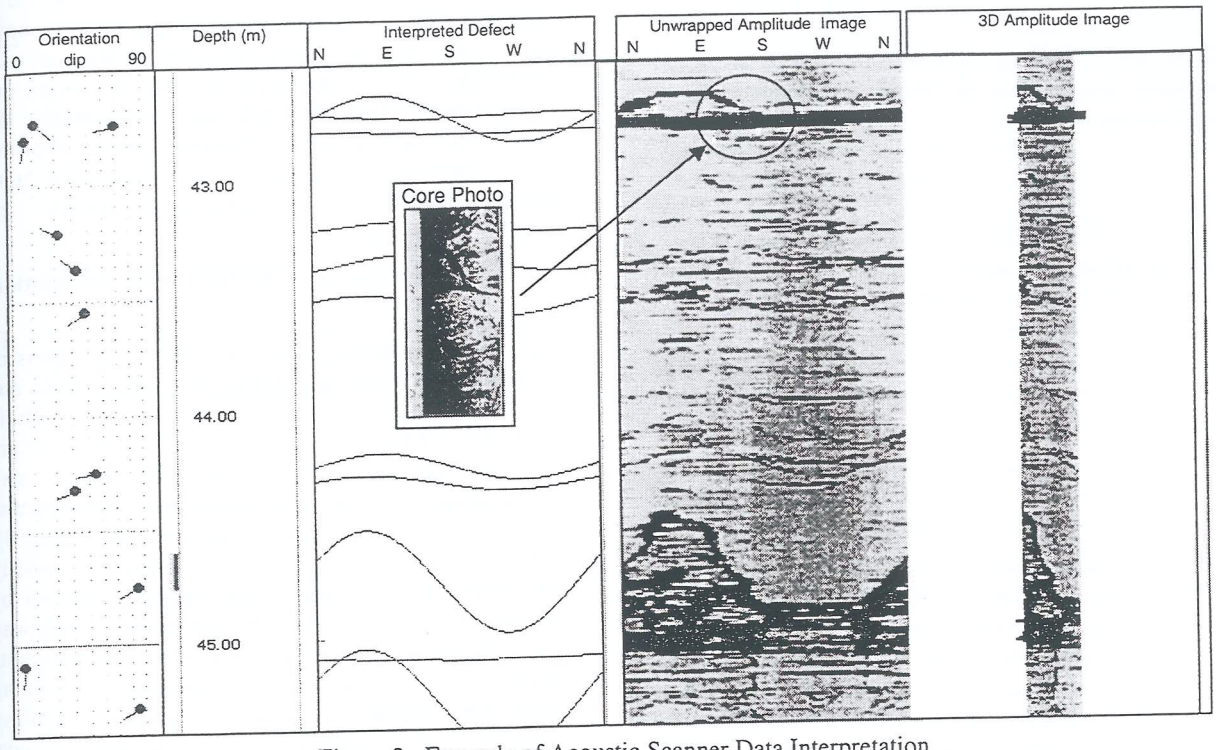

Figure 2: Example of Acoustic Scanner Data Interpretation

High quality, orientated data on rock defects were obtained from most of the drainholes. The quality of the acoustic scanner data appeared to be influenced by the condition of the drillhole wall. Overall, better results were obtained in diamond cored holes than holes redrilled by percussive means. Although different scanning equipment was used, data quality from drainholes that were not reamed was generally comparable with that of the cored surface holes.

The interpretation software allowed logs to be compiled for each drainhole showing the acoustic amplitude and travel time images, interpreted features and their classification and orientation, and drillhole azimuth and inclination. Consideration of the large amount of additional data gained from acoustic scanning at Roxburgh has contributed to a far more detailed understanding of rock mass properties at the dam site. It is unlikely that any other investigation tool would have given such detail and spatial coverage for the same cost.

4. ISSUES ASSOCIATED WITH USE OF THE ACOUSTIC SCANNER

4.1 Cored versus Non-Cored Drillholes

By providing orientated data the scanner represents a major advance over most conventional downhole geophysical methods.

The scanner is not regarded as a replacement for core investigation drilling. It does however have the potential to enhance the quality of geotechnical data obtained from both cored and non-cored holes.

Where highest quality orientated data is required the scanner may be used in conjunction with cored drilling. The two techniques are complementary and data from both may be combined on a single interpretive drillhole log for subsequent interpretation. The drillcore allows direct inspection and sampling of the strata encountered whilst the scanner provides defect orientations, 3D drillhole deviation data and additional information in zones of poor core recovery. The use of the scanner in this manner is more appropriate for projects where the orientation of rock mass defects can have major design and contractual implications. Examples include tunnels, cut slopes, deep excavations and landslide investigations.

The scanner may also be used to gain geotechnical information from non-cored holes drilled for other purposes. Examples include resource definition drilling in quarrying and mining, grouting holes, ground anchor holes, or as in the case of Roxburgh, drainage holes. Typically a large number of these holes are drilled rapidly and cheaply by open hole methods. Whilst the scanner data quality may be poorer than for cored holes, a wide spatial coverage of information on defect orientations and stratigraphy may be acquired at relatively low additional cost. Some "control" in the form of occasional cored holes is still desirable.

4.2 Drillhole Environment

There are a number of physical limitations on the drillhole environment in which the scanner may be used. These include:

- Drillhole fluid – the scanner requires a water or mud filled drillhole
- Drillhole diameter – the 75-mm diameter drainholes at Roxburgh were close to the lower limit of the equipment used.
- Headroom – the shortest tool used at Roxburgh was 2.6 m long. This precluded its use in some of the galleries
- Artesian groundwater/gassing - Data quality may be adversely affected by strong artesian groundwater flows or gas bubbles.
- Hole inclination - Vertical or steep downwardly inclined drillholes may be readily scanned using a conventional wireline winch. Lower angle and subhorizontal holes can be scanned in some cases, with the tool pushed into the hole with flexible fibreglass rods. Problems with tool centralisation may also be experienced. Upwardly inclined holes cannot be scanned due to the requirement for a drillhole fluid.
- Drilling method - Diamond cored holes provide a smoother drillhole wall than do percussive or wash bored holes. Data quality may be adversely affected by excess rugosity of the drillhole wall.
- Hole conditions - In softer rocks, excessive caving or smearing on removal of casing may effect data quality. Poor hole stability may also place the tool at risk of jamming or other damage.
- Casing - The scanner will not work through drillhole casing, screens or liners.

Specific requirements differ slightly between geophysical contractors and will no doubt change as new equipment is developed.

4.3 Cost Effectiveness

Depending on the site location, mobilisation costs may be significant, but the actual data acquisition is relatively quick. Cost effectiveness therefore increases with the number of holes scanned in one visit. This, however requires holes to be left open and uncased. In some situations this may not be possible, or may involve additional drilling costs to re-visit each hole after scanning to complete installations. The timing of investigation drilling must be carefully considered to maximise the cost effectiveness of a scanning programme.

Data interpretation and presentation costs can be a significant component of the overall investigation cost. Some contractors provide a data interpretation service while others do not. Interpretation may be carried out by the client's engineering geologist, in which case the cost of software purchase, training, and a "learning curve", must be considered. A third alternative is to make use of a "third party" interpretation service.

4.4 Determination of In Situ Stress Orientation

The scanner is being increasingly used as a means of estimating the direction of principal *in situ* stresses due to its ability to determine the orientation of drillhole breakout. When *in situ* deviatoric stress is high, breakout (spalling of the drillhole wall) may preferentially occur in the drillhole wall perpendicular to the axis of principal horizontal stress (see Figure 3). The occurrence and orientation of breakout is readily determined from the travel time images produced by the scanner. Stress orientation determined in this way has been shown to correlate well with measurements using other techniques[4]. Techniques are also being developed to deduce *in situ* stress directions for drilling induced fracture patterns[5]. These techniques have application in the design of underground mines, caverns and tunnels where *in situ* stress directions have the potential to influence excavation and stability.

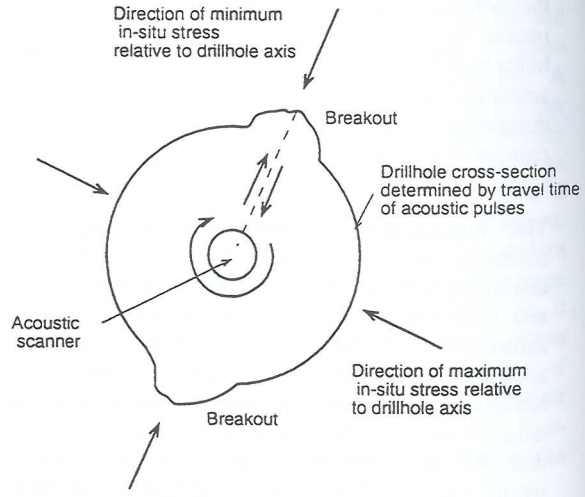

Figure 3: Determination of *in situ* stress orientation from drillhole breakout

Acknowledgements

Permission from Contact Energy Limited to present data from Roxburgh Dam is gratefully acknowledged, as is the assistance of Mr Peter Silvester (Contact Energy) and Mr Roland Turner (Reeves Wireline).

REFERENCES

1. Elkington, P., 1990: "The Acquisition and Analysis of Slim Acoustic Scanner Data" BPB Slimline Services, UK
2. Riddolls & Grocott Ltd., 1997: "Roxburgh Power Station. Review of Geophysical Logging techniques, Drillholes OW 12 and OW 13. Unpublished Consultants Report
3. Riddolls & Grocott Ltd., 1998: "Drainhole Acoustic Scanner Logs, Roxburgh Dam" Unpublished Consultants Report
4. Lamb, P.D. & Titheridge, D., 1989: "The Use of Borehole Breakout for Estimating Regional Changes in Horizontal Stress Directions" in Underground Coal Mining Exploration Techniques, Australian Coal Association
5. Aadnoy, B.S. & Bell, Sebastian J., 1998: "Classification of Drilling Induced Fractures and their Relationship to *In situ* Stress Directions". The Log Analyst, Nov-Dec 1999-11-02.

The Response of Suction Caissons to Catenary Loading

A.R. House

Geomechanics Group, The University of Western Australia

NEDLANDS WA 6907

Abstract

Research into the performance of suction caissons has developed in response to the demand from the offshore hydrocarbon industry for a versatile foundation solution capable of anchoring a range of alternative structures. Suction caissons are capable of providing large anchoring capacities in all directions. The simple installation procedure and high reliability has seen suction caissons employed in a range of water depths and within hydrocarbon fields from marginal to high potential. As exploration is directed toward increasing water depths, anchoring demands on the proposed structures become greater and subsequently a more detailed understanding of the limitations to caisson capabilities and performance is required.

Using the fixed beam geotechnical centrifuge facility at The University of Western Australia (UWA), the installation and response of a dimensionally scaled prototype caisson to inverse catenary chain loading was modelled with the objective of establishing a relationship between the caisson geometry, soil characteristics and the monotonic holding capacity. The installation and tensile resistances were recorded to determine the necessary installation pressures and uplift capacity of the caisson. Theory suggests that the lateral capacity is dependent upon the frictional resistance between the caisson and soil, which may be back derived through calibration of the theoretical and experimental response of the caisson to axial loading.

This paper presents the data from a series of centrifuge tests, comparing the results with the theoretical monotonic capacity of laterally loaded caissons. A smooth walled model caisson was installed and subsequently loaded with an anchor chain in normally consolidated kaolin clay. The data exhibited excellent repeatability between identical tests and a similar correlation with the adopted upper-bound plasticity solution for laterally loaded caissons.

1 INTRODUCTION

The versatility and cost effectiveness of suction caisson foundations has initiated significant research into the capabilities of and limitations to their applications.

In moderate water depths, suction caissons may be used within clusters as a mooring for such structures as floating, production, storage and offloading (FPSO) facilities. For these applications each caisson is attached to the structure with a chain that forms an inverse catenary profile within the soil between the mudline and the point of attachment, imposing a predominantly horizontal load on the anchor.

The first catenary moored structure using suction caisson foundations was at the Gorm field offshore Denmark (Senpere and Auvergne, 1982). The soil profile at Gorm comprises dense, fine sand overlying soft clay above stiff clay, proving the suitability of suction caissons in a diversity of soil types. Most recently, the first suction caisson installations within calcareous soils have been undertaken in the calcareous silty sediments of the Timor Sea for the Laminaria hydrocarbon field (Schrøder and Finnie, 1999).

As offshore hydrocarbon exploration exploits deeper waters, a greater understanding of the combined axial and lateral capacity of suction caissons is warranted.

Very little experimental research has been published on the response of suction caissons to lateral loading. Experimental work in progress at The University of Western Australia has the objective of developing a design methodology capable of specifying an optimal caisson geometry for a given soil profile and design load configuration. This research involves the experimental modelling of suction caissons (of various geometries) subjected to loads ranging form purely horizontal to purely vertical in a range of typical offshore soil profiles. This paper presents the results of the first series of centrifuge tests on a caisson monotonically loaded within normally consolidated kaolin clay.

2 BACKGROUND

2.1 Installation

Of concern during the installation of suction caissons is whether the caisson will reach the target installation depth before upheaval of the internal soil plug. Soil plug failure will not be further discussed in this paper since the aspect ratio of the model caisson and the adopted soil profile suggest a limiting aspect ratio well in excess of the model geometry, (House *et al.*, 1999). Furthermore, the adopted experimental installation method (jacked) eliminates the likelihood of soil plug upheaval due to the absence of the uplift force on the plug experienced during suction penetration.

A free body diagram of the caisson and internal soil plug during suction installation is shown in Figure 2.1.

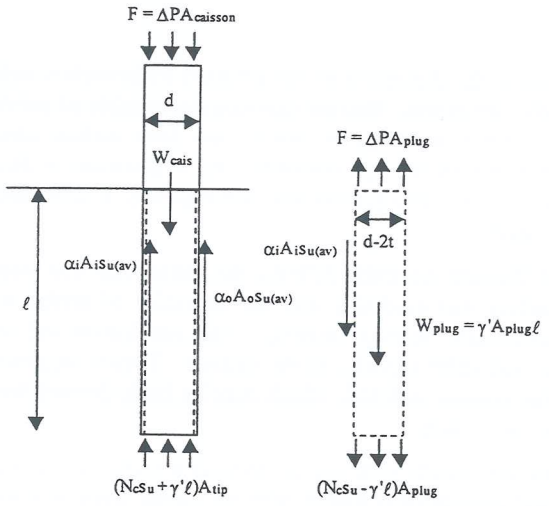

Figure 2.1 Free body diagram of caisson and soil plug

The required installation pressure is derived from the free body diagram of Figure 2.1(a) and is defined by

$$\Delta P_{caisson} = \frac{(N_c s_u + \gamma' \ell)A_{tip} + \alpha_i \overline{s_u} A_i + \alpha_o \overline{s_u} A_o - W}{A_{plug}} \quad (1)$$

where:
- N_c = bearing capacity factor (taken as 9)
- s_u = undrained shear strength (at caisson tip)
- γ' = bulk density
- ℓ = embedded caisson length
- A_{tip} = tip area of caisson
- A_{plug} = sectional area of soil plug
- A_i = internal area of caisson in contact with soil
- A_o = external area of caisson in contact with soil
- α_i = internal friction factor
- α_o = external friction factor
- W = submerged caisson weight

2.2 Lateral capacity

A least upper-bound to the undrained collapse load of a laterally loaded caisson in clay may be predicted using theory discussed in detail by Murff and Hamilton (1993) and refined for suction caisson analyses by Randolph *et al.* (1998). The iterative method (described below) varies three geometric parameters (defining the failure mechanism) and one optimisation parameter to solve for the minimum collapse load satisfying the kinematic constraints of the adopted failure mechanism.

(a) Assume a failure mechanism (geometry)

(b) Identify velocity field for failure mechanism

(c) Derive function between plastic strain rate and energy dissipation

(d) Set external work done by imposed loads to total plastic energy dissipation

(e) Repeat steps (a) to (d) until minimum collapse load is determined

A schematic representation of the proposed kinematic failure mechanism is shown in Figure 2.2. The geometric parameters are the depth of the failure wedge, radial extent of the failure wedge and depth to the centre of rotation.

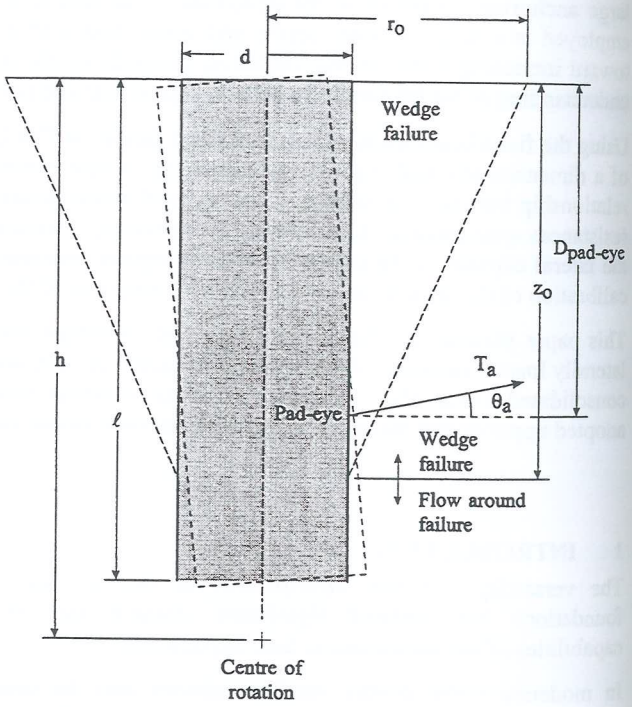

Figure 2.2 Upper bound failure mechanism

Subsequent to the experimental soil characterisation tests and using a mobilised friction coefficient calculated from the caisson installation data, the least upper bound to the caisson holding capacity is predicted using the aforementioned model.

3 EXPERIMENTAL MODELLING

A model suction caisson was fabricated in the UWA workshop from 6061 T6 aluminium and tested in the centrifuge within a sample comprising normally consolidated kaolin clay. The caisson had a dry mass of 32.3 g excluding attachments (representing a prototype submerged weight of approximately 550 kN), with a wall thickness of 0.5 mm and a

stiffened region at the padeye of 1 mm wall thickness. The geometry of the model suction caisson is identified in Figure 3.1.

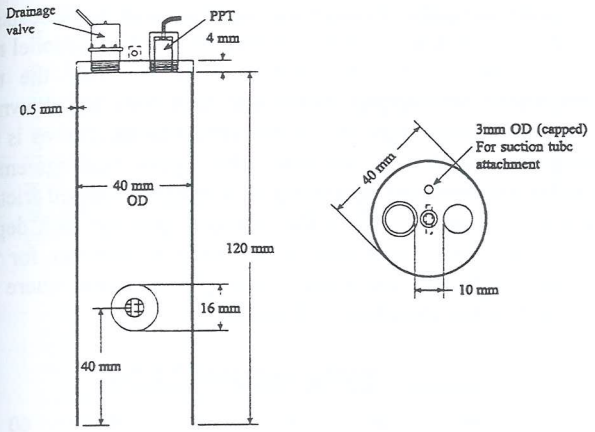

(a) Elevation (b) Plan

Figure 3.1 Geometry of model suction caisson

The normally consolidated kaolin sample was prepared by self-weight consolidation of a clay slurry on the UWA fixed beam geotechnical centrifuge (Randolph *et al.*, 1991). Commercially available dry kaolin clay powder was mixed to a slurry with a water content of 120 % (twice the liquid limit) and subsequently de-aired under a vacuum of approximately 100 kPa. A slurry depth of 280 mm was placed over a 10 mm sand drainage layer at the base of the strongbox and consolidated under an accelerated self-weight (120 g) for a period of approximately 2 days. Previous characterisation of the same clay at UWA (Stewart, 1991) suggested a fully consolidated model depth of 180 mm would be achieved with a target strength gradient (prototype scale) of approximately 1.1 kPa/m. Key properties of the kaolin clay are detailed in Table 1.

Soil characterisation tests were undertaken using the T-bar penetrometer (Stewart and Randolph, 1991) before each caisson installation associated with a catenary load test. The T-bar was penetrated and extracted at model rates of 3 mm/sec and 1 mm/sec respectively.

PROPERTY	VALUE
Specific gravity, G_s	2.60
Liquid limit, LL (%)	61
Plastic limit, PL (%)	27
s_u/σ'_v (Normally consolidated)	0.187
Consolidation coefficient, c_v (m^2/year)	1.3
Clay density, γ'_c (kN/m^3)	5.9

Table 1 Kaolin clay properties, after Stewart (1991)

The undrained shear strength of the normally consolidated kaolin clay samples was determined using the T-bar penetrometer (Stewart and Randolph, 1991). The T-bar has a load cell attached to the shaft above the tip from which the installation resistance is directly determined. The bearing pressure, q, is derived by dividing the installation resistance by the bar area and the shear strength is subsequently estimated by dividing the bearing pressure by a bar factor N_b.

$$s_u = \frac{q}{N_b} \qquad (2)$$

For the bar used it is standard convention to adopt an N_b value of 10.5, based on an average between the theoretical upper and lower bound plasticity solutions for a perfectly smooth (adhesion factor, $\alpha = 0$, $N_b = 9.14$) and a perfectly rough bar ($\alpha = 1$, $N_b = 11.94$), (Randolph and Houlsby, 1984).

The geometry of the experimental arrangement limited the modelling to two catenary load tests and a maximum of two installation / pull-out tests per strongbox. An elevation and plan schematic of the experimental arrangement is shown in Figure 3.2.

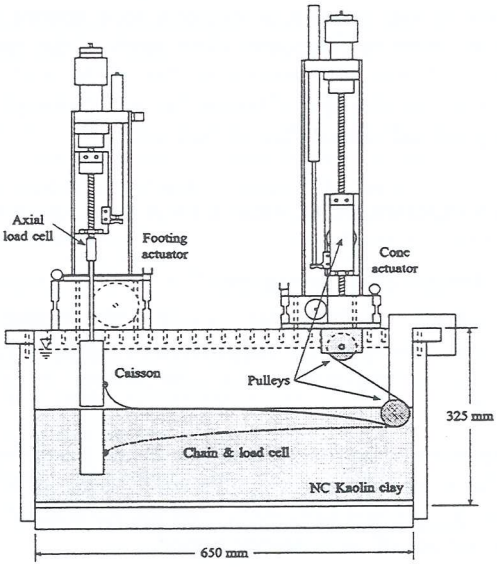

(a) Elevation

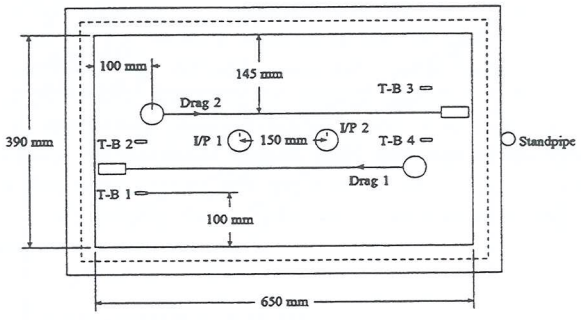

(b) Plan

Figure 3.2 Experimental arrangement

Each installation commenced with the caisson submerged and suspended above the mudline. The loading arm attached to the caisson was lowered into the sample with the drainage valve on the lid of the caisson open. Installation was undertaken at a model rate of 0.5 mm/sec. An axial load cell

(3 kN model capacity) attached to the loading arm measured the penetration resistance throughout the duration of the jacked installation. The anchor chain was pinned alongside the anchor wall throughout the penetration phase. A miniature pore pressure transducer (PPT) attached to the lid of the caisson recorded the internal caisson pressure.

After the caisson was installed to the target depth, the centrifuge was stopped, the chain unclipped and attached to the pulley arrangement and the drainage valve on the caisson lid was closed. The loading arm attached to the caisson was removed before the centrifuge was ramped back up to the target normal acceleration and the sample allowed to re-consolidate.

The catenary (inverse) load tests were performed by vertically displacing the actuator associated with the chain and pulley arrangement. The pulleys were geared such that one unit of vertical displacement of the actuator represented a chain displacement of 2 units. A chain drag rate of 0.2 mm/sec (monotonic) was adopted to maintain load control yet also ensure an undrained response. The depth of the end pulley was set such that the catenary profile of the anchor chain agreed with the solutions of Neubecker and Randolph (1995), for the predicted ultimate lateral capacity.

4 EXPERIMENTAL RESULTS & DISCUSSION

4.1 Sample characterisation

The normally consolidated kaolin clay sample was characterised by two T-bar tests before each of the two anchor tests. The undrained shear strength profiles are shown in Figure 4.1.

A comparison of the first (T-bars 1 & 2) and second series (T-bars 3 & 4) of T-bar tests highlighted evidence of a strength increase of approximately 40 % over the duration of the first anchor test and re-consolidation period.

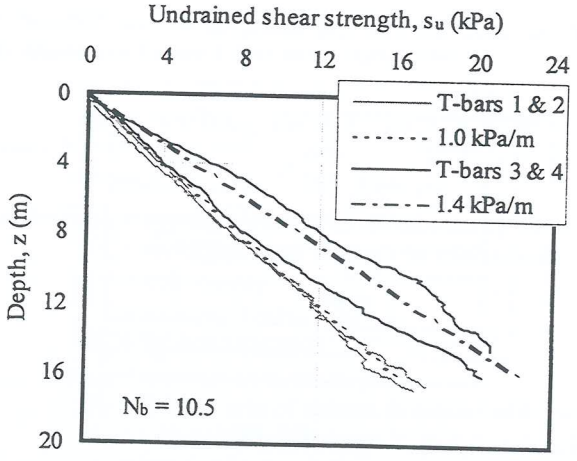

Figure 4.1 Undrained shear strength

The variability between the profiles of T-bars 3 and 4 suggests that the sites may have been subjected to soil disturbance upon extraction of the embedded end pulley used for monotonic drag test 1. T-bar pull out tests (immediately after penetration) showed a remoulded shear strength approximately 75 % that of the peak undrained shear strength.

4.2 Installation and axial loading

To ensure adequate drainage through the valve on the caisson lid, installation tests were undertaken at a constant model rate of 0.25 mm/s. The penetration resistances for the two installations preceeeding monotonic load tests are shown in Figure 4.2. Superimposed on the experimental curves is the theoretical installation response which gave best agreement with the experimental data using an average mobilised friction ratio of 0.3, and k is the shear strength gradient with depth. Note that minor corrections were made to account for the buoyancy effects in the initial stages of installation where the caisson was not completely submerged.

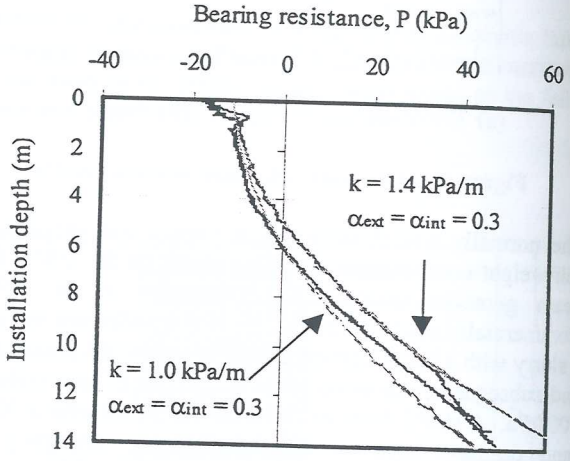

Figure 4.2 Installation resistances

The penetration resistance and internal caisson pressure rose sharply upon contact of the internal soil plug with the top cap of the anchor. Penetration was stopped at this point which for both installations was approximately 95 % of the target installation depth. Since the installation method was one of jacking, the internal soil plug upheaval may only be attributable to soil displaced by the caisson skirts.

Following the second monotonic load test, one installation / pull-out test was undertaken. The pull-out test was performed with a drained top cap at a constant rate (model) of 0.25 mm/sec. The experimental response is shown in Figure 4.3.

The caisson pull-out response is classically frictional, suggesting that the caisson-soil interface cohesion was mobilised with no contribution of reverse end bearing. The pressure response within the lid of the caisson showed that no negative pressures were developed between the top of the caisson and the internal soil plug, proving that the soil plug was not extracted with the caisson, verifying the expectations for a drained pull-out test.

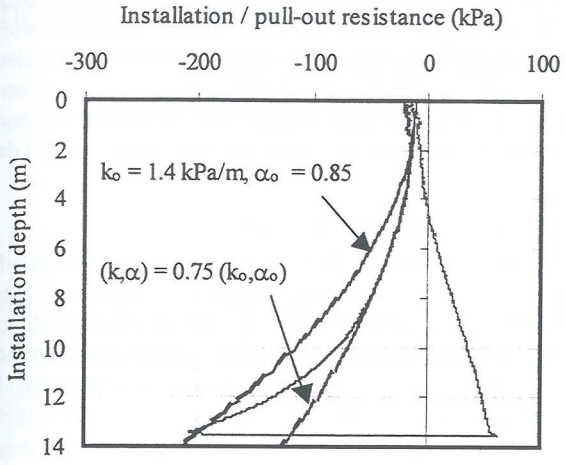

Figure 4.3 Axial pull-out response

The theoretical pull-out capacity is superimposed on the experimental data, showing that the experimental performance experiences a transition as the skirt friction apparently reduces quadratically. Best agreement is found by application of a reduction factor not only on the shear strength (as experienced in the T-bar pull-out tests) but inexplicably also on the mobilised friction ratio.

4.3 Inverse catenary loading

The load development response of the suction caissons subjected to monotonic chain loading is presented in Figure 4.4. Load development is slow as the initial slack in the chain was taken up. Post-peak behaviour exhibits significant strain softening of the kaolin clay.

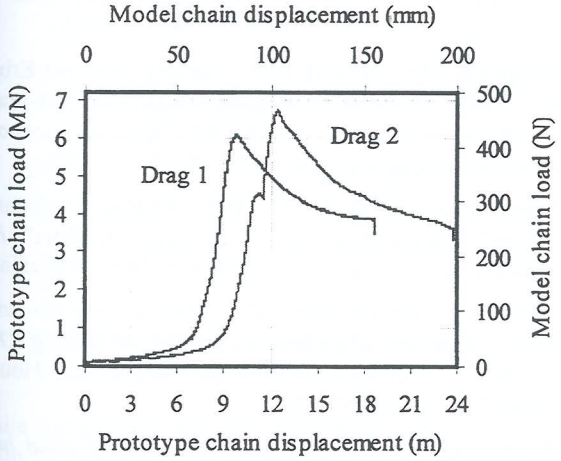

Figure 4.4 Load development (monotonic loading)

The pressure inside the lid of the caisson was monitored as the monotonic chain load was applied. It is observed that no significant pressure response was experienced up to the point of peak holding capacity, beyond which the differential pressure development is a response to the passive suction caused by caisson displacements.

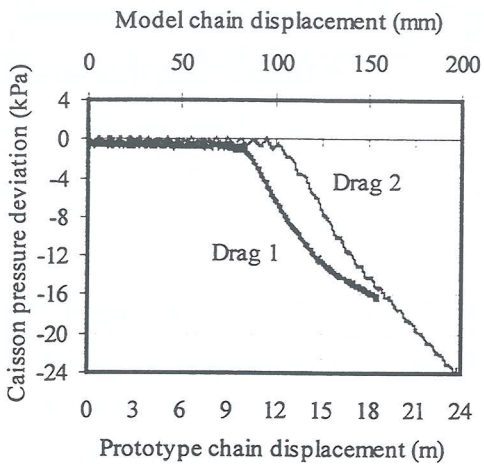

Figure 4.5 Pressure response (monotonic loading)

The total caisson displacement was approximately 1.5 and 2 diameters for drag tests 1 and 2 respectively.

Using the mobilised friction coefficient back derived from the installation data, the predicted least upper bound to the caisson holding capacity (2 sided failure mechanism) for each of the monotonic load tests is detailed in Table 2.

PARAMETER	TEST 1	TEST 2
Strength gradient, k (kPa/m)	1.0	1.4
Adhesion factor, α	0.3	0.3
Ultimate capacity, P_{ult} (MN)	4.7	6.7
Depth to centre of rotation, h (m)	14.4	14.4
Depth of soil wedge, z_o (m)	11.2	13.2
Radius of soil wedge, r_o (m)	10.1	11.0

Table 2 Predicted caisson holding capacity

Good agreement is observed between the experimental and predicted capacity for Test 2, although for Test 1 the theoretical model under-predicted the measured ultimate holding capacity by approximately 20 %. One possible reason for this under-prediction is that the sample may have experienced a strength increase over the period of reconsolidation between the caisson installation and lateral load tests. The reconsolidation period would also serve to increase the mobilised friction ratio, although as discussed in the following section this has a very minor influence on the predicted holding capacity for the experimental arrangement studied.

5 PARAMETRIC STUDY

To observe the sensitivity of the holding capacity model to the soil strength parameters and proportion of mobilised friction, a series of parametric analyses were undertaken using the experimental caisson geometry subjected to a purely lateral load. For normally consolidated soils (s_{uo} = 0 kPa) of various strengths, the predicted least upper bound to the caisson capacity is shown in Figure 5.1 for a two sided failure mechanism and a range of friction ratios.

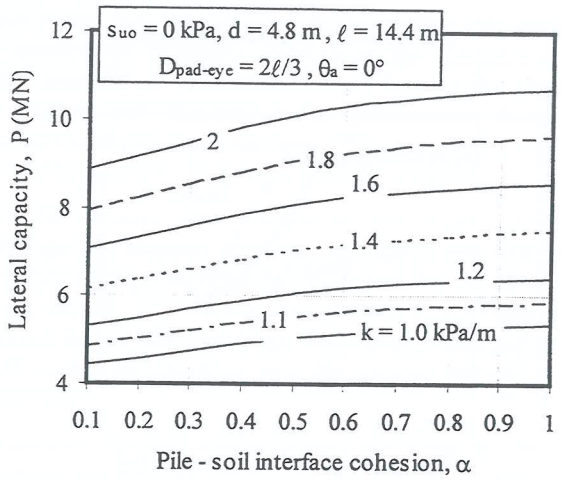

Figure 5.1 Influence of shear strength gradient

Similarly, the influence of mudline shear strength, s_{uo}, on the ultimate holding capacity of the same caisson within a 'typical' soil is shown in Figure 5.2.

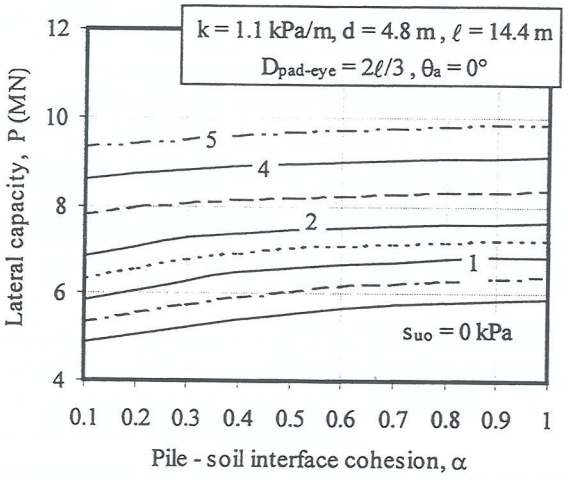

Figure 5.2 Influence of mudline shear strength

From the above two figures, it is apparent that for the experimentally modelled caisson, the predicted upper bound to the holding capacity is relatively insensitive to the caisson-soil interface cohesion ratio, α.

6 CONCLUSIONS AND FURTHER WORK

The results presented herein support the theory that the least upper bound plasticity solution provides a good prediction to the holding capacity of suction caissons subjected to quasi-lateral loading. Further refinement of the model will facilitate the prediction of caisson performance when subjected to load inclinations typical of those experienced when suction caissons are used for taut wire or fibre rope moorings.

More data are required on the performance of suction caissons in a range of soil profiles before a design methodology may be developed to assist in the optimal suction anchor selection for a specific requirement.

Kinematic data are essential in identifying the optimal pad-eye attachment depth on the anchor. Other proposed work at UWA includes a series of 3-dimensional finite element analyses to calibrate the theoretical load displacement response of caissons subjected to quasi-lateral loading and the predicted failure geometry of the soil with experimental data.

7 ACKNOWLEDGEMENTS

The research described here is part of the activities of the Special Research Centre for Offshore Foundation Systems, established and supported under the Australian Research Council's Research Centres Program. The author is supported by an Australian Postgraduate Award. The efforts of UWA workshop and centrifuge staff are gratefully acknowledged.

8 REFERENCES

1. House, A.R., Randolph, M.F. and Borbas, M.E. (1999). "Limiting aspect ratio for suction caisson installation in clay", *Proceedings of the 9th International Offshore and Polar Engineering Conference*, Brest, France, **1**, 676-683.
2. Murff, J.D. and Hamilton, J.M. (1993). "P-ultimate for undrained analysis of laterally loaded piles", *Journal of the Geot. Engineering Division, ASCE,* **119**(1), 91-107.
3. Neubecker, S.R. and Randolph, M.F. (1995). "Profile and frictional capacity of embedded anchor chain", *Journal of the Geot. Engineering Division, ASCE,* 121(11), 787-803.
4. Randolph, M.F. and Houlsby, G.T. (1984). "The limiting pressure on a circular pile loaded laterally in cohesive soil", *Geotechnique,* **34**(4), 613-623.
5. Randolph, M.F., Jewell, R.J., Stone, K.J.L. and Brown, T.A. (1991). "Establishing a new centrifuge facility", *Proceedings of the International Conference on Centrifuge Modelling - Centrifuge '91*, Colorado.
6. Randolph, M.F., O'Neill, M.P., Stewart, D.P. and Erbrich, C. (1998). "Performance of suction anchors in fine-grained calcareous soils", *Proc. of the 30th Offshore Technology Conference*, Houston, Paper OTC 8831, 521-529.
7. Schrøder, K. and Finnie, I. (1999). "Catenary and taut leg moored floating structures using suction anchors", *Proc. Australasian Oil and Gas Conference*, Perth, Australia.
8. Senpere, D. and Auvergne, G.A. (1982). "Suction anchor piles – A proven alternative to driving or drilling", *Proc. of the 14th Offshore Technology Conference*, Houston, Paper OTC 4206, 483-493.
9. Stewart, D. P. (1991). "*Lateral loading of piled bridge abutments due to embankment construction*", PhD Thesis, Department of Civil Engineering, The University of Western Australia.
10. Stewart, D. P. and Randolph, M. F. (1991). "A new site investigation tool for the centrifuge", *Proceedings of the International Conference on Centrifuge Modelling - Centrifuge '91*, Colorado, 531-538.

The Monitoring and Modelling of Ground Movements Caused by Open Pit Mining and Their Effect on Mine Infrastructure

Alison Jennings: Senior Geological Engineer, Geo-Eng Australia Pty Ltd.

Summary: This paper discusses the generation, and the extent of development, of ground strains in and around the large open pit mines of the Latrobe Valley in Victoria. These pits range in depth from 75m to 160m and individually cover areas of up to 16km^2. They supply coal to a number of large mine mouth thermal power stations. The station complexes and their related infrastructure are located close to the mine batters.

Extraction of overburden, coal and groundwater from the mines generates considerable vertical and horizontal ground movement in the base of the mines, in the batters and the surrounding areas. This paper discusses the methods used to predict the ground movements associated with current and future mining activities, in particular the computer programs FLAC (ground movements and subsidence) and COMPAC (subsidence modelling).

The paper discusses the mechanisms of ground movement experienced in and around the mines and how their effects are predicted. In addition, this paper broadly discusses the effectiveness of the modelling techniques, the benefits gained from modelling and the reasons for computer modelling not being adopted in some instances.

1. INTRODUCTION

The Latrobe Valley is located approximately 170km to the east of Melbourne (refer Figure 1). It is the centre of Victorian power generation with over 95% of Victoria's electricity generated from coal supplied by three mines to five large coal fired thermal power station complexes.

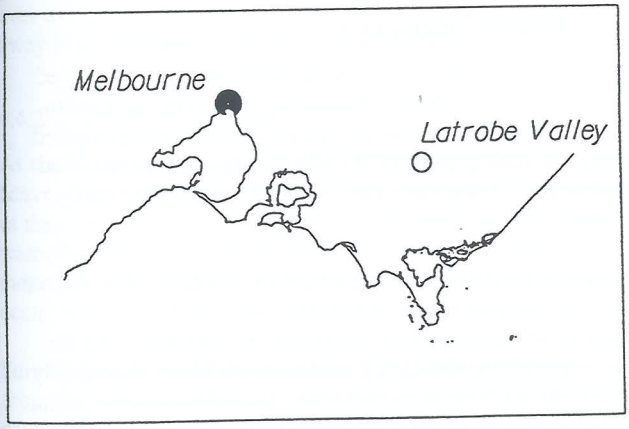

Figure 1: Locality Plan

Lignite (brown coal) was first discovered in the Yallourn area in 1866. Commercial exploitation of the coal commenced in the early 1900's and was used to supply businesses and homes. Coal was first mined for power generation in 1921 and the first coal fired power station was constructed in 1924.

Coal mining has continued at Yallourn Mine since that time. The Mine now covers an area of 16km^2. Planning is currently being undertaken for the expansion of the Mine into the Maryvale Field (refer Figure 2) which will supply coal to the Yallourn 'W" power station until 2027. The development of the field requires the diversion of the Morwell River. This paper will outline some of the geotechnical modelling undertaken for this project. Some of the geotechnical impacts at Hazelwood and Loy Yang mines are also mentioned.

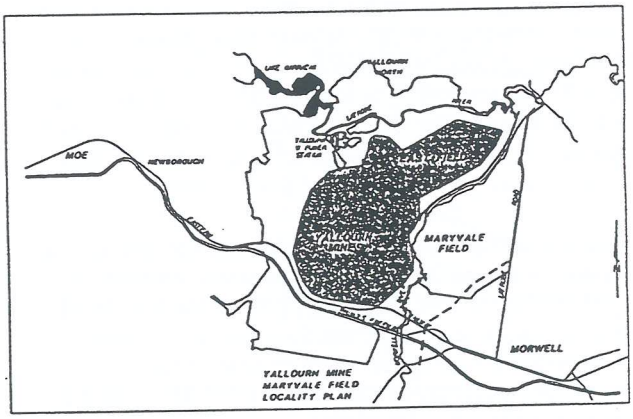

Figure 2: Yallourn Mine Fields

2. GEOLOGY

2.1 General

The Latrobe Valley Coal Measures are of Tertiary age and are found in the Latrobe Valley Depression. The Latrobe Valley Depression is the onshore extension of the Gippsland Basin, a major oil and gas field.

Five seams are mined in the Latrobe Valley, they are, in order of age, the Yallourn , the Morwell 1A, 1B, 2A and 2B. In some locations these seams are underlain by the Morwell 2C and the Traralgon seams that are not exploited due to their depth.

The coal seams range from 20m to 90m in thickness and are separated by up to 80m thick interseams made up of sandy aquifers, clays, ligneous clays, thin inferior coal and coals.

Faulting is not widespread within the relatively flat lying Tertiary sequences, however, major fault displacements have been observed adjacent to major geological structures such as the Yallourn Monocline Fault and the Loy Yang Dome. Faulting generally occurs in the basement rocks and is expressed in the coal measures as gentle folds, monoclines and occasional domes.

Jointing occurs extensively throughout the coal seams. The jointing is of tectonic origin, with a dominant NNW to SSE strike for the high angle (> 80°) and intermediate (40° - 80°) joints. Low angle joints (< 40°) strike predominantly NNE to SSE or ENE to WSW. Approximately 85% of all joints mapped are high angle joints.

Mapping has shown the joints are continuous along strike and fully penetrate the coal seam in which they are found. Joints can be up to 100mm wide and are often filled with sands and clays from the overlying Haunted Hill Formation (HHF), indicating continued reactivation of the stresses that formed the joints.

3. MINING METHODS

Mining of coal and overburden in Yallourn Mine is undertaken by a combination of Bucket Wheel and Bucket Chain Excavator (BWE and BCE). Mining takes place on faces with an average length of approximately 1.5km and height of 20m to 25m. Each 'pass', or block, advances the operating face by an around 50m. The time taken to complete a pass is dependent on the coal demand or set overburden production rate, but is usually in the region of 6 to 12 weeks.

During normal operations each overburden and coal face is separated by around 200m or approximately 9 months of normal production time. In periods prior to the transfer of operations into a new field these distances are increased so as to provide time for the re-establishment of conveyor systems without jeopardising coal supply reliability, which is required to be in the order of 98%.

4. INFLUENCE OF MINING ON BATTERS, MINE FLOOR AND SURROUNDING AREAS

4.1 General

Large scale open cut lignite mining faces can result in the following geotechnical events:

- Failure of individual overburden and coal faces or levels;
- Larger scale batter failures (two or more faces/levels);
- Ground movement of batters into the mined void due to the relief of tectonic stresses; and
- Ground movements related to water pressures and depressurisation of deep regional aquifers.

All have the potential to cause damage to mine infrastructure, both internal such as dredgers, conveyors and pipelines and external such is buildings, roads and services.

4.2 Individual Faces

Failure of individual faces, although sometimes quite extensive, generally does not generally generate ground strains significant distances from the mine batters. These types of failures are generally circular or piping failures in the overburden and joint controlled wedge or planar failures in the coal.

4.3 Large Scale Batter Failures

In extreme cases a planar or wedge failure can extend over more than one level. However large, batter scale, movements are generally block failures where a large block of coal moves under the influence of water pressures in joints within the coal. The block generally slides on the interseam clays, with lateral release being provided by the dominant sub-vertical joint sets mentioned in Section 2 of this paper. Movements such as these generally occur inside the mines, however in extreme cases movements have extended beyond the crest of the overburden batter up to a distance of 50m. Movements of large blocks by up to 1.5m have been recorded.

4.4 Stress Relief Related Ground Movements

Stress relief following mining produces the most significant horizontal and vertical ground movements and strains.

4.4.1 Horizontal Movements

Ground movements and strains are progressively generated as the mine is developed. Monitoring of survey pinlines in the mines has shown how ground movements are generated during the mining process. Ideally survey pins are installed on or near the proposed batter crest prior to mining commencing.

In general the magnitude and direction of stress relief related batter movements can be reasonably well predicted. For example, at Yallourn little movement is observed until the excavation of No. 2 Cut. By this point the Mine is generally in the order of 50 to 60m deep. The rate of batter movement reaches a maximum with the excavation of No's. 3 and 4 Cuts and then slowly reduces as No. 4 Cut moves away (refer Figure 3).

Significant ground movements continue for around 2 years following the excavation of No. 4 Cut. At the end of this time the following ranges of ground movement can be expected to have occurred.

Batter crest:	800 – 1000mm
Batter toe:	1400 – 2000mm

The shear movements along the coal/interseam interface at the base of the coal seam reduce the strength of the interface to residual values between the overburden batter crest and the toe of the batters. For the purposes of batter stability

analyses, and based on observations from inclinometers, this is assumed to occur between the excavation of No. 2 and 3 Cuts as this is when the first significant ground movements occur.

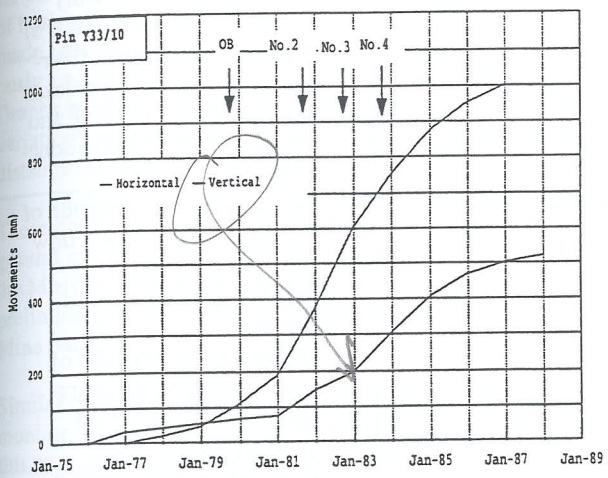

Figure 3: Graph Showing Generation of Ground Movements With Time and Progression of Excavation

The interseam strength is assumed to increase linearly to the peak shear strength between the batter crest and the 'Locus of X' (the point at which horizontal ground strains become insignificant). At Yallourn he Locus of X generally occurs between 400m and 600m from the crest of the batter, depending on the batter height and interseam strengths, however the Locus of X has been found to occur up to 900m away from the batter crest at Loy Yang Mine.

4.4.2 Vertical Movements

As coal is excavated it elastically rebounds resulting in heave. However survey data indicates the batters consolidate as they are excavated. This is due to the removal of groundwater from the coal batters and from the deep aquifers below the mines, which causes significant regional subsidence to occur.

Survey data shows that subsidence of the batter crest by around 300mm, in addition to the effects of regional subsidence (refer Figure 3) is not unusual.

4.5 Ground Movement Due to Regional Aquifer Pressures

The interseams between the coal seams of the Latrobe Valley contain extensive, high permeability sand aquifers. These aquifers are continuous across much of the Valley and extend towards the east where they becoming interbedded with the offshore oil and gas bearing marine sediments.

Aquifer depressurisation first commenced at Hazelwood Mine following a major episode of floor heave in 1960. Pumping rates in excess of 700 L/s have been maintained from the M1 and M2 aquifers since that time, with pumping reaching a maximum of around 1000 L/s in the early 1970's and again in the early 1990's.

Depressurisation of the M2B, M2C and Traralgon aquifers commenced at Loy Yang Mine in the mid 1980's and have now reached approximately 250 L/s, while pumping at Yallourn Mine commenced in the mid 1990's from the M1A aquifer and is continuing at around 15 to 20 L/s.

Aquifer pressures have been reduced by an average of 120m at Hazelwood Mine, 100m at Loy Yang Mine and around 40m at Yallourn Mine since pumping commenced.

Depressurisation of the aquifers has caused widespread subsidence of the Latrobe Valley. The Morwell Township, adjacent to the northern batters of Hazelwood Mine has the greatest impact from the extraction of groundwater with subsidences in the order of 2500mm recorded in the Township. Figure 4 shows the recorded subsidence at a number of points around the Latrobe Valley.

Regional subsidence appears to have caused no major environmental or infrastructure damage (eg: river gradients, pipelines etc.), despite the large movements that have occurred around Morwell. It appears that the rate of sedimentation in the streams has been able to keep up with the rate subsidence, while the subsidence 'bowl' has been relatively broad and gentle.

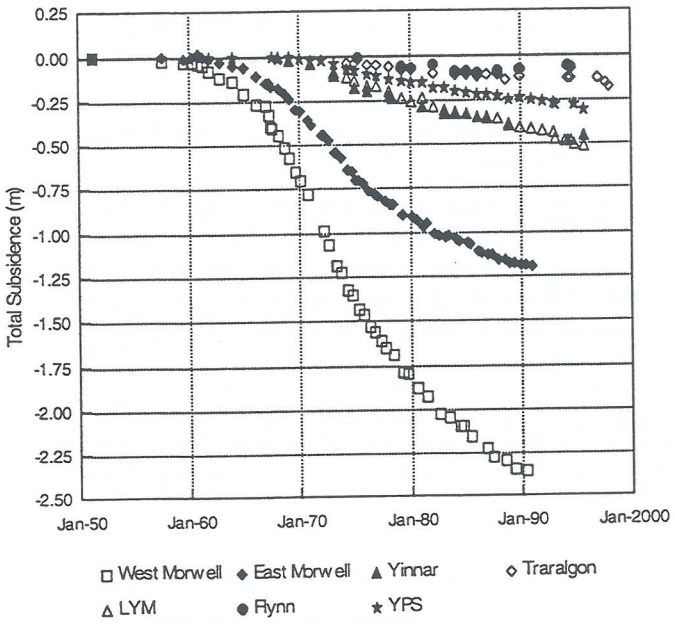

Figure 4: Recorded Subsidence Around The Latrobe Valley (Locations of points shown on Figure 1)

5. MONITORING OF GROUND MOVEMENT AND GROUNDWATER

5.1 Ground Movement Monitoring

Survey monitoring of pins and pinlines provide ground movement data that is used to:

- Assess the performance of a batter;
- Allow identification of areas of the batter which are not performing satisfactorily;
- Indicate when a batter design is too conservative which may allow an increased level of coal recovery; and
- Record ground movements.

Experience has shown that the following arrangement of pins generally produces an adequate amount of data for decisions regarding the stability of a batter system to be made;

- ***Crest Pinlines*** - located near the crest of the overburden batter over its entire length, where possible it is installed a minimum of 100m ahead of the overburden face to ensure it is able to collect a full history of ground movements. This pinline is the most important source of data in ground movement models such as FLAC.

- ***Radial Pinlines*** - extending from the Crest Pinline and away from the Mine. They should extend beyond the Locus of X. The complete pinline should be installed prior to any significant movement taking place.

- ***Batter Pinlines*** – extending from the crest to the toe of the batter. Ideally pins should be placed on the crest of each batter as it is developed. Placement of the pin on the crest allows maximum satellite coverage for the station when using GPS monitoring systems.

Regional subsidence is record on a series of settlement markers distant from the mines.

5.2 Groundwater and Ground Movement Bore Installations

Groundwater and pore pressure monitoring bores are used to confirm that water and pore pressures in and below the batter are at or below the design levels. High water levels can indicate that batter stability is being compromised and that the drainage system designed for the batters is not effective.

Ground movement bores are used to monitor movements along the coal/interseam interface. These bores help to identify the location and width of the failure/movement zone at the base of the coal and can give early warning of potential batter failures.

6. CONSEQUENCES OF GROUND MOVEMENTS

Impacts of excessive ground strains on infrastructure can include:

Failure Mechanism	Potential Damage to Infrastructure
Failure of individual faces	• Coal blocks falling on plant (potential loss of life). • Broken fire service pipes. • Damage to roads.
Large scale batter failures.	• Broken fire service pipes. • Damage to roads. • Damage to plant (mainly conveyors and occ. BWE's) • Opening of cracks in riverbeds close to the Mine leading to flooding of Mine and therefore lost power production.
Regional Subsidence	• Interruption and variation of natural and man made flow paths. • Variations in river flood plains. • Differential movement of structures build across regional faults (eg: No. 3 Cooling Tower, YPS) • Opening of cracks below dams (eg: LY Settling Pond)

As noted above individual face movements generally cause minor damage, with only occasional cases where damage has occurred to a BWE. These were a coal block failure in Yallourn Mine that damaged Dredger 3 in 1962 and a large scale overburden failure in Hazelwood Mine that damaged Dredger 10 in 1991. Similarly, while spectacular, larger scale batter movements have only caused relatively minor damage to pipes, roads etc. Both stress related movements and ground movement due to regional subsidence have the potential to impact on the serviceability of infrastructure and/or a natural system such as a river. For this reason effort is put into the prediction of such movements and their likely impact on the areas surrounding the mines.

7. PREDICTION OF GROUND MOVEMENTS AND STRAINS

Three main methods of predicting ground movements are used in the LV mines. The method adopted depends on the potential for damage to infrastructure.

For a batter with no important items of infrastructure, predictions of horizontal and vertical ground movements and the likely extent of ground movements are generally empirical and are based on historical data.

For more important batter systems, such as those carrying conveyor systems or those close to large masonry buildings, rivers or river diversion channels, historical predictions are used as a 'first pass' estimation. This is later confirmed using computer based models such as FLAC or in the case of regional subsidence related movements, COMPAC.

A recent example of this is the work carried out for the diversion of the Morwell River around the proposed Maryvale Field (MMRD), an extension of the Yallourn Mine. The aim of this modelling was to determine the distance between the Mine and the MMRD channel required to reduce the strains

generated by the mining to a level that will not result in cracking in the base of the channel following mining

7.1 Estimates Based on Historical Data

As part of preliminary definition studies for MMRD a series of horizontal and vertical ground movement predictions were made based on historical data collected from batters previously excavated with a similar orientation and geology. Graphs were plotted showing batter crest and toe movement variations with batter height and ground movement versus distance from the batter crest.

These correlations were used to predict the magnitude of the ground movements and strains likely to occur in the base of the MMRD channel and the width of the buffer zone. This preliminary buffer width was used to set the location of the Mine batters.

Similar data was collected on regional benchmarks that monitor subsidence in the Morwell and Yallourn areas. In this case correlations were made between the distance from the centre of pumping, drops in aquifer pressure and the thickness of sediments above the basement rock at a particular site.

Using this data the long term subsidence of the MMRD channel was predicted based on expected pumping rates from the aquifers below the channel. The preliminary modelling showed a differential subsidence of 400 to 500mm between the start and the end of the channel. This figure was input into the preliminary channel design.

7.2 FLAC Modelling

7.2.1 General

FLAC is a continuum stress analysis code, with a range of nonlinear models available for soil or rock material, interfaces and structural elements or modelling rock bolts, tunnel linings etc. FLAC can also be used to analyse transient groundwater flow in a porous medium, either alone or coupled with a stress analysis.

7.2.2 Mechanical Modelling

The first step in the modelling process is the generation of the model grid. The sections analysed for this project were in the order of 1200m to 1300m long and around 220m high. Sections of this length were adopted to ensure that boundary effects were minimised on the results of the calculations around the river, by allowing the boundary of the model to be located approximately 300m away from the outside edge of the Diversion channel. The height to length ratio suited a 10m horizontal by 5m vertical configuration. The model was developed so that the grid lines run parallel to the batter faces and the batters of the MMRD channel.
Observation of ground movements and coal cracking and jointing indicates that the coal behaves as a 'mass' rather than a series of individual blocks. For this reason the model does not model either individual joints or joint sets and the strata is modelled as an elastic material.

Experience shows that in order to maintain ground movements to the order observed in the field, the batter system had to be run as an elastic model. Efforts to model the batter system as a mohr–coulomb model proved ineffective as large vertical settlements occur during initialisation of the model which result in high unbalanced forces in the model. Efforts to combat this were ineffective.

Elastic parameters were applied to the model grid and an initial stress regime applied. A horizontal to vertical stress ratio varying from 1.0 to 1.5 was adopted, which combined the far field stress regimes common to the region and the overburden stresses.

Initial stresses were calculated using a subroutine which summed the stresses induced by each materials type over each column of the model. An interface capable of strain softening behaviour with ground movement was defined. The initial steady state water levels were input and the model was stepped to mechanical equilibrium. The model displacements and velocities were reset to zero.

As the problem to be solved assumed the river diversion channel existed and the effects to be studied were those of the mine excavation, the channel formed part of the ground surface in the initial equilibration.

The mine batters were progressively excavated with the water levels being redefined at each modelling step.

7.2.3 Probabilistic Modelling

Once the models were calibrated and initial modelling runs for a range of buffer widths were completed, a range of FLAC runs were undertaken to assess the impact of variations in the interface strength and their impact on the strains generated across the base of the MMRD channel.

Four FLAC runs were completed for each of the buffer analysed for each section. The runs were carried out for all the possible variations in the interface strength. A bivariate point estimate method was then used to estimate the probability of the strains in the base of the MMRD channel exceeding the tensile strain limits of intact coal which monitoring data has indicated is in the order of 0.65%.

7.3 Results of FLAC Modelling

Comparisons have been drawn between the results of the historical pinline survey based strain calculations and the results of the computer modelling for this project.

The pinline surveys have been carried out across ground with a generally flat surface at grass level. In the case of this study the MMRD channel excavation creates a large 'notch' in the surface. The effects of this are similar to those demonstrated in a notch ductility test on a metal plate, which exhibits large strain concentrations around the notch.

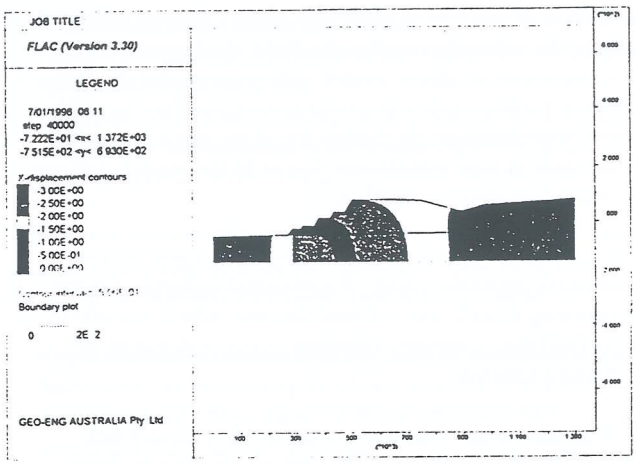

Figure 5: Typical X-Displacement Plot From FLAC

The variations in strain are shown by the x displacement plots from the FLAC analyses and indicate large strains at the batters, reducing across the buffer zone and then increasing around the area of the MMRD channel (refer Figure 5).

The magnitude of the computer predicted ground strains were larger than those determined from the historical data and indicate that the ground strains generated by mining Maryvale Field will exceed the tensile strain limits for remoulded clay but are acceptable for intact brown coal. It was therefore concluded that lining the channel with compacted clay was unlikely to improve its ability to hold water when effected by ground strains.

The results of the probabilistic analysis together with a check of the potential for block sliding failures indicates that a reduction in the buffer width as estimated in the preliminary assessment of historical data can be made. Accordingly the buffer widths were set as 250m (reduced from 295m) along the southern batter, widening to 300m (reduced from 335m) along the southern end of the eastern batters and increasing to 345m (reduced from 375m) in the northern part of the eastern batter. This releases an additional 17Mm^3 of coal from the batters, nearly a years production.

7.4 COMPAC Modelling

7.4.1 General

Future land levels are predicted using the COMPAC numerical model. The COMPAC model uses a non-linear generalisation of Terzaghi's 1-D theory of consolidation to compute land subsidence resulting from changes in hydraulic head within on or more aquifer systems. Virgin (non recoverable) compression and elastic (recoverable) rebound and recompression of sediments that lie either within an aquifer system or between aquifer systems are taken into account. The compression of permeable aquifer material (usually sand) is also calculated. The aggregate vertical movement at the ground surface, as a function of time, is computed by summing the individual contributions of the layers.

As the model is one dimensional is incorporates only the vertical subsurface profile and as such can only be used to predict land level changes at discrete sites. A feel for the regional effects of subsidence is gained by making predictions at a number of points across an area and contouring the results.

7.4.2 Regional Subsidence Mechanism

The magnitude and rate of land subsidence due to the depressurisation of the aquifers is dependent on a number of factors including:

- Material consolidation characteristic such as compression ratios (CR) and permeability.
- The preconsolidation pressure (P'c).
- Initial effective stresses.
- The increase in effective stress due to groundwater extraction.
- The thickness of the aquifers and separators.

The preconsolidation pressure is the maximum effective stress that a soil has been exposed to in its history. When the stress being applied to a soil exceeds the P'c, its compressibility increases by an order of magnitude. In the Latrobe Valley the sediments are heavily overconsolidated due to extensive erosion of the Tertiary sediments.

The depressurisation of the regional aquifers is causing an increase in the insitu effective stresses. The magnitude of the subsidence is proportional to the increase in the effective stresses and the compressibility of the materials. It is generally recognised that coal is more compressible than clay, which is more compressible than sand.

The larges subsidence is observed to occur adjacent to the mines. This is due to the localised combination of thick near surface deposits of coal and the largest drops in aquifer water pressures. It should be noted that consolidation settlement is inversely proportional to the initial effective stress, therefore for a given stress increase, the deeply buried strata produces much less subsidence than the near surface strata.

7.4.3 COMPAC Model Accuracy

In general adequate historical surface survey data exists, however most areas have little historical water level data from each of the aquifers that is being depressurised. In most areas only one or two aquifers are being monitored at any one time.

Model accuracy is highly dependent on the accuracy and amount of aquifer water pressure data available. In the case of the MMRD channel this area has only limited water pressure data an it was expected that models run with this data would produce an answer that was plus or minus 20% or around 250mm.

7.4.4 MMRD COMPAC Modelling

To carry out COMPAC modelling specifically for the MMRD channel would require the following:

- Drilling of 3 boreholes to basement rock (approx. 500m), one at either end and one in the middle of the proposed channel.
- Geological and geophysical logging of the bores.
- Installation of piezometers to monitor the water levels.
- 1-D consolidation testing of samples.
- Running of the regional groundwater model to determine the likely changes in groundwater levels (and therefore effective stresses) at each bore location.
- Creation of a COMPAC model for each site. Running the models for a number of water level scenarios.
- Interpreting the results of the modelling and their effect on the flow in the channel.

The estimated cost to undertake this program of works was significant. It was decided that the work was not economically justified for the improved accuracy of the results that would be obtained from the modelling. In addition, the River was likely to be able to compensate for the variations in the levels with time, this is despite the channel gradient being very flat.

8. CONCLUSIONS

In general the magnitude and direction of stress relief related batter movements can be reasonably well predicted using empirical methods. Ground movements of the following order are generally expected to occur:

Batter crest:	800 – 1000mm
Batter toe:	1400 – 2000mm

Depressurisation of regional aquifers has caused widespread subsidence of the Latrobe Valley, with movements in the order of 2500mm recorded in the Morwell Township. At this stage regional subsidence appears to have caused no major environmental or infrastructure damage (eg: river gradients, pipelines etc.)

Three main methods of predicting ground movements are used in the LV mines. They are:

- Empirical methods based on historical data.
- Completion of a 'first pass' empirical estimation later confirmed using computer based models such as FLAC and/or, in the case of regional subsidence related movements, COMPAC.

The method adopted depends on the potential for damage to infrastructure located around the mine batters.

The FLAC modelling completed for MMRD improved the definition of the buffer zone between the proposed mine and the river diversion channel. In this case the preliminary empirical estimate was considered to be very conservative and the potential returns from the modelling were believed to justify the expense of collecting the data for the model (drilling and laboratory testing) and the cost of the modelling. In this case approximately 17Mm^3 of extra coal will be recovered and will provide the mine with a significant return on the investment in the modelling.

9. BIBLIOGRAPHY

Bamford, W.E. 1979: Summary of 18 Sets of Strength Tests Carried Out on Yallourn Seam Coal. University of Melbourne.

Barton, C.M. 1981: Analysis and Prediction of Geological Structures in the Latrobe Valley. SECV Report, Exploration and Geological Division, Fuel Department.

Geo-Eng Pty Ltd 1997: Yallourn East Field, Coal Face Mapping and Operating Face Stability. Report 1150/5032/01.

Geo-Eng Pty Ltd 1997: Southern Batter Fringe Coal, River Diversion Buffer Width Assessment. Report 1150/5095/03.

Geo-Eng Pty Ltd 1998: Yallourn Energy. Morwell River Diversion Alignment Study. Report 1150/5119/10.

Geo-Eng Pty Ltd 1998: Maryvale Field, Preliminary Assessment of River Diversion Buffer Widths and Potential Ground Movements Due To Mining. Report 1150/5127/03.

HI 11 1975: Cracking of Clay Beams. SECV Report, Hydro and Investigations Design Division, Civil & Architectual Dept.

Trollope D.H., Rosengren K.J. & Brown E.T 1961: The Mechanics of Brown Coal.

Putting the Geo into Geotechnical - The Role of the Engineering Geologist During Construction of the Eastern Distributor Tunnel, Sydney, Australia

Richard Justice.
Engineering Geologist, Pells Sullivan Meynink Pty Ltd

SUMMARY

The 1.5km long Eastern Distributor Tunnel, to the east of Sydney's CBD, is Australia's first piggyback tunnel. The tunnel is excavated through a highly urbanised area with limited rock outcrop, hence the geotechnical model formulated for design purposes was heavily reliant on borehole information. During construction, detailed engineering geological mapping served to 'proof check' the assumptions and interpretation made in the design model.

This paper briefly summarises the design geotechnical model, the role of the Engineering Geologist during construction and the Geologist's position in the overall context of the construction team. The post construction model, formed on the basis of in-tunnel mapping, is then presented.

It is concluded that the mapping undertaken during construction largely confirmed the preconstruction model. Where encountered tunnelling conditions were different to those anticipated in the design model, the results of engineering geological mapping allowed appropriate support redesign in 'real time'.

The paper therefore provides a working example of the concept of 'putting the "geo" into "geotechnical'.

1. INTRODUCTION

The 1.5km long Eastern Distributor Tunnel, located to the immediate East of the CBD of Sydney (Figure 1), will carry three lanes of Northbound traffic over three lanes of Southbound traffic in Australia's first piggyback tunnel.

The geotechnical model for design purposes was based on field investigations comprising a sum total of 103 cored boreholes, supplemented by geotechnical mapping in old quarries and along the Cahill Expressway, to the north of the tunnel. Hence the preconstruction or design geotechnical model was heavily reliant on interpretation between boreholes. Engineering geological mapping undertaken during the construction phase of the project was used to validate the preconstruction model.

This paper outlines the design geotechnical model, tunnel construction sequence and the role of the Engineering Geologist during construction. Elements of the post construction geotechnical model are then compared to the design model. It is concluded that mapping and database upkeep during excavation allowed for effective and quick support redesign where needed, served to largely confirm the design geotechnical model and has provided a permanent record of excavation conditions for the future.

2. PRECONSTRUCTION (DESIGN) MODEL

2.1 Lithology

The tunnel excavation was expected to occur entirely within subhorizontally bedded Hawkesbury Sandstone which forms the basement rock for the majority of the CBD. However, the upper part of the main south portal at South Dowling St and the ramp tunnels to Anzac Parade and Moore Park Rd were anticipated to be excavated through weathered Mittagong Formation. The boundary between the Hawkesbury Sandstone and the Mittagong Formation was known to be gradational and it was considered that the base of the Mittagong Formation formed a shallow basin structure near Taylor Square (Figure 1).

Three main sedimentary facies are apparent within the Hawkesbury Sandstone as outlined below.

1. Massive Facies: typically internally homogenous in particle size and either massive or displaying a poorly to well developed undulose layering. This facies usually displays a discordant, erosional lower layer and a planar concordant upper surface, Herbert (1). Shale breccia commonly occurs within troughs above this erosional surface.

2. Sheet Facies: Sandstone in this facies consists of cosets of trough or tabular cross strata which are bounded by subhorizontal bedding surfaces. Cross bedded sets range from a few centimetres to more than 5m in thickness and commonly dip to the north to northeast. Syndepositional convolution and recumbent folding of foresets is common in this facies, Conaghan (2) and is probably due to mass movement events shortly after deposition involving the unconsolidated sediments
3. Mudstone Facies: This facies is laterally discontinuous and usually between 0.3 - 3m thick. It is composed of

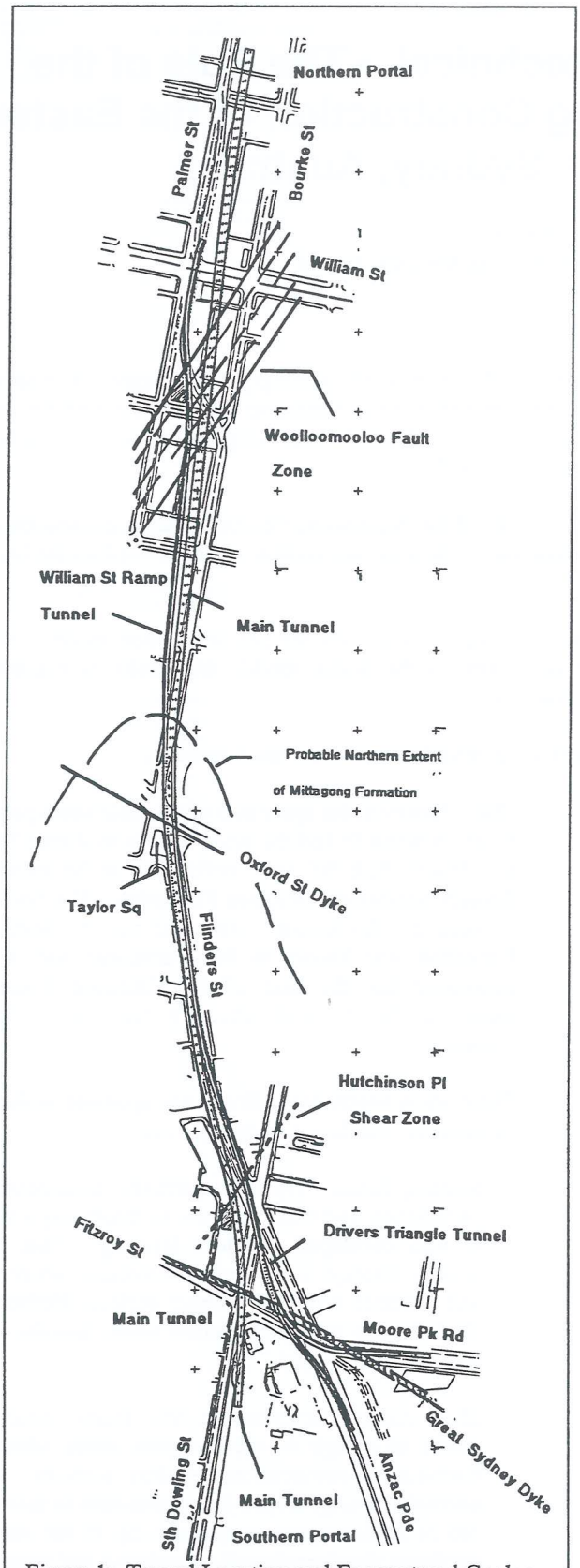

Figure 1: Tunnel Location and Encountered Geology

grey, fissile mudstone which in places is slightly carbonaceous and is often laminated with fine grained sandstone. The facies is often referred to by the terms "Shale lens" or "Laminite".

2.2 Bedding

The results of the site investigation indicated that bedding was typically subhorizontal and typically planer to undulose, with high horizontal continuities. Sand to Clay infill was encountered along approximately one third of the measured bedding defects.

2.3 Cross Bedding

Cross bedding was inferred to typically dip towards the northeast. In fresh or slightly weathered sandstone at the depths of the tunnel, cross bedding was not anticipated to form planes of weakness. However, in moderately to highly weathered sandstone the cross beds were considered likely to form surfaces of incipient parting or low shear strength.

2.4 Jointing

Based on oriented hole core and the limited surface mapping data, the dominant joints were inferred to be subvertical and strike north-northeast, although occasional vertical joints orthogonal to the main north-northeast system were interpreted. The joints were anticipated to have substantial horizontal and vertical continuity, and be planar, rough and mostly clean.

2.5 Faulting

Faulting in the Hawkesbury Sandstone is uncommon. However, a fault zone, termed the Woolloomooloo Fault Zone (WFZ) was encountered while drilling for the piers of the Eastern Suburbs Railway viaduct in the late 1960's. It was expected that the WFZ would intersect the main tunnel between 160m and 240m in from the northern portal, and at the William Street Ramp Tunnel portal. Minor sub-parallel faults or shears were expected to intersect the main tunnel up to approximately 450m in from the northern portal.

The zone was inferred to be steeply dipping to the southeast; vertical displacement across the zone was interpreted to be about 5m, with the eastern (hanging wall) side up-thrown, ie an overall reverse motion.

Stress measurements were undertaken in a borehole just to the north of Stanley Street, using hydrofracture techniques. The results indicated that the horizontal stress was about five times the overburden pressure which was considered to also indicate reverse motion across the WFZ.

Borehole data suggested that additional minor faults or shears could possibly occur near the intersection of Flinders Street and South Dowling Street, ie approximately 200m in from the southern portal of the main tunnel.

Low angle thrust faults, which merge into bedding plane shears, are known to occur within the Hawkesbury Sandstone but were difficult to detect in borehole core. A thrust fault was observed in an exposure to the north of

the tunnel. It was considered probable that thrust faults would be encountered along the tunnel route.

2.6 Igneous Dykes

Two near-vertical igneous dykes were interpreted to intersect the tunnel route (Figure 1):

- a relatively thin (0.3 to 0.6m wide) dyke underneath Oxford Street (the Oxford St Dyke), and
- the Great Sydney Dyke which runs along the alignment of Fitzroy Street. The dyke varies in thickness from 5 to 7m and, at the depth where it is penetrated by the tunnel, was inferred to comprise stiff fissured clay (extremely weathered dolerite).

3. TUNNEL EXCAVATION

3.1 Excavation Sequence

Excavation was mostly by roadheader. Excavation of the main tunnel typically involved the following sequence (Figure 2):

A. Excavation of 5 to 6m wide parallel headings at Northbound level
B. Pillar stripping
C. Southbound excavation.

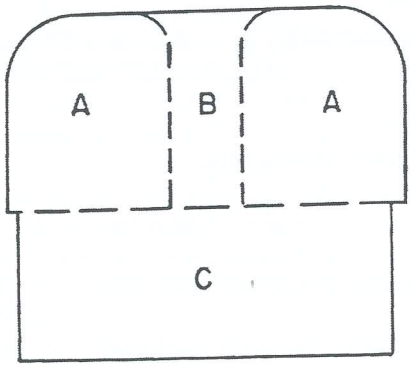

Figure 2: Tunnel Excavation Sequence
(see text for explanation)

At the peak of excavation activity, six roadheaders were operational with a maximum advance rate of 80m per week for a 6m wide heading attained.

3.2 Company Role and Personnel Objectives During Construction

Pells Sullivan Meynink Pty Ltd (PSM) had the responsibility for the design of roof and side wall support of the Eastern Distributor Tunnel. The basic philosophy for tunnel support involved the concept of a linear arch being formed in the rock above tunnel roof which was supported by rockbolts and shotcrete.

PSM's role on site was involved with the on-site "Surveillance" team, whose job it was to ensure that the support for the tunnel was installed as designed. Where ground conditions differed substantially from the design geotechnical model, it was the responsibility of Surveillance to provide support redesign. PSM's task was therefore to check that geological reality reasonably matched the design model and to undertake redesign when and where significant departures from the design model occurred.

Significant departures from the design geotechnical model would have included such scenarios as:

- relatively continuous moderately dipping defects,
- in conjunction with monitoring, evidence of low horizontal stress (eg. open joint planes),
- ground water inflows greater than expected,
- faults and shears other than predicted, and
- weathering conditions other than predicted.

The objectives of the Engineering Geologist's role were therefore to:

- modify and update the geotechnical models used for design purposes,
- forecast tunnel conditions, more particularly in twin headings, and through known structures,
- reduce the risk of 'geological surprises',
- allow quick response and localised redesign of tunnel support where 'geological surprises' were encountered, and
- provide a record of tunnel conditions for the future.

These objectives were achieved by:

- engineering geological tunnel mapping of all Northbound headings as well as Southbound walls,
- observation and interpretation of drilling for rockbolts and pipe canopy tubes to assess geotechnical conditions above the tunnel roof,
- routine sample collection for point load strength testing , and
- creation and management of a database containing the properties of mapped defects (orientation, length, persistence, roughness etc).

The major task was in-tunnel mapping. Detailed 1:100 scale maps were produced for all headings and included both sidewalls and the roof. When access allowed, the active face was logged. An example of a completed mapping sheet is shown in Figure 3.

Mapping of a particular heading typically lagged some 20 to 30m behind the tunnel face because the roadheader and haul trucks severely affected compass readings. Periodic logging of the face itself was necessary, however, as the face allowed a cross-tunnel section of the local geology to be viewed as well as assessment of the latest excavation conditions.

3.3 Data Flow

It was attempted where feasible to provide support redesign to the main contractor in what was termed 'real time'; or in other words with a minimum of delay. The theoretical data flow from in-tunnel mapping and monitoring through support redesign to support installation is shown in Figure 4.

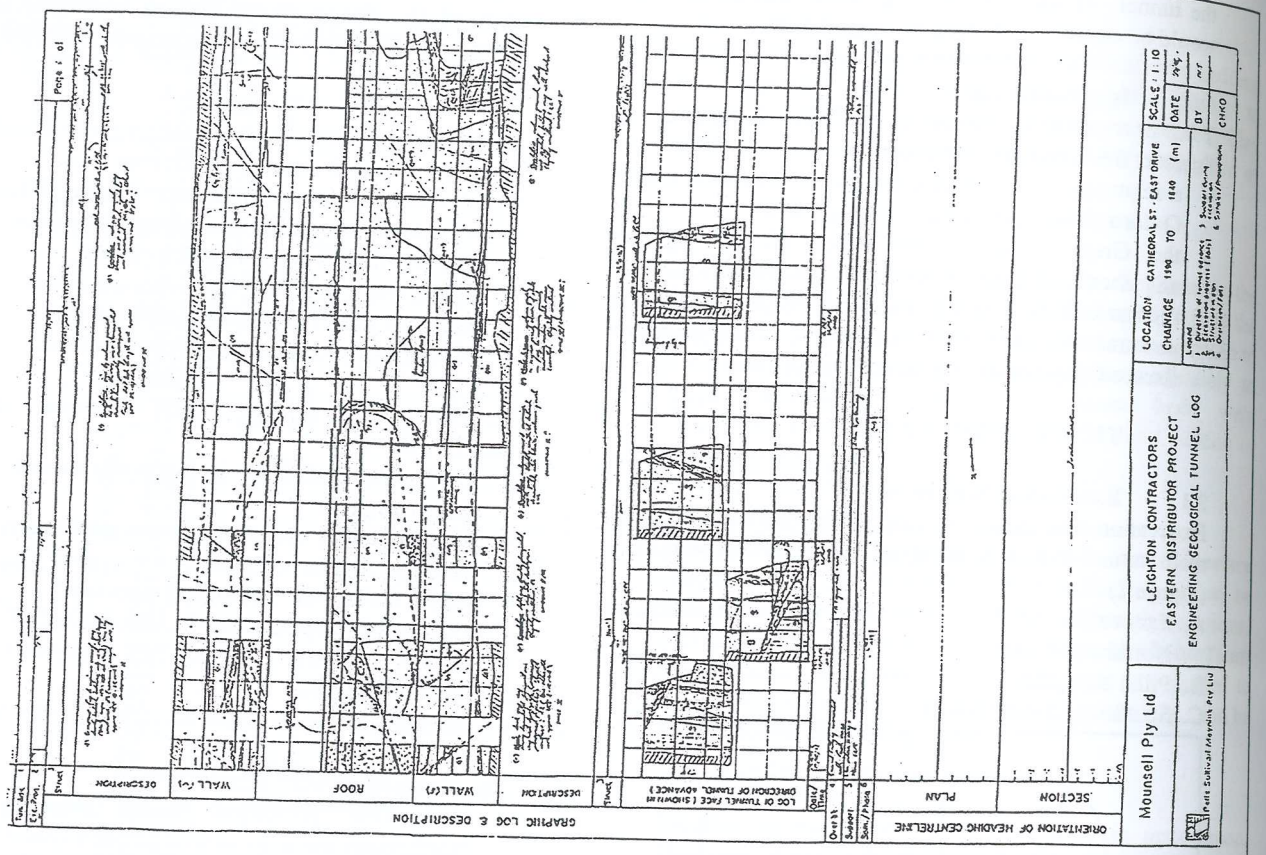

Figure 3: Example of a Completed Tunnel Mapping Sheet

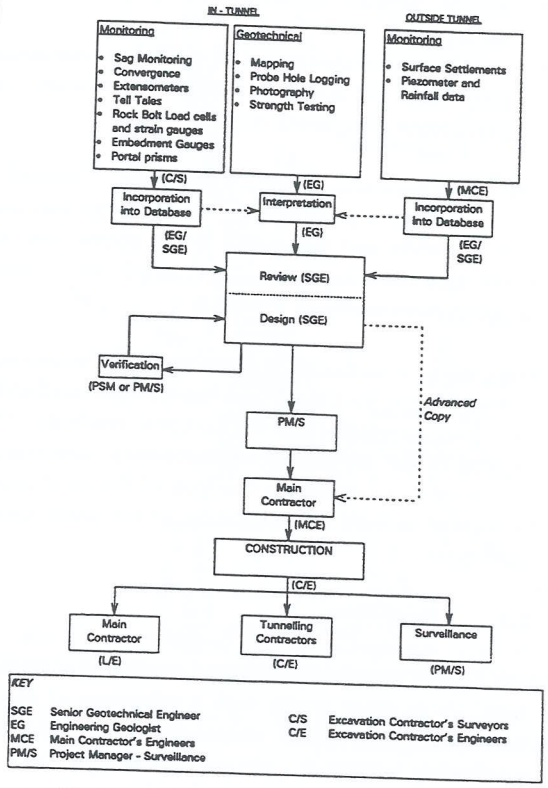

Figure 4: Theoretical Data Flow Sequence

Support review and redesign was carried out by a Senior Geotechnical Engineer, also from PSM, on the results of in-tunnel mapping and monitoring.

In reality, the roles performed by the Engineering Geologist and the Geotechnical Engineer were somewhat overlapping and became more so in the latter stages of the project. The Geotechnical Engineer sometimes performed mapping, whilst the Engineering Geologist routinely undertook support design, particularly sidewall bolting. This had the advantage of 'decompartmentalising' both roles, ie the data flow sequence did not come to a grinding halt because of personnel unavailability etc.

The collection of data from in-tunnel monitoring was the responsibility of the tunnelling excavation contractor. Surveillance had overall control of where monitoring points were installed, and the frequency of reading. It was the responsibility of Surveillance to maintain a monitoring database.

3.4 Data Collation

Data collation involved:

- daily updating of standard plans and sections in paper form,

- incorporation of structural data into a standard database from which defect stereoplots and defect histograms were produced, and
- inclusion of the results of Point Load, or other, testing into a testing database.

The histogram sheet and stereoplots were typically generated for 100 – 200m segments of the tunnel and allowed a quick visual check to be made between the design model and the encountered conditions.

3.5 Southbound Wall Bolting

The Eastern Distributor Tunnel is designed as a piggyback tunnel with Northbound traffic supported on a 600mm thick steel reinforced concrete decking, supported at each end on a 400 to 500mm wide sill beam.

Imposed loads of up to 827kN/m were calculated at the widest span of the tunnel. The orientation of the major joint set at an acute angle to the tunnel alignment and the imposed loads acting on the sill beam meant that potential "one sided" wedge failure, Pells and Dai (3), under the sill beam could occur. This failure mechanism involves release along an existing joint plane with shearing and tensile failure through intact rock (Figure 5).

Depending on the orientation of a joint beneath the sill beam and the local tunnel width, one of a series of four different patterns was installed adjacent to the joint. Support patterns were marked up during southbound wall mapping. This served to minimise the delay between mapping and support installation and allowed a 'one-pass' operation for the Engineering Geologist.

4. ELEMENTS OF POST CONSTRUCTION MODEL

For most of the length of the tunnel, the mapping confirmed the preconstruction model. The following sections provide a summary of the characteristics encountered for various features. Figure 6 summarises the post-construction engineering geological model.

4.1 Hawkesbury Sandstone

Sheet and Massive Facies Sandstone as well as the minor Mudstone Facies were encountered during mapping. In general the Hawkesbury Sandstone encountered was typically classified as Class II with Class III near the portals (after Pells et al, Reference 4). A general profile can be summarised as:

- Mixed Massive and Sheet Facies Sandstone with few shale horizons (encountered in the southern half of the tunnel) overlying;
- Sheet Facies Sandstone with relatively common shale or shale breccia horizons (encountered in the northern half of the tunnel).

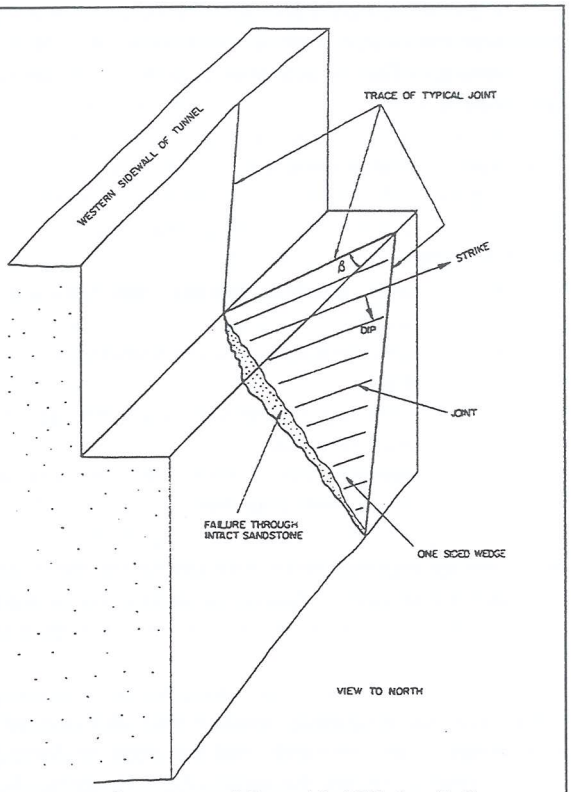

Figure 5: Geometry of One-sided Wedge Failure

The shale breccia was found to comprise zones of reworked and/or syndepositionally deformed shale within a fine to medium grained sandstone matrix. The horizons had a typical maximum thickness in the order of 1m and occurred at greater frequency than anticipated from borehole logging. Typically, the borehole logs indicated the horizons as one or two discontinuous shale lenses in a sandstone matrix, and were mostly noted as being minor features within the drill core. However, exposure within the tunnel indicated these apparently minor features typically formed part of a more extensive zone, with individual continuities of up to 100m.

4.2 Bedding

Figure 7 presents the stereographic projections of the structure mapped during tunnelling and shows that bedding was mainly sub-horizontal. Analysis of bedding defects recorded during tunnel logging indicate the following defect characteristics:

- bedding spacing averaged about 2.0m;
- 85% dip less than 10°, 95% dip less than 20°;
- 60% had some infill varying from a stain to over 50mm;
  - 5% of which are Clay,
  - 50% of which are sandy Clay with or without some iron oxide,
  - 25% of which are clayey Sand,
  - 10% are Sand, and
  - the remaining 10% either iron oxide or carbonaceous material.

Clay dominated infill typically occurred near the surface whereas sand dominated infill occurred at the depth of the tunnel. This is interpreted to be a weathering related effect.

4.3 Cross Bedding

Figure 7 shows that cross bedding typically dips at 15° towards 045°. The mapping also indicated the following characteristics:

- cross bedding spacing was typically less than 0.2m;
- average length of cross bedding is approximately 4m;
- 66% dip between 10 and 20° typically to the northeast; and
- approximately 50% of the measured defects had minor infill of up to 3mm.

During logging, focus was placed on those defects that had some infill. Hence, the proportion of infilled cross beddings calculated above is much higher than reality.

In Class II sandstone or better, the cross bedding surfaces were not noticeably weaker than the rest of the rock material, and as such, did not tend to form planes of separation within the rock mass. However, in zones of Class III, or poorer, sandstone (ie within the WFZ and adjacent to the Great Sydney Dyke), cross bedding planes acted as release surfaces for roof failures. In these sections roof failures were typically defined by 'feather edging' on cross bedding with side release on joints.

4.4 Mittagong Formation

The Mittagong Formation formed the roof of the Drivers Triangle Ramp tunnel. The sequence comprised highly to extremely weathered interbedded sandstone and black mudstone (Class IV/V), and displayed a gradational relationship with the underlying Hawkesbury Sandstone which was assessed to be Class II/III.

4.5 Joints

The major joint set was confirmed to strike north-northeast and the minor set east-southeast (Figure 7). Both defect sets occurred as discrete features or as swarms of about 3 to 10 defects. Defect spacings within the swarm range from 20 to 500mm, whilst spacing between swarms was up to 20m. Typical joint characteristics are outlined below.

- 15% are continuous out of both the floor and roof of the tunnel, crossing several bedding planes, with a vertical continuity greater than 10m.
- 45% are semicontinuous, and transgress one or more bedding planes, with a vertical continuity of between 3 and 10m.

No clear correlation exists between sandstone type and joint occurrence or characteristics. However, joints were much less frequent in the central part of the tunnel compared to near the portals. This may be an effect of near surface stress relief.

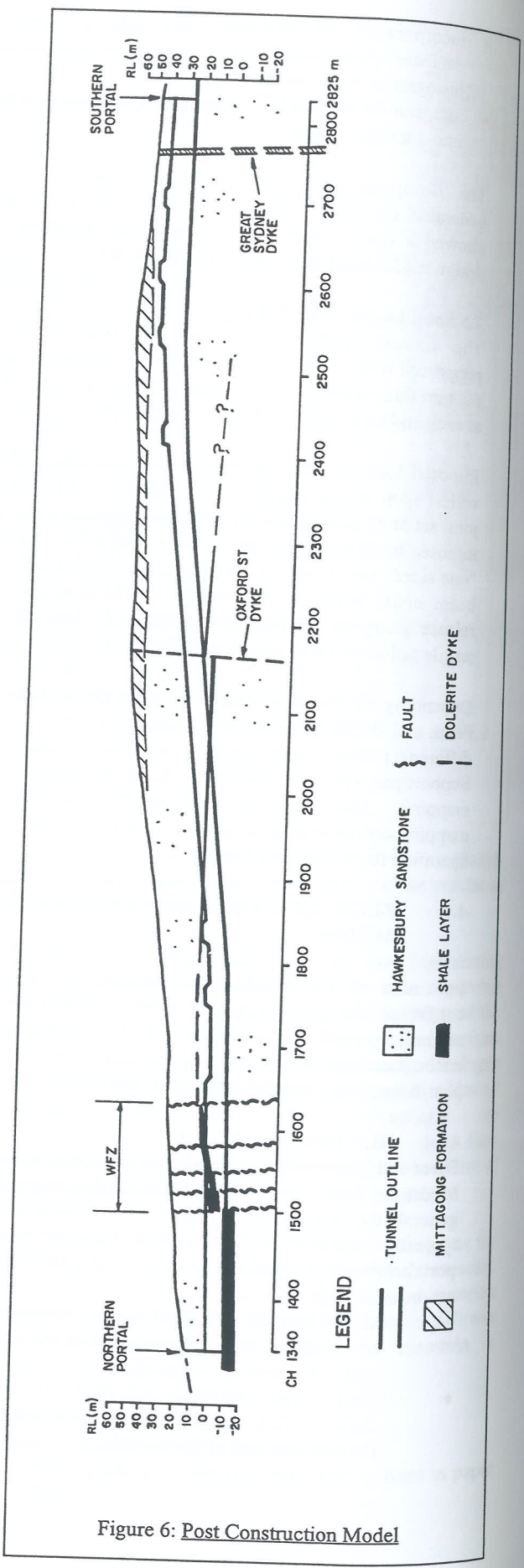

Figure 6: Post Construction Model

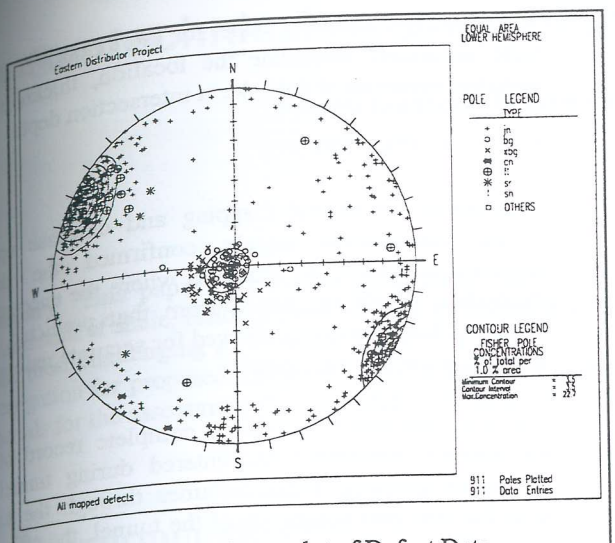

Figure 7 Stereoplot of Defect Data
(relative to true north)

4.6 Faults

The WFZ and low angle thrust faults were encountered during tunnelling. Low angle thrust faults were recognised on both sides of the Great Sydney Dyke, and adjacent to, or as part of the WFZ.

The low angle thrusts ranged in length from about 1m up to approximately 20m. A sandy clay infill of up to 50mm was typical. The faults were often formed between adjacent bedding planes. This characteristic is interpreted to mean that:

- some amount of movement occurs along bedding planes, and
- the low angle thrusts serve to provide a movement surface, or 'connection path', between adjacent bedding planes.

The WFZ was intersected in the main northern tunnel between Ch1521-1625m with parallel faulting extending to 1700m, and at the portal of the William St Ramp tunnel. The WFZ is approximately 50m wide, dips at about 70° towards the southeast, and intersects the tunnel at about 25°. The WFZ comprises five major fault splays, (Figure 8) comprising 50 to 1000mm of crushed sandstone within a soft to firm clay matrix. Smaller faults and shears were apparent between the major splays. These minor faults had a maximum width of about 20mm. Rock quality between the fault splays improves towards the south, starting as poor between splays 1 and 2 and becoming very good between splays 4 and 5.

Overall movement of the zone is interpreted to be reverse (ie northwest side up relative to the southeast), although some of the fault splays are normal. Mapping indicated a displacement across the fault of approximately 8m. The component (if any) of strike slip motion was not able to be determined.

The gross characteristics and the overall sense of movement of the WFZ was accurately determined in the design geotechnical model, however, the number and position of the major fault traces was not realised.

The zone of minor faulting near the intersection of Flinders Street and South Dowling Street interpreted in the design model was intercepted during tunnelling, and was termed the "Hutchinson Place Shear Zone" (Figure 1). The zone was intercepted some 190m in from the main tunnel southern portal and comprised a number of closely spaced joints shears and faults. Vertical displacement of up to approximately 8mm was observed on some planes. The overall orientation of the zone is interpreted to be subparallel to both the WFZ and the major joint set, ie northeast - southwest.

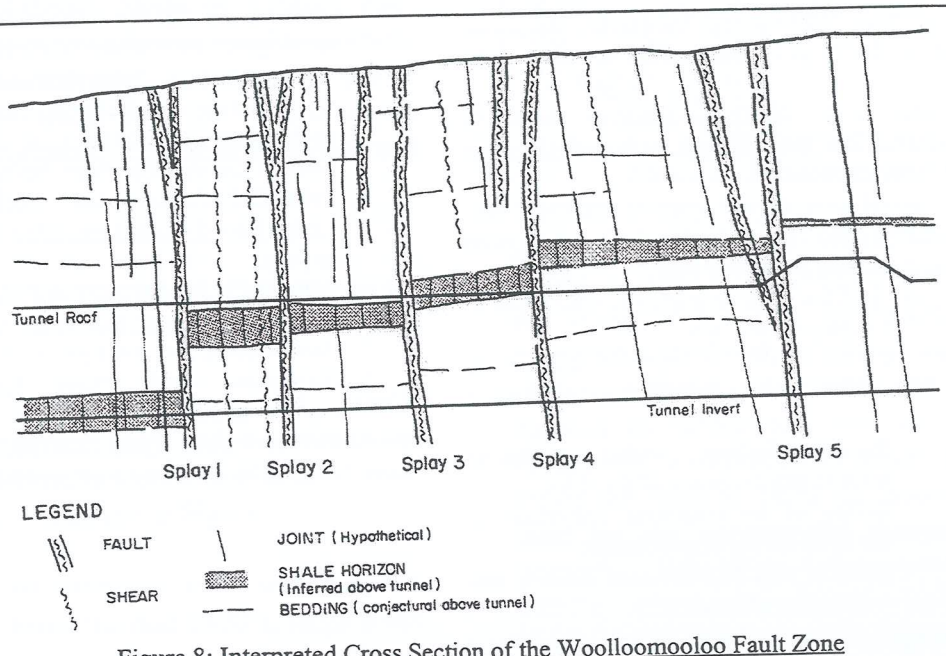

Figure 8: Interpreted Cross Section of the Woolloomooloo Fault Zone

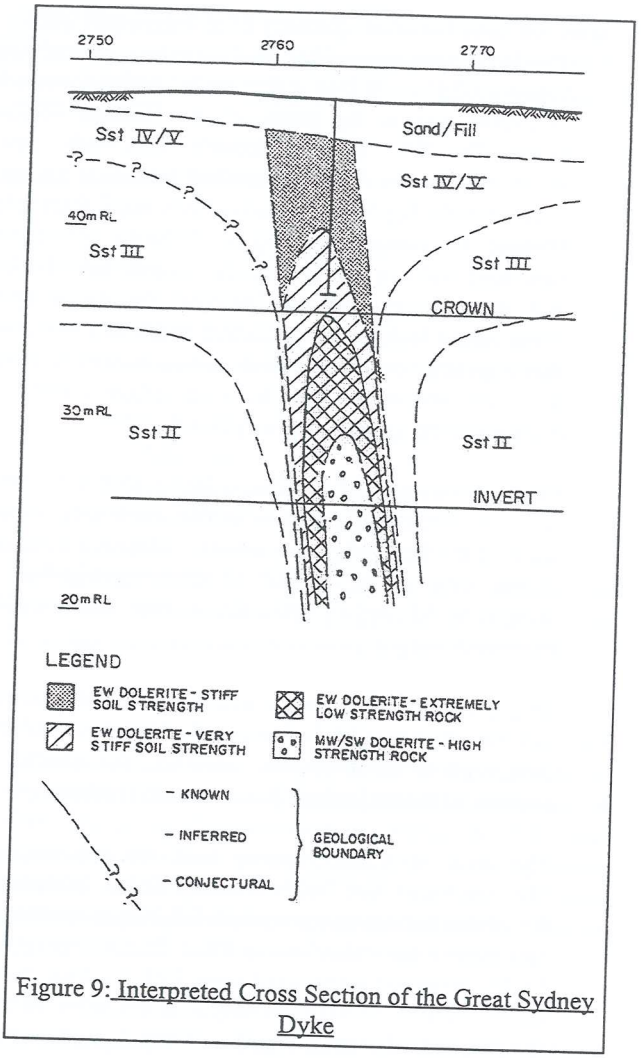

Figure 9: Interpreted Cross Section of the Great Sydney Dyke

4.7 Dykes

Both the Great Sydney Dyke and the Oxford Street Dyke were intersected within 1m of their expected positions.

The post-excavation geotechnical model for the Great Sydney Dyke is shown in Figure 9. Key features of the model are:

- at tunnel level, the dyke comprises extremely weathered low strength rock with stiff clay near the sandstone contacts,
- the central core of the dyke is relatively less weathered than material near the contacts with the surrounding sandstone rock,
- the quality of the dolerite improves with depth to very high strength rock, and
- sandstone rock quality is degraded adjacent to the dyke. This is likely to reflect a combination of;
  - fracturing/faulting within sandstone prior to emplacement of the dyke,
  - baking of the sandstone immediate to the dyke during emplacement,
  - possible post emplacement faulting and weathering effects.

The design geotechnical model for the tunnel was able to quite accurately determine the location, thickness and material properties of the dyke at intersection depth.

5. CONCLUSIONS

Engineering Geological mapping and database upkeep during construction largely confirmed the design geotechnical model. In situations where the encountered excavation conditions varied from that predicted, data collected during mapping allowed for accurate redesign of tunnel support in 'real - time'.

The mapping sheets provide a complete record of the geotechnical conditions encountered during tunnelling. Given the potential traffic volumes through the tunnel over the 100 year design life of the tunnel, the effort put in to the engineering geological mapping and data collection during construction is considered appropriate.

This paper therefore provides a working example of the issue raised by Stapledon (5) of 'putting the "geo" into "geotechnical", by

- using graphic representation of data on excavation logs,
- presenting detailed logs of high standard, and
- regular and on-going comparison between the encountered tunnelling conditions and the design geotechnical model.

ACKNOWLEDGEMENT

The author wishes to thank Leighton Contractors Pty Ltd and Maunsell Pty Ltd for their permission to publish this paper.

REFERENCES

1. Herbert, C, "Sydney Basin Stratigraphy", 1983, in Geology of the Sydney 1:100 000 Sheet
2. Conaghan, P. J., "The Hawkesbury Sandstone: Gross Characteristics and Depositional Environment", 1980 in Herbert, C and Helby, R (eds) "A Guide to the Sydney Basin Geol. Surv. NSW Bull 26 pp188 - 254
3. Pells, PJ.N.P. and C.Dai. Rockbolt Design for Rock Ledge Based on the One Sided Wedge Failure Model in prep.
4. Pells, P.J.N.P, Mostyn G and Walker B.F. Foundations on Sandstone and Shale in the Sydney Region (1998) Aust. Geom. Dec 1998 pp17 - 36
5. Stapledon, D.H. "Lets Keep the 'Geo' in Geomechanics". (1986). Proc Speciality Geomechanics Symp. On Insitu Testing, Adelaide, Aug 1986. Inst Eng Aust pp 18-29

Geotechnical Aspects of the Sydney 2000 Olympic Site

Roberta Lindbeck, Douglas Partners Pty Ltd, Sydney, Australia

Summary This paper reviews the geotechnical aspects of the Sydney 2000 Olympic Site at Homebush Bay: a geological environment of shale, residual clays, alluvial sediments, and filling. Of these materials, the soft alluvial sediments provided some of the most challenging geotechnical conditions. The paper focuses on one particular geotechnical case study, which was the investigation for proposed irrigation ponds in the former landfill areas. The work involved the investigation of the soft alluvial materials for the assessment of slope stability of the ponds.

1 INTRODUCTION

The site for the 2000 Olympic Games is located at Homebush Bay in Sydney's inner west. Homebush Bay is a low-lying area, which was previously covered by natural wetlands and has been utilised for industrial and land filling purposes since the early 1940's.

The redevelopment of the Homebush Bay area for the Olympic Games involved the development of the previously industrial area into major sporting, recreational, and residential facilities. The construction activities have resulted in much geotechnical investigation being undertaken in the area over the past decade.

The geological environment in the Homebush Bay area consists of Ashfield Shale of Triassic age, residual clays, Quaternary alluvium, and man-made filling. The development therefore required construction to be undertaken in a challenging geotechnical environment, comprising filling and soft alluvial deposits.

2 HISTORY OF THE HOMEBUSH BAY AREA

Originally, the Homebush area was greatly influenced by Homebush Bay and its tributaries: Haslam's Creek, Powell's Creek, and Duck Creek. A map of the area is included in Figure 1.

The area comprised extensive tidal wetlands and thick woodlands. From the mid 1800's, large areas

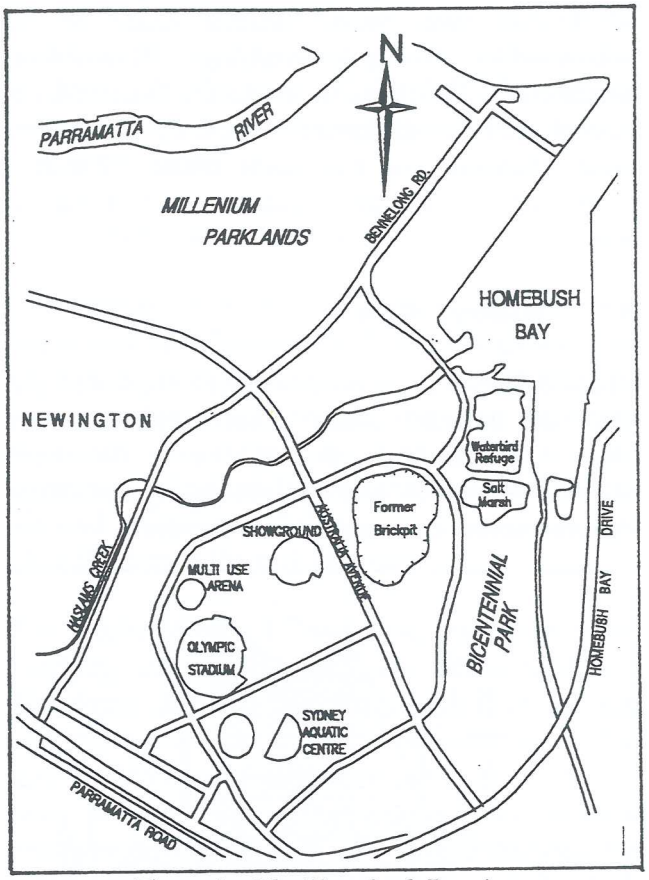

Figure 1. - The Homebush Bay Area

of the wetlands were gradually reclaimed, and the forests cleared. The low-lying areas of Newington and along the fringes of Homebush Bay have been extensively modified by filling operations[1]. The area comprised a number of industrial and commercial enterprises, such as a brickworks, a racecourse, an armaments depot, and an abattoir. From the 1960's, parts of Homebush Bay were used for the uncontrolled dumping of industrial wastes[2]. Extensive development began in the 1980's when recreational facilities, such as Bicentennial Park, were opened. Sydney's

successful bid for hosting the 2000 Olympic Games resulted in the next surge of development for Homebush Bay.

3 GEOLOGY OF THE HOMEBUSH BAY AREA

The following section details the geology of the area, with examples of geotechnical work undertaken as part of the Olympic development.

The prevailing geology of the area comprises rocks of Triassic age, with Ashfield Shale of the Wianamatta Group overlying Hawkesbury Sandstone[3]. Overlying the rocks are Quaternary to Recent alluvial sediments deposited within the creek channels, and man-made filling. Figure 2 shows the different geological areas of Homebush Bay.

3.1 Ashfield Shale

The Ashfield Shale is predominantly black and grey shale and laminite, which is heavily jointed. The shale is present in the upland areas of the nearby suburb, Newington, and underlies filling and alluvial deposits across the remainder of the site[2].

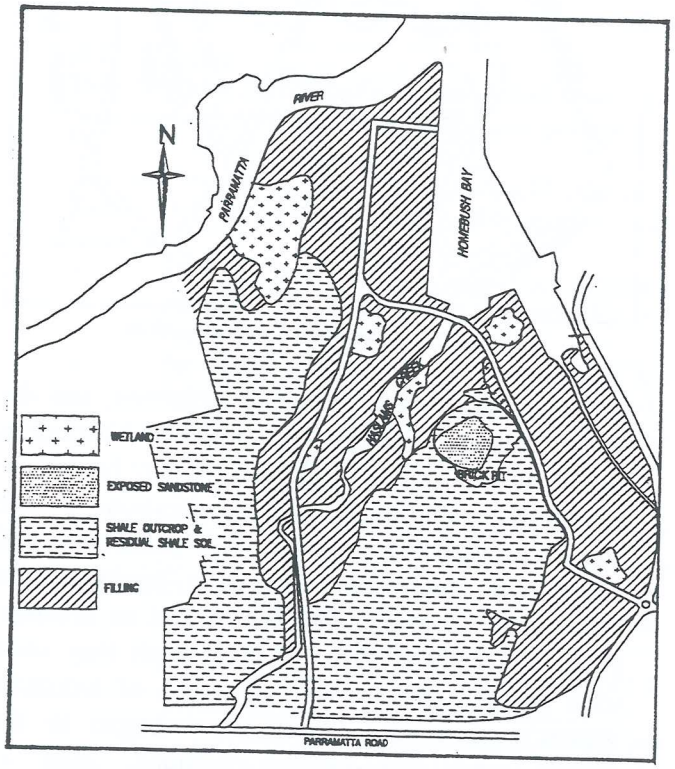

Figure 2. - The Geology of Homebush Bay

Some excellent exposures of the shale are evident in a previous quarry, known as the 'Brickpit', which was, at one stage, proposed for use as a water treatment facility for the Olympic site and surrounds, but now may be used for recreational purposes. Geotechnical projects undertaken at the 'Brickpit' site have included the assessment of stability of the existing excavation walls, to determine the suitability of the area for public access.

3.2 Residual Soils

The residual soils are red brown clays and silty clays which grade into stiff grey and red brown clays. The layer of residual clays is typically 3m to 4 m thick, although the soils range from a variable thin cover on the uplands to a thick laterised profile which has been locally preserved. Excavation has been so extensive that the residual soils are now limited to the upland areas of Newington, although some have been preserved below the alluvial sediments in Haslam's Creek and the wetlands[4]. As the extent of the residual soils is quite limited, most of the geotechnical work in these materials comprised design of shallow footings and bulk earthworks for facilities such as the Olympic Village.

3.3 Alluvial Sediments

The alluvial sediments mainly comprise black to grey, silty and sandy clays, and occasional peat layers. The sediments are up to 11 m thick in places, but are typically 2 m to 4 m thick[4]. The estuarine or alluvial deposits are variable in thickness, but are consistent in lithology. Shell fragments are common and are concentrated in discrete layers, which confirm the sediments' marine origin. The Irrigation Ponds case study as detailed later in this paper, investigates the geotechnical properties of these alluvial sediments.

3.4 Filling

The filling of the Homebush Bay area shows a great variability, and comprises putrescible waste, vegetation, paper, rubber, timber, plastics, building rubble, metallic debris, bituminous waste, batteries, asbestos, and excavated spoil. Much of the filling was placed in low-lying areas and the relocation of

the filling was required as part of the redevelopment. The filling has now been stored in a number of mounds, designed to be landscaped as recreational features. Geotechnical investigation related to this development comprised assessment of the slope stability of the mounds.

4 CASE STUDY - IRRIGATION PONDS

As mentioned earlier, whilst the geology of the site for the 2000 Olympic Games comprises a variety of different sequences, some of the most interesting geotechnical work comprised investigation of the soft alluvial sediments, in particular. The remainder of the paper provides discussion of one particular case study - the Irrigation Ponds on Hill Road.

The redevelopment of the Homebush Bay site for the 2000 Olympic Games resulted in the removal of uncontrolled filling from low-lying areas of Newington, and replacement with imported clay filling material. The resultant refilled area was proposed for recreational use, comprising a number of water features that could be used as irrigation ponds and for flood control. A plan showing the area of the proposed ponds is included as Figure 3.

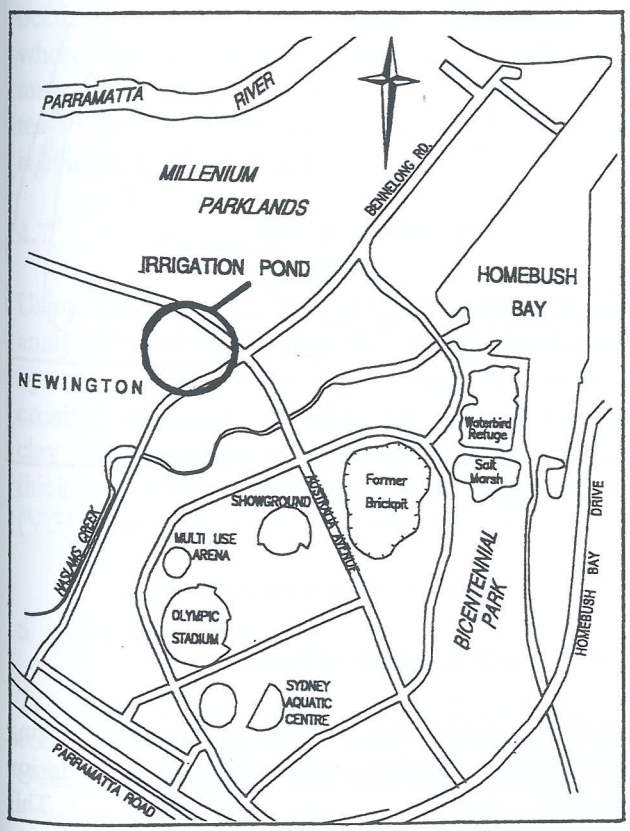

Figure 3. - The Irrigation Ponds

During the removal of the waste filling, it became evident that the proposed pond area was underlain by soft clay, and as a result, investigation was carried out by Douglas Partners Pty Ltd (DP) to assess the stability of the proposed ponds[4].

4.1 Site Description and Geology

The area of the proposed irrigation ponds is located between Hill Road and the Olympic Village, in a flat area which is part of the flood plain of Haslam's Creek. Reference to geological maps and previous investigations undertaken in the area indicated that the site's geology comprised man-made filling, overlying alluvial clay ranging in strength from soft to hard. In the area of the failed ponds, the uncontrolled filling had been replaced by 4 m to 5 m of clay filling.

4.2 Field Investigation

The initial investigation was undertaken in September and October 1997, and comprised cone penetration tests to determine the soil profile and characteristics. A series of test pits were also excavated, and these were used to assist in the estimation of strength parameters. The test pits allowed sampling of the subsurface soils and identification of the soft silty clay.

The results of the CPT indicated man-made filling overlying soft silty clay and very stiff to hard clay. The depth of filling and the thickness of the soft silty clay varied across the investigation area. The layer of filling was found to be generally 4 m to 5 m thick, however, was as thin as 1 m to 2 m in some locations. The layer of soft clay underlying the filling was found to be about 0.8 m to 2 m thick[4]. The soil profile can be seen in Figure 4.

The CPT results had indicated total cone resistance, q_c, of between 200 kPa and 500 kPa. and sleeve frictions of less than 10 kPa. Pore pressures were not measured during the testing.

4.3 Stability Analyses

Stability analyses were undertaken in December 1997 to determine safe design slopes for the irrigation ponds. Analysis for circular slip failures, using a computer slope stability program, were

undertaken. The analyses assumed typical strength parameters for the soft clay layer, based on previous experience and the results of the CPT undertaken in the area of the Irrigation Ponds.

The previous CPT had indicated a cone resistance, q_u, of 200-500 kPa in the layer of soft clay. Lunne et al.[5] (1997) provide a method of calculating the undrained shear strength of fine grained soils using the total cone resistance, the total in situ vertical stress, σ_{vo}, and an empirical cone factor, N_k, using equation (1).

$$s_u = \frac{(q_c - \sigma_{vo})}{N_k} \qquad (1)$$

The total cone resistance is provided by the CPT, and the total in situ vertical stress is determined from the pressure applied by the overburden clay filling. Lunne and Kleven (1981)[6] showed that for normally consolidated marine clays, the cone factor varied between 11 and 19, with an average of 15.

Using this method, the undrained shear strength of the soft clays can be calculated as ranging between 12 kPa and 29 kPa.

Thus, in the stability analyses of December 1997, a strength of S_u=10 kPa was assumed, based on the results of site specific field data. The results of the analyses indicated that the factor of safety of the ponds would be satisfactory if the slopes were maintained at no steeper than 1:2 (V:H)[7] . The graphical output of the stability analyses are shown in Figure 4.

4.4 Failure of the Irrigation Ponds

Whilst the initial design slopes for the ponds were specified to be 1:2 (V:H), excavation conditions during construction allowed slopes of 1:1.3 (V:H). In January 1998, during construction, an entire section of the edge of one of the ponds slumped, resulting in post failure slopes of 1:6 (V:H). It was found that the layer of soft clay had failed, causing the overlying clay filling to move along the soft clay layer. Large transverse cracks were visible at the head of the slide.

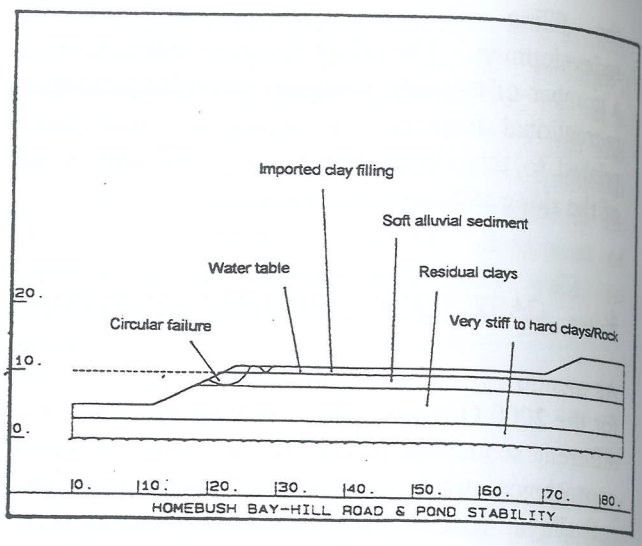

Figure 4. - Stability Analysis of the Pond Slopes

A plan of the pond, showing the cracks is included in Figure 5.

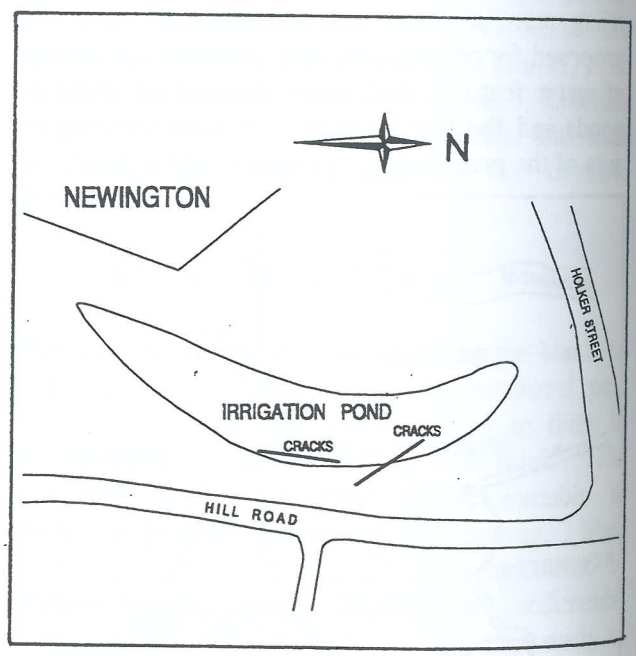

Figure 5. - Plan of the Failed Pond

4.5 Back Analysis of Failure

Following subsequent failures of the ponds during construction, further investigation of the design strength parameters was undertaken. This comprised back analysis of the observed failures to

assist in determination of shear strength. Revised stability analyses were then performed and these allowed stabilisation measures to be designed and ultimately implemented.

Using the pre-failure geometry of the slope, and trialling various combinations of strength parameters, stability analyses were undertaken to achieve a factor of safety less than 1.0. This back analysis indicated that the strength of the soft clay was as low as c_u=5 kPa[8] , as opposed to the value of 10 kPa, which had been used in the stability analyses and was based on field CPT results.

4.6 Discussion of Differences in Undrained Shear Strength

There are obvious differences between the strength assumed for the purpose of stability analyses and the strength calculated from the back analysis of the failed pond. It is considered that the differences could be attributed to variations in conditions between the CPT locations and where the pond failure actually occurred.

The CPT were located near the Irrigation Ponds, but not directly at the locations where failures occurred. Thus, the resistance of the soft clay where failure occurred had not actually been measured. The importance of accurately locating tests when relying heavily on site-specific field data is evident in this case study.

4.7 Subsequent Design of Stabilisation

Using the amended strength parameters, stability analyses were undertaken on various stabilisation options. It was found that a supporting layer of crushed sandstone, covering the face of the soft clay layer, resulted in improved stability. A 3 m thick layer of sandstone with a slope angle of 1:3.5 (V:H) resulted in a factor of safety of 1.4[9] .

5 CONCLUSIONS

The geological environment in the Homebush area consists of Ashfield Shale, residual clays, Quaternary alluvium, and man-made filling. The development of the area for the Sydney 2000 Olympic Games therefore required construction to be undertaken in a challenging geotechnical environment. The Irrigation Ponds case study investigated the geotechnical properties of the alluvial sediments. Geotechnical investigations in the area of the proposed ponds comprised cone penetration testing, excavation of test pits, and stability analyses. Following the failure of part of the Irrigation Ponds, back analysis revealed that the undrained strength of the soft clays was as low as 5 kPa, which was much lower than anticipated. Furthermore, it was about half of that back calculated from previous failures in the vicinity. The variations in ground conditions between test locations and the position of the ponds. It pointed to a clear need to carry out site specific investigations rather than rely on global strength parameters determined elsewhere in the region.

---

[1] CH2MHill (1995), " Site Assessment Report, Homebush Bay/Newington, Stage 2 Contamination Study", (unpublished)

[2] INTERNET SEARCH (1999), "Building for the Games - Planning for the Future", www.magna.com.au/~knight/fsgen.htm.

[3] DEPARTMENT OF MINERAL RESOURCES (1983), "1:100 000 Geological Series Sheet 9130 - Sydney"

[4] DOUGLAS PARTNERS PTY LTD (1997) "Stability Assessment, Hill Road, Homebush Bay, Project 24341B", (unpublished).

[5] LUNNE, T., ROBERTSON, P.K., AND POWELL, J.J.M. (1997) "Cone Penetration Testing in Geotechnical Practice", Blackie Academic & Professional

[6] LUNNE, T. AND KLEVEN, A. (1981) "Role of CPT in North Sea foundation engineering". Session at the ASCE National Convention: Cone Penetration Testing and Materials, St. Louis, 76-107, American Society of Engineers, (ASCE)

[7] DOUGLAS PARTNERS PTY LTD (1997), "Pond Stability, Hill Road, Homebush Bay, 24341B", (facsimile - unpublished).

[8] DOUGLAS PARTNERS PTY LTD (1998), "Stability of Haslam's Creek Widening, 24341B", (facsimile - unpublished)

[9] DOUGLAS PARTNERS PTY LTD (1998), "Stability, 24341B", (facsimile - unpublished)

A New Model for the Behaviour of Granular Filters

Mark Locke and Buddhima Indraratna
PhD Student and Associate Professor, University of Wollongong, NSW.

Summary Filters are used in Geotechnical Engineering to control seepage and to prevent erosion of soil due to the drag forces of seeping water. Filters act as barriers to retain the base soil while allowing seepage flows to exit without causing high hydraulic gradients or pore pressures which may damage the structure. This paper describes a new analytical model of filtration. The model is based on a three dimensional lattice model of the filter pores, and the equations of conservation of mass and momentum which govern the rate of particle transport. The model has application in the design of granular filters for non-cohesive base soils in embankment dams, retaining walls, drainage wells or road pavements.

1. INTRODUCTION

Filters are used, in geotechnical engineering, where it is necessary to protect soils from erosion due to seepage and groundwater. As water flows through a soil, fine soil particles can be washed out, leading to internal erosion (or piping) and eventual failure. A correctly designed filter will retain the loose soil particles while allowing seepage water to flow; thus preventing piping and avoiding a build up of high internal pore pressures. Filters are used in embankment dams, road pavements, behind retaining walls, coastal protection, in landfills and wastewater treatment, sand beds in oil wells and chemical engineering filtration. This study deals predominantly with the problem of filters for embankment dams.

Filters are used where water seeping out of fine grained soils may cause erosion of the soil, by removing particles under hydraulic forces. To function correctly, filters must be:

1. Fine enough that the pore spaces between the filter particles are able to capture some of the larger particles of the protected materials in place (see Figure 1).
2. Coarse enough to allow seepage flow to pass through the filter, preventing build up of high pore pressures and hydraulic gradients.
3. Non cohesive, so that no cavities or cracks can form within the filter.

Figure 1 shows a stable base - filter interface. Seepage forces have washed some base soil particles into the filter. Initially, some fine base particles may be washed completely through the filter, but in a stable filter the larger base particles will be trapped by the void constrictions (connections between voids) of the filter material. These trapped particles will then form smaller voids, retaining smaller base particles and the entire interface becomes stable. This process is called "self filtration". Water flow will be reduced during this process but generally reaches a steady state as self filtration occurs. If a filter is too coarse, the base soil particles will be able to move through the pores of the filter material and self filtration will not occur. If a filter too fine, it may not have sufficient permeability to allow the seepage flows to leave the base soil and high pore pressures can develop. Also, manufacturing a fine filter is often considerably more expensive than a coarse filter; hence the economic benefits of correct filter design are significant.

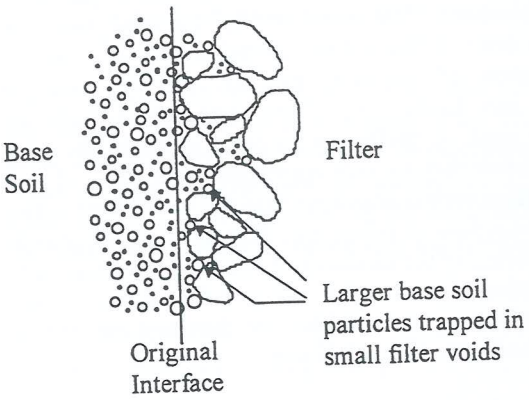

Figure 1 Stable Base-Filter Interface During Seepage.

There is an increasing push to replace granular filters with geotextiles which perform the same function. The advantages of geotextiles are numerous, often they are cheaper to install than granular filters and they are manufactured and placed under strict specifications, so the uncertainties involved with using natural materials are removed. However, there is still a concern that the long term performance of geotextiles (remembering a dam usually has a design life in excess of 50 years) may be unsatisfactory. A particular concern is that a geotextile may tear due to differential settlement within the structure, or earthquake motion. Because of these concerns, granular filters are more commonly used in important structures such as embankment dams. This study will focus solely on the performance of granular materials as filters.

2. EXISTING DESIGN METHODS

Terzaghi (1) was the first to develop filter design requirements. He envisaged two requirements which must be fulfilled:

- The filter should be many times more pervious than the base soil, to allow the free seepage of water, without causing excessive head loss (the permeability requirement). To ensure this he recommended:

$$D_{15F}/d_{15B} \geq 4 \quad (1)$$

- The filter should be fine enough to prevent the washing through of the base soils and arrest piping (the stability requirement). To ensure this he recommended:

$$D_{15F}/d_{85B} \leq 4\text{-}5 \quad (2)$$

Where D_{15F} is the diameter of filter particles where 15% by pass of particles are smaller, and d_{85B} is the diameter of base particles with 85% of the particles, by mass, smaller. These requirements describe, basically, the conflicting requirements on grain size, of a suitable filter. Some engineers still use these criteria for designing granular filters.

Subsequent research into filter behaviour has been predominantly empirical; a series of experiments on sets of base soil - filter combinations, has lead the researcher to recommend an empirical relationship for a stable combination. Research has lead to empirical design criteria which provide simple to apply relations for stable base soil - filter combinations. The most widely accepted empirical criteria are those of Sherard and Dunnigan (2). A review of the application of empirical methods can be found in Indraratna and Locke (3). These empirical criteria are extensively used, in preference to other methods, for filter design. However they are only applicable to the range of soils tested, and have certain laboratory bias due to different testing methods, definitions of failure etc. They also do not provide an understanding of the mechanisms involved with base soil - filter interaction. Hence they do not give the designer a clear picture of what may occur within the dam and the level of safety involved with design decisions.

Many researchers are now concentrating on numerical analysis of filtration, particularly modelling particle movement through filters. These approaches recognize that soil masses are made up of a random distribution of many sized particles. The most important part of base soil movement through a filter is the geometric requirement, that a base soil particle must be smaller than the pore void (and void constriction joining pores) through which it is passing. Additionally, some researchers have considered the hydraulic conditions (seepage forces) necessary to carry soil particles through the filter. The basis of the numerical analysis is:

1. to represent the filter by some form of a pore model, usually based on the particle size distribution of the filter material;
2. to simulate the movement of base soil particles by an analysis of the movement of individual base soil particles through the pores of the filter, caused by seepage forces, up to a point where the particle passage is blocked by a pore constriction, or the seepage forces are insufficient to move the particle further.

There are two general approaches to modelling particle movement, either: geometric - probabilistic, where the expected depth of infiltration of a particle, into the filter, is determined by probabilistic analysis of particle and void sizes; or mass transport equations using flow laws and conservation of mass and momentum to examine the rate of particle movement.

Analytic methods provide detailed models of what may be occurring at a base soil - filter interface. They give an idea of the thickness of filter required and also can estimate a probability of failure. The assumptions used in developing the model are very important. Often the assumption of spherical particles or a certain particle size distribution curve shape etc. cannot be applied to a real soil. The models are often difficult to apply to real design situations because of their reliance on a number of empirical parameters or impractical mathematical models.

3. NEW ANALYTICAL FILTER MODEL

Existing numerical models of filtration have some limitations. They generally adopt simplified void models, and very few consider the time rate of formation of a stable filter interface. Indraratna and Vafai (4) have developed a particle migration model, considering conservation of mass and momentum to model particle movement. This model is capable of showing the variation with time of particle size distribution, permeability and porosity of elements of the base soil and filter. Some criticism has been directed at the simplified void model adopted in this analysis. Hence there is some room for improvement and adaptation of Indraratna and Vafai's method. A new model for filtration is described below, based on the model of Indraratna and Vafai (4), and a modified three dimensional pore void model, based on the work of Schuler (1996). The entire model includes:

Filter void model - based on a cubic lattice network described by Schuler (5). Void sizes are determined by an adaptation of the method described by Silveira (6).
Particle infiltration depth - Schuler (5) developed an equation, based on Monte Carlo simulation, for infiltration depth, dependent on particle size.
Particle transport equations - the equations of conservation of mass and momentum, developed by Indraratna and Vafai (4), are used to determine the rate of particle transport.

3.1 Filter Void Model

There are many models of filter voids which have been adopted in modelling filtration. The commonly used models include; parallel channels of varying diameter (Indraratna and Vafai (4)), layers of filter voids perpendicular to the direction of flow (Silveira (6)), or pore networks (Schuler (5)). A granular soil is a three dimensional collection of particles which form voids of different size and shape, with constrictions between the voids, also of different size, shape and orientation. It is not feasible to model this completely random arrangement of voids and constrictions. However, the pore network models appear to provide a reasonable model of the soil structure. Schuler (5) suggests that after examination of the pore voids of a real soil, there are on average 5.7 constrictions from every pore. Based on this, Schuler (5) developed a regular cubic lattice model of pores and constrictions, shown in Figure 2.

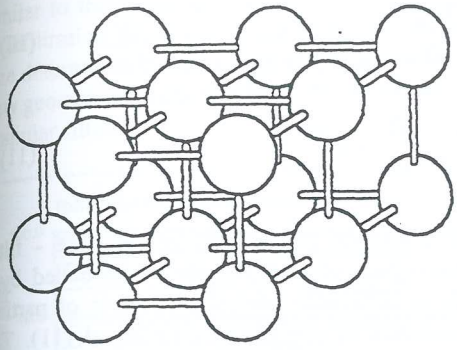

Figure 2 Cubic lattice void model (Schuler (5))

It remains then, to determine the size of the voids and void constrictions in the void model. The void constrictions, represented as bonds between the voids in Figure 2, form the smallest link between voids, capturing moving particles. Hence the important factor for modelling filtration is the void constriction size distribution, hereafter called the CSD. Schuler (5) has examined the CSD of a soil at varying relative density and found that the CSD curves all have the same shape. Hence, if we find the CSD for most dense and least dense states, then the actual CSD will have the same shape and lie somewhere in between. A reasonable assumption is that there is a linear change in CSD size from the most dense to least dense states.

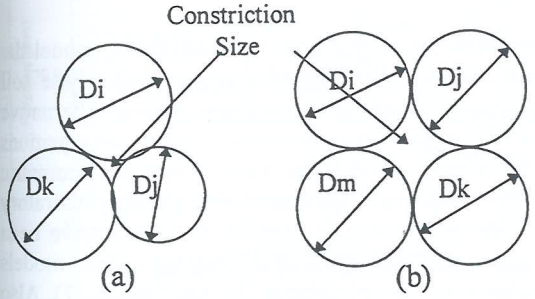

Figure 3 Void Constriction Size for a) Most Dense and b) Least Dense states.

The two geometric conditions to be considered, are shown in Figure 3. Humes (7) presents a method to calculate the CSD for the most dense case (Figure 3a), based a method described by Silveira (6) using the filter PSD. The PSD by mass (as determined by sieve analysis) tends to over-estimate the influence of larger particles, which form a large proportion of the mass of the soil, but are few in number and unlikely to meet to form large voids. Humes (7) recommends using the PSD by surface area of grains, and has shown this to better represent the pore constriction sizes for well graded materials. Equation (3) can be used to convert the PSD by mass to a PSD by surface area, assuming all particles have the same specific gravity.

$$P_{i,SA} = \frac{P_{i,mass}/D_i}{\sum_{j=0}^{n} P_{j,mass}/D_j} \qquad (3)$$

The PSD is divided into a number of discrete particle diameter intervals (D_0, D_{10}, D_{20}, etc.), so that it then represents the cumulative frequencies (P_0, P_{10}, P_{20} etc.) of the medians of these intervals. Humes (7) presents an equation, (4), to find the void size, D_v, for the most dense particle packing, when the void is formed by three tangent spheres of diameter D_i, D_j and D_k, as shown in Figure 3a.

$$\left(\frac{2}{D_i}\right)^2+\left(\frac{2}{D_j}\right)^2+\left(\frac{2}{D_k}\right)^2+\left(\frac{2}{D_v}\right)^2 = 0.5\left[\left(\frac{2}{D_i}\right)+\left(\frac{2}{D_j}\right)+\left(\frac{2}{D_k}\right)+\left(\frac{2}{D_v}\right)\right]^2 \qquad (4)$$

The probability of occurrence, P_v, of void size D_v, is a function of the probability of occurrence of the three particles, taken from the discretised PSD. P_v is calculated using (5), where r_i, r_j and r_k represent the number of times particle diameters D_i, D_j, and D_k appear in the combination of three particles being considered. Hence r_i, r_j and $r_k = 1,2$ or 3 and $r_i + r_j + r_k = 3$.

$$P_v = \frac{3!}{r_i!\,r_j!\,r_k!}(P_i)^{ri}.(P_j)^{rj}.(P_k)^{rk} \qquad (5)$$

Silveira et al. (8) present equations for the least dense packing of a granular material; where the void constrictions are formed by four tangent grains as shown in Figure 3b. Silveira (8) note that the geometry of the problem is very difficult to solve directly and hence assumes the void is equivalent to a circle with the same area as that formed by four tangent particles as shown in Figure 4b and c. Silveira's equations for the diameter of the equivalent circle are not presented here.

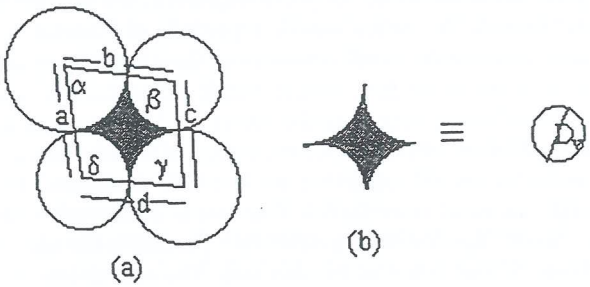

Figure 4a) Pore constriction formed by 4 particles
b) Constriction Area formed by tangent particles
c) Circle of equivalent area

Pore constrictions usually do not form on a plane through the centres of the three or four particles making up the constriction. Hence it is suggested that the mean of all possible chords through the circlular particle be used to represent the size of particles, rather than the diameter. Thus the particle diameter to be considered for determining constriction size, D_{model}, is given by (6).

$$D_{model} = 0.82\, D_{actual} \qquad (6)$$

The CSD of a granular material, at different relative densities, will have the same shape. Also the assumption was made, that

the difference between two constriction size distributions will be directly proportional to the difference in relative density. Hence, using relative density, defined in (7), then the actual CSD can be calculated from (8). We then have a pore void model, consisting of a 3D cubic lattice of pores with six constrictions connecting each pore to its neighbours, as shown in Figure 2. The size of each constriction is randomly generated from the CSD.

$$RD = \frac{e_{max} - e}{e_{max} - e_{min}} \tag{7}$$

Actual Void Diameter = Most Dense Diameter +
RD x (Most Dense Diameter - Least Dense Diameter) (8)

3.2 Particle Infiltration Depth

Previous laboratory and analytical research has shown that a filter has a controlling constriction size, d_c* (Kenney et al., 9). Where base particles finer than d_c* can pass through a filter of large thickness. As base particles larger than d_c* are considered, their depth of infiltration into the filter decreases rapidly as the particle diameter increases. Schuler (5) executed a detailed Monte Carlo simulation of the cubic lattice pore model, shown in Figure 2. It was shown that, as predicted by percolation theory, a percolation threshold, p_c, exists for this model. The percolation threshold represents a probability of meeting a constriction larger than the particle, so the particle can move through that constriction. Above the percolation threshold, a particle can move an infinite distance through the lattice. Below the threshold the infiltration depth reduces very quickly. The percolation threshold was found to be, approximately, the size of the 63% largest pore constriction. Based on the results of the analysis, Schuler (5) determined an equation, (9), for the depth of infiltration, up to the percolation threshold. In (9), E represents the number of levels, through the lattice model, a particle will travel. The physical distance of travel depends on the distance between pores or levels in the filter model, this is called the unit step. Since constrictions form near the centre of a particle and the next constriction will form near the centre of the next particle, the constrictions are separated by two half diameters. This suggests the mean filter particle diameter is a reasonable unit step. Finally, the distance travelled by a particle is the number of levels, E, multiplied by the unit step. The probability, p, is the probability density of constrictions larger than the particle.

$$E(p) = 123(36.3 - p)^{-0.88}; p < 36.3\% \tag{9}$$

3.3 Particle Migration Model

Indraratna and Vafai (4) have developed a particle transport approach to model particle movement. They also consider the hydraulic forces required to mobilise the particles. If seepage forces exceed the critical hydraulic gradient and the particle is smaller than the pore constriction, it will move. Moving particles are controlled by governing differential equations of conservation of mass (10) and momentum (11).

$$\frac{d(\rho_m u)}{dz} = \frac{d\rho_m}{dt} \tag{10}$$

$$\sum F = \rho_m V_m \left(\frac{du}{dt} + u \frac{du}{dz} \right) \tag{11}$$

By considering a number of elements at the base - filter interface, the movement of particles can be modelled by a forward step, finite difference analysis. The rate of particle erosion and movement is governed by (10) and (11). The geometric constraint to movement is modelled by the depth of infiltration into the cubic lattice (9). If the predicted infiltration of a particle size is equal the length of an element then particles smaller than that diameter can pass through; larger particles will be captured. The base and filter particle size distributions can be recalculated at each time step and the procedure repeated. This analysis predicts the gradual change in particle size distribution of the base and filter elements and hence describes what is occurring at the base - filter interface with time for the entire particle size range. Indraratna and Vafai (4) describe a method to determine permeability of a non-cohesive soil based on the particle size distribution, thus the time dependent changes in filter permeability can also be modelled.

3.4 Application of the Model

The model presented in this paper is intended to model the time rate of particle migration of a non-cohesive base soil through a granular filter. No laboratory data or alternative models are available to verify the particle migration equations proposed by Indraratna and Vafai (4). However, the geometric model of filter voids can be compared with existing laboratory data and model predictions. A number of models have been proposed for particle infiltration depths. The models considered here are that of Schuler (5), and Humes (7). Also the equations for controlling constriction size developed by Kenney et al. (9) and Witt (10), from experimental and theoretical modelling, describe the particle range at which a large infiltration depth will occur. The pore channel model adopted by Indraratna and Vafai (4) gives a minimum pore diameter, where smaller particles will pass through the filter. These five models are compared with the newly developed model for two cases. These are a uniform sand, with C_u=2, as shown in Figure 5, and a well graded sand, with C_u=6, as shown in Figure 6.

The models of Schuler (5) and Humes (7) both predict particle infiltration as a function of particle diameter, and these models are plotted in Figure 5 and Figure 6. Kenney et al (9), Witt (10) and Indraratna and Vafai (4) predict a single value for the approximate boundary between the retained and free particle diameters. These models are shown as a single vertical line in Figure 5 and Figure 6. As can be seen, in both examples the model of Schuler (5) predicts a percolation diameter very close to that of Kenney et al. (9) and Witt (10). The model of Humes (7) predicts a lower infiltration depth. The pore channel model of Indraratna and Vafai (4) is reasonable for uniform filters but overestimates pore channel diameters for broadly graded materials. The new model,

similar to the model of Schuler (5), predicts a rapid increase in infiltration depth very close to the controlling constriction size determined by Kenney et al. (9) and Witt (10). Hence the new geometric model is suitable for modelling infiltration into granular filters.

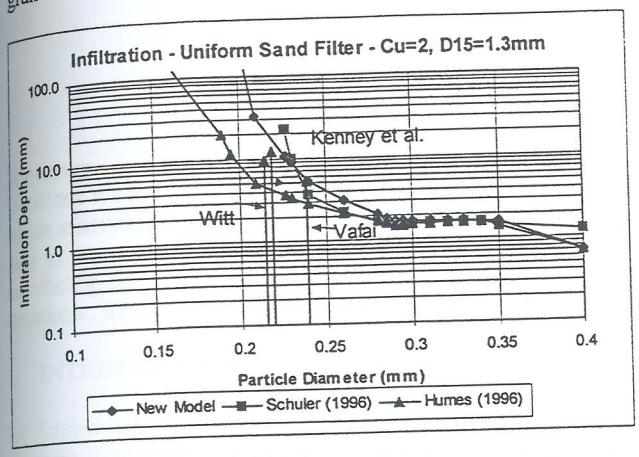

Figure 5 - Comparison of Predicted Infiltration Depth of Base Particles into a Granular Filter - Uniform Sand

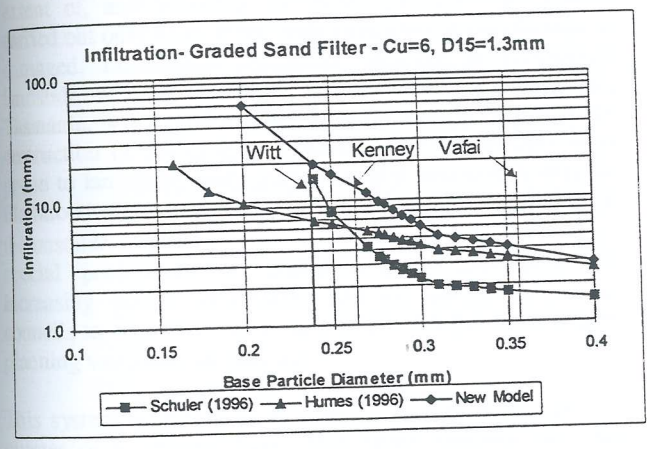

Figure 6 Comparison of Predicted Infiltration Depth of Base Particles into a Granular Filter - Well Graded Sand

4. CONCLUSIONS

Granular filters are an essential element of earthfill dams, providing protection from erosion and piping to the dam core. The role of a filter is to retain any eroded particles, while allowing seepage water to drain from the base material. This requires careful selection of filter particle size; the pores of the filter must be small enough that the larger base soil particles are captured within the pore constrictions. A new analytic model has been presented which describes the time rate of infiltration of base soil into a filter. The filter pores are modelled by a three dimensional lattice of pores, connected by constrictions. The size of these constrictions is randomly generated from the constriction size distribution; which is determined from the filter particle size distribution and relative density. The rate of movement of particles is modelled by a finite difference approximation of the differential equations of conservation of mass and momentum. The model has been shown to predict infiltration depths of base soil particles; similar to those determined, by other researchers, from both experimental and theoretical work. The analytical model presented here has several advantages over others in the literature including:

- A three dimensional pore model, more representative of real soil conditions than simple pore channel or layered void models.
- Modelling of the rate of particle movement. Hence predicting the time to reach steady state or large scale piping of the base soil.
- Modelling of time dependent changes in the base soil and filter. As particles are eroded or captured they alter the particle size distribution of the soil or filter. By re-calculating the constriction size distribution and permeability of each element in the model at each time step, time dependent changes are considered.

5. REFERENCES

1. Terzaghi K. "Der Grundbruch an Stauwerken und Seine Verhuntung" Forcheimer Nummer Der Wasserkraft, 17, 1922, pp. 445-449.
2. Sherard J. and Dunnigan L. "Filters and Leakage Control in Embankment Dams" Proc. Symposium on Seepage and Leakage from Dams and Impoundments, R.L. Volpe and W.E. Kelly (eds.), ASCE 1985, pp 1-30.
3. Indraratna B. and Locke M. "Design methods for granular filters - critical review", Proc. Instn. Civ. Engrs Geotech. Engng, 1999, Vol. 137, pp. 137-147.
4. Indraratna B. and Vafai F. "Analytical Model for Particle Migration Within Base Soil - Filter System", Jour. Geotechnical and Geoenvironmental Engineering, ASCE, 1997, Vol 123, No. 2, pp. 100-109.
5. Schuler U. "Scattering of the Composition of Soil - An Aspect for the Stability of Granular Filters" Proc. GeoFilters '96, Montreal, Canada, 1996, pp. 21-34.
6. Silveira A. "An Analysis of the Problem of Washing through in Protective Filters", Proc. 6th Int. Conf. Soil Mechanics and Foundation Engineering, Canada, 1965, Vol. 2, pp. 551-555.
7. Humes C. "A New Approach to Compute the Void-Size Distribution Curves of Protective Filters", Proc. GeoFilters '96, Montreal, Canada, 1996, pp. 57-66.
8. Silveira A., Peixoto T., Nogueira J. "On Void Size Distribution of Granular Materials", Proc. 5th Pan-American Conf. Soil Mechanics and Geotech. Engng., 1975, pp. 161-176.
9. Kenney T., Chahal R., Chiu E., Ofoegbu G., Omange G., Ume C. "Controlling Constriction Sizes of Granular Filters", Canadian Geotechnical Journal, 1985, Vol. 22, pp. 32-43.
10. Witt K. "Reliability Study of Granular Filters", in *Filters in Geotechnical and Hydraulic Engineering*, Brauns, Heibaum & Schuler (eds.), Balkema, Rotterdam, 1993, pp.35-42.

LANDSLIDES: AN ALTERNATIVE METHOD OF LANDSLIP ZONATION IN THE TAMAR VALLEY, NORTHERN TASMANIA

Rochelle Macdonald
BSc., Hons (geol)
Thompson & Brett Consulting Engineers, Tasmania, Australia

Summary
Decisions made concerning the management and landuse of sloping areas subject to landsliding are dependent on a set of criteria which assessments can be based around. This paper offers a revised method of grading landslip risk by the integration of additional data to that used by Mineral Resources Tasmania. The method is assisted by the evaluation and development of geological, morphological and hydrological models using Geographic Information Systems (GIS). Two active landslides, Gaunts and Native landslides, were used to test the validity of the GIS method.

1. INTRODUCTION

Landslides are amongst the most common of natural disasters affecting regional landscape development. However, while slope failure is an ever present risk in many hilly suburban areas and on farming properties, studies of the extent of, and potential for future problems are usually carried out only when man-made structures are threatened, or damaged. Legislation restricting building in proclaimed landslide areas, including most of the Tamar Valley, Tasmania, was introduced in the early 1970's following the destruction of dwellings by landslides. Areas thought most prone to landslides were mapped and it was shown that the likelihood of damage can be reduced by: (1) not building on the unstable slopes, with slopes in excess of 10-11° requiring special precautions to minimise slope movement, (2) increasing public awareness; and (3) encouraging local councils to zone areas according to the risk factors, and then planning variations in land use.

This system is still in use, with no further refinements, a quarter of a century later. This paper suggests how the zoning system can be improved. Much of the work, upon which this paper relies, was carried out by the author in the Windermere area, northwest of Launceston, in the Tamar Valley. Landslip zonation in this area has attracted only minimal attention from other workers, although the area was used as a laboratory for method tests and assessment of risk factors [Ingles (1991), Telfer (1988), Leaman (1972/73)]. The area was not, then, reviewed as part of the broader Tamar Zonation studies using the zoning system. Although the Windermere area has a long history of slope failure it was not included in any detail by Telfer (1988) who constructed part of a series of Tamar Valley zone maps, which were recently updated by Forsythe (1997). Current maps only show the location of existing landslide zone boundaries, classified according to the perceived risk of failure associated with the area. The regional classification dervised by Minerals Resources Tasmania, outlined in Table 1, makes no allowance for hydrology and vegetation, both of which are shown here to have important implications for slope stability.

This paper offers a revised method of analysing field and laboratory data by integration of additional data, including vegetation and flow relationships, to grade individual risks of failure. Assessment of landslip risk assisted by the development and evaluation of geological, morphological and hydrological models using Geographic Information Systems (GIS) (Clarke, 1986). The GIS computer assisted system used was ARC/INFO version 7.0.4. Two active landslides, Gaunts and Native landslides, were used to test the validity of the GIS method.

2. BASIS OF CLASSIFICATION

2.1 Methods of Acquiring Data

A geological map was compiled, using rock outcrops, geophysical surveys and interpretation of core and auger holes. Geology, vegetation and areas of past movement were digitised into an ARC/INFO database.

2.2 Data Modelling

A slope map classified into several zones, and a flow accumulation map, were produced from 1: 5,000 topographical maps. Production of a digital elevation model (DEM) in ARC/GRID, which assigned a particular value to each cell within the grid, was used to develop the slope class map. The supplied contour interval for the area (Tasmanian Terrain Model) was 5 metres; an interval of 1 to 2 metres would have provided a more accurate representation of the slope.

The flow accumulation model was also derived from the DEM using ARC/GRID. Wet areas are of particular interest when studying landslides. Initially, however, attempts to produce a flow accumulation model were constrained by problems related to non-continuous drainage lines. These problems were resolved by incorporating a stream layer into a comprehensive flow accumulation model (Figure 1), which indicated the potential for a given cell to receive water.

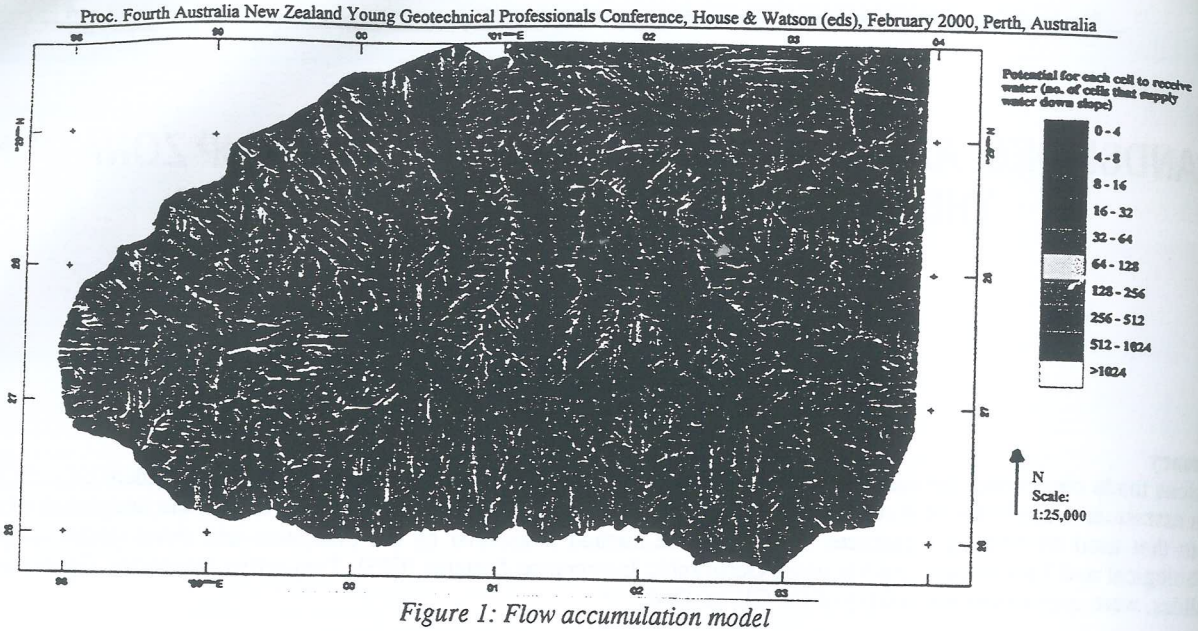

Figure 1: Flow accumulation model

2.3 Data Integration

A risk zonation map of Windermere was created by the addition of a series of attribute data[1]. Each layer was split into a series of classes, each of which was weighted according to its likely effect on slope stability, irrespective of any correlation between layers.

The geology layer was subdivided into five main classes according to the rock types present (Figure 2). Each rock unit was assigned a weighting of 1 to 10, depending on material strength or properties. Solid outcrops of Tertiary basalt and Jurassic dolerite were assumed to provide a firm foundation base and were assigned a weighting of '1'. Alluvium, mainly confined to the shorelines and thin cover on low angle slopes, and being devoid of expansive clays, was given a comparatively low weighting of 3. Thick basalt talus was given a moderate value '5', although such basalt talus benches are thought to have originated from previous landslide activity. In many cases, where the basalt talus has a matrix composed of Tertiary clay it has been assigned a weighting of '8'. Tertiary sediments were assigned the highest value '10', due to the low resistance to shear forces that the sediment exhibits. Shear box tests completed on the sediment suggest an internal friction angle of $\phi'=10$, supporting this statement.

The vegetation layer was subdivided into three classes (Figure 3), based on field observations. Dense forested areas have the most stable slopes and were assigned a weighting of '1', the lowest value in the table. Medium density forest was classed as '3' and bare ground '10', as providing no vegetal resistance to movement.

Active areas, dormant areas, and areas that have never moved (Figure 4) have also been assigned weightings. The highest value was assigned to the currently active landslide areas (10), because they are clearly unstable. Areas now dormant were assigned a slightly lower value (7) because, they have a high risk of failure. Movement reduces sediment strength, and these regions which are failing or have failed recently have a greater potential for failure than those which have not previously failed (e.g. Gaunts Landslide is the reactivation of an old landslide). Areas where movement has not occurred were given the lowest risk rating (1).

A number of the layers, namely geology, vegetation and areas of movement, were categorised using vector layers[2]. In contrast, the slope and flow accumulation layers were categorised using raster format[3]. Both of these formats require the operation of 'slicing' of data into classes to ensure each class or data range specified in a lookup table[4] is separated within each layer. The vector layers were converted to raster format to allow both forms of data to be combined.

Critical slope angles beyond which sediments are believed to be unstable, have been based conventionally, upon regional estimates of sediment strength. For example, Young (1972) suggested that sandy clays are only stable to angles of between 5 – 7°; Forsythe (1997), in his landslide zonation maps of Launceston, proposed a critical angle of 7° for deep soils and 10° for dolerite gravel. However useful such generalisations may be as regional estimates, they do not necessarily apply to individual localities. Sediment stability angles depend upon a wider variety of interacting local variables, including pore water pressure and composition of clay minerals, which are difficult to predict. Critical slope analysis in this study distinguishes areas with slope gradients 0-2°, 2-4°, 4-6°, 5-6°, 6-7°, 8-9°, 9-10°, 10-11°, 11-12° and > 12° (Figure 5).

Weightings assigned to the flow accumulation map were modelled on the perceived potential for the supply of water from cells up-slope to produce wetter areas down slope. The weightings thus differ from those of Heath (1997), who did not take account of areas of active, dormant[5] and non-landsliding conditions.

[1] attribute: a non-graphic characteristic of a map feature described by numbers or characters, usually stored in tabular format, and linked to the feature by a user assigned identifier (ESRI, 1990)

[2] vector layer – data consisting of lenses, points and polygons (Burrough, 1986)

[3] raster format – layers comprising grids or cells (Burrough, 1986)

[4] lookup table – method of linking different data sets together

[5] Dormant – active in the past, but has been stable for some time

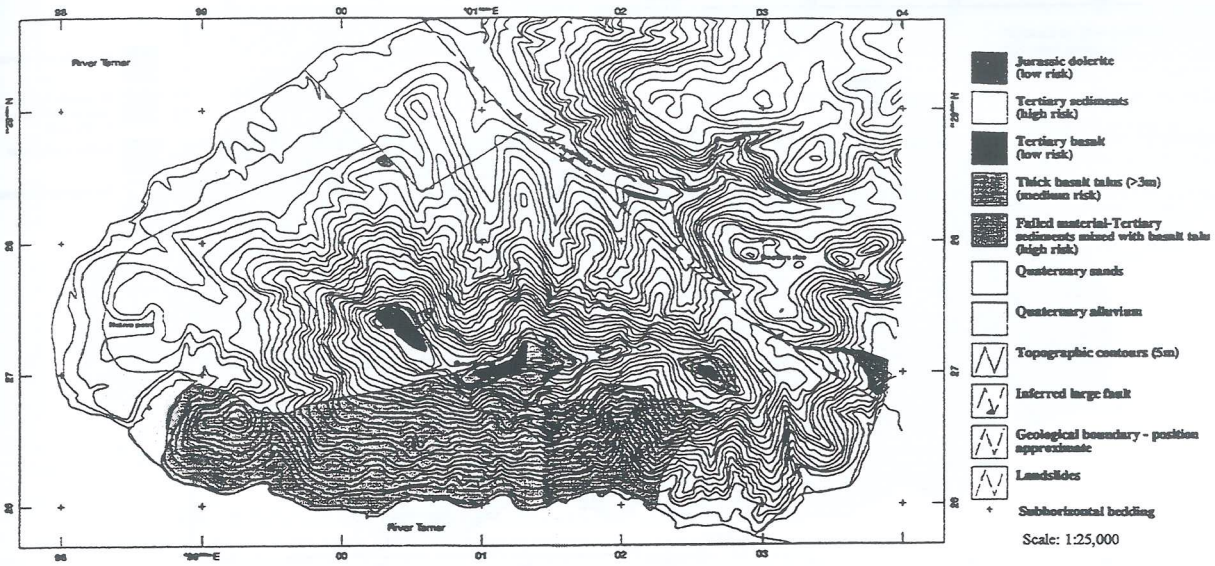

Figure 2: Geology map of the Windermere area

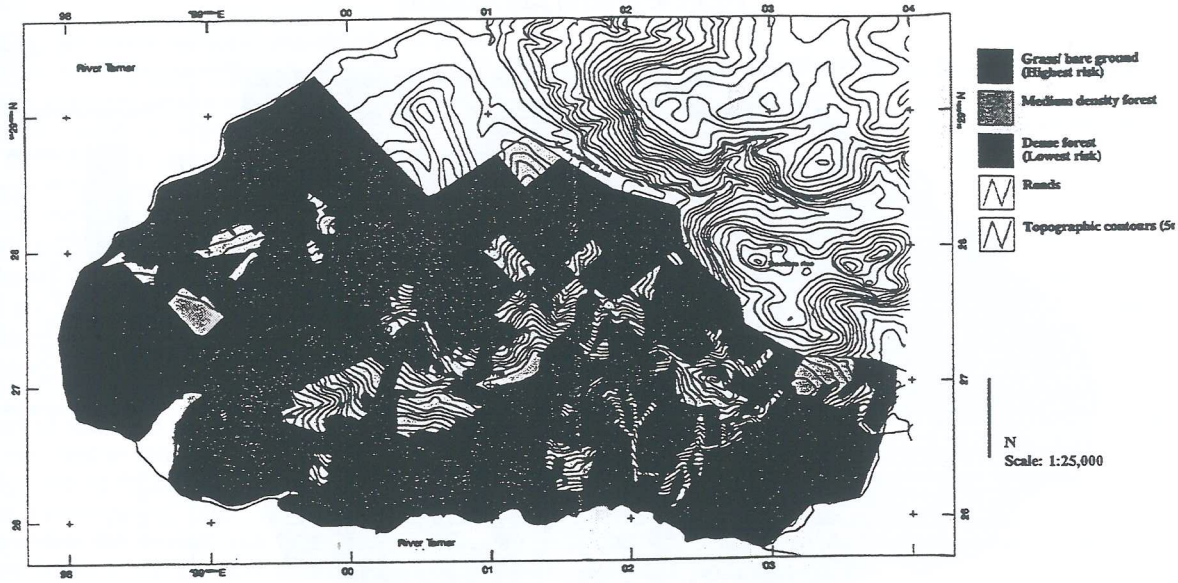

Figure 3: Vegetation map of the Windermere area

2.4 Classification Criteria

Within each class, each layer was assigned weightings relative to its potential to cause failure by assessing the influence of each on slope stability. For example, in order to predict the areas of greatest potential for movement, the relative weightings of four layers (Table 1), excluding the active movement layer, were combined as in Figure 6. This method identified those areas most likely to fail as a result of a reduction in sediment strength (residual values). Maps derived from these parameters, as listed in table 1, demonstrate the effect of the movement layer.

Figure 6: Risk zonation excluding the active movement layer

Slope was assigned the next highest weighting after movement, because the resistance to movement of slope materials is directly related to the slope gradient. Geology was ranked next, because of the varied resistance of slope materials to shear stress. Flow accumulation in the form of water-promoted land instability, particularly during periods of intense rainfall, ranked next. Vegetation was considered to be the least important parameter, because failure at the site is observed on both vegetated and unvegetated areas e.g. Native Landslide. Telfer (1988) awards a much more important role to vegetation than was used in this model. However, the discovery that previous failure occurred at depths mainly below root penetration is evidence in support of a low weighting.

Table 1: Weightings assigned to individual parameters

Layers used	Parameters used in Figure 6	Parameters used in Figure 7
Movement		0.5
Slope	0.2	0.2
Geology	0.15	0.15
Flow accumulation	0.1	0.1
Vegetation	0.05	0.05

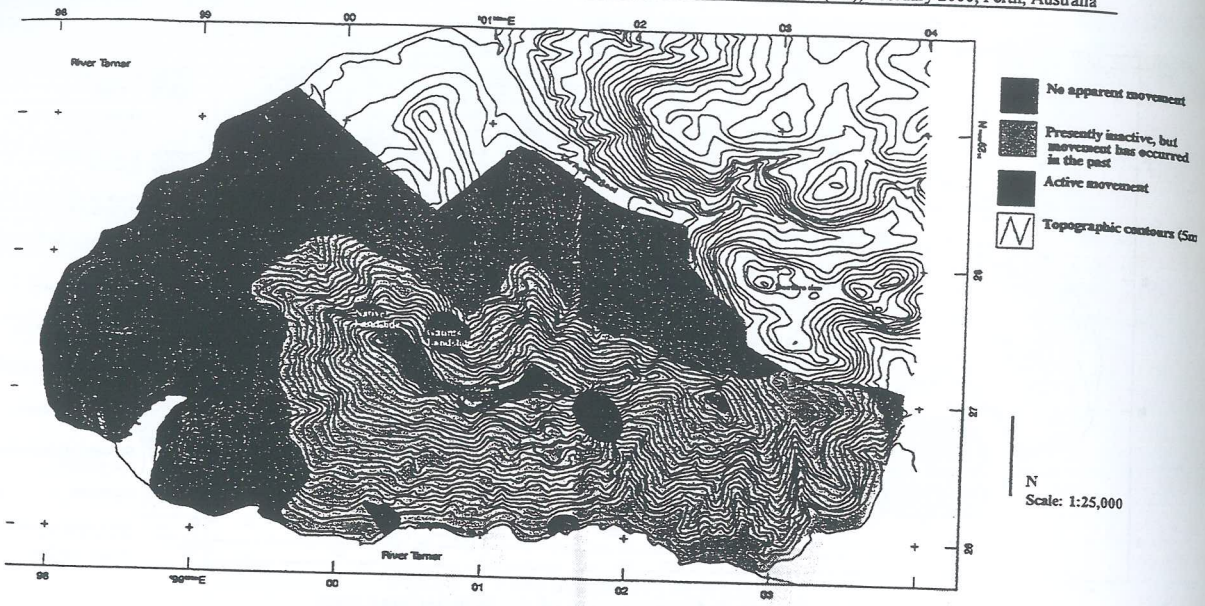

Figure 4: Areas of past movement

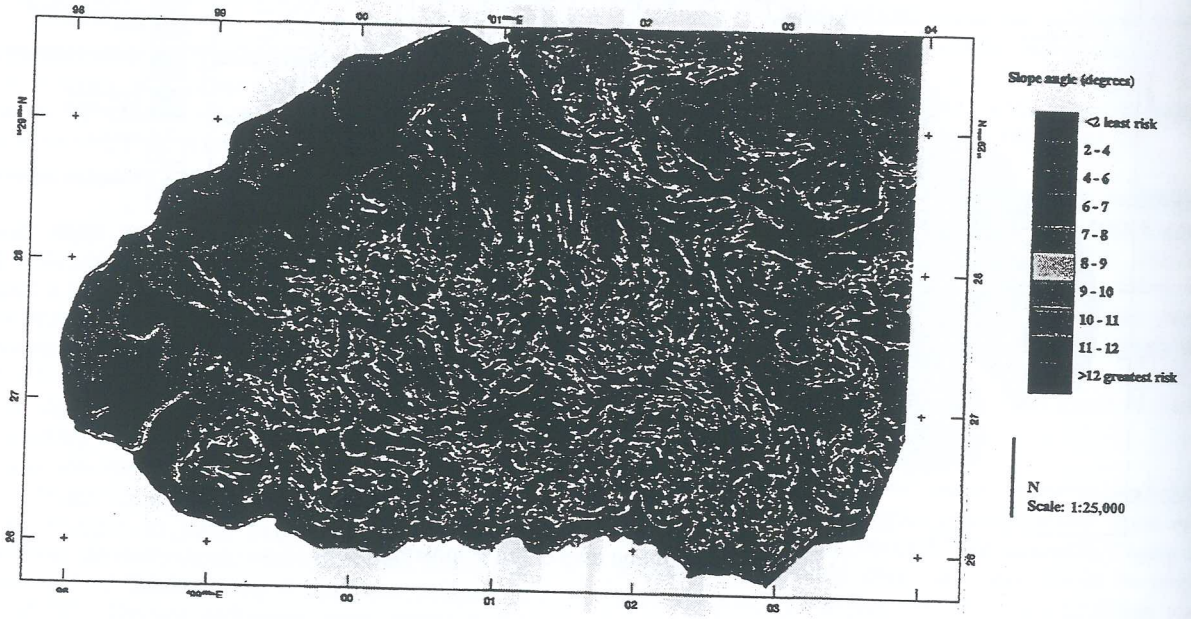

Figure 5: Slope class map

2.5 Data Overlay

All layers in the same format, geology, slope, vegetation, movement and flow accumulation were overlain and modelled in ARC/GRID using the relative weights assigned to each layer in Table 1. The resultant map, which illustrates the gradual change from high to low risk over the Windermere area, was then 'sliced' into five distinct categories, to show the relative potential of each risk factor for land instability (Figure 2). *It should be noted, however, that the information is of a general nature, and applies only at a regional scale, because site specific parameters were unavailable on a property basis and could not be employed.* Thus, when considering building construction, a detailed investigation is needed on a site by site basis by a qualified engineer or geologist to differentiate between stable areas and areas of potential risk.

3 MODEL RISK POTENTIAL FOR INSTABILITY

The Windermere area has potential for further instability. Stability problems are known throughout the Tamar Valley, generally associated with the Launceston Beds. Areas of movement appear dependent upon geology, slope, drainage and vegetation. The steep slopes around Gaunts Hill, in which two active landslides occur, have the greatest landslip risk in the Windermere area.

It is apparent from the flow accumulation model that two major, previously unrecognised drains of significant proportions run through Gaunts Landslide (Figure 6), whereas the adjacent stable areas do not exhibit similar concentrations of predicted flow. However, while surface topology influences flow accumulation, the derived flow accumulation model (Figure 1), is unlikely to have been influenced by the movement on Gaunts Landslide: a 1984

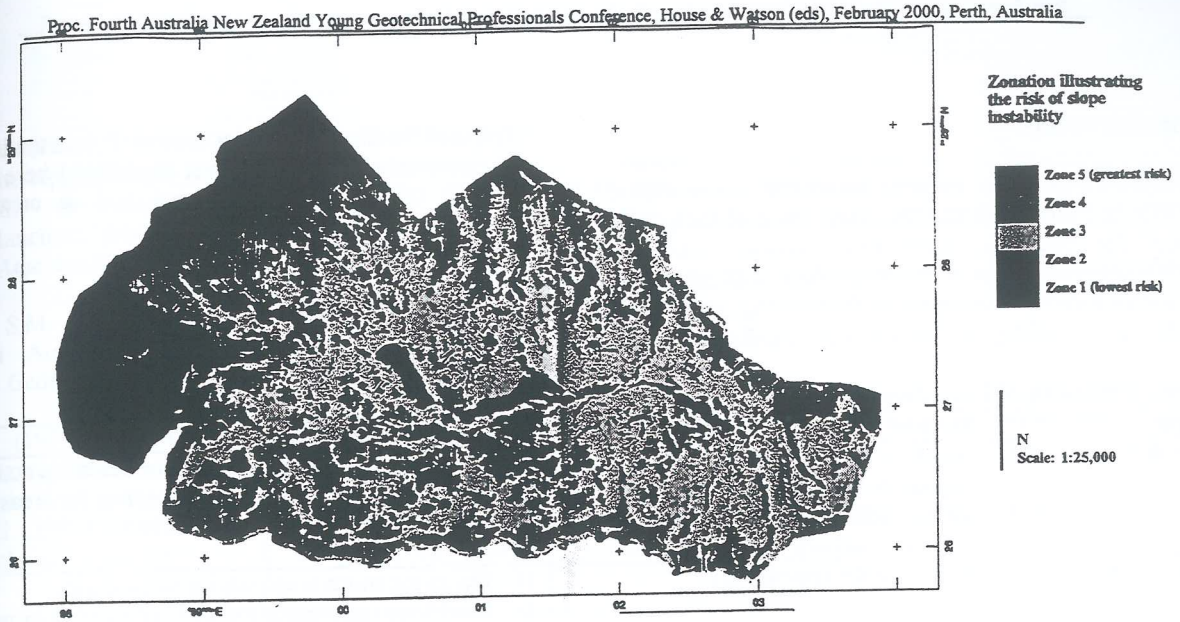

Figure 6: Landslip risk zonation map without the past movement layer

ortho-image, the source of data, was developed before the major part of the landslide occurred. Native Landslide also has a major drainage pattern associated with it, and failure has occurred despite a vegetated cover comprising trees. Indeed, all recorded areas of past instability in the Windermere area have large water channels running through them and it can be inferred that where these are normal to slope there is a higher potential for failure. In general, if an area is already failing the risk is extreme; it will continue to fail until the shear strength exceeds the shear stress. Risk should therefore also include movement history as well as the other outlined factors.

Areas marked black are unlikely to fail, the dark grey areas have the potential to fail and the light grey and white areas have a high risk of failure. This model is based partly upon theoretical assumptions, and while it provides useful information for the overall risk potential map, it needs refinement before it can be used with complete confidence by the construction industry.

4.0 PROBLEMS ASSOCIATED WITH THE CURRENT ZONATION METHOD

Telfer (1988) classifies the southern slope riverfront area as zone III in his risk zonation map. Because of past slope movements which have affected the entire slope, it is more appropriately classed as zone IV. Moreover, it does not seem reasonable to classify the region along the foreshore, immediately east of where a house fell into the river is zone III. Two houses have been affected along the foreshore on the southern slope in the past decade. The derived risk model (figure 6) shows a high risk potential for this area and the official classification should be revised accordingly. Another reason for updating Telfer's (1988) map is that not all active areas are illustrated. The rate of occurrence of failure in recent years suggests, also that landslip zoning on the basis of slippage should be revised at no longer than 5-year intervals.

The geological and geophysical data derived from this investigation showed the basalt to be less extensive than first thought, so that only a small portion of the ridge top was ultimately classified with confidence as zone I.

5 FINAL CLASSIFICATION

Figure 7 is a final classification map for construction and subdivision of the Windermere area. The zonation used is based upon Minerals Resources Tasmania criteria, as outlined in Table 2.

Table 2: Zone classification for levels of land stability in the Windermere area

Zone 1:	Stable hard ground, e.g. Tertiary basalt, or Jurassic dolerite.
Zone 2:	Generally stable ground on soft rock all slopes < 7°
Zone 3:	Potential landslide areas on soft rock, with slope > 7°
Zone 4:	Old landslip and adjacent areas
Zone 5:	Recent/active landslip and adjacent areas

Based on the zonation used by Minerals Resources Tasmania.

6 LANDSLIDE CLASSIFICATIONS USED IN AUSTRALIA

A number of landslide risk classifications have been developed throughout Australia. Some of the most important models and associated problems, as illustrated in Table 3 are of general importance but, nevertheless, landslide mapping schemes should always be tailored for each location to ensure they are as accurate as possible.

Geographical information systems (GIS) have been used increasingly in recent years to create landslide zonation maps. GIS allows a series of data sets to be combined independently of possible human error so that model parameters can be adjusted and new variables interspersed (Heath, 1997).

7 CONCLUSIONS

Investigations of slope stability inevitably raises difficult questions and this paper has discussed some of the possible methods for obtaining satisfactory solutions. Causes of instability are not always obvious and factors affecting slope stability need careful examination. By locating areas that are at high risk of failing, precautions can usually be taken to prevent the likelihood of movement. It is essential, therefore, to undertake risk assessments, as outlined here on all areas where construction is proposed and in areas of future subdivision.

Table 3: Summary of Landslide Zonation Models Used in Australia

Author	Method	Problems associated with model
Joyce & Evans, 1976	**Stability rating:** focus on slope angle, vegetation, landuse, proximity to springs, jointing, bedding planes and previous land activity	1) Gives too much emphasis to prior landslide activity. 2) Slope classifications are inappropriate for areas where low strength materials exist
Ingles, 1976	**Problematic approach:**	1) Places too much emphasis on steep slopes. 2) Insufficient allowance for signs of existing or past instabilities. 3) Over emphasis on drainage.
Stevenson, 1977	**Relative risk**: Assigns scores for clay factor (p) and water factor (w), slope angle (s), slope complexity © and landuse (u). Denoted by the equation : Risk (r) = [(p+2w) x (s+c)] Slope failure is said to occur when r > 60.	1) Crude method; values of r> 50 should be treated as a warning sign of possible instabilities. 2) Plasticity Index is not necessarily a good guide to instability.
Walker et. al., 1985	**Specifically for residential development:** Risk of instability, active or ancient, and evidence for creep.	1) Designed for soil slopes overlying interbedded siltstones, shales, sandstones and coal in the Sydney Basin. 2) Not directly applicable to other areas or geological environments.

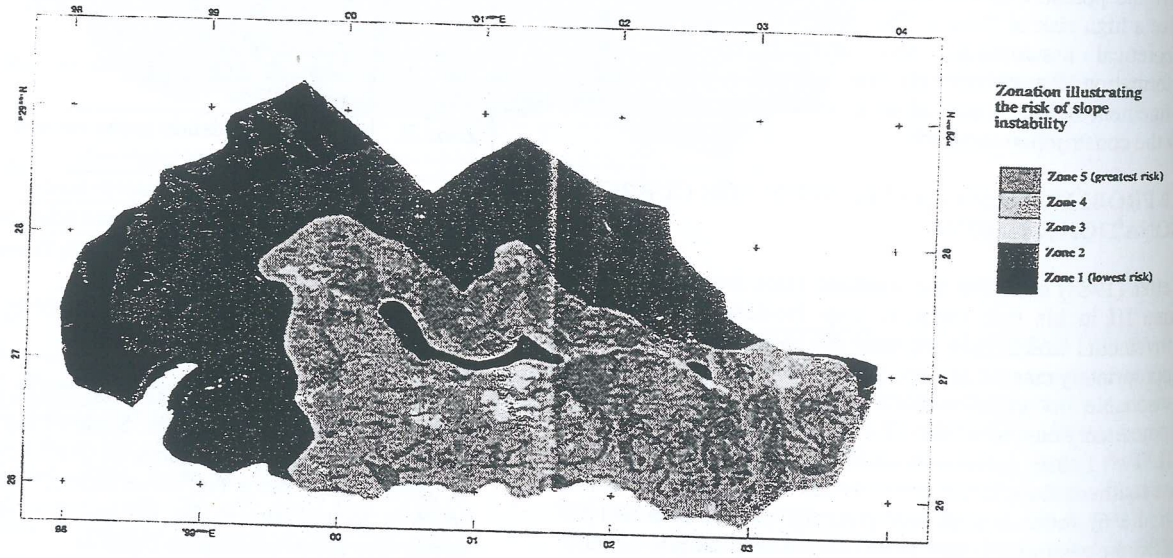

Figure 7: Final landslip risk zonation map

8 ACKNOWLEDGMENTS

I would like to thank Dr. David Leaman, Dr. Garry Davidson and Dr. Michael Roach, for their willingness to provide constructive suggestions during the writing of this paper.

9 REFERENCERS

Burrough, P.A. (1986), Principals of geographic information systems for land resource assessments, *Monographs on Soil and Resources Survey*, 12, 194p.

Clarke, G.M. (1986), Debris slide & Debris Flow Historical Events in the Appalachians, South of the Glacial Border: in Costa, J.E., & Wieczorek, G.F., editors, Debris Flows/Avalanches: process, recognition and mitigation, *Geol. Soc. America Rev. Eng Geology 7*, pp. 125-137.

Forsythe, S.M. (1996), Land stability zonation map, Launceston Area, Urban Engineering Geology Series, *Tasmanian Geological Survey*.

Heath, R. (1997), *Geotechnical risk assessment of the Claremont area*, Hobart, Tasmania, Honours Thesis, 92pp.

Ingles, O.G. (1991), *Land stability, Windermere Farm, East Tamar*, Technical report for T. Hodgman, Unisearch Limited.

Leaman et. al. (1973), Gravity Survey of the Tamar Region, Northern Tasmania, Tasmanian Department of Mines, *Geological Survey Paper, no. 1*.

Leaman D.L. & Stevenson P.C. (1972), Proposed Subdivision at Windermere, *Unpublished Tasmanian Mines Department Report*, 1972/23.

Stevenson, P.C. (1977), Stability of Land at Windermere, East Tamar, *Unpublished Tasmanian Mines Department Report*, 1977/91.

Walker et.al (1985), Geotechnical Risk associated with hill side development, *Aust. Geomech. News*, vol 10, pp. 29-35.

Young, A. (1977), *Slopes*, I & A Constable Ltd, Great Britain, 288p.

Construction and Quality Management of a Bentonite-Cement Slurry Containment Wall, Perth, W.A.

Robyn Mason BE(Hons) GradIEAust
MPA Williams and Associates, Perth, Australia

Summary The Omex site, located in the eastern suburb of Bellevue in Perth Western Australia, is undergoing remediation. The site is contaminated with heavy metals, sulphuric acid, polynuclear aromatic hydrocarbons (PAH) and hydrocarbons from the past disposal of wastes from an oil-refining plant to a series of shallow clay pits. As part of the remediation program a Bentonite-Cement Slurry Containment Wall was constructed to isolate the contamination. Given the levels of contamination and the sensitive nature of the remedial works, Quality Management systems represented an important aspect of the project. It involved detailed on-site supervision and testing and extensive laboratory testing of excavated materials and the containment wall slurry. This paper documents the practical aspects of the Quality Management System developed, gives details of the supervision and testing of the containment wall installation required to ensure compliance with design requirements as well as an outline of the procedures adopted for management of excavated material and surface water during construction.

1 INTRODUCTION

The Omex site, located in the eastern suburb of Bellevue in Perth Western Australia, is undergoing remediation. The site is contaminated with heavy metals, sulphuric acid, polynuclear aromatic hydrocarbons (PAH) and hydrocarbons from the past disposal of wastes from an oil-refining plant to a series of shallow clay pits.

As a part of the remediation program, a Bentonite-Cement Slurry Containment Wall was constructed over the period 2 September to 2 December 1998, for the Department of Environmental Protection (DEP). The project involved the potential risk of human exposure to hazardous material and further contamination of the environment.

2 SITE DESCRIPTION

2.1 Location

The Omex site is located 17 km east of the Perth Central Business District, in the suburb of Bellevue. The surrounding area is comprised of a mix of light industrial and residential land uses.

2.2 Hydrogeological Setting

The site is located close to the Darling Fault, on the Swan Coastal Plain with a surface elevation of approximately 19 m AHD. The Quaternary superficial formation consists of Guildford Clay, which is underlain at an approximate depth of 16 m by the Cretaceous Leederville Formation.

Guildford Clay contains layers of sandy clay, clayey sand and minor sand beds with local groundwater flow systems as well as individual confined aquifers formed in discontinuous sand beds. At the site the formation is about 16 m thick with approximately 13 m saturated thickness (1). The regional groundwater flow is to the south west towards the Helena River.

The Leederville Formation contains layers of sands and clays and forms part of the Leederville aquifer, a major confined aquifer which flows regionally to the west. Its potentiometric head at the site is approximately 15 m AHD (1).

2.3 Contamination History

During the 1940's the site was mined for clay leaving a series of shallow clay pits as shown on Figure 1. Between approximately 1957 to 1975, the site was utilised for a waste oil recycling operation. The process involved the refining of used lubricating oils by mixing with concentrated sulphuric acid to remove non-oil material and unstable oil. The waste sludge consisted of bitumen residue, spent Fullers Earth, acid and traces of heavy metals and was deposited into the clay pits.

Subsequently the major pit was progressively backfilled with building rubble, sand, clay, plaster wastes, car bodies and drums from 1976 onwards. In 1989 the major pit and minor pits 1 and 3 were infilled and covered with yellow sand and then in 1996 a 1 mm thick HDPE (high density polyethylene) cover was placed over the major pit. Between 100 and 500 mm of clean sand was placed over the pit prior to covering to ensure runoff directed to the perimeter drain and sump.

The contaminated wastes are known to be located within at least two of the clay pits. The major pit is about 7 m deep and contains approximately 12 400 m^3 of waste. The second (minor pit 1) is about 2 m deep containing approximately 240 m^3 of waste (1). Typical concentrations of the main contaminants in the clay pits and the current DEP landfill classifications are set out in Table 1. Generally the solid wastes fall into Class III and occasionally Class IV of the

DEP Waste Classification Guidelines (2). Groundwater samples taken in the vicinity of the clay pit were generally found to be of low pH with elevated levels of sulphate and sulphur.

The line of the slurry wall lies approximately 4 m outside the edge of the major pit, therefore the level of contamination expected during the installation of the containment wall was thought to be fairly limited. Prior investigation along the line of the wall suggested that the soil to be excavated during the installation was generally suitable for disposal at a Class II landfill site (3).

The waste within the major pit is partly submerged beneath the watertable. Groundwater contamination has been found below the pit and laterally at least 13 m from the edge of the pit (1).

2.4 Remediation Process

The remediation process developed for the site involves two stages.

STAGE 1: Isolation of the contaminants within the major pit to prevent further lateral migration to the surrounding aquifers, achieved through the construction of a bentonite cement slurry containment wall. The containment wall also acts to prevent the inflow of groundwater into the pit, facilitating Stage 2 works.

STAGE 2: Removal of all wastes, solid and liquid, to a suitable waste disposal facility.

3 BENTONITE-CEMENT SLURRY CONTAINMENT WALL

3.1 Design

To prevent further lateral migration of contaminated groundwater, an impermeable boundary both around and beneath the clay pit was required. The black clay of the Leederville Formation identified at approximately 27 m depth has low permeability, thus forming a relatively impermeable base. To contain the contaminants, the surrounding bentonite cement slurry containment wall had to:

i. be continuous, uniform and of low permeability;
ii. have its base intersect the black clay layer by at least 1 m;
iii. have sufficient strength to support loading imposed by its construction and subsequent remediation works; and
iv. be chemically resistant to low pH and high sulphate groundwater conditions.

The required characteristics of the containment wall imposed by these conditions are described in Table 2. The layout of the containment wall around the waste pit is depicted on Figure 1 while Figure 2 shows a typical cross section through the containment wall and major pit.

	SAMPLE		WA DEP LANDFILL WASTE CLASS		
Contaminant	CMA	CMB	Class II	Class III	Class IV
Phenol	<0.2	1.6	1	10	100
PAH's	18	45.8	20	200	2 000
Total Petroleum Hydrocarbons (TPH) C6-C9	14	79	100	1 000	10 000
Total Petroleum Hydrocarbons (TPH) >C9	1 100	9 400	1 000	10 000	100 000
Benzene (TCLP)	- 0.004	- 0.025	- 0.01	- 0.1	- 1.0
Benzo-a-pyrene (TCLP)	- <0.000 1	- <0.000 1	- 0.000 1	- 0.001	- 0.01
pH	3.1	1.6	-	-	-
As (TCLP)	1 0.02	1 <0.01	30 0.07	300 0.7	3 000 7.0
Cd (TCLP)	<0.01 <0.002	<0.01 <0.002	5.0 0.02	50 0.2	500 2.0
Cr (TCLP)	36 1.4	13 0.77	250 0.5	2 500 5	25 000 50
Cu (TCLP)	7 0.04	22 0.15	100 20	1 000 200	10 000 2 000
Hg (TCLP)	<0.02 <0.000 2	<0.02 <0.000 2	2.0 0.01	20 0.1	200 1.0
Ni (TCLP)	4 0.13	2 0.06	100 0.2	1 000 2.0	10 000 20
Pb (TCLP)	190 0.6	1 200 2.8	300 0.1	1 000 1.0	30 000 10
Zn (TCLP)	420 17	170 9.4	300 0.1	1 000 1.0	30 000 10

Table 1: Typical contaminant concentrations within main pit (mg/kg) (3), the location of samples CMA and CMB are shown on Figure 1. TCLP is the Toxicity Characteristic Leaching Procedure test.

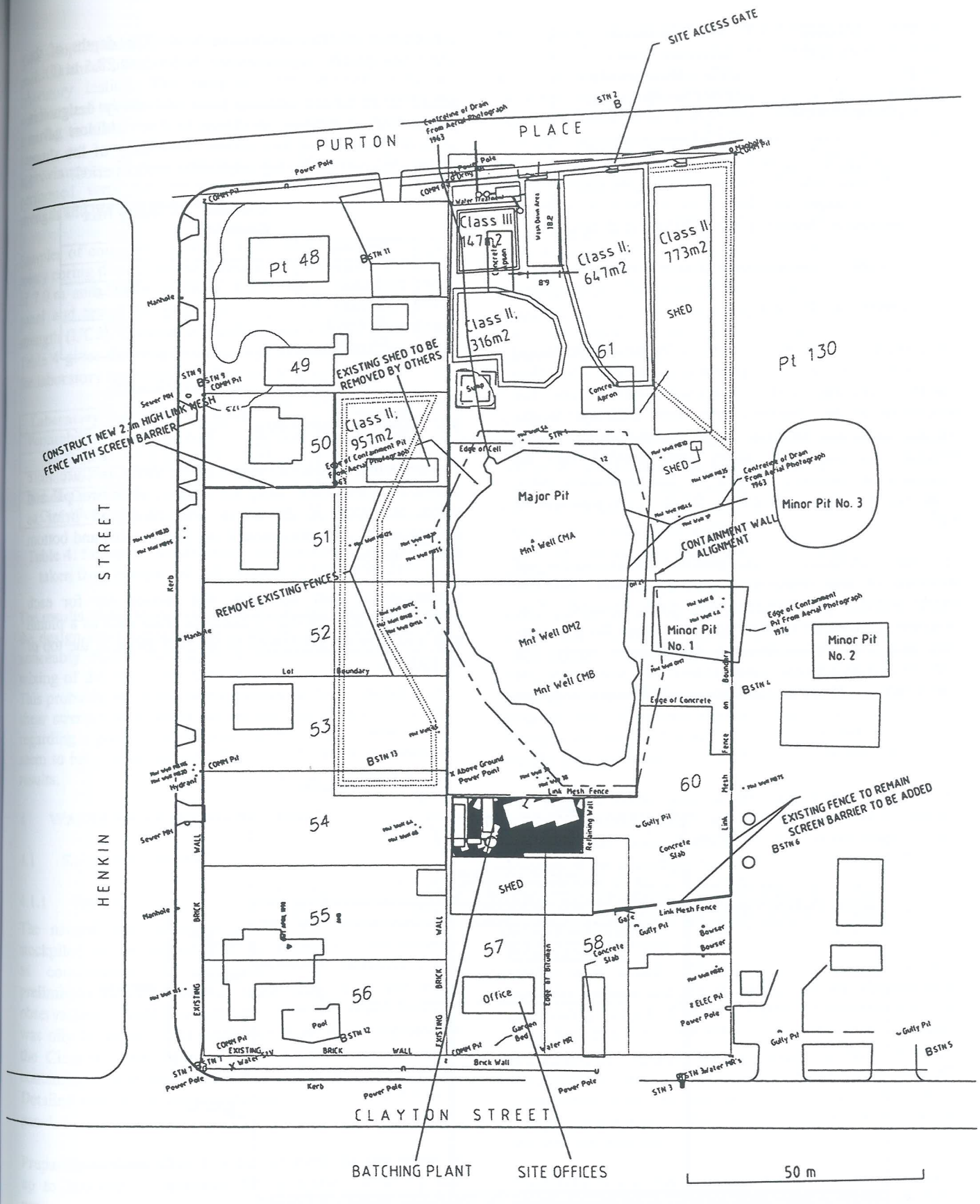

Figure 1: Omex site plan (4).

Property	Compliance
Permeability	Max of 1×10^{-8} m/s at 60 days under 150 kPa water pressure
Erosion Resistance	Pinhole test classification of ND1.
Unconfined Compressive Strength	Min of 150 kPa at 90 days.
Undrained Shear Strength	Min of 25 kPa at 14 days.
Modulus of Elasticity	Min of 20 MPa at 28 days.

Table 2: Containment wall characteristics.

3.2 Installation Process

The containment wall was constructed by the excavation and placement of 88 slurry wall panels created by a mechanical clamshell grab suspended from a track-mounted crane. The dimensions of the clamshell grab were 2800 mm length, 600 mm width and 6000 mm height. As the natural ground material was excavated, slurry was pumped into the excavation to maintain stability of the excavation sides. When set, this slurry formed the fabric of the containment wall.

The panel installation process involved the excavation and placement of three consecutive 'primary' panels (2800 mm length) within a prefabricated steel guide assembly. Two 'secondary' panels (2000 mm length) between the primaries were then completed to intersect the adjacent panels. The 400 mm overlap between panels ensured the integrity of the wall structure. This process was repeated to complete the construction of the containment wall. The depths of the slurry wall panels ranged between 24.5 m and 28.5 m (5).

Mixed in an on-site batching plant, the slurry design mix proportions are shown in Table 3. The addition of an additive (Thermathin) to improve workability of the slurry mix was carried out during most of the works period.

	Hydrated Bentonite	Slurry Mix
Bentonite	50 kg	-
Water	1000 L	-
Marine Cement	-	200 kg
Hydrated Bentonite	-	940 L

Table 3: Design mix proportions (5).

3.3 Quality Management

To ensure that the characteristics of the slurry mixture were consistent it was tested daily for density, viscosity, pH and bleed. Sampling of the slurry was conducted prior to placement and after placement from the top third and bottom third of the trench.

Monitoring of wall verticality was carried out for each panel. This was achieved by using the clam shell as a plumb with measurement referenced to the steel guide at the top of the panel.

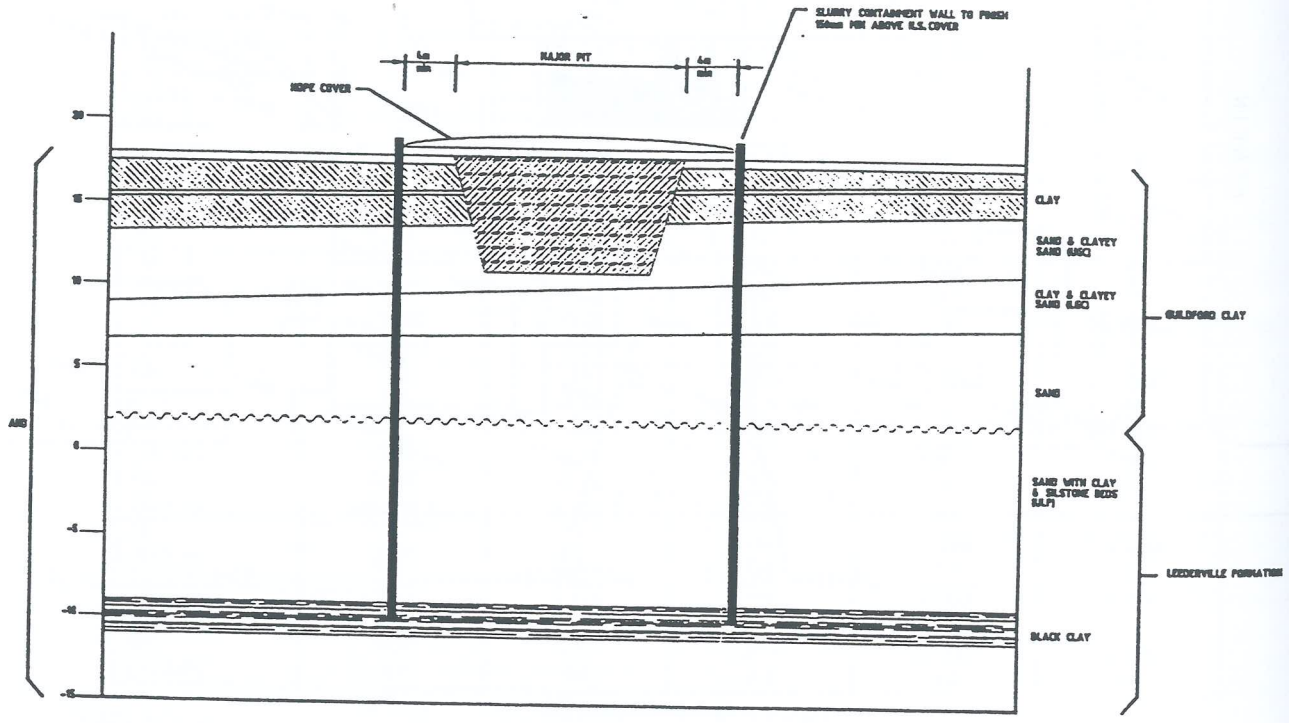

Figure 2: Typical cross section of containment wall (4).

Two samples, taken from the top third and bottom third of each finished panel, were recovered for the purpose of laboratory testing. The samples were obtained using a wireline steel tube and ball sampling device and then stored in a curing tank on site prior to testing. Laboratory tests were carried out on selected slurry samples at periods of approximately 28 days, 60 days and 90 days. The tests performed were for permeability, UCS, modulus, shear strength and pinhole dispersion.

Samples of completed sections of the wall were obtained by rotary coring through the structure at four locations. At depths of 7.0 m and 15.0 m, cores of 1.5 m were taken from each panel and tested for permeability, unconfined compressive strength (UCS), modulus of elasticity and pinhole dispersion. Table 4 gives the range and average values of the results of the laboratory tests conducted on the rotary cores.

Laboratory Test	Range	Average
Permeability (m/s)	$2.7\times10^{-10} - 1.2\times10^{-8}$	5.3×10^{-9}
UCS (kPa)	503 – 1528	938
Modulus (Mpa)	54 – 299	196
Pinhole Dispersion (Classification)	-	ND1

Table 4: Summary of laboratory test results of rotary cores taken from completed wall sections at 60 and 90 days.

The results of the tests were generally found to greatly exceed the design requirements. Slurry density after placement was noticeably higher than prior to placement because of the mixing of the slurry and the natural sandy soil in the trench. This probably attributed to the increase of UCS, modulus and shear strength well above the design specification. Concerns regarding a possible corresponding reduction in permeability seem to have been discounted by the laboratory permeability results.

4 WASTE QUALITY MANAGEMENT

4.1 Excavated Material

4.1.1 On-site

The natural soil excavated for the wall installation was stockpiled on-site according to its preliminary classification as contaminated or non-contaminated material. The preliminary classification was made using visual and odour observations. Visibly contaminated material, which typically was oily in texture, was stockpiled in an area designated as the Class III area. Material with very low or no visible contaminants was stockpiled in the designated Class II areas. Detailed logs of the excavated material were made for each panel.

Preparation of the Class II areas involved the placement of up to 300 mm of limestone fill to enable trafficking and prevent potential mixing of contaminated material with the clayey surface soils. Drainage of these areas was directed to the existing sump receiving stormwater from the HDPE liner. Volumes of the Class II stockpiles ranged between approximately 800 to 1 500 m^3. The total amount of excavated Class II material was approximately 7 000 m^3.

The Class III area formed part of a purpose built concrete washdown and sump area and was 10 m × 10 m in plan with 1 m high walls. The Class III area was covered by tarpaulins and drainage of the area was via four oil and silt interceptor tanks to the sewer. The volumes of the Class III stockpiles ranged between approximately 100 to 150 m^3. The total amount of Class III material excavated was approximately 500 m^3. The location of the Class II and 3 stockpile areas is shown on the site plan, Figure 1.

Once a stockpile area was filled to its maximum capacity the excavated material was then placed in one of the alternate stockpile areas. The completed stockpile was then tested, classified and disposed of at the appropriate land fill facility. After the removal of the excavated material the area was reused for stockpiling.

4.1.2 Disposal

For each completed stockpile one soil sample for every 100 m^3 of stockpiled waste, with a minimum of six samples, were taken for laboratory testing. The samples were tested for TPH, PAH, As, Cd, Cr, Cu, Pb, Hg, Ni, Zn, pH, Phenol and Sulphate. In addition, TCLP tests were carried out (1 per 500 m^3) for heavy metals, Benzene and Benzo-a-Pyrene.

Based on the results of the laboratory tests, the stockpiled waste was classified according to the DEP Waste Classification Criteria (2). Class II material was sent to the Flynn Drive waste disposal facility at Wanneroo and Class III material was sent to the waste disposal facility at Red Hill. Detailed chain of custody records prepared for each stockpile included the results of laboratory tests, estimated volume and weight, and gate dockets for trucks entering landfill sites.

The removal trucks were covered and washed down in a special washdown facility before leaving the site to ensure no additional contamination of the environment. The location of the washdown facility is shown on Figure 1.

4.2 Surface Water

4.2.1 Site Drainage

HDPE liner runoff, Class II stockpile runoff, Class II stockpile seepage and general site runoff was directed to a pre-existing sump as shown on Figure 1. Overflow from this sump was directed to the local stormwater drain. The sump was monitored regularly for any changes in the sump water chemistry as part of the Quality Management Process. Contingency plans for dealing with contamination involved pumping sump water to the Class III treatment area, however this was not required.

Potentially contaminated surface runoff from the washdown facility, Class III stockpile runoff and Class III stockpile seepage passed through an interceptor system before being discharged to the sewer. The interceptor system comprised of a concrete lined silt trap and four covered concrete ring sumps. Discharge from the sumps was controlled by valve operation as required by the Water Corporation. This system

separated suspended solids and oil components prior to discharge to sewer. Details of the design of the Water Treatment Facility, Washdown Facility and the Class III stockpile can be seen on Figure 3.

4.2.2 Monitoring

Daily monitoring of the pH of water discharged to sewer was required to ensure compliance with the water quality standards set by the Water Corporation. The acceptable pH of the water was between 6 and 10.5. On a small number of occasions, the pH was above 10.5 and was consequently dosed with Hydrochloric Acid (38% industrial grade) to lower the pH. Initially it was anticipated that lime dosing would be required due to the low in-situ pH. However, the mixing of alkaline slurry appeared to have effectively altered the pH environment from acidic to alkaline.

The pH of the Class II sump was also monitored daily to ensure the water chemistry was not changing dramatically. The measured pH was within the range of 7.7 to 9.0.

Samples from the last interceptor to the sewer and from the Class II sump were periodically taken and tested for TPH, PAH, As, Cd, Cr, Cu, Pb, Hg, Ni, Zn, pH, Phenol, Sulphate, Conductivity and BTEX (benzene, toluene, ethyl benzene and xylene). The Water Corporation also carried out periodic testing to ensure compliance of the water quality for discharge to sewer.

5 SAFETY PROCEDURES

The potential exposure of site personnel to hazardous materials created a need for well defined safety procedures. All site personnel attended a site induction outlining safety procedures and hazards associated with the site. Protective equipment required to be worn by people on site included protective gloves, protective goggles, protective footwear, overalls/long trousers and head protection. A gas monitor was worn daily by the site engineer in case of the disturbance of noxious gas pockets (SO_2, H_2S) during panel excavation. Appropriate respiratory equipment (gas masks) were also kept on site for this reason.

Areas containing contaminated material were defined as contaminated zones. Only authorised personnel were allowed to work in these zones wearing their protective equipment, no food or drink was allowed to be consumed within the zone. Dust generation was controlled using tarpaulins and sprinkler systems.

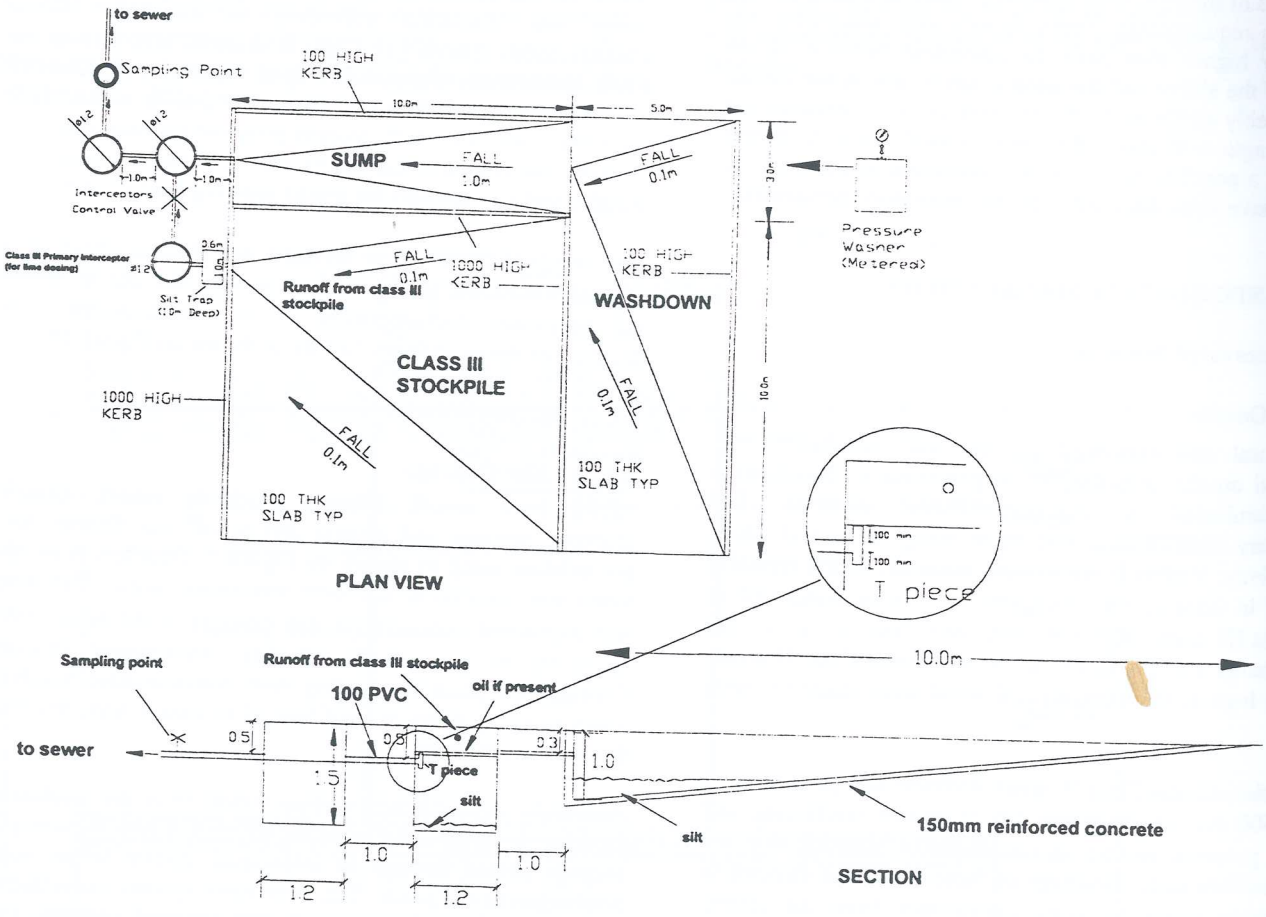

Figure 3: Waste water treatment facility (4).

6 CONCLUSIONS

6.1 Slurry Wall

Extensive testing of the containment wall to ensure compliance with the design criteria was conducted. The results of all tests complied with the requirements thus the containment wall should perform its desired role effectively.

6.2 Waste Management

The management of waste material on site was dealt with efficiently. The preliminary classification of excavated waste using visual and odour observations worked adequately. There was one instance where material with the preliminary classification of Class II contained Class III material. One sample taken from the stockpile contained elevated levels of copper. The material within the area containing this sample and extending to the surrounding sites of samples with Class II copper levels was transported separately to the landfill. Upon arrival it was lime dosed and mixed with inert material to reduce copper levels before disposal.

7 ACKNOWLEDGEMENT

MPA Williams and Associates acted as sub-consultants to Bachy Pty Ltd in this project who were responsible for the construction of the bentonite cement slurry containment wall. The author would like to thank Bachy and the DEP for permission to publish this paper.

8 REFERENCES

1. Golder Associates, "Extent of Contamination and Options for Remediation: Omex Petroleum Site (Clayton Street, Bellevue)", February 1997.
2. Department of Environmental Protection, "Landfill Waste Classification and Waste Definitions", 1996.
3. CMPS&F, "Omex Remediation Project Containment Strategy Specification", May 1998.
4. Bachy Pty Ltd, "Omex Site Bellevue, Design Report", August 1998.
5. MPA Williams & Associates, "Omex Site Bellevue, Construction report", February 1999.

The Kogai Waste Dump
A Case Study of the Observational Method

Patricia A. Murison, CPEng, Senior Geotechnical Engineer, Porgera Joint Venture

Summary This paper describes the design and development of the Kogai waste dump using the Observational Method. The Kogai waste dump is an engineered structure located at the Porgera Gold Mine in Papua New Guinea. The main objective of the paper is to demonstrate through the example of Kogai that the Observational Method is valuable to many geotechnical projects, and to mine waste dump development in particular. The case history of the Kogai dump also highlights an innovative engineering solution that has allowed construction of a stable waste dump in an adverse geotechnical environment. "Lessons learned" from using the Observational Method for construction of the Kogai dump are also summarised.

Keywords: Observational Method, mine waste dump, Papua New Guinea

1 NOTATION AND UNITS

tpd: metric tonnes per day
Mt: million metric tonnes
Bt: billion metric tonnes
M7.0: Richter scale magnitude 7.0 earthquake.
m/yr: metres per year

2 INTRODUCTION

The Observational Method is a systematic "learn-as-you-go" procedure developed by K. Terzaghi for applied soil mechanics. When correctly applied, the Observational Method is the ideal approach for the design and construction of mine waste dumps.

Located in the highlands of Papua New Guinea (see Figure 1), the Porgera Gold Mine has designed and developed the Kogai waste dump using the Observational Method. From the project inception, the Kogai waste dump was viewed as an "engineered" structure. This approach has allowed for informed risk taking, which is a necessary element in the mining industry for maximising cost effectiveness without compromising safety. Given the extreme conditions that exist at Porgera, the Observational Method was in fact essential to the development of a large stable waste dump.

A brief history of the Kogai waste dump since its inception in 1993 is presented herein. This case history highlights the use of the Observational Method to optimise an aggressive waste dump design based on performance, thereby minimising the cost to the mine development. Uncertainties in storage requirements and design parameters have been addressed, and will continue to be refined over the life of the mine. The conclusions and "lessons learned" from the continued successful development of the Kogai dump using the Observational Method are also summarised.

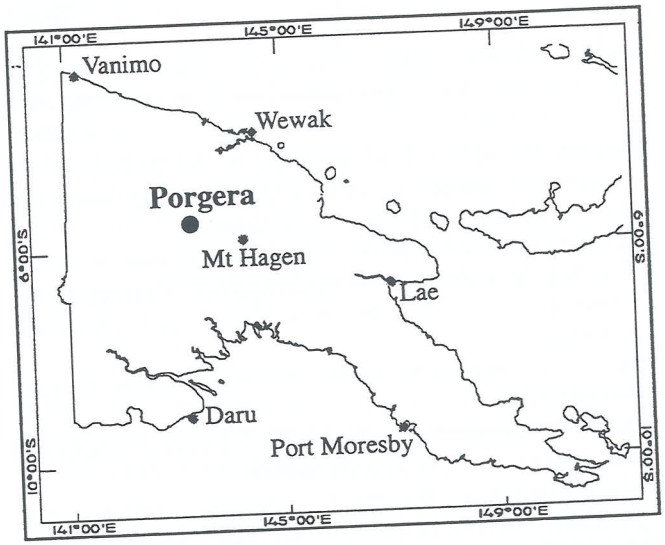

Figure 1: Location Plan

3. REVIEW OF OBSERVATIONAL METHOD

The Observational Method was well documented by R. Peck (1) as the 9th Rankine Lecture. This method is ideally suited to mine waste dump development due to the typically large foundations, where no practical amount of investigation can disclose all variations.

A brief summary of the essential steps is presented below, and has been tailored specifically for mine waste dumps:

1. Complete field, laboratory and office investigations sufficient for establishing the condition of the foundation and waste materials.
2. Assess the most probable conditions and the worst case deviations, and then determine the corresponding consequences in dump performance.
3. Establish the design of the waste dump based on the most probable conditions (a working hypothesis).

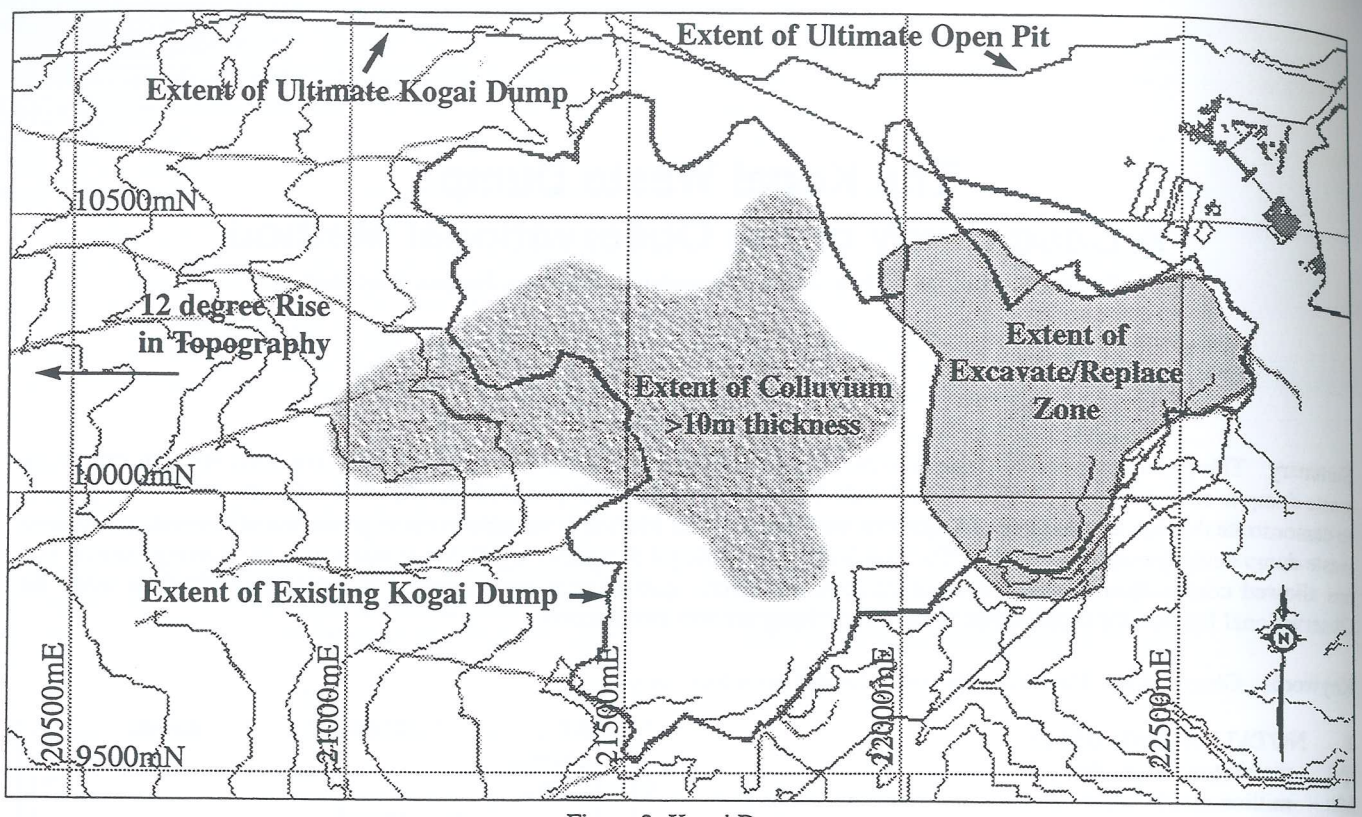

Figure 2: Kogai Dump

4. Define and select key quantities to be monitored as construction proceeds. Calculate the anticipated values for both the probable and worst case conditions.
5. As part of the design stage, identify the appropriate course of action or design modification required to handle every foreseeable serious deviation from the predicted performance.
6. Develop a monitoring system for measurement of key parameters.
7. Using the monitoring system, evaluate actual conditions during construction in a timely fashion.
8. Act according to the results collected; control waste placement, modify the design, and adjust the monitoring program as appropriate.

The above feedback loop which funnels the performance monitoring data back into design is essential to the correct application of the Observational Method. This allows the gaps in knowledge to gradually be closed, and the design modified during construction as necessary. As a result, great savings in time, money or risk reduction can be realised. The Observational Method must not be applied to a design which can't be modified during construction.

Unlike some civil engineering projects, waste dump development is typically stretched over several years of the mine life. This creates an ideal timeframe to collect data and experience to optimise the design and construction procedures, often without impacting production.

4 CASE STUDY - KOGAI WASTE DUMP

4.1 General Setting

The Porgera Gold Mine is located in the remote Enga Province, at the heart of the Papua New Guinea highlands. Rugged limestone and sandstone peaks up to El. 4,000 m surround the Porgera valley, and active colluvium landslides blanket most of the valley floor. The peaks and colluvium slides are underlain by highly folded mudstone, which is the basal unit for the region. This complex geological setting combined with an average rainfall of over 3m/yr and recorded seismic activity of M7.0 has resulted in a very adverse geotechnical environment for mine development.

Underground mining of the Porgera gold deposit began in 1989 and development of the open pit commenced in 1991. Over the past 8 years, the open pit operation has expanded and now produces an average of 210,000tpd of waste, while the underground was decommissioned in 1997. Three waste dumps are currently used by operations, of which the Kogai stable waste dump is the primary facility for storage of competent waste material.

4.2 Investigation and Initial Design

The Kogai valley, located in the main Porgera valley, is immediately adjacent to the open pit (see Figure 2). The foundation ranges from colluvium and residual soils over 20m thick to fresh mudstone outcrops at the base of some active stream channels and local ridges. Five major creeks and associated tributaries flow through the valley. The original ground surface rises to the west at about 12 degrees.

In 1993, drilling, surface mapping, and geophysical methods were used to investigate the foundation conditions. The Observational Method was adopted, and the initial design was completed in 1994. The storage requirement of the dump, set at 160Mt over the life-of-mine (LOM), was determined from mine planning projections.

Based on the 1993 investigations, the most probable foundation conditions were ascertained and a design concept was developed. The main aspects of the design concept for Kogai were as follows:

- The colluvium would be excavated from the toe area of the dump to expose a more competent mudstone foundation.
- The dump would be constructed to abut into the ridges forming the sides of the Kogai valley, thereby maximising three-dimensional confinement.
- The dump would be constructed of competent waste only.
- The upper portion of the dump would be founded on colluvium and buttressed by the dump toe founded on mudstone.
- "Flow-through" drains of coarse, competent rock would be used to direct the creeks through the dump. An emergency southern perimeter ditch would also be included and the ultimate dump was to be graded to slope towards the perimeter channel.

Stability criteria were set at a factor of safety of 1.1 during construction, 1.3 for long term closure conditions, and less than 5m horizontal displacement under seismic loading (long term closure conditions). These criteria are lower than the conventionally used factors of safety for engineered waste dumps, which are virtually impossible to economically achieve given the combination of weak foundation materials, moderate ground slope, and slow pore pressure dissipation rates characteristic of the Porgera minesite.

The critical geotechnical parameters which governed stability of the dump were identified as follows:

- The strength of the mudstone and colluvium foundations under undrained and drained conditions.
- The thickness and extent of the colluvium.
- The dip and dip direction of bedding planes in the mudstone.
- The pore pressure response in the colluvium and the mudstone foundations.
- The level of saturation within the dump during construction and upon closure.
- The strength of the mine waste materials.

Limit equilibrium stability analyses were carried out using both the probable and worst case values for the above critical parameters. The critical mode of failure resulting in overall dump instability was shearing through the mudstone foundations in the toe buttress area. Potential mitigative actions ranged from revised dumping procedures to full cessation of dumping.

To better understand the foundation response to loading and quantify dump performance for comparison to the design intent, a monitoring program was developed and implemented. The program consisted of the following components, and is directed by the on-site senior geotechnical engineer:

- detailed mapping and point load testing of the exposed mudstone foundation after colluvium was stripped from the toe buttress area.
- daily visual inspection of waste placement areas.
- regular full dump visual inspection, which is also required after extreme events.
- survey monuments on dump surface for movement measurement (waste and foundation together)
- inclinometers for separate measurement of movement in waste and foundation materials.
- shear strips in inclinometers after they become too warped for measurement with the inclinometer probe.
- piezometers and load cells in the foundation to measure pore pressure response due to loading.
- piezometers in the waste materials to measure the fluctuation of water within the dump, and the effectiveness of the flow through drains.

4.3 1994-1995 Construction

Construction of the access road for excavation of the colluvium in the toe area commenced in May 1994, after appropriate land negotiations were finalised. Almost 2Mt of colluvium was excavated from the toe buttress area, which was roughly 2500m² in size when completed in November 1995 (see Figure 2).

The exposed mudstone foundation was immediately mapped and backfilled with competent waste to prevent excessive weathering and strength reduction in the mudstone. This particular aspect of the development program was critical to prove the design assumption that the mudstone bedding was steeply dipping and a large-scale failure along bedding was not possible. Following external review, a second drilling program was also undertaken to assess the potential for a large deep-seated failure in the mudstone.

In accordance with the Observational Method, the initial design was re-evaluated and no design modifications were considered necessary based on the additional mudstone mapping and strength testing data.

Survey monuments, inclinometers, and load test sites in the mudstone were installed progressively as the toe buttress area was constructed. Daily visual inspections were also carried out and feedback from the monitoring program was given to the engineering and operations staff, which focused in particular on quality control of waste material type and surface water control. No serious deviations from expected performance occurred during this construction period.

A formal qualitative risk assessment was also completed in 1995 to complement the design work already completed.

4.4 1996-1997 Construction and Design Optimisation

4.4.1 1996 Design Optimisation

Due to continued exploration, the size of the open pit had substantially increased by 1996 and approximately 460Mt of competent waste storage was required (see Figure 3). The question arose whether the toe buttress founded on mudstone would have to be extended to provide the additional storage capacity.

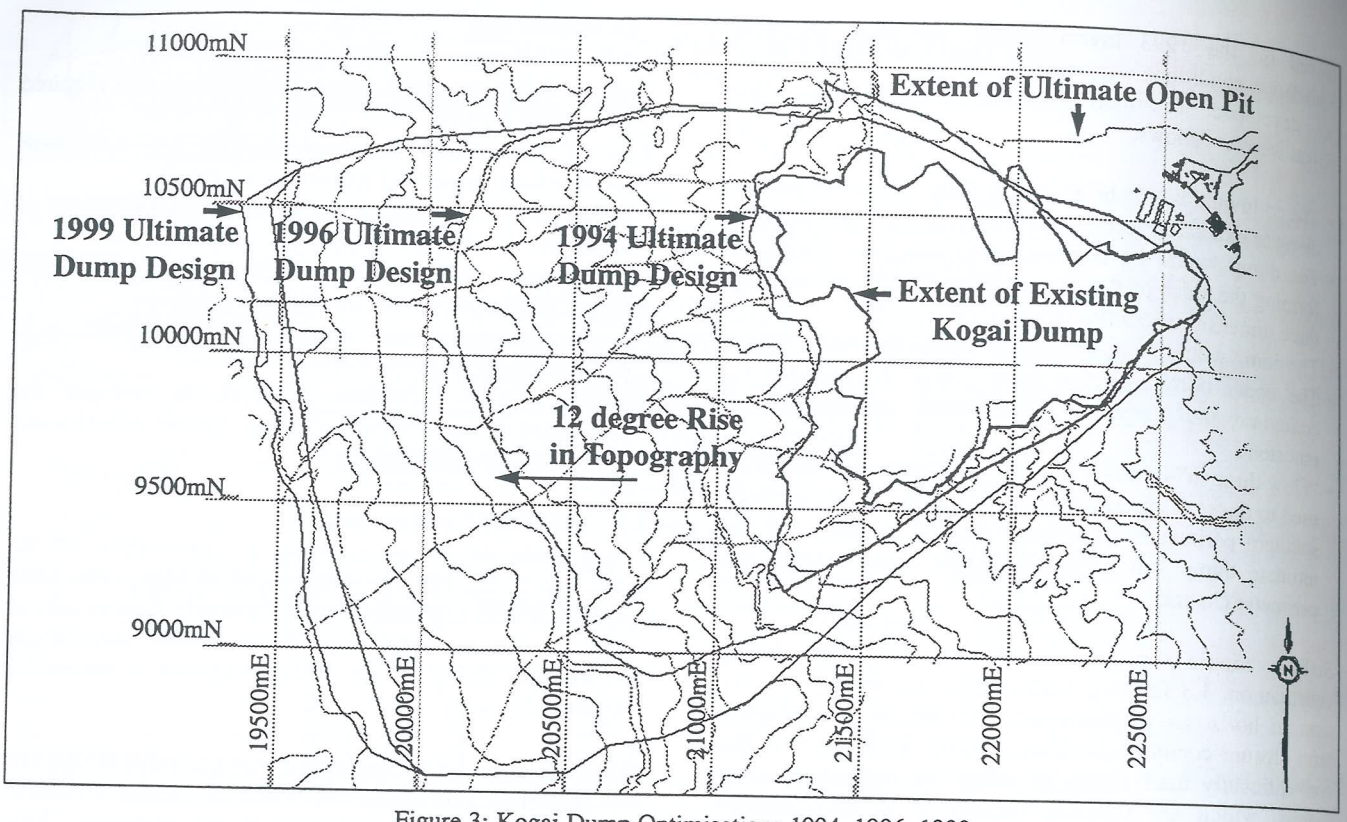

Figure 3: Kogai Dump Optimisations 1994, 1996, 1999

A conceptual optimisation of the Kogai dump was completed in 1996 using all of the investigation and monitoring data collected since construction began. The optimisation process complied with the principles of the Observational Method, and used a mixed team of on-site staff, external consultants, and academic professionals.

Many benefits were realised as a result of the optimisation based on performance data. In particular, the likely average values and ranges of the critical parameters were refined using the field performance data. Also, it was concluded on a conceptual level that the dump capacity could be expanded without additional excavation and replacement of colluvium. The latter outcome was achieved by modifying the waste dump geometry behind the design toe buttress to eliminate internal dump failure through the upper colluvium foundation.

4.4.2 1996 Construction

By the start of 1996, the excavate/replace zone was complete and waste placement directly onto a colluvium foundation commenced. Towards the end of 1996, significant deformations occurred over colluvium foundations. The movements were attributed to:

- the lack of adequate buttressing by the toe, which was underbuilt compared to design due to the presence of ore stockpiles.
- high pore pressure generation in the colluvium due to rapid loading.

Additional survey monuments were immediately installed adjacent to tension cracks to track the rate of deformation. The rate of dumping over colluvium foundations was significantly reduced, and the toe buttress area was reinforced with additional waste placement. Dump construction proceeded normally following the above modifications.

Flaws in application of the Observational Method were evident both in lack of adequate monitoring and feedback into design modification to proactively minimise the deformations. Also, no instrumentation was installed to measure colluvium pore pressure dissipation after movements had stabilised, and post-failure documentation or back analysis was lacking.

4.5 1998-1999 Construction and Optimisation

From 1996 to 1999, the ultimate open pit had again expanded, and up to 1.1Bt of competent waste storage will be required over the LOM which will cover about 6km² (see Figure 3). For reference, the dump configuration as of mid 1999 is also shown in Figure 3.

Unlike 1996, a very detailed optimisation was undertaken in 1999. All monitoring data collected since initial construction was used to re-evaluate the critical parameters. In particular, additional data collected from dump deformations that occurred in early 1999 over the same area affected in 1996 was utilised.

With the expansion of the pit, the interaction between the pit and the dump was also evaluated. The optimisation process strictly complied with the principles of the Observational Method, and both on-site staff and external consultants were involved in the process.

The study concluded that a 1.1Bt dump was feasible, provided the excavate/replace was extended to the north. This design

modification was necessary given the deep colluvium upstream of this area. Priorities for future monitoring were identified and included additional data collection for defining pore pressure generation and dissipation in the colluvium and recording of dump saturation levels.

5 CONCLUSIONS AND "LESSONS LEARNED"

The Observational Method is the ideal approach for waste dump development: if not applied, only two options remain as stated by Terzaghi in 1915:

"...either to adopt an excessive factor of safety, or else to make assumptions in accordance with general average experience. ...The first method is wasteful; the second is dangerous."

Proper application of the Observational Method will be critical for continued safe and economic development of the Kogai engineered waste dump over the LOM. Further open pit optimisations will undoubtedly influence both the future storage requirements and the interaction between the ultimate pit and the dump.

With such adverse geotechnical conditions and low operating factors of safety for Kogai, vigilance in monitoring and design modifications can not be relaxed without incurring significant risk. Close cooperation between geotechnical engineering, mine engineering, and operations staff with full support by management is essential.

From the case study of the Kogai stable dump presented in this paper, several more general conclusions or "lessons learned" can also be gleaned. They are applicable to a wide range of geotechnical engineering projects that can benefit from the use of the Observational Method:

- Many engineers may instinctively apply several aspects of Observational Method to geotechnical projects. However, unless the observations are a part of a conscious and systematic program containing all essential steps, adverse outcomes can result. Many case histories will attest to this, where the absence of an essential step in the Observational Method has led to failure.
- When applying the Observational Method, constant stewardship by personnel fully cognisant of the design assumptions and historical development is an absolute necessity. A gap in the continuity of this knowledge caused by staff turnover must be avoided through overlap and proper documentation. Significant risks could otherwise be incurred.
- Sufficient human and material resources for maintaining an adequate monitoring program must be available.
- The Observational Method is best used when more than one qualified engineer is involved in identifying the critical parameters, potential failure modes, and suitable monitoring program. There is no substitute for experience, making the involvement of senior engineers invaluable.

6. ACKNOWLEDGEMENTS

The author wishes to thank many staff at Porgera who assisted in preparation of this paper. In particular, Cam Grundstrom of Porgera and Bryan Watts of Klohn-Crippen Consultants provided many insightful comments to improve the quality of the paper. Shona Smith of Shonart Graphic Design also helped immensely in preparation of the paper format.

7. REFERENCES

1. PECK, R. B., "Advantages and Limitations of the Observational Method in Applied Soil Mechanics", Geotechnique 19, No. 2 pp. 171-187, June 1969.

2. KLOHN-CRIPPEN, "Kogai Engineered Waste Dump Evaluation", September 1994.

3. KLOHN-CRIPPEN, "1996 Kogai Waste Dump Optimisation", March 1996.

4. KLOHN-CRIPPEN, "1999 Kogai Waste Dump Optimisation", June 1999 (DRAFT Report).

5. PORGERA JOINT VENTURE, "Annual Waste Dump Summary Report", December 1998.

6. BRITISH COLUMBIA MINE WASTE ROCK PILE RESEARCH COMMITTEE, "Mined Rock and Overburden Piles, Methods of Monitoring", Interim Report, March 1992.

A Micro-Mechanical Approach into the Shear Behaviour of Rock Joints

HELEN PEARCE, PhD Student, Department of Civil Engineering, Monash University

Summary: Current methods to estimate the peak shear strength of rock joints rely predominantly on empirical relationships. The empirical nature of these models requires conservatism on the part of the designer. The Geotechnical Group at Monash University is currently developing a theoretical approach where the behaviour of the rock joint is being modeled. By understanding the mechanisms involved during shearing, it is hoped that the uncertainty of design can be minimized. This paper outlines the difficulties in correctly modeling rock joint behaviour and gives a brief outline of the theoretical approach being taken.

1.0 INTRODUCTION

Rock masses are inherently intersected by discontinuities that are typically the weakest part of the rock mass and hence may govern its strength. The presence of these discontinuities has been known to cause catastrophic failure in many engineering structures where the design has not incorporated accurate properties of these defects.

To understand the mechanisms of failure within the rock mass, it is first necessary to understand the behaviour of a single discontinuity. Considerable research has been undertaken during the last three decades to determine the behaviour of rock joints under the application of shear load. Much of this research has involved the use of empirical models due to the complexity of the joint interface and shearing behaviour.

This paper outlines the complexities of the joint shearing process and the many factors that may affect its behaviour. A theoretical approach to rock joint behaviour that is currently being investigated by Monash University is discussed.

2.0 FACTORS AFFECTING ROCK JOINT SHEAR BEHAVIOUR

To accurately predict the shear response of a rock joint, it is important to identify and understand the many factors that will affect the joint behaviour. These factors are often very difficult to quantify.

There are many stresses that act on a rock joint. These can be in-situ stresses; such as gravitational stresses, tectonic stresses, residual stresses from such processes as magma cooling, terrestrial stresses such as seasonal variation; or induced stresses from such processes as mining, drilling or pumping. These stresses are often difficult to accurately measure and with little to compare answers to, unavoidably require large confidence intervals.

The boundary conditions for a rock joint vary according to the deformability of the surrounding rock. The deformability of the surrounding rock can be measured in terms of its stiffness. If the rock surrounding the joint is deformable enough to allow dilation of the joint without reaction forces, then shearing will take place under zero normal stiffness. An example of this would be a rock slope where sliding along a joint occurs under the constant normal load of the block's weight. In most underground rock situations and in rock slopes where rock bolts or cables have been used, rock blocks cannot slide freely due to intimate contact with surrounding rock blocks. Dilation of the joint causes a reaction from the surrounding rock mass that applies additional stress to the rock joint. This is known as Constant Normal Stiffness. It is also possible to have conditions where the normal stiffness may vary.

Rock joint surfaces possess many irregular departures from the plane both on the large scale and on the small scale. These departures of varying angle and width (referred herein as asperities) are dependent on the rock's mode of origin, weathering and mineralogy. Due to the random and irregular nature of the asperities, it is difficult to assign a statistical value to represent the roughness of the surface. This is made more difficult as the roughness is scale dependent. Roughness measured on a 10 cm core sample may not indicate the overlying waviness visible when looking at an exposed joint surface from some distance. At very small stress levels or very small scales the grain size can even be seen to affect the shear behaviour. To further complicate a roughness analysis, the joint surface roughness will also typically decrease during shearing as steeper asperities are sheared.

Shearing of asperities may be dependent on the rock strength. If the rock joint is not weathered then the joint wall strength is that of the intact rock. However, weathering of the joint surface will alter the joint wall strength properties. Weathering will typically weaken the joint wall strength although in some cases such as the occurrence of iron penetration, the joint wall strength can be stronger than the strength of the intact rock. Laboratory testing can be performed to determine the strength of the joint surface although very small depths of penetration often make this testing very difficult. A field tool, called the Schmidt Hammer, has been developed to provide characteristic data. It

involves dropping a spring-loaded plunger onto the joint surface and recording the number of rebounds. From an average of at least ten tests the surface unconfined compressive strength can be estimated. Damage to the surface can cause an inaccurate measurement as can voids or compressive layers hidden in the rock mass and therefore, unless calibrated extensively, the results should not be relied upon.

Joint aperture, a measure of the perpendicular distance separating the adjacent joint faces, can affect the shear response as partially open joints only allow the higher asperities to come into contact and hence become involved in the shearing process. Measuring the aperture can be quite difficult as typical drilling techniques would tend to disturb the joint interface.

Many joint walls are separated by material that will typically reduce the shear strength of the joint (such as carbonaceous material, clay, silt, breccia or minerals). The effect on the shear behaviour will be dependent on the infill's thickness, composition, water content, extent of consolidation, previous shear history and roughness of the joint walls. Laboratory direct shear tests have indicated that a rock joint containing infill will produce two peak shear strengths – failure of the infill followed by failure of the asperities (Checcia de Toledo and de Freitas, 1995).

Laboratory testing has indicated that the shear displacement velocity can affect the magnitude of the shear resistance at stress levels applicable to engineering structures (Crawford and Curran, 1981). The extent of the effects appears dependent on the rock type and level of the normal stress.

The presence of water in the joint has been documented to either reduce, increase or have no effect on the shear strength of the rock joint (Barton, 1973). These results are dependent on the mineralogy and roughness of the joint surface and the resulting development of pore pressures.

In the determination of a realistic but useable rock joint model capable of accurately predicting the performance of the joint under the application of a shear load, an understanding and method of quantifying all factors affecting the joint is required.

3.0 TRADITIONAL APPROACHES TO ROCK JOINT SHEAR STRENGTH MODELLING

During the past three decades extensive research has been conducted on the behaviour of rock joints under the application of a shear load.

According to the classical law by Amonton, the shear resistance, τ, is related to the normal stress, σ_n, and the coefficient of friction,μ, by the following relationship:

$$\tau=\mu\sigma_n \qquad (1)$$

where $\mu=\tan\phi$

ϕ=friction angle of the material

By investigating over 300 slopes in the Rocky Mountains and performing laboratory tests on synthetic rock profiles with constant angled asperities, Patton, (1966) highlighted the presence of two failing mechanisms - sliding and shearing. He produced a bilinear failure model whereby under a predetermined transition stress, σ_T, sliding occurs and above this stress shearing occurs. He extended Amonton's shear stress relationship to include the asperity angle, i, as shown in equation (2).

$$\tau=\sigma\tan(i+\phi) \qquad (2)$$

Although this model highlights two basic mechanisms of rock joint behaviour, it is simplistic in that real rock joint surfaces are irregular, comprising many different asperity angles. This allows shearing and sliding to occur simultaneously and would produce curved failure envelopes.

Given the non-linear failure envelopes of natural rock joints, Barton, (1973) believed that empiricism was required to correctly describe the shear strength. He proposed the following relationship based on extensive testing and observations of rock joints:

$$\tau=\sigma_n\tan(JRC\log_{10}(JCS/\sigma_n)+\phi_b) \qquad (3)$$

where τ = peak shear strength

σ_n = effective normal stress

JRC = joint roughness coefficient

JCS = joint compressive strength

ϕ_b = basic friction angle

This equation can be compared to the Patton model with the asperity angle, $i=JRC\log_{10}(JCS/\sigma_n)$.

The JCS is a measure of the joint compressive strength and can be roughly measured using the Schmidt Hammer. This takes into account any alterations to the joint surface.

The JRC represents a sliding scale of roughness where the roughness is visually assessed from ten roughness profiles. These profiles have been given the ranges 0-2, 2-4, etc up to 18-20 and are 100mm long. Scale effects are therefore not considered in the measurement of the JRC. A further empirical relationship was later added to the model to take into account scale effects.

The standard roughness profiles together with the empirical relationship has been accepted by the International Society for Rock Mechanics as a useful method to estimate peak shear strength in their Commission on Standardization of Laboratory and Field tests (ISRM, 1978). Due to this endorsement and ease of use, this method has gained significant popularity and is perhaps the most widely used approach today. However, its empirical nature may limit its applicability to all situations and rock types.

In an attempt to produce an understanding of the shear behaviour, Ladanyi and Archambault, (1970) used energy principles to extend Patton's bilinear model to take into account various failure modes of rock joints occurring simultaneously. They considered that the total shearing force would comprise of four components:

- component due to external force done in dilating against the external force, N
- component due to additional internal work done in friction due to dilatancy
- component due to the work done in internal friction if the sample did not change in volume in shear.

- component due to shearing through the base of the asperities

The summation of these components combined with several empirical constants was used to predict the total shear force.

Although introducing combined concepts of shear failure of asperities and dilation, the Ladanyi and Archambault model relies on several parameters that are either difficult to predict or rely on empirical methods. Its approach to boundary conditions, rigidity of asperities and elasticity of the rock is also overly simplified.

4.0 MONASH APPROACH

The Geotechnical Group at Monash University has for the past 20 years being developing a theoretical approach to the determination of rock socket pile performance. This work has concentrated on developing a micro-mechanical approach to the behaviour of the concrete-rock interface during shear. The model uses several of the energy principles adopted in Ladanyi and Archambault but is based on a more fundamental approach without the use of empiricism. The model is reported in detail in Seidel, (1993).

It was considered that the shear model developed for concrete-rock interfaces could be modified to represent rock joints. Initial testing has suggested that the main mechanisms are consistent (Fleuter, 1997). A simplified description of the model details will be briefly outlined.

The model represents the roughness as a series of irregular triangular elastic asperities. When a shear force is applied, sliding will initially occur on the steepest asperity slopes. As the asperities are elastic (in particular with soft rock) sliding will also occur on several of the lower sloped asperities. Sliding on these asperities causes dilation and other asperities are lifted out of contact. This reduces the contact area causing an increase of the normal stress on areas still in contact. If the normal stress increases beyond the intact strength of the asperity then the asperity will shear. Further movements in the shear direction will cause a displacement of the sheared material. Due to the irregular nature of the surface, sliding, dilating and shearing can all occur simultaneously. With some materials the surface can also experience inelastic deformations where the surface is worn away. These simplified components are shown diagrammatically in Figure 1.

To date this model has been developed using simplified roughness profiles on either synthetic rock or reasonably homogeneous sandstone samples. To be able to realistically extrapolate the model to real rock joints of varying rock type and strength, further detailed laboratory testing is currently being undertaken.

5.0 TESTING OF MODEL

Most of Melbourne is underlain by Silurian and Lower Devonian Age siltstones, sandstones and mudstones called Melbourne Mudstone. This formation can be encountered in a range of weathering states that can vary from very low strength rock to very high strength in its fresh state.

Due to its importance in the Melbourne area, initial testing was conducted on a synthetic rock called Johnstone that has similar properties to Highly to Moderately Weathered siltstone. This rock was developed specifically for testing of the concrete – rock interface in pile sockets (Johnston and Choi, 1986). It has an unconfined compressive strength of approximately 4MPa when its saturated moisture content is approximately 14%.

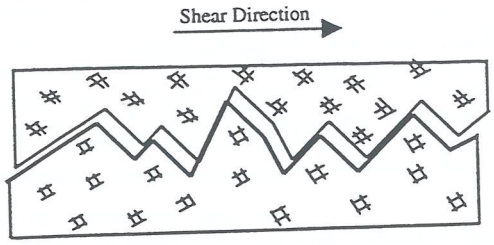

Sliding and Dilation

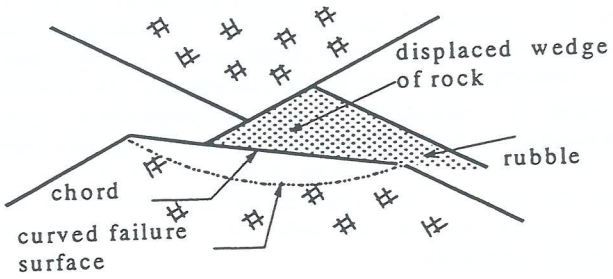

Shear Failure of Single Asperity

Figure 1 Idealized Sketches of sliding, dilation, shearing

Direct shear tests conducted on intact and planar Johnstone samples obtained peak and residual friction angles of 35^0 and 24.5^0 respectively. Tests were undertaken on regular triangular 2-dimensional profiles to be able to observe and model the sliding, shear and wear behaviour. This was then extended into 2-dimensional irregular triangular profiles.

All direct shear tests were conducted in a specially designed device that is capable of testing samples up to 600mm long under constant normal stiffness conditions.

These direct shear tests indicated that sliding was initially occurring on the steepest asperities and on some shallower asperities due to elasticity effects. This caused dilation and some asperities moved out of contact. Due to the increase in load on the steeper asperities, failure occurred transferring the load to lower asperities. Due to the irregular nature of the surface, sliding and failure was observed to occur simultaneously. Later inspection of the surface also indicated wear was occurring. With these observations, the basic model developed for concrete-rock interfaces could be extrapolated to rock joints (Fleuter, 1997).

Recent testing has extended this work into 3-dimensional profiles. These profiles were obtained by tensile splitting Johnstone blocks. Several 2-dimensional profiles were taken of each split surface using laser profilometry techniques. The laser device used was the Monash *Socket-Pro* that was developed for pile socket roughness inspections (Collingwood et al., 1999).

A visual comparison of the profiles from each surface indicated a close similarity across the face. Several of the 2-dimensional profiles for one split face are shown in Figure 2.

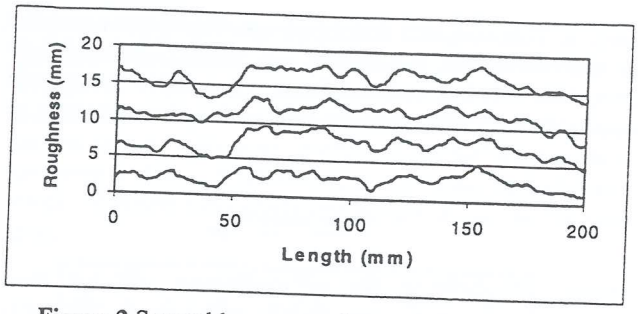

Figure 2 Several laser scans from a Johnstone split face

A statistical analysis was also completed by using the compass walking method. This method, which has been suggested as one method to estimate the fractal dimension of the joint roughness, involves walking a compass opened to a specified chord length along the profile. Considerable debate still rages over the application of this method, amongst others, in determining accurate fractal dimensions. As a result, analysis has been restricted to the determination of the variation of the standard deviation of chord angle with chord length. Correlation coefficients determined for the between each profiles range of standard deviation of chord angle with chord length were in the order of 0.99. This indicates excellent correlation.

These comparisons have suggested that the 3-dimensional surface can be modeled using a 2-dimensional profile. Limited laboratory testing has agreed with these comparisons although further work will be required to confirm this.

By testing Johnstone, a synthetic rock, problems associated with natural variations in the material are avoided allowing the basic model to be developed. Testing is currently being conducted on natural Slightly weathered to Fresh Melbourne mudstone. Samples were obtained from the tunneling work conducted for the Melbourne City Link project. The rock obtained has an unconfined compressive strength of approximately 60MPa and saturated moisture content of approximately 1.5%. These samples are therefore considerably stronger than previous samples tested in the development of the rock socket model.

A series of direct shear tests have been conducted on regular triangular asperities of chord length 16mm at angles of 5^0,10^0 and 15^0. The profiles were cut using waterjet cutting techniques. Waterjet cutting involves spraying water mixed with fine sand through a nozzle under high pressure. The resulting jet is approximately 1.2mm in diameter. The shear test results indicated that under the normal stresses applied (up to 3000 kPa), sliding on the asperity faces occurred with no shearing and very little wear. An example profile and the resulting direct shear test results are given in Figure 3.

Tests were also conducted on 2-dimensional irregular triangular profiles. An example profile together with the direct shear test results is shown in Figure 4. Some shearing of the higher asperities can be seen in these results. Dilation caused some of the interface to move out of contact causing the stresses became highly localized. When these were greater than the strength of the intact rock shearing of the asperity occurred. The results from these tests can be used to confirm the basic model.

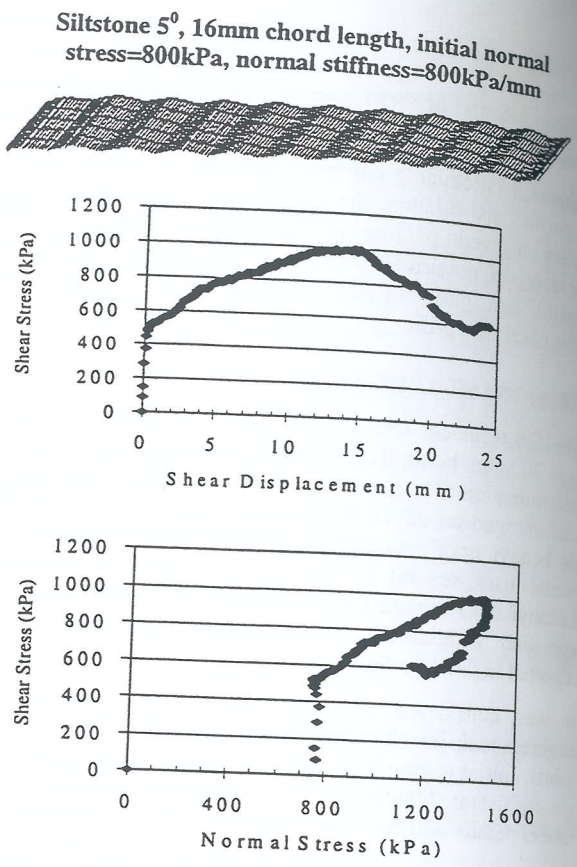

Figure 3 Shear results of 5^0 siltstone sample

Several blocks of siltstone have been split parallel to their bedding direction These surfaces have been compared to natural bedding joints in the slightly weathered to fresh siltstone. The split surfaces were visually and statistically similar to the natural bedding joints. Direct shear tests will be conducted on these samples to extend the existing model into more realistic 3-dimensional profiles.

6.0 CONCLUSIONS

Empirical models to predict the peak shear stress of natural jock joints fall short of explaining the behaviour of the joint. Although simple to use, they cannot be confidently extended to all rock joint situations thus requiring considerable conservatism.

The Geotechnical Group at Monash University is currently investigating a theoretical approach to model the behaviour of a rock joint under the application of a shear load. This work is being extended from previous investigations that were related to the performance of pile rock sockets. Testing to date has indicated that the model can be modified for rock joint analysis.

To maximize the potential application of the proposed model, confidence is required in its ability to model all situations. To provide this level of understanding, considerable testing of the many factors that effect the rock joints behaviour is still required. Once this level of understanding is achieved, it is hoped that a computer aided design tool can be developed.

Siltstone standard deviation angle = 5^0, 5mm chord length, initial normal stress=800kPa, normal stiffness=800kPa/mm

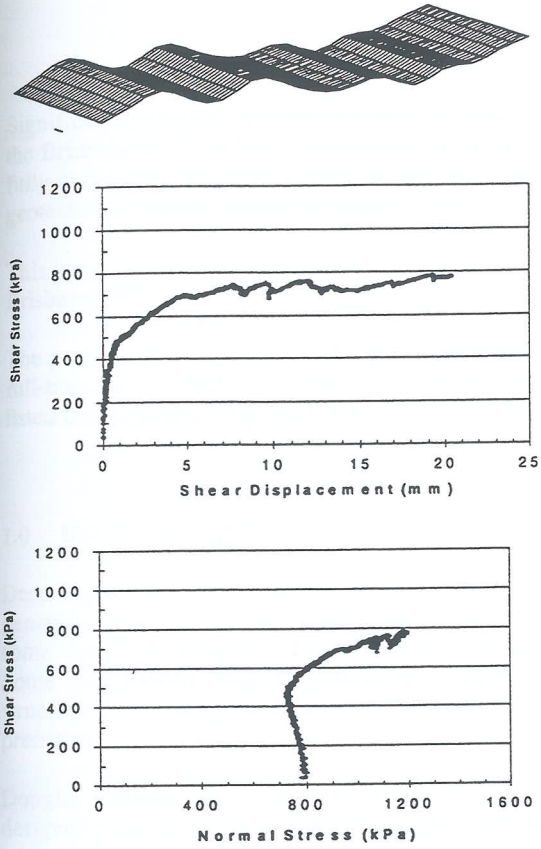

Figure 4 Shear results of s=5^0 siltstone sample

7.0 ACKNOWLEDGEMENTS

The work described in this paper forms part of the ongoing research into the behaviour of rock joints under the application of a shear load funded through the Australian Research Council. The author is financially supported by the Australian Postgraduate Award Council. Grateful acknowledgement of the support provided by the Department of Civil Engineering, its technical staff and in particular my supervisors Chris Haberfield and Julian Seidel is also given.

8.0 REFERENCES

Barton, N. (1973). Review of a new shear - strength criterion for rock joints, *Engineering Geology*, **7**, pp. 287-332.

Checcia de Toledo, P. E. and de Freitas, M. H. (1995). The peak shear strength of filled joints, Fractured and Jointed Rock Masses, pp. 385-392

Collingwood, B., Seidel, J. and Haberfield, C. (1999). Laser based roughness measurement for design and verification of rock socketed piles, 8th ANZ Conference on Geomechanics, pp.

Crawford, A. M. and Curran, J. H. (1981). The influence of shear velocity on the frictional resistance of rock discontinuities, *Int. J. Rock mech. Min. Sci. & Geomech Abstr.*, **18**, pp. 505-518.

Fairhurst, C. (1964). On the validity of hte 'Brazilian' test for brittle materials, *Int. J. Rock Mech. Mining Sci.*, **1**, pp. 535-546.

Fleuter, W. T. (1997). Analytical and experimental investigation into the shear performance of joints in soft sedimentary rocks, Masters Thesis, Civil Eng. , Monash University.

ISRM (1978). Suggested methods for the quantitative description of discontinuities in rock masses, *Int. J. Rock Mech. Min. Sci.*, **15**, pp. 319-368.

Johnston, I. W. and Choi, S. K. (1986). A synthetic soft rock for laboratory model studies, *Geotechnique*, **36**(2), pp. 251-263.

Ladanyi, B. and Archambault, G. (1970). Simulation of shear behaviour of a jointed rock mass, Proc. 11th Symp. on Rock Mech., Rock Mechanics: Theory and Practice, pp. 105-125

Patton, F. D. (1966). Multiple modes of shear failure in rock, Proc. 1st Cong. Int. Soc. Rock Mech., pp. 509-513

Seidel, J. P. (1993). The analysis and design of pile shafts in weak rock, PhD Thesis, Civil Eng. , Monash University.

Excavations In The Brisbane CBD

David Qualischefski
Douglas.

Significant geological non-conformities (ie. shear zones or contact zones) exist within the geological formations that underlie the Brisbane CBD. Where deep excavation is proposed geotechnical modeling of these excavations must be undertaken to fully understand the possible slope failure mechanisms and to design appropriate positive support requirements. Site specific geotechnical models must be verified by inspection and monitoring of the respective excavations.

This paper highlights the geological and geotechnical engineering aspects of some recently completed deep excavations in the Brisbane CBD.

The projects discussed include the Brisbane Casino Carpark which comprised a 22m deep by 80m square excavation where full-time slope stability assessment and inclinometer monitoring were undertaken. The excavation was adjacent to heritage-listed buildings and the project won an ACEA 'Award of Excellence' for Douglas Partners Pty Ltd.

1.0 INTRODUCTION

Deep excavations (ie. deeper than 6m) in soil and rock generally require battering or where space does not permit, some form of temporary support during construction. Some excavations require permanent support if the structure is not designed to support the excavation earth pressures.

Douglas Partners Pty Ltd (DP) Brisbane office have designed excavations on a number of significant projects within the Brisbane CBD in the past seven years. The work included design of support measures and monitoring of the excavation during construction.

Significant shear and contact zones were encountered within these excavations which required detailed stability assessment and ongoing monitoring to ensure that significant failures did not occur. This paper presents an overview of two of these projects namely the Brisbane Casino Carpark and the Central Energy Building at the Royal Brisbane Hospital .

2.0 BRISBANE CASINO CARPARK

2.1 Project and Geotechnical Investigation

The Brisbane Casino underground carpark excavation was 22m deep by 80m square. The site is bounded between George Street, Elizabeth Street, William Street and the Lands Administration Building and is located one city block east of the Brisbane River in the Brisbane CBD.

Field investigations comprised the following:-

- drilling and sampling of nine (9) test bores
- excavation and sampling of five (5) test pits
- pressuremeter testing
- water pressure tests
- rock stress measurements in one bore
- seismic traverses
- mapping of rock exposures

A site plan showing the location of the excavation and the test locations is given in Figure 1.

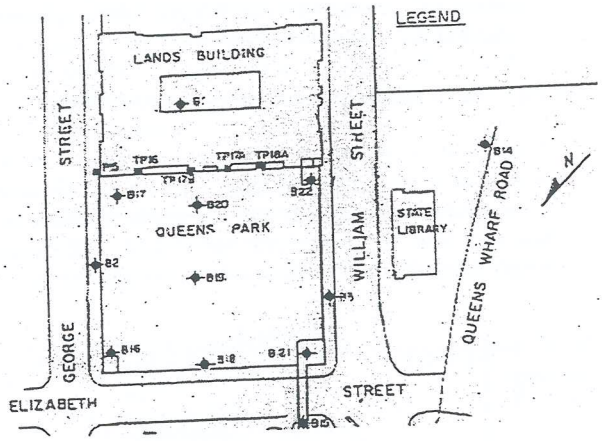

Figure 1 Site Plan

2.2 Subsurface Profile and Regional Geology

The generalised subsurface profile on this site comprised a mantle of variable filling materials and natural very stiff to hard silty clays typically 0m to 5m thick. These soils were overlying bedrock.

Bedrock comprised phyllite, argillite (cleaved shale), and greywacke of the Palaeozoic Age Neranleigh-Fernvale Group which is in close contact with the Pre-Cambrian Bunya Phyllite Group which comprises phyllite, chert and greywacke. Documented information and the results of previous work in the CBD indicated that the "Normanby Fault" was situated close to the site.

The sediments from which the rocks were derived were originally deposited in a deep sea marine environment and have been regionally metamorphosed, folded, tilted, and uplifted. During the deformation and folding processes, the various interbedded rock types have been moved differentially to produce zones of shearing which appear mostly along contacts between essentially 'competent' sandy materials (greywackes) and 'non-competent' muddy materials (argillites, and phyllites).

The original bedding is generally preserved as a strong, parallel and/or slatey cleavage, which can be either straight or tightly folded (crenulated). These rocks are commonly interbedded, steeply (40° to 60°) dipping, and well jointed.

Most joints form as a result of tensile stresses imposed within the rock mass. Such stresses may develop during lithification of strata or during subsequent phases of deformation and folding as the rocks become lithified. Joints often occur along the crests of folds and/or other areas of stress relaxation. Faults, shears and other related geologic structures develop as a result of compressive stresses in the rock. Complex structural patterns may exist in rock strata which have been subjected to multiple phase of tectonic deformation and metamorphism. On this site, jointed rock mass strength and the superimposed surficial weathering processes controlled the geotechnical characteristics of the rock mass.

2.3 Rock Slope Stability and Support Design

The dominant joint and cleavage directions were derived from measurement of rock core samples and site mapping of outcrops near the site and are given in Table 1. All bearings and dip directions are staked with respect to AMG North (True North).

Table 1

Joint Set	Dip (°)	Dip Direction (°)
1	50-80	235-245
2a	80-88	115-145
2b	70-80	295-325
3	45-65	170-180
4	35-45	270-285
Cleavage	**Dip (°)**	**Dip Direction (°)**
C1	30-50	060
C2	55-65	075

The potential failure modes predicted prior to excavation for each face are detailed below:

William Street (Trend 131^0)

Planar failures along cleavage planes which dip out of this face at 40-65^0 to the north-east and wedge failures caused by the intersection of Joint Set 4 and the cleavage plunge out of this face at 40-45^0. Shears zones that parallel the cleavage, also cut this face and were possible causes of planar failures.

Elizabeth Street (Trend 049^0)

Planar failures along Joint Set 2 which dips out of this face at 30-55^0 and which are truncated by the cleavage were considered to be the most likely mode of failure on this face. Wedge failures resulting from the intersection of Joint Sets 2 and 4, which plunge out of this face at 40-45^0. Wedges caused by the intersection of Joint Set 2 and cleavage, which plunges out of this face at approximately 40-65^0.

George Street (Trend 131°)

Wedge failures caused by the intersection of either Joint Sets 1 and 2 which plunge to the south-west at 50-70^0 or Joint Sets 2 and 3 which plunge to the south-west at 55-65^0 and are truncated by the cleavage.

Lands Administration Building (Trend 049°)

Wedge failures caused by the intersection of Joint Sets 1 and 3 which plunge at about 50^0 to the south-west and are truncated by the cleavage.

Geotechnical modelling of the proposed excavation was undertaken. The rock anchor loads required to maintain excavation stability (and hence basement wall loads) were estimated using a 'sliding wedge' analysis for a range of unsurcharged, 'drained', excavation depths to 23m.

The base of the sliding wedge analysis was considered to comprise a continuous, planar joint filled with clay. This was considered to be an upper bound value as it was considered that continuous clay filled joints existed only in the upper portions of deep excavations.

The clay coatings on joints encountered in the bores could not be sampled and the properties used in the stability analysis were estimated based on correlation with Atterberg limit results. The properties used are given in Table 2.

Table 2

Rock Joint Infill Property	Excavation Face	
	George & Elizabeth Sts, Land Administration Building	William Street
Effective cohesion (c') kPa	5	2
Effective friction angle (Ø') degrees	28	22

The maximum estimated anchor loads per metre length of excavation face, calculated for a factor of safety (FOS) of 1.0, are given in Table 3.

Table 3

Excav -ation Depth (m)	Anchor Inclination (°)	Required Anchor Load (kN/m of face)	
		George & Elizabeth Sts, Lands Administration Building Faces	William Street Face
6	10	190	N/C
8	10	360	N/C
1	10	560	N/C
12	10	800	1050
17	10	1900	2300
23	10	4000	4500

N/C Not calculated

Support for the straight sided excavation faces was then designed. The top 2m to 4m depth comprising surface filling, soils, and extremely low strength rock which required continuous support to prevent instability, was supported by anchored, cantilever soldier piles socketed into rock, with timber lagging.

The ground below the soldier pile and lagging comprised competent rock (ie slightly fractured, medium strength phyllite, argillite or greywacke) and was supported by a regular grid of prestressed rock anchors. An anchor spacing of 2m to 3m horizontally was suggested for initial design.

Loose rock zones between the anchors were to be supported by shotcreted and meshed panels.

A diagrammatic representation of the general support details for the excavation faces is given in Figure 2.

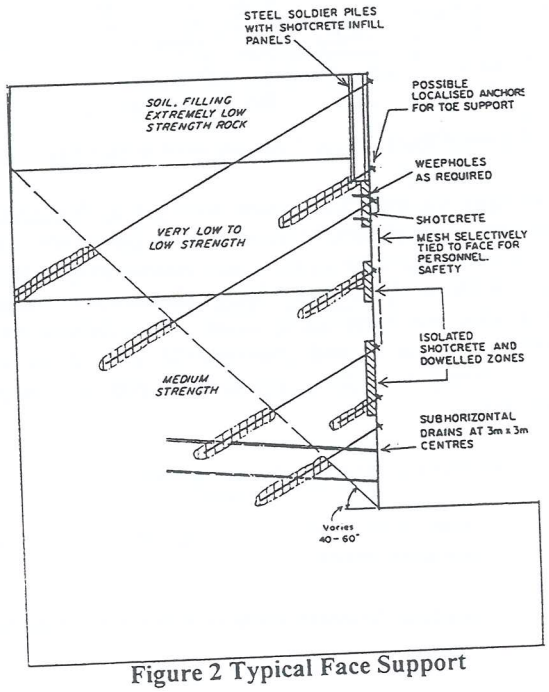

Figure 2 Typical Face Support

Estimated settlement of the ground behind the crest of the excavation due to relaxation of the upper soils and filling materials for a 3m deep vertical cantilevered retaining wall are given in Table 4.

Table 4

Distance from wall (m)	Estimated Settlement (mm)
1	7-9
6	4-5
12	3-4
18	1-2
24	0

The insitu rock stress measurements undertaken in Bore 20 indicated that to the depth tested (ie 14m) no significant stress exists in the rock in excess of geostatic stresses. It was predicted that significant lateral movement of the excavation faces would not occur due to release of 'locked in' tectonic stresses.

3.0 CONSTRUCTION MONITORING

DP monitored the excavation as the work proceeded. This involved progressive mapping of the excavation faces, in particular the locations of support measures, and monitoring lateral movement via inclinometers. Surveying of the condition of the adjacent heritage listed buildings was part of the program. Monitoring results were compared with original predictions - failure mechanisms and excavation face displacements.

About 440 geological discontinuities were mapped during the course of the works. Mapping data were assessed using the 'DIPS' computer software. Figure 3 shows the resulting lower hemisphere stereographic projection contoured plot.

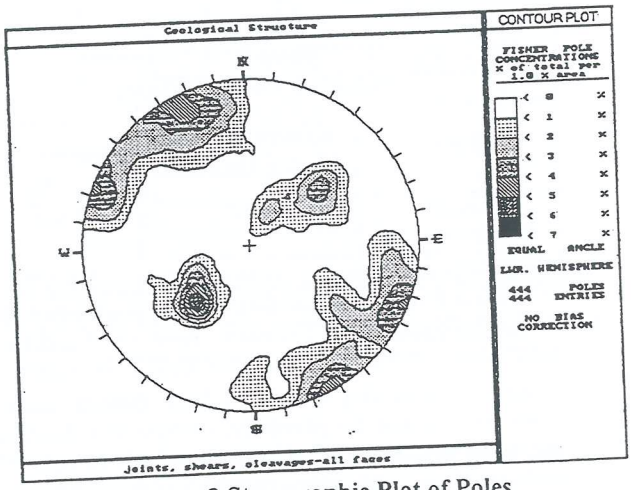

Figure 3 Sterographic Plot of Poles

Two persistent cleavage directions C1 and C2 were identified, one superimposed on the other (i.e. both sets are present within the strata). These are summarised in Table 5.

Table 5

Cleavage Orientations		
Cleavage	Dip	Dip Direction
C1	35-50°	035-060°
C2	55-65°	055-070°

The face mapping also revealed that sheared zones were generally parallel to the cleavage, but often dipped more steeply. Conjugate shear zones were also noted on the George Street face and dip at 20^0 to 45^0 opposite to the cleavage.

Mapped cleavage orientations compared well with the predicted ones.

Five joint sets were interpreted, including two steeply dipping, conjugate sets (1a and 1b) trending at 20^0 to 30^0 and 55^0 to 65^0. These steep joints strike approximately parallel and up to 15° on either side of the cleavage dip direction. Set J2 almost parallels the cleavage but dips 90° in the opposite direction. Joint sets 3 and 4 are minor sets. Table 6 lists the joint sets.

Table 6

Joint Set Orientations			
Joint Set	Measured		Corresponding Predicted Joint Set
	Dip	Dip Direction	
1a	80-90	325-335 145-155	Joint Set 2b
1b	80-90	110-120 290-300	Joint Set 2a
2	15-25	210-220	Joint Set 3
3	50-60	230-240	Joint Set 1
4	60-70	302-312	Joint Set 2b

Potential wedge failures identified by mapping are summarised in Table 7

Table 7

Potential Wedge Failures		
Face	Excavated Wall Facing Direction	Joint Combinations (°M)
Lands Administration	319°	2 and 1
Elizabeth Street	139°	C2 and 1
William Street	041°	C2 and 1a
George Street	221°	3 and 1a

Samples of silty clay recovered from sheared zones and joints were tested for plasticity, particle size distribution and shear strength to check the initial predictions. This testing indicated an effective friction angle (Ø') in the range of 23^0 to 36^0 and an effective cohesion c' of 4kPa and 22kPa. A comparison of the initial failure plane joint properties used in the design and those used on the basis of the laboratory testing are presented in Table 8

Table 8

Rock Joint Infill Property	Predicted Design		Measured
Effective cohesion (c') kPa	5	2	4
Effective friction angle (Ø') degrees	28	22	26

Monitoring of the excavation faces, including mapping and laboratory testing of joint infill materials, verified the initial geotechnical assumptions. The dominant failure mechanisms identified during excavation were planar wedges.

The distribution of the principal rock types ie argillite, phyllite, and greywacke, is shown on Figure 4. A number of shear zones are also shown.

Zones identified in the investigation were mapped as continuous structures across the excavation. These sheared zones were generally less than 200mm wide and comprised firm clays grading to extremely low strength rock as infill materials. Some clay seams within the crush and shear zones extended below full excavation depth.

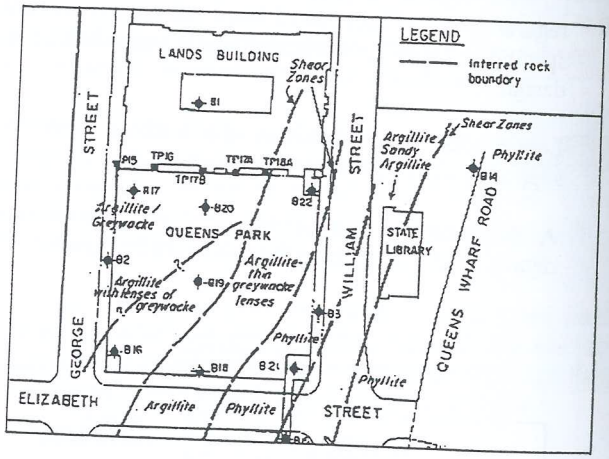

Figure 4 Rock Types Encountered in the Excavation

Generally the excavation faces were stable throughout the duration of the project, however a minor instability occurred in the corner bounded by the Lands Administration Building and William Street. A 6mm displacement into the excavation was noted along a rock wedge defined by Joint Set 4, Joint Set 1a and Cleavage C2. Part of the wedge failed during excavation and the resulting overhang was removed.

The contributing factors to this failure were:

- water from services entering the face along joints and shear zones.
- omission to install anchors in this area of the face.

The encountered sheared zones tended to deteriorate quickly once exposed. These materials slake, potentially undermining the slope if not locally stabilised. Rock bolts which fasten shotcrete and mesh panels were used to seal these sub-vertical clay filled shear zones which were relatively continuous (i.e. 10m to 20m long) in the Elizabeth Street, George Street corner.

The results of inclinometer monitoring along the Lands Administration Building face indicated maximum movement of 8mm into the excavation.

4.0 ROYAL BRISBANE HOSPITAL

4.1 Project and Geotechnical Investigation

The Royal Brisbane Hospital is located in the suburb of Herston, approximately 5kms north-west of the Brisbane CBD. The construction of the Central Energy Building at this hospital required the enlargement, benching, and stabilisation of an existing three sided, 13m high excavation (originally a quarry).

A low cost geotechnical investigation was undertaken comprising:

- drilling and sampling of five (5) shallow test bores
- (ie to maximum depth of 5m)
- mapping of rock exposures

The layout of the proposed excavation is shown on Figure 5

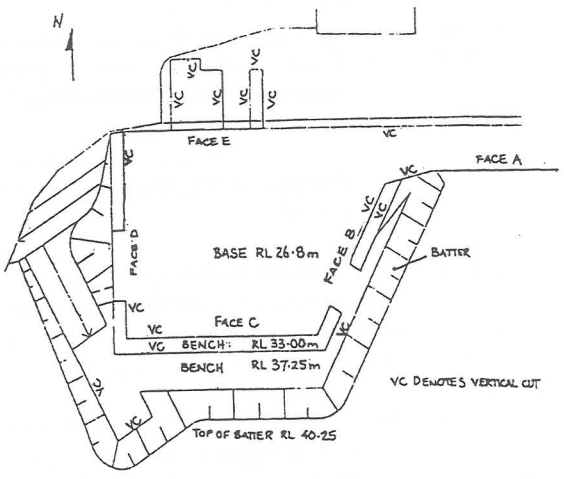

Figure 5 Site Plan

4.2 Subsurface Profile and Regional Geology

The generalised subsurface profile around the top slopes of the quarry comprised a mantle of variable filling materials and natural very stiff to hard silty clays typically 0m to 2m thick. These soils were underlain by bedrock, comprising rhyolitic tuff and ignimbrite of the Triassic Age Brisbane Tuff Formation.

The Brisbane Tuff generally overlies phyllite, argillite (cleaved shale), and greywacke of the Palaeozoic Age Neranleigh-Fernvale Beds in the Brisbane inner city area. The zone between these two rock formations is known as the contact zone. This typically comprises silty clays or weathered rock and varies in thickness. The tuff immediately above the contact zone is often highly brecciated.

The Brisbane Tuff originated as ash ignimbrite ejected by volcanic explosions. The ash flowed down gullies and infilled low lying areas of the original landscape. The rapidly cooling ash typically formed a high strength massive rock mass.

Preferential weathering of the weaker underlying strata has resulted in the development of some tuff cliffs within inner areas of Brisbane. The tuff formation is typically characterised as high strength, massive to jointed. On this site jointing of this rock mass controlled the geotechnical characteristics.

4.3 Rock Slope Stability and Support Design

Dominant joint sets recorded during site mapping of exposed quarry faces are given in Table 9.

Table 9

Joint Set	Dip (°)	Dip Direction (°)
1a	75-90	030 –350
1b	75-90	190 – 220
2a	75-90	305-330
2b	65-85	150-180
3	65-75	250-290
4a	20-35	55-85
4b	30-50	290-330

The geotechnical model for the initial design comprised a uniform rock mass of Brisbane Tuff that was slightly weathered to fresh. Potential failure mechanisms for the existing excavated tuff faces comprised planar slides and block toppling.

Analysis of the proposed 13m high, benched profiles indicated that rock anchors would be required for temporary excavation stability.

Design parameters for the clay coatings on the jointed rock mass were based on past experience and are given in Table 10.

Table 10

Rock Joint Infill Property	All Faces
Effective cohesion (c') kPa	5
Effective friction angle (Ø') degrees	26

Excavation faces A to E were indicated in Figure 5.

The excavation profile of faces B and C was to be a vertical slope, benched at 6m and 9m above the base. The bench widths were to be 3m and 5m wide respectively. Face D was to have a single bench 3m wide at 6m above the base. Face E was to be a vertical 6m high face. Faces B, C, D and E were anchored for temporary support.

Face A, was to be left in its original condition with only localised support provided to wedges. A typical excavated and anchored profile is shown on Figure 6.

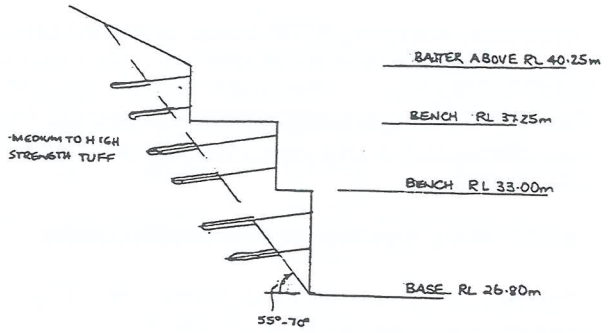

Figure 6 Typical Face Support

Each excavation profile was modeled using planar sliding wedge stability analyses incorporating various surcharge loadings for a factor of safety (FOS) of 1.5. The design estimated anchor loads per meter of excavation face are given in Table 11.

Table 11

Face (m)	Anchor Inclination (°)	Required Anchor Load (kN/m of face)
A	15	NR
B	15	1240
C	15	1775
D	15	1200
E	15	900

NR – not required

5.0 CONSTRUCTION MONITORING

The ground was excavated in a controlled manner Anchors were installed after each bench level was reached before the excavation was deepened to the next bench level. On all sides, high strength, jointed, slightly weathered tuff rock was encountered down to approximately RL 35.0 ie just above the lower bench level. The joints were generally up to 15mm wide, non-continuous, sub-vertical, either rough oxide coated or clay filled.

In the south-western corner of the excavation, at the intersection of faces C and D, the tuff rock strength deteriorated rapidly with depth (ie 1m to 2m) below RL 35.0 to reveal the contact zone. Further localised excavation on face D was undertaken to assess the quality, thickness and orientation (ie. dip/dip direction) of the contact zone materials and the underlying Neranleigh-Fernvale formation.

The mapping confirmed that the contact zone on face D dipped at 17° to 26° to the north-east and plunged to the north.

A typical cross section profile through the tuff, contact zone, and underlying phyllite on face D comprised:

1.2m to 1.5m thick very high strength rhyolitic tuff overlying a 1.5m thick contact zone (ie the older land surface). The latter comprised:

0.1m thick	low strength ash fall tuff
0.15m thick	extremely low strength, tuffaceous claystone, fissured, and slickensided
0.25m thick	very low strength carbonaceous mudstone which contained tree fragments and represented the old land surface.
1.0m thick	very low strength with zones of low to medium strength "scree breccia" and comprising fragments of the underlying phyllite.

Below the contact zone the phyllite rock mass was generally low to medium strength, moderately weathered with a cleavage dipping at 18° to 32° to the north-east and plunging to the north.

The intersection of faces C and D showing the orientation of the contact zone as it daylights in faces and dips below the floor of the excavation is shown in Figure 7 below.

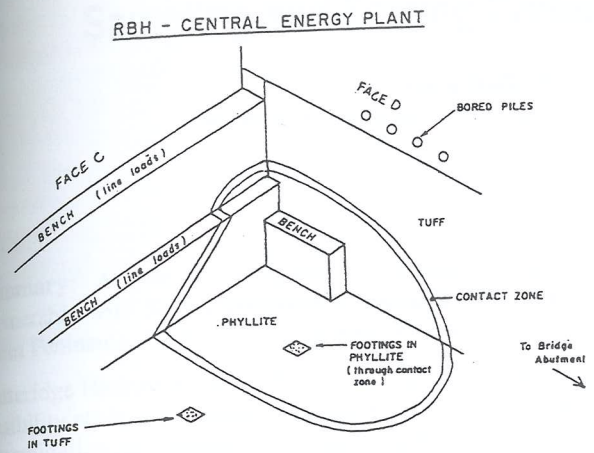

Figure 7 Intersection of Faces C & D

Due to the orientation of the contact zone and the vertical excavation of face D, a 5m to 13m high block of jointed high strength tuff was surcharging the 10m long planar surface of the contact zone. A large planar failure into the excavation was possible.

A check of the orientation of the contact zone behind the face and the length and capacity of the anchors installed above the contact zone indicated an adequate factor of safety (FOS) against planar slide.

An intrusive dyke was encountered below RL 29 in the south-west corner of the excavation, at the intersection of faces B and C. The dyke comprised very low to low strength tuffaceous mudstone which was friable and highly fissured. The mudstone dipped at 45° to 50° into the excavation and plunged north.

The remainder of the excavation encountered jointed, high strength, slightly weathered tuff with some minor moderately weathered zones.

The different rock types encountered in the excavation and the location of the contact zone and the intrusive dyke structure are shown in Figure 8.

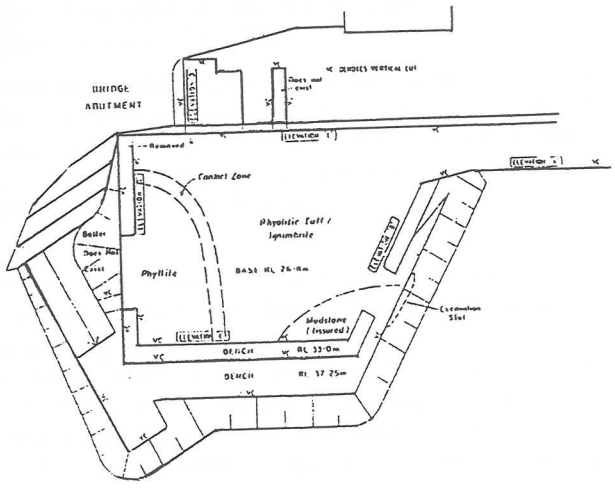

Figure 8 Plan showing rock types and discontinuities

Additional building loads were imposed on the benches as the building design evolved during construction. This necessitated the re-analysis of both local bench and global face stability.

5.1 Implications for the Development

The contact zone and intrusive dyke, which both dipped beneath the floor of the excavation and behind faces B,C, and D, had stability implications for the proposed building and excavation faces.

Due to the poorer quality materials of these major discontinuities, careful assessment of the bearing capacity and associated settlement of high level building foundations located at the floor of the excavation was required. Where insufficient depth of competent tuff existed above the contact zone/dyke materials,. bored piles were redesigned to transfer building loads to the underlying phyllite.

On face D where a major plane of instability was present the building foundations were changed to bored piles which were sleeved through tuff and contact zone and transferred the building loads to the underlying competent phyllite.

6.0 CONCLUSIONS

Where significant excavations are planned an appropriate scale of geotechnical investigation must be undertaken. The potential failure mechanisms can then be identified via modelling of the excavation . The appropriate excavation support can then be designed.

This investigation and modelling process provides a window into the site conditions. Monitoring of the excavation faces must be undertaken as it progresses to check the relevance of the model. Where conditions change, re-analysis must be undertaken and the support methods altered as required. Sometimes this has implications for the proposed development.

In the projects discussed in this paper significant shear zones or contact zones were encountered during the excavation process. In the RBH site the contact zone was not anticipated and in the Casino Carpark the extent of the shear zones could not be accurately gauged prior to excavation.

Only the on-site monitoring during excavation identified how continuous these discontinuity zones were. Proper geotechnical supervision and analysis was required on almost a continuous basis to ensure stability of the excavation and safety of the personnel working on-site.

Sampling and Testing Cretaceous Claystone near Darwin, NT

Greg Ralls BE(Hons), BSc, Grad IEAust
Geotechnical Engineer, Gutteridge Haskins & Davey Pty Ltd, Perth, Western Australia

Summary: As part of a proposed $10 billion development of Timor Sea gas reserves, Woodside Energy Ltd in joint venture partnership with Shell Development Australia evaluated an onshore LNG processing plant to be situated at Glyde Point, on the Gunn Peninsula about 45 km north-east of Darwin, in the Northern Territory.

Gutteridge Haskins & Davey Pty Ltd was commissioned to perform a preliminary geotechnical investigation as part of the project feasibility study. The work included an assessment of the suitability of the site for the proposed development, to facilitate the determination of foundation design parameters for 120,000 cubic metre capacity LNG storage tanks and the prediction of settlements of shallow footings.

The site was found to be underlain by a monotonous sequence of weathered, lateritised kaolinitic claystone and shale, or clay shale, becoming montmorillonitic with depth. Difficulties experienced during the investigation included a slower than anticipated rate of drilling in "soft" rock, disturbance during drilling, remoulding of cored samples, and difficulty in recovering "undisturbed" samples.

The evaluation of the field and laboratory data included reconciliation of field and laboratory test results and charting variation in basic soil parameters with depth. A large discordance was found between various methods of strength and deformation characteristic evaluation. Due to lateritisation of an overconsolidated profile, the usual strength and depth relationships were not observed, and these anomalies had to be taken into account in developing a geotechnical site model.

The paper summarises the main conclusions drawn from the work, including identification of limitations of the investigation procedures and a recommendation of alternative testing methods for future detailed geotechnical investigations on the site.

1 PROJECT BACKGROUND

Details of the proposed Northern Australia Gas Venture (NAGV) were released for public access in 1999 by Woodside Energy Ltd and Shell Development Australia. The NAGV project was established in May 1997, to evaluate the feasibility of producing LNG from gas fields in the Timor Sea.

The feasibility study was finalised in December 1998, and included assessment of offshore production facilities, a 600 km subsea pipeline, and the proposed onshore LNG processing facility at Glyde Point.

The onshore plant site covers about 600 hectares, and was selected following consideration of land access in light of land claims, proximity to Darwin, marine access to deep water and environmental, and operational considerations regarding potential future development.

Process facilities were planned to comprise a LNG Plant consisting of two Propane-Mixed Refrigerant LNG trains, a 500 million standard cubic feet per day capacity domestic gas plant, and two train 5300 tonnes per day Condensate Stabilisation Plant. LNG storage facilities comprise two 120,000 cubic metre capacity containment tanks, with prestressed concrete walls and reinforced concrete base slab and roof, and condensate storage facilities comprising two 70,000 cubic metre floating roof tanks.

Relatively little existing data was available for the onshore plant site location, and substantial site survey and surface and subsurface investigations were therefore essential to the feasibility study.

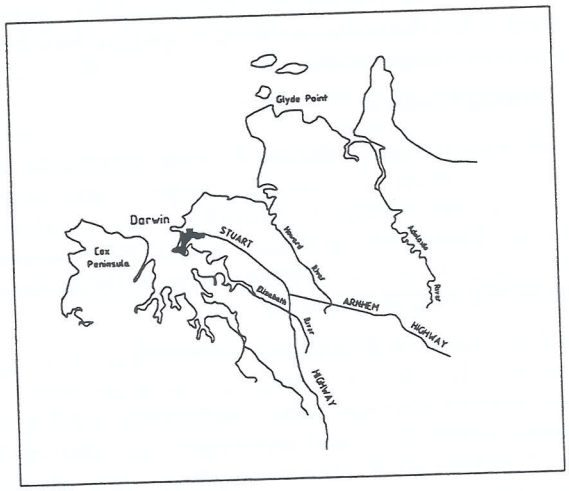

Figure 1: Locality Plan

2 GEOLOGICAL SETTING

According to published geological information (Pietsch, 1983 & 1985), the region is underlain by flat-lying Early Proterozoic and Cretaceous fluviatile, shallow-marine, and chemical sediments of the Bathurst Island Formation (BIF).

Glyde Point itself is underlain by a BIF member known as the Wangarlu Mudstone Member (WMM). The WMM is reported to be conformable with, lithologically similar to, and visually indistinguishable from an underlying unit called the Darwin Member (DM). Both units are reported to consist of weathered, kaolinitic claystone and minor, silty claystone, which becomes montmorillonitic at depth. The claystone is silicified in places and calcareous at depth, with shelly fragments commonly present. The lower boundary of the DM consists of a marker horizon of bioturbated material contained within thin carbonate beds. The combined thickness of the WMM and DM is inferred to be greater than 70 m.

3 FIELD INVESTIGATIONS

3.1 Locality Description

The Glyde Point site has low topographic relief, and is fringed on three sides by tidal mangrove swamps. Medium density vegetation comprising eucalyptus and mixed scrub plant species such as pandanus, melaleuca, grevillea and acacia is characteristic of the area. The coastal mangrove fringe is a saltwater crocodile habitat. Accordingly, the project-specific Health, Safety, Environment and Aboriginal Heritage Management Plan which was written to comply with client health and safety requirements also included a section titled "Crocodile Safety Plan", prepared in consultation with Wildlife Management International Pty Ltd and the Parks & Wildlife Commission of the Northern Territory. This document served as a training tool for the protection of field personnel.

3.2 Drilling Program

The site work comprised drilling 25 vertical boreholes on a grid pattern across the site, by washbore and wireline diamond drilling techniques. The drilling was performed by contractor, Bachy, who mobilised a TRH tractor-mounted rotary drilling rig, and the boreholes were drilled to varying depths up to a maximum of 60 m.

Each of the holes was drilled by washbore to a nominal depth of 5 m, then HQ diamond coring to the target depth. A polymer mud additive was used to stabilise the holes during washboring, however, water flush only was used during diamond drilling in weathered claystone, with the hole typically cased over the top 3 m. Sixteen boreholes were drilled to 10 m, five of which were drilled by washbore only to allow in situ testing.

3.3 In Situ Sampling & Testing

Recovery of "undisturbed" U65 tube samples was attempted in soil, however, the ground was too hard and sampling proved to be impracticable. Intact, "semi-undisturbed" samples for laboratory testing were recovered removing diamond drill core from the triple tube inner core barrel. After cleaning off the mud cake from the outside of the core, it was placed inside transparent lay-flat plastic, and taped and stored inside HQ-sized split PVC tubing for transport to the testing laboratory. Shrinkage cracking of the core tended to occur on exposure to air, due to the effect of sun-drying, therefore placement of moistened rags was necessary whilst the logging was performed, prior to sampling of the core.

Standard Penetration Tests (SPT) were carried out at 1 m intervals in each of the washbore holes, to depths of either 5 m or 10 m, depending on the depth of washboring. The testing was carried out in accordance with the Australian Standard procedure, using a drive hammer of 63.5 kg mass falling 760 mm with automatic trip mechanism. Disturbed SPT split-spoon samples were retained for laboratory classification testing.

Pocket penetrometer tests were carried out on the drill core.

4 SUBSURFACE CONDITIONS

4.1 Soil Profile

The borehole results revealed materials in the upper 5 m consisting of surficial colluvial lateritic gravels overlying inorganic, low to high plasticity, red-brown and orange mottled clays. The clays were typically very stiff to hard in consistency, in dry condition and characterised by variable weak iron-cementing.

Beyond about 5 m depth, the ground conditions comprised partly-indurated residual soil, generally red-brown, orange and grey mottled or grey, and often containing iron-oxide coated joints and microfractures in a random pattern and orientation. The indurated zones tended to be brittle and to fragment easily, and were assessed as being weak rock, with strength in the extremely low to low range. Induration can be attributed mainly to silicification, which has occurred through mobilisation of silica and precipitation through groundwater fluctuations within the soil profile (Nyland & Gerner, 1984; Clarke et al, 1999).

The nature of the materials is consistent with the Tertiary chemical weathering described by Pietsch (1983), and is typical of deep trizonal lateritised soil profiles found throughout the region, and comprises zones described on the basis of colour, soil mineralogy and formation processes as either ferruginous, mottled, or pallid. The uppermost layers are enriched in iron and aluminium oxides, and the underlying pallid zone material is depleted, as a result of leaching of iron and aluminium. Nyland & Gerner (1984) have previously reported the presence of rock within the profile. Lateritised siltstone is common in a hardened mottled zone, and silicified claystone, referred to locally as "porcellanite", and kaolinitised siltstone can occur within the pallid zone. The uppermost ferruginous zone also often contains an indurated, strongly-cemented layer of pisolitic laterite, of variable thickness and lateral extent, however, this layer was mostly absent from Glyde Point, and had probably eroded away, leaving behind the layer of colluvial gravel.

Significant loss of drilling circulation fluid occurred in one of the boreholes, the loss occurring within the mottled portion of the profile through sub-horizontal cavities up to 20 mm in diameter. Similar features, locally termed "rat holes", are reported to exist in the Darwin area and form active channels of high secondary permeability through otherwise relatively impervious materials (Nyland and Gerner, 1984).

The transition between the pallid zone and underlying bedrock was typically not sharply defined, and occurred between 20 - 50 m depth.

4.2 Bedrock

The bedrock was found to consist of dark grey interbedded claystone and shale. The claystone is massive, and based on simple field identification criteria ranges from extremely low to medium strength. The shaly zones characteristically had a penetrative horizontal fabric, and as a result of marked strength anisotropy drilling breaks were closely-spaced. The widely-used classification scheme proposed by Moye (1955) was used to describe degree of weathering, according to which the material appeared to be mainly in the extremely weathered to slightly weathered range. Since claystone and shale are composed of clay minerals, however, weathering is predominantly a process of reverse induration, and a clear distinction between the various grades of weathering is therefore difficult to make. An alternative classification scheme is that proposed for Sydney shale by Pells et al (1978), under which the material at Glyde Point can be categorised as Class IV to Class V shale. According to the text book definition of Attewell and Farmer (1976), materials comprising soil / rock with a high clay content and a tendency towards fissility can also be grouped collectively under the term clay shale. Johnston (1991) reports a definition of "soft" rock material with overlapping boundaries between Unconfined Compressive Strength (UCS) values for clay and rock, based on International Society for Rock Mechanics (ISRM) classification, and describes several shortcomings of in situ and laboratory testing of materials which fall into this category.

Recovery greater than 100% was recorded on many of the drilling runs in the more shaly zones, and the rock material was therefore inferred to be composed of indurated expansive montmorillonitic clay particles. The swelling, common in weak shale, occurs because of the combined effect of unloading from overburden removal and the wetting caused by drilling resulting in volumetric expansion.

Blocking of the diamond drill bit waterways occurred several times in the deeper boreholes, typically in zones of transition between competent claystone and weathered or weaker shaly material. Drilling progress was slow as a result of the need to remove the drill rods from the hole in order to unblock bit waterways. To reduce the frequency of blocking, a relatively low bit pressure, high rate of rotation and high water pressure were maintained through most of the drilling. A face discharge bit was used initially but was replaced by a stepped bit, with side discharge waterways.

4.3 Groundwater

Standpipe piezometers consisting of 50 mm slotted PVC were installed in five of the boreholes, and groundwater samples recovered for laboratory testing, in accordance with British Standard BS 5930. Chemical analyses performed on the samples revealed low pH values of the order 3.0, which was initially suspected to indicate prevailing acid-sulphate soil conditions. Further sampling and testing revealed low sulphate (SO_4) concentrations, and it was later found that acidic groundwater is widespread in coastal areas of the Northern Territory, and occurs as a result of dissolved CO_2 originating from the high CO_2 respiration rate of tree and plant roots in aquifer recharge areas during the wet season (Marks and Jolly, 1987).

Acidic groundwater conditions would have an impact on foundation construction, particularly piled foundations. According to the American Concrete Institute (ACI) Guide to Durable Concrete (1992), a protective barrier system would be necessary to prevent the corrosion of concrete. Similarly, a protective barrier system would also be required to prevent the corrosion of steel piles.

5 IN SITU AND LABORATORY TESTING

The laboratory testing which is summarised in Table 1 below was carried out on selected core samples recovered from diamond drilling:

Test	Qty	Purpose
Moisture Content and Dry Density	55	Indirect determination of material strength and deformation parameters
Point Load Index	10	Indirect assessment of material strength
Unconfined Compression	33	Direct assessment of strength and indirect assessment of deformation parameters
Unconsolidated Undrained Multi-stage Triaxial	2	Direct assessment of strength and deformation parameters
Consolidated Undrained Multi-stage Triaxial	3	

Table 1: Laboratory Testing

Core sample selection in soil and rock materials was restricted by the minimum length of intact sample required for testing and fragmented nature of the core. Triaxial testing of soil materials was carried out under the presumption that confining pressures would reinstate the sample to a condition of integrity close to that of an undisturbed sample.

6 ANALYSIS OF DATA

6.1 Laboratory Test Data

The results of the laboratory testing showed that the soil strength was relatively high, and the rock material strength generally low. For example, the maximum measured UCS value was 2.7 MPa, recorded for a sample recovered at a depth of 57 m, and pocket penetrometer testing with an upper limit of 450 kPa was able to be carried out throughout the profile. Johnstone (1991) reports a definition of "soft" rock material with overlapping boundaries between UCS values for clay and rock, for strengths between 0.5 and 25 MPa, under which basis the materials can largely be termed "soft" rock. The UCS results are similar to those reported by Sales (1988), for the testing of the foundations of the bridges constructed to provide access to the Channel Island Power Station, at Elizabeth River and Channel Island. The UCS values in the upper 12 m of the profile ranged between 0.5 MPa and 2.5 MPa. By contrast, Clarke et al (1999) reported the range of compressive strengths for silicified material, or porcellanite, in the Darwin region as being between 2 and 160 MPa, which is significantly higher than for the silicified materials at Glyde Point. Strictly speaking, therefore, the materials at Glyde Point cannot be referred to as porcellanite.

For the materials at depth, a simple least squares linear regression analysis was performed to investigate the relationship between UCS and Young's Modulus, (E). Assuming the material behaviour to be like that of a cohesive soil, the undrained shear strength, (S_u,) was taken as half of the UCS value, and the ratio E/S_u compared with ratios published in the literature and available in standard soil mechanics texts. A relationship $E = 228\ S_u$ was derived, which is comparable with the relationship reported for overconsolidated clays by Bromham and Styles (1971), namely, $E = 250\ S_u$. The minimum plasticity index (PI) value for materials at Glyde Point was determined to be 32%, and Bowles (1997) quotes the relationship $E_s = (100$ to $500)\ S_u$, for materials which have a PI greater than 30.

A comparison was also made between the various other parameters, either measured or derived from field and laboratory data. The relationship between moisture content versus dry density was examined, and an inverse linear trend observed, and the relationship between moisture content versus E was examined, to determine whether a simple correlation could be made allowing E to be derived from moisture content tests, which are cheap and easy to perform, rather than unconfined compression and triaxial tests.

Correlations between E and UCS and moisture content exist for other similar geologic materials both in Darwin and elsewhere in Australia, and form the basis for an expected relationship between these parameters at Glyde Point. Nyland and Gerner (1984) presented a chart which shows moisture contents ranging from 4 to 24% and corresponding UCS values between 6 and 20 MPa, for BIF siltstone and claystone in the Darwin region. Ghafoori et al (1993) reported a relationship between moisture content and unconfined compressive strength for Ashfield Shale, from the Sydney Basin, in New South Wales, for a range of moisture contents between 1 and 9% and corresponding UCS values between 2 and 35 MPa, and Johnston (1992) reported the trend of saturation moisture content against secant modulus values for Melbourne mudstone, with moisture contents ranging from 3 to 16%, and modulus values in the range 100 and 6000 MPa.

The range of results at Glyde Point, for both E and UCS values was lower and moisture contents greater than for each of the three regions above. The results also showed a wide scatter and no clearly defined trend. The lack of a relationship between the measured parameters reflects the varying degrees of sample disturbance which inevitably occurred due to the drilling and sampling procedures which were used.

6.2 Standard Penetration Tests

Johnston (1991) has described several shortcomings of in situ and laboratory testing of materials which fall into the "soft" rock category, including mention of the fact that SPT is generally precluded because of the effort required to penetrate the materials.

At Glyde Point, a plot of the results of SPT versus depth for the upper 10 m revealed a wide scatter of results, reflecting varying degrees of cementing caused by lateritic weathering and / or silicification of the soil profile. The SPT N-values were therefore found to be most useful as a crude indicator to discriminate between materials behaving as either soil or as weak rock.

Look (1997) discusses the interpretation of SPT N-values when SPT refusal occurs. SPT refusal, defined in Australia as 30 blows for less than 100 mm penetration or hammer bounce on 5 consecutive blows, is typical in hard soils and weak rock. Equivalent N-values can be determined, although there is no standard procedure for doing so. The simplest method of determining equivalent N-values is to assume a linear increase in blows with depth. If the values obtained fall within the range of 80-200, as was typically encountered at Glyde Point, the result is considered to be characteristic of weak rock.

6.3 Point Load Testing

The limited number of point load test results Point Load Index (Is_{50}) were compared with UCS values and a relationship $UCS = 13\ Is_{50}$ found by linear regression, with a corresponding correlation coefficient of 0.55. The constant in this equation is about half of the value reported by Pells (1975), but is consistent with the relationship reported by Nyland and Gerner (1984). It can be concluded, however, that since there is a poor correlation between Is_{50} and UCS values, point load testing is an inappropriate testing procedure for predicting the compressive strength of material such as the clay shale encountered at Glyde Point. The test results, however, did confirm that the rock material strength is in the extremely low to very low range ($Is_{50} < 0.1$ MPa).

6.4 Rock Mass Rating

An assessment of the Rock Mass Rating (RMR) was made using the method established by Bieniawski (1989). RMR determination was deemed to be appropriate for rock mass

characterisation as it takes into account the strength of intact material, RQD, discontinuity spacing, the condition of discontinuities, and the presence of groundwater. From the RMR values, E was derived using the Bieniawski formula. The RMR method, however, generally has applicability to higher strength rock masses. The derived moduli values were generally an order of magnitude higher than those established by laboratory methods, and were therefore considered to be an upper bound estimate.

6.5 Geotechnical Model

The end result of the interpretation of data was a seven-layer geotechnical model, comprising zones of relatively low strength surficial soil, higher strength indurated weak rock, low strength hard clay, weak interbedded clay shale and intact claystone, and finally higher strength massive claystone bedrock. Unique strength and deformation properties were identified for each zone, and as the properties based primarily on the results of the laboratory UCS and triaxial testing.

7 ALTERNATIVE TESTING METHODS

In light of difficulty experienced obtaining good quality samples for laboratory testing, in situ testing is generally the most suitable means of determining strength and stiffness parameters for detailed design. Typical in situ testing methods include surface seismic refraction surveying, crosshole seismic measurements, high range pressuremeter and self-boring pressuremeter testing (Ervin, 1983). The latter of these methods would be likely to produce the most reliable results, because the test procedure does not rely upon insertion of the testing equipment into a pre-bored hole. Pre-boring in low strength clay shales is likely to result in softening and possibly erosion of the sides of the hole and therefore adversely affect the testing results. Pile load testing is another routine procedure however is the most costly means of establishing design parameters.

Sales (1988) reports the results of pressuremeter and pile load tests carried out for the design of foundations for the Channel Island bridges. The ground conditions comprised completely to moderately weathered, sub-vertically bedded siltstone and phyllite. The results showed a backfigured rock modulus of twice the measured pressuremeter modulus under compressive loading, and approximately equal values under lateral loading. At Glyde Point, it is evident that since the clay shale is horizontally bedded, the modulus under lateral loading conditions will be higher than under compressive loading, and pressuremeter testing is therefore likely to underestimate the true range of rock mass modulus values for compressive pile loading conditions.

8 APPLICATION TO PILED FOUNDATIONS

8.1 Pile Types

As a part of the work carried out, an assessment and recommendations were made regarding suitable piling techniques. Due to the presence of alternating strata of hard soil and "soft" rock, there are significant disadvantages to driven pile footings:

- the near-surface cemented layer would be impenetrable to all except small solid section or tubular steel piles
- alternating bands of weak rock and hard clay would result in slow and erratic penetration rates. Although pre-boring would be possible it would be uneconomic to use a two-stage installation system to any significant depth
- the high level of energy required to drive piles would significantly disturb weak, brittle rock, and would reduce rather than increase the capacity gained by side adhesion.

Bored cast-in-place piles, on the other hand, were assessed as having several advantages:

- more reliable adhesion because of lesser disturbance
- the larger pile diameter which can be used provides a significant end-bearing component
- larger diameter piles enable inspection of the base and adjustment to the founding depth is not costly

Rock socketed piles were used in construction of foundations for the Elizabeth River and Channel Island bridges (Sales, 1988).

8.2 Pile Design

Preliminary design calculations were carried out to determine pile capacities, using parameters from the geotechnical model to derive ultimate shaft adhesion and end bearing resistance values. Ultimate fully mobilised adhesion for stiff to hard clays in the literature (Poulos & Davis, 1989; Winterkorn & Fang, 1975) is recommended as not greater than 0.4 - 0.5 S_u for both driven and bored piles, and the geotechnical strength reduction factor in AS 2159 - 1995 is taken as 0.45. With an average load factor of 1.35, this is equivalent to a factor of safety of 3. For brittle soil conditions, such as at Glyde Point, a skin friction of slightly less than 0.4 S_u was recommended. The ultimate end bearing resistance was calculated as 4.5 times the unconfined compression strength, consistent with 9 times the undrained cohesion for clays, as recommended by Poulos (1989) and AS 2159. Since very little definition was given of the actual design loading conditions, the calculations performed were limited to prediction of pile capacities for only two simple example pile diameters and lengths, namely piles of 0.5 m and 1.5 m diameter and 15 m and 40 m length, with predicted ultimate capacities of 2,500 kN and 22,000 kN respectively.

9 CONCLUSIONS

A geotechnical investigation has been carried out as part of the feasibility study for a proposed LNG processing facility at Glyde Point, near Darwin, in the Northern Territory. The local geology comprises material which can be described as lateritised clay shale, forming part of a geological unit named

the Wangarlu Mudstone Member, within the Bathurst Island Formation.

The nature of the material encountered is similar to that in the Darwin city area. The material strength is low and typical of a group of materials which can be referred to as "soft" rock. Conventional investigation sampling and testing techniques, namely SPT and "undisturbed" thin-walled tube sampling are generally inadequate, as the material strength is too high both for meaningful results to be obtained and for samples to be recovered.

Good core recovery can be obtained from diamond drilling operations, however sampling disturbance is difficult to avoid due to low material strength, wetting of lateritised material and remoulding and swelling during drilling of shaly material, and mechanical disturbance during removal from the inner core barrel.

In situ pressuremeter testing is recommended as a more suitable method of determining elastic deformation parameters, and combined with the results of unconfined compressive strength testing is considered likely to be the most suitable method for obtaining parameters for design of piled foundations.

10 ACKNOWLEDGEMENTS

The author wishes to thank Woodside Energy Ltd for giving their kind permission to publish the paper, and senior geotechnical engineering staff at GHD for their assistance.

10 REFERENCES

1. American Concrete Institute. *Guide to Durable Concrete ACI 201.2R-92*. 1992.
2. American Petroleum Institute. *API Recommended Practice 2A-LRFD (RP 2A-LRFD) - Recommended Practice for Planning, Designing and Constructing Fixed Offshore Platforms - Load and Resistance Factor Design*. First Edition, July 1, 1993.
3. AS 2159 - 1995. *Piling - Design and Installation*. Standards Association of Australia.
4. Attewell, P.B. & Farmer, I.W. *Principles of Engineering Geology*. John Wiley & Sons Inc., New York, 1976, pp. 104-181.
5. Bieniawski, Z.T. *Engineering Rock Mass Classifications*. Wiley, 1989.
6. Bowles, J.E. *Foundation Analysis and Design, 5th Ed.* McGraw-Hill, Singapore, 1997, p. 317.
7. Bromham, S.B. & Styles, J.R. *An Analysis of Pile Loading tests in a Stiff Clay*. Proc. First Australia - New Zealand Conference on Geomechanics, Melbourne, 1971, pp. 246-253.
8. Clarke, G., McNally, G., Nyland, G. *Geotechnical Characteristics of the Darwin Porcellanite*. Proceedings, 8th Australia New Zealand Conference on Geomechanics, Hobart, 1999, pp. 911-914.
9. Ervin, M.C. (Ed.). *In-Situ Testing for Geotechnical Investigations*. A.A. Balkema, Rotterdam, 1983.
10. Ghafoori, M., Airey, D.W. & Carter, J.P. *Correlation of Moisture Content with the Uniaxial Compressive Strength of Ashfield Shale*. Australian Geomechanics, August 1993, pp. 112-113.
11. Gutteridge Haskins & Davey Pty Ltd. *Northern Australia Gas Venture Darwin Onshore Geotechnical and Topographical Surveys - Report on Geotechnical Investigation* (unpublished). July 1998.
12. Gutteridge Haskins & Davey Pty Ltd. *Northern Australia Gas Venture Darwin Onshore Geotechnical and Topographical Surveys - Report on Geotechnical Data Analysis and Interpretation* (unpublished). July 1998.
13. Johnston, I.W. *Geomechanics and the Emergence of Soft Rock Technology*. Australian Geomechanics, No. 21, December 1991, pp. 3-26.
14. Johnston, I.W. *Silurian and Lower Devonian Engineering Properties*, in "Engineering Geology of Melbourne", Peck, Neilson, Olds & Seddon (Eds), Balkema, Rotterdam, 1992, pp. 95-108.
15. Look, B.G. *Standard Penetration Test Procedure in Soil Rock*. Australian Geomechanics, No. 32, December 1997, pp. 66-68.
16. Marks, A.R. & Jolly, P. *Extreme Corrosivity of Northern Territory Coastal Groundwater Supplies - Origin, Effects and Materials of Construction*. IEAust Annual Conference, Darwin 1987.
17. Moye, D.G. *Engineering Geology for the Snowy Mountains Scheme*. Journal IEAust, Vol. 27, 1955, pp. 281-299.
18. Nyland, G.W. & Gerner, P.R. *Engineering Geology and Foundation Conditions in Darwin, Northern Territory*. Fourth Australia - New Zealand Conference on Geomechanics, Perth, 14 - 18 May 1984, pp. 235-239.
19. Pells, P.J.N. *The Use of the Point Load Test in Predicting the Compressive Strength of Rock Materials*. Australian Geomechanics Journal, Vol. G5, No. 1, 1975, pp. 54-56.
20. Pells, P.J.N., Douglas, D.J., Rodway, B., Thorne, C. & McMahon, B.K. *Design Loadings for Foundations on Shale and Sandstone in the Sydney Region*. Australian Geomechanics Journal, 1978, Vol. G8, pp. 31-39.
21. Pietsch, B.A. *1:100,000 Geological Map Series Explanatory Notes, Koolpinyah 5173*. Northern Territory Geological Survey. 1985.
22. Pietsch, B.A. *1:100,000 Geological Map Series Explanatory Notes, Darwin 5073*. Northern Territory Geological Survey. 1983.

23. Poulos, H.G. & Davis, E.H. *Pile Foundation Analysis And Design (Series in Geotechnical Engineering).* John Wiley & Sons Inc., 1980.

24. Poulos, H.G. *The 29th Rankine Lecture - Pile Behaviour - Theory and Application.* Geotechnique, Vol. 39, No. 3, pp. 365-415, September 1989.

25. Sales, A.A. The Performance of Rock Socketed Piles in Low Strength Siltstone. Australian Geomechanics, No. 16, December 1988, pp. 9-18.

26. Winterkorn, H.F. & Fang, H.Y. (Eds.). *Foundation Engineering Handbook.* Van Nostrand Reinhold Company, 1975.

27. Woodside Energy Ltd & Shell Development Australia Pty Ltd. *Northern Australia Gas Venture - Feasibility Study for Timor Sea Gas Development.* Perth, Western Australia, 1999.

Organo-Clay Reactive Barriers in Contaminated Site Remediation

Sarah Richards: Department of Civil Engineering, Monash University, Clayton, Victoria.

Summary: *Increased awareness of the total environmental impact and economics of many common site remediation strategies has led to interest in natural attenuation. Natural attenuation is any process that reduces the concentration or toxicity of environmental contaminants, without the aid of human intervention. The most commonly cited reasons for not utilising natural attenuation are that the process takes longer than the project timeframe and there is no guarantee that contaminants will not migrate into the air or groundwater. A barrier system could be used to allow development to continue and provide the time required for the processes to run their course. It would also provide a guarantee against further migration. Conventional barrier systems rely on minimising advective flow, however contaminants can still travel quite effectively by diffusion. Reactive barrier systems utilise contaminant reactions to reduce contaminant transport. This paper outlines some of the research being conducted into natural and organically modified clay barriers for the immobilisation of environmental contaminants.*

1 INTRODUCTION

Contaminated site management in Australia is currently in a state of change. New technologies are continually being presented as the waste management cure all. However, many of these strategies require high energy input or involve exposing the contaminants. In industrial production, increased emphasis is being placed on total environmental impact. If a life cycle analysis is performed on many contaminated site remediation projects, the results indicate that the least environmental impact is achieved by not doing anything [1]. This has led to increased interest in natural attenuation.

Natural attenuation is any process that reduces the concentration or toxicity of environmental contaminants, without the aid of human intervention. Examples of such processes are biodegradation of organic compounds and adsorption of heavy metals onto soil particles. Both of these processes have been proven to reduce the concentration of certain contaminants [2]. However, these processes do have limitations. Bioremediation takes time to be effective and high concentrations of organic compounds can kill the bacteria that are responsible for biodegrading lesser concentrations. Adsorption of inorganic ions to soil particles is governed by the concentrations of ions available and is limited by a maximum capacity. These limitations make it hard to confidently rely on these processes to manage contaminant concentrations and movement.

Currently natural attenuation is only utilised in conjunction with extensive monitoring programs. A barrier system could be used to isolate the site to ensure contaminants are unable to pass across site boundaries or enter environmentally sensitive systems, such as groundwater or surface waters, then the natural attenuation processes could be left to manage the contaminants within the isolated zone. Some monitoring would still be required, but on a much lesser scale.

The commonly used barriers to contaminant migration focus on minimising advective and/or diffusive transport. To achieve sufficiently low contaminant movement this approach often requires the placement of thick compacted clay liners or high density polymer materials. Both of these options are expensive, time consuming and interfere with the natural hydraulic movement across the site. Reactive barriers increase retardation of the contaminants. By incorporating materials that adsorb contaminants in a porous matrix, contaminant transport can be reduced without affecting hydraulic flow.

The same principle can be used in solid waste management. The adsorbent materials can be incorporated in a low permeability material to minimise hydraulic flow and contaminant movement. Layers can be used as part of a landfill liner system and are commonly referred to as attenuating layers.

2 REACTIVE BARRIER TECHNOLOGIES

Contaminant transport comprises of three components; advection, diffusion and reaction [3]. Contaminant mobility can be minimised by minimising advection and diffusion and/or maximising reaction.

Advection is governed by hydraulic gradient and hydraulic conductivity. The hydraulic gradient is a characteristic of the given site conditions and can not be varied greatly. Low hydraulic conductivity is the major selection criterion for barriers. Compaction is used to minimise the hydraulic conductivity of the material chosen. Advection is the component of transport most commonly investigated and is generally minimised as much as practicable. Diffusion is governed by the diffusion coefficient of the particular contaminant and porosity of the material. The diffusion coefficient is constant for a given compound at a constant temperature and pressure. Porosity for a particular material is generally minimised, along with hydraulic conductivity, by

compaction. Reaction can describe many different processes, none of which are commonly used in barriers or liners.

Different contaminant groups can be immobilised by different techniques. Therefore, to utilise reactive barriers a good understanding of the contaminants present is required. Some of the mechanisms which can be utilised are briefly described below [4], [5].

2.1 pH Control

pH control is the most common mechanism used for metal fixation. Most techniques employing pH control, raise the pH to within the range where metal hydroxides have the lowest solubility by using a material which has a high pH and high acid buffer capacity. That is, addition of acid does not necessarily lower the pH of the material. This results in precipitation of the metals. Figure 1. shows the solubilities of metal hydroxides as a function of pH.

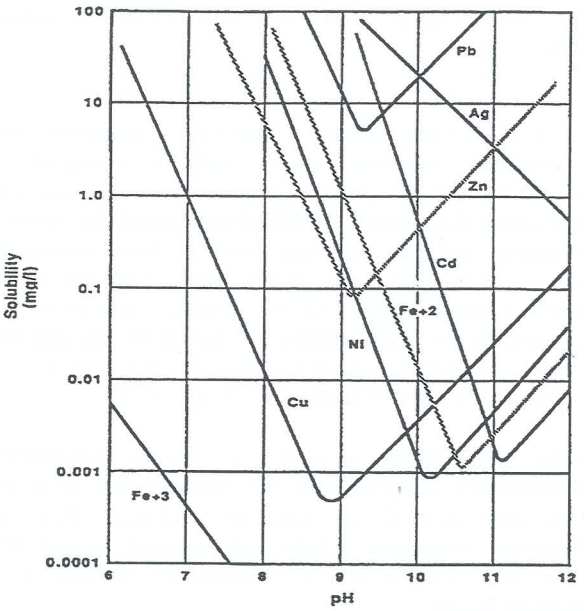

Figure 1: Solubility of metal hydroxides as a function of pH. [4]

As can be seen from Figure 1, there is no pH range that is ideal for minimising the solubility of all metals. However, pH above 8 is generally considered to be beneficial. A good understanding of the metals of concern and the species present in the waste is necessary for the successful employment of this mechanism.

2.2 Oxidation or Reduction

Oxidation or reduction can change the valence of some metals such as chromium and arsenic. These changes in valence can result in a significant change in mobility. The redox potential can be used to identify if oxidation or reduction is likely to occur. Little work has been done to provide an estimate of the mobility of metals based on the redox potential.

2.3 Adsorption of Contaminants to Clay Minerals

Clay minerals consist of various arrangements of tetrahedral and octahedral silicate sheets. This construction results in clays having a large specific surface area. Substitution of atoms in the sheet structure results in a net negative charge over the clay surface. This charge is usually balanced in nature by calcium, sodium or magnesium ions. However, these cations are exchangeable and can be replaced by almost any positively charged ion. A schematic of this process is shown in Figure 2. This mechanism can be quite effective for immobilisation of metal ions. The maximum adsorption is limited to the cation exchange capacity of the clay.

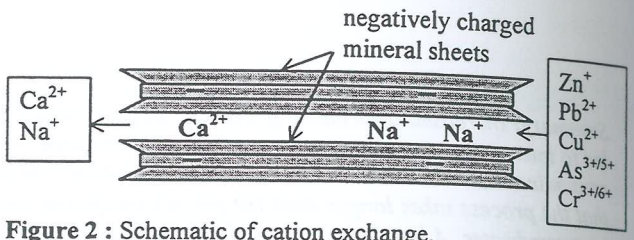

Figure 2 : Schematic of cation exchange.

2.4 Adsorption of contaminants to organically modified clays

By the mechanism described above, organic cations can be bonded to clay mineral surfaces [6]. Organic cations usually consist of a cationic end (often ammonium) and a long organic tail. Adsorption of these cations leads to pillaring of the interlayer spaces in the clay material. That is, the long organic chain keeps the silicate sheets apart. This enables organic compounds to access the interlayer spaces where they can be adsorbed onto the mineral surfaces [7]. In addition, organic compounds are attracted to the organic ends of the cations and form micelles [8]. A schematic of organic compound adsorption is shown in Figure 3. By this process the clay surface is modified from hydrophilic to organophilic. Adsorption on to the mineral surfaces is limited by the physical space available whereas adsorption through organic-organic attraction does not seem to be limited.

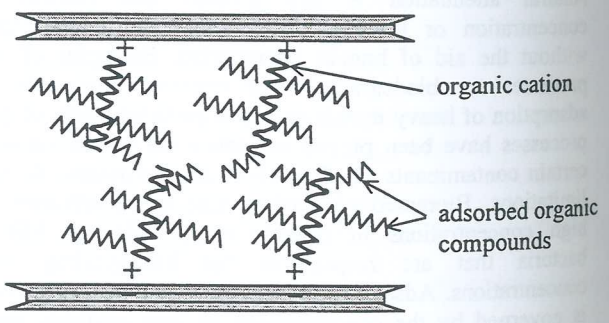

Figure 3 : Schematic of organic compound adsorption to organically modified clay.

Organically modified clays are prepared by adding organic cations, generally quaternary amines, to the natural clay in quantities up to the cation exchange capacity. Organic cations with differing organic groups are used to target different organic contaminants.

3 IMPLEMENTATION OF REACTIVE BARRIERS

There is no single formulation for a reactive barrier, containing natural or organically modified clay, that

effectively immobilises all contaminants. As with compacted clay liners, a thorough investigation is necessary prior to use. Several combinations of clay types and organic modifiers may be trialed using actual contaminated samples or samples prepared to simulate expected conditions. Ionic strength and pH greatly affect the performance of adsorption to natural clays. Therefore, it is vital that expected site conditions are induced during laboratory trials. Laboratory tests can include: batch adsorption tests (see Figure 4), which involve total particle-solution contact and provide an indication of the relative efficiency of adsorption of various contaminants to clays, or column advection-diffusion tests (see Figure 5), which test combination of barrier materials in the condition they will be used and provide an indication of how the barrier material will actually perform.

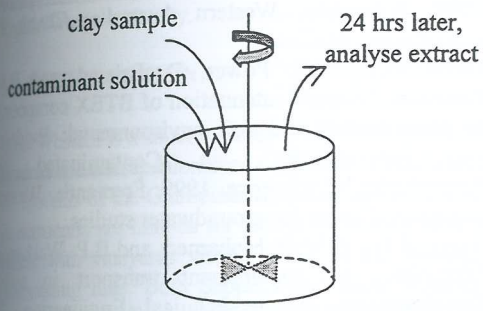

Figure 4: Schematic of batch adsorption test [9].

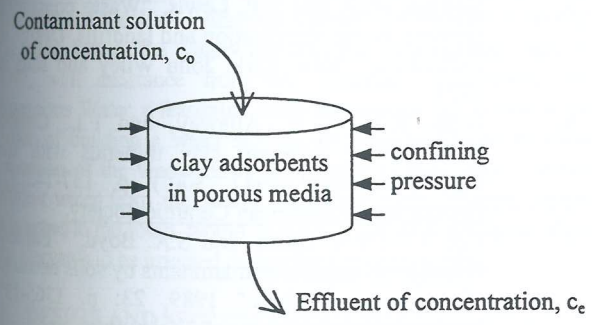

Figure 5: Schematic of column advection-diffusion test.

Since reactive barriers are prepared specifically for site conditions, it is worth investigating the use of natural clay from the site. There are a few preliminary tests that are useful to assess the suitability of clay for contaminant immobilisation. High surface area and cation exchange capacity are desirable characteristics.

4 CURRENT RESEARCH

Research, currently being undertaken at Monash University, is focussing on the retardation of selected metals and organics by three Australian clays; Saponite from Perth, basaltic clay from Melbourne and commercial bentonite from Brisbane.

Tests have been conducted to assess the physical characteristics of the clays. Surface area, cation exchange capacity, particle size distribution and mineralogy were all investigated. The results of the surface area and cation exchange capacity tests are presented in Table 1.

Table 1 : Clay surface properties.

Clay Type	Surface Area (m^2/g)	Cation Exchange Capacity (meq/100 g)
Saponite	270.4	32.1
Basaltic	252.4	45.3
Bentonite	410.2	63.5

meq = milliequivalents

The surface area and cation exchange capacity results indicated that all three clays had a good potential for use as contaminant adsorbents in a reactive barrier.

Acid buffer capacity has also been investigated. A high acid buffer capacity can be valuable in acidic applications, such as mine tailings dams. Metals can be immobilised by a material with high acid buffering capacity despite being in an acidic environment. However, it must be noted that there is a limit to acid buffering capacity. In long-term projects there is a risk of the pH in the material suddenly dropping and the immobilised metals being released. Results of the acid buffer capacity tests are presented in Figure 6.

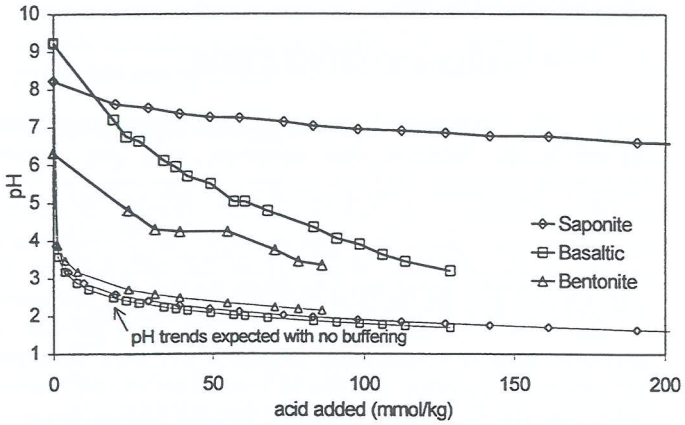

Figure 6: Acid titration curves.

The set of curves that lie between pH of 2 and 3 represent the pH expected if there was no buffering action by the clays. The results of the acid buffering tests show that basaltic clay and bentonite have a low resistance to change in pH, whereas saponite has a very high acid buffering capacity.

Batch adsorption tests have been conducted for adsorption of copper, lead and zinc to the clays. It was expected that the adsorption of metal ions would be limited to a maximum capacity equal to the cation exchange capacity. This was the case for bentonite and basaltic clay. However, saponite achieved adsorption in excess of the estimated cation exchange capacity. There are two potential explanations for this. The estimated cation exchange capacity may be incorrect or there may be other mechanisms acting to increase immobilisation. When the pH of the equilibrium solution and the concentration of metal ions remaining in the solution were plotted together, the curves were very similar. This was not

the case for basaltic clay and bentonite. This leads to the conclusion that the high pH buffer capacity of the saponite increased the immobilisation of metal ions.

The adsorption of organic compounds to natural soil is related to the organic carbon content of the soil and the organic partitioning coefficient of the organic compound of interest [9]. In other words, how much organic material is there in the soil and how strongly are the contaminants attracted to other organic matter. The three clays were analysed for total organic carbon. The basaltic clay and bentonite had very low organic contents, approx. 0.1%, whereas the saponite had a relatively high organic carbon content, approx. 5%. This suggests that the basaltic clay and bentonite would have a very low potential for adsorption of organic compounds in their natural condition. However, by utilising their high cation exchange capacities, through organic modification, it is anticipated that the organic compound adsorption potential of these clays can be greatly increased.

Future testing is planned to focus on the performance of these clays in a matrix of low permeability material, as would be used in an attenuating layer for solid waste management. Flexible wall permeability testing equipment has been modified to facilitate the use of contaminant solutions [10], [11]. It is proposed to correlate the results of this testing with a contaminant transport model that has been developed at the University of Turin, Italy.

5 DISCUSSION AND CONCLUSION

Many of the contaminated site remediation strategies gaining popularity in Australia and overseas, rely on natural attenuation processes that can be time consuming and have variable efficiency. A reliable barrier system could be incorporated into these strategies to isolate the contaminants present at the site. This would allow the development to continue and provide the time required for natural processes to immobilise the contaminants. It would also provide a guarantee against contaminant migration off site. Reactive barriers utilise chemical reaction to immobilise contaminants, rather than relying on flow reduction through minimisation of advective and diffusive transport.

Preliminary tests have shown that three Australian clays have a good potential for use as contaminant adsorbents in reactive barriers. Basaltic clay from Melbourne and commercial bentonite from Brisbane adsorb metal ions through cation exchange. Saponite from Perth adsorbs metal ions in excess of the cation exchange capacity, which indicates a second mechanism. It is considered that this is due to precipitation of metal hydroxides due to the high acid buffer capacity of the saponite.

None of the clays is expected to naturally immobilise organic compounds. However, their high cation exchange capacity can be utilised, through organic modification, to create organophilic clays. The modified clay is then able to adsorb some organic compounds.

These mechanisms of contaminant immobilisation have been shown to be almost irreversible under common environmental conditions. It is hoped that this research will improve the knowledge base on contaminant soil interactions in some Australian clays and may promote the use of reactive barriers in contaminated site remediation and attenuating layers in solid waste management.

6 AKNOWLEDGEMENTS

The financial support of the Australian Research Council, ENRID Pty Ltd and Envirotreat Ltd (U.K.) has made this research possible. In addition, the author would like to thank Dr Malek Bouazza for his supervision.

7 REFERENCES

1. Cramer, D. "To Clean up or not to clean up? Life cycle analysis in contaminated land management.". in Contaminated Site Remediation Conference. 1999. Fremantle, Western Australia: Centre for groundwater studies.
2. Davis, G.B., T.R. Power, D. Briegel, and B.M. Patterson. "Natural attenuation of BTEX compounds in groundwater and soil environmental: Evidence and Uncertainties". in Contaminated Site Remediation Conference. 1999. Fremantle, Western Australia: Centre for groundwater studies.
3. Yong, R.N., A.M.O. Mohamed, and B.P. Warkentin, "Principles of contaminant transport in soils". Developments in Geotechnical Engineering, 73. Amsterdam: Elsevier. 1992 .
4. Conner, J.R., "Chemical fixation and solidification of hazardous wastes". New York: Van Nostrand Reinhold. 1990 .
5. Sharma, H.D. and S.P. Lewis, "Waste containment systems, waste stabilisation and landfills. Design and evaluation.". New York: John Wiley and sons inc. 1994 .
6. Grim, R.E., W.H. Allaway, and F.L. Cuthbert, "Reaction of different clay minerals with some organic cations." 1947, 30(5): p. 137-142, The Journal of the American Ceramic Society.
7. Lee, J.-F., J.R. Crum, and S.A. Boyd, "Enhanced retention of organic contaminants by soils exchanged with organic cations." 1989, 23: p. 1365-1372, Environmental Science and Technology.
8. Boyd, S., M. Mortland, and C. Chiou, "Sorption characteristics of organic compounds on hexadecyltrimethylammonium-smectite." 1988, 52: p. 652, Soil science society of America.
9. Roy, W.R., I.G. Krapac, S.F.J. Chou, and R.A. Griffin, "Technical Resource Document - Batch-type procedures for estimating soil adsorption of chemicals.", United States Environmental Protection Agency: Washington. 1992.
10. Shackelford, C.D., "Critical concepts for column testing." 1994, 120(10, Oct 1994): p. 1804, J of Geotechnical Engineering.
11. Redmond, P.L. and C.D. Shackelford, "Design and evaluation of a flow pump system for column testing." 1994, Sept 1994: p. 269, Geotechnical testing J.

Great Western Winery Storage Pond

Anthony Spiteri, Victorian Sales Manager, Geofabrics Australasia Pty Ltd

SUMMARY:

This paper details the investigation, design and construction of an artificially lined 200ML treated effluent water storage pond. The base of the pond incorporated a clay liner and a geosynthetic clay liner, due to the differing geological features present at the site. The pond is situated outside the township of Great Western, a small regional town two hundred and twenty kilometres northwest of Melbourne. The construction of the pond was essential as the treated effluent water, piped from the Ararat Treatment Plant, is required to irrigate vineyards situated in the district. Major expansion of the vineyards could not take place without these major infrastructure works being carried out by the Grampians Region Water Authority.

1 INTRODUCTION

Great Western is a small regional town situated approximately two hundred and twenty kilometres northwest of Melbourne, nestled in the foothills of the Grampians mountain range. The township and its surrounds are famous for producing quality table and fortified wines, with vineyards visible as far as the eye can see on the surrounding hills. Both Seppelts and Bests wineries have been present in the district since the 1880's, their wines famous throughout the world.

Vineyards in the district have traditionally relied on rainfall to irrigate their vines. Expansion of the vineyards has always been looked at, but a lack of confidence amongst the wineries in enough rainfall to sustain the winery has held this development back. In 1997, with assistance from the Victorian Government and Grampians Water, a feasibility study was carried out to look at the option of building a water storage off Sugarloaf Road to allow expansion of the vineyards in the district to take place. Treated effluent water from the Ararat Treatment Plant, situated sixteen kilometres to the south, would be piped to the new storage to allow the vineyards to be irrigated during the summer months.

2 DESIGN AND SITE INVESTIGATION

Fisher Stewart were engaged by Grampians Water to design the proposed storage and pipeline. Piper and Associates in turn were engaged to provide geotechnical information for the proposed works, and Nolan ITU being engaged to provide a hydrogeological assessment. The project comprised the construction of a 200 megalitre storage dam, located within the Sugarloaf Creek catchment.

It also incorporated the following works:

* Earth-fill embankments complete with geofabric and rock beaching erosion protection;

* A clay liner and Geosynthetic Clay Liner (G.C.L) lagoon floor, including an under drainage system for the clay lagoon floor area. This was required to reduce uplift pressure on the liner systems, and was seen as environmentally sound, as salinity was an issue.

* Laying of a 200 mm diameter pipeline from the Ararat Treatment Plant to pipe treated effluent to the storage. Grampians Water previously discharged treated wastewater to the Hopkins River, with some minor reuse.

2.1 Geology

The proposed winter storage is located in an area of alluvial deposits overlying weathered granite. The following primary soil profile was encountered by Piper and Associates (1) :

* Rootmatter extending to a depth of 20 mm.
* medium density, brown, fine to medium grained, silty sand (SP) or sandy or clayey silt (ML) extending to a depth of between 0.2 and 0.6 metres.
* very stiff to hard, mottled grey, orange - brown and red - brown, slightly sandy silty clay (CH), often highly fissured with slickensided joints extending to a depth of between 1.8 and 6.1 metres.
* low to very low strength, orange - brown, white - grey, highly to completely weathered granite (HW-CW) extending to the full depth explored of 12.5 metres.

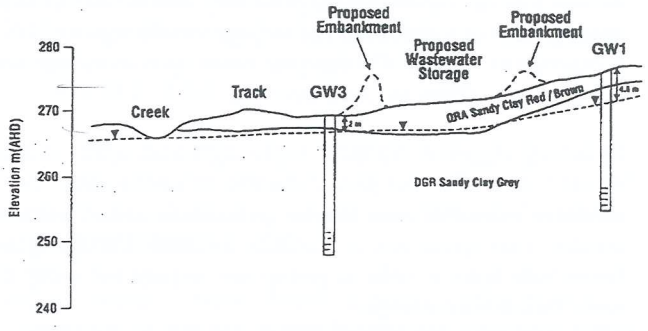

***Figure 1:** shows a cross section (East/West) through the site. Note the location of sand, silt and clay deposits (QRA) and the granite (DGR). (Piper and Associates (1))*

2.2 Laboratory Test Results

Laboratory permeability tests were conducted on samples drilled from the site. The remoulded compacted clay samples achieved an average hydraulic conductivity of 5.7 x 10^{-9} m/s. (Piper and Associates (1)). The test results varied considerably and reflected the variability of the ground encountered.

2.3 Slope Stability of the Embankments

A slope stability analysis of the embankments was carried out in order to assess stability under the following conditions:

i) steady state seepage
ii) construction conditions with excess pore water pressures
iii) seismic condition in the event of an earthquake
iv) drawdown condition.

Factors of safety of 1.5, 1.3, 1.1 and 1.2 respectively were adopted for the above analysis. The steady state seepage (downstream) results varied between 1.43 and 1.48. (Piper and Associates (1)). These were lower than first desired, but could be tolerated provided there was a high level of construction quality control.

Construction conditions factor of safety varied between 1.27 and 1.9. (Piper and Associates (1)). This will generally be adequate and did not cause construction delays, provided that these pressures were monitored by vibrating wire piezometers placed within the embankments and the floor of the lagoon.

2.4 Hydrogeological Design

The floor on the western half of the storage (uniform elevation) was lined with a 600 mm thick layer of compacted clay. The assumed design hydraulic (vertical) conductivity was 7 x 10^{-9} m/s. (Piper and Associates (1)).

The eastern half of the storage has a shallow depth to the granite. Due to this condition, an inclined floor was designed (difference in elevation of two metres) and was lined with Bentofix X2000, a geosynthetic clay liner. It has a design thickness of 10 mm and a vertical hydraulic conductivity of 3 x 10^{-11} m/s. (Fisher Stewart (2)).

The head of water in the storage is a maximum of 6 metres on the clay liner and reduces from 6 to 5.4 metres on the G.C.L. The seepage loss rate expected through the clay liner is 1803 mm/year (average head of 4.3 metres). The seepage loss through the G.C.L. is expected to be about 630 mm/year, based upon an average head of 6.65 metres. (Piper and Associates (1)).

Modelling suggested that there maybe significant uplift pressures on the G.C.L. when the storage water level was lowered. Clearly excessive leakage of water into the groundwater stream was to be avoided. One option was to introduce an under drainage system below both liners in order to pickup any seepage and pump this water back into the storage.

2.5 Geofabric Specification

The geofabric specification for both the embankments and the gravel drains consisted of the following (Fisher Stewart (2)):

i) Manufacture: ultra violet stabilized, needle punched polyester.
ii) Mass: 180 gsm
iii) Thickness: 1.7 mm
iv) Wide Width Tensile Strength: 14.5 kN/m (mean)
v) Trapezoidal Tear Strength: 310 N (mean)
vi) Drop Cone (h50): 1500 mm
vii) CBR Burst: 2700 N (mean)
viii) G Rating: 2000
ix) Mullen Burst: 2400 kPa
x) Pore Size (O95) Dry: 190 microns (maximum)

All values stated are minimum unless otherwise noted.

3 TENDER PROCESS

Tenders were advertised by the Grampians Authority in late January 1999. In May, following consideration of all tenders, the contract was awarded to Midwest Earthmovers. The contract duration for practical completion was set at 22 weeks.

4 CONSTRUCTION

Works were carried out on site by Midwest Earthmovers, an experienced construction company based in Ballarat. The construction sequence was dependent upon both a mild winter and area limitations on site. The following sequence was carried out:

i) Materials were stripped, separated and stockpiled from the lagoon floor and embankment area: topsoil; clayey silt; clayey and silty sand; silty and sandy clay; and weathered granite. The topsoil, clayey silt and clayey sand overlaid the site in depths ranging from 0.2 to 1.8 metres. The sandy and silty clay varied in thickness from 0.2 to 6.1 metres and was located beneath the silt. The weathered granite was found beneath the above materials.

ii) Construction of the under drainage system in the western flat area of the lagoon floor. A herringbone gravel underdrainage system was constructed, consisting of geofabric lined trenches, slotted Class 18 pipe, and 6 mm diameter gravel screenings. Overall 8000 square metres of Bidim A24 geofabric was used to line the trenches.

iii) Removal of clay from the stockpile and place and compact to form embankments. All sand filter and coarse gravel finger drains were constructed concurrently with the clay placement.

iv) Installation of a G.C.L. on the sloping eastern area of the lagoon floor. A 300 mm layer of silty and clayey sand, won from the borrow pit area, was evenly spread over the liner and lightly compacted in two layers. To monitor pore pressures beneath the liner, three vibrating wire piezometers were installed underneath it. The piezometers were also required to monitor embankment stability throughout the construction phase. Overall 19,500 square metres of Bentofix X2000 G.C.L. was installed.

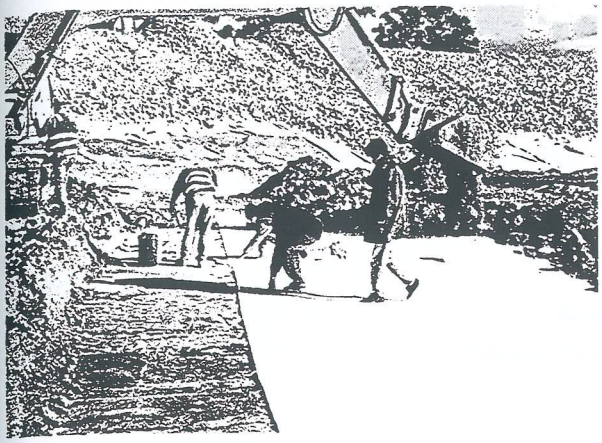

Figure 2: Installation of the Bentofix X2000 G.C.L. on the sloping lagoon floor.

v) Construction of a 600 mm thick layer of compacted clay to form the lagoon floor liner in the flat western area. The clay was moisture conditioned to between 0 and 3 % above Optimum Moisture Content, and compacted to a minimum of 96 % Standard Maximum Dry Density. In order to monitor pore pressures beneath the clay liner, a further three vibrating wire piezometers were installed beneath it. Overall 25,600 square metres of clay was installed.

***Figure 3:** Piezometers being installed beneath the clay liner*

vi) Placement of geofabric and rip rap armour rock on the upstream embankment to prevent erosion. The geofabric filter was anchored in a trench at the top of the embankment and laid down the slope. A minimum overlap of 500 mm was provided between adjacent geofabric runs, and pinned down with galvanized staples at two metre centres along the overlap. An overall 14,000 square metres of Bidim A24 was placed on the embankments.

Following the placement of the geofabric, a minimum 200 mm layer of rip rap rock was placed over it. The specification (Fisher Stewart (2)) for the rip rap rock stated:

i) nominal maximum diameter shall be 150 mm
ii) not more than 5 per cent by mass to pass a 50 mm sieve
iii) not more than 15 per cent by mass to pass a 100 mm sieve.

***Figure 4**: placement of rip rap rock over the Bidim A24 geofabric filter cloth.*

5 CONCLUSION

Overall the project proceeded smoothly with the earthworks and lining operations taking place between May and September. The contractor was able to install the Bentofix liner with a minimum of fuss, as they had installed Bentofix on a number of occasions. The completion of the project has ensured that the wineries in the Great Western region can carry out capital works and expand their vineyard area significantly. The existance of a 200 megalitre water storage now ensures expansion can proceed without the risk of water shortages in the summer months.

6 ACKNOWLEDGEMENTS

I would like to thank the following people for their assistance in preparing this technical paper :

Mr. Bernhard Resenberger – Fisher Stewart ;
Mr. Luis Batista – Fisher Stewart ;
Mr. John Piper – Piper and Associates ;
Mr. David McMaster – Grampians Region Water Authority ;
Mr. Kevin Francis – Midwest Earthmovers ;
Mr. Matthew Eberle - Geofabrics Australasia.

7 REFERENCES

Piper and Associates "Geotechnical and Hydrogeological Investigation for Proposed Winter Storage, Pipeline and Tank, Great Western, Victoria – Volume 1 – Text and Volume 2 – Appendices" (December 1998).

Fisher Stewart "Ararat Reuse Scheme – Specification for Construction of 200 ML Winter Storage and Associated Works" (January 1999).

Piling for Extensions to the International Terminal Building at Sydney (Kingsford-Smith) Airport

Bruce Stewart
Douglas Partners Pty Ltd, Sydney

Summary The International Terminal at Sydney (Kingsford-Smith) Airport is located on a geologically complex site, with dredged sand filling overlying deep alluvial sediments. The design and construction of foundations for numerous extensions to the original terminal building has been further complicated by the need to comply with vibration, noise and settlement criteria, that satisfy existing structures and day-to-day airport operations. This paper presents a review of the site investigation, design, construction method and foundation testing undertaken on two specific extensions to the terminal building with reference to these conditions.

1 INTRODUCTION

The continuing development of the International Terminal at Sydney (Kingsford-Smith) Airport has provided many challenges for foundation design and construction. Extensions to existing buildings are regularly undertaken and often utilise the same foundation type as the existing structure. However, in this project the original foundation type is unsuitable for construction in close proximity to buildings, and other foundation types that satisfy vibration, noise and settlement criteria in a complex geological environment must be considered.

2 HISTORY OF SYDNEY AIRPORT

Sydney (Kingsford-Smith) Airport started in the early 1920s as a private aerodrome in a low lying swampy area beside the Cooks River on the northern foreshores of Botany Bay. Since conception the airport has undergone extensive changes including a diversion of the Cooks River, construction of terminal facilities, extension of the north south runway into Botany Bay and construction of the third runway.

The International Terminal is located in the northeastern sector of the airport, with parts of the terminal building situated over the former Cooks River channel. Filled with dredged sand during the 1950's, the river is now located west of the terminal building.

Prior to construction of the terminal building, this area was used for dumping of flyash from a local powerstation. This material was removed and replaced with dredged sand in the early 1960s, and surcharged with up to 2 m of sand for 2 years in an attempt to reduce the consolidation of underlying soft soils. Review of settlement data over the past 30 years indicates that this surcharging was not successful in eliminating settlement, albeit reducing it to an extent.

From 1967 to 1970, the International Terminal and Concourse (Terminal B and Pier B) was constructed, comprising a three storey prestressed concrete structure. Construction of a southerly extension to the terminal and new concourse (Terminal C and Pier C) commenced in 1988, comprising a similar structure with the addition of two basement levels to the new terminal and associated surrounding aircraft pavements. The latest development, "Sydney Airport 2000" commenced in 1998, and incorporates a variety of new expansions. These include northerly and southerly extensions to Piers B and C respectively, westerly and easterly extensions to the terminal building, upgraded road network including elevated overpasses, extensive expansions to existing aprons and a number of smaller associated projects.

3 GEOLOGY OF SYDNEY AIRPORT

The regional geology of the International Terminal area consists of dredged sand overlying quaternary alluvium. Extensive investigation of the area has identified a number of distinct layers:

- sand filling dredged from Botany Bay, generally medium dense to very dense up to 4 m thick
- soft organic clay up to 10 m thick, undergoing consolidation due to filling and now firm in some locations
- dense or very dense silty sand up to 3 m thick
- stiff or very stiff sandy clay
- dense sand between 0.5 and 4 m thick
- very stiff clay possibly of residual origin, and
- Hawkesbury sandstone bedrock at depths generally ranging between 25 and 50 m, occasionally up to 80 m

The lithology at the location of the terminal building is complicated by the fact that it was constructed over the former river channel, as shown in Figure 1. Geotechnical investigations at the site refer to the possibility of deeply incised river channels, filled with soft and loose soils in recent geological times.

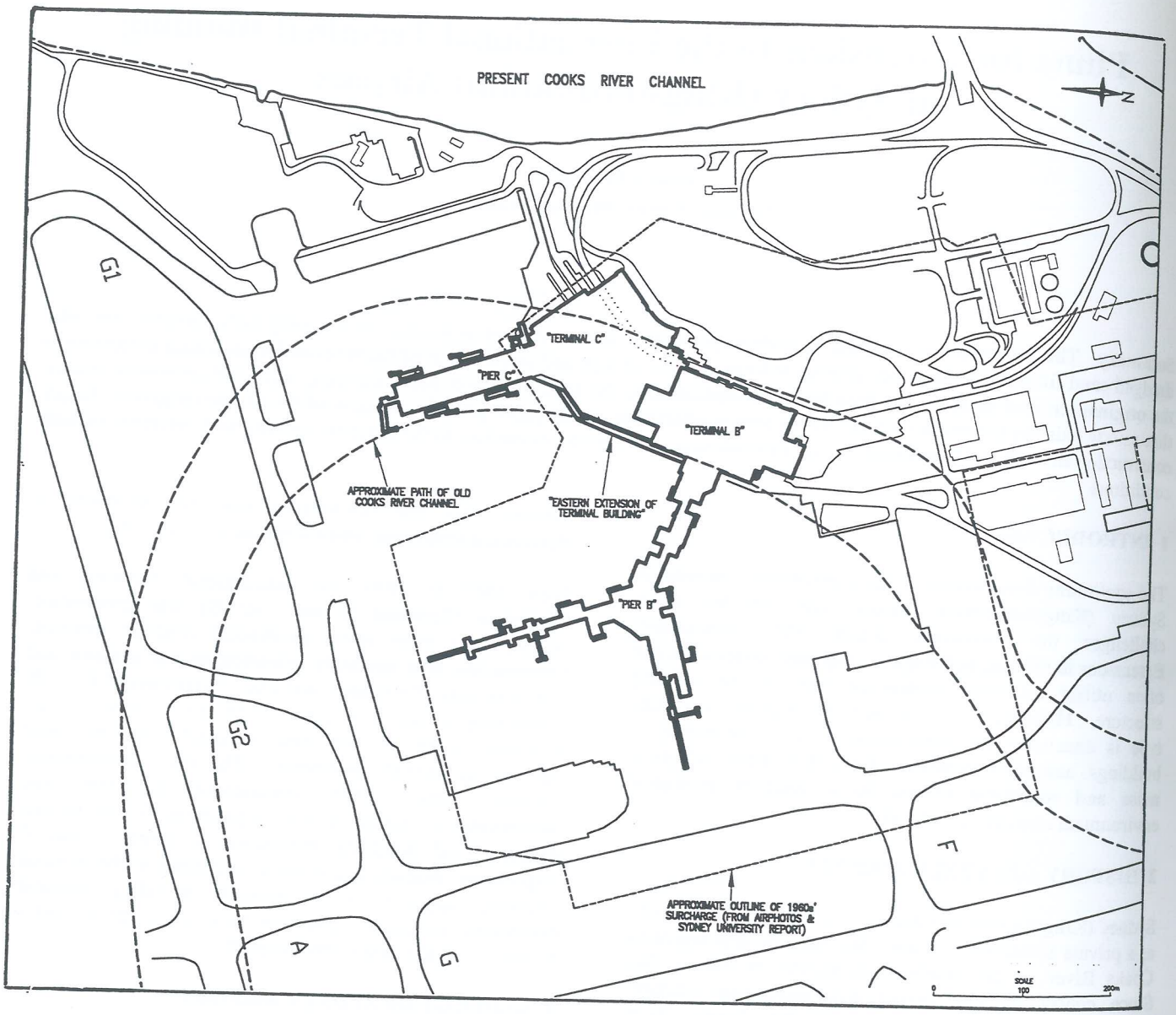

Figure 1: Location of terminal building and former river channel

4 INTERNATIONAL TERMINAL AND CONCOURSE

The original terminal building and concourse (Terminal B and Pier B), was constructed following a number of small geotechnical investigations and an extensive surcharging and testing program undertaken by the University of Sydney. The failure to induce the majority of consolidation in soft clays over a 2 year period by surcharging, has led to the preclusion of shallow footings under moderate loads at this site.

As a result the original terminal building and concourse are founded on tar epoxy coated steel H-piles driven to rock. Founding depths are in the range 24 to 36 m. Providing a simple cost effective construction method, these piles were driven by a 7 tonne hammer falling from a maximum drop height of 20 m.

A silico-iron anode buried approximately 9 m below the ground provides cathodic protection to most of these piles and buried service pipes. Subsequent monitoring of piles not protected cathodically indicates no structural deterioration after 30 years of service

5 CASE STUDY 1 - TERMINAL C AND PIER C

The Terminal C and Pier C expansion comprised a five storey reinforced concrete southerly extension to the terminal building, with a two level fully tanked basement and three storey steel concourse.

5.1 Geotechnical Investigation

The initial investigation comprised 5 bores and CPTs installed on a 100 m square grid over the site, as a part of a larger investigation of the airport. Results of this work indicated the presence of a 2 m thick dense sand layer at approximately 11 m depth beneath some of the site. This layer was suitable for founding enlarged base piles, but it was necessary to prove the thickness and continuity of the layer. Therefore in order to confidently design piles, further investigation was suggested. The Stage I investigation comprising 70 bores and CPTs highlighted the variability of the aforementioned sand layer towards the centre of the concourse and north of the terminal, but provided reasonable data for cost estimation and design. Further investigation was recommended at all column locations where this dense layer was not present, and less frequent testing in other areas. As a result, the Stage II investigation incorporated 77 bores and CPTs, and facilitated the design of piles based on three areal classifications, as shown in Figure 2.

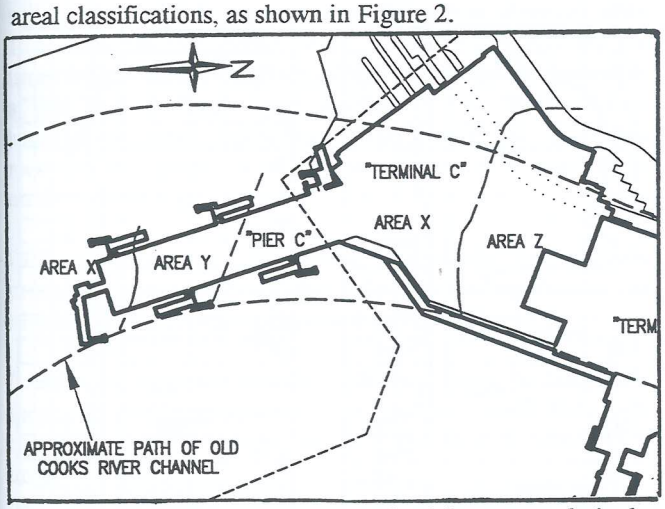

Figure 2 Areal classification derived from geotechnical investigation

5.2 Pile Design

The primary concern for design of piles on this project was the support of a compressive serviceability load of 1800 kN and restraint of a maximum possible tension load of 630 kN in the terminal area. The proposed foundation design for the terminal building was a beam and slab system, with piles supporting/restraining the beams at 2.5 m and 5 m intervals on longitudinal and transverse beams respectively.

For the concourse, compressive serviceability loads of 2000 kN per pile and no tension loads were expected.

Differential settlements between the existing building and new extension also had to be within a 15 mm tolerance.

5.3 Piling Method

Selection of pile types was based on the areal classifications (Figure 2) determined during the investigation stages of the project.

Area X, with its consistent dense sand layer at 11 m depth was considered suitable for founding of cast insitu enlarged based piles. A deeper dense sand layer at approximately 16 m depth in Area Y, was also considered suitable for founding of cast insitu enlarged based piles. However, the depth of this sand layer increased to 19 m in the area close to the terminal, requiring deep piling. Vibration effects in the existing structure precluded selection of driven piles, and as a consequence, grout injected piles or Atlas piles were suggested in this area. Area Z, with a 1.5 m very dense sand layer at depths up to 21 m was considered suitable for application of driven precast piles.

5.4 Pile Testing

Three tension pile tests and five trial penetration tests were undertaken to confirm the ultimate tension load capacity, penetration resistance and basing conditions for 500 mm enlarged base piles, prior to commencement of construction.

Tension pile construction was typical for a pile of this type with the exception that tension capacity was developed by replugging the tube and driving it through the first base enlargement to a lower level so a second base enlargement could be carried out. The pile shafts were then poured to level similar to the proposed basement level, so as not to contribute shaft resistance in the upper 4 m of the pile. Trial driving was undertaken by driving the pile tube to depths of 12 m where a variety of base combinations similar to the tension piles were attempted. Upon completion of basing the pile tube was withdrawn, while recording the load required to pull the tube. A summary of depth and basing details for the three tension piles is shown in Table 1.

Test Pile No.	1	2	9
First Base			
Depth (m)	11.5	10.5	11.5
Volume (m^3)	0.14	0.70	0.14
Location	Just in sand	In firm clay	Just in sand
Second Base			
Depth (m)	12.3	11.8	13
Volume (m^3)	0.14	0.28	0.28
Location	In sand	Just above sand	1.5 m in sand

Table 1 Summary of depth and basing details

The results of tension testing, shown in Figure 3 indicate ultimate uplift loads between 1100 and 1400 kN. However,

it should be noted that these tests were not an actual simulation of constructed piles. With basement level approximately 4 m below surface level, the decrease in overburden pressure was considered to reduce the tension capacity of the piles by up to 30 %. Theoretical estimates used in this capacity reduction could estimate the effect of overburden pressure reduction on lateral pressure, but no reasonable account of the densification effect while driving and basing the piles could be made. Overall the reduction was estimated unlikely to be greater than 15 %, but a value of 20 % was adopted to remove all doubt.

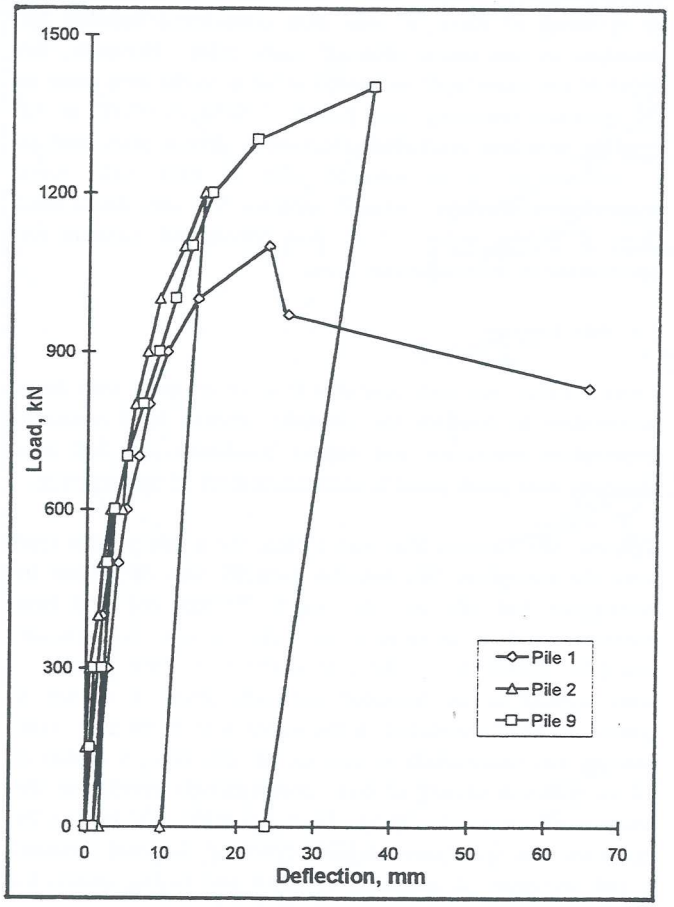

Figure 3 Load response of tension piles

From this it was concluded that test piles needed to restrain a test load of 750 kN. Given that the serviceability load was an extremely unlikely event, and should one pile fail the shedded load would be shared along the beam system and furthermore, pile testing was also to be undertaken during construction, a factor of safety of 1.5 on tension loads was considered reasonable. Hence, this required the piles to have an ultimate tension capacity of 1140 kN. With a modification of the construction procedure for the pile with an ultimate capacity of 1100 kN, the tension trials indicated that this capacity could be achieved.

6 CASE STUDY 2 - EASTERN EXTENSION OF TERMINAL BUILDING

The eastern extension, or "Clip On" is approximately a 10 m wide three storey structure extending along the entire eastern side of the terminal building between Piers B and C.

6.1 Geotechnical Investigation

Initial investigation of the site was undertaken to supplement data available from earlier investigations in the area, and determine founding conditions for piles. Investigation confirmed the presence of a dense to very dense sand layer at approximately 12 m depth at the southern end of the site. This layer was utilised in support of foundation loads in a large proportion of the Terminal C and Pier C expansion, however this layer had been eroded towards the north end of the site and ideal founding conditions for piles in this area no longer existed. The variation in soil conditions is illustrated in the CPT results for the south and north of the site shown in Figure 4.

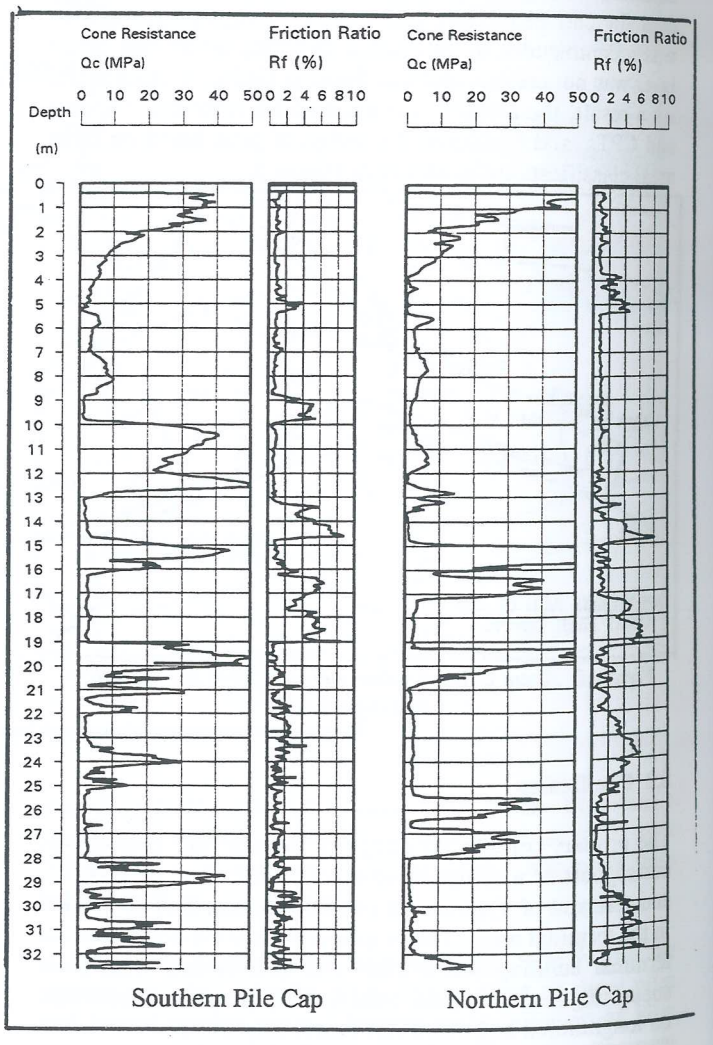

Figure 4: Typical CPT results for southern and northern pile caps

As a result, further testing was undertaken at each pile cap location prior to the commencement of piling.

6.2 Pile Design

Maintaining differential settlement between the existing building and new extension at tolerable limits was the primary concern for this project. Experience gained from earlier extensions suggested piles founded in soil could achieve acceptable differential settlements, when compared to the steel H piles beneath the existing terminal building. A serviceability load of 675 kN was adopted for each pile in a three pile group.

Driven piles were considered to involve unacceptable noise and vibration given the proximity to the existing building, and subsequently only drilled and jacked piles were considered. The final design adopted for construction was a jacked in precast 230 mm square concrete pile.

6.3 Piling Method

The "Grip-Pile", or "G-Pile" hydraulic jacking pile installation system utilises a Chinese developed technology where an electric hydraulic rig, ballasted to provide 100 tonnes thrust, pushes jointed 6 m pile segments into the soil until no visible movement of the pile is observed after 15 seconds at 100 tonnes load. This load represents 1.1 times the design action effect (S*) of 90 tonnes and simulates a pile test for every pile installed. Pile loads during installation were calculated from hydraulic pressures recorded by a geotechnical engineer from a calibrated gauge on the driving rig.

CPTs undertaken at pile locations indicated pile driving pressures consistently higher than cone resistance, as illustrated by a typical comparison in Figure 5

It has been suggested that this difference could be due to the increased frictional resistance of the pile, when its rough concrete surface is compared with the smooth metal CPT probe.

Variations between pile termination depths at the same pile cap were thought to be caused by the densification of soil by the first pile, leading to driving difficulties for subsequent piles. Piles were generally spaced at 350 to 400 mm centres, and installed as in-line groups of 3 or 4. Termination depths for the final pile were up to 30 % higher than the first pile installed. During construction, driving difficulties lead to the failure of only one pile, the third pile to be driven in a four pile group. This failure could not be directly attributed to the densification of soil around the existing piles because the toe of the pile was in loose sand at the time of failure. The pile was removed and later reinstalled

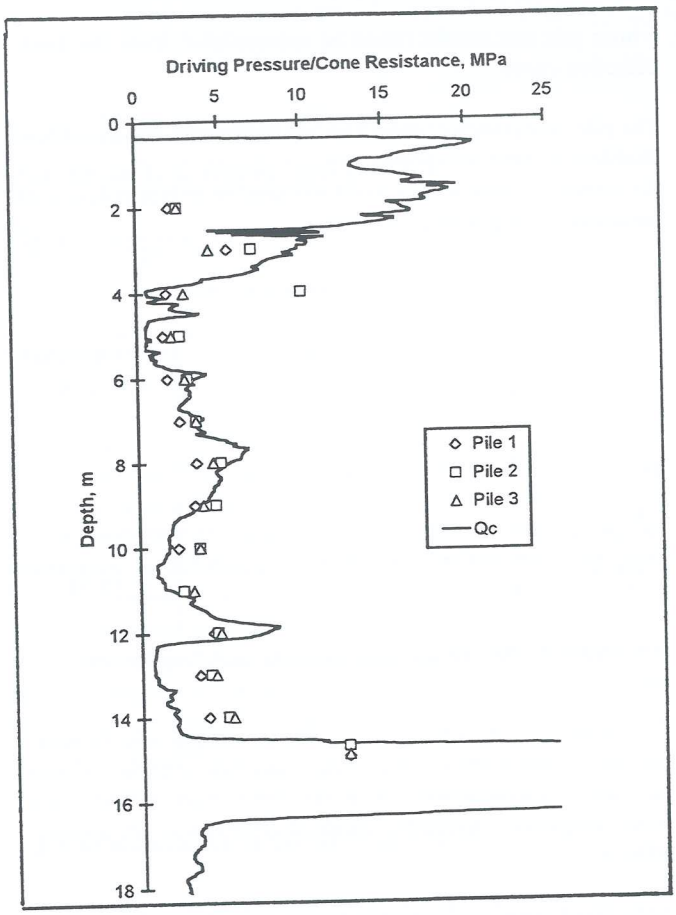

Figure 5: Comparison of Pile Driving Pressure and Cone Resistance

6.4 Pile Testing

A static load pile test was undertaken during pile installation to compare the response of a typical pile with the Australian Standard AS 2159.8.3.5.6. The pile was tested according to the following site specific procedure, created to accommodate curfew and rig limitations:

- install pile to desired depth
- record load and deflection at the top of the pile at 1 minute intervals as the pile is forced into the ground at a constant penetration rate of 0.5 mm/min
- when the design serviceability load (approximately 75 % S*) is reached, sustain the load for as long as possible (preferably 6 hours) while measuring deflections at the top of the pile.
- unload pile and record nett deflection after 10 minutes
- record load and deflection as the pile is reloaded to 100 tonnes at constant penetration rate (maximum test load normally 150 % S* = 135 tonnes however this was beyond rig capacity)
- sustain load at 100 tonnes for 10 minutes and record nett deflections
- unload pile and record nett deflection after 10 minutes

Time restrictions due to the airport curfew restricted the maximum test load interval to 110 minutes. At the end of this period, deflections were considered to be uniform and

6 hour pile test results could be extrapolated from the load-defection curve.

The pile acceptance criterion as outlined by the Standard was modified to meet acceptance criteria adopted in other areas of the airport. These values are compared with pile deflections measured during testing in Table 2.

Load	Deflection (mm)		
	Criteria		Extrapolated 6 hour test
	AS 2159	DP	
75 % S*	15		8.95
S*		10	
0 kN	7	3	0.93
150 % S*	50	15	
110 %S*			16.68
0 kN	30	5	2.5

Table 2 Pile Acceptance Criteria and Test Results

The measured maximum deflections exceeded site criteria, but were significantly lower than Standard criteria. Creep deflections extrapolated for a six hour load period were below suggested Australian Standard criteria and site specific criteria.

Analysis of creep performance results and observations made on site during pile installation suggest that this type of pile satisfied the design objectives.

7 CONCLUSIONS

The soil lithology at the International Terminal at Sydney Airport is complex and highly variable. The two case studies have demonstrated that conditions cannot be reliably predicted without detailed site investigation, prior to design and construction of foundations. However, with this data accurate estimates of pile performance can be made, and supplementary testing of specific piles during construction confirms that the new pile types satisfy their design objective, and comply with construction restrictions at this location.

DEPARTMENT OF HOUSING AND CONSTRUCTION (1983) "Engineering History of the Development of Sydney (Kingsford-Smith) Airport, 1947 to 1972, Department of Housing and Construction

D.J. DOUGLAS & PARTNERS PTY LTD (1989) "Report on Tension Pile Tests, Sydney (Kingsford-Smith) Airport, Project SSI/10900-1", (unpublished).

D.J. DOUGLAS & PARTNERS PTY LTD (1989) "Interim Report on Foundations, Stage 1 Geotechnical Investigation, International Terminal Extensions, Sydney (Kingsford-Smith) Airport, Project SSI/10900-2", (unpublished).

D.J. DOUGLAS & PARTNERS PTY LTD (1989) "Final Report - Stage II Investigation, International Terminal Extensions, Sydney (Kingsford-Smith) Airport, Project SSI/10900-2", (unpublished).

DOUGLAS PARTNERS PTY LTD (1998) "Report on Geotechnical Investigation, Proposed Eastern Extension to Existing International Terminal Building, Sydney (Kingsford-Smith) Airport, Project 10900V", (unpublished).

DOUGLAS PARTNERS PTY LTD (1999) "Report on Pile Observations, Eastern Extension, International Terminal Building, Sydney (Kingsford-Smith) Airport, Project 10900V", (unpublished).

THE UNIVERSITY OF SYDNEY (1968) "Settlement Analysis of International Terminal Area and QANTAS Running Up Area, Investigation Report No S86", (unpublished).

THOM, Michael (1999) (pers. comm.)

Investigation, Design & Construction of a Composite Road Embankment Raroa Road, Wellington

Bruce Symmans
MIPENZ, Tonkin & Taylor Ltd, Wellington, New Zealand

Summary Cracking and subsidence was observed in the Raroa Road carriageway following a period of heavy rain. The site is located 500m from the main Wellington Fault. The topography of the site is steep. Remedial works have been designed and constructed to reinstate the 200m length of road to modern stability requirements including seismic design. Remedial works include a combination of a geogrid reinforced slope, fill buttress, drainage improvements, cantilever pile and tied-back pile retaining walls.

The project encountered difficult and variable surface and sub-surface conditions and unforeseen groundwater flows during construction. Flexibility and contingency provided in the design and ongoing design involvement throughout the construction enabled the project to be completed efficiently. Modifying and fine-tuning the design throughout the project and challenging standard design and construction techniques resulted in an innovative, efficient solution.

1 INTRODUCTION

Wellington City Council engaged Tonkin & Taylor Ltd (T&T) to investigate the causes of subsidence observed in the carriageway of Raroa Road, Wellington. T&T have undertaken:

- inspection and assessment of immediate risk
- monitoring to identify the magnitude and frequency of on-going deformation
- sub-surface investigation
- assessment of the risk of further movement
- review of remedial options and associated costs
- design of three specific retaining solutions
- supervision of construction

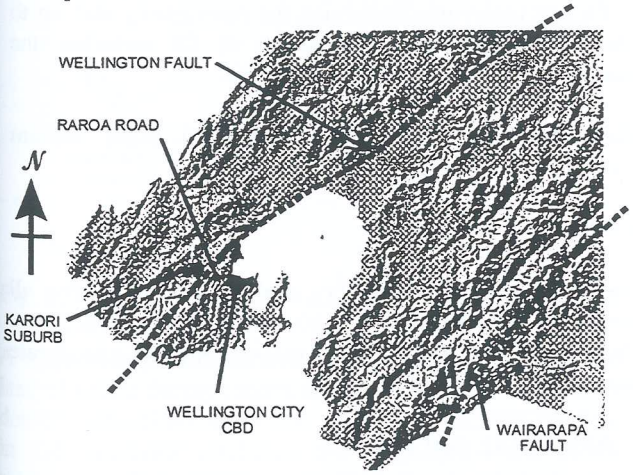

Figure 1: Location Plan

2 GEOLOGICAL AND GEOGRAPHICAL SETTING

New Zealand straddles the boundary of the Australian and Pacific tectonic plates. Caught in the wrenching action between the two plates sliding past each other, the Wellington region has fractured into blocks and long splinters of crust. The Wellington and Wairarapa Faults mark the edges of the larger blocks with many smaller faults crisscrossing the region. Minor earthquakes are common in the Wellington area. Since European settlement major earthquakes have been recorded in 1848, 1855 and 1942. The 1855 earthquake, the result of a rapture of the Wairarapa fault, is estimated to have been magnitude 8 (Richter) or higher (Begg Mazengarb) [2].

The active Wellington Fault bisects the City of Wellington. The signature earthquake for the Wellington fault is a magnitude 7.6 event with a predicted return period of 500 years. The last movement of the Wellington fault is dated at 340 to 480 years (Begg Mazengarb)[2]. This major fault lies 500m to the west of the Raroa Road site.

The site extends along a 200m section of roadway that ascends the side of the Aro Valley. The Aro valley follows the alignment of a minor dormant fault. The basement rock is interbedded greywacke sandstone and argillite with complex structure (Ruscoe) [4]. The steep side slopes of the underlying basement rock range from 30° to 60°. The floor of the valley is infilled with well-graded alluvial gravel. The side slopes are mantled with generally 0m to 1.0m thickness

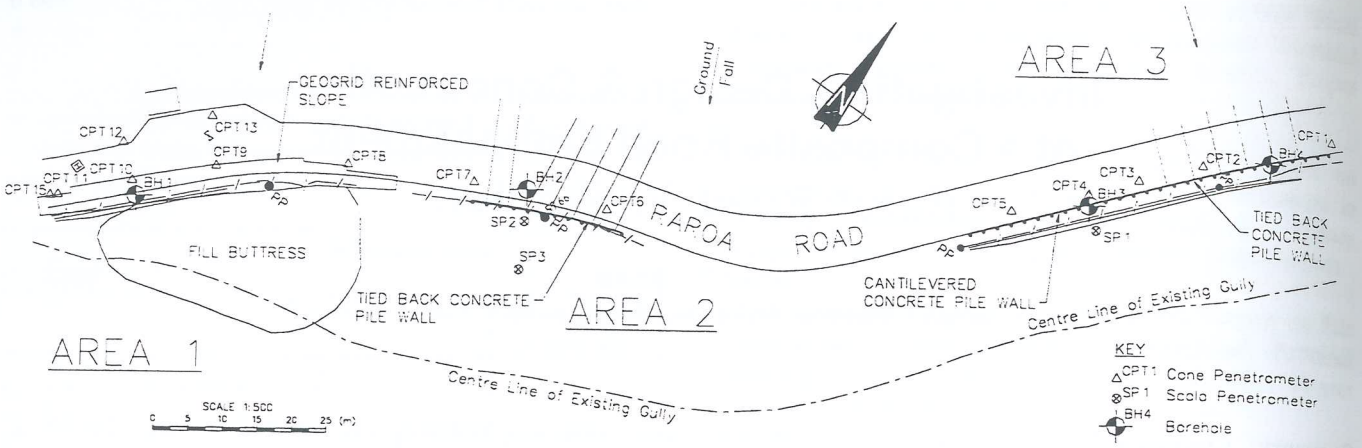

Fig. 2: Remedial Works Site Plan.

of colluvial and residual soils. Investigations indicate that the road embankment was formed early last century as a sidling cut to fill with local and imported greywacke rock placed as fill. The fill appears to have been placed directly on to the original slope. The original topsoil horizon is still in place and there is no evidence of benching or under-drainage. The fill is nominally compacted and generally consists of loose, fine to coarse silty gravel.

Artesian ground water was encountered in the basement rock with bored drains under the fill embankment encountering spring flows of up to 8 litres per minute.

The cut slopes above the road range from 35° to 70°. The fill embankment below the road stands at 35° to 45° and extends to the valley floor some 20 to 30m below the level of the road. At several locations the top of the fill embankment was retained with low concrete crib walls up to 3m in height.

Raroa Road is one of three arterial routes that link the city centre (on the down-thrusted side of the Wellington fault) and the suburb of Karori (on the up-thrusted side of the fault).

3 SUBSIDENCE

Deformation and subsidence of the carriageway was noticed following a large rainstorm event in October 1998. The deformation included significant cracking and subsidence in the downslope lane of the carriageway, resulting in arcuate depressions and cracking patterns with up to 50mm vertical offset.

Three discrete areas (Areas 1, 2 and 3 on Figure 2) along the road alignment were identified as having significantly deformed. Two of the three areas were supported by cribwalls. The cribwalls had noticeable deformation in both the horizontal and vertical alignments.

4 INVESTIGATION

4.1 Movement Monitoring

A monitoring regime was initiated to identify if further movement was occurring and if a major circular type failure beneath the carriageway was imminent. Only very minor movements were recorded following subsequent heavy rain and it was decided to keep the road open and maintain regular monitoring while a remedial investigation and design was carried out.

4.2 Sub-surface

Investigation of the site included four machine drill holes, 15 CPTs and 6 Scala penetrometer tests. Standpipe piezometers were installed in the boreholes to provide information on groundwater conditions.

The investigation confirmed that the road was constructed on silty, gravel fill, founding on a steeply inclined rock interface. At the western end of the road (Area 1), the depth of fill and colluvium underlying the carriageway was up to 15m. Typically 5m to 7m depth of fill underlies the remaining sections of road (Areas 2&3).

The existing cribwalls were constructed using 900mm concrete units connected with steel pins.

4.3 Stability Analysis

Site observations and stability analysis confirmed that all three sites were marginally stable under existing conditions. There was a high risk of further movement under a moderate seismic event or major rainstorm.

5 REMEDIAL SOLUTION

Findings of the investigation and stability review were discussed with Wellington City Council. Given the importance of the road as an arterial route, a low risk (high

security) type solution was recommended. For the 200m length of road identified as having a moderate to high risk of instability, remedial designs were adopted.

5.1 Area 1

5.1.1 Design Philosophy

Properties (see Figure 3)

- 15m depth of variable fill and colluvium
- narrow infilled valley with original valley centre under the carriageway
- an existing cribwall 3.0m in height above a 35° fill batter slope
- assumed existing failure mechanism is a circular shear plane encompassing the existing cribwall.

The remedial solution adopted to provide adequate factors of safety for both static and seismic cases was:

- construct a flexible gravity type retaining structure to support the edge of the carriageway
- fill the valley to form a buttress to support the new retaining structure.

The significant depth of fill and colluvium (15m) and depth to a suitable bearing stratum ruled out piled or anchored wall solutions. A geogrid reinforced fill with a 68° wrap around face (see Figures 3 & 4) was constructed to support the carriageway. Using a deformation tolerant retaining system reduced the difficulties with variable founding properties and also reduced the design requirements for ultimate limit state seismic design.

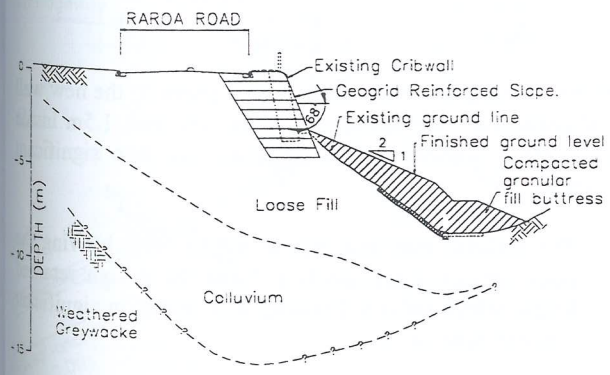

Fig. 3: Remedial Works Area 1. Schematic Cross Section

A major design consideration was to maintain at least one lane of traffic during construction as there were no alternate detour routes close to the site. In order to provide one lane in safe operating condition, the depth and width of the retaining wall excavation was limited. A relatively low retaining wall and large fill buttress was adopted to achieve this goal.

5.1.2 Seismic Design

Seismic design was undertaken using the following assumptions:

- The ultimate limit state horizontal ground acceleration was taken as 0.4g (approximately 1000 year return period)
- The serviceability limit state horizontal ground acceleration was taken as 0.2g (approximately 150 year return period)

The structure is designed to prevent yield in the serviceability limit state with a FOS greater than 1.1. The probable displacement of the wall in the ultimate limit state is estimated to be between 25mm to 100mm. Probable displacements have been calculated using Newmark [3] and Ambraseys and Menu [1] charts. Deformations of this magnitude are unlikely to result in structural failure of the reinforced slope or buttress however some cracking of the road surface would be expected. These predicted magnitudes of deformation are considered to be acceptable for the ultimate limit state design case.

5.1.3 Modifications During Design

Because construction was to be undertaken over winter, both the buttress and the geogrid-reinforced fill were constructed with compacted granular hardfill. The existing fill materials were not reused because of the high organic and clay contents.

The use of hardfill instead of clay fill or re-using existing fill cost an extra 5% of the original (summer) estimated contract value. However, the use of hardfill resulted in a higher strength fill, easy construction, lesser fill testing and monitoring requirements. Only two days were lost due to adverse weather conditions over the two months of construction. In hindsight, the correct decision was made and resulted in efficiencies in completing the contract.

The contract was let as a measure and value contract with design build elements. This enabled different geogrid suppliers to submit specific designs. Regan Brothers, Ltd, using Maccafferri New Zealand as geogrid supplier and designer won the contract. The geogrid used was "Fortrac 35/20-20", at 500mm vertical centres with a wrap-around face.

The design was modified during tender evaluation to minimise excavation widths in order to maintain one lane of traffic. For the critical loading case, greater geogrid embedment lengths are required at the top of the wall reducing in length with depth. It is typical practice (mainly to simplify details and specifications) to use a single geogrid embedment length for the full wall height. By challenging this typical practice and constructing a tapered wall with longer geogrid at the top shortening up at the base, the excavation width at the base of the excavation was

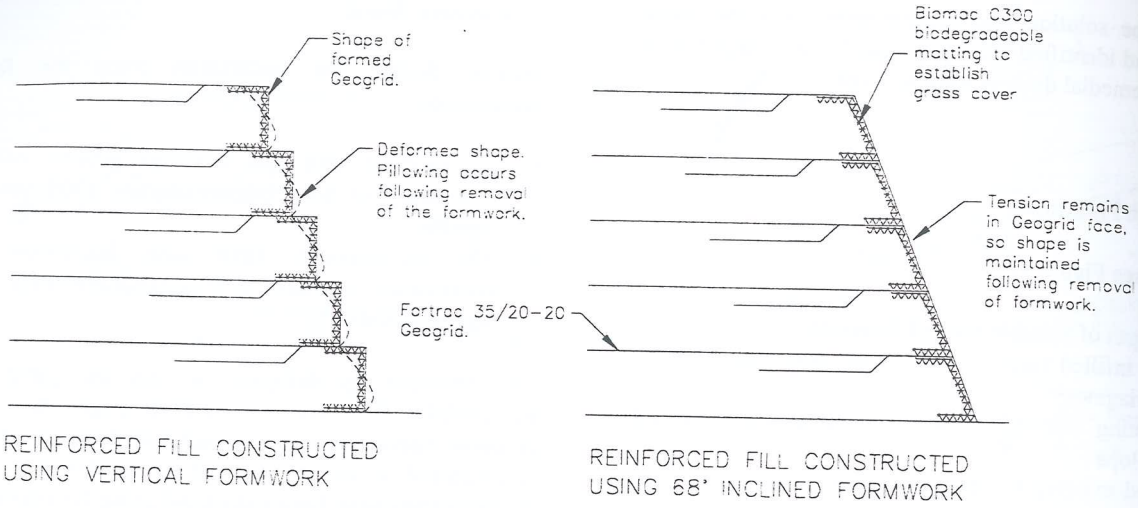

Fig. 4 Geogrid Reinforced Slope Face Detail

significantly reduced, allowing a flatter temporary batter and reducing the risk of instability of the temporary excavation.

5.1.4 Construction

Initially, the templates (formwork) used to form the face were 500mm high vertical sections with each successive layer setback 300mm to form an overall face angle of 68°. This practice was found to be unacceptable because the square edges of the geogrid provide minimal tension in the grid and the hardfill soon loosens up and the face bulges to form an unsightly pillow type appearance.

The templates were modified to provide a 68° face slope. Each successive layer was constructed immediately above the other. This was successful as tension in the front face is maintained and resulted in a superior finish. The template, as a consequence of the angled face was stiffer and much easier to handle and extract from each lift.

5.2 Areas 2 and 3

The two lower sections of road were retained with cantilevered pile retaining walls. The piles are bored, cast insitu reinforced concrete. Each pile is placed at 3D centres in order to provide soil arching between adjacent piles and negate the requirement to install rails or lagging.

The new retaining structures at both Areas 2 and 3 are rigid and not tolerant of deformation. Both structures are therefore designed to resist an ultimate limit state seismic load of 0.4g without yielding.

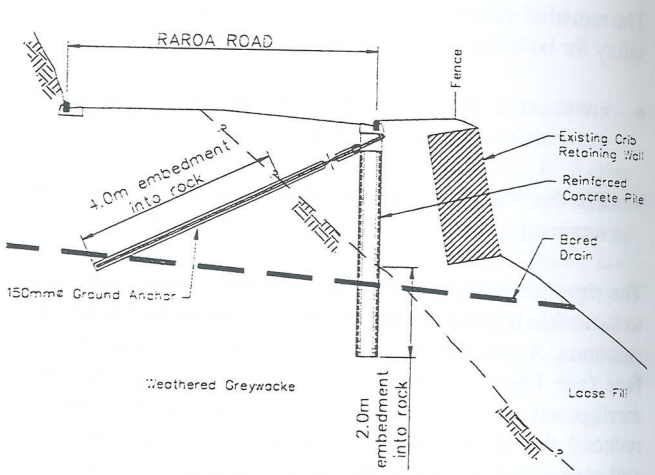

Fig. 5: Typical Section (Area 3).

5.2.1 Area 3

Where existing cribwalls were present (Area 3) the new wall is aligned under the existing kerb and channel, 1.5m inside the existing cribwall. This alignment has two significant benefits.

- The rock/fill interface dips at 40° to 50°. Moving the piles upslope significantly reduces the design retained height which reduces loadings and results in significant cost and time savings.

- Installing the piles upslope of the existing cribwall minimised the excavation required. Construction was rapid and access to both traffic lanes could be maintained for the majority of the works.

Locating the wall on the inside of the footpath leaves the pedestrian footpath unprotected by the new wall. The new wall will however significantly reduce the loadings applied to the existing cribwall, which may prolong the design life of the aging cribwall. When the existing cribwall deteriorates, pedestrian access can be maintained either by lowering the

footpath alignment or cantilevering a suspended timber path from the new retaining wall piles.

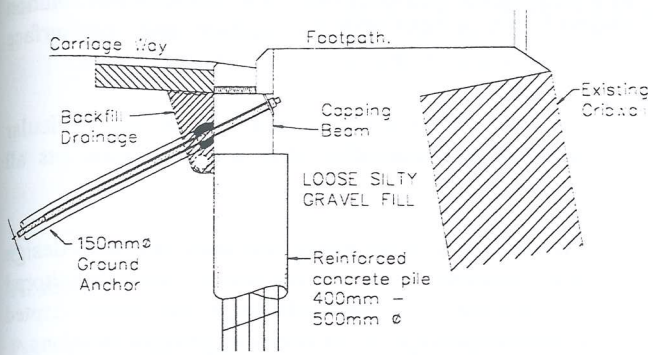

Fig. 6: Remedial Works Area 3, Typical Section

At Area 3, the design retained height of the wall varies between 2 and 5m depth. Where the designed retained heights of the walls are greater than 3.5m tieback anchors have been used to reduce the bending and overturning moments in the piles. The use of tieback anchors resulted in a cost saving to the principal of 30% over a simple cantilever type wall.

5.2.2 Area 2

In Area 2 there was no existing crib wall and the rock level (between 5m and 7m depth) was less steeply inclined than in Area 3. Minimal advantage was gained by moving the wall alignment upslope so Area 2 piles are aligned along the downslope edge of the footpath.

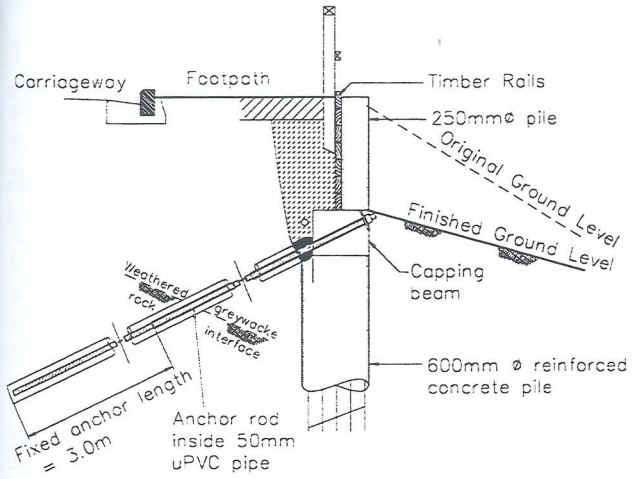

Fig. 7: Remedial Works Area 2

Tied-back reinforced concrete piles were used (see Figure 7) for Area 2. A tieback beam is set 1.2m below the footpath level with 600mm diameter concrete piles at 2m centres below the beam. Above the beam, the pile diameters were reduced to 250mm diameter mainly for aesthetics but this reduction in pile diameter also economises on materials where the bending moments are minimal.

The soil behind the 250mm diameter piles is supported with timber rails. The small wedge of fill in front of the timber rails was removed to facilitate anchor installation and also to relieve some loading from the top of the fill slope.

Downslope of the retaining wall there is potential for further instability in the unsupported fill slope. The Area 2 wall is designed to retain 5m depth. This depth of retention was established by estimating the worst probable long-term regression of the slope below. The regression profile was estimated by taking the deepest probable failure surface of the fill slope, and projecting a 26° line (tangent) from the base of the failure surface. This resulting regression line has a FOS under saturated conditions of 1.3 or greater. If such regression occurs, remedial lagging (sprayed concrete) will be required between the palisade wall piles.

5.2.3 Ground Anchors

Ground anchors have been designed to derive pull out resistance from the weathered greywacke rock. The anchors are RB 32 Reidbars set in a 150mm-diameter cement grout. The anchors with an ultimate tensile load of 430kN were designed assuming an ultimate rock-grout bond stress of 300kPa.

The anchors have a long non-bonded length so that a majority of the grout column will work in compression. Because the grout column is in compression tensile cracking of the grout is minimised and the elasticity of the anchor is controlled by the stiffness of the grout in compression. Anchor loads are therefore transferred more evenly to the founding rock at low strains minimising the risk of gradual unraveling of the rock/grout bond.

The anchors are in a relatively low corrosive environment however two to three levels of corrosion protection are provided for steel rods and components. Levels of protection are:

- all rods and components are galvanised
- the grout column is designed to be continuous to the surface
- the anchor tendon over the free length is coated in grease and enclosed in a uPVC tube
- exposed surfaces are coated in grease and wrapped in Denso tape.

A foam cushion was detailed between the top end of the grout column and the tieback beam so that when the anchors are stressed and tested, the grout/rock bond is stressed rather than putting the grout column/concrete beam joint into compression.

All anchors have been proof-loaded to 90% of yield and then locked off at design working stresses. The tieback wall analysis assumes rotation of the wall about the anchors. The anchors need to be pretensioned because the concrete piles have low elastic properties (stiff) compared to non-tensioned

anchors. If the anchors were non-tensioned they may stretch taking up the load, this may result in the rigid concrete piles attracting higher proportions of the design load and possibly failing.

5.2.4 Construction

The construction works for the concrete pile walls (Areas 2 and 3) was let as a separate contract to the geogrid reinforced slope (Area 1). Construction proceeded generally as anticipated with the exception of the following:

- Minor variations in depth to rock between test locations were encountered. These variations were accommodated by varying pile details and introducing additional anchors for some sections of the Area 3 wall.

- Large quantities of groundwater were unexpectedly encountered in a crush zone in the centre of Area 3. One ground anchor intercepted artesian ground water within the greywacke. The water was flowing from the top of the anchor hole at approximately 2 to 5 litres per minute. After three attempts, the anchor holes (in this area) were successfully grouted with grout return to the surface.

- Two anchors failed under test loading. Both anchors were extracted and re-drilled. The anchors were unable to take load because two couplings joining sections of anchor rod failed. Both couplings had been modified by the drilling contractor to fit down the inside of a smaller drill casing. These modifications weakened the couplings.

5.2.5 Sub-surface Drainage

Due to the artesian groundwater encountered during anchor installation, inclined bored drains were drilled into the slope to relieve water pressures.

The drains were drilled from below the existing cribwall inclined upwards at 5° (see Figure 5). There was concern that the drains would transfer groundwater from the rock and into the more permeable gravelly fill, reducing slope stability below the new retaining wall.

To overcome this a permanent casing was drilled through the fill and socketed 1.0m into the rock. The hole and casing were then cement grouted. A smaller diameter inclined bored drain was advanced through the grout and into the rock, forming a sealed pipe through the fill material. Two bored drains were installed and each has a constant flow of about 8 litres per minute.

6 CONCLUSIONS

The client received an innovative and cost-efficient solution despite difficult and variable surface and sub-surface conditions. Elements that have contributed to this are:

- Different design solutions were used to suit particular ground conditions rather than a one solution fits all approach

- Flexibility and contingency was built into each design and specification. Soil conditions were monitored during construction and each design was easily adapted to accommodate local variations in ground conditions.

- The engineer throughout the project has provided design input. Each stage has been reviewed, fine-tuned and modified to suit construction methods used and the conditions encountered.

- "Standard" construction and design techniques for the geogrid-reinforced slope were challenged and reviewed for this application. Large benefits were achieved by providing small amendments to "standard" procedures.

7 REFERENCES

1. Ambraseys N.N. and Menu J.M., 1988, "Earthquake Induced Ground Displacements", Earthquake Engineering and Structural Dynamics, Vol. 16.

2. Begg J.G. and Mazengarb C., 1996, "Geology of the Wellington Area", Institute of Nuclear and Geological Sciences Limited

3. Newmark N.M., 1965, "Effects of Earthquakes on Dams and Embankments", Geotechnique 15, 139-160.

4. Ruscoe Q.W., 1974, "Microzoning for Earthquake Effects in Wellington", Bulletin 213, New Zealand Department of Scientific and Industrial Research.

8 ACKNOWLEDGEMENT

The author wishes to thank Wellington City Council for permission to publish this paper and acknowledges the assistance of Dianne Shirer for drafting, Bruce McLean, Stuart Palmer and Gary Smith for their contribution to this project and for the review of this paper.

GEOTECHNICAL INVESTIGATIONS ASSOCIATED WITH THE AXIS FERGUSSON EXPANSION

Nicola Ridgley

Beca Carter Hollings & Ferner Ltd, Auckland, New Zealand

Abstract:

Ports of Auckland Ltd (POAL) are upgrading Axis Fergusson Terminal to increase container handling capacity in order to meet a projected increase in trade. The upgrade includes construction of a piled wharf 320m long, mooring dolphins, 1000m length of perimeter bunds and a reclamation which will be 9.4 hectares in area and will contain 1.5 million cubic metres of fill.

The existing seabed lies between 1m and 12m below Chart Datum, with the surface of the reclamation at around 5.4m above chart datum, resulting in fill depths of up to 18m. The site is located in Auckland, New Zealand in the Waitemata Harbour which is a drowned river valley system and which has significant depths of weak sediments. The existing terminal is constructed over the top of an old remnant ridge. The proposed reclamation is located to the east of the ridge over a valley with thick layers of weak sediments.

The main geotechnical design issues associated with this development include stability (static and seismic) of the 18m high bunds and reclamation on weak sediments, settlement of the reclamation and bunds, suitability of reclamation fill materials to obtain a reclamation of relatively low compressibility, reuse of marine dredgings, and piling options to support the wharf structure.

Geotechnical investigations have been undertaken at various stages of the project from prefeasibility to detailed design in order to obtain information about the underlying soil conditions. Investigations comprised a series of machine boreholes and Geonor in situ large vane testing undertaken from a barge in the harbour and laboratory testing.

This paper describes the geotechnical design issues associated with the development, the extensive geotechnical investigations to address these design issues, and summarises the results of these investigations.

1 INTRODUCTION

POAL propose to upgrade the capacity of the existing Axis Fergusson Terminal by expanding the reclamation, extending the existing wharf, and constructing a new wharf.

The upgrade is proposed to involve construction of a 320m long wharf (concrete piled flat slab structure) adjacent to the northern edge of the existing reclamation, mooring dolphins, perimeter bunds and a reclamation of approximately 9.4 hectares in area located to the south of the proposed new berth and east of the existing terminal. The reclamation bunds and quay structure will be constructed to a level of about 5.4m above Chart Datum. (+ 5.4CD).

The piled wharf will be required to support container cranes. The reclamation will be used for the storage of containers stacked up to 4 high in the future and will be trafficked by heavy duty vehicles such as straddle carriers.

Dredging of the seabed to the north and east of the existing terminal is proposed to provide the required navigational water depth. Construction of the bunds will also require dredging to remove unsuitable soils from below the bund and allow a keyed toe to be formed. The proposed dredged level along the northern edge of the proposed wharf for the ship berth is -13.5CD with an allowance to dredge to -14.0CD in the future.

2 GEOLOGY

The site is located in Auckland, New Zealand in the Waitemata Harbour (Refer Figure 1).

The Waitemata Harbour is a drowned river valley system. During previous periods of glaciation (i.e. low sea levels) the landform was eroded, forming valleys in the weathered Waitemata Group rocks. As the sea levels subsequently rose, the valleys became submerged and infilled with sediments. These infill materials typically comprise very weak to stiff fine grained materials i.e. sands, silts and clays.

The Geological Map of the Auckland area (Sheet R11, Scale 1:50000) indicates that the underlying rock is the Waitemata Group sandstone and siltstone of East Coast Bays formation. This formation is expected to also contain mudstone with occasional lenses of coarser cemented grit (i.e. "Parnell Grit").

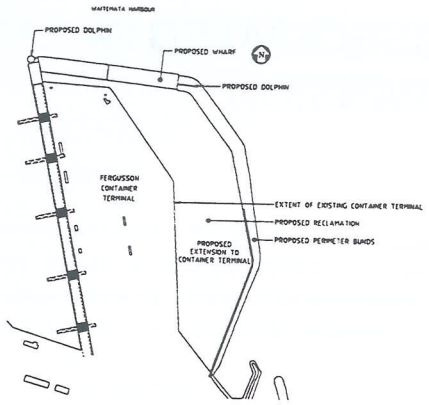

Figure 1 - Site Layout Plan

3 GEOTECHNICAL DESIGN ISSUES

The key geotechnical design issues for this development include:

a) overall stability of the bunds and reclamation;
b) settlement of the bunds and reclamation;
c) suitability of various reclamation fill materials;
d) piling to support the wharf structure; and
e) seismicity

These issues are briefly described in turn below.

a) Overall Stability of the Bunds and Reclamation Fill

The bunds will act as a containment structure to hold the reclamation fill. Two modes of failure will need to be considered in design of the bunds:

- Shallow surface slumping of the bund materials, and
- Deep seated failure through the underlying soils.

The shallow failures are mainly a function of the bund material while the deep seated failures are mainly a function of the strength of the underlying soils. The short term (i.e. during and immediately following construction) stability of the bund is likely to be critical and can be managed by staged construction, limiting surface loadings and sizing of the toe key or improvement of the underlying soils. For design of the bunds it is necessary to define the shear strength of the underlying soils and the depth and extent of very soft soil layers.

b) Settlement of the Bunds and Reclamation

Weak sediments underlying the site will consolidate and contribute to settlement of the reclamation, bunds and structures founded above these materials. Settlement of the reclamation and bund will be due to consolidation of the underlying soils and of the reclamation fill under the weight of the fill and applied (container stacking) loads. Design of the surface gradings, pavements, drainage and other structures will need to take into account predicted settlements. Geotechnical investigations are necessary to define the underlying soil types and consolidation characteristics in order to estimate the magnitude and rate of potential settlements for design.

c) Suitability of Various Reclamation Fill Materials

The majority of the reclamation and bund fill will be placed below water, and therefore will not be compacted. The selected fill materials must however be of low compressibility so as not to add to settlements that will occur due to consolidation of underlying soils and must not be susceptible to liquefaction during earthquake shaking. Selected suitable fill types are likely to be either granular in nature or stabilised mud.

Dredging of marine sediments will be required during construction to remove unsuitable soils and obtain the required berth depth. Material will also be made available for maintenance dredgings around the port. These materials have been found to form a high strength fill of low compressibility when mixed with cement. Cement stabilised marine dredgings (named "mudcrete") has been used successfully as a high strength structural fill material on other local marine projects. The cement has also been shown to "lock up" contaminants within the marine dredgings.

d) Piling to Support the Wharf Structure

Piles will need to support the quay structure, container cranes containers and vehicles. Piling options including both driven and bored piles will be evaluated to obtain an economic solution. While the properties of Waitemata Group rock are relatively well understood, geotechnical investigation is required to determine the location of the rock surface for founding the piles.

e) Seismicity

Seismic hazard is an important aspect of the design of structures in New Zealand which lies on tectonic plate boundaries. For this project seismic effects must be considered in the design of the wharf structure, bunds and reclamation. A site specific seismic hazard assessment has been undertaken to determine the seismic design parameters for this site. Geotechnical investigations were considered necessary to determine the type and strength of the soils to allow an assessment of the performance of these soils under seismic loads and their susceptibility to liquefaction.

A series of geotechnical investigations has been targeted and undertaken to address the various design issues described above. These investigations are described in Section 4.

4 GEOTECHNICAL INVESTIGATIONS

Geotechnical investigations have been undertaken at various stages of the overall development of Fergusson Terminal and in particular to resolve the design issues related to this project. In 1993 preliminary site investigations, comprising machine boreholes, were conducted in the harbour adjacent to the two main container terminals as part of an overall development plan for the wharves and reclamation. In 1997 a more detailed geotechnical investigation comprising machine boreholes, limited large shear vane testing and laboratory testing was undertaken to determine subsoil conditions for designing the extension to the Fergusson Container Terminal

and obtaining environmental approvals (i.e. Resource Consents). In 1998 large in situ shear vane testing was carried out along the eastern side of the proposed reclamation, and several machine boreholes were drilled through the existing reclamation for detailed design of the bunds. In situ large shear vane testing was performed to obtain a direct measurement of the shear strength of the weak marine soils for design of the bunds. The locations of the investigations are shown on Figure 2.

The investigations have typically been carried out over the water from a barge, and as such were limited to periods of calm water. At times the drilling operation had to contend with water currents of 2 knots when drilling was undertaken in the main harbour channel. The machine boreholes were advanced using open barrel sampling in soil and triple tube coring in the Waitemata Group rock. Undisturbed samples were taken in tubes as required for selected laboratory testing, and standard penetrometer testing was undertaken at 1.5m centres through the length of the borehole. Pilcon vane shear strength tests were undertaken on core in the open barrel. Large shear vane test holes were carried out in sections at 50m centres along the length of the bund. Each section comprised 3 test holes each around 25m apart across the width of the bund. Shear vane tests were undertaken at 1m intervals in each test hole until a shear vane strength of 80kPa or greater was recorded. A Geonor vane was used with a diameter of around 50mm and a height of 100mm. The purpose of this testing was to obtain a profile of the shear strength of the soil in sections across the width of the bund and with depth.

Laboratory testing was undertaken on a range of soil samples obtained during the investigation. The laboratory testing comprised soil classification tests such as natural moisture content and Atterberg limits, gradings, consolidation tests, consolidated undrained triaxial tests and unconfined compressive strength tests.

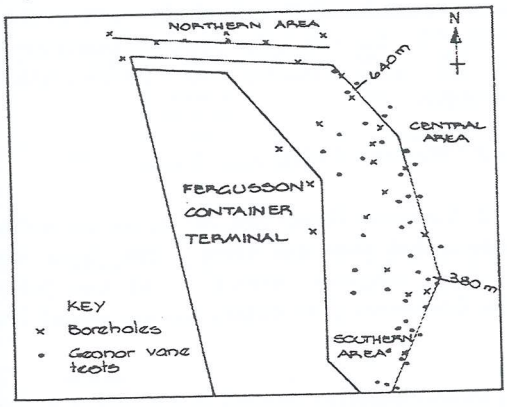

Figure 2 - Location of Investigations

5 SOIL PROFILE

In summary, the foundation conditions encountered during these investigations typically comprised weak marine sediments overlying residual soils of the Waitemata Group (i.e. sands, silts and clays) grading to interbedded layers of Waitemata Group sandstone and siltstone. Figures 7 and 8 show schematically the soil profile encountered along the northern and eastern edges.

The results of these investigations indicated that Fergusson Terminal was built along the top of a ridge and that the sandstone/siltstone surface generally dipped gently northwards. A gully has been identified along the eastern side of Fergusson Terminal. Contours of the sandstone/siltstone surface have been interpolated from historical and recent site investigation results and are shown on Figure 3.

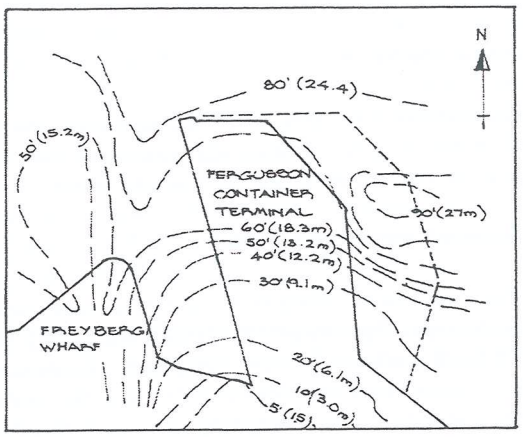

Figure 3 : Contours of Waitemata Group Rock

The relatively weak sediments have been divided into two categories: very weak Holcene sediments (i.e. deposited the last 10,000 years), overlying stronger Pleistocene sediments (i.e. deposited within the last 1.6 million years). The categorisation between the two layers was assessed based on the shear strength of the soil, the natural moisture content and the plastic and liquid limits.

The in situ large shear vane testing along the eastern bund indicated three distinct areas of relatively consistent soil shear strength profile.

At the Southern end (Chainage 0 to 380m) the strength profile typically recorded was around 3-5m of very soft Holocene sediments with shear strengths of 2-10kPa overlying stiff Pleistocene sediments and residual (weathered) Waitemata group soils with shear strengths around 80kPa.

Soils underlying the Central section (Chainage 380 to 640m) of the bund typically comprised 2-5m very soft Holocene sediments (as above) overlying firm Pleistocene sediments with shear strengths of around 30 to 50kPa. These in turn were all underlain by stiffer weathered Waitemata group soils.

Towards to Northern end, around 1-2m of very soft Holocene sediments was encountered overlying stiff Pleistocene sediments and weathered Waitemata group (i.e. soils with shear strength 80kPa+).

Boreholes drilled in the eastern side of the reclamation indicated an extensive gully infilled with very weak Holocene sediments within the Central bund section. The Geonor vane shear strength testing confirmed the presence of this infilled gully.
Three machine boreholes were also drilled through the

reclamation along the existing eastern edge. The location of these are shown on Figure 2. Soils encountered in these boreholes typically comprised stiff clayey silt and medium dense sand. In situ testing indicated Pilcon vane shear strengths of 80 to 120kPa and standard penetrometer tests recorded typically 11 to 50 blows per 300mm in the Pleistocene sediments below the old rock bund.

The soil types encountered are described below. A summary of the soil test results is shown on Table 1.0.

(a) Layer A : Sediments

The sediments encountered in the machine boreholes typically comprised recent very weak Holocene sediments overlying older slightly over-consolidated Pleistocene sediments.

(i) Layer A1: Holocene Sediments

The very weak Holocene sediments encountered were typically around 0.5-2m thick along the Northern edge of the proposed reclamation increasing to around 5m thick beneath the Central eastern side. In situ testing indicated relatively consistent strengths with large vane shear strengths of typically around 2 to 10kPa and Pilcon shear strength measurements of 4 to 30kPa. Figure 4 shows a general increase in shear strength with depth.

It is noted that the Pilcon vane tests carried out in the open barrel measured higher soil shear strengths than the large in situ vane testing. This is considered to be due to the soil sample becoming compressed in the open barrel during sampling. Also the Pilcon vane is rotated faster than the large Geonor vane, resulting in a faster rate of shearing and hence higher apparent soil shear strengths.

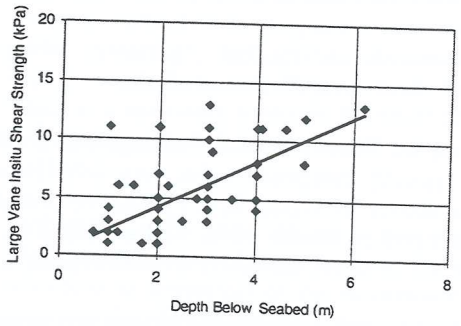

Figure 4 : Shear Strength vs Depth Below Seabed HOLOCENE LAYER

Atterberg limit tests on samples of these soils indicate that the material is highly plastic and has a natural water content close to the liquid limit. Soil particle size gradings carried out on these soils indicate that the soils are typically silty clays/clayey silts.

(ii) Layer A2: Pleistocene Sediments

In-situ strength testing and laboratory consolidation tests of the Pleistocene sediments indicate that these deposits are overconsolidated. Pilcon vane shear strengths measured in this material typically varied between 30 and 100kPa and standard penetrometer tests recorded typically 4 to 20 blows/300mm penetration. Large vane shear strengths recorded in these soils to the east of the existing reclamation varied between 20 and 80kPa.

Figure 5 shows that generally the shear strength of the Pleistocene sediments also increases with depth below seabed.

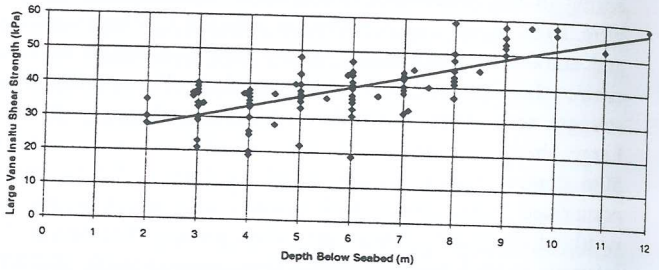

Figure 5 : Shear Strength vs Depth Below Seabed PLEISTOCENE LAYER

Atterberg limit tests on these Pleistocene materials indicates this material is also moderately to highly plastic. The natural moisture content of these soils is typically closer to the plastic limit. Soil particle size gradings carried out on these soils indicates that the soils are typically sandy or clayey silts.

A hard lens of material was located in boreholes located along the alignment of the northern bund between -12 and -16 CD. Standard penetrometer tests recorded typically 40+ blows/300mm penetration.

(b) Layer B : Weathered Waitemata Group

The weathered Waitemata Group typically comprises stiff to very stiff interbedded silts and clays. This layer was encountered in the boreholes between 6 and 14m below seabed (10 and 24m below chart datum) and was around 2 to 5m thick.

In situ testing indicated that the soils are stiff to very stiff with standard penetrometer test results of between 12 and 41 blows per 300mm penetration and Pilcon vane shear strengths between 80 and 130kPa. Figure 6 shows a plot of normal stress versus shear stress from results of triaxial tests on the Pleistocene and weathered Waitemata Group soils collected during various investigations for development of the Fergusson Container Terminal. The line on this graph indicates this soil has a cohesion (c') of around 5kPa and an angle of friction (ϕ') of around 35º.

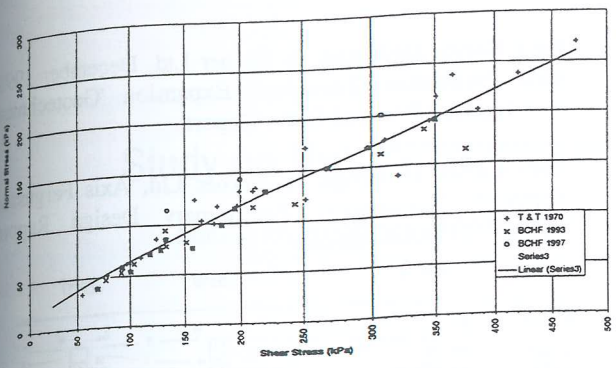

Figure 6 : Normal Stress vs Shear Stress

(c) *Layer C : Waitemata Group Sandstone and Siltstone*

This layer generally comprises interbedded extremely weak to very weak (in terms of rock strength) grey fractured sandstone and siltstone. Figure 3 shows approximate contours of the surface of sandstone/ siltstone. Along the alignment of the proposed piled quay structure (ie northern edge) sandstone/siltstone was encountered in the boreholes between -22 CD and -29CD (ie 10 to 17m below seabed).

Along the eastern edge sandstone/siltstone was encountered between -11 and -26CD. The depth to sandstone encountered in the boreholes indicates that the sandstone/ siltstone surface slopes from the southern end of the reclamation towards the north. A gully was located at around distance 500m, to the east of the existing terminal.

Standard penetrometer tests produced penetrations of between 95 and 290mm for 50 blows ie N = 50 - 150 blows/300mm. This layer is considered suitable for pile foundations.

6 CONCLUSION

In order to resolve the design issues described in Section 3 geotechnical investigations comprising the drilling of machine boreholes, large vane in situ shear strength testing and laboratory testing have been undertaken.

Boreholes were drilled to obtain samples of the soils for logging, laboratory testing and determining the depth to Waitemata Group rock. In situ strength testing such as standard penetrometer tests and large vane shear tests down the borehole and Pilcon vane tests on soil samples in the open barrel provided information to allow a general assessment of the soil conditions across the site. The laboratory testing has provided additional information on the nature of the soils (ie. particle size gradings for a liquefaction assessment) and geotechnical parameters for an assessment of consolidation settlements and shear strength parameters from triaxial tests for stability analysis.

The boreholes revealed significant depths of weak soils across the site. The assessment of the shear strength of these soils is considered critical to the stability of the bunds. In situ large shear vane testing was considered the most appropriate method of determining the actual shear strength of the underlying soils and this testing was undertaken as described earlier. Indirect measurement of the shear strength of very weak soils using Pilcon vane in a sample can provide misleading results due to sample disturbance and rate effects of testing. Direct measurement of soil shear strength in situ is considered necessary, particularly where very weak soils are present and where the actual shear strength of the soil is critical to the design of the structure.

Staging of the geotechnical investigations has allowed the appropriate testing at each stage by focusing on resolving each of the geotechnical design issues, as the various stages of investigations revealed the critical soil conditions.

TABLE 1 - SUMMARY OF SOIL PROFILE AND LABORATORY TEST RESULTS

Layer	Description	Depth below seabed to top of layer (m)	Thickness (m)	SPT N (Blows/ 300mm)	Pilcon Vane Shear Strength (kPa)	Geonor Vane Strength (kPa)	Atterberg Limits LL (%)	Atterberg Limits PL (%)	Natural Moisture Content (%)	Grading Sand (%)	Grading Silt (%)	Grading Clay (%)	Consolidation $\frac{C_c}{1+e_o}$ (%)	Consolidation Pc' (kPa)	Triaxial CU c' (kPa)	Triaxial CU Ø' deg	Bulk Density t/m³	UCS (MPa)
A1	Holocene Sediments	0	0.5-5	0-1	4-30	2-10	82 to 93 Avg =88	27 to 33 Avg =30	77 to 98 Avg =82	1 to 36 Avg =10	36 to 66 Avg =52	33 to 51 Avg =38	23 to 24 25	70 to 50 70	12	24	1.48 to 1.56 Avg =1.52	
A2	Pleistocene Sediments	0-12	2-14	3-50 typically 15	30-130 Typically 70	20-80	49 to 98 Avg =76	23 to 45 Avg =30	32 to 72 Avg =48	2 to 63 Avg =21	28 to 64 Avg =44	9 to 64 Avg =35	15 to 23 26	180 to 200 250	25	24	1.52 to 1.78 Avg =1.65	
B	Weathered Waitemata Group	6-14	2-5	12-41 typically 30	80-130 typically 100	80+							10 to 14 17	150 to 300 350	25 to 12 50	30 to 33 34		
C	Waitemata Group Sandstone & Siltstone	8-15	-	50+	-	-												1020 to 4000

Note: (i) LL = Liquid Limit, PI = Plasticity Index; Pc' = Preconsolidation Pressure; $\frac{C_c}{1+e_o}$ = Compressibility; Ø' = Effective Angle of Friction; c' = Effective Cohesion; CU = Consolidated Undrained with Pore Pressure Measurement; UCS = Unconfined Compressive Strength

7 ACKNOWLEDGMENTS

The writer would like to thank Ports of Auckland Ltd for permission to publish details on the proposed Axis Fergusson Container Terminal Expansion and Stephen Priestley and Gavin Alexander of Beca Carter Hollings and Ferner Ltd for reviewing this paper.

8 REFERENCES

1. Beca Carter Hollings & Ferner Ltd, December 1998, Axis Fergusson Terminal Expansion 'Geotechnical Investigation Factual Data Report'.

2. Beca Carter Hollings & Ferner Ltd, Axis Fergusson Terminal Expansion Preliminary Design Report, Volume 2 Geotechnical.

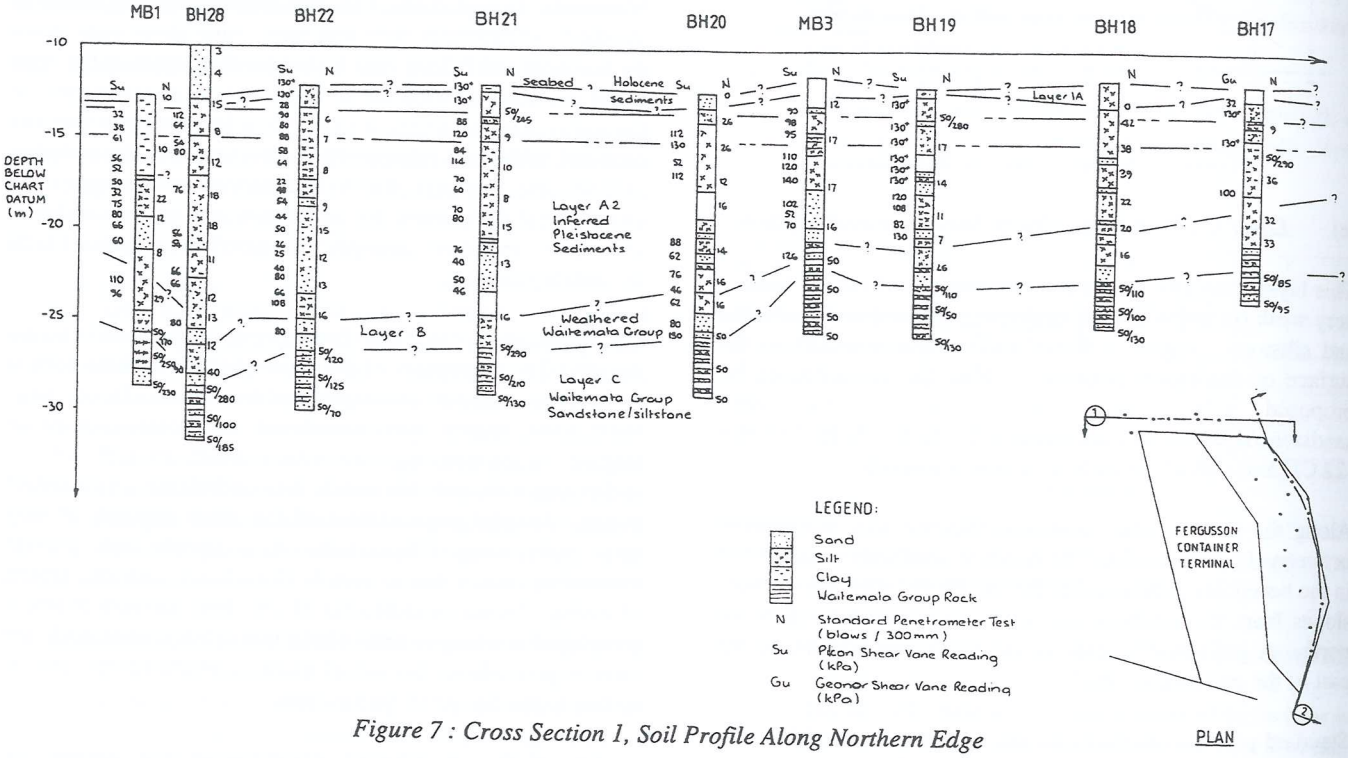

Figure 7 : Cross Section 1, Soil Profile Along Northern Edge

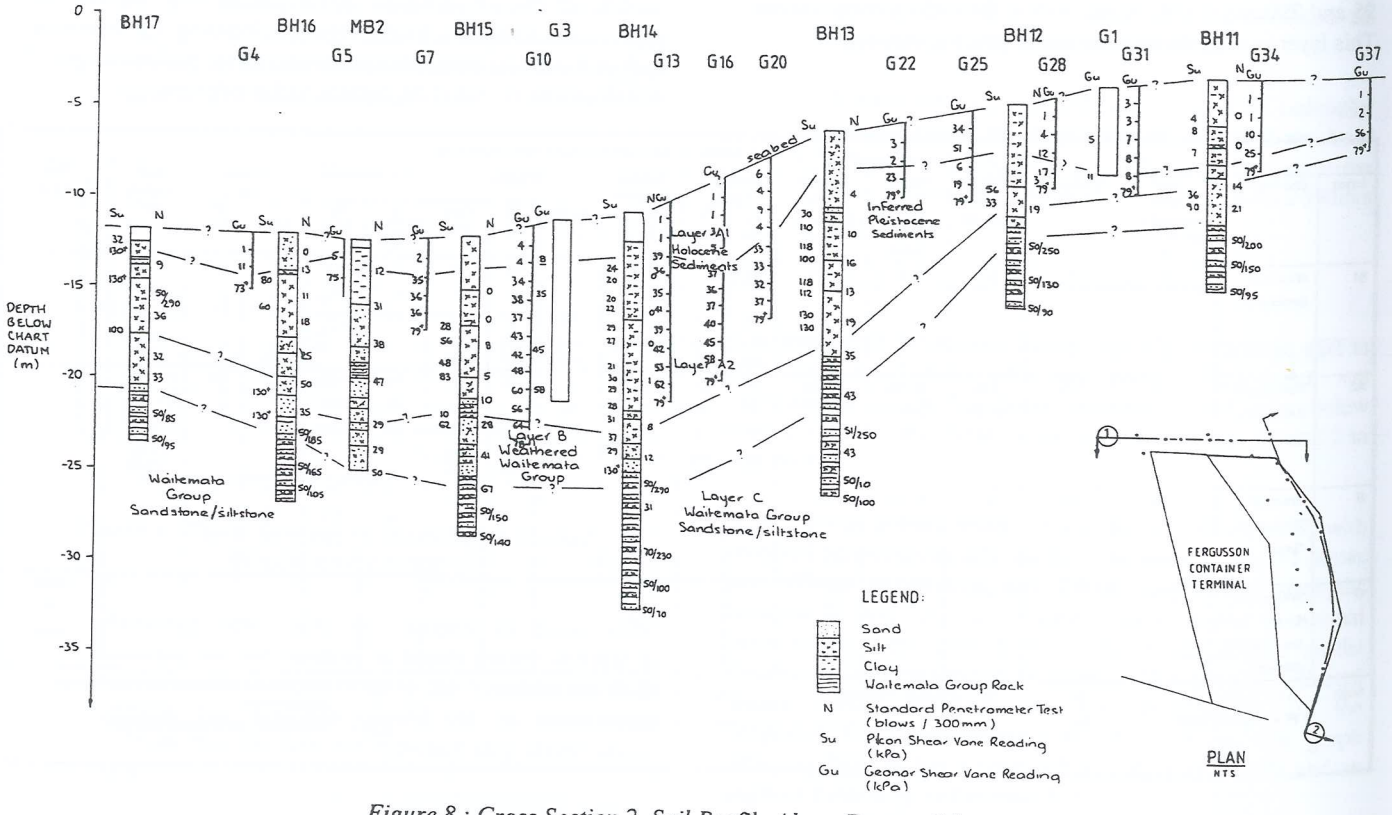

Figure 8 : Cross Section 2, Soil Profile Along Eastern Edge

Study on the Properties of Cemented Saline Tailings Backfill

Caigen Wang
Mining Engineering Program, Western Australian School of Mines, Kalgoorlie, Australia

Summary This paper deals with the properties of tailings fill cemented by two different binding agents: Ordinary Portland Cement (OPC) and a special binding agent called High Water and Quick Setting cement (HWQS). Specific emphasis was placed upon the exploration of potential applications of saline tailings prevailing in the Goldfields region of Western Australia for mine backfill purposes. Included in this paper are the testing results of the properties of tailings fill with a range of salinity and cemented by either OPC or HWQS. Recommendations for the selection of binding agent for the design of tailings-based mine backfill are provided.

1 INTRODUCTION

In the Goldfields region of Western Australia, fresh water is in serious shortage, and with this reality, saline ground water is the only choice for most of the mineral processing plants. Consequently, the tailings slurries from mill plants are also highly saline. The typical salinity of the ground water and the water in the tailings slurries in the Goldfields range from 80000 to 200000mg/L TDS (Total Dissolved Solids), of which 90% is Na^+ and Cl^-[1].

In general, the salinity of the water used to prepare cemented products has an adverse impact on their properties, especially their strength characteristics. The higher the salinity of water, the lower the strength of cemented products mixed with this kind of water. In view of the highly saline ground water and tailings prevailing in the Goldfields region of Western Australia, a challenge is to determine the degree of influence of water salinity on the properties of cemented tailings fill. This would allow the economical and technical evaluation of the application of saline tailings for cemented backfill. With these initiatives, an investigation on the properties of cemented tailings fill was initiated in early 1997, with the preliminary laboratory testing results[2] being reported by Wang (1997). This study showed the technical potential for the application of saline tailings for mine backfill.

The backfill investigation started in Jan., 1998 with the saline tailings slurry provided by the Mill Plant of Kalgoorlie Consolidated Gold Mines Pty Ltd (KCGM). The binding agents used in this investigation were Ordinary Portland Cement (OPC) and HWQS separately. HWQS used in this investigation was supplied by China University of Mining and Technology. For both types of binders, water with a range of salinities was used to mix the tailings solids. A comparison between the properties of tailings-fill including water having different salinity and different types of binders was then undertaken.

2 TESTING MATERIALS

In total, three types of materials were combined in this study, i.e. tailings, water with different salinity and binding agents (OPC and HWQS).

2.1 Tailings

Fresh unclassified gold tailings slurry from the KCGM mill plant, comprising almost 50% tailings solids and 50% highly saline water was sampled. The Total Dissolved Solids (TDS) determined was 208000mg/L. Separation of saline water and tailings solids was conducted so that the fill samples could be prepared according to a designed solids/water ratio.

The particle size distribution of the tailings provided by KCGM [3] is presented in Table 1.

Table 1. Particle size analysis results

Particle size (micron)	Cumulative percent passing (by weight)
300	97.5
212	91.3
150	82.2
106	73.6
75	65.4
53	60.8
38	55.5
0	0

2.2 Binding agents

One binding agent used was Cockburn Cement for General Purpose.[4] .

The other binding agent used was HWQS cementitious material, which was specifically designed for underground

use[5]. This material is composed of two kinds of solid powder material, i.e. substance A and substance B. A and B are usually separately packed before they are put into use (mixed). The method of using HWQS is to mix A with water (or plus aggregates) and mix B with water (or plus aggregate) separately and transport slurry A and B separately. After being transported to the destination where fill placement is to take place, slurry A and B are put together and placed into mined-out voids. As HWQS is capable of reacting with a large amount of water, the water/cement ratio by weight can reach 2.5-3.0 or even higher. The volume of solidified water in pure HWQS-water compound after the completion of hydration can be as high as over 88-90%. The pumping life of slurry A and B before being mixed together is up to 3 days.

The other distinctive properties of HWQS compared to OPC are quick setting and high early strength. After slurry A and B are mixed together (at A/B ratio of 1), the chemical reaction and solidification take place immediately with an initial setting time ranging from 10 to 20 minutes and a final setting time being 30 to 40 minutes. Uniaxial compressive strengths of HWQS with a series of W/C ratio at different stages of curing process are presented in Table 2.

2.3 Water

Two types of water were used to prepare the fill samples, i.e. saline water and fresh water. The salinity of the water used to mix the tailings solids and binding agents varied from 0, 5%, 10% and 20.8% for fill samples of different recipe. (1% water salinity is equivalent to a TDS of 10,000ml/L.)

3 TEST SAMPLE PREPARATION AND CURING

3.1 Sample size and preparation

Samples 50mm in diameter and 100mm high were cast in a mold made of PVC pipe. Both ends of the sample were trimmed and made parallel after the sample had set and hardened. The samples were demolded and cured in a curing tank with the relative humidity and temperature being controlled at 96-98% and 23-27°C respectively.

3.2 Sample batches

Two categories of samples were prepared and tested, i.e. OPC-based tailings fill and HWQS-based tailings fill. For both categories of fill samples, 70% solids by weight was designed as a fill slurry density, which is the typical density for hydraulic fill in practice. Tailings solids/binder ratios of 92:8, 94:6 and 96:4 by mass were adopted for both fresh water samples and saline water samples. The salinity of the water used is as mentioned above. Table 3 lists all the sample compositions of this investigation.

Table 3 Compositions of samples with 70 Wt% density

Type of binder	Tailings/binder proportion, Wt %		Water salinity
	Tailings solids	Binder	(%)
Either HWQS or OPC	92	8	0
	94	6	0
	96	4	0
	92	8	5
	94	6	5
	92	8	10
	94	6	10
	92	8	20.8
	94	6	20.8
	96	4	20.8

4 TESTING EQUIPMENT

The samples were tested under Triaxial Compression. A confining pressure of 0.1MPa was applied, which was achieved by using a pressure-adjustable air compressor and air pressure reservoir. The loading rate of the test machine was set at 1~2 kN/min. The testing system is presented in Figure 1.

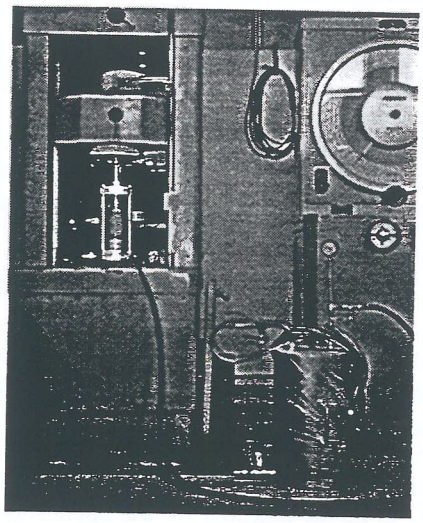

Figure 1. Testing system

Table 2 Mechanical properties of High Water and Quick Setting cement at different W/C ratios

Batch No	W/C Ratio	Water Content (% volume)	HWQS Consumption (kg/m^3)	Initial setting time (minutes)	Uniaxial Compressive Strength (MPa)				
					2h	24h	3d	7d	28d
1	1.00:1	74.36	743	1~1.5	12	18	20	25	30
2	2.00:1	85.20	426	14	3.33	6.26	7.27	7.92	8.70
3	2.25:1	86.60	385	15	2.42	4.74	5.38	6.19	7.08
4	2.50:1	88.00	352	15	1.78	3.93	4.64	4.74	5.32
5	2.75:1	88.80	323	14	1.30	3.08	3.57	3.84	4.22
6	3.00:1	89.70	299	15	0.92	2.54	2.99	3.22	3.60

5 TEST RESULTS

Compressive failure stress of cemented fill samples were determined under a confining pressure of 0.1 MPa and at a curing age of 24 hours, 3 days, 7 days and 28 days.

The values for the early mechanical properties (at a curing time of 24 hours, 3 days and 7 days) were calculated from the mean of two tests. The values for the 28 days mechanical properties were calculated from an average of three tests. Each value reported is the total stress on the specimen at the failure, that is, the applied vertical stress plus the cell pressure [6].

5.1 Properties of Tailings Fill Constituted with Fresh Water

The properties of backfill containing tailings solids and fresh water (using OPC and HWQS as binding agents) are presented in Table 4 and Figure 2.

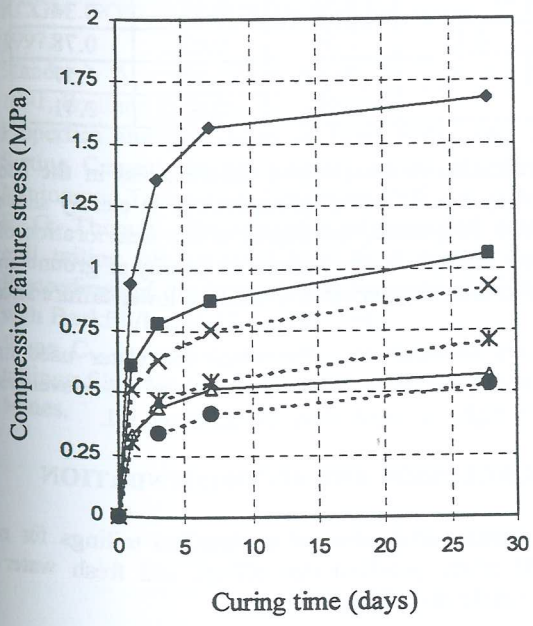

Figure 2. Compressive failure stress of cemented tailings fill containing fresh water at a confining pressure at 100kPa
♦, ■, Δ—HWQS-based fill at Tailings/Binder ratios of 92:8, 94:6 and 96:4 respectively
×, ∗, •—OPC-based fill at Tailings/Binder ratios of 92:8, 94:6 and 96:4 respectively

It can be seen, from Figure 2, that, for fresh water based samples, the compressive failure stress of HWQS-based fill is almost two times that of OPC-based fill for all curing times. For example, a backfill sample containing 6 Wt% HWQS showed a higher failure stress than a sample containing 8 Wt% OPC for each stage of curing.

Monitoring the physical behavior of fill samples immediately after the fill samples were cast revealed the drainage situation of backfills containing different types of binder. For HWQS based backfill samples, neither percolation nor sample shrinkage were observed. By contrast, both water percolation and shrinkage were observed in the OPC-based samples for all the ranges of OPC content. The conclusion reached is that a potential exists for the application of unclassified tailings in conjunction with HWQS.

5.2 Properties of Backfill Constituted with Saline Water

As was previously described, samples containing water having a salinity of 5%, 10% and 20.8% were prepared and tested separately for both HWQS-based fill and OPC-based tailings fill. The properties gained are presented in Table 5 and 6.

5.2.1 Backfill Containing 5% and 10% Water Salinity

The backfill properties are presented in Table 5, which shows that, for 5% water salinity, HWQS-based tailings fill still has a 28 days failure stress 10% higher than an OPC-based tailings fill for both Tailings/Binder ratios of 92:8 and 94:6. However, for a sample containing 10% water salinity, no difference on failure stress of fill cemented by either binder was determined (28-day curing age).

5.2.2 Backfill containing a 20.8% water salinity

The properties of backfill containing 20.8% water salinity are presented in Table 6.

A comparison between the failure stresses of HWQS-based fill and OPC-based fill indicates that, for tailings fill containing water of 20.8% salinity, OPC-based fill would achieve a higher failure stress than HWQS-based fill.

Table 4 Properties of cemented tailings fill made of fresh water at a density of 70 Wt %

Type Of Binder	Tailings/Binder Proportion		Salinity of Water	Shrinkage	Water Percolation	Compressive Strength (MPa) (A Confining Pressure of 100kPa)			
	Tailings	Binder	(%)			24h	3d	7d	28d
HWQS	92	8	0	NO	NO	0.94	1.36	1.57	1.68
	94	6	0	NO	NO	0.61	0.78	0.87	1.06
	96	4	0	NO	NO	0.33	0.44	0.52	0.57
OPC	92	8	0	Observable	YES	0.52	0.63	0.76	0.93
	94	6	0	Observable	YES	0.30	0.47	0.55	0.71
	96	4	0	Observable	YES		0.34	0.42	0.53

Table 5 Properties of tailings fill containing 5% and 10% water salinity

Type of Binder	Proportion of Tailings to Binder		Salinity of Water	Shrinkage	Water Percolation	Compressive Failure Stress (MPa) (A Confining Pressure of 100kPa.)
	Tailings	Binder	(%)			28 days
HWQS	92	8	5	NO	NO	0.94
	94	6	5	Observable	YES	0.66
	92	8	10	NO	NO	0.82
	94	6	10	Observable	YES	0.57
OPC	92	8	5	Observable	YES	0.84
	94	6	5	Observable	YES	0.60
	92	8	10	Observable	YES	0.81
	94	6	10	Observable	YES	0.58

Table 6 Properties of tailings fill containing 20.8% water salinity

Type of Binder	Proportion of Tailings to Binder		Salinity of Water	Shrinkage	Water Percolation	Compressive failure stress (MPa) (A Confining Pressure of 100kPa.)			
	Tailings	Binder	(%)			24h	3d	7d	28d
HWQS	92	8	20.8	NO	NO	0.45	0.57	0.62	0.76
	94	6	20.8	Observable	YES	0.31	0.38	0.44	0.49
	96	4	20.8	Observable	YES		0.28	0.31	0.34
OPC	92	8	20.8	Observable	YES	0.42	0.54	0.63	0.78
	94	6	20.8	Observable	YES		0.40	0.48	0.57
	96	4	20.8	Observable	YES		0.33	0.37	0.41

6 INFLUENCE OF WATER SALINITY ON THE PROPERTIES OF TAILINGS FILL

The compressive failure stresses of fills containing 8% and 6% binder content in solids with salinity of water are presented in Figure 3.

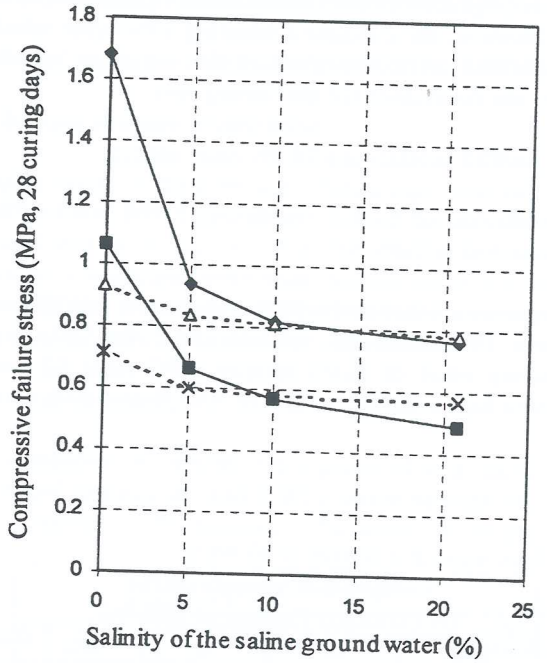

Figure 3 Backfill failure stress with water salinity (A confining pressure of 100kPa was applied.)
◆, ■—HWQS-based fill at Tailings/Binder ratios of 92:8 and 94:6 respectively
Δ, ×—OPC-based fill at Tailings/Binder ratios of 92:8 and 94:6 respectively

The reduction in compressive failure stress in the backfill caused by the salinity of ground water is clearly shown in Figure 3. In general, the degree of the deterioration of fill strength depends on the amount of salinity of ground water. For all cases, a higher salinity means a lower failure stress.

Figure 3 also indicates that when the water used has a salinity higher than 10%, OPC-based fill developed a slightly higher strength than HWQS-based fill.

7 CONCLUSION AND RECOMMENDATION

The potential application of unclassified tailings for mine backfill exists, provided that HWQS and fresh water are used to make the tailings fill.

The salinity of water used to make cemented fill has larger influence on the strength of HWQS-based fill than on OPC-based fill. For cases of low salinity (<10%), HWQS is preferred to OPC for the application of saline tailings fill. Otherwise, the OPC based fill is recommended.

As far as the Goldfields tailings is concerned, with their typical TDS of 80000~200000 mg/L as introduced previously, the option between HWQS and OPC for cemented backfill binding agent should be made on the base of the individual salinity of the ground water which is proposed to be used to prepare the cemented backfill.

The preference of using either OPC or HWQS for a potential cemented backfill application would also be identified by comparing OPC vs. HWQS for the cost implications and handling implications

ACKNOWLEDGEMENT

The author acknowledges the Visiting Research Fellowship granted by the Department of Mining Engineering and Mine Surveying at the Western Australian School of Mines. It facilitated conduct of studies presented in this paper. Permission of China University of Mining and Technology to accept this scholarship is very much appreciated. Mr. Dick Cowling's instruction for the start of this investigation was significantly helpful and appreciated. KCGM's provision of tailings slurry for the preparation of fill samples is acknowledged.

REFERENCES

1. Laboratory reports for ground water samples, KCGM, Nov. 1995.
2. Wang C., Properties of High Water and Quick Setting Cementitious Fill, Western Australian School of Mines. June, 1997.
3. KCGM GOLD/SULFUR Distribution report, 17 Dec., 1997.
4. Standards Australia, Amendment No. 2 to AS 3970-1991, Portland and blended cements.
5. Properties and production of High Water and Quick Setting Cement, Research report. China University of Mining and Technology, November 1995.
6. E. G. Thomas, Characteristics of cemented deslimed mill tailing fill prepared from finely ground tailing, Proceedings of the International Symposium of Mining with Backfill/Luleå/17-9, June, 1993
7. Wang C., Investigation on the properties of cemented tailings fills, May 1998, Western Australian School of Mines.

Large Deformation Analysis of Strip Footing on Layered Purely Cohesive Soils

C.X.Wang
Department of Civil Engineering, The University of Sydney, Australia

Summary The bearing capacity of footings on layered soils has already received significant attention of researchers, however, most of the reported studies are limited to footings resting on the surface of soil, and are based on the assumption that the displacement of the footing is very small. In this paper, an approach developed by Hu and Randolph (15), which combines the Arbitrary Lagrangian Eulerian (ALE) approach and the finite element (FE) method, is adopted to allow the large penetration analysis of footings on layered soil. The FE configurations and ALE approach were verified by comparing the FE small deformation analysis results with available analytical and semi-empirical predictions, and the results of ALE large deformation analyses with available solutions for homogeneous soil.
Large deformation analyses of strip footings on strong-over-weak layered cohesive soils were carried out. The load - displacement curves and the bearing capacity factors predicted by the large deformation analysis are given in the paper. It is shown that during footing penetration, both the increased bearing resistance from the soil above the footing base and the decreased bearing resistance from the weaker bottom soil affect the overall bearing capacity. Bearing capacity factors are given for various cases of different layer thickness and different cohesion ratios for the two soil layers. Unlike the small deformation analysis for cohesive soil, it is found that the soil self-weight can have a significant effect on the bearing capacity in large penetration problems.

1 INTRODUCTION

The bearing capacity of footings comprises quite an extensive literature today. The methods for calculating the bearing capacity of multi-layer soils range from averaging the strength parameters (1), using limit equilibrium considerations (2, 3, 4), to a more rigorous limit analysis approach (5, 6, 7). Semi-empirical approaches have been adopted based on some experimental studies (8, 9). The Finite Element Method (FEM) was also applied to this problem more recently (10, 11, 12, 13).

However, most of these studies are limited to footings resting on the surface of the soil, and are based on the assumption that the displacement of the footing is very small. These solutions may be applied to a footing which partially penetrates the soil, by ignoring the strength contribution of the adjacent soil above the plane of the footing base and the change of depth of the top layer soil during footing penetration. In many cases, the footings or other structures will experience a significant settlement, and sometimes even penetrate through the top layer to the deeper layer. In these cases, the small displacement assumption is no longer appropriate, and a large displacement theory should be introduced into the analysis.

For large deformation or large strain analysis, it is well known that the two main approaches are the Eulerian and Lagrangian formulations. The latter can be further classified as Total Lagrangian and Updated Lagrangian methods. As pointed out by Cheng and Tsui (14) and Hu and Randolph (15), each of these three approaches has its own limitations.

In an attempt to overcome the limitation of the pure Lagrangian and Eulerian approaches, a more flexible approach called the Arbitrary Lagrangian-Eulerian (ALE) method has been developed by Ghosh and his co-workers (16). Hu and Randolph (15, 17) adopted the ALE approach along with a fully automatic finite element mesh generation method to analyse large deformation problems of footings on a single-layered soil and spudcan penetration. In this paper, Hu and Randolph's method is used, and the analysis was extended to two-layered purely cohesive soil. The top layer is assumed stronger than the bottom layer. In the cases investigated, the ratio of the bottom layer strength to the top layer strength varies from 0.1 to 1, and the thickness of the top layer is either one half or the same as the footing width.

First, small deformation analysis was done to verify the FEM adopted for this problem. Then large deformation analysis of the ALE approach was carried out to give the full load-displacement curve and the mobilized bearing capacity of the layered soil. A discussion about the bearing resistance of layered cohesive soils under large penetration is made, based on the comparison of the small and large deformation analysis results. The effects of soil weight on the large deformation analysis were also investigated.

2 NUMERICAL MODELS

In this paper, six-noded triangular elements with a three-point Gauss integration rule were adopted. The small displacement analysis was carried out using the AFENA finite element package developed by Carter et. al. (18), and the large displacement analysis was based on using Hu and Randolph's program with some modification to suit two-layered soils. The solution algorithm adopted was based on a tangent stiffness approach.

Plane strain meshes were designed such that the elements were concentrated in highly stressed zones and the boundaries were sufficiently distant from the footing to ensure that the mesh contained the entire plastic zone. To ensure that the equilibrium errors and the discretization errors were small, several calculations of different meshes and increment sizes

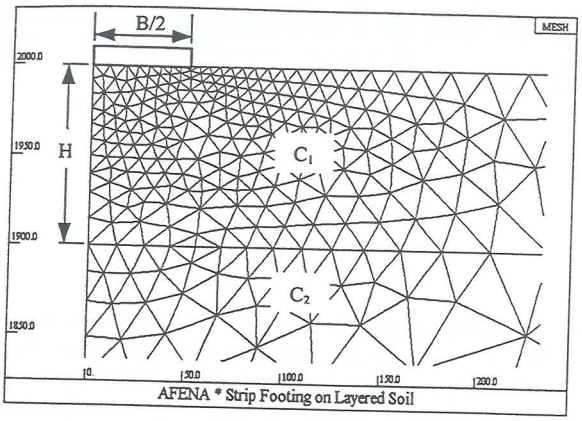

Figure 1 Typical mesh used in the analysis

were repeated. The typical mesh configuration finally adopted in this paper is shown in Fig. 1. The loading of a rigid footing was simulated by specifying incremental displacements of appropriate surface nodes. The increment size was taken as 0.02% of the footing width. The footing base and sides were assumed to be perfectly smooth.

The soil was assumed to be an elastic-perfectly plastic Tresca material, with modulus ratio $G/c_1 = 100$ or 200 (where G is the shear Modulus of both layer, c_1 is the cohesion of the top layer). Undrained analysis was carried out by adopting Poisson's ratio $\nu = 0.49$.

As to the large deformation analysis, full details of the algorithm are given by Hu and Randolph (15). While for the small deformation analysis, the mesh configuration remains the same as the original mesh; in the ALE large deformation analysis, the mesh was updated after certain steps of penetration. To obtain the results, in this paper, the mesh was updated every 20 steps. As the displacement increment size is 0.02% of the footing width, this means the updating interval is 0.4% of the footing width.

3 BEARING CAPACITY FACTOR BY SMALL DEFORMATION ANALYSIS

The ultimate bearing capacity q_m of a strip footing without a surcharge on two-layered cohesive soil can usually be expressed as

$$q_m = c_1 N_c \qquad (1)$$

where N_c is the modified bearing capacity factor that depends on the ratio of the cohesion of the two layers c_1/c_2 and H/B (the thickness of the top layer divided by the footing width).

The available values of N_c for two-layered cohesive soil have been given by Button (2) and Reddy et al. (3) using the assumption of a cylindrical yield surface, and Brown and Meyerhof (8) based on some experimental studies. Button and Reddy et. al. gave very similar figures for the values of N_c indexed by c_2/c_1 and H/B. Their approach gave the upper bound solution to this problem, and returned the bearing capacity factor for homogeneous soil (a special case for two-layered soil) to be 5.51, which is 7% above Prantl's exact solution of $(2+\pi)$. The factors given by Brown and Meyerhof

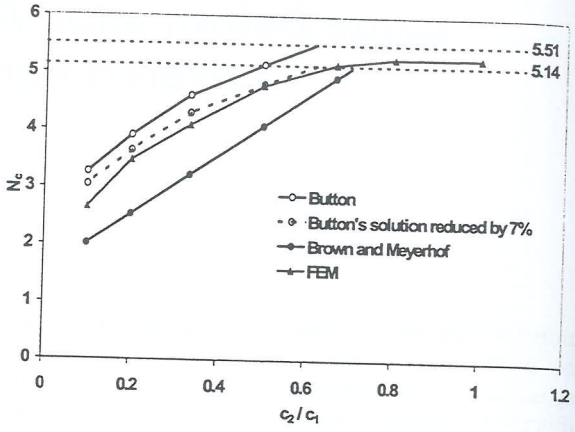

(a) H/B = 1

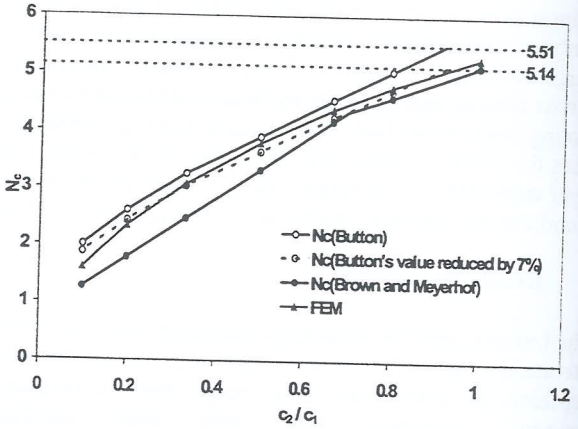

(b) H/B = 0.5

Figure 2 Comparison of bearing capacity factors for layered soil under surface footing

are lower, and in better agreement with the value of $(2+\pi)$ for homogeneous soil, and are given by the following equation:

$$N_m = 1.5\frac{H}{B} + 5.14\frac{c_2}{c_1} \le 5.14 \qquad (2)$$

The bearing capacity factors given by the FE small deformation analysis were compared with the values given by Brown and Meyerhof (8) and Button (2). Various cases were investigated, and the comparison is shown in Figs. 2(a) and (b).

It can be seen from Fig. 2, that the bearing capacity factors given by the FEM are lower than Button's solution, but higher than the empirical values given by Brown and Meyerhof. As Button's solution is an upper bound, and for the special case $c_1/c_2 = 1$ it is 7% higher than the accurate value $(2+\pi)$, it can reasonably be assumed that for other cases, his solution is also approximately offset by about the same amount. The dashed curve in Fig. 2 shows Button's solution reduced by 7%. The FE results agree well with the reduced Button's solution.

The FE prediction is about 10-15% higher than the empirical values given by Brown and Meyerhof's formula. Georgiadis and Michalopoulos (19) proposed a "slip surface"method for the same problem, and their prediction was also 10% higher than the value given by Brown and Meyerhof, but agrees well

with their FE analysis results and Giroud (20)'s prediction. Thus the adopted FE mesh configuration and solution algorithm can be regarded as suitable for solving this bearing capacity problem.

4 LIMITATIONS OF SMALL DEFORMATION ANALYSIS

The above-mentioned analytical solution and the FEM small displacement analysis for the bearing capacity of layered soil are only applicable to footings resting on the surface of the soil deposit. For the large penetration problem, they are not valid approaches. First, when the footing penetrates into the top layer, the actual value of H/B under the footing base decreases. Second, in the case that the footing penetrates through the top layer and force it into the bottom layer, it will trap a certain amount of top layer soil into the bottom layer. Also, the penetration will cause the soil heave close to the footing edges, which will affect the bearing capacity. All of these factors make it difficult and unreasonable to use H/B to refer to the existing figures and formula in the literature to determine the bearing capacity factors for footings undergoing deep penetration.

The geometry change makes assumptions for some analytical solutions (eg. cylindrical yield surface) not suitable to the penetration problem. The FEM with ALE, however, makes no a priori assumption about the failure mechanism, and thus it can reflect the natural development of the failure zone and give good predictions of the bearing behaviour.

5 LARGE DEFORMATION ANALYSIS AND RESULTS

5.1 The Bearing Response

Hu and Randolph (17) used the ALE approach to compute the bearing response of shallow foundations penetrating into a single layered non-homogeneous soil. In this paper, the bearing response of the strong-over-soft two-layered soil under a strip footing is examined by comparing the results given by the small and large deformation analysis. Various cases of H/B = 0.5 and 1, and c_2/c_1 = 0.1, 0.2, 1/3, 0.5, 2/3 and 1 (homogeneous soil) were investigated. Typical normalized load-displacement curves are shown in Fig. 3(a).

The curve given by the small deformation analysis reaches an ultimate value after a relatively small displacement (penetration), this value is the bearing capacity factor shown in Fig. 2(a). The curves given by the large deformation analyses are quite different from those given by the small displacement analysis.

For the homogeneous soil (c_2/c_1 = 1), the curve continues to rise until an ultimate value is reached (see Fig. 3(b) for the whole curve). The ultimate bearing capacity for a deep footing in homogeneous soil was investigated by Meyerhof (21) and Skempton (22), among others. Skempton's prediction was based on both theoretical and experimental results and can be simply estimated from the equation:

$$N_c = 5(1+0.2\frac{s}{B}), \qquad (3)$$

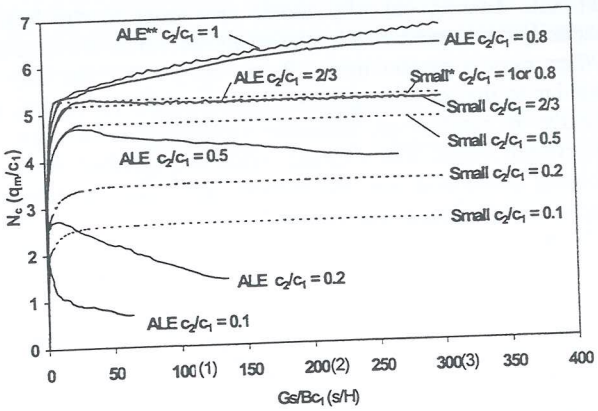

(a) H/B = 1, G/c_1 = 100, c_2/c_1 = 0.1~1

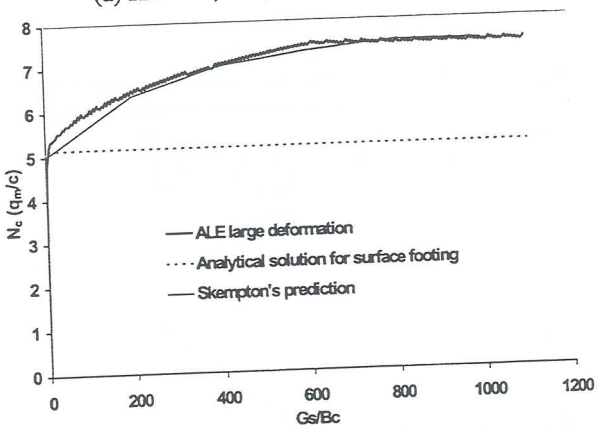

(b) G/c = 100, c_2/c_1 = 1 (complete curve)

Figure 3 Typical normalized load-displacement curves

when $s/B < 2.5$. At $s/B \geq 2.5$, N_c *is* constant and equal to 7.5, where s is the penetration depth of the footing. It can be seen from Fig. 3(b) that the curve given by the ALE large deformation analysis agrees very well with Skempton's prediction. The FE analysis scheme and the ALE method were verified again by this agreement.

For the layered soil, it is difficult to give an analytical solution for the bearing capacity factor of a large penetration problem, thus it is the very problem that needs the FEM to conduct the analysis. For the cases of a top layer over a much weaker bottom layer (eg. c_2/c_1 = 0.1, 0.2, and 0.5), the curve given by the ALE method rises to a peak value (see Fig.3(a)), which is lower than the bearing capacity predicted by the small deformation analysis, then it declines with further penetration, finally it reaches a stable value after the footing settles into the bottom layer. The peak values of these curves are the maximum bearing capacity factors given by the large deformation analysis and the values reached after large penetration are referred to as the ultimate bearing capacity factors in this paper. For the small deformation analysis, the ultimate bearing capacity factor is also the maximum bearing capacity factor.

It is interesting to note that at c_2/c_1 = 2/3, the curves given by the large deformation analysis and small deformation analysis are almost coincidental. Thus both the maximum and the

ultimate bearing capacity factor are equal to the bearing capacity factor predicted by the small deformation analysis. When c_2/c_1 is greater than 2/3, eg. $c_2/c_1 = 0.8$, the curve is similar to that of homogeneous soil, it continues to rise, and finally it reaches an ultimate value, which is also the maximum value. The ultimate value was reached when the footing penetrated into the bottom layer and the top layer broke into two parts (see section 5.2).

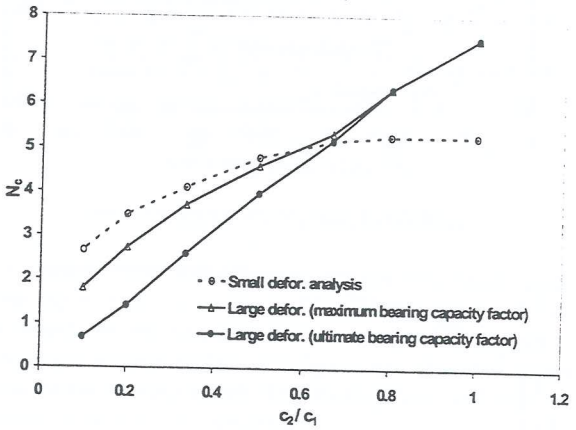

(a) H/B = 1

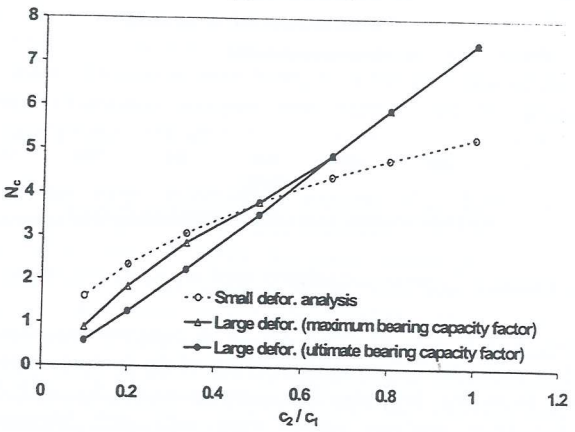

(b) H/B = 0.5

Figure 4. Bearing capacity factors given by large deformation analysis

The analyses of the cases of H/B = 0.5 gave similar curves after normalization but with different maximum and ultimate bearing capacity factors. In Fig. 4(a) and (b), the values of the bearing capacity factors for the case H/B = 1 and H/B = 0.5 are shown respectively with those predicted by the small deformation analysis.

It can be seen that for the case H/B = 1, when $c_2/c_1 = 0.5$ to 2/3 (or $c_2/c_1 = 0.4$ to 0.6 for H/B = 0.5), the maximum bearing capacities given by the small deformation analysis and large deformation analysis are very close to each other. When the bottom layer is weaker than this, i.e. the ratio of c_2/c_1 is less than the above-mentioned values, the ALE predicted maximum values of N_c are lower than those given by the small deformation analysis. For a stronger bottom layer, i.e. the ratio of c_2/c_1 is greater than the above-mentioned values, but still less than 1, the ALE predicted maximum values of N_c are higher than those given by the small deformation analysis. The reason for this can be explained as follows.

When a rigid footing penetrates into a two-layer soil system, the bearing capacity is contributed by two parts of the soil. One is the soil beneath the footing. The other is the soil above the level of the footing base and besides the footing edge. This part of the soil usually heaves at the surface during penetration. If a small deformation analysis is done, only the first part is considered, as the mesh configuration remains unchanged during the analysis and thus the soil is always beneath the footing base. For the large deformation analysis, the mesh is updated regularly and thus the ratio of the contribution to the bearing capacity from the two parts varies during penetration, i.e. the surcharge and burial effect varies during penetration.

At early stages of penetration, most of the soil is beneath the footing, and thus the load-displacement curves are almost identical to those given by the small displacement analysis. As the deformation gets larger, the footing penetrates into the soil, the soil of the top layer flows from beneath the footing, leading to less top layer soil under the footing. As the bottom layer is weaker than the top layer, the contribution of the bearing capacity from the soil beneath the footing becomes less. Meantime, more and more soil is above the level of the footing base, and additional bearing resistance comes from this part of the soil. Whether the predicted bearing capacity by the ALE analysis is higher or lower than that given by the small deformation analysis depends on how these two factors interact. From the above analysis, it can be seen that when $c_2/c_1 < 0.5$ - 2/3 for the case of H/B = 1 (or $c_2/c_1 < 0.4$ - 0.6 for H/B = 0.5), the loss of the bearing capacity because of the top layer's "flow away" beneath the footing is greater than the gain from the soil above the footing base. Thus the predicted bearing capacity factor is lower than that given by the small deformation analysis. The smaller the value of c_2/c_1, the lower is the bearing capacity.

When $c_2/c_1 = 0.5$ - 2/3 for H/B = 1(or $c_2/c_1 < 0.4$ - 0.6 for H/B = 0.5), the loss and the gain are approximately balanced as the footing settles to a certain distance into the soil, and at this point, the soil provides the maximum bearing capacity. Then the loss starts to surpass the gain and the load-settlement curve begins to decline. But there is a critical value for c_2/c_1, at this value, the loss and the gain can always be compensated, so the curve given by the large deformation analysis is the same as the one given by the small deformation analysis. For the case H/B = 1 this value is approximately $c_2/c_1 = 2/3$; while for H/B = 0.5 it is about $c_2/c_1 = 0.6$. From Fig. 4, it can be seen that at this point, the three curves give almost the same bearing capacity factors.

In the cases of $c_2/c_1 > 0.5$ - 2/3 for H/B = 1 (or $c_2/c_1 > 0.4$ - 0.6 for H/B = 0.5), the gain is always greater than the loss, which leads to the load - settlement curve continuing to rise. Thus the maximum bearing capacity factors are the ultimate bearing capacity factors and they are greater than those given by the small deformation analysis.

5.2 The Development of Plastic Zones

As the footing settles, the top soil layer gradually flows out from under the footing base. However, not all of the top layer soil will flow out of the footing base, some soil will be trapped under the footing. Thus the top layer soil tends to

break into two parts, one part remains under the footing during further settlement, the other flows to the side of the footing. In the FE program, if the minimum width of the long strip of top layer soil at the side of the footing became less than 3% of the footing width, the top layer soil was broken into two parts. This is shown in Fig. 5. Then the footing and the trapped soil settle together into the bottom layer soil, at this stage, the value for the bearing capacity factor usually does not change much. This is because the contribution of the bearing capacity from the above-defined two parts of soil vary very little after this, and thus the final stable value for the ultimate bearing capacity is obtained.

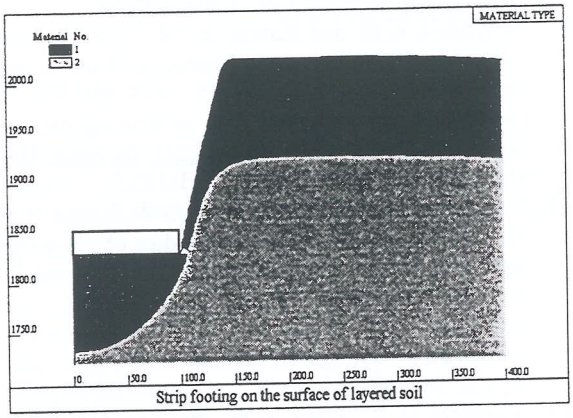

Figure 5 Footing settles into the bottom layer with some top layer soil trapped underneath (H/B = 0.5)

As mentioned before, to ensure the mesh contains the entire plastic zone for various cases, an extensive mesh was used in this paper. In Fig. 6(a), the plastic zone upon failure for the case $c_2/c_1 = 0.5$ of H/B = 1 is shown. This figure shows that the plastic zone was restricted to a very small area. A much smaller mesh domain could have been used for analyzing this case. However, for a weaker bottom layer soil, eg. $c_2/c_1 = 0.1$ of H/B = 1, the plastic zone is much more extensive and developed to the boundary of the FE mesh (Fig. 6(b)).

It is found that for case $c_2/c_1 = 0.5$ of H/B = 1, the failure of the soil occurred first in the top layer soil, and immediately after that, the bottom layer just beneath the top layer began to fail. Then the failure developed in both layers, but faster in the bottom layer. For a weaker bottom layer soil than this, e.g. $c_2/c_1 = 0.1$ of H/B = 1, failure began from the bottom layer, and only after it developed to a considerably large area within the bottom layer, did failure start to occur in the top layer. After that the plastic zone developed very fast in the bottom layer. The weaker the bottom layer compared to the top layer, the more extensive is the plastic zone developed in the bottom layer. The values of the ultimate bearing capacity factors, which were obtained when the footing settled into the bottom layer, were mainly affected by the bottom layer's strength and plastic zone development.

5.3 The Effect of Soil Weight

It is well known that for a surface footing, the ultimate bearing capacity given by the undrained analysis is independent of the soil self-weight for purely cohesive soil. However, in large deformation analysis, the footing is not a surface footing once it begins to settle and penetrate, and the self-weight of the soil affects the results. The previous analyses were carried out without considering soil self-weight

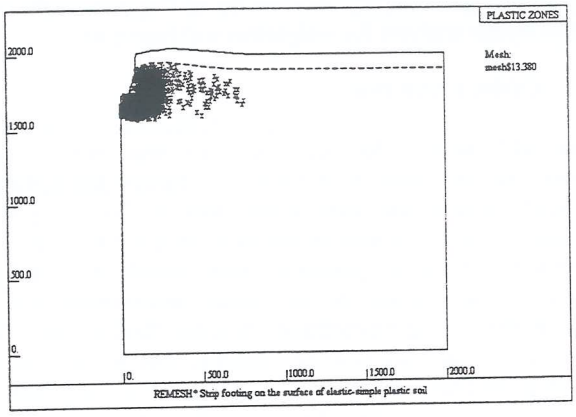

(a) $c_2/c_1 = 0.5$ of H/B = 1

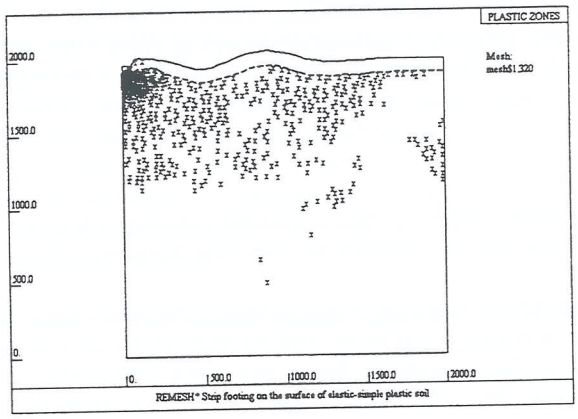

(b) $c_2/c_1 = 0.1$ of H/B = 1

Figure 6 Plastic zone upon failure

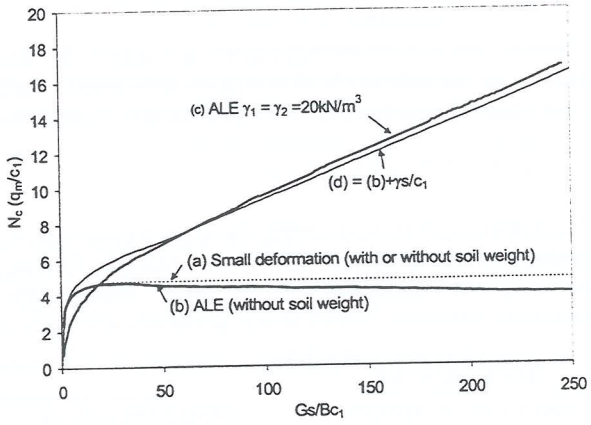

Figure 7 Normalized load-deflection curves given by analysis with and without soil self-weight

to investigate the effects of the large deformation analysis on the bearing capacity factor N_c. If the self-weight is included, the large deformation analysis results, for $c_2/c_1 = 0.5$ and H/B = 1, are as given in Fig.7.

Fig. 7 shows the small and large deformation analysis results of weightless soil and soil of unit weight 20kN/m^3. It can be seen that if soil weight is included, the results given by large deformation analysis are quite different from those without

considering soil weight. However, if both layers are of the same unit weight, the large deformation analysis result (curve c) can be approximately obtained by adding $\gamma s/c_1$ to the result given by the analysis for weightless soil (curve d).

6 CONCLUSIONS

The ALE large deformation analysis was carried out to investigate the bearing response and failure mechanism of layered cohesive soil under a strip footing. For the specified strong-over-soft problem investigated in this paper, the load-displacement curves generally were significantly different from the ones given by the small deformation analysis. During the footing's penetration process, there are two major factors affecting the bearing capacity, one is the increased bearing resistance from the soil above the footing base and the other is the decreased bearing resistance from the weaker underlying soil. For a specified value of H/B, a corresponding value of c_2/c_1 can be obtained, where the two effects can be exactly offset, and the load-displacement curve is the same as the one given by the small deformation analysis. For a greater c_2/c_1 value than this, the load-displacement curve rises continuously until the footing penetrates into the bottom layer and a stable ultimate bearing capacity is achieved, which is also the maximum bearing capacity. For a smaller c_2/c_1 value, the curve rises to the maximum bearing capacity, then declines until the ultimate bearing capacity is reached.

The failure zone may either develop first in the upper layer (for a greater c_2/c_1) or the bottom layer (for a smaller c_2/c_1), but it develops much faster and more extensively in the bottom layer. The smaller is c_2/c_1, the more extensive is the plastic zone developed in the bottom layer. Thus a very extensive area should be modelled in the FE large deformation analysis for a small value of c_2/c_1, eg. 20B×20B or bigger for $c_2/c_1 = 0.1$ for the case of H/B = 1.

Although the soil self-weight does not affect the bearing response of the cohesive soil in a small deformation analysis, it has a significant effect in the large deformation analysis.

7 ACKNOWLEDGMENT

The author wishes to express sincere appreciation to Dr. Yuxia Hu in the University of Western Australia for her kind providing the remeshing source code. Support by the Australian Research Council is also gratefully acknowledged.

8 REFERENCES

1. Bowles, J.E., Foundation analysis and design, Mcgraw-Hill, New York, N.Y., 1988.
2. Button, S. J., "The bearing capacity of footings on a two-layer cohesive subsoil", Proc., 3rd Int. Conf. on soil mechanics and foundation engineering, Zurich, Vol.1, 1953, 332-335.
3. Reddy, A. S., and Srinivasan, R. J. "Bearing capacity of footings on layered clays", J. Soil Mech. Found. Div., ASCE, Vol. 93, No. 2, 1967, 83-99
4. Meyerhof, G. G., "Ultimate bearing capacity of footings on sand layer overlaying clay", Can. Geotech. J., Vol. 11, No. 2, 1974, 223-229.
5. Chen, W.F., and Davidson, H.L., "Bearing capacity determination by limit analysis", J. Soil Mech. Found. Div., Vol. 99, No.6, 1973, 433-449.
6. Florkiewicz, A., "Upper bound to bearing capacity of layered soils", Can. Geotech. J. Vol. 26, 1989, 730-736.
7. Michalowski, R. L. and Lei Shi, "Bearing capacity of footings over two-layer foundation soils", ASCE, J. Geotech. Eng. Vol. 121, No. 5, May, 1995, 421-427.
8. Brown, J. D. and Meyerhof, G. G., "Experimental study of bearing capacity in layered clays", Proc., 7th Int. Conf. on soil Mechanics and foundation engineering, Mexico, Vol. 2, 1969, 45-51.
9. Meyerhof, G.G. and Hanna, A. M., "Ultimate bearing capacity of foundations on layered soils under inclined load", Can. Geotech. J., Vol. 15, 1978, 565-572.
10. Griffiths, D.V., "Computation of bearing capacity on layered soils", Proc., 4th Int. Conf. on Num Meth. In Geomechanics, Vol. 1, 1982, 163-170.
11. Love, J.P., Burd, H.J., Milligan, G.W.E., and Houlsby, G. T., "Analytical and model studies of reinforcement of a layer of granular fill on a soft clay subgrade", Can. Geotech. J., Vol. 24, 1987, 611-622.
12. Burd, H. J. and Frydman, S. "Bearing capacity of plane-strain footings on layered soils", Can. Geotech. J., Vol. 34, 1997, 241-253.
13. Merifield, R. S., Sloan, S. W., and Yu, H. S, "Rigorous plasticity solutions for the bearing capacity of two-layered clays", Geotechnique, Vol. 49, No. 4, 1999, 471-490.
14. Cheng, Y. M. and Tsui,Y., "Limitations to the large strain theory", Int. J. Num. Meth. Eng., Vol. 33,1992, 101-114.
15. Hu, Y. and Randolph, M. F., "A practical numerical approach for large deformation problems in soil", Int. J. Num. Analy. Meth. Geomechanics., Vol. 22,1998, 327-350.
16. Ghosh, S. and Kikuchi, N., "An arbitrary Lagrangian-Eulerian finite element method for large deformation analysis of elastic-viscoplastic solids", Comp. Meth. Appl. Mech.Eng., Vol. 86, 1991, 127-188.
17. Hu, Y. and Randolph, M. F., "Deep penetration of shallow foundations on non-homogeneous soil", Soils and Foundations, Vol. 38, No. 1, Mar. 1998, 241-246.
18. Carter, J. P., and Balaam, N., AFENA Users Manual, Geotechnical Research Center, Univ. of Sydney, 1995.
19. Georgiadis, M. and Michalopoulos, A. P., "Bearing capacity of gravity bases on layered soil", J. Geotech. Eng. Vol. 111. No. 6, June 1985, 712-727.
20. Giroud, J. P., Tran-Vo-Nhiem and Obin, J. P., "Table pour le calcul des foundations", Tome 3, Force Portante, Dunod, Paris, France, 1973.
21. Meyerhof, G. G., "The ultimate bearing capacity of foundations", Geotechnique, Vol. 2, No.4, 1951, 301-332
22. Skempton, A. W., "The bearing capacity of clays", Build. Res. Cong., Division 1, Part 3, London, 1951, 180-189.

The Development of Water Balance Models for Tailings Management

S. J. Watson
Golder Associates

Summary The management of water on a tailings storage facility (TSF) is an important aspect of the overall management of a TSF. A useful tool to assist with TSF water management is a water balance model that tracks water inflows and outflows, and the change in surface water storage on a TSF. This paper discusses the components of a TSF water balance model and the uses of such a model. A case study illustrating the development of a water balance model for the TSFs at Kalgoorlie Consolidated Gold Mines is then presented.

1. INTRODUCTION

In recent years the management of tailings storage facilities (TSFs) has received increasing attention from government regulators and operators within the mining industry. One important aspect of tailings management that relates to the safe operation and efficient management of a TSF is the control of water within the storage area.

Water management in a TSF largely involves controlling the size and position of the decant pond through careful management of slurry deposition and decant water return to the processing plant. External influences such as rainfall, evaporation and seepage complicate the overall management of water on a TSF.

A useful tool to assist with the water management in a TSF is a water balance model, which accounts for all of the water inflows and outflows, and the change in water storage within the TSF. TSF water balance models can be developed for individual paddocks within a TSF, for an entire TSF, or for a series of TSFs that are independent or interconnected.

Two types of TSF water balances can be developed to assist with water management. An overall water balance can be developed for a TSF by accounting for the change in surface water storage and interstitial void storage. This requires all of the internal and external water flows to be accounted for in the water balance model.

Alternatively, the model can be simplified to account for the change in surface water storage only. In this case some of the external flows, such as seepage from the facility, and the processes that cause a change in interstitial void storage can be neglected. This has the advantage of simplifying the model by reducing the number of parameters and processes that have to be included in the model. A disadvantage of this approach is that the overall water balance for the TSF facility can not be evaluated.

This paper focuses on this second approach for TSF water balance model development, although most of the information presented is also applicable to the first approach.

2. COMPONENTS OF A WATER BALANCE

2.1 General

A water balance is an account of all quantities of water added to, stored within, or removed from a system over a specified period of time, such as a day, week, or month. In general, a water balance for a TSF is dynamic, which means that the components of the water balance vary continuously with time.

The main components of a TSF surface water balance are classified as storages, inflows or outflows, and are presented in Table 1.

Table 1: Components of a TSF Surface Water Balance

POND INFLOWS	POND OUTFLOWS
Slurry Bleed Water	Seepage / Drainage
Seepage / Drainage Return	Return Water
Rainfall	Evaporation
Additional Pumped Water	Spillway Overflow
Consolidation Water	

The difference between the inflows and the outflows is the quantity of water that is added to (positive difference) or removed from (negative difference) water storage upon the TSF.

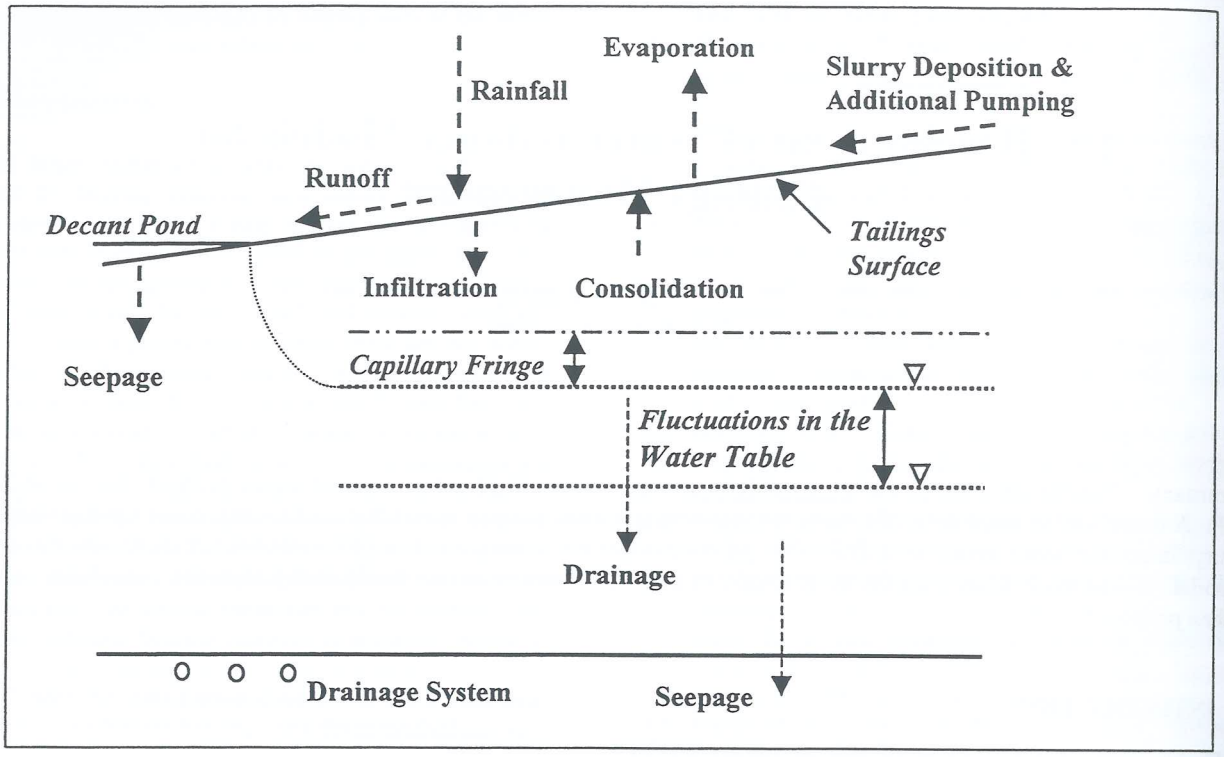

Figure 1: Schematic representation of the water inflows into a TSF and outflows from a TSF.

A schematic representation of the internal and external water flows is given in Figure 1, and a description of the inflows and outflows is given below.

2.2 Slurry Deposition

Mine tailings are generally deposited in TSFs as a slurry from single or multiple discharge points. Slurry deposition is therefore an external inflow of water into the facility.

In TSFs under active deposition, the rate at which slurry water is discharged into the facility is generally the largest of the water inflows into the facility. Slurry water deposition is also the water inflow that is most easily managed by the operators of a TSF.

Using the simplified (surface water) approach for TSF water balance model development, the volume of slurry water that reaches the surface water pond (decant pond) has to be evaluated. The volume of slurry water being deposited into the facility can be readily calculated from the tonnage being deposited, the slurry solid content, the specific gravity of the tailings solids and the density of the slurry water. However the volume of water discharged into the facility is greater than the volume of water that reaches the decant pond because some of the slurry water is held in interstitial voids, some infiltrates into the underlying tailings, and some is lost to evaporation.

A rough estimate of the volume of slurry water that inflows into the decant pond can be obtained by assuming that a fixed percentage of the slurry water reaches the pond. A more accurate approach is to account for the processes that have a *significant* effect on the volume of water that reaches the decant pond. These processes include sedimentation of the tailings with release of slurry water (termed bleed water), followed by loss of the bleed water to evaporation and infiltration, as a function of the area under active deposition.

2.3 Tailings Consolidation

Water that is released to the tailings surface during consolidation of the tailings is an inflow of water into the decant pond. The volume of water released by consolidation depends on:

- the mineralisation, physical and chemical properties of the tailings
- the depositional history of the tailings, particularly the rate of tailings deposition
- the thickness of tailings
- the permeability of the TSF foundations.

Generally, in a facility that has a small decant pond, the majority of water that is released to the surface during consolidation of the tailings evaporates. However, if the tailings has been deposited with a rapid rate of rise, or the majority of the tailings surface is covered by the decant pond, then a larger proportion of consolidation water is likely to inflow into the decant pond.

An estimate of the volume of water released into the decant pond by consolidation of the tailings is best obtained from a consolidation model of the facility.

It should be noted that if an overall water balance is being developed for a TSF, water release due to consolidation not only results in an inflow into the decant pond, but also reduces the volume of water stored in interstitial voids.

2.4 Return Water

Most TSFs are constructed with a decant facility to remove surface water off the TSF. The majority of operations return water to the processing plant, whereas some allow for evaporation or disposal of the water. Returning process water to the plant reduces overall raw water and reagent consumption, thereby reducing costs. It has the added advantage of minimising the volume of contaminated slurry water that requires treatment or storage.

At any point in time, the volume of water returned to the process plant from a TSF depends on a number of factors including:

- the volume of decant water available on the TSF
- the pumping capacity of the water return system
- the maximum volume of process water able to be used by the processing plant.

Plant return water is generally the outflow from a TSF that is most readily controlled by the TSF operator.

2.5 Seepage and Drainage

Seepage and drainage from a TSF is an external outflow from the facility into either an underdrainage collection system, if such a system has been installed, or into the surrounding environment.

It is important to minimise seepage from a TSF for both environmental and economic reasons, to minimise adverse environmental impacts, such as groundwater contamination and salinisation of the root zone, and to minimise the loss of process water and chemicals.

In some cases the seepage that is collected in seepage collection dams or from recovery bores is returned to the plant. In others, the seepage water is returned back into the TSF from which it has emanated. In the latter case, the seepage water that is recovered becomes a surface inflow into the facility.

If the water balance is being developed to account for changes in surface water storage only, the seepage from the decant pond into the underlying tailings is more important than seepage from the base of the TSF. The rate of seepage from a decant pond is a function of the tailings depth, tailings permeability, pond size and to some extent the facility size. The rate of seepage from a decant pond can either be estimated using Darcy's law, or can be evaluated using 2-dimensional sectional seepage models.

2.6 Rainfall and Evaporation

Rainfall is an external water inflow and evaporation is an external water outflow from a TSF, but unlike slurry deposition and water return, these water flows are largely unable to be controlled by the operators of the TSF.

The volume of rainfall that reaches the decant pond of a TSF depends on the amount of runoff and evaporation that occurs from various regions of the decant pond catchment.

A decant pond catchment can generally be divided into five main regions, discussed below:

- Wet Beach - is the area of tailings beach under active deposition. In this area the tailings are already saturated so 100% of the rainfall is likely to become runoff.
- Drying Beach - is the area of tailings beach that has recently undergone deposition, but is no longer an active beach. The tailings in a drying beach are also close to saturation, so 100% of the rainfall can be assumed to runoff. There will be some evaporative losses from the runoff.
- Dry Beach - is the area of tailings beach that has dried to the point that the voids are no longer fully saturated. In this case some (or all) of the rainfall is lost to infiltration and evaporation, depending on the intensity and duration of the rainfall event. There may also be significant cracking of the tailings surface in a dry beach area, which can affect the volume of water lost to infiltration and evaporation. The remaining volume of rainfall can be assumed to report to the decant pond.
- Decant Pond - rainfall falling directly on the decant pond is a direct inflow into the pond. Water loss from the decant pond due to evaporation also needs to be included in the water balance.
- Surrounding Catchment – Some TSFs located within valleys may receive runoff from the surrounding catchment during a rainfall event if drainage channels or bunds are not constructed to divert the catchment runoff.

If a TSF water balance model is being developed to account for changes in surface water storage, then only the volume of rainfall and runoff reaching the decant pond, and the volume of evaporative loss from the pond need to be accounted for in the model.

Alternatively, if an overall water balance model is being developed to account for changes in surface and interstitial storage, then the volume of rainfall infiltrating into the residue and the volume of water lost to evaporation in the various regions of the TSF must be included in the model.

2.7 Climatic Data

One aspect of TSF water balances that requires special consideration is the climate data to be used in the simulation.

It is not possible to predict future rainfall and evaporation rates, so various techniques are used to obtain climate data for the simulations.

One approach is to use measured historical daily rainfall and evaporation data for the area. A long period of historical record is preferential because it allows a number of simulations to be run, starting at different times in the historical records. This allows a range of climatic conditions to be applied to the simulated deposition strategy. The simulation results can then be interpreted to give probabilistic results, such as daily water return volumes and decant pond elevations. An advantage of this approach is that it can be used to examine the effect of climatic extremes by simulating a series of wet or dry years.

A less accurate approach is to use average monthly rainfall and evaporation rates. The main disadvantage of this technique is that the averaging procedure smooths out the rainfall, moderating the effects of irregular rainfall events.

2.8 Spillway Overflow

Some TSFs are designed with spillways to remove excess water from the decant pond when the elevation of the water surface in the decant pond exceeds the elevation at the base of the spillway. Typically spillways are used to transfer excess water into other TSFs (or other water storage facilities) to maintain sufficient freeboard within an interdependent system of TSFs.

2.9 TSF Geometry

To account for the changing geometry as slurry is deposited into a TSF, a water balance model must incorporate the following:

- The depth of the decant pond as a function of pond volume
- The surface area of the decant pond as a function of the pond volume (or depth)
- An approximate rate of rise of the tailings during the period that tailings is being deposited.

These geometrical relationships are extremely important as they affect many of the water balance components, including evaporation and seepage from the decant pond, rainfall runoff from most of the beach areas, rainfall recharge of the decant pond, and consolidation water flow into the decant pond.

3. USES OF A WATER BALANCE MODEL

A TSF water balance model, which accounts for the storages, inflows and outflows discussed in Section 2, can be used to:

- Improve deposition strategies in the short or long term to maximise water recovery or maximise water evaporation, depending on the water return requirements
- Estimate the likelihood of exceeding the maximum operational water elevation for a range of climatic conditions
- Estimate the freeboard necessary to contain extreme rainfall events, such as a 1:1000 year storm event
- Estimate the likelihood and extent of a return water shortfall under average or extreme climatic conditions
- Manage the water in TSFs containing acid generating tailings that may require a permanent water cover
- Provide inputs for a qualitative and quantitative risk assessment of a TSF.

4. DEVELOPMENT OF A TSF WATER BALANCE MODEL FOR KCGM

4.1 Background

KCGM is Australia's largest gold producer from one operation, with annual gold production in excess of 23 tonnes. Approximately 13.7 million tonnes of ore are processed annually to produce the gold, which results in approximately 13.7 million tonnes of waste tailings being generated annually.

The waste product is a sandy (fine-grained) silt tailings which is discharged as a slurry into the KCGM TSFs. In excess of 23,000 kL of slurry water are discharged daily into the TSFs. A proportion of this slurry water reports to the decant ponds and is available for return to the processing facilities.

KCGM spends several million dollars a year on process water for the plant. It was therefore considered desirable to develop a water balance model for the KCGM TSFs to enable reasonably accurate prediction of return water from the TSFs. Another purpose of the model was to enable comparison of differing tailings management strategies and/or TSF construction options to maximise water recovery.

4.2 KCGM Tailings Storage Facilities

KCGM has three active TSFs called Fimiston I, Fimiston II and Gidji. Tailings from the Fimiston processing plant is predominantly discharged into Fimiston II, with excess tailings directed to Fimiston I. A much smaller volume of tailings is discharged into the Gidji TSF from the Gidji roaster.

Fimiston II is the largest TSF covering approximately 3.6 km^2. Tailings discharge is cycled between three paddocks, with each paddock receiving approximately 2 months of deposition, followed by 2 months of drying and 2 months of wall raising.

Fimiston I and Gidji are also divided into paddocks so that tailings deposition can be cycled between paddocks to allow for drying of the tailings. This allows for upstream raising of the perimeter walls with tailings borrowed from the adjacent beach.

An important consideration in the development of the water balance model was the incorporation of a flexible deposition strategy to enable the cycling between facilities to be

modelled, and also to enable different deposition strategies to be evaluated.

4.3 Model Framework

The model was developed in Microsoft Excel as it was desirable to have a model that could be readily adapted in the future, and which allowed for the incorporation of add-in programs, such as @RISK, at a later date.

The model structure incorporates a graphical menu to direct the user to various sheets in the model and a control menu to enter simulation parameters and run the water balance simulations. There are a number of data entry sheets setup in the model, including an operational data sheet which allowed for the entry of different deposition strategies. A climatic data sheet has also been included in the model, containing 25 years of historical rainfall and evaporation data to be used for the model simulations. The model also contains a master calculation sheet for the water balance calculations and various report sheets to view the simulation results.

The model was developed to track water flow into and through each TSF paddock on a daily basis and daily return water availability.

The model was also developed to track three water quality parameters, namely pH, magnesium ion concentration and the concentrations of total dissolved salts (TDS). This functionality was included so that the model could simulate the quality of the water returned to the processing facilities.

The chemical species of interest (hydrogen ions, magnesium ions and other salts) were assumed to be conservative solutes. This allowed the chemical concentrations to be tracked using a mass balance approach.

4.4 Water Balance Components

The following components were incorporated into the KCGM TSF water balance model:

- slurry deposition
- rainfall and evaporation
- water return to the plant
- seepage losses.

Consolidation water release to the decant pond was not included in the water balance model, as this inflow was considered negligible given the overall water flow volumes for the KCGM TSFs.

Some other important processes that were incorporated into the model equations include:

- the loss of slurry (and therefore slurry water) to borrow pits around the perimeter of the tailings surface following upstream raising of the perimeter embankment
- loss of rainfall to cracks
- effect of salinity on evaporation
- runoff factors for each month for a range of rainfall events
- varying rates of seepage from each decant pond as a function of the pond size, residue depth and paddock area.

4.5 Model Simulations

The model has been developed so that different water balance simulations can be run once all of the operational and tailings data has been entered into the model. Water balance simulations can be run for a specified period of deposition using either wet, dry or randomly selected sets of daily historical rainfall and evaporation data. If the climate sets are set to be randomly selected, up to 25 different climate scenarios can be run against the specified depositional strategy.

4.6 Model Calibration

Although historical and operational data has been used during the development of the model, many of the lookup tables upon which the model relies have been estimated from experience, or using surface or groundwater models with little hard data available for their calibrations.

The model is now in a stage of calibration to real data to refine various parameters, such as runoff coefficients for the various beach areas, seepage rates from the decant pond, beach drying times and dry beach crack volumes.

4.7 Model Output

The results from a water balance simulation are presented in tabular and graphical form in the KCGM TSF model. Results are generated for each TSF paddock and for user specified paddock combinations to obtain total processing facility results.

The output results generated for each paddock include:

- the volume of water returned to the process plant
- the percentage of total slurry water that is returned to the plant
- the TDS and magnesium ion concentration of the return water
- the pH of the return water.

The output results generated for each paddock are tabulated and produced graphically against the simulation time. An example of a paddock graph showing the volume of water available for return to the processing plant from a paddock in the Fimiston II TSF is given in Figure 2. This example has been generated from a simulation using 5 different climate sets (CS1 to CS5). As the model has not yet been calibrated, the volumes presented in Figure 2 are not an actual indication of water return volumes for the single paddock.

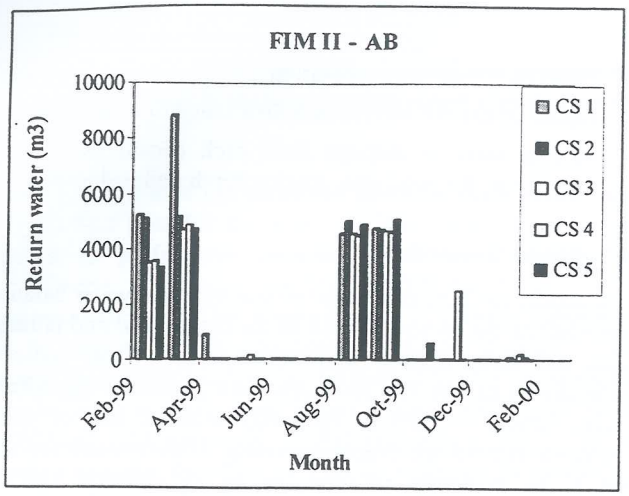

Figure 2: Example graph for a TSF paddock

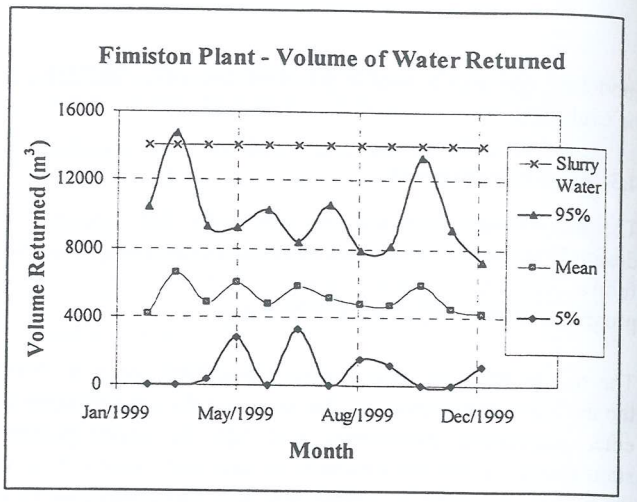

Figure 3: Example of a facility graph

The output results generated for each paddock for each climate set are combined to generate processing facility results. The paddock results are evaluated statistically to give the mean and 90% confidence interval (90% CI) values for the parameters listed above (for the paddock results).

The statistical results for the processing facilities are tabulated and produced graphically against the simulation time. An example of a facility graph showing the mean and 90% confidence interval limits for the volume of water returned to the Fimiston processing facility is presented in Figure 3. The 90% CI curves give the upper and lower limits within which there is a 90% confidence that the predicted values will fall. As for Figure 2, the volumes presented in Figure 3 are not an actual indication of water return volumes to the KCGM Fimiston processing plant because the model has not been calibrated to site data.

5. CONCLUSIONS

A water balance model is a useful tool to assist in water management in and around a TSF, and to indicate how much water is likely to be available for return to the processing plant. A water balance model can also be used to assist in the development of deposition strategies that are appropriate to the water return requirements of the mining operation.

It is generally not necessary to do an overall water balance for a TSF, as a surface water balance model provides reasonable estimates of surface water storage volumes, and the volume of water available for return to the plant.

The reliability of a water balance model is controlled by the accuracy of the input data. Some of the input data can be measured, but some data has to be estimated. In general, it is possible to make reasonable estimates of the input and output flows resulting in reliable output results from the water balance simulations.

6. ACKNOWLEDGEMENTS

The author wishes to thank KCGM for their permission to publish this paper, and David Williams and Shaun Davidge of Golder Associates for their assistance with the development of the KCGM model and the review of this paper.

The Channel Tunnel: Construction and The Marine Service Tunnel Breakthrough

James Weller BE (Hons) Grad IE Aust
Hydro Electric Corporation, Hobart, Tasmania
(Transmanche-Link, UK, Feb 90 - Feb 91)

SUMMARY: This paper provides an overview of how the Channel Tunnel project was accomplished. The emphasis is on construction of the tunnel system. The main aim is to illustrate the magnitude and complexity of the overall task so that the various remarkable achievements of the project, especially in the areas of logistics and surveying, can be recognised. Following a description of the Eurotunnel twin bore "Rolling Road" system, the geological and geotechnical features of the tunnel are described. The various construction methods and the overall construction programme are then outlined. The construction of the Marine Service Tunnel is then detailed, including tunnel boring machine operation, survey control, and the breakthrough and junctioning procedures.

1 INTRODUCTION

[The reference used in this section was Irwin (1)]

The Channel Tunnel is one of this century's largest and most ambitious civil engineering projects. Testament to this fact is that it was voted the greatest construction achievement of the 20th century by construction engineers around the world, beating Chek Lap Kok airport in Hong Kong, the Panama Canal, and 97 other nominations for the award. The announcement was made at the Conexpo exhibition in Las Vegas (one of the largest construction meetings in the world) in March 1999 and was the result of a poll made by readers of an array of construction magazines. Its technological achievements and utility surpassed the others, they said.

In addition, in 1997 the American Society of Civil Engineers voted it one of the seven modern wonders of the world.

This paper provides an overview of how the Channel Tunnel project was accomplished. The emphasis is on the construction of the tunnel system, concentrating on the role of the Marine Service Tunnel. The main aim is to illustrate the magnitude and complexity of the overall task so that the various remarkable achievements of the project, especially in the areas of logistics and surveying, can be recognised.

2 BACKGROUND TO THE EUROTUNNEL PROJECT

[Unless stated otherwise the references used in this section were Henderson (2) and Essig et al (3)]

2.1 Selection of the Fixed Link Scheme

The construction of a tunnel under the English Channel has been proposed at various times over the last 200 years. In 1974 4.3km of tunnel was driven from England to demonstrate the ideal mechanical boring conditions that exist in the ground beneath the Channel. With cross-Channel traffic on the surface and in the air heavily congested and a move towards decreasing trade barriers within the European Community; the British and French Heads of Government announced their enthusiastic support for a privately funded fixed link on the 30th November 1984.

In response to an Invitation to Promoters, four projects were tendered. The competing schemes included bored tunnels, submersed tubes, artificial islands and bridges; and embraced both rail and road transport solutions.

On the 20th January 1986 the two Governments decided on the Eurotunnel Scheme because:

- it was the soundest financially;
- it carried the fewest technical risks;
- it was the safest for the traveller;
- it presented no navigational hazard;
- it was the least vulnerable to terrorist action; and
- its environmental impact could be contained.

2.2 Parties to the Project

A concession agreement signed on the 14th March 1986 gave the Eurotunnel promoters, a consortium of banks and construction companies, 55 years from the 29th July 1987 to construct and exclusively exploit the rail link.

After the concession was awarded the promoters formed two separate organisations. Eurotunnel was established as the concessionaire to own and operate the system and raise the necessary finance of £6billion (~$A12billion in 1986).

Transmanche Link (TML) was formed as the contractor. This was an umbrella organisation for the purposes of liaison and coordination between the UK and French halves of the project. Each original group of five construction firms formed their own joint venture: Translink JV in the UK and Transmanche Construction GIE in France.

2.3 Progress of the Project

Work began in May 1986 and the fast-track design-and-construct program called for a construction period of seven years with a completion date of May 1993.

The project was plagued by cost, schedule and safety problems and consequently took eight years to complete. At a final cost of £9billion it became one of the world's largest privately financed engineering endeavours. [Irwin (1)]

It is interesting to note that the civil works were completed to program (although not to budget), the overall project time overrun being mainly due to problems with commissioning the incredibly complex control systems.

3 THE EUROTUNNEL SYSTEM

[The main reference for this section was Crighton et al (4)]

- The Eurotunnel system is a twin bore rail tunnel for "Rolling Road" shuttles and through trains.
- From portal to portal the tunnel system is 50.5 km long, 37.9km of which are under the sea.
- The two 7.6m internal diameter running tunnels (one for each direction of travel) are 30m apart and straddle a central service tunnel of 4.8m internal diameter (See Figure 2).
- Access cross passages of 3.3m internal diameter link the running tunnels to the service tunnel at 375m centres (See Figure 2)
- 2m internal diameter piston-effect relief ducts connect the running tunnels at 250m centres (See Figure 2).
- Two crossover chambers approximately 160m long x 20m wide x 15m high, at the third points, are required for single track working during maintenance periods and emergencies.
- Numerous signalling rooms, electrical substations and equipment rooms of 3.3m - 4.8m internal diameter are located throughout the tunnel system.
- There are three distinct low points on the alignment, each of which has a pumping station. Additional pumping stations are located at the coasts, to prevent any seepage flow from the under-land tunnel sections entering the undersea sections.
- Terminals at each end provide the road-to-rail interface and a loop section that connects the two running tunnels. The French terminal covers 470ha while the smaller UK terminal occupies 170ha.

4 TOPOGRAPHY, GROUND CONDITIONS, TUNNEL ALIGNMENT AND STRUCTURE SITING

[The main references used for this section were Crighton et al (4), Destombes et al (5), Missoffe (6), Eurotunnel (7), Biggart et al (8) and Fermin (9)]

4.1 Site Investigation History

The possibility of a fixed link between Great Britain and France has led to the geology of the Dover Strait being given considerable attention for over a hundred years. Samples of the seabed were taken between 1872 and 1883, further work was carried out in 1958-59 and a major site investigation in 1964-65 included nearly 100 marine boreholes, 20 land boreholes and a thorough seismic survey at sea. Further work was also carried out in 1972-74.

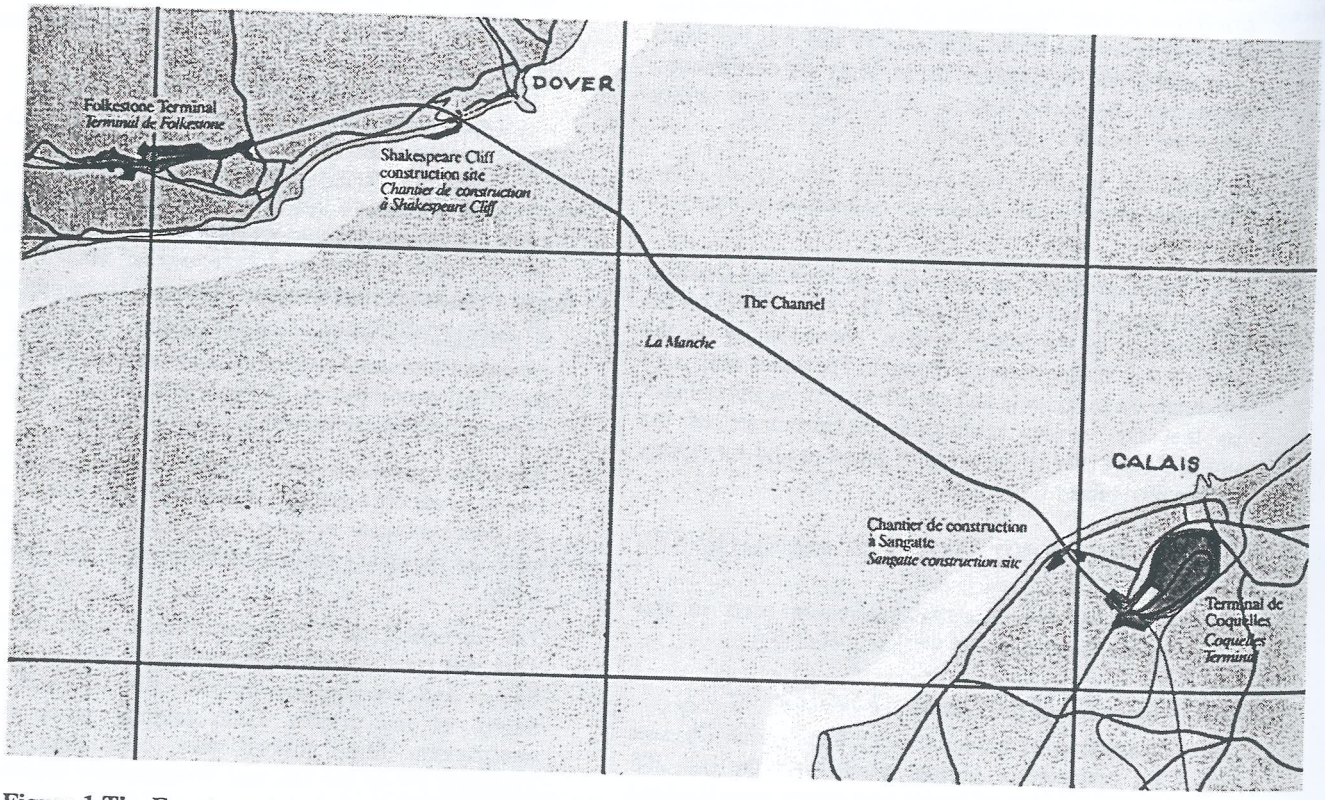

Figure 1 The Eurotunnel System route, showing inland terminals and coastal construction sites.

Recent geotechnical and geophysical surveys were carried out in 1986 and again in 1988. The main objectives were to supplement existing information, particularly in areas where significant changes were made to the alignment from previous schemes; and to gain detailed site specific information at the location of the crossovers and the Fosse Dangard (a major alluvium-filled erosional valley near the centre of the main channel).

4.2 Topography and siting of the Terminals

The Dover Strait is an erosional channel some 37km wide running approximately SW-NE. The maximum water depth is around 60 metres near the middle. The cliffs along each coast attain heights of between 50 and 75 metres at the neck of the Strait between Dover and Calais.

On the British Coast the ground rises towards Folkestone where the cliffs are up to 160 metres high. Consequently, the only relatively level area suitable for a terminal site is at the head of an erosional valley to the north west of Folkestone, about 13km west of Dover (See Figure 1).

On the French side however, the land flattens out almost immediately inland from the coast. Consequently a suitable site for the main terminal, two and a half times the area of the Folkestone site, was found just 3km south west of Calais (See Figure 1). This larger facility includes the rolling stock maintenance workshops.

4.3 Geology

The geological structure of the region comprises a Palaeozoic basin on which is superimposed an anticline of Cretaceous and Jurassic sedimentary beds. The major axis of the anticline is roughly at 90^0 to that of the Strait, ie running SE-NW. Dover and Sangatte are to the east of the anticline, so that due to erosion, successively older rocks outcrop on the seabed as one progresses westwards. The upper beds of the Cretaceous system in descending order from the seabed are the Upper, Middle and Lower Chalk, Gault Clay and Lower Green Sand. Only the Lower Chalk remains beneath the seabed at the line of the tunnel. It is further subdivided into White Chalk (15-25m thick), Grey Chalk (15-28m thick), Chalk Marl (20-35m thick) and a thin layer of Glauconitic Marl. Further secondary anticlinal structures, running perpendicular to the main anticline, cause the strata to dip severely at the French coast. Some faults were identified within the French tunnel section. One substantial one caused deep penetrative weathering within the Grey Chalk, but this was not expected to penetrate to tunnel level within the Chalk marl. (See Figure 2)

4.4 Geotechnical Properties

The White and Grey Chalks, carbonate content 85 and 80 per cent respectively, are of relatively hard, brittle and fractured material. Flint, which is very hard, is generally found in the Middle Chalk but was expected in the upper layers of the Lower Chalk as well.

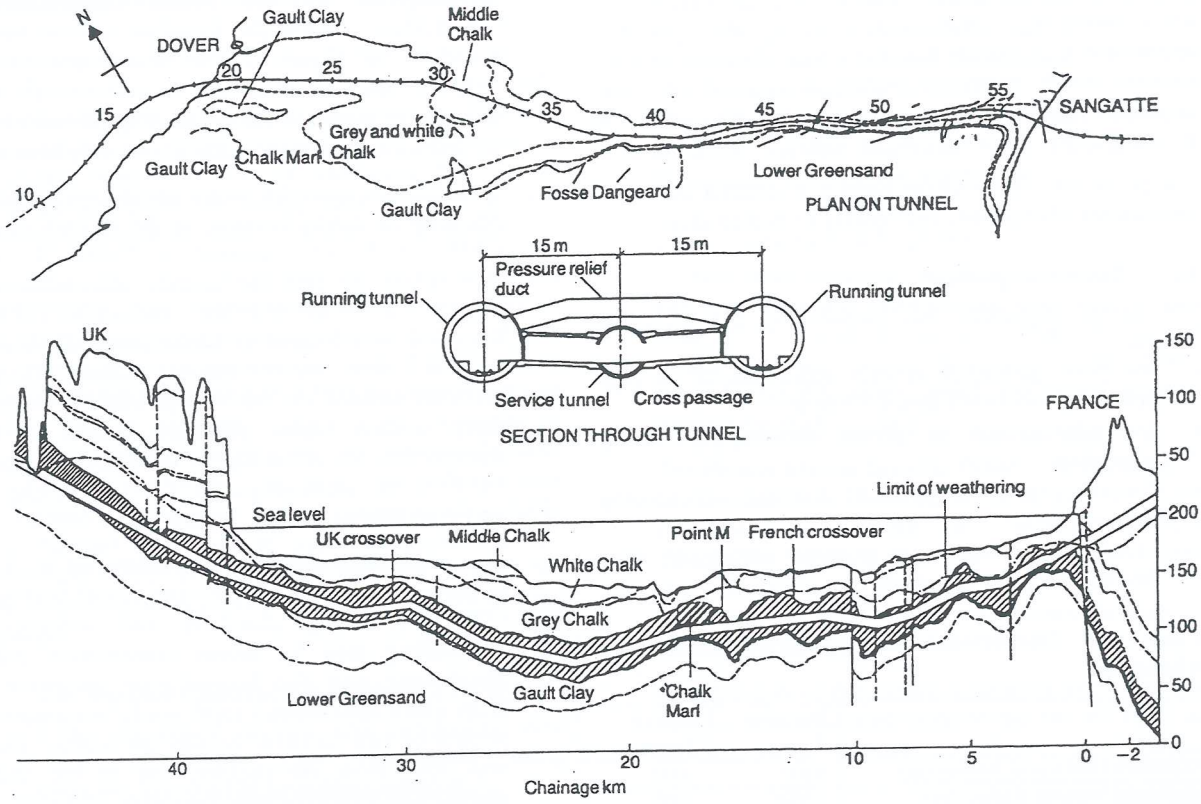

Figure 2 Geological plan and cross-section, and section through the tunnel system.

Table 4.4 Geotechnical Properties of the Lower Chalk and Gault Clay

	Compressive Strength (MPa)	Deformation Modulus (MPa)	Permeability (m/s)
Weathered White Chalk	7 –11	N/A	5×10^{-5}
Sound Grey Chalk	8 – 15	4700	1×10^{-5}
Chalk Marl	2 - 50	1300 – 2000	2.5×10^{-7} - 1×10^{-6}
Glauconitic Marl	6 – 35	N/A	1×10^{-7}
Gault Clay	1 – 4	350	1×10^{-7}

The Grey Chalk was estimated to have 3-5 discontinuities per cubic metre, with thicknesses in the order of centimetres and marked chemical degradation in the upper parts. The estimated ingress per metre length of tunnel was 2 L/s for weathered Chalk reducing to 0.5 L/s for sound Grey Chalk. This renders the Grey Chalk highly aquiferous but with no risk of solution cavities.

The Chalk Marl, is a mixture of clay and carbonate-mudstone with an average carbonate content of 70% and moisture content of 11%. It is of low strength, homogeneous and slightly plastic, but retains a brittle mode of failure. It was considered to be essentially impermeable with 1-2 discontinuities per cubic metre, in the order of millimetres and generally filled with calcite, giving an estimated tunnel ingress per metre length of 0.1L/s.

The underlying Gault clay, while also virtually impermeable, is weaker than the Chalk Marl and exhibits strongly plastic behaviour leading to non-uniform time-dependent deformation when stressed. It is also subject to swelling action when exposed to water.

The permeable Lower Green Sand is a complex system of alternations of clay beds and weakly cemented sand.

4.5 Tunnel Alignment

The tunnel alignment was dictated by the following criteria:

- the basic geometric criteria applicable to a high speed railway (see Table 4.5 below);
- the minimisation of power consumption during operation;
- the establishment of optimum drainage and pumping regimes; and
- to be located as far as possible within the most favourable tunnelling medium.

Table 4.5 Operational Design Criteria for the Alignment

	Running Tunnels	Service Tunnel
Minimum Horizontal Radius (m)	4200	1000
Minimum Vertical Radius (m)	15000	1000
Maximum Gradient (%)	1.1	3.5
Minimum Gradient (%)	0.18	0.18

The Chalk Marl was considered to be a medium ideally suited to mechanised tunnelling techniques: easy to excavate yet competent with a good stand-up time suitable for the use of an expanded unbolted tunnel lining. As a result 90% of the tunnel's alignment is in the Chalk Marl at a depth at mid channel of approximately 115m below sea level and a cover of 70m, reducing to 19m near the French coast. Here, due to the dipping of the strata, the alignment goes through the upper beds of the Lower Chalk and then into the Middle Chalk to reach the inland portal at Beussingue, which is 3 km from the coast. On the UK side the tunnel alignment essentially stays within the Chalk Marl all the way to the portal on the western side of Castle Hill, 9km from the coast.

The tunnel profile is dictated by that of the strata: an elongated triple U. Similarly the plan alignment of the undersea section of tunnel follows the major axis of the Cretaceous anticline: i.e. a line running SE-NW. To remain in the Chalk Marl the alignment runs parallel to and about 3-4km to the west of a line linking Dover and Calais. Inland from the UK coast, it then swings round to the west and heads directly for the terminal. In France the portal remains on roughly the same NW-SE line as the undersea alignment. (See Figure 1)

4.6 The Tunnel Construction Sites

In order to reduce the length of the tunnel construction programmes, construction was to be carried out concurrently on two fronts, on both sides of the channel. Tunnelling would commence from a single location, but proceed both seaward and landward. In addition it was advantageous for the tunnel commencement and construction support site to be as near to the coast as possible (See Figure 1). This was in order to keep the length of the seaward drive to a minimum. The reason for this was to minimise the logistical problems of supplying an undersea construction face from a very long distance.

Providing the space for such a major construction site and reaching the tunnel horizon, in the vicinity of the White Cliffs of Dover presented a formidable challenge. Fortunately the task had already been achieved by the Service Tunnel demonstration project in 1974. A split-level site was located at Shakespeare Cliff, about 3km west of Dover. The site offices, canteen, change rooms, etc were situated on the high ground above the cliff. A steep decline tunnel provided access to the main construction site at the foot of the cliff. A further decline led from this sea-level platform to the existing 4.3km of undersea Marine Service Tunnel.

A second, larger decline was constructed to provide rail access to what were initially the tunnel-boring machine (TBM) launching chambers and subsequently the marshalling area for tunnel construction traffic. The marshalling area also housed spoil collection bunkers, from which each tunnel's spoil would be transported to the surface by belt conveyor through the original adit. A shaft was sunk from the cliff-top site to the underground marshalling area to provide personnel access to the tunnel system.

On the French side the fractured aquiferous nature of the weathered ground, rather than the topography of the site, presented the obstacle to reaching the tunnelling horizon. In this case a huge access shaft, 55m in diameter and 65m deep, was sunk at Sangatte about 4km west of Calais.

5 CONSTRUCTION OVERVIEW

[The references used in this section were Crighton et al (4) and Biggart et al (10)]

5.1 Implications of the Geotechnical Investigations

By 1988 the Channel Tunnel area had probably become the most thoroughly investigated site ever. To be able to carry out a site investigation, the aim of which is to confirm and supplement a hundred years worth of exisiting information is unprecedented. This situation provided a high level of confidence in the knowledge of the ground conditions, of what was essentially a straightforward geological structure.

Consequently the design of the underground structures and the selection of the construction technique could be accurately tailored to the local conditions, allowing a high level of efficiency. In any other situation a conservative all encompassing approach would probably have been employed due to the lack of familiarity with the ground conditions.

An example of the successful use of this approach occurred when the type of TBM for each of the tunnel drives was selected. Closed face Earth Pressure Balance (EPB) machines were selected for the French drives to deal with the waterladen fractured ground near the coast. This technology although expensive is well-proven and reliable in bad ground conditions. On the UK side on the other hand, fissured water-bearing ground was only expected in isolated instances. In this case open face (i.e. at atmospheric pressure) machines were employed in conjunction with a method of confirming the ground conditions ahead of the tunnel face, so that ground treatment contingencies could be employed if required.

In addition, the level of confidence in the structural quality of the Chalk Marl presented the opportunity to introduce a construction technique that had previously not been used in soft rock applications in the UK. The New Austrian Tunnelling Method (NATM) provided a fast and efficient method of constructing one-off structures or structures whose cross section was not uniform. Initially trialled and confirmed on the marshalling area development works, which comprised fairly straightforward structures, it was then applied to the construction of the UK Crossover chamber, one of the most ambitious underground chambers ever constructed in Europe.

5.2 The Various Construction Methods Employed

- All the UK tunnel horizon and marshalling area development works were constructed using roadheaders and NATM tunnelling methods.
- The French shaft at Sangatte was constructed using diaphragm wall techniques.
- For the most part the tunnels were constructed using TBMs: open-face machines on the UK side and EPB machines on the French side.
- There is a half kilometre section of cut-and-cover tunnel at Holywell Combe just east of the UK tunnel portal.
- Between Holywell Combe and the UK portal there is a half kilometre section through Castle Hill that was constructed using road headers and NATM techniques.
- The UK Crossover chamber was constructed using NATM techniques with roadheaders and excavators.
- The French Crossover chamber employed the parallel drift method of construction.
- Ancillary structures such as the cross passages, piston effect relief ducts and pumping stations were all constructed using hand held pneumatic equipment and lined with cast iron segments.

5.3 Spoil Disposal

The 4.3 million cubic metres of UK spoil was used to reclaim the site at the foot of Shakespeare Cliff from its original 5 hectares to a final area of approximately 30 hectares.

The 3 million cubic metres of French spoil was slurried and pumped to a purpose built settling lagoon 1 km from the Sangatte site.

5.4 Precast Concrete Lining Manufacture

The precast concrete segments used to line the tunnels were manufactured by two purpose built facilities. In France, the main tunnel construction site at Sangatte was large enough to accommodate their plant. In the UK however, limited site space necessitated the construction of a plant on the Isle of Grain in the Thames estuary. Granite aggregate was shipped from a dedicated quarry in Scotland and the segments were transported to the Shakespeare Cliff Lower Site by rail.

5.5 Construction Logistics

On both sides tunnelling by TBM commenced at the coast and proceeded both seaward and landward. Therefore, a total of 12 tunnel drives were required. The shorter French landward running tunnel drives were constructed using the same machine, which was turned around in the Beussingue portal cutting.

The French Marine Service Tunnel TBM was the first to be launched from the Sangatte shaft, in March 1988, and maintained a 10 month lead over the running tunnel TBMs (See Figure 3). This was so that ground conditions could be confirmed ahead of them, and to meet the UK marine Service TBM for the initial breakthrough in order to close the survey traverse.

Construction of the French Crossover and other ancillary structures commenced towards the end of TBM activity (See Figure 3).

5.6 The Strategic Role of the UK Marine Service Tunnel Drive

The UK Marine Service Tunnel began on January 1st 1988, nearly a year ahead of the UK running tunnel machines and maintained a 10km lead for the following reasons (See Figure 3).

5.6.1 Ground Treatment

The Service Tunnel acted as a pilot tunnel, to investigate and confirm ground conditions and provide enough time for any necessary treatment to be carried out so that running tunnel progress was not affected.

The necessity for ground treatment arose just off the UK coast where fissured water-bearing ground was encountered. A fan of holes was drilled and a silica based cement grout was injected to provide a protective hood over the path of the running tunnels.

5.6.2 Excavation of the Crossover Chamber and other Ancillary Structures.

The Marine Service Tunnel provided the access and supply route for construction of the UK Crossover chamber. This was in order to construct the Crossover chamber before the arrival of the running tunnel machines. Similarly most of the ancillary structures that were excavated by hand were constructed from the Service Tunnel.

5.6.3 Initial Breakthrough

The French Marine Service Tunnel drive began soon after the corresponding English tunnel drive was begun; so the two drives had the distinction of making the initial contact for their country's construction team, providing the opportunity to close the two survey traverses.

6 CONSTRUCTION OF THE MARINE SERVICE TUNNEL BY TBM

[The main references for this section were Biggart et al (10) and an unpublished TBM operator's manual written by James Howden & Company, Scotland]

6.1 Operation of the UK Open Face TBM

The 15m long main body or "shield" of the Marine Service Tunnel TBM had two sections, which moved telescopically relative to each other. When advancing, the cutting head section thrust off the gripper section. The cutter head rotated at a top speed of 4.5rpm. There were 16 thrust rams each normally delivering 90t; that is a total thrust of 1440t. There were 270m of trailing backup gantries and the total weight of the TBM was 700t. The following is a description of one production cycle:

- The machine pulls up its gripper section and trailing backup gantries after having just completed a 1.5m long cut.
- A pre-cast concrete ring of 6 segments is built in the exposed tunnel bore. A wedge key is thrust into the ring to expand it and lock it against the excavated ground.
- Cementitious grout is pumped behind the ring to create a uniform contact service between the ground and the concrete lining and to stop any water flow.
- During ring building an empty skip train is positioned under the conveyor discharge of the TBM.

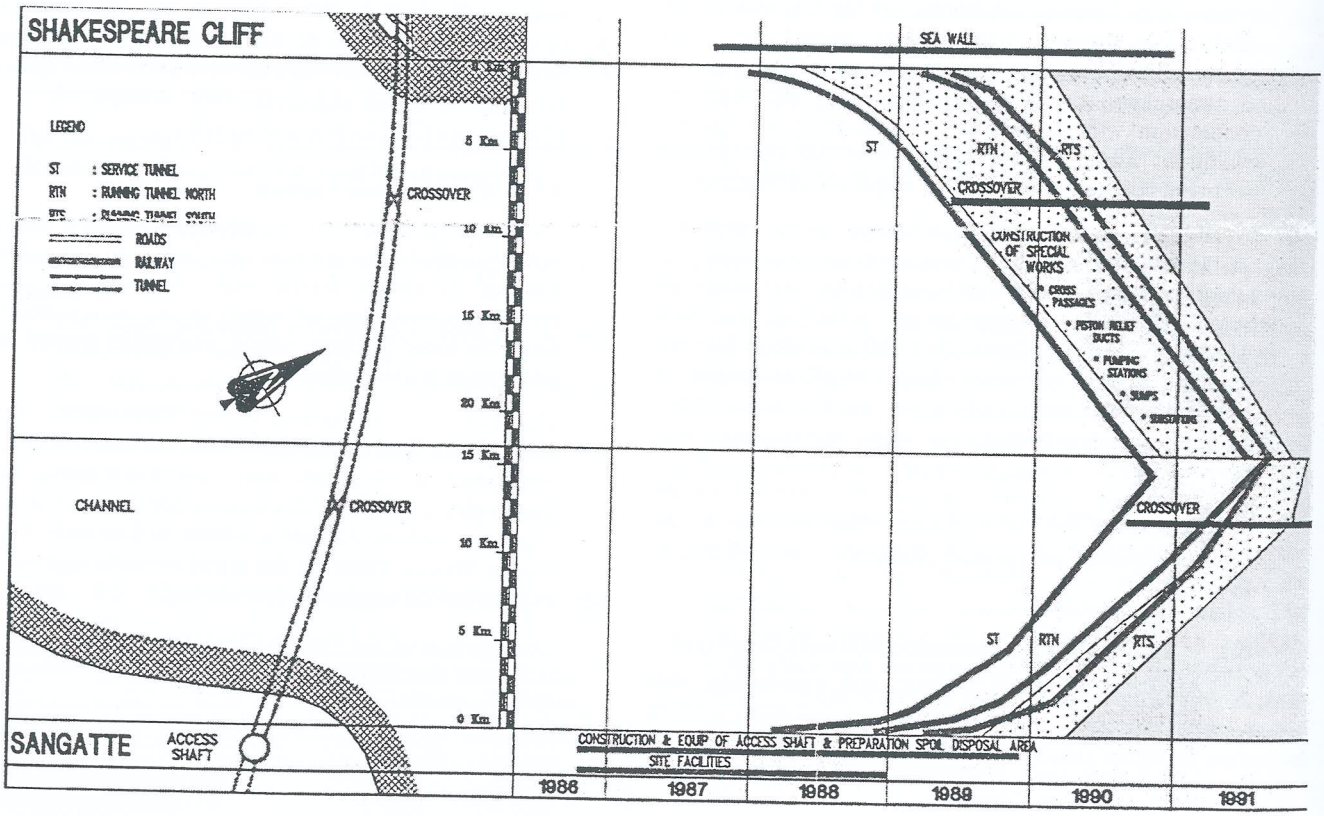

Figure 3 The undersea works construction programme

- A new cut is commenced. Spoil is transported from the head to the muck skips by conveyor belt.
- The cycle repeats.
- Each train brings in the lining segments and takes out the spoil, for 1 production cycle.
- The rate of advance is 1.5 m in about 40 min.
- Best day 60 m.
- Best month 1.04 km.

It was necessary to investigate ground conditions ahead of the open face TBM. Every week a 250m destructive probe hole was drilled to determine the water bearing state of the ground. Also, vertical core samples were taken near the low point of the alignment to determine the distance to the underlying unfavourable Gault Clay.

If a potential inundation situation was encountered, the muck conveyor could be retracted from the head very quickly and a trap door automatically sealed the face off. In addition, a circumferential blade seal could be thrust out into the ground to seal off the annular space (provided for manoeuvring) between the shield and the excavated ground.

6.2 Operation of the French EPB TBM

The French earth pressure balanced machine had similar characteristics to, and operated in much the same way as, the UK open-face machine except that it was designed to operate in full static head conditions, which reached a maximum of 95m of water. The TBM main body acted as a pressurising piston against the ground water. The cut spoil was ground up and mixed with the water to create a paste plug within the cutter head. The spoil was evacuated from the head by Archimedian screw and then transferred to the skips by belt conveyor.

The pre-cast concrete segmental lining was bolted together within the tail skin of the shield. Seals at the end of the tail skin prevented water ingress into the shield. When the TBM advanced the ring was left behind in the tunnel bore. Grout was then placed behind it.

The French EPBs were able to operate in either closed or open mode, depending on the present water content of the ground. In open mode the gripper section was used, to thrust against. In closed mode the ground conditions were usually such that the shield had to thrust off the concrete lining.

7 SURVEYING TECHNIQUES & TUNNEL ALIGNMENT CONTROL

[The main reference for this section was Winney (11)]

7.1 Primary Control Network

Overall primary control for the entire site was based on a network of sightings across the channel established over many years with recent input from a satellite global positioning system (GPS). A rectangular grid based on a transverse Mercator projection, with its central meridian near the middle of the project, was used to convert from a curved geodetic co-ordinate system to a planar rectangular one.

A local network of survey stations was established at both coastal sites, to transfer the primary survey underground. On the UK side, at Shakespeare Cliff, this included a traverse running through the two adits to the enlarged marshalling area of the service tunnel, where the baseline for the tunnel primary traverse was established. At Sangatte in France the corresponding transfer underground was done by taking a series of steeply inclined theodolite sights down the access shaft. This produced a very short baseline from which to extend the primary traverse.

7.2 Tunnel Control Traverse

The primary traverse was extended down the tunnel using a 75m zigzag pattern with wall-mounted stations on alternating sides of the tunnel. This method enabled the systematic error due to refraction, introduced when taking sights along one side of the tunnel, to be effectively cancelled out. The refraction is caused by a temperature gradient along the tunnel radius due to warm air from the face flowing through a tunnel whose concrete lining is damp and cool. If not accounted for, this phenomenon would have put the tunnel on a 3000km radius, which would have resulted in the UK drive being off line by several diameters after the 22 km of drive towards France.

Settlement of the lining as the ground loading came on meant that revisions to the zigzag survey were required to account for the 5mm to 10mm spread of the tunnel lining.

A second separate traverse was carried forward on tripods along the tunnel invert to provide a check of the zigzag traverse.

Weaknesses introduced into the primary traverses, by both short baselines and refraction, were picked up by check sightings with high-precision north-seeking gyro theodolites. These instruments were able to provide a true reading of azimuth anywhere in the tunnel.

On several occasions a separate traverse was carried out by a German team in order to provide a completely independent check on the in-house primary traverse.

7.3 Production Traverse

A separate production traverse was carried forward along one side of the tunnel only, by the TBM shift engineers. This traverse was used to set out laser stations for machine guidance. On a regular basis the primary survey team would extend their control traverse into the TBM and pickup the production traverse stations. The co-ordinates of these stations were then adjusted accordingly.

7.4 Tunnel Alignment Control

The information used to steer the TBM is provided by a laser-guided system:

- The laser is set out parallel to the Designed Tunnel Axis (DTA).
- On curves the laser defines a chord and is taken around the curve using a Prism Beam Deflector.
- The "ZED" onboard computer guidance system is fed with a data set of points (coordinates) that define the DTA and information describing the position and orientation of the laser.

- An electronic target on the TBM picks up the laser spot. The computer can then calculate the position of the machine.
- The machine's actual position is then compared with that of the DTA at the present chainage.
- "Off" line and level information is displayed in the operator's cab.
- The operator steers to reduce these figures to zero by individually selecting thrust rams.

8 BREAKTHROUGH AND JUNCTIONING PROCEDURE OF THE MARINE SERVICE TUNNEL

[Unless stated otherwise the information for this section was taken from unpublished internal TML design and construction documents.]

8.1 Desired Criteria for the Breakthrough Procedure

The two Marine Service tunnel drives were of unprecedented length, undersea and between separate landmasses. Therefore, the logistics of junctioning the two tunnels, including the safe disposal of the boring machines, were challenging in the extreme.

In addition, the precise relative position of the two tunnels would not be known until the separate survey traverses could be closed. The final design had to be capable of accommodating this potential variance whilst minimising the impact on the running tunnel alignments and associated structures.

Many schemes were suggested and several reports compiled on the best junctioning method. Some, like the one entailing the construction of a large cavern (similar to the crossover) in which all six machines could be preserved in an undersea museum, could only be described as fantasy. Others like the head on junction, cutting out one TBM and sliding the second into its place were wishful thinking. In practice, considering the issues mentioned above, this task would have become an engineering nightmare.

The "ideal" solution had to be:

- engineeringly practicable;
- capable of meeting the overall programme;
- cost effective;
- politically acceptable to both parties; and
- above all it had to be safe.

To achieve these criteria the following specific conditions were applied:

- The meeting point should not be predetermined and should be independent of the other tunnels.
- The scheme should not involve dismantling and removal of the TBMs.

This last condition however, was modified following discussions with specialist sub-contractors who confirmed that removal of all but the structural skin was both a feasible and safe option for the French TBM.

8.2 Solution Options

The development of the options concentrated on the construction of the junction and disposal of the TBMs irrespective of location. This was possible as the tunnel alignment in the likely area of the junctioning was of consistent plan and profile.

From the various schemes which were identified, 3 options were chosen which best met the objectives and warranted further analysis. A cost and programme comparison was then carried out to identify the most suitable proposal.

8.2.1 Option 1: Double curve; both TBM main-bodies buried; duration 14 weeks; cost £5.8M. (See Figure 4)

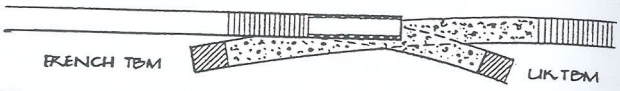

Figure 4 Marine Service Tunnel Junction Option 1

8.2.2 Option 2: Single curve; UK TBM main-body buried; French TBM main body stripped leaving the hollow shield; final Service Tunnel connection by manual heading into the French shield chamber; duration 9 weeks; cost £3.83M. (See Figure 5)

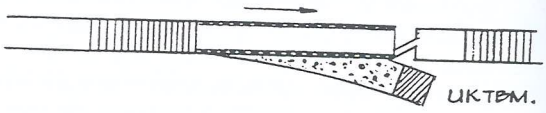

Figure 5 Marine Service Tunnel Junction Option 2

8.2.3 Option 3: Single curve; UK TBM main-body buried; French TBM driven towards the UK to complete the Service Tunnel; duration 12 weeks; cost £3.9M. (See Figure 6)

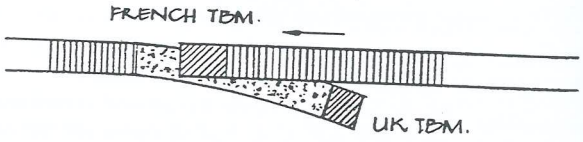

Figure 6 Marine Service Tunnel Junction Option 3

8.3 The Chosen Solution

Option 2 was clearly the cheapest and quickest scheme and is now presented in detail, as it happened (See Figure 7).

Phase 1

At the end of October, after driving 22km on the British side and 16km on the French side, the two machines were stopped with 100m separating them. A probe hole was drilled from the UK machine towards the French. It broke through into the French face on the 30th November 1990. A sophisticated Maxibor hole-surveying device (used for the first time horizontally in tunnelling and accurate to 1:1000) was used to determine the relative positions of the two tunnel drives. It was found that there was a horizontal

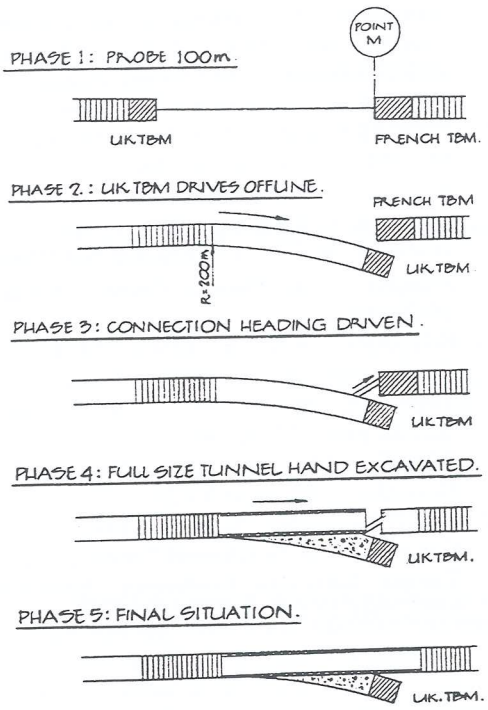

Figure 7 Junction Option 2, phase by phase.

misclose of 500mm (+/- 100mm) between the two headings. A level check was also performed with a water tube giving a vertical misclose of 50mm.

Phase 2

The UK TBM was then driven off the Service Tunnel alignment on a 200m radius curve, using a temporary lining to support the tunnel. Modifications to the TBM were necessary, as the minimum design radius of curvature for the Service Tunnel was 1000m. The TBM backup train was then disconnected from the shield, dismantled and removed from the tunnel.

Meanwhile, the French TBM backup train was de-coupled from the main body and withdrawn from the tunnel. The remaining shield was then gutted.

Phase 3

On the 1st of December 1990 a hand-dug adit from behind the UK shield broke through into the French shield chamber and parties from either side made the first land crossing of the Channel since the Ice Age. A conventional precise closure between the two survey traverses was also carried out, giving the following misclose details: horizontal 361 mm; vertical 58 mm; chainage 69 mm [Korritke (12)]

Phase 4

The offline UK drive was then backfilled with concrete, burying the TBM main body. The Service Tunnel was realigned by manual excavation from the UK end and lined with cast iron segments.

Phase 5

The tunnel was completed by extending the cast iron lining into the French TBM shield at the end of January 1991.

8.4 Discussion

Option 2 was clearly the cheapest and quickest scheme. It had the feature that UK and French operations were carried out independently until a very late stage in the procedure. This had considerable benefits in terms of coordinating operations and to a lesser extent in border control formalities. In particular, from a safety point of view, there were major advantages in containing and controlling fumes from French flame cutting operations during gutting of the shield.

Options 1 & 3 required a TBM to remain static for significant periods, which presented a considerable exposure to risk. For Option 2 the UK TBM was only temporarily stopped while probing, the breakthrough and surveying occurred. Options 2 and 3 involved stripping the French TBM, leaving the skin in place. Option 2 provided an advantage by allowing this exercise to commence at the earliest opportunity with some degree of programme float.

All three of the schemes allowed for the initial 100m probe hole in order to permit the low-precision closure of the survey traverses prior to the final TBM burial curve(s). This provided enough precision to ensure that the TBM that was being turned off on its burial curve would not hit its stationary counterpart. But, only options 2 and 3 allowed for precise closure before manually completing the remaining 100m of Service Tunnel. This course of action allowed the misclose to be gradually and subtly reduced over the full 100m length, rather than creating an obvious kink or step in the final tunnel alignment.

Once chosen, Option 2 was further refined to include the deviation of the southern running tunnel alignment to provide for an extra 3m separation distance required, between it and the Service Tunnel alignment, to accommodate the buried TBM.

9 CONCLUSION

In order to realise the vision of the Eurotunnel system significant achievements were made in almost every aspect of its design and construction. The milestone that epitomised the collective achievements of the Channel Tunnel project was the breakthrough of the Marine Service Tunnel on 1st December 1990. The UK Marine Service drive at 22km is the longest undersea heading ever accomplished. The French, after reaching the tunnelling horizon through extremely bad ground, drove 16km to link up with the UK drive.

In addition, the UK Marine Service Tunnel was of pivotal strategic importance to the UK marine-tunnelling programme, acting as a pilot tunnel for the main running tunnels and providing the access and supply route for the construction of the majority of the ancillary structures.

The fact that the overall production programme was met and the junctioning procedure was successful is testament to the outstanding logistic and surveying achievements of both construction teams.

10 REFERENCES

1. IRWIN, A. "Channel Tunnel Voted Century's Top Construction", The Daily Telegraph, London, 25th March 1999.
2. HENDERSON, N. "Channel Tunnel- The Early Stages", The Channel Tunnel- papers from a conference organised by the Institution of Civil Engineers, London and the Société des Ingénieurs et Scientifiques de France, Paris in September 1989, Thomas Telford, 1989, pages 1,2,4,7,10,11,14 & 17.
3. ESSIG, P. & McDOWELL, A.D. "Project Management by Transmanche Link J.V.", The Channel Tunnel, Thomas Telford, 1989, pages 183 & 186.
4. CRIGHTON, G. & LEBLOND, L. "Tunnel Design", The Channel Tunnel, Thomas Telford, 1989, pages 97-99, 101, 103, 104 & 127.
5. DESTOMBES, J.P. & SHEPARD-THORN, E.R. "Geological Results of the Channel Tunnel Site Investigation 1964-65", N.E.R.C./I.G.S., pages 2.2, 3.2, 2.3.
6. MISSOFFE, Y. "Conception des Terminaux", The Channel Tunnel, Thomas Telford, 1989, page 158.
7. EUROTUNNEL, "The Channel Tunnel- A Technical Description", Eurotunnel, 1987, pages 12 & 23.
8. BIGGART, A.R., KING, J.R.J., MacKENZIE, R.D., MOORE, G. A., & MILES, J.A. "U.K. Tunnels Construction" The Channel Tunnel, Thomas Telford, 1989, pages 232, 234 & 235.
9. FERMIN, J. "Le Creusement des Tunnels Côté Français ", The Channel Tunnel, Thomas Telford, 1989, page 252.
10. BIGGART, A.R. & KING, J.R.J. "Design & Construction of the Channel Tunnel", Tunnels & Tunnelling, spring 1991: The Channel Tunnel Special, page 10 U.K. side.
11. WINNEY, M. "Level Best", New Civil Engineer, November 1990, pages 35-38.
12. KORITTKE, N. "Check Surveys During The Construction of the Channel Tunnel", The First Trans Tasman Surveyors Conference, Newcastle, April 1997, page 27.13.

Centrifuge Modelling of Pipeline-Soil Interaction in Calcareous Sand

Jianguo Zhang

Department of Civil and Resource Engineering
The University of Western Australia

Summary Previous research work on modelling pipe–soil interaction has been focused on pipelines in terrigenous sands and clays of the North Sea and the Gulf of Mexico. The foundation response in such soils is very different from that in the calcareous sediments that predominate off the coast of Australia. An investigation into pipeline/soil interaction in calcareous sediments conducted on a centrifuge is presented in this paper. A total of 25 model tests were undertaken on a segment of pipe modelling a 1 m diameter prototype pipeline shallowly embedded in four uncemented calcareous sand samples. The test facility, experimental program and test results are described. The effects of the loading history, the installation method and the depth of embedment are discussed.

1. INTRODUCTION

In offshore hydrocarbon development, pipelines are the most efficient method of transporting oil and gas products from offshore fields to onshore production plants. The cost of the pipelines represents a significant proportion of the development budget of a new hydrocarbon field. To minimise the cost, the selection of pipe on-bottom weight and protection method, as determined by the geotechnical stability, is critical. As a consequence, pipeline-soil interaction under different loading environments is a pivotal issue in pipeline design.

In an attempt to achieve good predictions of pipeline-soil interaction, a large amount of research work has been carried out during the last two decades. A variety of physical model tests have been performed in terrigenous sands and clays of the North Sea and the Gulf of Mexico. Some representative results from these work were given by Paulin et al. (1995), Brennodden et al. (1986), Lieng et al. (1988), Morris et al. (1988), and Brennodden et al. (1992) for buried and unburied pipelines respectively.

Among all these physical modelling results, none of them has shown pipeline performance in calcareous soils. All results for unburied pipelines are obtained from full-scale tests with the potential of high cost and long period. To avoid these shortcomings, a centrifuge was employed to perform the experiments in this project. All tests were conducted in uncemented calcareous soils. The centrifuge, soil samples, pipe installation method, test procedure and test results are described in the corresponding sections.

2. EQUIPMENT AND SAMPLE PREPARATION

2.1 Centrifuge

The centrifuge is an Acutronic Model 661 Geotechnical Centrifuge (Randolph et al., 1991). It has a swinging platform at a radius of 1.8 m with nominal working radius of 1.55m, and is rated at 40 g-tonnes. The platform seats standard "strongboxes" which have internal dimensions of 390 mm wide by 650 mm long by 325 mm high. The headroom of 900 mm allows for mounting equipment above the box to allow "in-flight" events to be performed.

2.2 Actuators

Apart from the strongbox that contains the soil, the key pieces of equipment relevant to these tests are the cone actuator. It sits on top of the strongbox, and permits vertical and horizontal movements to be imposed on models. The horizontal travel on the cone actuator allows repositioning of the actuator in-flight, to allow multiple cone model tests to be performed without stopping the centrifuge.

2.3 Model Pipeline Segment

The 160 mm long model pipeline segment is a 20mm diameter, 3 mm wall thickness aluminium pipe, with a solid section at the centre into which the load cell and the loading actuator were fitted. No attempt was made to model the self-weight of a prototype pipe, as the effective self-weight is controlled entirely by the loading actuator. All centrifuge tests were

conducted at 50g so that the pipe represents a prototype pipe of 1 m diameter.

2.4 Sample Preparation

The testing was commenced using a seabed soil. The soil was sieved through a 1 mm screen prior to sample preparation. Particle size distributions for the material, after removing the coarse particles, are shown in Figure 1.

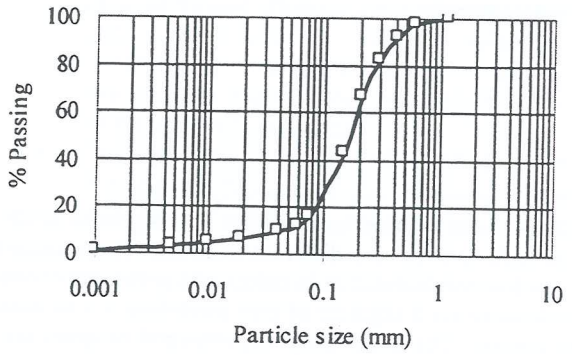

Figure 1 Particle distribution

The dry soil was mixed with water under a vacuum for several hours to remove air from the mixture. The slurry was then carefully placed in the strongbox above a fine to medium grained sand drainage layer of 120 mm thickness. The initial thickness of the slurry was about 140 mm. The sample was then consolidated under 50 kPa on the compressor for about 18 hours. The weight and the thickness of the soil were then measured for soil density calculation.

3. TESTING PROGRAM AND PROCEDURE

3.1 Testing Program

A total of 25 pipe tests were conducted on the model pipeline segment, with four soil samples being prepared. The general arrangement was shown in Figure 2. The types of tests undertaken are as follows.

- Pipe installation without horizontal loading, monotonically penetrating the pipe to prescribed load V_{max}, and unloading to the load level V_0 at which the pipe sideswipe or probe tests will be conducted.
- Sideswipe tests, where the vertical position of the pipe was held constant while it was pushed laterally. The tests were performed both on normal-penetrated (V_0=V_{max}) pipe and on over-penetrated (V_0<V_{max}) pipe.
- Probe tests, where the vertical load on the pipe was held constant while the pipe was pushed laterally. Two different pipe installation methods were adopted in probe tests, pushed-in method and trenching method. Both normal-penetrated pipe probe tests and over-penetrated pipe probe tests were conducted on the pushed-in pipe, while V_0 = 4 kN/m was selected for all trenched pipe probe tests.

3.2 Testing Procedure

Prior to starting self-weight consolidation of the samples on the centrifuge, a cone penetrometer and actuator were mounted on the strong box. At the completion of consolidation at 50 g, two cone penetration tests were conducted. The penetrating rate was 0.1 mm/s to ensure the test was performed fully drained.

After the completion of the two cone penetration tests, the centrifuge was stopped and the cone penetrometer was replaced by the model pipeline segment and load cell. The actuator was positioned over the pipe test site and the centrifuge accelerated to 50 g. Pipe tests were then carried out.

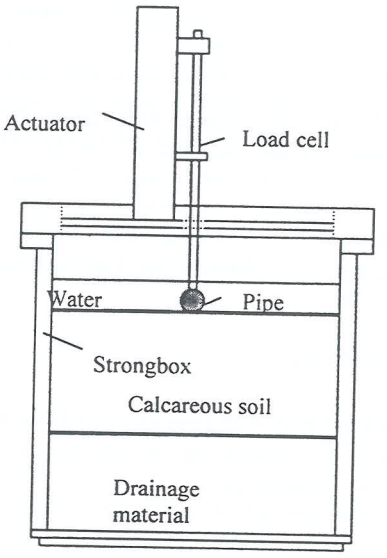

Figure 2 General arrangement of test package

4. TEST RESULTS

4.1 Sample Conditions

The method of sample preparation and the loading rate was kept as constant as possible to minimise differences between each sample, and to minimise the error in soil resistance caused by drainage conditions. The average density and water content measured for each sample are listed in Table 1. The average gradients of cone penetration resistance measured with the 2 MPa (10 mm diameter) cone before and after pipe tests are also listed in this table.

4.2 Pipeline Installation – Pipe Load-Unload Tests

During over-penetrated pipe tests, the pipe was firstly penetrated into the soil until the vertical load was equal the prescribed value V_{max} and then unloaded to get the vertical stress hold load V_0. Hence a load-unload test was actually performed in this installation process. Typical results from these load-unload tests are shown in Figure 3.

Table 1 Summary of soil sample conditions

Sample	γ (kN/m^3)	ω (%)	γ_d (kN/m^3)	e*	CPT Gradient (kPa/m)
1	18.1	30.5	13.9	0.824	340
2	18.5	31	14.1	0.837	480
3	18.6	31.3	14.2	0.845	420
4	18.6	31.6	14.2	0.853	410

*Obtained by assuming $G_s = 2.70$ and soil was fully saturated.

Table 2 Summary of k_{ve} and k_{vp} values

Test	V_{max} (kN/m)	V_0 (kN/m)	k_{vp} (kN/m/m)	k_{ve} (kN/m/m)
1-7	80	40	400	7200
1-8	80	20	260	10000
1-9	80	10	370	6300
2-4	80	4	330	8600
2-5	80	8	350	6000
2-6	80	20	340	7000
2-7	80	20	350	7500
3-1	20	4	320	10500
3-2	40	4	380	6900
3-3	80	4	390	7500
4-8	100	4	420	7700

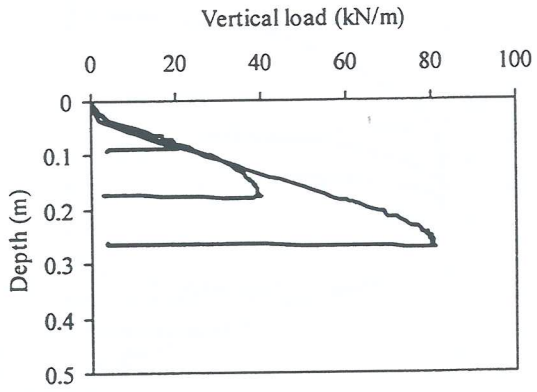

Figure 3 Pipeline vertical load-displacement response

The vertical load required for penetrating the pipe increased approximately linearly with depth, despite an increase in the contact area between pipe and soil as penetration increased. The gradients of the loading line and unloading line are listed in Table 2. In this table, k_{vp} describes the gradient of loading line while k_{ve} describes the gradient of unloading line. The gradient of loading line is around 350 kN/m/m, and the gradient of unloading line around 7000 kN/m/m. It may be concluded that the gradient of the unloading line is about 20 times greater than that of the loading line for the soil samples used in this study.

4.3 Horizontal Load-Displacement Response

4.3.1 Sideswipe tests

Sideswipe tests were undertaken to effectively trace out the shape of the yield surface (Tan, 1990, and Martin, 1994) of the foundation under combined vertical and horizontal loading. This technique has been successfully applied to pipe-soil interaction problems (Zhang et al., 1999b). Test results are summarised in Table 3 with typical ones shown in Figures 4 and 5.

Table 3 Summary of sideswipe test data

Test	V_{max}, V_0 (kN/m)	H_{max} (kN/m)	V_1 at H_{max} (kN/m)	H_{max}/V_{max}	V_1/V_{max}
1-1	3.7, 3.7	0.43	1.66	0.12	0.46
1-2	9.6, 9.6	1.3	4.8	0.14	0.5
1-3	19.1, 19.1	2.6	9.9	0.14	0.52
1-4	39.5, 39.5	6.6	17.1	0.17	0.43
1-5	79.1, 79.1	14.2	34	0.18	0.43
1-6	77.7, 10	7.6	10.4	-	-
1-7	80, 20	9.5	20.1	-	-
1-8	78.9, 39	12.6	34	0.16	0.43
1-9	77, 57	14.4	40.2	0.19	0.52

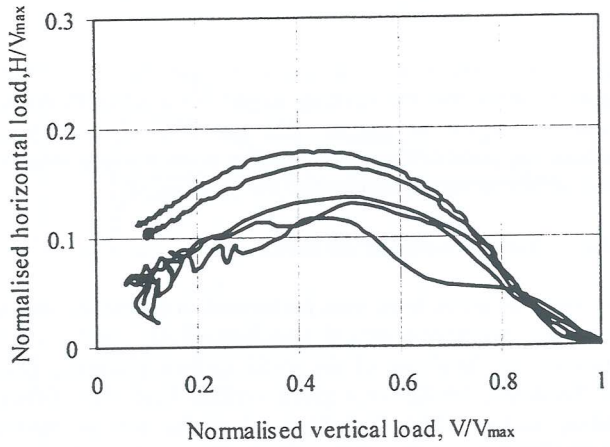

Figure 4 Sideswipe at $V_0 = V_{max}$

The relationship between horizontal load and displacement, as well as the yield surface agreed very well for the two series of sideswipe tests. As the pipe was displaced laterally, the horizontal load initially increased to a peak, while the vertical load dropped. After the peak horizontal load was reached, both vertical and horizontal loads reduced to approximately constant values.

The yield envelopes shown in Figure 4 are approximately parabolic in shape, with the horizontal load reaching a peak of about 15% of the peak vertical load. The vertical load corresponding to the peak horizontal load was between 43% and 52% with an average of 47% of the peak vertical load. It is worth mentioning that Tan (Tan, 1990) has suggested H_{max} occurred at a value of $V/V_{max} \approx 0.46$. This feature probably suggested that the yield envelope has a vertical load axis intercept at negative vertical load (thus intersecting the horizontal load axis at a positive value). An intercept on the horizontal load axis represents passive soil resistance, and the negative intercept on the vertical load axis does not indicate that the pipeline has significant uplift capacity.

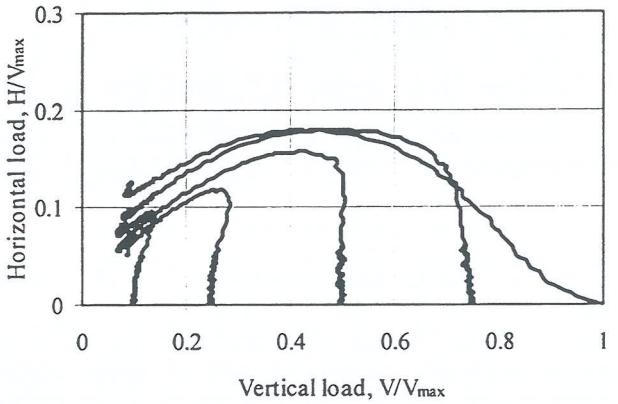

Figure 5 Sideswipe at $V_0 < V_{max}$

Results from over-penetrated pipe sideswipe tests, as plotted in Figure 5, show that the loading points initially travel through an elastic region at almost constant vertical load before reaching the yield surface. The loading point moving along the yield surface as soon as it reached the yield point.

4.3.2 Pushed-in pipe probe tests

Two types of probe tests were performed to define the limiting horizontal resistance (Gottardi and Butterfield, 1993), and the expansion or shrinkage of the yield surface (Stewart, Zhang and Randolph, 1998), for a given vertical load after different loading history. The first type of probe test is normal-penetrated pipe probe test, where the vertical load was corresponding to the initial embedment, i. e., $V=V_{max}=k_{vp}z_0$. The second type of probe test is the over-penetrated probe test. In these tests, the vertical load was fixed at a predetermined value, say, 4 kN/m, at different initial penetrations.

Normal-penetrated pipe probe tests

The results from normal-penetrated pipe probe tests are summarised in Table 4 with typical results shown in Figure 6. For each test the maximum horizontal load was estimated from the data, although the pipe was not always pushed far enough to define this load exactly, or the capacity of the load cell was reached. The horizontal loading curve levelled when the horizontal load approximately equals the vertical load.

Test data revealed that the expansion of the yield envelope was related to the vertical load or the initial embedment of the pipe, as the vertical displacement increment increased with the increasing of pipe initial embedment. The initial gradient of displacement was about 0.6, and has been shown not to depend on the initial embedment. The data did not indicate a direct relation between initial stiffness of horizontal loading with pipe initial embedment or load level, but most likely a constant value, as shown in Figure 6.

Table 4 Summary of normal-penetrated pipe probe tests

Test	V (kN/m)	z_0 (m)	H_{max} (kN/m)	δz (m)	Initial (dz/dx)
2.1	4	0.073	3.9	0.043	0.4
2.2	10	0.085	11.6	0.226	0.6
2.3	20	0.104	20.9*	0.31	0.6
3.1	4	0.037	3.3	0.067	0.7
3.2	8	0.085	7	0.122	0.4
3.3	16	0.104	18.1	0.25	0.7
3.4	4	0.082	3.4	0.03	0.3
4.6	4	0.018	3.0	0.049	0.4

* Limited by load cell capacity.

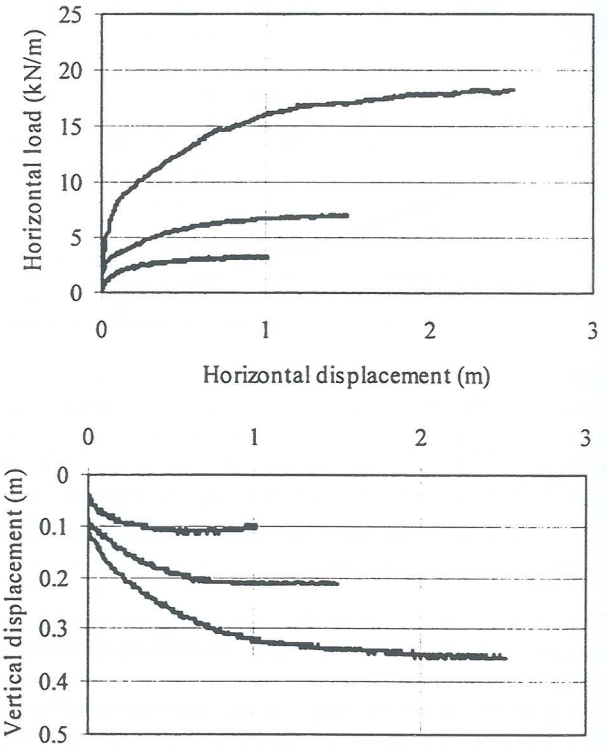

Figure 6 Normal-penetrated pipe probe test results
a) Horizontal load development; b) Pipe displacements

Over-penetrated pipe probe tests

As shown in Table 5 and Figure 7, over-penetrated pipe probe tests revealed different trends compared with those from the normal-penetrated pipe probe tests. During the first stage of horizontal displacement, pipe movement was always upwards when the over-penetration ratio V_{max}/V_0 was larger than about 10, and there was considerable post-peak softening of the horizontal load.

Table 5 Data from over-penetrated pipe probe tests

Test	V_{max}, V_0 (kN/m)	z_0 (m)	H_{max} (kN/m)	δz (m)	Initial dz/dx
2.4	80, 4	0.24	3.6	-0.1	-0.15
2.5	80, 10	0.24	4.2	-0.01	-0.03
2.6	80, 20	0.24	16.8	0.056	0.06
3.5	40, 4	0.17	3.7	0.012	0.08
3.6	80, 4	0.27	4.6	-0.19	-0.19
3.7	100, 4	0.30	4.4	-0.213	-0.21

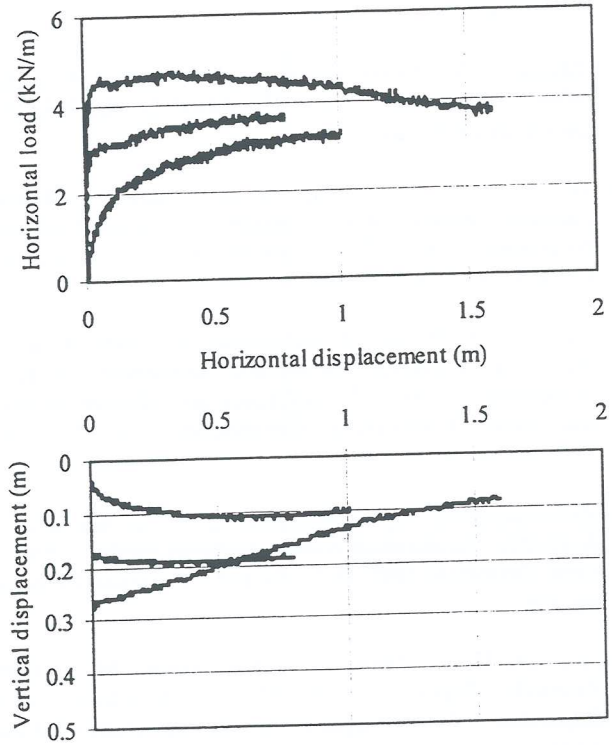

Figure 7 Over-penetrated pipe probe test results
a) Horizontal load development; b) Pipe movement

4.3.3 Trenched pipe probe tests

Some probe tests were conducted on trenched pipelines in order to investigate the effects of installation method. The trench depth varied from 0.16 m to 0.84 m in prototype scale. A 4 kN/m vertical load was applied to the trenched pipe after spinning up in order to model the pipe self weight, and then horizontal load was applied and the probe test performed.

Test data is summarised in Table 6 with typical results shown in Figure 8. The data suggested that the peak horizontal load, the gradient of pipe initial displacement and pipe upward movement all increased with the increasing trench depth. However, the values of upward movement and the initial displacement gradient were much smaller than that from pushed-in pipe probe tests at a similar initial embedment.

Figure 8 shows that the initial stiffness of the pipe horizontal load-displacement curve was much lower than that given in Figures 6 and 7, suggesting that the pushed-in process resulted in a larger horizontal load, a higher initial horizontal stiffness and a larger gradient in pipe displacement curve. This is probably caused by the densification of the soil around the pipe by the push-in process.

Table 6. Data from trenched pipe probe tests

Test	Depth (m)	H_{max} (kN/m)	δz (m)	Initial dz/dx
4.1	0.16	3.7	-0.05	-0.116
4.2	0.28	4.8	-0.13	-0.123
4.3	0.67	8.8	-0.34	-0.398
4.4	0.84	11.7	-0.92	-0.483

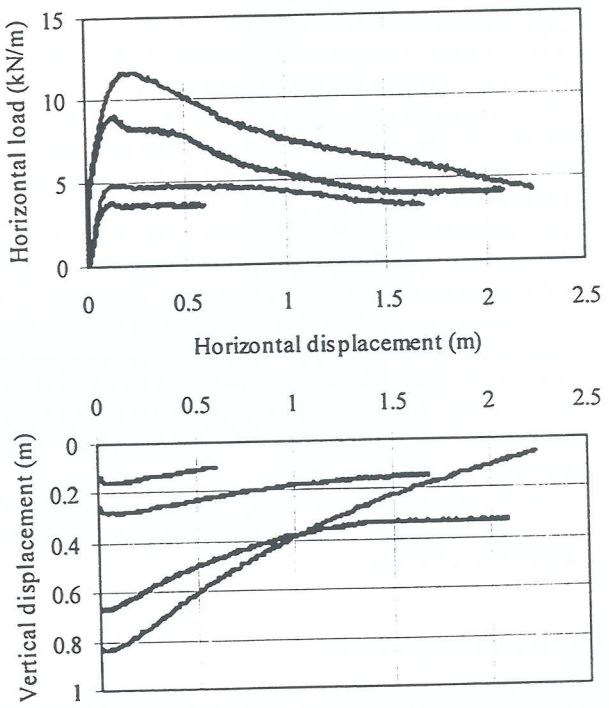

Figure 8 Trenched pipe probe test results
a) Horizontal load development; b) Pipe movement

5. SUMMARY AND COUNCLUSIONS

Twenty-five pipe tests were carried out on a fixed beam centrifuge at 50 g to investigate pipeline load-displacement response in calcareous sand. The three primary objectives of this experimental work were to define the yield surface for a pipeline under combined vertical and horizontal loads, to derive the hardening parameters of pipe-soil interaction and to investigate the effects of load history and installation method on pipeline response. As a result, the following conclusions were reached.

- Centrifuge modelling is a suitable technique for determining the features of pipe-soil interaction of shallowly buried pipelines in calcareous sand.
- The vertical stiffnesses of pipe loading and unloading are about 350kN/m/m and 7000 kN/m/m respectively. It implies that the stiffness of pipe reloading may be much greater than that in the initial loading. A further test programme is required to investigate this property of pipe-soil interaction.
- The yield surface of pipe-soil interaction under combined vertical and horizontal loads is parabolic in shape. At the critical state of pipe-soil interaction, pipe horizontal load of about 15% of its maximum vertical load was reached when the vertical load was about 47% of the maximum vertical load.
- The peak horizontal loads approximately equal to the vertical loads were recorded from the normal-penetrated pipe probe tests. Data from these tests did not show a direct relation between initial displacement gradient and horizontal stiffness and initial embedment.
- Over-penetrated pipe probe test data revealed that the pipe movement was upwards when the over-penetration ratio larger than about 10, and there was considerable post-peak softening of the horizontal load.
- For trenched pipes, the peak horizontal load, the initial displacement gradient and the initial horizontal stiffness were much smaller compared with those of pushed-in pipe.
- The results presented in this paper form a part of the data base of the geotechnical stability of offshore pipelines on calcareous soils. This database provides a corner stone not only for the development of a plasticity based pipe-soil interaction model, but also for the design of offshore pipelines in calcareous soils.
- A further test programme is required to elucidate the effect of cyclic loading and excess pore water pressure on this interaction problem.

ACKNOWLEDGEMENTS

The work described here is a part of a continuing research program on offshore foundation systems at the University of Western Australia. Research funding from the Australian Research Council, and the technical support in centrifuge testing from Mr Don Herley are gratefully acknowledged.

The author is supported by a University Postgraduate Award and an Ernest and Evelyn Havill Shacklock Scholarship in Civil Engineering at the University of Western Australia.

REFERENCES

1. Brennodden, H., Sveggen, O., Wagner, D. A. and Muff, J. D. (1986). "Full-Scale Pipe-Soil Interaction Tests". Proceedings of the 18th Offshore Technology Conference, pp. 433-450, OTC 5338, Texas.

2. Brennodden, H. and Stokkeland, A. (1992). "Time-Dependent Pipe-Soil Resistance for Soft Clay". Proceedings of the 24th Offshore Technology Conference, pp.339-348, OTC 6846, Texas.

3. Gottardi, G., and Butterfield, R. (1993). "On the Bearing Capacity of Surface Footings on Sand under General Planar Loads". Soils and Foundations, Vol. 33, No. 3, pp.68-79.

4. Lieng, J. T., Sotberg, T. and Brennodden, H. (1988). Energy Based Pipe-Soil Interaction Models. SINTEF Report, STF69-F87024.

5. Martin, C. M. (1994). Physical and Numerical Modelling of Offshore Foundations under Combined Loads. PhD thesis, University of Oxford.

6. Morris, D. V. and Dunlap, W. A. (1988). "Self-burial of Laterally Loaded Offshore Pipelines in Weak Sediments". Proceedings of the 20th Offshore Technology Conference, pp. 421-428, OTC 5855, Texas.

7. Paulin, M. J., Phillips, R. and Boivin, R. (1995). "Centrifuge Modelling of Lateral Pipeline-Soil Interaction – Phase II". Proceedings of the 14th Conference on Offshore Mechanics and Arctic Engineering, Copenhagen, Vol. 5, Pipeline Technology, pp. 107-123.

8. Randolph, M. F., Jewell, R. J., Stone, K. J. L., and Brown, T. A. (1991). "Establishing a new centrifuge facility". Proc. Int. Conf. Centrifuge 1991, H. Y. Ko (ed.), Balkema, Roteerdam, pp. 2-9.

9. Stewart, D. P., Zhang, J. and Randolph, M. F. (1998). Research Report, Geo:97193, Geomechanics Group, Department of Civil Engineering, The University of Western Australia.

10. Tan, F. S. (1990). Centrifuge and theoretical modelling of conical footings on sand. PhD thesis, University of Cambridge.

11. Zhang, J, Randolph, M. F. and Stewart, D. P. (1999b). "An Elasto-Plastic Model for Pipe-Soil Interaction of Unburied Pipelines". Proc. ISOPE'99, Brest, Vol. 2, p185-192.

House, ANdrew (ed); Watson, Phil (ed). PROCEEDINGS OF THE FOURTH (4TH) AUSTRALIA-NEW ZEALAND YOUNG GEOTECHNICAL PROFESSIONALS

The 4th Australia New Zealand Young Geotechnical Professionals Conference is generously supported by:

ADVANCED GEOMECHANICS

Centre for Offshore Foundation Systems

Douglas Partners
Geotechnics · Environment · Groundwater

EQC
EARTHQUAKE COMMISSION
Earthquake Commission Research Foundation

Golder Associates

GHD
Gutteridge Haskins & Davey Pty Ltd

MARINE & CIVIL CONSTRUCTION CO PTY LTD

PSM Pells Sullivan Meynink Pty Ltd
Engineering Consultants
Rock-Soil-Water

RIO TINTO

Worley Ltd

The Australian Centre for Geomechanics

Centre for Geotechnical Research at the University of Sydney

Dames & Moore Pty Ltd

Department of Civil Engineering, Monash University

Kalgoorlie Consolidated Gold Mines Pty Ltd

MPA Williams & Associates

Soil & Rock Engineering Pty Ltd

Western Australian School of Mines